

YUKON
EXPLORATION
& GEOLOGY
2005

Edited by

D.S. Emond, G.D. Bradshaw, L.L. Lewis and L.H. Weston

Yukon Geological Survey

Energy, Mines and Resources

Government of Yukon

Published under the authority of the Minister of Energy, Mines and Resources, Government of Yukon

<http://www.emr.gov.yk.ca>

Printed in Whitehorse, Yukon, 2006.

Publié avec l'autorisation du ministre de l'Énergie, des Mines et des Ressources
du gouvernement du Yukon

<http://www.emr.gov.yk.ca>

Imprimé à Whitehorse (Yukon) en 2006.

© Minister of Energy, Mines and Resources, Government of Yukon

ISBN 1-55362-271-5

This, and other Yukon Geological Survey publications, may be obtained from:

Geoscience and Information Sales
c/o Whitehorse Mining Recorder
102-300 Main Street
Box 2703 (K102)
Whitehorse, Yukon, Canada Y1A 2C6
phone (867) 667-5200, fax (867) 667-5150

Visit the Yukon Geological Survey web site at www.geology.gov.yk.ca

In referring to this publication, please use the following citation:

Yukon Exploration and Geology 2005. D.S. Emond, G.D. Bradshaw, L.L. Lewis and L.H. Weston (eds.),
2006. Yukon Geological Survey, 339 p.

Production by K-L Services, Whitehorse, Yukon.

PHOTOGRAPHS

Front cover: Jeff Bond is sampling stream sediments for heavy minerals in Mendocina Creek,
Big Salmon Range. Photo by Amber Church, Yukon Geological Survey.

Back cover: Wally Hyde, Yukon's 2005 Prospector of the Year, receiving his award at the 2005 Yukon
Geoscience Forum, November 2005. Photo provided by V. Fedoroff, Whitehorse Star.

PREFACE

Yukon Exploration and Geology (YEG) continues to be the main publication of the Yukon Geological Survey (Energy, Mines and Resources, Yukon government). This is the 28th volume of the series.

YEG 2005 contains up-to-date information on mining and mineral exploration activity, studies by industry, and results of recent geological field studies. Information in this volume comes from prospectors, exploration and government geologists, mining companies and students who are willing to collectively benefit the scientific community, general public, as well as the mineral and petroleum industries of the Yukon. Their assistance and patience is sincerely appreciated.

Sincere appreciation is extended to the YEG co-editors. We were fortunate to have Leyla Weston rejoin the team this year; and Geoff Bradshaw and Lara Lewis also continued in this role. Thanks go to all of them for their help in making the editorial process effective, efficient and fun. We thank the Translation Bureau, Public Works and Government Services Canada for translating the French abstracts. Appreciation is also extended to Maurice Colpron of the Yukon Geological Survey (YGS) for his able assistance in the review of French translations of abstracts. We also thank all the geologists who contributed by critically reviewing YEG manuscripts: S. Sutherland, S. Traynor, L. Pigage, G. Bradshaw, C. Hart, J. Bond, L. Kennedy, S. Piercey, T. Lynch, D. Gibson, L. Groat, R. Friedman, R. MacNaughton, J. Scoates, J.G. Abbott and M. Burke.

Wynne Krangle and Peter Long of K-L Services continue to provide excellent service in putting this production together, including editing suggestions, design of diagrams, volume layout, and working under the pressure of a tight deadline. Sherry Tyrner of the Queen's Printer once again ensured that the printing process went smoothly.

The 2005 volume has four parts. The first – Mineral Industry – includes overviews of hardrock and placer mining, development and exploration in the territory as well as a summary of the Yukon Mining Incentives Program. The second part – Government – outlines the activities and organization of the Yukon Geological Survey, and includes announcements of the sixth Mining Land Use Reclamation Awards, the Robert E. Leckie Awards. The third part – Geological Fieldwork – contains reports describing regional mapping, and more detailed geoscience studies. The last part – Property Description – is meant for submissions from the mineral industry on mineral occurrences and deposits. This year there is only one paper on a mineral occurrence in the Mayo area.

We welcome any input or suggestions that you may have to improve future YEG publications. Please contact me at (867) 667-3203 or by e-mail at diane.emond@gov.yk.ca.

Diane Emond

PRÉFACE

Yukon Exploration and Geology (YEG) continue d'être la publication principale de la Commission géologique du Yukon (Énergie, Mines et Ressources, gouvernement du Yukon). Ce volume est le 28e de la série.

YEG 2005 contient une mise à jour sur l'exploitation et l'exploration minières, les études réalisées par l'industrie et les résultats des travaux géologiques exécutés récemment sur le terrain. L'information est fournie par des prospecteurs, des géologues prospecteurs et du gouvernement, des sociétés minières et des étudiants qui veulent en faire bénéficier la communauté scientifique, le grand public, ainsi que les industries minières et pétrolières du Yukon. Nous apprécions leur aide et leur dévouement.

Nous tenons à remercier les co-rédacteurs du YEG. Cette année, Leyla Weston s'est jointe à notre équipe et nous avons continué à recevoir l'appui de Lara Lewis et de Geoff Bradshaw. Nous tenons à tous les remercier de nous avoir aidés à rendre efficace, efficient et amusant le processus de rédaction. Nous remercions le Bureau de la traduction, Travaux publics et Services gouvernementaux Canada, d'avoir traduit les résumés en français. Nous remercions également Maurice Colpron de la Commission géologique du Yukon pour son aide précieuse en matière de révision des traductions de résumés en français. Il faut aussi souligner la contribution de plusieurs géologues à la lecture critique des manuscrits, au cours de cette année; il s'agit notamment de S. Sutherland, S. Traynor, L. Pigage, G. Bradshaw, C. Hart, J. Bond, L. Kennedy, S. Piercey, T. Lynch, D. Gibson, L. Groat, R. Friedman, R. MacNaughton, J. Scoates, J.G. Abbott et M. Burke.

Wynne Krangle et Peter Long de K-L Services ont une fois de plus fourni un excellent service de production, incluant des suggestions de révision, la conception de diagrammes, la mise en page et le respect d'échéances serrées. Sherry Tyrner de l'Imprimeur de la Reine a, pour sa part, veillé au bon déroulement de l'impression.

Le volume de 2005 comprend quatre parties. La première – Industrie minérale – renferme des survols sur l'exploitation, le développement et l'exploration minières de roches dures et de placers dans le territoire, de même qu'un résumé sur le Programme d'encouragement des activités minières du Yukon. La deuxième partie – Gouvernement – décrit dans les grandes lignes les activités et l'organisation de la Commission géologique du Yukon, et présente la sixième édition des prix Robert E. Leckie, récompensant les meilleurs travaux de remise en état des sites miniers. La troisième partie – Travaux géologiques sur le terrain – contient des rapports décrivant la cartographie régionale et des études géoscientifiques plus détaillées. La dernière partie – Descriptions des propriétés – vise les présentations des sociétés minières concernant des occurrences et des gîtes minéraux. Cette année, on ne présente qu'une seule étude sur une occurrence minéralisée dans la région de Mayo.

Pour tout commentaire ou suggestion afin d'améliorer les futures publications du YEG, vous être priés de communiquer avec moi par téléphone au (867) 667-3203 ou par courriel à l'adresse suivante : diane.emond@gov.yk.ca.

Diane Emond



TABLE OF CONTENTS

MINERAL INDUSTRY

Yukon Mining, Development and Exploration Overview 2005	
M. Burke	2
Appendix 1: 2005 exploration projects.....	38
Appendix 2: 2005 drilling statistics	40
Yukon Placer Mining Overview 2005	
W. LeBarge.....	41
Yukon Mining Incentives Program 2005	
S. Traynor.....	47

GOVERNMENT

Yukon Geological Survey	
G. Abbott and staff	51
La Commission géologique du Yukon	
G. Abbott et M. Colpron.....	67
Robert E. Leckie Award for Outstanding Reclamation Practices	
J. St. Amand	71

GEOLOGICAL FIELDWORK

Triassic overlap assemblages in the northern Cordillera: Preliminary results from the type section of the Jones Lake Formation, Yukon and Northwest Territories (NTS 1051/13)	
L.P. Beranek and J.K. Mortensen	79
Geology and mineral potential of Yukon-Tanana Terrane in the Livingstone Creek area (NTS 105E/8), south-central Yukon	
M. Colpron.....	93
Gold mineralization in the upper Hyland River area: A non-magmatic origin	
C.J.R. Hart and L.L. Lewis.....	109
Unconformity-related uranium potential: Clues from Wernecke Breccia, Yukon	
J. Hunt, G. Abbott and D. Thorkelson.....	127
Bedrock geology of the Duke River area, parts of NTS 115G/2, 3, 4, 6 and 7, southwestern Yukon	
S. Israel, A. Tizzard and J. Major	139
Placer geology and prospective exploration targets of Sixtymile River area, west-central Yukon	
W. LeBarge.....	155
Active-layer detachments following the summer 2004 forest fires near Dawson City, Yukon	
P.S. Lipovsky, J. Coates, A.G. Lewkowicz and E. Trochim.....	175

continued

Anatomy of a Late Jurassic Gilbert-type delta in basal strata of the Tantalus Formation, Whitehorse Trough, Yukon D.G.F. Long and G.M. Lowey.....	195
Summary of Rock-Eval data for the Whitehorse Trough, Yukon: Implications concerning the hydrocarbon potential of a frontier basin G.W. Lowey and D. Long	207
Geology of the Quartet Mountain lamprophyre suite, Wernecke Mountains, Yukon D. Milidragovic, D.J. Thorkelson and D.D. Marshall.....	231
Compositional studies of placer and lode gold from western Yukon: Implications for lode sources J.K. Mortensen, R. Chapman, W. LeBarge and E. Crawford.....	247
Uranium-lead ID-TIMS and LA-ICP-MS ages for the Cassiar and Seagull batholiths, Wolf Lake map area, southern Yukon J.K. Mortensen, C. Sluggett, T. Liverton and C.F. Roots	257
Stratigraphy Summary for southeast Yukon (NTS 95D/8 and 95C/5) L.C. Pigage	267
Geochronological and lithochemical studies of intrusive rocks in the Nahanni region, southwestern Northwest Territories and southeastern Yukon K.L. Rasmussen, J.K. Mortensen and H. Falck	287
Paleomagnetism of the ~91 Ma Deadman pluton: Post-mid-Cretaceous tectonic motion in central Yukon D.T.A. Symons, M.J. Harris, C.J.R. Hart and P.J.A. McCausland.....	299
Structural constraints for oil and gas assessment in the Whitehorse Trough: New results from seismic profiling D. White, M. Colpron, G. Buffett and B. Roberts	315

PROPERTY DESCRIPTIONS

Sediment-hosted disseminated gold occurrence, northeast Mayo Lake area G. Lynch.....	327
---	-----

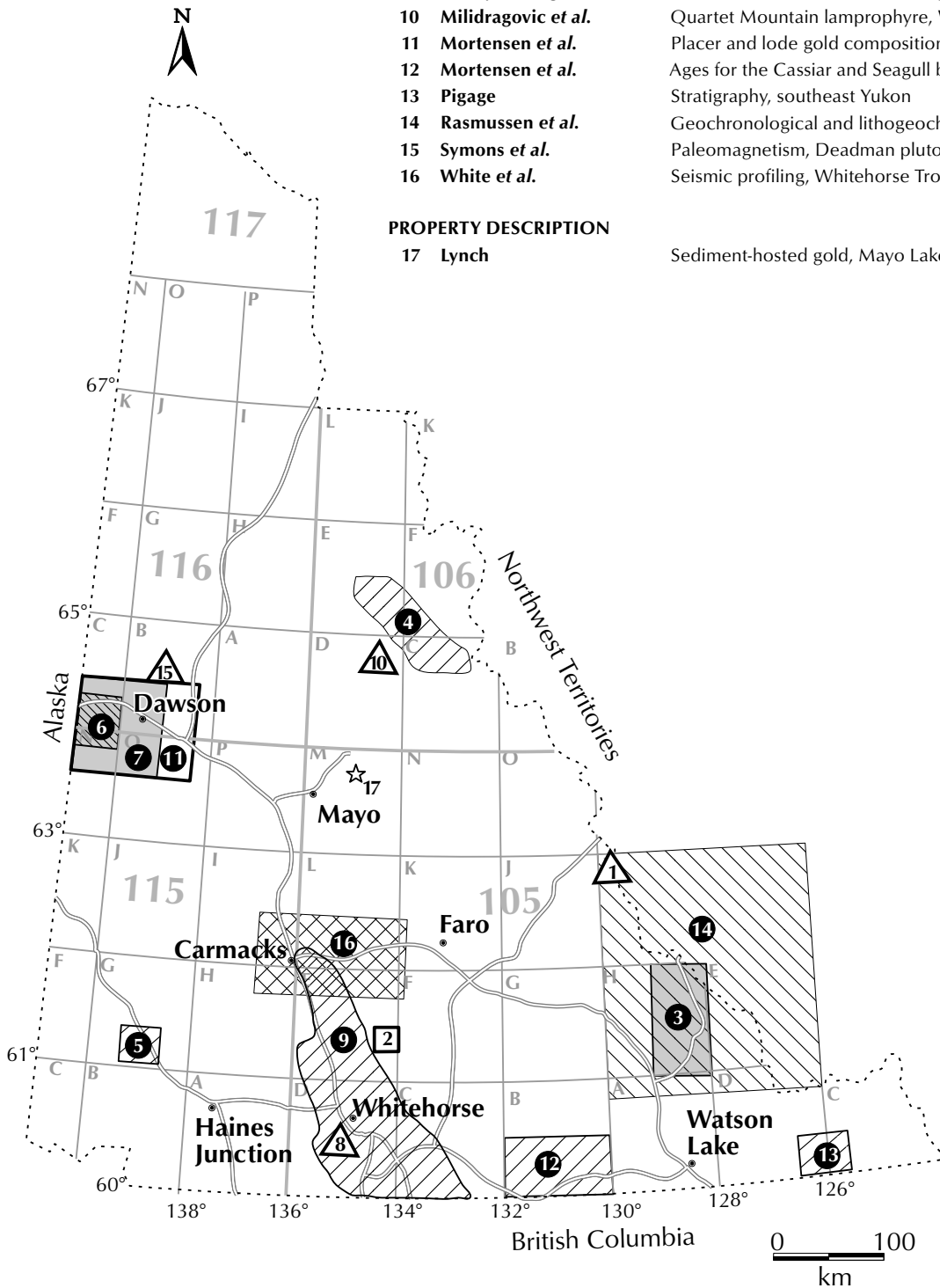
YUKON EXPLORATION AND GEOLOGY 2005

GEOLOGICAL FIELDWORK

<p>1 Beranek & Mortensen 2 Colpron 3 Hart and Lewis 4 Hunt <i>et al.</i> 5 Israel <i>et al.</i> 6 LeBarge 7 Lipovsky <i>et al.</i> 8 Long & Lowey 9 Lowey & Long 10 Milidragovic <i>et al.</i> 11 Mortensen <i>et al.</i> 12 Mortensen <i>et al.</i> 13 Pigage 14 Rasmussen <i>et al.</i> 15 Symons <i>et al.</i> 16 White <i>et al.</i></p>	<p>Triassic overlap assemblages, Jones Lake Formation Geology and mineral potential, Livingstone Creek area Gold mineralization, upper Hyland River area Unconformity-related uranium Geology, Duke River area Placer geology and exploration targets, Sixtymile River Active-layer detachments, Dawson City area Tantalus Formation, Whitehorse Trough Rock-Eval data, Whitehorse Trough Quartet Mountain lamprophyre, Wernecke Mountains Placer and lode gold compositions, western Yukon Ages for the Cassiar and Seagull batholiths Stratigraphy, southeast Yukon Geochronological and lithochemical studies, Nahanni region Paleomagnetism, Deadman pluton Seismic profiling, Whitehorse Trough</p>
---	---

PROPERTY DESCRIPTION

<p>17 Lynch</p>	<p>Sediment-hosted gold, Mayo Lake area</p>
------------------------	---



MINERAL INDUSTRY

Yukon Mining, Development and Exploration Overview 2005

Mike Burke
Yukon Geological Survey

Yukon map.....	2
Abstract	3
Résumé.....	3
Introduction	4
Base metals	7
Volcanic associated	7
Mafic/ultramafic associated.....	10
Porphyry/sheeted vein associated	12
Wernecke Breccia	16
Sedimentary rock associated.....	19
Vein/breccia associated.....	22
Skarn.....	23
Precious metals	24
Porphyry/sheeted vein.....	24
Skarn/replacement.....	26
Vein/breccia associated.....	28
Bulk sample valuations.....	35
Coal.....	36
References	37
Appendix 1: 2005 exploration projects.....	38
Appendix 2: 2005 drilling statistics.....	40

Yukon Placer Mining and Exploration Overview 2005

William LeBarge
Yukon Geological Survey

Placer mining	41
Placer exploration.....	43
Aperçu	45

Yukon Mining Incentives Program 2005

Steve Traynor
Yukon Geological Survey

.....	47
Résumé.....	48

Yukon Mining, Development and Exploration Overview 2005

Mike Burke¹

Yukon Geological Survey

Burke, M., 2006. Yukon Mining, Development and Exploration Overview 2005. In: Yukon Exploration and Geology 2005, D.S. Emond, G.D. Bradshaw, L.L. Lewis and L.H. Weston (eds.), Yukon Geological Survey, p. 2-40.

ABSTRACT

Exploration expenditures in Yukon have continued their dramatic rise for the third consecutive year, with an estimated \$53 million spent exploring for a wide range of commodities. Base metal exploration (mainly zinc) has benefited the most from this resurgence. Exploration for copper, tungsten and uranium has also substantially increased this year, as has exploration for precious metals. The majority of expenditures were on advanced stage projects. Approximately 30 properties were subjected to drilling programs, many with the intent to upgrade existing resources, while several other projects were subjected to their first ever drilling.

Three projects are currently approaching production decisions: Yukon Zinc Corp.'s Wolverine (zinc-silver-lead-copper-gold), Sherwood Copper Corp.'s Minto (copper-gold-silver) and Cash Minerals Ltd.'s Division Mountain (coal) deposits. All three projects conducted advanced exploration in support of feasibility studies, which are expected to be released in the last quarter of 2005 and the first quarter of 2006.

RÉSUMÉ

Les dépenses d'exploration au Yukon ont encore augmenté de manière saisissante et ce pour la troisième année consécutive; on estime qu'il s'est dépensé 53 millions de dollars en travaux d'exploration à la recherche d'une gamme étendue de produits. Cet accroissement a profité surtout les projets d'exploration à la recherche de métaux communs (et surtout du zinc). Les travaux d'exploration à la recherche de cuivre, de tungstène et d'uranium ont aussi considérablement augmenté cette année tout comme ce fut le cas pour les métaux précieux. Les dépenses ont été en majorité consacrées à des projets qui en étaient aux stades avancés. Des programmes de forages ont été menés dans environ 30 propriétés, dans plusieurs cas dans le but d'ajouter aux réserves existantes de ressources alors que pour plusieurs autres projets il s'agissait des premiers forages exécutés.

Des décisions d'entreprendre la production sont imminentes aux trois gisements suivants : Wolverine (zinc-argent-plomb-cuivre-or) de la Yukon Zinc Corp., Minto (cuivre-or-argent) de la Sherwood Copper Corp. et Division Mountain Ltd. (charbon) de Cash Minerals. Dans le cadre de chacun de ces projets des travaux d'exploration préliminaires ont été exécutés à l'appui d'études de faisabilité qui devraient être diffusées au dernier trimestre de 2005 et au premier trimestre de 2006.

¹mike.burke@gov.yk.ca

INTRODUCTION

Mineral exploration expenditures have continued their dramatic rise for the third consecutive year, with an estimated \$53 million spent in 2005 exploring for a wide range of commodities. Expenditures in 2004 were \$22 million (Fig. 1). Approximately 70% of expenditures were spent on the exploration of base metals, 20% for precious metals and the remainder on gemstones and coal. The location of projects with expenditures greater than \$25 000 is shown in Figure 2 (on previous page spread). Claim staking remained at significant levels (5716 claims, Fig. 3) and claims in good standing (Fig. 4) have increased slightly over 2005 (50 373 claims). Three projects are currently approaching the production stage; these consist of Yukon Zinc Corporation’s Wolverine (zinc-silver-lead-copper-gold), Sherwood Copper Corporation’s Minto (copper-gold-silver) and Cash Minerals Ltd.’s Division Mountain (coal) deposits. All three projects conducted advanced exploration in support of feasibility studies which are expected to be released in the last quarter of 2005 and the first quarter of 2006.

The Government of Yukon continued to support the mineral industry in several areas including: 1) the Yukon Mining Incentives Program which offered approximately \$1.09 million to 63 successful applicants (Traynor, 2006); and 2) the Yukon Mineral Exploration Tax Credit which offers a refundable corporate and personal income tax credit of 25% of eligible mineral exploration expenditures incurred by qualified individuals and corporations conducting off-minesite exploration in the Yukon between April 1, 2004 and March 31, 2007. Control over the territory’s natural resources was recently transferred from Canada to the Yukon government. Decisions regarding oil and gas, mining, lands, forests and water are now made by the Yukon government. Internally, the government has initiated an Integrated Resource Management Strategy. This strategy streamlines the review process by addressing policies and legislation gaps, and it establishes better collaboration between departments.

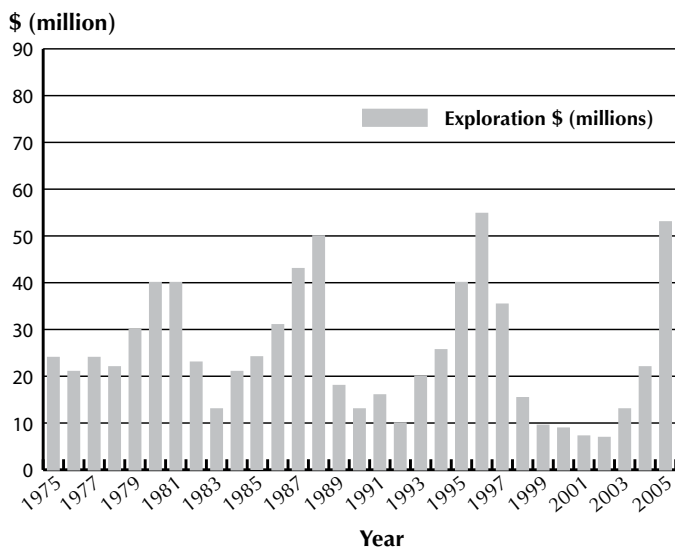
An example of this strategy is the Project Management Process that assists mining companies in their efforts to secure permits for development proposals. Project coordinators are assigned to individual projects to assist with the reviews and

timely resolution of issues for each project. The project coordinators report to a team of deputy ministers that is responsible for regulatory approvals. This committee is chaired by Energy, Mines and Resources.

Currently, five Yukon projects have been assigned project coordinators. These consist of Yukon Zinc Corporation’s Wolverine (zinc-silver-lead-copper-gold), Sherwood Copper Corporation’s Minto (copper-silver-gold), Cash Minerals Ltd.’s Division Mountain coal, Western Silver’s Carmacks Copper (copper-gold) and Tintina Mines Ltd.’s Red Mountain (molybdenum) deposits.

The Government of Yukon also continued to maintain current levels of funding for geoscience projects under the auspices of the Yukon Geological Survey. Of further interest, 11 of 13 Yukon First Nations have ratified their land claim agreements.

Figure 1. Exploration expenditures 1971 to 2005 (estimated).



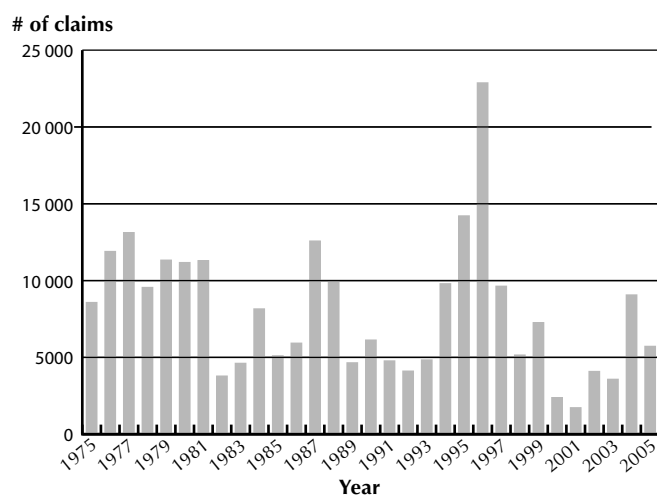


Figure 3. Claims staked 1975 to 2005.

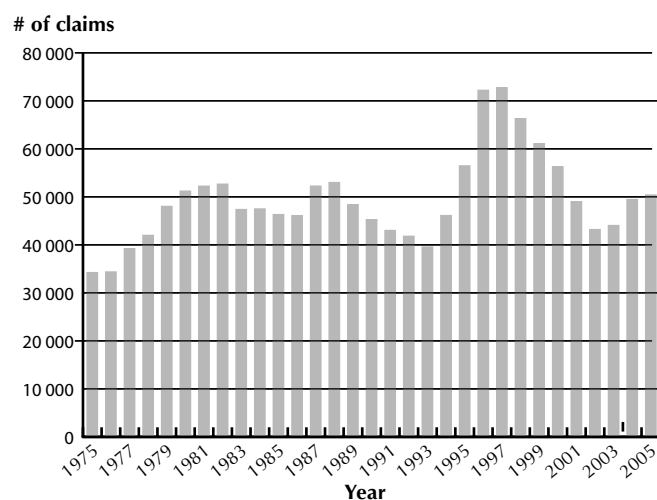


Figure 4. Claims in good standing 1975 to 2005.

Base metal exploration (mainly zinc) has benefited most from the resurgence in exploration expenditures. The largest exploration program in Yukon was the Wolverine project of Yukon Zinc Corporation in the Finlayson Lake volcanogenic massive sulphide (VMS) district; over \$20 million were spent on this project. Yukon Zinc also conducted exploration on several of their other projects in the Finlayson Lake district. Exploration for zinc has resumed in the Selwyn Basin, within a late Precambrian-Devonian depositional basin, which is well known to host significant zinc-lead-silver sedimentary exhalative deposits. Pacifica Resources acquired the Howard's Pass sedimentary exhalative deposits and conducted a major drilling program on the shallow portions of the known deposits, as well as on exploration targets within other areas of prospective stratigraphy.

Exploration for copper, tungsten, uranium and molybdenum has also substantially increased this year. Copper exploration was targeted in several different geological settings throughout Yukon. The largest project was conducted by Sherwood Copper Corporation after acquiring 100% of the Minto deposit. The Minto deposit is an intrusion-related magmatic-hydrothermal system that displays characteristics of both porphyry (R. Tafti and J.K. Mortensen, 2004) and iron-oxide-copper-gold (IOCG) systems. Other projects that have copper as the primary commodity of interest are the Lucky Joe project of Kennecott Canada/Copper Ridge Exploration, which is a new intrusion-related magmatic-hydrothermal target in the Stewart River area south of Dawson, as well as several projects targeting IOCG mineralization hosted in Wernecke Breccias in the northern Yukon. Copper-gold skarn and porphyry mineralization in the Whitehorse Copper Belt also continued to receive some attention. Copper-nickel-platinum group element (PGE) mineralization in the Kluane mafic-ultramafic belt of western Yukon had an increase in activity; exploration programs were conducted at Northern Platinum/Coronation Minerals Wellgreen property, Golden Chalice/Strategic Minerals Burwash property and Resolve Ventures' Klu property (optioned from Inco Ltd.). Falconbridge Ltd. also became active in the Kluane mafic-ultramafic belt late in 2005 by optioning the Canalask property from StrataGold Corporation.

The strength in the tungsten price has resulted in a resumption of production at North American Tungsten Corporation's Cantung mine located in the

Northwest Territories but accessed through the Yukon. The first tungsten concentrates from the mine were shipped in mid-October, 2005. The annual concentrate production capacity from the mine is 400 000 metric tonne units.

Tungsten exploration increased as a result of drill programs at North American Tungsten's MacTung deposit and at Copper Ridge Exploration's Kalzas occurrence.

Uranium exploration was focused mainly in the Wernecke Mountains area of northeast Yukon where many occurrences of uranium-enriched IOCG mineralization are known to exist. Companies such as Cash Minerals Ltd. and Signet Minerals Inc. are active in the region, having recognized the under-explored potential of unconformity-related uranium occurrences.

Molybdenum has re-emerged as a commodity of interest for exploration companies, and in 2005, the Red Mountain deposit of Tintina Mines conducted engineering and environmental studies on their project in preparation for a proposed underground exploration program for 2006. Furthermore, small exploration programs were performed on the Stormy molybdenum deposit, acquired by E-Energy Ventures, and the Rams Horn molybdenum occurrence of Ordorado Resources.

Exploration for precious metals has also benefited from the increase in exploration expenditures. Epigenetic gold mineralization is recognized in several different settings within Yukon. These consist of intrusion-related gold, associated with mid-Cretaceous plutonism; orogenic gold, related to Jurassic and Eocene events; epithermal gold, related to late Cretaceous to Eocene sub-aerial volcanism; and gold skarns, related to Cretaceous, oxidized and reduced intrusions. Exploration for intrusion-related gold occurred mainly within the western portion of the Tintina Gold Belt between Dawson and Mayo where accessibility is greatest. StrataGold Corporation conducted the largest drill program at the Dublin Gulch deposit, north of Mayo. Drilling also occurred at Acero-Martin Industries Ice property, as well as at the Mike Lake project of Bashaw Capital which was drilled for the first time. A large number of orogenic, gold-vein targets are being explored in the Dawson-Stewart River area, with the most advanced program being the Lone Star property of Klondike Star Corporation. Recent work by Craig Hart of the Yukon Geological Survey (Hart and Lewis, 2006) has classified the belt of gold occurrences in the Hyland River area of eastern Yukon as orogenic. Epithermal gold was targeted at the Grew Creek deposit of Freegold Ventures Inc. in the Faro area and by Tagish Lake Gold Corporation at their Skukum Creek deposit south of Whitehorse.

Exploration of properties with high silver potential has also increased as is shown by the renewed exploration of several projects in the Rancheria district of southern Yukon. Work in this area included a drilling program by CMC Metals Ltd. at their newly acquired CMC property. Furthermore, exploration for silver is expected to increase substantially in 2006 with recent developments in the Keno Hill Silver mining camp; Alexco Resource Corp. has an Agreement for Purchase and Sale for United Keno Hill Mines (UKHM). The Agreement of Purchase and Sale allows until March 31, 2006, if necessary, for the completion of an initial closing that is subject to negotiation of a subsidiary agreement between Alexco and the governments of Canada and Yukon. The subsidiary agreement addresses possible solutions to the long-term environmental care, maintenance and remediation of the UKHM mine site. Negotiations regarding the key terms of the subsidiary agreement were satisfactorily carried out during the fall of 2005.

True North Gems conducted bulk sampling for emeralds on their Tsa Da Glisza property. The company also processed the bulk sample acquired in 2004 from their True Blue property, and it was proven to contain blue beryls.

BASE METALS

VOLCANIC ASSOCIATED

Exploration for volcanic-hosted massive sulphide (VHMS) deposits occurred mainly in variably metamorphosed Upper Paleozoic sedimentary and volcanic rocks of the Yukon-Tanana Terrane and in Selwyn Basin, a predominantly off-shelf metasedimentary and metavolcanic sequence deposited west of ancestral North America. In Yukon-Tanana Terrane the massive sulphide deposits formed in continental-arc and back-arc-basin settings during rifting from the continental margin. Since the initial discovery of the **Kudz Ze Kayah** (Yukon MINFILE² 105G 117) deposit by Cominco Ltd. in 1994, four additional deposits (**Wolverine**, **GP4F**, **Fyre** and **Ice**; Yukon MINFILE 105G 073, 143, 034, 118, respectively) and numerous occurrences have been discovered in the Finlayson Lake district of southeastern Yukon. The majority of the exploration activity for VHMS deposits occurred in the Finlayson Lake district, however, exploration resumed in rocks of the Selwyn Basin with a drilling program at Yukon Gold Corporation's **Marg** deposit northeast of Mayo (Yukon MINFILE 106D 009).

The largest exploration program in Yukon was carried out by Yukon Zinc Corporation (formerly Expatriate Resources Ltd.) at their **Wolverine** zinc-silver-copper-lead-gold deposit (Yukon MINFILE 105G 073). The company conducted a program of test mining, definition drilling, metallurgical studies and other related work in support of completion of a bankable feasibility study being conducted by Hatch Associates Ltd. The program began early in the year with the construction of a winter road into the property to mobilize the equipment and materials necessary for the underground test mining (Fig. 5). The company submitted its environmental

²All Yukon MINFILE references are found in Deklerk and Traynor (2005).



Figure 5. Exploration portal at the Wolverine deposit.

assessment report (EAR) on October 28, 2005. The submission of the EAR sets in motion a public review and permitting process. The issuance of a water and mine-production licence will allow mine construction to begin. The company also reached a socio-economic participation agreement with Ross River Dena Council for formalizing its participation in the exploration and development of the Wolverine deposit and Yukon Zinc's extensive exploration lands in the Finlayson district. Ross River Dena Council represents the Kaska Nation, whose traditional territory encompasses Yukon Zinc's mineral claims within the Finlayson Lake district.

The Wolverine deposit, in all categories, is a 6 237 000-tonne resource, grading 12.66% Zn, 1.55% Pb, 1.33% Cu, 371 g/t Ag and 1.76 g/t Au. Currently, the probable diluted mining reserve (determined by Hatch Associates Ltd. in a November, 2000 pre-feasibility study) is 3 470 000 tonnes grading 12.43% Zn, 1.44% Pb, 1.37% Cu, 336.6 g/t Ag and 1.59 g/t Au (using a 4-m minimum thickness of the sulphide deposit) and will provide an eight-year mine life. The deposit was intersected with 56 drill holes totalling 11 713 m in the 2005 exploration program. This will upgrade the current resource figures and provide a more detailed outline of the orebody. This orebody has been intersected by 190 drill-holes to date. The deposit was accessed by a 5 x 5-m decline that will serve as the main haulage ramp during production. An access from the main haulage exposed a 110-m strike length of the deposit in a test stope. The ground conditions, particularly in the hanging-wall argillite, were better than expected, considering the poor quality of the host rocks in drill core.

Figure 6. First piece of sulphide mineralized rock from the test mining at Yukon Zinc Corporation's Wolverine deposit.



Test mining was successfully conducted in both the thinner margins of the deposit and within the thicker portions of the massive sulphide mineralization (Fig. 6). A five-tonne bulk sample was collected and will be used for completion of the metallurgical test work, as well as providing detailed paste backfill and additional dense media separation information. Dense media separation studies indicate that dilution encountered in the thinner portions of the deposit can be separated before material is processed in the mill. This will allow mining of the thinner, high-grade portions of the deposit and potentially upgrade thicker intersections of the orebody that contain some internal bands of barren argillite. The bankable feasibility study is scheduled for release in the first quarter of 2006, with a production decision to follow shortly thereafter.

Yukon Zinc holds title to over 640 km² of claims in the Finlayson Lake district. The company conducted a small drill program on the **Thunderstruck** (NTS 105G/8) discovery where zinc-silver-copper-lead-gold-bearing massive sulphide mineralization was intersected during drilling in 2004. Yukon Zinc

also optioned the **Money** copper-zinc-silver-gold property (Yukon MINFILE 105H 078) from YGC Resources. The Money claims are located approximately 5 km east of the Wolverine deposit. The claims encompass a younger succession of Pennsylvanian- to Permian-aged rocks, known as the Campbell Range succession, which hosts pyritic massive sulphide mineralization with minor copper, zinc, silver and gold. Yukon Zinc conducted a program of geological mapping and sampling on the claims.

Strategic Metals Ltd. explored the **Four Corners** Cu property (Yukon MINFILE 105G 146) located north of the Fyre Lake deposit in the Finlayson Lake District. The company conducted a program of prospecting and soil geochemistry surveys, and discovered a copper soil anomaly from limonitic float which assayed up to 0.97% Cu. The property is underlain by mafic metavolcanic rocks, and was previously explored for its emerald potential.

Strategic also conducted detailed prospecting and hand-pitting on the **Convert** lead-zinc-silver property (Yukon MINFILE 105B 143) in southern Yukon. Recent mapping by the Ancient Pacific Margin NATMAP project assigned rock units in this area to Yukon-Tanana Terrane. The company reported that assays from a float boulder of mineralized, felsic exhalative mineralized rock assayed up to 12.30% Pb, 4.09% Zn and 411 g/t Ag. The float was discovered in an area marked by the following: a series of strong gossans; a 2500-m-long zone of moderately to strongly anomalous lead-zinc soil geochemical values; and a laterally extensive barite horizon. The float was located 1.3 km from the closest drill hole. Previous drilling in the zone intersected values of 9.41% Zn, 0.03% Pb and 25.6 g/t Ag across 0.6 m.

Yukon Gold Corporation explored the **Marg** copper-lead-zinc-silver-gold deposit (Yukon MINFILE 106D 009) with a late-season diamond-drilling program. The Marg deposit is located approximately 80 km northeast of Mayo in central Yukon and is hosted in Devonian- to Mississippian-aged Earn Group volcanoclastic and sedimentary rocks of the Selwyn Basin. The property was last drilled in 1997. In 2000, a program of geological mapping, core re-logging, soil sampling and prospecting led to an updated structural interpretation of the deposit, leading to new potential stratigraphy, and expansion of the deposit. Most recent drilling indicated resources of 4 646 200 tonnes grading 1.80% Cu, 2.57% Pb, 4.77% Zn, 65 g/t Ag, 0.99 g/t Au, and an inferred resource of 880 800 tonnes grading 1.55% Cu, 1.90% Pb, 3.75% Zn, 50.4 g/t Ag, 0.95 g/t Au on the property. This year's program of four drill holes, totalling 1200 m, was completed in November. Drill holes 84 and 85 were drilled within the existing deposit to upgrade the inferred resource, while drill hole 86 and 87 were drilled outside the known resource, and will expand the deposit (Table 1).

A new three-dimensional model of the Marg deposit will be constructed in anticipation of an updated resource and preliminary economic assessment study due in 2006.

Klondike Star Mineral Corporation conducted a program of geological mapping, prospecting and ground geophysics on the **Ultra** zinc-copper-lead property (Yukon MINFILE 115B 008) located approximately 40 km northwest of Haines Junction, in southwestern Yukon. The Ultra property hosts two styles of mineralization: volcanic-associated copper-zinc-silver-gold, and mafic/ultramafic-

Table 1. Drill intersection results from the Marg property.

Hole number	Intersection (m)	Cu %	Pb %	Zn %	Au g/t	Ag g/t
84	3.17	2.17	2.45	5.04	0.64	57
85	6.12	2.84	2.38	5.48	0.55	48
86	3.59	2.19	2.89	5.81	0.84	69
87	2.37	2.20	2.84	5.36	1.18	56
	2.70	2.08	1.93	4.02	0.71	48

associated nickel-copper-platinum-palladium-gold. Pre- to Late-Triassic Kluane suite mafic-ultramafic sills have intruded a northwest-trending package of volcanic and sedimentary rocks. The sills are thought to be part of a subvolcanic system that fed the Mid- to Late-Triassic mafic volcanic rocks of the overlying Nikolai formation (Israel *et al.*, 2006). The exploration program was following up on an airborne geophysical survey flown in 2004, designed to locate the source of volcanogenic massive sulphide boulders and trace mafic-ultramafic sills on the claims. Massive sulphide boulders, up to 13.6 tonnes, occur on the property in a cluster on a terminal moraine. The boulders assay an average of 6.9% Zn, 1.8% Cu, 24.0 g/t Ag, 0.2% Pb and trace Au. Mineralization associated with ultramafic sills on the property have assayed up to 4.1% Cu, 1.73% Ni, 0.46 g/t Au, 5.54 g/t Pt and 13.46 g/t Pd.

MAFIC/ULTRAMAFIC ASSOCIATED

Exploration for mafic/ultramafic-associated copper-nickel-platinum group element (PGE) deposits was concentrated within the Kluane mafic-ultramafic belt of western Yukon. The Kluane region lies within the Insular Superterrane, which is largely composed of Devonian to Triassic island arc and ocean floor volcanic rocks, with thick assemblages of overlying sedimentary rocks (Israel *et al.*, 2006). In northern British Columbia, Triassic volcanic rocks are host to the world's largest Besshi-type

massive sulphide deposit (Windy Craggy, BC Minfile 114P-002, 2005). Sill-like, mafic-ultramafic bodies that are believed to represent subvolcanic magma chambers of the Triassic volcanic rocks, host numerous nickel-copper-PGE deposits in the Kluane Ranges, the most important of these being the former **Wellgreen** mine near Burwash Landing (Yukon MINFILE 115G 024).

Coronation Minerals optioned the **Wellgreen** mine property from Northern Platinum. The historic resource at Wellgreen is 42.3 Mt grading 0.35% Cu, 0.36% Ni, 0.51 g/t Pt, 0.34 g/t Pd. Exploration on the property consisted of geological mapping, excavator trenching and percussion drilling. Work concentrated on an east-striking shear zone conformable with the mineralized ultramafic sill in the north (JPS) zone and overlying sedimentary and volcanic rocks (Fig. 7). The shear consists of a rusty, gossanous and clay-altered zone exposed in intermittent trenches along strike for approximately 2.6 km. Chip samples across the shear zone have returned numerous assays enriched in platinum, palladium, gold and silver. The highest grade chip sample assayed 38.9 g/t Pt, 65.0 g/t Pd, 3.9 g/t Au, 39.9 g/t Ag, 0.07% Ni, 0.10% Cu over 1 m. Results from the percussion drilling were pending at year-end. In 2006, plans are to continue testing the new zone of high-grade shear-hosted mineralization and to confirm the historical resources contained in the Wellgreen deposit.

Golden Chalice Resources is earning a 75% interest in the **Burwash** copper-nickel-PGE property

Figure 7. Shear zone with high-grade platinum-palladium at the Wellgreen deposit.



(Yukon MINFILE 115G 100) from Strategic Metals. The Burwash property is located 7 km east of the Wellgreen deposit. Exploration work in 2005 consisted of mechanized trenching, road building and diamond drilling of seven holes totalling 520 m. Trenching and drilling focused on the Tom zone, which hosts net-textured and disseminated sulphide mineralization within a mafic-ultramafic sill defined by the trenching and drilling over a strike length of 200 m (Fig. 8). Geochemistry results suggest that the zone could be up to 2 km long. Drilling intersected mineralization with grades similar to that of the Wellgreen deposit (Table 2).

The Burwash property hosts numerous showings which were evaluated during the 2005 exploration program. Several of the showings, such as the Lower showing, have high-grade mineralization. The Lower showing is a mineralized shear zone in talc-chlorite schist that has been exposed intermittently over a minimum strike length of 25 m and a true width of up to 1.1 m. A grab sample collected in 1987 assayed 6.25% Cu, 0.11% Ni, 18.5 g/t Pt and 13.6 g/t Pd.

Resolve Ventures optioned the **Klu** copper-nickel-PGE property (Yukon MINFILE 115G 003, 098, 099) from Inco Ltd. The Klu is located in the Kluane mafic-ultramafic belt, approximately 40 km southeast of the Wellgreen mine property.

Mineralization was discovered on the Klu property in 1994 by Inco Ltd. during a reconnaissance survey of the area. A grab sample from a chalcopyrite-pyrrhotite lens, taken during the 1994 survey,

graded 2.6% Ni, 10.4% Cu, 75.8 g/t Pt, 7.9 g/t Pd and 7.0 g/t Au. Subsequent exploration programs on the property have consisted of an airborne magnetic and electromagnetic survey, ground geophysical surveys, geological mapping, and soil/stream sediment geochemical surveys. No diamond drilling has been completed on the property. Resolve Ventures performed a review of the historical data, including re-interpretation of the airborne magnetic/electromagnetic survey, and then completed a field examination and ground-truthing survey of the numerous geophysical anomalies on the property in preparation for an expanded program in 2006.

Falconbridge Ltd. entered into an agreement with StrataGold Corporation in October to option the **Canalask** nickel property (Yukon MINFILE 115F 045). The

Table 2. Drill intersections from the Burwash property.

Hole number	Intersection (m)	Cu %	Ni %	Pt g/t	Pd g/t	Au g/t
05-01	31.9	0.30	0.13	0.2	0.15	0.07
including	22.43	0.57	0.25	0.55	0.30	0.15
05-02	18.9	0.21	0.10	0.16	0.09	0.07
05-03	43.58	0.34	0.15	0.25	0.13	0.09
including	12.65	0.47	0.16	0.48	0.26	0.15
05-04	4.47	0.35	0.16	0.27	0.15	0.14
05-05	2.18	0.36	0.10	0.46	0.24	0.16
05-06	5.45	0.38	0.15	0.14	0.06	0.09
and	23.86	0.27	0.12	0.14	0.05	0.07
05-07	30.9	0.25	0.11	0.20	0.11	0.07
including	17.99	0.35	0.16	0.34	0.19	0.10

Figure 8. Geologists Bill Wengzynowski (centre), Archer Cathro & Associates, and Steve Israel (right), Yukon Geological Survey, examining nickel-copper-PGE-mineralized core from the Tom zone on the Burwash property.



Canalask property is located approximately 80 km northwest of the Wellgreen mine property and covers the White River mafic-ultramafic sill. Historical resources at the Canalask property are 390 235 tonnes grading 1.35% Ni. Falconbridge conducted additional claim staking in the area. The agreement with StataGold has a \$500 000 work commitment to December 31, 2006.

PORPHYRY/SHEETED VEIN ASSOCIATED

Sherwood Mining Corporation acquired 100% of the **Minto** copper-gold-silver deposit (Yukon MINFILE 1151 021,022) in early 2005. In the late 1990s, a feasibility study was completed by previous owners and permits were obtained. It was at this time that construction of an open-pit mine commenced. Construction was suspended after expenditures of approximately \$10 million, due to depressed copper prices. During that period, the mill foundations were poured; the ball and SAG mills were purchased and moved to the site; the mine accommodations were constructed; and the site was connected to a permitted Yukon River crossing by a 29-km production-standard access road. All of this infrastructure has been well maintained and is available for future operations (Fig. 9). The Type A and Type B Water Licences were recently renewed and permit a continuation of construction once a production decision has been made.

The deposit is an intrusion-related, magmatic-hydrothermal system that displays characteristics of both porphyry and iron-oxide-copper-gold (IOCG) systems.

Mineralization consists of bornite-chalcopyrite-magnetite in gneissic zones containing abundant biotite within a Jurassic granodiorite. The company completed an independent National Instrument 43-101 compliant resource calculation which resulted in an approximate 10% increase in total copper and gold contained in the deposit (Table 3).

Sherwood Mining Corporation commenced a 57-hole, 6772-m diamond drilling program on the Minto deposit. This program was designed with three objectives in mind: (1) to independently

Table 3. Minto resource (National Instrument 43-101 standard compliant), June 27, 2005.

Mineral resource Category	Cutoff (Cu%)	Tonnes (x1000)	Average grade		
			Cu (%)	Au (g/t)	Ag (g/t)
Measured	0.5	3600	1.74	0.45	4.37
Indicated	0.5	4730	1.90	0.65	8.40
Additional inferred	0.5	700	1.41	0.45	6.00

Figure 9. Semi-autogenous grinding mill, ball mill and mill footings at the Minto mine property.



confirm the existing resource; (2) to upgrade the approximate 8% of inferred resource within the proposed pit boundaries to the indicated category; and (3) to expand the overall resource on the margin of the existing resource. The drilling program was highly successful with step-out holes to the south and southeast of the deposit, intersecting significant mineralization. Hole 05SWC-29 intersected 14.6 m grading 2.6% Cu, 1.1 g/t Au and 9.9 g/t Ag, while hole 05SWC-30 intersected 9.6 m grading 3.9% Cu, 0.8 g/t Au and 11.1 g/t Ag.

Confirmation drilling returned numerous high-grade intersections such as 14.0 m grading 10.2% Cu, 1.8 g/t Au and 42.3 g/t Ag in hole 05SWC-02, and 24.6 m grading 6.9% Cu, 1.7 g/t Au and 25.2 g/t Ag in hole 05SWC-26 (Fig. 10). Gold grades intersected in the 2005 drilling program indicate a significant increase over the historical drilling of 1973 and 1974. Considerable exploration potential exists on the property. The northern boundary of the deposit is cut-off by the Def fault and the offset portion has not been located, however, an excellent drill target indicated by a magnetic high and induced polarization anomaly remains untested. Several other untested geophysical and geochemical targets exist on the property, in addition to three areas to the south of the main deposit which have returned historical ore-grade drill intersections up to 15.8 m grading 3.2% Cu and 1.7 g/t Au.

The overall size and grade of the deposit is expected to increase when the results from the 2005 drilling program are incorporated into a new resource calculation. The new resource calculation, confirmatory metallurgical studies and geotechnical studies are being utilized by Hatch Associates Ltd., to update a bankable feasibility study expected in April, 2006. The project may also benefit from a potential infrastructure development initiative in Yukon that could see the Whitehorse-Aishihik hydro grid connected to the northerly Dawson-Mayo transmission line.

Kennecott Canada conducted a 6-km single-line induced-polarization (IP) survey and diamond drilling of 5 holes totalling 1035 m on the **Lucky Joe** copper-gold project (Yukon MINFILE 1150 051) optioned from Copper Ridge Exploration. Kennecott Canada has worked on the property since 2003 and has spent over \$1 million on geochemistry and geological mapping programs prior to this year's drilling. The claims cover an assemblage of metasedimentary and meta-igneous rocks of the Yukon-Tanana Terrane. Kennecott Canada has proposed that the occurrence is a metamorphosed porphyry system hosted by Devonian to Mississippian meta-igneous intrusions. The single-line IP survey was conducted over the core of the Papa Bear copper-gold soil anomaly. The soil anomaly is 11 km long by 2 km wide with values up to 3060 ppm Cu and 235 ppb Au. The drill holes targeted geophysical anomalies identified in the survey. Four holes (LJ05-01, 02, 04, 05) were drilled within a 1.6 km section of the trend, and one hole (LJ05-03) was a



Figure 10. High-grade core from in-fill drilling on the Minto deposit.

Table 4. Drill results from the Lucky Joe project.

Hole number	Intersection interval (m)	Cu %	Au ppb
LJ05-01	24.1	0.060	
	33.5	0.071	
LJ05-02	94.7	0.130	52.4
	22.7	0.217	88.5
LJ05-03	74.1	0.135	320
LJ05-05	24.4	0.057	

Table 5. Drill results from the Kalzas tungsten property.

Drill hole	From m	Interval m	WO ₃ %
KZ05-01	11.0	48.0	0.153
	includes 29.6	11.4	0.304
	includes 29.6	8.4	0.393
	includes 29.6	2.4	0.688
KZ05-02	36.1	1.9	1.122
	33.0	29.0	0.130
KZ05-03	includes 50.0	2.1	0.391
	3.0	8.0	0.246
	includes 28.0	2.0	0.240
	49.2	4.6	0.260
KZ05-04	69.6	9.8	0.211
	16.0	5.5	0.221
	includes 64.9	19.8	0.145
	64.9	3.6	0.231
KZ05-05	0.0	24.4	0.304
	includes 7.0	7.0	0.419
	includes 9.0	8.4	0.533
	includes 9.8	0.5	1.220
	includes 16.9	0.5	1.390
	58.4	1.6	0.380
	84.0	1.0	0.720

2.1-km step-out along the trend to the northwest. The drill holes intersected disseminated pyrite-chalcopyrite mineralization in metamorphosed intrusive rocks. The strongest copper mineralization correlates with potassic (biotite) and magnetite-silica alteration with 3-5% disseminated pyrite. Overlying this zone of alteration is a shell with lower copper values and 5-10% disseminated pyrite. The highest-grade intervals were in hole LJ05-02, which intersected 22.7 m averaging 0.217% Cu and 88.5 ppb Au; and hole LJ05-03 which intersected 74.1 m grading 0.135% Cu and 0.032 g/t Au (Table 4). Kennecott opted to return the project to Copper Ridge. A large portion of the Papa Bear copper-gold soil anomaly and the Ryans Creek copper-gold geochemical anomaly remains to be tested by drilling. The Ryans Creek copper-gold geochemical anomaly is parallel to the Papa Bear and is defined by a 7.2-km-long anomaly with values up to 4400 ppm Cu and 611 ppb Au.

Copper Ridge also conducted smaller-scale programs consisting of prospecting and geological mapping on its **Thistle** and **Shamrock** copper-gold properties located a few kilometres south of the Lucky Joe property. The Thistle and Shamrock properties cover areas having similar geochemical and geophysical signatures as the Lucky Joe property.

Copper Ridge Exploration conducted a helicopter-supported diamond drilling program on their **Kalzas** tungsten property (Yukon MINFILE 105M 066). The company completed a 5-hole, 397-m drill program that tested areas of high-grade mineralization identified by surface-sampling from previous exploration programs. Wolframite occurs with minor scheelite, molybdenite, cassiterite, galena and beryl in a broad, sheeted vein and stockwork complex, approximately 1000 m by 500 m in size. This vein and stockwork complex cuts gritty, hornfelsed Yusezyu Formation quartzite and phyllite of the Upper Proterozoic Hyland Group. The drilling was successful, intersecting quartz veins with coarse wolframite and minor coarse scheelite mineralization (Table 5). The coarse-grained nature of the mineralization (Fig. 11) could have a significant

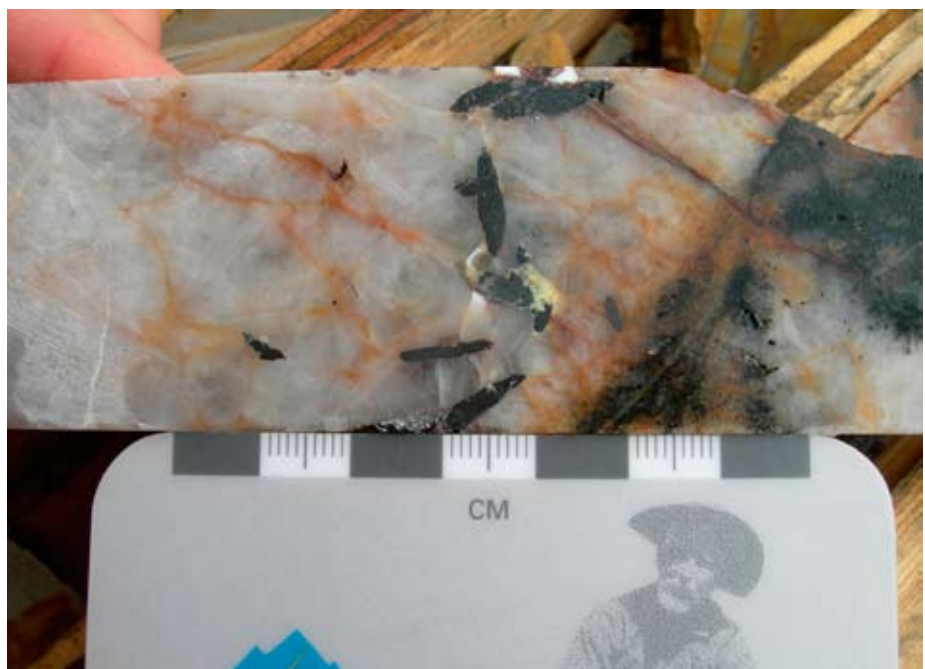


Figure 11. Coarse wolframite in drill core from the Kalzas tungsten property.

nugget effect on the intersections and the company is considering an expanded drill program with larger diameter drill core to test the occurrence.

Strategic Metals conducted minor exploration and environmental clean-up at their **Logtung** tungsten-molybdenum project (Yukon MINFILE 105B 039). The project is the largest intrusive-hosted tungsten deposit in the world. Historical resources calculated by Amax Potash Ltd., outlined 162 million tonnes grading 0.13% WO_3 and 0.052% MoS_2 that are minable by open-pit methods including a higher grade core of 55 million tonnes grading 0.16% WO_3 and 0.062% MoS_2 that are also minable by open-pit methods.

The **Red Mountain** (Yukon MINFILE 105C 009) molybdenum deposit of Tintina Mines Ltd. is a large porphyry deposit that was last explored by Amoco Canada in the 1960s and 1970s. Exploration at that time established a historical resource of 187.27 Mt grading 0.167% Mo including a high-grade core with 21.296 Mt grading 0.293% Mo (Fig. 12). Tintina Mines Ltd. performed engineering and environmental studies in support of its application to the Yukon government to conduct an underground exploration program proposed for 2006. This program will consist of driving a decline, underground drifting, drilling, test mining and bulk sampling.

Ordorado Resources Corp also performed a small exploration program consisting of geochemical sampling, geological mapping and prospecting on their **Rams Horn** molybdenum property (Yukon MINFILE 105D 004) in southern Yukon. The occurrence is underlain by altered volcanic and clastic sedimentary rocks assigned to the Cache Creek Terrane. An undated Cretaceous(?) biotite-quartz monzonite stock intrudes the volcanic/sedimentary sequence. Rich pockets and rosettes of molybdenite are associated with quartz veins, 0.3 cm to 5 cm wide, that form a stockwork zone about 760 m long and 150 m wide within the monzonite stock.



Figure 12. Exploration camp on the Red Mountain molybdenum deposit. Work was last conducted in the 1970s.

WERNECKE BRECCIA

At least 65 iron oxide-copper-gold ± uranium ± cobalt (IOCG) prospects are associated with a large-scale Proterozoic breccia system in north-central Yukon. The breccia system, known as Wernecke Breccia, consists of numerous individual breccia bodies that occur in areas underlain by the Early Proterozoic Wernecke Supergroup, an approximately 13-km-thick deformed and weakly metamorphosed sequence of sedimentary rocks (Hunt, 2005b). Wernecke Breccia occurrences have been explored in recent years mainly for their copper-gold content, however, in the last year, a significant amount of claim-staking has occurred based on the uranium potential of the breccia bodies. Unconformity-related uranium potential has also been recognized within Wernecke Supergroup (Hunt, 2006).

Janina Resources Ltd. conducted a 5-hole, 504-m diamond drill program on the **Yukon Olympic** copper-gold property (Yukon MINFILE 116G 082) optioned from Copper Ridge Exploration. In 2004, detailed geophysical surveys were conducted at the eastern end of the previously defined 12- km-long gravity and magnetic anomaly. The survey successfully defined a strong, roughly circular, magnetic anomaly, with a partially fringing gravity anomaly, locally in excess of two milligals. The southeastern portion of the gravity anomaly, correlates with known, copper-bearing hematite (iron oxide) breccia in Spectacular Creek, while, for the most part, the source of the combined magnetic and gravity feature is hidden under younger, overlying rocks. One drill hole was abandoned in overburden, while the other four were drilled on the fringes of the gravity anomaly in Spectacular Creek. Hematite-breccia with chalcopyrite was intersected in drilling. Drill hole YO-05-02 intersected 0.071% Cu over 9.8 m, and an additional 30 m grading 0.02% Cu. Hole YO-05-03 intersected 0.061% Cu over 6.75 m.

Copper Ridge Exploration conducted an exploration program including helicopter-supported gravity surveying, geological mapping and rock sampling on their **Ironman** (formerly Hart River) copper-gold property (Yukon MINFILE 116A 017). Previous work on the property identified several showings of copper-gold

mineralization associated with hematite-rich breccias. The now fully defined gravity anomaly is 4 milligals in strength and the core of the anomaly measures approximately 1.5 km by 2 km.

International KRL Resources conducted a 1155-line-km high-resolution airborne magnetometer survey, a gravity survey, a 50.5-line-km induced polarization survey, geochemical sampling, geological mapping and prospecting on the **Nor** copper-gold-uranium property (Yukon MINFILE 106L 061) in northern Yukon. Results from programs run between 1978 and 1980 by previous owners returned assay values of up to 4% U₃O₈, 4% Cu and 2.0 g/t Au in grab samples from the Nor heterolithic diatreme breccia,

Figure 13. Jesse Kirby (student, Yukon Geological Survey) and Paul Kilkenny (International KRL Resources) at the Nor copper-uranium property.



which has surface dimensions of 800 m by 1800 m (Fig. 13). Initial evaluation of the exploration results has shown conductivity and resistivity anomalies coincident with copper and uranium geochemical anomalies, gravity anomalies and a zone of potassic alteration. Drill testing of several coincident anomalies is planned for 2006.

Cash Minerals Ltd optioned the **Igor, Lumina, Steel** and **Bond** copper-gold-uranium properties (Yukon MINFILE 106E 009, 106C 069, 106D 049, 065) from Twenty Seven Capital Corp. On the **Igor** property, seven diamond drill holes totalling 1121 m were drilled (Fig. 14). Drilling intersected Wernecke Breccia with chalcopyrite and pitchblende mineralization. Partial results from the 2005 drill program were available by year-end with the highlight being hole IO5-4 which intersected 74.44 m of mineralized breccia, which assayed 1.88% Cu and 0.069% U_3O_8 (1.38 lbs/ton U_3O_8 ; Table 6).

On the **Lumina** property, the company conducted geological mapping, sampling and radiometric prospecting. Previous operators on the property in the 1980s had identified uranium-bearing float samples in sedimentary rocks, which were assumed to originate from a glacial ice-covered cirque. The company reported that most of the mineralization consists of sooty to compact pitchblende-filling fractures and vein breccias. Brannerite is also present in a few areas and yellow secondary uranium minerals coat some weathered surfaces. Although the uranium mineralization is structurally controlled, it is relatively young in age (~510 Ma); and proximity to the discordant younger rocks lying above a regional unconformity to the immediate north and east of the showing suggests it is probably unconformably related. Glacial melting has exposed an inaccessible showing (Jack Flash) high on the cirque wall, consisting of fracture filling and veins in sedimentary rocks. A total of 31 float boulders derived from the Jack Flash showing were collected over a 1.4-km-long talus train. The average value assayed from the boulders was 1.22% U_3O_8 (24.4 lbs/ton U_3O_8). The Ram showing, located 4.5 km north of the Jack Flash showing, consists of a pitchblende-bearing vein exposed in a creek valley.

Table 6. Drill intersections from the Igor property.

Hole no.	From m	To m	Interval m	U_3O_8 %	U_3O_8 lb/ton	Cu %	
I05-1	10.74	33.04	22.28	0.005	0.10	0.32	
	88.08	99.10	11.02	0.006	0.12	0.38	
	115.51	124.97	9.46	n.r.	n.r.	0.26	
I05-2	8.95	13.36	4.41	n.r.	n.r.	0.35	
	17.68	19.22	1.54	n.r.	n.r.	0.42	
	29.00	30.35	1.35	n.r.	n.r.	0.33	
I05-4	103.87	178.31	74.44	0.069	1.38	1.88	
	includes	111.87	24.30	12.43	0.192	3.84	4.79
	includes	160.27	174.81	14.54	0.215	4.30	4.79
includes	160.27	164.59	4.32	0.400	8.00	6.62	

n.r. = none reported



Figure 14. Helicopter-supported diamond drill on the Igor copper-uranium property.

Sampling by previous operators has returned values up to 0.91% U_3O_8 (18.2 lbs/ton U_3O_8). A late-season (November) drill program was conducted near the Ram showing; seven holes totalling 504 m were drilled. The drill, as well as the all-season camp, remain on the property, ready for an early start to the 2006 field season. Drill results were not available at year-end.

On the **Steel** property, three holes totalling 581 m were drilled on a broad magnetic and gravity anomaly in an overburden-covered valley. None of the holes explained the source of the anomalies, nor did they intersect any significant copper or uranium mineralization. Drilling of seven holes totalling 735 m on the **Bond** property intersected weak uranium mineralization. The companies conducted additional claim staking in the vicinity of the Lumina and Igor properties and optioned the **Delores** property (Yukon MINFILE 106C 013) that adjoins the Lumina property to the south.

Signet Minerals conducted an exploration program of prospecting and radiometric sampling on the **Curie** uranium-copper-gold property (Yukon MINFILE 106E 3, 6, 11, 22, 27-31). Based on the positive results of the exploration program, the company staked additional claims in the area. The claims cover a number of MINFILE occurrences. These occurrences exist as uranium and copper mineralization in an area underlain by Wernecke Breccia cutting Middle Proterozoic Quartet Group. Mineralization is associated with breccias and structural zones within Quartet Group sedimentary rocks. The company obtained significant uranium assays collected from float and grab samples of sheared and hydrothermally altered, quartz-feldspar-chlorite-veined, fine-grained sedimentary rocks (Fig. 15). Samples ranged from 0.07% to 52.3% U_3O_8 . The company is also assessing the potential of unconformity-related uranium on the property.

Figure 15. High-grade uranium in sheared and hydrothermally altered, quartz-feldspar-chlorite-veined, fine-grained sedimentary rocks at the Curie property. Photo by Aurora Geosciences.





Figure 16. Fine-grained sphalerite, pyrite and galena occur in rhythmically laminated carbonaceous chert and calcareous mudstone at the Howard's Pass deposits.

SEDIMENTARY ROCK ASSOCIATED

Selwyn Basin is a continental margin basin characterized by the deposition of thick sequences of black carbonaceous shales in euxinic conditions, and by the development of second-order basins through periodic extensional tectonism, subsidence and faulting. Over 800 mineral occurrences have been discovered within the outline of Selwyn Basin; 19 of these have been identified as sedimentary-exhalative (SEDEX) deposits. An additional 89 occurrences have been described as SEDEX-type mineralization. Of the three main SEDEX districts (Anvil, MacMillan Pass and Howard's Pass), only those of the Anvil district have been mined, although all three still have potential for significant new discoveries.³ With the rising price of zinc, interest in the deposits and exploration potential of the Selwyn Basin has been expected to rise. Interest to date has been minimal with the exception of the large exploration program in the Howard's Pass district by Pacifica Resources.

In July 2005, Pacifica Resources Ltd. completed an option to purchase agreement with Placer Dome Inc. and Cygnus Mines Ltd. (a subsidiary of US Steel) to acquire the **Howard's Pass** zinc-lead-silver deposits (Yukon MINFILE 105I 012, 037) in order to consolidate their current claim holdings in the district. The Howard's Pass deposits (XY, Anniv and OP) are sheet-like, stratiform sulphide deposits hosted by black shale of the Ordovician-Silurian Road River Formation within the Selwyn Basin. Fine-grained sphalerite, pyrite and galena occur in rhythmically laminated carbonaceous chert and calcareous mudstone (the 'active member') (Fig. 16). Historical resources that pre-date National Instrument 43-101 standard include an indicated reserve of 60 million tonnes grading 5.51% Zn and 2.38% Pb in the XY zone, and 55.5 million tonnes grading 5.29% Zn and 1.79% Pb in the Anniv zone. The tabulation of reserves and resources also included 367 million tonnes of inferred resources grading 5.12% Zn and 1.90% Pb within the Anniv and XY zones.

³www.geology.gov.yk.ca/metallogeny



Figure 17. Howard's Pass exploration camp.

Pacifica Resources Ltd. completed an extensive exploration program consisting of camp construction (Fig. 17), geochemical sampling, geological mapping, metallurgical testing and diamond drilling of 8317 m in 53 holes. The focus of Pacifica's exploration program was to 1) drill-test areas of favourable stratigraphy with potential for near-surface mineralization in the area of the known deposits; 2) drill-test areas with geological and geochemical potential on Pacifica's wholly owned claims; and 3) infill drill in the area of the known deposits. The strike length of the known favourable stratigraphy in the district, which is approximately 40-50 km, highlights the immense scope and potential of this program. The XY and Anniv deposits are separated by 22.5 km.

Table 7. Drill results from the Brodel zone.

Hole	From m	To m	Interval m	True thickness m	Pb %	Zn %
BR-01	Hole abandoned in hanging-wall stratigraphy					
BR-02	169.50	194.10	24.60	18.00	0.99	3.18
includes	169.80	186.30	16.50	12.07	1.19	4.20
includes	169.80	182.40	12.60	9.22	1.36	4.90
BR-03	94.00	141.10	47.10	40.00	0.58	2.13
includes	94.00	103.50	9.50	8.07	1.35	4.62
includes	129.80	141.10	11.30	9.60	1.04	4.09
BR-04	Hole abandoned in hanging-wall stratigraphy					
BR-05	49.12	68.30	19.18	17.50	1.28	4.03
includes	49.58	59.77	10.19	9.30	1.40	5.66
includes	55.40	60.80	5.40	4.93	2.14	7.95
BR-06	167.30	177.71	10.41	10.25	1.17	3.75
includes	168.94	175.00	6.06	5.97	1.58	5.57
BR-07	215.42	235.56	20.14	19.38	1.06	3.31
BR-08	137.01	144.90	7.89	7.4	0.79	2.94
BR-09	87.16	105.51	18.35	16.63	1.02	3.04
includes	87.16	100.12	12.96	11.75	1.10	3.96
BR-10	121.95	147.57	25.62	22.19	0.76	3.10
includes	121.95	137.20	15.25	13.21	0.90	4.10
includes	115.2	121.42	6.22	5.76	1.95	7.17

Highlights from drilling include the discovery of two new areas of mineralization, the Brodel zone and the Don Valley. The Brodel zone is located 4 km northwest of the XY deposit and was tested with 10 drill holes, 8 of those intersecting significant mineralization (Table 7).

Drilling in the Don Valley resulted in a new discovery. The drilling tested an area with favourable stratigraphy and geochemical anomalies. The Don Valley stretches 11 km between the Brodel discovery and the Anniv deposit. Eight widely spaced stratigraphic drill holes were collared in the Don Valley with seven holes abandoned in hanging-wall stratigraphy or stratigraphy representing the footwall to the 'active member'. Hole Don-04 was successful in intersecting the mineralized 'active member' and returned 34.1 m grading 0.99% Pb, 3.64% Zn, including 7.81 m of 1.80% Pb, 7.93% Zn and 7.13 m of 1.74% Pb and 4.71% Zn. The drilling has led to a better understanding of the structure that offset stratigraphy in the Don Valley, while the intersection in hole 4 has demonstrated that the 'active member' in the area is mineralized.

Drilling in the area of the XY, Anniv and OP deposits resulted in numerous intersections with grades similar to that indicated by the historical drill results.



Figure 18. High-grade zinc-lead mineralization in drill core from the XY deposit at Howard's Pass.

Highlights include XY-105 intersecting 16.25 m of 3.17% Pb and 7.47% Zn, including 5.62 m grading 6.97% Pb and 17.23% Zn (Fig. 18); Anniv-76 which intersected 31.0 m grading 1.49% Pb and 4.37% Zn, including 21.51 m grading 1.89% Pb and 5.16% Zn; and OP-11 intersecting 14.0 m of 0.97% Pb and 2.84% Zn, including 8.18 m grading 1.51% Pb and 4.24% Zn. The OP is located 7 km northwest of the Anniv deposit. Complete drill results are available at Pacifica Resources website⁴.

In addition to the on-site work, Pacifica Resources Ltd. initiated preliminary metallurgical testing consisting of Dense Media Separation (DMS) gravity testwork at SGS Lakefield Research. The initial work used a grab sample from the mine dump of the XY deposit. The combined zinc + lead head grade of this sample was 21.8% which was upgraded to 29.0%, with lead and zinc recoveries at 98% and 97%, respectively. A larger sample collected from the mine dump, and compiled from drill core, has been submitted to SGS Lakefield for further testing. The positive, preliminary testwork results illustrate the potential for pre-concentration of mineralization from a wide range of run-of-mine (ROM) grades in the Howard's Pass deposits. The nature of the mineralization lends itself to DMS technology because there are high-density bands of zinc-lead mineralization with very little pyrite, separated by barren shale beds of lower density.

Manson Creek Resources conducted a small geological program on their **Tanner** lead-zinc property (Yukon MINFILE 106C 098), located in the northeast portion of the Selwyn Basin, near its boundary with the Mackenzie Platform. Reconnaissance-scale drilling of two holes by Manson Creek Resources in 2002 intersected bedded barite. The bedded barite exceeded 20 m (down hole) in length and returned an average assay of 26.9% BaO. The presence of barite suggests the area is potentially underlain by Devonian to Mississippian Earn Group stratigraphy which is host to the MacMillan Pass SEDEX deposits and the Marg volcanogenic massive sulphide deposit.

⁴www.pacificaresources.com

Figure 19. Drill core storage area at the Blende lead-zinc-silver deposit.



VEIN/BRECCIA ASSOCIATED

Blind Creek Resources optioned the **Blende** lead-zinc-silver deposit (Yukon MINFILE 106D 064) from Eagle Plains Resources and conducted an exploration program of re-logging historical diamond drill core (Fig. 19), geological mapping, geochemical sampling and prospecting. The Blende property, located on the south edge of the

Mackenzie Platform is hosted by Middle Proterozoic Gillespie Group dolomite and contains an inferred resource of 15.3 Mt grading 3.23% Pb, 3.04% Zn and 67.5 g/t Ag. Examination of the drill core, and reviews of previous work, concluded that “epigenetic mineralization consisting of sphalerite, galena, smithsonite and minor chalcopyrite is spatially associated with a middle-Proterozoic structural zone. The highest grade mineralization is associated with veining and breccia zones with grades typically running 8-20% Pb+Zn over 1-2 m” (B. Sharp, 2005⁵). The companies have announced plans for a 7000-m drill program in 2006 to infill existing drilling, evaluate underground high-grade mining potential, and test other targets along the 6-km mineralized trend.

Figure 20. Regan Chernish (centre of photo), President, Manson Creek Resources sampling at the Cuprum copper-zinc-silver property.



⁵Blende Property Update – Presentation at the 33rd Annual Geoscience Forum, November, 2005.

SKARN

Manson Creek Resources explored the **Cuprum** copper-zinc-silver property (Yukon MINFILE 105E 008), located near Whitehorse. They conducted an exploration program consisting of geochemical sampling (Fig. 20), prospecting, geological mapping and ground magnetometer surveys. Copper-zinc mineralization is associated with magnetite and calc-silicate skarn. Grab samples from the magnetite skarn have returned values of up to 7.5% Cu, 2.2% Zn and 123 g/t Ag.

Strategic Metals Ltd. explored the **Tidd** copper-lead-zinc-silver property (Yukon MINFILE 105J 029) and completed a program of prospecting, geochemical surveys, geological mapping and geophysical surveys (magnetic, horizontal-loop electromagnetic, gravity and induced polarization). Chip sampling in areas of trenching by previous operators yielded values of up to 1.08% Cu, 68.5 g/t Ag, 46 g/t In and 0.02% Bi over 10.5 m. Float samples have returned values up to 6.85% Cu, 411 g/t Ag, 157 g/t In, 0.34% Bi, 3.61% Pb and 2.39% Zn.

North American Tungsten Corporation explored their **MacTung** deposit (Yukon MINFILE 106D 064) with a 25-hole, 6668-m diamond drill program. The company also rehabilitated the mine portal (Fig. 21), conducted underground channel sampling, and collected a 100-tonne bulk sample for processing. Historical resources are reported as 5.02 Mt at 1.2% WO_3 in the Lower skarn and 8.62 Mt at 0.8% WO_3 in the Upper skarn. Tungsten mineralization consists of scheelite in pyrrhotite skarn within Lower Cambrian sedimentary rocks. The drilling was conducted to upgrade resources within the deposit and to expand the deposit to the west. Drilling intersected grades consistent with the previous drilling, with the highest grade intersection in MS146 assaying 1.60% WO_3 over 32.2 m. The resource was expanded 60 m to the west. A new resource calculation is being conducted utilizing the results of this year's program.

E-Energy Ventures Inc. conducted an initial prospecting program on the **Stormy Mountain** molybdenum project (Yukon MINFILE 105F 011). Molybdenite occurs with lesser amounts of scheelite in a garnet-diopside-pyrrhotite skarn zone. The deposit formed in Lower Cambrian limestone, in a shallow-dipping contact aureole above the Rose Lake Stock. Prospecting in a new area on the property located three samples of molybdenum-bearing float, which assayed 10.4%, 8.63% and 3.16% Mo.

Figure 21. Rehabilitated portal at the MacTung tungsten deposit.



PRECIOUS METALS

PORPHYRY/SHEETED VEIN

The **Dublin Gulch** project (Yukon MINFILE 106D 025) of StrataGold Corporation was the largest gold exploration project in Yukon this year. The program consisted of 34 holes totalling 8102 m, and was designed to upgrade resources within the Eagle Zone (Fig. 22), expand the resources to the west, and test areas with sulphide-mineral veins and alteration in metasedimentary rocks for higher grade

mineralization. The Dublin Gulch property hosts indicated resources in the Eagle Zone of 55.228 Mt grading 0.934 g/t Au and an additional 17.255 Mt grading 0.723 g/t Au in the inferred category. Mineralization in the Eagle Zone consists of gold in sheeted quartz veins, shears and fractures within the granodiorite intrusion. This style of mineralization appears to be the exact same style of mineralization found at the producing Fort Knox mine in Alaska. Results from this year's drilling program will be used to upgrade and expand the resource estimate in the Eagle Zone. The first four holes were successful in expanding the deposit 150 m to the west of the current resource area (Table 8). The remaining holes, including individual results, were scheduled for release by year-end with the upgraded resource estimate.

A number of targets on the **Mike Lake** gold property (Yukon MINFILE 116A 012) of Bashaw Capital Corporation were drill-tested for the very first time. Exploration on the property consisted of camp construction, geological mapping, prospecting, geophysical surveys and diamond drilling of

Table 8. Drill results from the Eagle Zone of the Dublin Gulch gold property.

Hole DG05	Length m	From m	To m	Interval m	Au g/t
276C	258.00	60.96	258.00	197.04	0.983
includes		119.59	256.03	136.44	1.133
includes		196.06	212.14	16.08	2.021
277C	198.12	19.81	175.26	155.45	0.608
includes		134.81	175.26	40.45	0.949
279C	201.17	15.24	201.17	185.93	0.697
includes		16.76	64.01	47.25	0.923
includes		80.77	110.29	29.52	0.957
includes		160.57	201.17	40.60	0.923
281C	222.50	35.06	185.24	150.18	0.561
includes		56.19	75.56	19.37	0.858
includes		105.80	149.35	43.55	0.927

Figure 22. View of the Dublin Gulch camp and placer workings. The Eagle Zone (arrow) is visible in the background. Photo by StrataGold Corporation.



18 holes totalling 2200 m. The property hosts a number of intrusion-related gold targets which are as follows: vein- and fracture-related gold-copper mineralization within the Cretaceous-aged syenite intrusive rocks (Spartan vein); shear zones within Paleozoic sedimentary rocks (Birdie-Bindie); and skarn- and replacement-style mineralization proximal to the intrusive rocks (Skarn and North zone). The best results from the drilling program came from the North zone (Fig. 23), where 12 holes were drilled. The drilling tested a 1000-m conductor identified in a max-min electromagnetic survey. Approximately 500 m of the conductor were tested, with the best results revealed from a 150-m section of the conductor. Drilling intersected a 3- to 15-m-wide skarn horizon with pyrrhotite, arsenopyrite and chalcopyrite mineralization (Table 9).

The only hole drilled at the Spartan vein, tested about 70 m down-dip from a strong, well mineralized surface exposure, resulted in 43.7 g/t gold across 0.91 m. The vein narrowed in the hole to only 15 cm; however, the interval that included the vein material still assayed 5.80 g/t gold across 1.00 m. Previous drilling at the Spartan vein yielded intersections of 4.39 g/t Au over 1.40 m and 21.51 g/t Au over 1.28 m. Follow-up drilling based on results obtained in 2005, plus drilling on five other untested targets, will commence in 2006.

Acero-Martin Exploration Inc. continued to drill the Jethro zone at its **Ice** property (Yukon MINFILE 115P 006). The Jethro zone is a northeasterly striking structural zone in which gold mineralization is hosted by sheeted quartz-sulphide mineral veins, fractures and shear zones within the Cretaceous, Red Mountain quartz-

Table 9. Drill results from the North zone of the Mike Lake property.

Hole number	From m	To m	Interval m	Au g/t
NV05-1*	1.40	3.66	2.26	0.50
and	7.80	9.10	1.30	1.15
NV05-2	42.37	60.80	18.43	7.67
includes	57.61	60.80	3.19	38.60
NV05-3	71.32	72.49	1.17	1.49
NV05-5	59.73	61.87	2.14	0.71
NV05-7*	106.74	107.75	1.01	0.67
NV05-12	75.74	83.32	7.58	12.42

*only crossed a portion of the mineralized zone

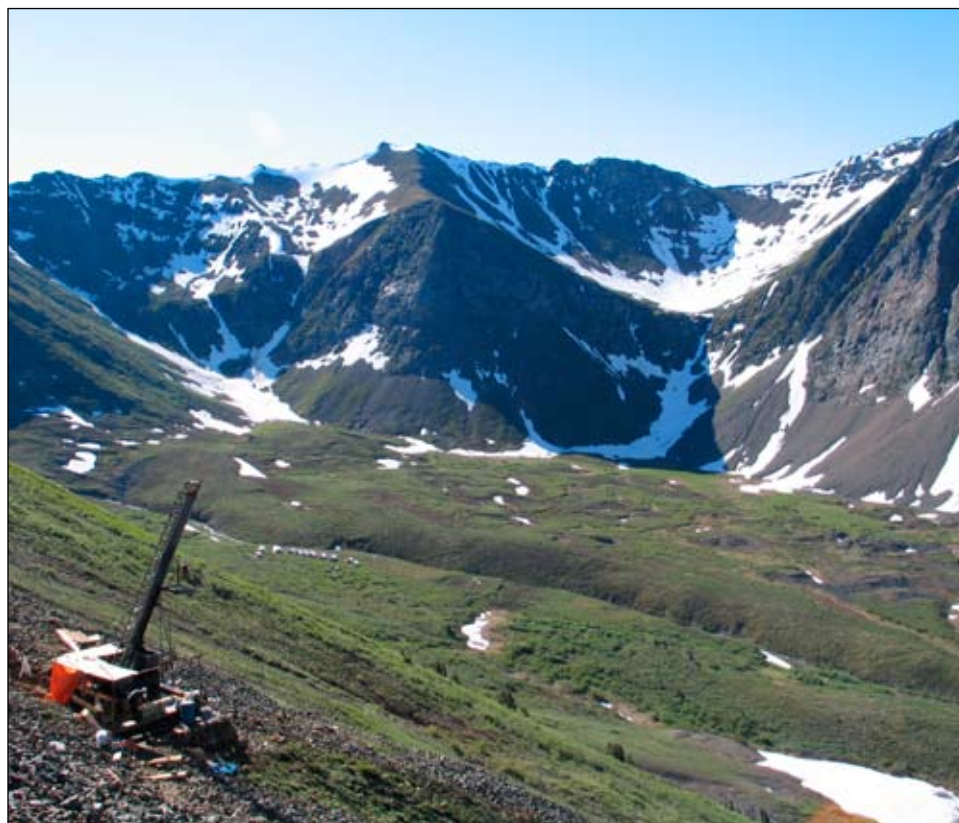


Figure 23. Diamond drill on the North zone at the Mike Lake project. Photo by Bashaw Capital Corporation.

Table 10. Drill results from the Ice property.

Drill hole	From m	To m	Interval m	Au g/t
DD-05-20	122.47	227.38	104.91	1.07
includes	122.47	148.90	26.43	0.81
includes	148.90	186.23	37.33	1.47
includes	186.23	227.38	41.15	0.88
	227.38	304.00	76.62	0.67
DD-05-21	42.83	106.40	63.57	1.13
includes	42.83	74.15	31.32	0.64
includes	74.15	106.40	32.25	1.60
	161.10	183.18	22.08	0.62
DD-05-22	4.27	32.48	28.21	1.24
	32.48	60.65	28.17	0.53
	60.65	75.36	14.71	0.70
	75.36	94.60	19.24	0.54
	119.30	135.30	16.00	0.55
DD-05-23	118.00	132.16	14.16	0.94
DD-05-24	6.66	19.77	13.11	0.74
	60.86	79.74	18.88	1.07
	148.50	165.80	17.30	0.56
DD-05-25	107.46	113.34	5.88	1.15
	124.28	145.28	21.00	0.68

Figure 24. Diamond drill on the Jethro zone at the Ice property.



monzonite intrusion and adjacent hornfelsed sedimentary rocks. Eight holes were drilled, with six intersecting significant mineralization (Fig. 24, Table 10).

Curlew Lake Resources Inc., together with partner Select Resources Corp., performed a program of soil geochemical sampling and magnetometer surveys on the **Typhoon** gold property located in the Clear Creek area (Yukon MINFILE 115P 060). Results from soil geochemistry defined an anomalous gold, arsenic, antimony and bismuth signature consistent with intrusive gold-related systems.

Firestone Ventures Inc. conducted an exploration program of geophysics consisting of induced polarization, magnetometer and very low frequency (VLF) surveys on the **Sonora Gulch** gold property (Yukon MINFILE 115J 008). The property is located within the Dawson Range Gold Belt and is host to high-grade, gold-tetradymite veins in structural zones, and copper-gold mineralization in stockwork and disseminated mineralization within a quartz-feldspar porphyritic intrusion. The geophysical surveys are designed to identify targets for a proposed diamond drill program, which is scheduled to begin in 2006.

SKARN/REPLACEMENT

YGC Resources initiated a large year-round exploration program on the **Ketza River** gold property (Yukon MINFILE 105F 019) in May of 2005. As of the end of November, 95 holes totalling 12 285 m had been drilled on the property. Mineralization at Ketza consists of massive, pyrrhotite-pyrite manto deposits (Fig. 25) hosted in Lower Cambrian limestones, as well as quartz-pyrrhotite-pyrite veins (Fig. 26) hosted in Lower Cambrian argillites which stratigraphically underlie the limestone

unit. Oxidized mantos mined at the Ketza River deposit between 1988 and 2000 produced approximately 3.1 million grams of gold.

YGC Resources Ltd. is concentrating on increasing the sulphide mineral resources on the property that have not been mined. The company has completed an upgrade of the camp, as well as road maintenance to make the camp and mine site suitable for year-round operation. The company has also performed a large amount of environmental clean-up and reclamation work at the site. YGC Resources Ltd. has signed a memorandum of understanding (MOU) with Ross River Dena Council for its participation in the exploration activities, as well as continuing environmental monitoring and

remediation. The Kaska First Nation is provided with opportunities for employment, training and service contracts related to the activities performed at the Ketz River property.

Exploration at the property has targeted both the Manto zone hosted in the limestones, as well as the quartz-sulphide mineral veins of the Shamrock zone, hosted in argillites. Drilling on the Manto zone has expanded the deposit to the west. Based on 37 holes from the summer drilling program, the Manto resource in the measured and indicated mineral resource category has been upgraded from 4.25 Mt grading 2.82 g/t Au (10.9 million g Au) to 5.95 Mt grading 3.0 g/t Au (16.3 million g Au) at a 1 g/t Au cut-off. In addition, the inferred mineral resource of 6.27 Mt grading 1.76 g/t Au (10 million g Au) have been increased to 10.55 Mt grading 2.37 g/t Au (22.8 million g Au) at a 1 g/t Au cut-off. Numerous intersections



Figure 25. Massive pyrrhotite-pyrite manto-style mineralization from Ketz River.



Figure 26. Quartz-pyrite vein mineralization from the Shamrock zone at Ketz River.

of the flat-lying manto were in the 0.5 m to 3.0 m range, with a higher grade example assaying 18.91 g/t Au over 3.1 m in hole 601. Complete assays of drill results received to date are available on the YGC Resources Ltd. website⁶, as well as in press releases. A new resource calculation will be determined with receipt of assays from additional intersections of the Manto zone in the fall and winter drill programs. Results from drilling on the Shamrock zone were pending at year-end.

Eagle Plains Resources conducted an exploration program of geophysics (magnetometer survey) and blast trenching on the **Dragon Lake** gold property (Yukon MINFILE 105J 007). Pyrrhotite-rich calc-silicate skarn is developed proximal to a small Cretaceous quartz-monzonite stock. The property was last explored in 1999. At that time, four holes were drilled, which intersected up to 3.66 g/t Au over 1.2 m.

VEIN/BRECCIA ASSOCIATED

Orogenic gold mineralization in Yukon is mostly associated with the polydeformed, greenschist-grade, pericratonic, meta-sedimentary and meta-igneous rocks of the Yukon-Tanana Terrane. The orogenic lode sources occur as low-sulphide quartz veins in fissures and shears that post-date metamorphism. The oldest veins are ~170-145 Ma, having formed after Early Jurassic (~185 Ma) terrane accretion and metamorphism. The youngest veins occur in more outboard (coastal) locations and are likely ~55 Ma, having formed in response to metamorphism and uplift associated with emplacement of coastal batholiths (Coast Plutonic Complex).

Orogenic gold has not traditionally been a focus of exploration in Yukon, despite approximately 20 million ounces (600 million g) of placer gold having been recovered from the historic Klondike placer district, and associated goldfields. An orogenic source is suspected for the Klondike placer district, but significant lode sources have not yet been discovered. Recent exploration activity, however, has focused on orogenic gold lode targets in the Klondike, and in other areas underlain by Yukon-Tanana Terrane that also yield significant placer gold (e.g., the Stewart River area). Much of this region was not glaciated during the Quaternary glaciations. As a result, bedrock exposure is poor with thick colluvial cover, which in turn inhibits effective exploration (Burke *et al.*, 2005).

The **Lone Star** deposit (Yukon MINFILE 115O 072) is currently being explored by Klondike Star Mineral Corporation. The property, located at the headwaters of Bonanza Creek in the heart of the Klondike, is one of the few, small historical lode producers in the district, with a reported production from the early 1900s of 7650 tonnes grading 5.1 g/t Au. Ore was produced from discordant quartz and quartz-pyrite veins. Gold grades are erratically distributed in the nuggety veins; consequently, new exploration efforts at Lone Star include bulk sampling. Controls on vein location and gold enrichments in the Klondike are poorly understood, but are pivotal for successful exploration of orogenic vein gold mineralization in this region. Klondike Star's exploration program included trenching, bulk sampling and a diamond drilling program that consisted of 32 holes totalling 4830 m on the Lone Star property (Fig. 27). Twenty Seven of the holes tested the Lone Star deposit (4268 m), while the remaining five were directed at the Dysle and Veronika zones (Fig. 28). Drilling at the Lone Star intersected gold mineralization over an 800-m strike length on drill sections spaced at 50 m. Gold is present as coarse, free

⁶www.ygcr.ca



Figure 27. Diamond drill on the Lone Star property.

Table 11. Drill results for Lone Star property.

Hole	Intersection m	Au g/t
05LS-02	62.55	1.14
includes	6.0	5.46
05LS-12	44.0	0.84
includes	8.4	2.74
05LS-15.	24.0	2.10
includes	1.0	13.43

gold, with disseminated pyrite, and locally is associated with narrow discordant quartz veins. The mineralized zones are associated with quartz-carbonate-pyrite alteration and are hosted by felsic metavolcanic schist. The mineralized horizon at Lone Star trends northwest and dips gently to the northeast. Results for 15 of the holes drilled at Lone Star were released by year-end with all holes intersecting gold mineralization (Table 11).

New World Resource Corp. conducted a percussion drilling program totalling 1800 m in 43 holes on their **McFaul** property (Yukon MINFILE 116B 157) located in the Klondike. The percussion drilling was conducted in a systematic grid pattern to better define the known listwaenite alteration zone located in the bedrock of the Paradise Hill placer gold mine workings, and to explore for gold-bearing veins proximal to this zone. Anomalous gold values were intersected at the contact of ultramafic rocks and underlying schists. Partial results from drilling included an intersection of 0.63 g/t Au over 12.2 m in hole PPH-46.

Ryanwood Exploration Inc. conducted an exploration program of soil sampling, ground magnetometer surveying and geological mapping on the **Crown Jewel** property in the

Figure 28. The Veronika zone on the Lone Star property was discovered during road building and camp construction.



Klondike (Yukon MINFILE 115O 088). The exploration program targeted low-sulphide, gold-bearing orogenic veins.

Other exploration programs in the Klondike included trenching, prospecting and sampling on the **King Solomon's Dome** property of J.A.E. Resources (Yukon MINFILE 115O 068). The property covers an area containing the gold-bearing Mitchell and Sheba veins. Trenching concentrated on new areas of the property that have favourable geochemistry. This trenching was successful in discovering new areas of gold mineralization.

Approximately 80 km south of the Klondike district, active placer mining in the White River-Thistle Creek area has been targeted for orogenic gold potential, as it is an area underlain by prospective Yukon-Tanana Terrane rocks.

Madelena Ventures Inc. expanded the grid soil sampling and magnetometer surveys on the **White River** property (Yukon MINFILE 115O 012). Exploration in 2004 discovered two parallel gold-bearing quartz veins with trace galena, chalcopyrite and visible gold. The veins vary from 1 to 5 m in width and are each exposed over a 12-m length. The veins dip steeply, and are hosted in Devonian to Mississippian quartz-sericite schist with a shallow foliation, which is in turn intruded by a large, mid(?) to late Paleozoic gabbroic body.

In the Thistle Creek area, Ryanwood Exploration conducted soil sampling, magnetometer surveys (Fig. 29) and excavator trenching on their **Blackfox** property (Yukon MINFILE 115O 014). Trenching exposed a low-sulphide, gold-bearing quartz vein, which had returned float samples found prior to trenching that assayed up to 26.0 g/t Au (Fig. 30).

Gold mineralization occurs in a northerly trending linear belt in the Hyland River area of southeastern Yukon. Recent work in the area by Craig Hart of the Yukon

Figure 29. Mike Lindley with Ryanwood Exploration conducting magnetometer surveying on the Blackfox property.





Figure 30. Gold-bearing quartz vein from the Blackfox property.

Geological Survey has suggested an orogenic model for the numerous gold occurrences that occupy this trend (Hart and Lewis, 2006).

StrataGold Corporation and joint venture partner Northgate Exploration Ltd. conducted a 4-hole, 985-m, helicopter-supported diamond drill program on the **Hyland Gold** property (Yukon MINFILE 095D 011). Previous workers have suggested an intrusive-related source for the mineralization at the Hyland Gold property; however, recent work by Hart and Lewis (2006) includes the Hyland Gold property in a newly outlined belt of orogenic gold occurrences. The claims are underlain by the Neoproterozoic to Lower Cambrian Hyland Group phyllite and quartzite. In the main area of exploration on the property, these Hyland Group rocks are characterized structurally as having formed an east-verging, overturned anticline. There is intense silica and sulphide mineral replacement of the phyllite and quartzite in the core of the anticline. No results were reported from this year's drilling.

The **Hy** property of Dentonia Resources Ltd. is located to the north of the Nahanni Range road, which provides access to the Cantung mine (Yukon MINFILE 105H 102). The property is underlain by Neoproterozoic to Lower Cambrian carbonate and clastic metasedimentary rocks assigned to the Hyland Group. Dentonia drilled three short holes on the property, targeting two areas identified by soil geochemistry and gold-bearing, low-sulphide quartz in float. The West gold zone, which trends north-northwest, is 1.4 km in length, with a width of 50 to 100 m, and contains quartz veins with values in grab samples ranging up to 144 g/t Au. Soil geochemical values range up to 909 ppb Au and 253 ppm As. The East gold zone is located 800 m east of the West gold zone, and also trends north-northwest. It is 900 m long and up to 350 m wide. Values in grab samples range up

Figure 31. Helicopter-supported drilling on the Hy property.



to 37.6 g/t Au. Soil geochemical values range up to 1259 ppb Au and 1783 ppm As. No significant results were reported from the drilling (Fig. 31).

North American Tungsten Corporation explored the **3 Aces** property which is located adjacent to the Nahanni Range Road (Yukon MINFILE 105H 036). North American Tungsten Corporation conducted a small exploration program of line-cutting, soil sampling and geophysical surveys. Gold-bearing quartz vein in float is reported from an area underlain by Neoproterozoic to Lower Cambrian carbonate and clastic metasedimentary rocks assigned to the Hyland Group.

Logan Resources Ltd. conducted an airborne magnetic survey, induced polarization/resistivity surveys, a gravity survey, soil and silt geochemical surveys, and geological mapping on their **Shell Creek** gold-copper property (Yukon MINFILE 116C 029). The property, located northwest of Dawson City, is underlain by Neoproterozoic to Cambrian Hyland Group. Preliminary mapping completed by Logan Resources revealed that, in the occurrence area, the Hyland Group is composed of recrystallized limestone at its base overlain by siliceous argillite, siltstone and sandstone. Within the siliceous sedimentary rocks, there occurs a narrow, banded iron formation composed of a magnetite-bearing slate (magnetite facies) interlaminated with a thin-banded, grey chert containing pyrite and pyrrhotite. Minor chloritic schist of probable volcanic origin overlies the iron formation. Gold mineralization is hosted in a series of quartz reefs, of which four are exposed within the Hyland Group meta-volcanic rocks. The quartz reefs are roughly 50 m to 75 m wide across the region of fold closure. Individual reefs consist of a number of stacked quartz veins that range from less than half a metre, to several metres in thickness, and contain visible gold and minor copper mineralization.

Epithermal gold mineralization in Yukon is associated with one of the following associations: 1) porphyry to epithermal transitions (e.g., Mount Nansen, Mount Freegold); 2) arc-like calderas (Mt. Skukum); or, 3) rift-related subaerial volcanic rocks (Grew Creek). Most systems are characterized by low-sulphidation,

Figure 32. Quartz-adularia mineralization from the Grew Creek deposit.

epithermal characteristics, but those in the epithermal-porphyry transition are of ‘intermediate’ sulphidation. ‘Intermediate sulphidation’ characteristics yield high silver contents, but lack copper enrichments or acid-related alteration.

Freegold Ventures Ltd. conducted an exploration program of geochemical surveys, a geophysical survey (induced polarization) and diamond drilling on the **Grew Creek** epithermal gold property (Yukon MINFILE 105K 003). Freegold acquired the Grew Creek property last summer and completed 12 diamond drill holes. Drilling was based on a new geological theory proposing that mineralization trends north-south, as opposed to previous interpretations which suggested that the mineralization trended east-west. Furthermore, this new interpretation suggests that the original deposit area may be open for potentially significant expansion. Results from last year’s drilling program indicate that the mineralization does trend north, and that the quartz-adularia vein (Fig. 32) and vein stockwork system in the Golden Spike zone is faulted into at least four separate segments. Geochemical and geophysical surveys were conducted over the main deposit area to characterize the geochemical and geophysical signature of the deposit. The geophysical survey produced a good chargeability anomaly that coincided with the main deposit. Surveys in the area of Rat Creek and the Tarn zone, located 1 km and 1.5 km east of the main deposit respectively, produced targets with similar geophysical and geochemical signatures to the main deposit. A drill program began in late November to test the new zones.

Tagish Lake Gold Corporation continued to drill-test the **Skukum Creek** epithermal gold deposit south of Whitehorse (Yukon MINFILE 105D 022). Underground drilling (Fig. 33) tested the Rainbow Two zone. The Rainbow Two zone is hosted in the same mineralized structure as the Rainbow zone, located 250 m to the northeast, and the Two zone, located 240 m to the southwest. The drilling outlined a significant zone of gold-silver mineralization in the Rainbow Two zone. Highlights from drilling include 17.95 g/t Au and 140.5 g/t Ag over 2.65 m in hole SC05-35 (Table 12).



Table 12. Drill results from the Rainbow Two zone.

Hole	From m	To m	Length m	Au g/t	Ag g/t
SC05-25	No significant results				
SC05-26	No significant results				
SC05-27	66.45	67.25	0.80	2.62	208.0
	70.75	71.60	0.85	3.51	1400.0
SC05-28 includes	68.90	72.20	3.30	4.15	56.1
	71.30	72.20	0.90	9.26	111.0
SC05-29 includes	5.00	6.00	1.00	1.35	6.4
	35.35	36.27	0.92	3.86	35.8
	35.35	35.97	0.62	5.01	40.9
SC05-30 includes	40.85	41.45	0.60	5.23	34.7
	50.90	51.20	0.30	2.23	74.6
	52.90	54.55	1.65	24.44	121.7
SC05-31 includes	52.90	53.30	0.40	25.90	148.0
	53.65	54.10	0.45	61.30	290.0
SC05-31 includes	25.30	36.80	10.50	10.59	89.4
	25.55	26.80	1.25	44.70	130.0
SC05-31 includes	32.50	34.00	1.50	24.90	216.0
	19.10	23.80	4.70	5.40	82.2
SC05-32 includes	19.10	19.80	0.70	34.20	198.0
	15.50	16.10		1.14	36.0
SC05-33	20.70	21.50		1.98	11.4
	No significant results				
SC05-34	No significant results				
SC05-35 includes	25.30	27.95		17.95	140.5
	25.30	26.05		21.80	236.0
SC05-35 includes	27.20	27.95		28.10	226.0
SC05-36	26.82	27.20		3.04	607.0

Figure 33. Underground drill at the Rainbow Two zone at the Skukum Creek deposit.



Table 13. Kuhn Zone drill results.

Hole	From m	To m	Au g/t	Ag g/t
SC05-37	125.05	130.60	0.99	13.1
includes	125.05	126.05	2.35	22.9
	139.10	142.85	2.83	106.1
including	141.90	142.85	5.04	172.0
SC05-38	93.90	95.10	1.23	16.0
	97.26	97.71	2.20	38.9
	109.12	110.46	1.03	15.6

Drilling was also directed at the depth extent of the Kuhn zone which is located on a structure that is sub-parallel to that hosting the Rainbow zone. Two holes were drilled which indicated that the gold-silver mineralized structure remains open to depth (Table 13).

Tagish Lake also contracted Laxey Mining Services Limited to update the preliminary feasibility study on the Skukum Creek deposits. MineTech prepared a measured and indicated resource estimate for Skukum Creek. The updated preliminary feasibility study indicates that the internal rate of return of the project would be 20.7% at gold and silver prices of \$500 (U.S.) and \$7.50 (U.S.) per troy ounce, respectively, for the base case.

CMC Metals Ltd. explored the **CMC** property (Yukon MINFILE 105B 021) with induced polarization surveying, trenching and diamond drilling directed at high-grade, silver-zinc veins. Trench samples returned values up to 2206 g/t Ag with 2.34% Zn. Drilling was directed at a number of historical veins that are known on the property. High-grade silver was encountered in a number of holes. Hole DH05-08 intersected 2.45 m grading 4.21% Pb, 3.12% Zn and 899 g/t Ag. The historical work on the property did not assess the zinc content of the veins. By contrast, hole DH05-07 intersected 22.7 m of 4.63% Zn and 76 g/t Ag. Results from the program will be used to re-evaluate historical resources that are reported for the property.

GEMSTONES

True North Gems continued with an expanded program of plant upgrading, camp construction, geological mapping, prospecting and bulk sampling at the **Tsa Da Glisza** emerald property. The company released results of the combined 2003 and 2004 bulk sampling programs, which led them to perform the expanded program in 2005. The program of extensive trenching and mini-bulk sampling (Fig. 34) was carried out in order to confirm grade, continuity of grade, and mineralization along strike and to depth. The program of trenching and mini-bulk sampling will also allow for the recovery of sufficient emeralds to permit completion of a pre-feasibility study in winter 2005/spring 2006.

A total of 3306 tonnes of mini-bulk samples, from material stockpiled from the 2003 underground program and from 2004 and 2005 trenching, were processed in the on-site plant that achieved production rates up to 125 tonnes per day. A total of 12 kg of clean emerald rough was recovered from 254 kg of hand-picked mineralized material. A total of 4044.67 g of gem and near-gem emerald rough was sent for cutting, and by year-end, True North had received the first shipment of cut stones from the cutting factory. Results from all shipments are expected in the first quarter of 2006. In addition to the material processed, 1600 tonnes of material were excavated in 2005 and stockpiled for processing in 2006.

Table 14. Tsa Da Glisza bulk sample rough stone grades.

	Tonnes extracted	Gem g/t	Near-gem g/t
2003 surface	963.6	0.39	3.77
2003 underground	987.2	0.30	3.09
2004 surface	582.3	1.44	12.88
combined	2533.1	0.59	5.66
	Tonnes extracted	Non-gem g/t	Total beryl kg
2003 surface	963.6	2.91	6.8
2003 underground	987.2	6.43	9.1
2004 surface	582.3	22.79	21.1
combined	2533.1	9.09	15.3



Figure 34. Bulk sampling at the Tsa Da Glisza emerald property.

BULK SAMPLE VALUATIONS

The wholesale valuation of emerald polished goods was completed by three valuers and focused on the inventory derived from the 2003 to 2004 surface and underground bulk sample. The wholesale value of the bulk sample in US dollars per tonne ranged from \$5.61 to \$33.61 with an average of \$19.43, while the retail value ranged from \$46.93 to \$134.

COAL

Cash Minerals Ltd. completed a scoping study on the **Division Mountain Coal** project. The deposit is located 20 km west of Highway 2 and Yukon's main power grid, and 300 km from the closest tidewater port at Skagway, Alaska. The study supports the potential for the economic development of an open-pit mine based on the annual production of approximately 1 375 000 tonnes of saleable coal. The scoping study is also based on a measured and an indicated resource of 51.5 million tonnes as defined by Norwest Corporation, a leading North American coal and engineering consultancy (Norwest Corporation, unpublished data). Cash Minerals Ltd. completed a 5-hole, 2800-m diamond drilling program (Fig. 35) designed to upgrade indicated resources into the measured category. The drilling and sampling program will provide information on coal-quality variation within each seam. It will also increase drill-hole density, thus increasing the confidence level in resource estimates. The data from the exploration project will provide the company with enough information to complete a bankable feasibility study which is anticipated for release in the first quarter of 2006.

Cash Minerals Ltd. and Alaska Industrial Development and Export Authority (AIDEA) are negotiating the use of the Skagway ore terminal for the shipping of Division Mountain coal. AIDEA is the contractual owner of the terminal, and it has use of the docking facility in conjunction with White Pass and Yukon Rail.

Figure 35. Diamond drill at the Division Mountain Coal project.



ACKNOWLEDGEMENTS

This report is based on public information gathered from a variety of sources. It also includes information provided by companies through press releases, personal communications and property visits conducted during the 2005 field season. The cooperation of companies and individuals in providing information, as well as their hospitality, time and access to properties during field tours, is gratefully acknowledged. Safe, reliable helicopter transportation provided by Helidynamics, TransNorth and Fireweed helicopters during the field season is always appreciated. The editing skills of Leyla Weston, Diane Emond, Lara Lewis and Geoff Bradshaw are also appreciated.

REFERENCES

- BC Minfile, 2005. Ministry of Energy, Mines and Petroleum Resources, British Columbia.
- Burke, M., Hart, C.J.R., Lewis, L.L., 2005. Models for Epigenetic gold exploration in the northern Cordilleran orogen, Yukon, Canada. *In: Mineral Deposit Research: Meeting the Global Challenge*, F. Bierlein and J. Mao (eds.), Proceedings of the Eighth Biennial SGA Meeting, Beijing, China, August 18-21, 2005, p. 525-528.
- Deklerk, R. and Traynor, S., 2005. Yukon MINFILE – A database of mineral occurrences. Yukon Geological Survey, CD-ROM.
- Hart, C.J.R. and Lewis, L.L., 2006 (this volume). Gold mineralization in the Upper Hyland River area: A non-magmatic origin. *In: Yukon Exploration and Geology 2005*, D.S. Emond, G.D. Bradshaw, L.L. Lewis and L.H. Weston (eds.), Yukon Geological Survey, p. 109-125.
- Hunt, J.A., Abbott, J.G. and Thorkelson, D.J., 2006 (this volume). Unconformity-related uranium potential: Clues from Wernecke Breccia, Yukon. *In: Yukon Exploration and Geology 2005*, D.S. Emond, G.D. Bradshaw, L.L. Lewis and L.H. Weston (eds.), Yukon Geological Survey, p. 127-137.
- Israel, S., Tizzard, A. and Major, J., 2006 (this volume). Bedrock geology of the Duke River area, parts of NTS 115G/2, 3, 4, 6 and 7, southwestern Yukon. *In: Yukon Exploration and Geology 2005*, D.S. Emond, G.D. Bradshaw, L.L. Lewis and L.H. Weston (eds.), Yukon Geological Survey, p. 139-154.
- Tafti, R. and Mortensen, J.K., 2004. Early Jurassic porphyry(?) copper (-gold) deposits at Minto and Williams Creek, Carmacks Copper Belt, western Yukon. *In: Yukon Exploration and Geology 2003*, D.S. Emond and L.L. Lewis (eds.), Yukon Geological Survey, p. 289-303.
- Traynor, S., 2006 (this volume). Yukon Mining Incentives Program, 2005. *In: Yukon Exploration and Geology 2005*, D.S. Emond, G.D. Bradshaw, L.L. Lewis and L.H. Weston (eds.), Yukon Geological Survey, p. 47-48.

APPENDIX 1: 2005 EXPLORATION PROJECTS

PROPERTY	COMPANY/OWNER	MINFILE # or (1:50 000 NTS)	WORK TYPE	COMMODITY
Blackfox	RyanWood Exploration	115O 014	G,GC,GP	Au
Clear Creek	Stratagold Corporation	115P 012,013	G	Au
Crown Jewel	RyanWood Exploration	115O 088	GC,GP,P	Au
Dragon Lake	Eagle Plains Resources Ltd.	105J 007	G,GP,T	Au
Dublin Gulch	Stratagold Corporation	106D 025	G,DD	Au
Heidi	Logan Resources	116A 037	G,GC,GP	Au
Hy	Dentonia Resources Ltd.	105H 102	G,DD	Au
Hyland Gold	Stratagold Corporation/Northgate Minerals Corp.	95D 011	G,DD	Au
Ice	Acero-Martin Exploration Inc.	115P 006	G,DD	Au
Indian River	Boulder Mining Corporation	115O 054	G,P	Au
Ketza River	YGC Resources Ltd.	105F 019	G,GC,DD	Au
King Solomons Dome	JAE Resources	115O 068	G,GC,T	Au
Lone Star	Klondike Star Mineral Corporation	115O 072	G,GC,DD	Au
McFaul	New World Resource Corporation	116B 157	G,PD	Au
Mike Lake	Bashaw Capital Corporation	116A 012	G,GP,GC,P,DD	Au
Tin	Madelena Ventures Inc.	116B 157	G,GC,GP	Au
Typhoon	Curlew Lake Resources Inc.	115P 060	G,GC,P	Au
White River	Madelena Ventures Inc.	115O 011,012	G,GC,GP	Au
Grew Creek	Freegold Resources Inc.	105K 009	G,GP,DD	Au-Ag
Skukum Creek	Tagish Lake Gold Corporation	105D 022	DD	Au-Ag
Sonora Gulch	Firestone Ventures Inc.	115J 008	G,GP	Au-Ag
Spice	Klondike Gold Corporation	105G 150	G	Au-Ag
Shell Creek	Logan Resources Ltd.	116C 029	G,GP,GC	Au-Cu-U
Pigskin	Strategic Metals Ltd.	105B 107	G,GC	Ag-Zn
CMC Silver (Silver Hart)	CMC Metals Ltd.	105B 021	G,GP,GC,T,DD	Ag-Zn
Meister	Tanana Exploration	105B 114	G,P,GC	Ag-Zn
Cuprum	Manson Creek Resources Ltd.	105E 008	G,P,T,GP,GC	Cu-Au
Hat (Whitehorse Copper)	Kluane Drilling	105D 125	DD	Cu-Au
Lucky Joe	Kennecott Canada/Copper Ridge Explorations Inc.	115O 051	G,GP,DD	Cu-Au
Thistle/Shamrock	Copper Ridge Explorations Inc.	(115O/6)	G,GC,P	Cu-Au
Carmacks Copper	Western Silver Corporation	115I 008	ES,PF	Cu-Au
Minto Project	Sherwood Copper Corporation	115I 021,022	G,GP,DD,F	Cu-Au-Ag
Bond	Cash Minerals Ltd./ Twenty Seven Capital Corporation	106D 065	G,DD	Cu-Au-U
Ironman	Copper Ridge Explorations Inc.	(116A/15)	G,GP,P	Cu-Au-U
Yukon Olympic	Janina Resources Ltd./ Copper Ridge Explorations Inc.	116G 082	G,GP,DD	Cu-Au-U
Rusty Springs	Eagle Plains Resources Ltd.	116K 003	DD	Cu-Pb-Zn-Ag

Abbreviations

BS - bulk sample

D - development

DD - diamond drilling

ES - environmental studies

F - feasibility

G - geology

GC - geochemistry

GP - geophysics

IOCG - iron-oxide copper gold

M - mining

PD - percussion drilling

PF - prefeasibility

R - reconnaissance

T - trenching

U/GD - underground development

Appendix 1 (continued): 2005 EXPLORATION PROJECTS

PROPERTY	COMPANY/OWNER	MINFILE # or (1:50 000 NTS)	WORK TYPE	COMMODITY
Marg	Yukon Gold Corporation Inc.	106D 009	G,DD	Cu-Pb-Zn-Ag-Au
Four Corners	Strategic Metals Ltd.	105G 146	G,P	Cu-Zn
Money	Yukon Zinc Corporation	105H 078	G,GC	Cu-Zn
Tsa da Glizsa	True North Gems Inc.	105G 147	G,P,BS	emerald
Moly	Strategic Metals Ltd.	105F 001	G,P	molybdenum
Rams Horn	Ordorado Resources Corporation	105D 002,3,4	G,GC,P	molybdenum
Red Mountain Moly	Tintina Mines Ltd.	105C 009	PF,ES	molybdenum
Stormy Mountain	E-Energy Ventures Inc.	105F 011	G,P	molybdenum
Burwash	Strategic Metals Ltd./Golden Chalice Resources	115G 100	G,DD	Ni-Cu-PGE
Canalask	Falconbridge Limited/StrataGold Corporation	115F 045	G	Ni-Cu-PGE
Klu	Resolve Ventures Inc.	115G 003,098,099	G,P	Ni-Cu-PGE
Ultra	Klondike Gold Corporation	115B 008	G,GC,P	Ni-Cu-PGE
Wellgreen	Coronation Minerals Inc./Northern Platinum Ltd.	115G 024	G,GC,T,PD	Ni-Cu-PGE
Blende	Eagle Plains Resources Ltd./Blind Creek Resources	106D 064	G,GP,GC	Pb-Zn-Ag
Convert	Strategic Metals Ltd.	105B 143	P,T	Pb-Zn-Ag
Howard's Pass	Pacifica Resources Ltd.	105I 012	G,GC,GP,DD	Pb-Zn-Ag
Kathleen Lake area	Manson Creek Resources Ltd.	106C 098	G,P	Pb-Zn-Ag
Thunderstruck	Yukon Zinc Corporation	(105G/8)	G,DD	Pb-Zn-Cu-Ag-Au
Tidd	Strategic Metals Ltd.	105J 029	G,GC,GP,P	Pb-Zn-Cu-Ag-Au
Wolverine	Yukon Zinc Corporation	105G 073	G,DD,BS,F,ES	Pb-Zn-Cu-Ag-Au
Alle	Cash Minerals Ltd./ Twenty Seven Capital Corporation	105B 126	G,P	U
Curie	Signet Minerals Inc.	106E 031	G,GC,GP	U
Igor	Cash Minerals Ltd./ Twenty Seven Capital Corporation	106E 009	G,DD	U
Lumina	Cash Minerals Ltd./ Twenty Seven Capital Corporation	106C 069	G,GP,DD	U
Pedlar	Cash Minerals Ltd./ Twenty Seven Capital Corporation	115J 092	G	U
Steel	Cash Minerals Ltd./ Twenty Seven Capital Corporation	106D 049	G,DD	U
U	RyanWood Exploration	115J 093	G,GC,P	U
Nor	International KRL Resources Corporation	106L 061	G,GC,GP,P	U-Cu-Au
Pike	Strategic Metals Ltd.	106E 040	G,DD	U-Cu-Au
Kalzas	Copper Ridge Explorations Inc.	105M 066	G,DD	WO ₃
Logtung	Strategic Metals Ltd.	105B 039	G	WO ₃
MacTung	North American Tungsten Corporation	105O 002	G,DD,BS	WO ₃
Division Mountain	Cash Minerals Ltd.	115H 013	G,DD,F	Co

Abbreviations

BS - bulk sample

D - development

DD - diamond drilling

ES - environmental studies

F - feasibility

G - geology

GC - geochemistry

GP - geophysics

IOCG - iron-oxide copper gold

M - mining

PD - percussion drilling

PF - prefeasibility

R - reconnaissance

T - trenching

U/GD - underground development

APPENDIX 2: 2005 DRILLING STATISTICS

Company	Property	MINFILE # or (1:50 000 NTS)	Drill holes	
			# holes	metres
Acero-Martin Exploration Inc.	Ice	115P 006	8	1514
Bashaw Capital Corporation	Mike Lake	116A 012	18	2220
Cash Minerals Ltd.	Division Mountain	115H 013	5	2800
Cash Minerals Ltd./Twenty Seven Capital Corporation	Bond	106D 065	7	735
Cash Minerals Ltd./Twenty Seven Capital Corporation	Igor	106E 009	7	1121
Cash Minerals Ltd./Twenty Seven Capital Corporation	Steel	106D 049	3	581
Cash Minerals Ltd./Twenty Seven Capital Corporation	Lumina	106C 069	7	504
CMC Metals Ltd.	CMC Silver (Silver Hart)	105B 021	12	1000
Kennecott Canada/Copper Ridge Explorations Inc.	Lucky Joe	115O 051	5	1049
Janina Resources/Copper Ridge Explorations Inc.	Yukon Olympic	116G 082	5	504
Copper Ridge Explorations Inc.	Kalzas	105M 066	5	397
Dentonia Resources Ltd.	Hy	105H 102	3	232
Eagle Plains Resources Ltd.	Rusty Springs	116K 003	2	405
Freegold Resources Inc.	Grew Creek	105K 009	6	960
Klondike Star Mineral Corporation	Lone Star	115O 072	32	4830
Kluane Drilling	Hat (Whitehorse Copper)	105D 053	4	838
North American Tungsten Corporation	MacTung	105O 002	25	6668
New World Resource Corporation	McFaul	116B 157	43*	1800
Pacifica Resources Ltd.	Howard's Pass	105I 012	53	8317
Sherwood Copper Corporation	Minto	115I 021,022	57	6772
Stratagold Corporation	Dublin Gulch	106D 025	34	8102
Stratagold Corporation/Northgate Minerals Corporation	Hyland Gold	95D 011	4	985
Strategic Metals Ltd./Golden Chalice Resources	Burwash	115G 100	7	520
Strategic Metals Ltd.	Pike	106E 040	3	278
Tagish Lake Gold Corporation	Skukum Creek	105D 022	14	850
YGC Resources Ltd.	Ketza River	105F 019	95	12485
Yukon Gold Corporation	Marg	106D 009	4	1200
Yukon Zinc Corporation	Wolverine	105G 073	61	11713
Yukon Zinc Corporation	Thunderstruck	(105G/8)	3	1476
Total				80 856

*Drilled using rotary percussion. All other holes were drilled using a diamond drill.

Yukon Placer Mining Overview 2005

William LeBarge¹
Yukon Geological Survey

LeBarge, W., 2006. Yukon Placer Mining Overview 2005. *In: Yukon Exploration and Geology 2005*, D.S. Emond, G.D. Bradshaw, L.L. Lewis and L.H. Weston (eds.), Yukon Geological Survey, p. 41-45.

PLACER MINING

Today, more than 100 years after the discovery of gold in the Yukon, placer mining is still an important sector in the Yukon's economy. Over 16.6 million crude ounces (517 tonnes) of placer gold have been produced to date in the Yukon – at today's prices that would be worth more than \$7 billion.

Approximately 450 people were directly employed at 128 placer mines in 2005 – and at least several hundred more were employed in businesses and industries that serve the placer mining industry. Most of the placer operations are small and family-run, with an average of three or four employees. The majority of active placer mining operations were in the Dawson Mining District, followed by the Whitehorse Mining District and the Mayo Mining District. No active mines are currently in the Watson Lake Mining District. The total Yukon placer gold production in 2005 was 70,322 crude ounces (2 187 260 g), compared to 76,152 crude ounces (2 368 610 g) in 2004. The value of this 2005 gold production was \$29.9 million.

Approximately 87% of the Yukon's placer gold was produced in the Dawson Mining District, which includes the unglaciated drainages of Klondike River, Indian River, west Yukon (Fortymile and Sixtymile rivers, and the Moosehorn Range) and lower Stewart River. The remaining gold came from the glaciated Mayo and Whitehorse mining districts, which include the placer areas of Clear Creek, Mayo, Dawson Range, Kluane, Livingstone and Whitehorse South.

Reported placer gold production from Indian River drainages in 2005 decreased compared to the previous year, from 2004's 27,366 crude ounces (851 178 g) to 26,473 crude ounces (823 403 g). Some of this decrease came from operations in Dominion Creek, but this was partially offset by some increases which were the result of new operations on Indian River.

In Klondike area drainages, production dropped slightly to 12,627 crude ounces (392 744 g) from 2004's 13,546 crude ounces (421 328 g), partially because of a decrease in gold coming from operations on Last Chance Creek. An increase in production came from bench deposits ("White Channel Gravels") on Bonanza and Hunker creeks.

A decrease was also seen in West Yukon (Sixtymile, Fortymile and Moosehorn Range) placer gold production, from 2004's 15,065 crude ounces (468 574 g) to 12,314 crude ounces (383 008 g). Matson Creek and Sixtymile River had fewer

¹bill.lebarge@gov.yk.ca

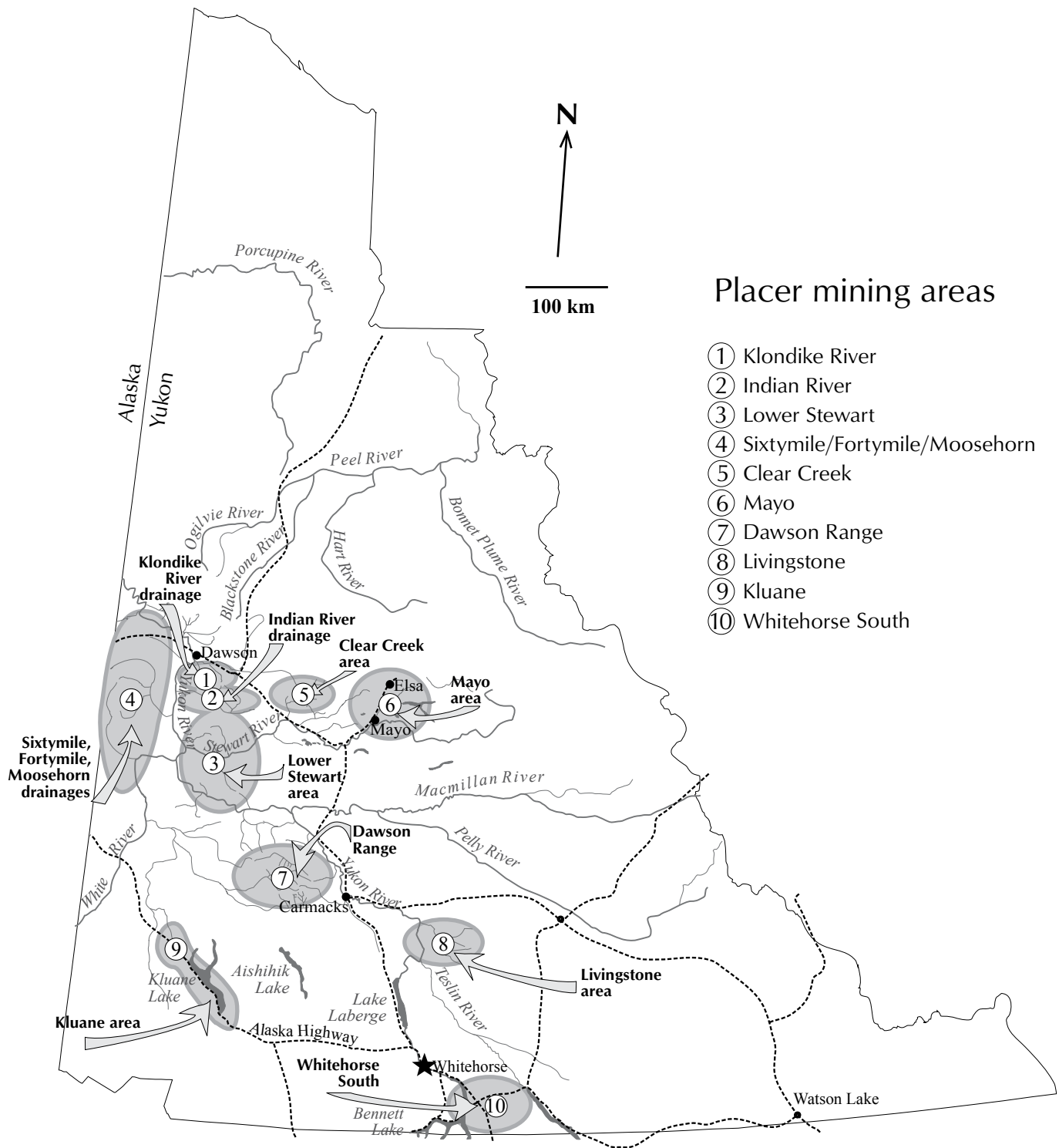


Figure 1. Yukon placer mining areas.

royalties reported, while figures increased from Kate Creek. Fifty Mile Creek, a tributary of Sixtymile River, began producing for the first time in 2005.

Reported production from operations in the Lower Stewart drainages was also down in 2005, to a total of 9572 crude ounces (297 722 g) from 11,496 crude ounces (357 565 g) the previous year. All operations, including those on Thistle and Black Hills creeks, reported less gold.

As usual, little gold was reported from Clear Creek drainages although several operations were active in 2005. The total reported gold from royalties increased slightly to 255 crude ounces (7931 g) from 207 crude ounces (6438 g).

In the Dawson Range, reported placer gold production dropped slightly from 1619 crude ounces (50 372 g) to 1545 crude ounces (48 054 g).

In the Mayo area, gold production decreased from 2502 crude ounces (77 821 g) to 2340 crude ounces (72 782 g).

In the Kluane area, reported placer gold production rose significantly from 1912 crude ounces (59 470 g) to 2667 crude ounces (82 953 g). The increase came mainly from Gladstone Creek.

The Livingstone area was inactive, although 17.2 crude ounces (535 g) of gold were reported the previous year in royalties.

In the Whitehorse South area, some mining and testing activity took place on Moose Brook and Wolverine Creek, although no royalties were recorded. Iron Creek, a tributary of Sydney Creek, had 27.4 crude ounces (852 g) reported in royalties.

PLACER EXPLORATION

Although it is generally unrecorded, exploration on placer mining properties has been a part of the process for many miners since they began to mine. Traditional methods of sampling and exploration include auger, reverse circulation and churn drilling, and geophysics including seismic surveys, ground-penetrating radar and

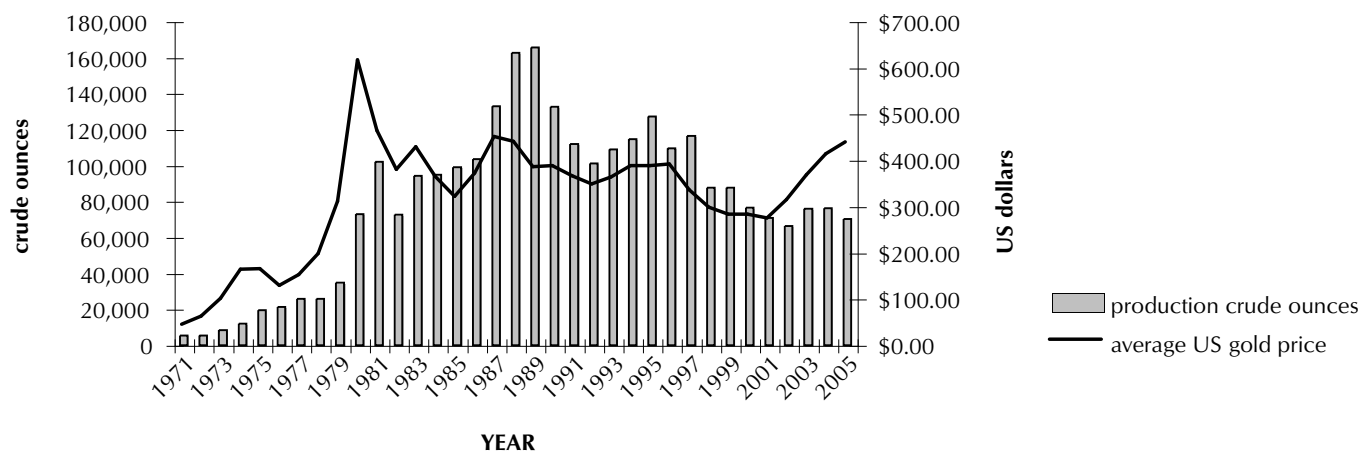


Figure 2. Yukon placer gold production figures and average US gold price, 1971-2005.

magnetometer surveys. Trenching and bulk sampling also continue to be well used methods of testing placer ground.

The Yukon Mining Incentives Program contributed funding to nine placer exploration programs in 2005. More information about this program can be obtained from Steve Traynor, Economic Geologist, Steve.Traynor@gov.yk.ca, (867) 456-3828 or at <http://www.emr.gov.yk.ca/mining/programs/ymip.html>.

One of the highlights of placer exploration in 2005 was the continued activity by Boulder Mining Corporation on their Indian River property 30 km south of Dawson City. The company produced a total of 436 crude ounces (13 561 g) of gold from three areas in two separate pits. The property consists of a large-volume bench deposit which lies above the modern valley of Indian River. Generalized stratigraphy consists of a Tertiary-age, 'White Channel' gold-bearing gravel on a bedrock terrace, which is in part overlain by glaciofluvial and glaciolacustrine sediments deposited during the earliest pre-Reid glaciation.

Exploration on this property in 2005 consisted of an extensive program of alluvial bulk sampling, alluvial sampling, and hard-rock mapping and sampling. Average grades from each of the three areas mined were 0.14 g/m³, 0.23 g/m³ and 0.18 g/m³. A total of 76 828 cubic metres were sluiced. A production-scale program for the property is being considered for the 2006 season.

Similar geologic and geomorphic settings to that of Indian River exist in other unglaciated drainages in the Yukon, specifically in Fortymile and Sixtymile areas. Although limited amounts of placer exploration have taken place on alluvial terraces in these areas, they remain poorly understood. It may be possible that significant quantities of gold lie in these bench deposits which have yet to be methodically evaluated.

The long-term health of the Yukon's placer mining industry requires that new placer gold reserves be discovered as traditional mining areas become depleted. With the application of new placer exploration and research techniques and new ideas, additional placer gold reserves may be found in non-traditional, more complex geological settings.

The staff at the Yukon Geological Survey and the Client Services and Inspection Division (Department of Energy, Mines and Resources, Yukon government) can provide information and advice regarding placer mining in the Yukon. Publications on placer mining in the Yukon are available through the Yukon Geological Survey office at Room 102, Elijah Smith Building, 300 Main Street, Whitehorse, Yukon. Many recent publications and maps can be downloaded for free from our website at www.geology.gov.yk.ca.

APERÇU

Approximativement 450 personnes trouvaient directement de l'emploi dans 128 exploitations minières de placers au Yukon en 2005 et au moins plusieurs centaines d'autres étaient à l'emploi d'entreprises et d'industries desservant l'industrie minière des placers. La production totale d'or tirée de placers au Yukon au 5 décembre 2005 s'élevait à 70 317 onces brutes (2 187 115 g), comparativement à 76 152 onces brutes (2 368 610 g) en 2004. La valeur de cette production pour 2005 s'élevait à 29,9 millions de dollars. Environ 87 % de la production d'or des placers du Yukon provient du district minier de Dawson, qui couvre les bassins versants non glaciés de la rivière Klondike, de la rivière Indian, de la branche ouest du fleuve Yukon et de la basse rivière Stewart. Le reste de la production d'or provenait des districts miniers glaciés de Mayo et de Whitehorse englobant les régions placériennes de Clear Creek, de Mayo, de la chaîne de Dawson, de Kluane, de Livingstone et de Whitehorse Sud.

L'exploration des propriétés minières de placers fait partie du processus pour un grand nombre de mineurs depuis qu'ils ont entrepris l'exploitation minière; elle s'effectue à la tarière, par forage à circulation inverse et au battage, par levés sismiques, par géoradar et par levés magnétométriques ainsi que par excavation de tranchées et échantillonnage en vrac. La poursuite des activités de la Boulder Mining Corporation dans sa propriété Indian River à 30 km au sud de Dawson City a constitué l'un des faits saillants de l'exploration à la recherche de placers en 2005. À cet endroit, un volumineux dépôt de terrasse domine la vallée contemporaine de la rivière Indian. La stratigraphie générale consiste en gravier aurifère de «White Channel» du Tertiaire reposant sur une terrasse du substratum et en partie recouvert par des sédiments fluvio-glaciaires et glacio-lacustres déposés pendant la plus précoce des glaciations antérieures à la glaciation de Reid. Un programme d'échantillonnage en vrac et d'échantillonnage d'alluvions ainsi que de cartographie et d'échantillonnage de la roche dure a été exécuté et un programme à l'échelle de production est envisagé pour la campagne de 2006. Des cadres géologique et géomorphologique similaires à celui de la rivière Indian existent dans d'autres bassins versants non glaciés au Yukon, en particulier dans les régions de Fortymile et de Sixtymile. D'importantes quantités d'or pourraient reposer dans ces dépôts de terrasses qui restent à évaluer méthodiquement.

La vitalité à long terme de l'industrie de l'exploitation minière de placers au Yukon exige que de nouvelles réserves d'or placérien soient découvertes à mesure que s'épuisent celles des régions traditionnellement exploitées. L'application de nouvelles méthodes d'exploration et de recherche de gîtes placériens combinée à des idées nouvelles pourrait permettre de découvrir des réserves additionnelles d'or placérien dans des cadres géologiques non traditionnels plus complexes.

Yukon Mining Incentives Program 2005

Steve Traynor¹
Yukon Geological Survey

Traynor, S., 2006. Yukon Mining Incentives Program, 2005. *In: Yukon Exploration and Geology 2005*, D.S. Emond, G.D. Bradshaw, L.L. Lewis and L.H. Weston (eds.), Yukon Geological Survey, p. 47-48.

The Yukon Mining Incentives Programs (YMIP) received 75 applications for funding by the March 1, 2005 submission deadline. Contribution agreements totaling \$1 009 000 were subsequently issued to 63 successful applicants. Proposals approved for funding included 12 under the Grassroots–Prospecting module, 12 under the Focused Regional module, and 39 under the Target Evaluation module.

The continuing trend of increasing gold prices, combined with copper prices that have doubled in the past two years, has resulted in high levels of exploration targeting these two commodities. This focus was mirrored by nearly three-quarters of the 54 exploration projects (see Fig. 1) which proceeded this year with a portion of their risk-capital provided by YMIP (approximately \$728 000 in 2005).

Reported highlights of this year’s YMIP activities already include the signing of a handful of option deals, a significant increase in expenditures relating to the evaluation of new occurrences, and a corresponding increase in claim staking directly related to these activities. The recent creation of the Focused Regional module, designed to appraise the potential of under explored areas of Yukon, has already resulted in significant new discoveries.

Year-to-year statistics routinely show expenditure levels are typically two to three times the portion funded by YMIP. At the upper end of this scale, and over the longer term of the past two decades, expenditures on a number of specific projects have exceeded twenty times the value of the initial YMIP contribution.

Significant discoveries made with initial assistance from YMIP include the Andrew (Zn, Pb, Ag), Canalask (Ni), Curie (U), Indian River (Au), and Yukon Olympic (Cu, Au) projects, to name a few. In the past five years, together these projects have accounted for total exploration expenditures of nearly \$4 million of which over \$3 million was spent in Yukon.

Regardless of what ‘yardstick’ is used to measure the successes of YMIP and other similar programs, these programs are continuing to result in grassroots discoveries of new mineral occurrences. Many of these discoveries, which develop into viable early stage projects, are now beginning to attract the attention of upper tier junior and major mining companies.

Over the past few years, grassroots exploration has consistently been identified as lacking in many jurisdictions.

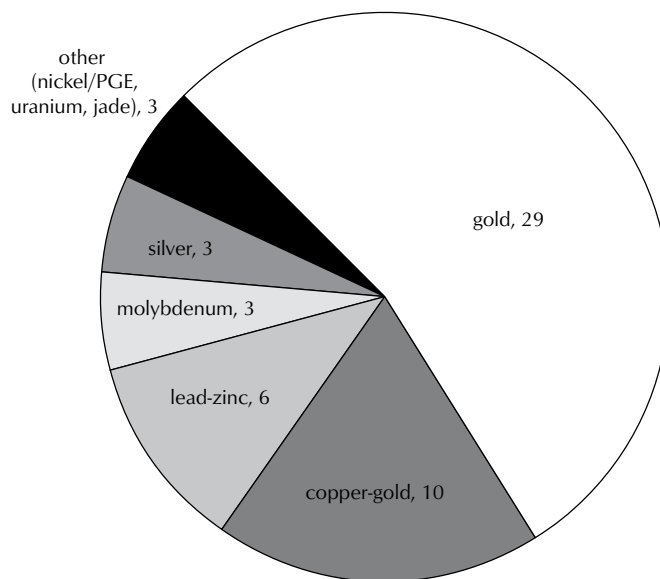


Figure 1. Number of 2005 Yukon Mining Incentives Program projects targeting various commodities.

¹steve.traynor@gov.yk.ca

As mining companies exhaust their current project inventories, it is likely that the need for new projects will increasingly be filled by the generative capacity of mining incentive programs such as YMIP.

RÉSUMÉ

Le Programme d'encouragement des activités minières du Yukon (PEAMY) a reçu 75 demandes de financement cette année. Les accords de contribution ont permis à 63 demandeurs d'obtenir 1 009 000 \$ au total. Parmi les demandes approuvées, 12 ont obtenu un soutien dans le cadre des programmes d'exploration primaire et de prospection, 12 dans le cadre du programme régional d'exploration de régions sous-explorées et 39 dans le cadre du programme d'évaluation de cibles.

La tendance constamment à la hausse du prix de l'or, combinée au doublement du prix du cuivre au cours des deux dernières années, a suscité la majeure partie des activités d'exploration au Yukon et justifié la plupart des octrois dans le cadre du PEAMY concernant ces deux produits de base. Au nombre des faits saillants rapportés pour cette année, on compte déjà la signature de quelques ententes d'options, une augmentation notable des dépenses engagées pour l'évaluation de nouvelles occurrences et une augmentation correspondante des jalonnements de concessions minières en rapport direct avec ces activités. Une analyse plus poussée de cette tendance indique que la récente création du programme régional, conçu pour évaluer le potentiel de régions sous-explorées du Yukon, donne lieu à d'importantes découvertes.

GOVERNMENT

Yukon Geological Survey

Grant Abbott and staff
Yukon Geological Survey

Overview	51
Projects	53
Programs.....	56
Information management and distribution.....	57
2005 publications and maps	60

La Commission géologique du Yukon

Grant Abbott et Maurice Colpron
La Commission géologique du Yukon

Aperçu	67
Travaux sur le terrain	68
Diffusion de l'information.....	69

Robert E. Leckie Awards for Outstanding Reclamation Practices

Judy St. Amand
Mining Lands, Energy, Mines and Resources

Quartz Reclamation Practices Award.....	71
Placer Reclamation Practices Award.....	73
Résumé.....	75

Yukon Geological Survey

Grant Abbott¹ and staff

Abbott, J.G. and staff, 2006. Yukon Geological Survey. *In: Yukon Exploration and Geology 2005*, D.S. Emond, G.D. Bradshaw, L.L. Lewis and L.H. Weston (eds.), Yukon Geological Survey, p. 51-66.

OVERVIEW

The Yukon Geological Survey (YGS; Fig. 1) took a significant step forward in its evolution and development when, in September of this year, it became a Directorate within the Oil, Gas and Minerals Division of the Department of Energy, Mines and Resources. YGS is no longer part of the Mineral Resources Division and now has an expanded mandate to provide information to support exploration, development and management of not only mineral resources, but also oil and gas and to a lesser extent, other resources such as forests. YGS is currently being reorganized to effectively meet its new responsibility for both a higher level of management and a wider mandate. YGS is now divided into Technical Services, Mineral Services, Regional Geology, and Mineral and Hydrocarbon Assessments (Fig. 2). As an interim step, Don Murphy has been appointed acting manager of Regional Geology and Craig Hart has been appointed acting manager of Technical and Mineral



Figure 1. Yukon Geological Survey staff from left to right: Julie Hunt, Amy Tizzard (student), Mike Burke, Steve Israel, Olwyn Bruce, Steve Traynor, Lee Pigage, Erin Trochim (student), Charlie Roots, Don Murphy, Lara Lewis, Craig Hart, Geoff Bradshaw, Leyla Weston, Jeff Bond, Rod Hill, Maurice Colpron, Kelly Coventry, Diane Emond, Panya Lipovsky, Ali Wagner, Grant Lowey, Robert Deklerk, Amy Stuart, John Mair, Bill LeBarge, Grant Abbott, Karen Pelletier.

¹grant.abbott@gov.yk.ca

Services. Other functions report to Grant Abbott, who has been appointed acting director. Rod Hill remains as operations manager.

The past year also saw a number of staff changes. We are pleased to welcome Tammy Allen and Tiffany Fraser to YGS. They are filling two petroleum assessment geologist positions provided by the Oil and Gas Branch. Ken Galambos is on a temporary assignment with the Department of Economic Development until March 31, 2006. Steve Traynor is taking his place as Yukon Mining Incentives Program (YMIP) coordinator. Jo-Anne van Randen is filling in for Steve as economic geologist. Amy Stuart is back with us on a short-term assignment as GIS technician. Monique Raitchey is on temporary assignment with another department until the fall of 2006. She is being ably replaced as office manager by Kelly Coventry. We were also fortunate to have John Mair with us for part of the year on a post doctoral fellowship from the Mineral Deposit Research unit at the University of British Columbia. Congratulations to Craig Hart for completing his PhD thesis at the University of

Western Australia in Perth, and for winning both the Julian Boldy Award for one of the three best economic geology presentations at the annual meeting of the Geological Association of Canada, and a service award for his years of work as editor of GEOLOG, the Association newsletter. Julie Hunt is also to be congratulated for completing her PhD thesis at James Cook University in Townsville, Australia.

YGS continued to enjoy stable core funding, but a department-wide shortfall in salary dollars forced the elimination of one vacant GIS technician position. We hope to reallocate resources to fill this position in the New Year. We did suffer from a shortfall in short-term funding with the winding down of the DIAND (Indian and Northern Affairs Canada) Knowledge and Innovation Fund and NRCan Targeted Geoscience Initiative, but more than made up for it with funding for geophysical surveys from the new DIAND Northern Economic Development program. Although the renewed TGI-3 was not available to Yukon, and the NRCan Cooperative Geological Mapping Strategy was not funded by the

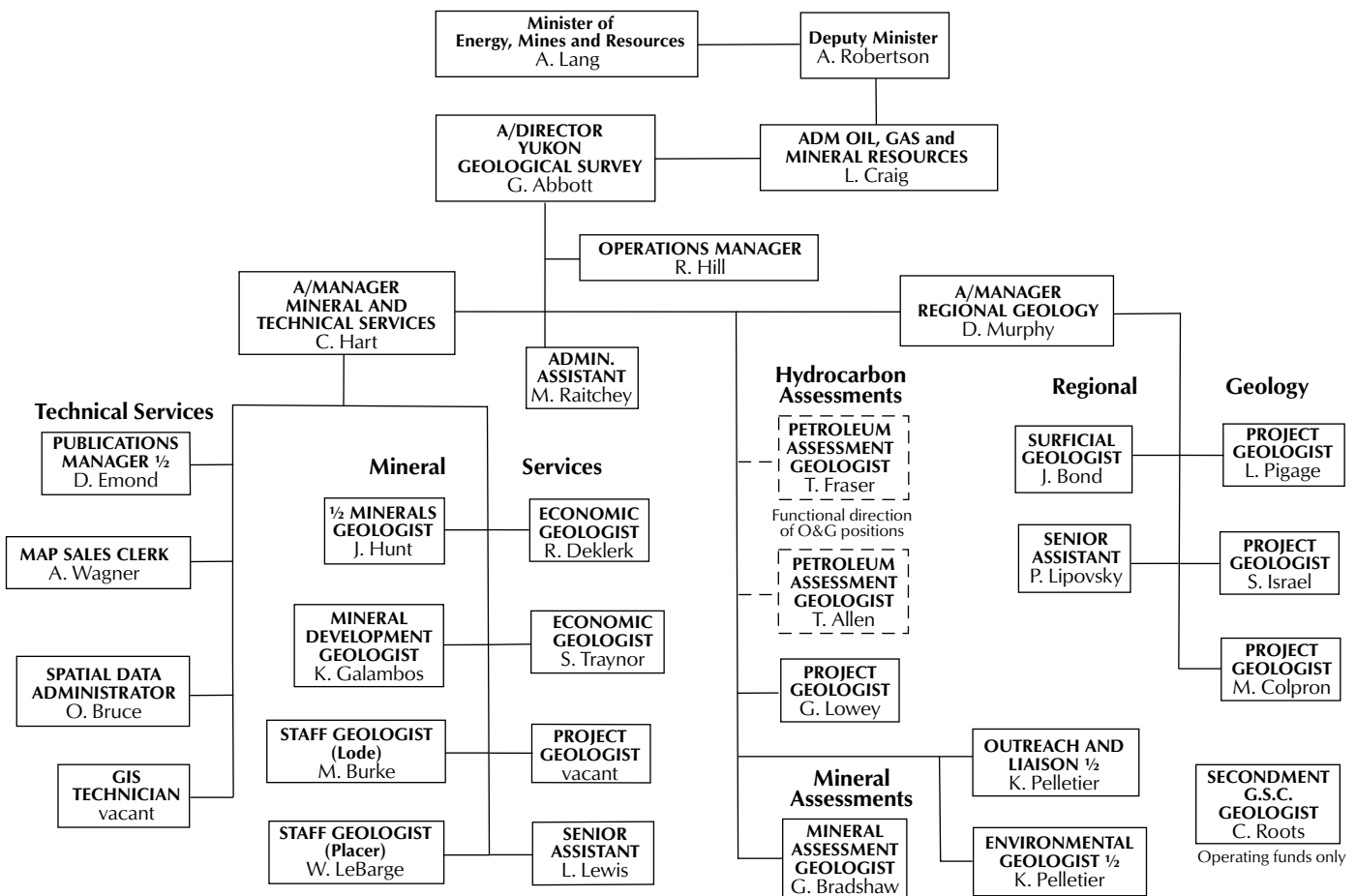


Figure 2. Yukon Geological Survey organization chart.

support hydrocarbon development and to meet increased demands for baseline data to address environmental and development issues while continuing to support our primary client, the mineral industry. Projects included 1:50 000-scale bedrock mapping, mineral deposit studies, surficial studies and mapping, regional stream sediment geochemistry, and topical geology studies. In addition, several office-based projects were undertaken to advance the Yukon Geoscience database.

BEDROCK MAPPING

1. Lee Pigage continued work in southeast Yukon near Toobally Lakes, where studies last year revealed significant new information on lower Paleozoic structure and stratigraphy, with implications for our understanding of the mineral potential of southeast Selwyn Basin.
2. Don Murphy continued work in Watson Lake map area, outlining the belts of volcanic rocks in Yukon-Tanana Terrane that host volcanogenic massive sulphide (VMS) deposits in the Finlayson Lake district, and determining both the internal structure of the terrane and its relationships to Slide Mountain Terrane and the rocks of the North American continental margin.
3. Maurice Colpron mapped in the Livingstone Creek area, where a lode source for gold placers in the area has yet to be found. This work builds on previous studies of Yukon-Tanana Terrane farther north and will help to set the stage for a future mapping program immediately to the west in the northern Whitehorse Trough.
4. Steve Israel continued mapping in the Kluane Ranges to better define the setting of magmatic copper- nickel- platinum group element deposits like Wellgreen. This project is also investigating the possibility that Windy Craggy stratigraphy occurs in the project area by focusing on the relationship between Alexander and Wrangellia and the Triassic volcanic successions found within both terranes. A secondary study of neotectonics within and surrounding the Alaska Highway corridor is also underway in partnership with the US Geological Survey.

MINERAL DEPOSIT STUDIES

1. Craig Hart and Lara Lewis continued to gather data on tungsten and beryl properties for future compilations. Fieldwork in the Hyland River area concentrated on the numerous gold properties in this undermapped area that appear to be structurally controlled rather than intrusion-related.
2. Jim Mortensen (UBC) and Bill LeBarge are studying trace element characteristics of placer gold in the Klondike to identify distinct populations and potential lode sources.
3. John Mair (MDRU/YGS), a post-doctoral fellow from Australia, is developing a database of the lithological, geochemical and isotopic characteristics of Cretaceous igneous rocks in the Yukon to help to differentiate mineralized plutons from unmineralized ones.
4. Julie Hunt continued her studies of iron oxide-copper-gold occurrences associated with the Wernecke Breccias. This work is expanding on earlier research that identified lithological, structural and fluid compositional influences on mineralization in the Wernecke Mountains with a focus on uranium.
5. Jake Hanley (U. of Toronto) with partial support from YGS is beginning a post-doctoral study at the University of Toronto on the evolution and generation of magmatic fluids and their relationship to gold mineralization.

WHITEHORSE TROUGH OIL AND GAS POTENTIAL PROJECT

1. Grant Lowey continued studies of the sedimentology and stratigraphy of the Laberge Group and Tantalus Formation.
2. Darrel Long (Laurentian U.) continued studies of the Lewes River Group and Tantalus Formation.
3. Steve Piercey (Laurentian U.) is studying the chemistry and origin of volcanic assemblages in the Whitehorse Trough.
4. Amy Tizzard (U. of Victoria) is nearing completion of her M.Sc. thesis on the tectonic evolution of the western margin of Stikinia.
5. The Geological Survey of Canada/Yukon Geological Survey seismic survey across northern Whitehorse Trough is now processed and results will be published in various publications over the next year.

SURFICIAL STUDIES

1. Bill LeBarge visited active placer mining operations throughout the Yukon to sample pay gravel and heavy minerals, complete stratigraphic descriptions, and update the placer database. Ongoing studies by Bill, coordinated with Mark Nowosad of Client Services and Inspections, will further define the relationship between water quality and placer sediment on the Klondike, Indian, McQuesten, and Sixty Mile rivers and put the information into a geological context.
2. Erin Trochim and Panya Lipovsky, in partnership with the GSC, began compilation of Yukon Department of Highways borehole data from the Alaska Highway corridor as part of a national permafrost database compilation. This data will assist with development of predictive models for permafrost distribution and allow testing of geophysical techniques for detecting permafrost.
3. Jeff Bond began a study of element distribution patterns in soil profiles on the Lone Star, Clip and Lucky Joe properties. This project will aid understanding of how to interpret soil geochemical data obtained from the unglaciated terrain of west-central Yukon.
4. Brent Ward (Simon Fraser U.) in collaboration with Jeff Bond and John Gosse (Dalhousie University) sampled boulders for cosmogenic dating in the Aishihik Lake area in an attempt to determine the age of the Reid Glaciation. This information is essential to developing a clear understanding of placer deposit evolution in west-central Yukon. This study also addresses broader questions pertaining to northwestern North America's climate history.
5. Jeff Bond began a glacial history reconstruction project for the Big Salmon Range in order to describe the ice-flow history for the McConnell glaciation. This will better enable mineral exploration companies to trace float and soil anomalies to their sources, and also provide insights into placer potential for the Big Salmon Range.
6. Panya Lipovsky monitored an active permafrost thaw-related landslide near Carmacks. She also monitored turbidity levels in the sediment-laden creek issuing from the landslide, which drains into an important salmon spawning ground.
7. Panya Lipovsky collaborated with Antoni Lewkowicz (U. of Ottawa) on studies documenting the effect of extensive recent forest fires on slope stability in areas underlain by permafrost. Large numbers of active-layer detachment slides have already increased sedimentation into drainages surrounding Dawson and could impact efforts to monitor the effects of placer mining on water quality. Dr. Lewkowicz is also studying the origin and dynamics of thermokarst lakes and palsen in the Wolf Creek watershed and developing new permafrost mapping techniques in southwest Yukon.
8. Panya Lipovsky recently completed a 1:50 000-scale surficial map at Watson Lake as a contribution to a Department of Environment (Government of Yukon) project to develop standards for a biophysical mapping framework for southeast Yukon. Biophysical mapping is an important planning tool that integrates physical and biological parameters to allow systematic classification of land for forest management and other activities.

TOPICAL STUDIES

1. Dejan Milidragovic under the direction of Dr. Derek Thorkelson (Simon Fraser U.) began a petrologic study of lamprophyre dykes in the Wernecke Mountains.
2. Luke Beranek (UBC) under the direction of Dr. Jim Mortensen began a doctoral study of Triassic sedimentary overlap assemblages in central Yukon to better understand the timing and nature of terrane accretion in the Canadian Cordillera.

REGIONAL STREAM GEOCHEMISTRY

1. GSC, in collaboration with Geoff Bradshaw, completed a survey in north Yukon, west of Fishing Branch Territorial Park, to assist with development of the North Yukon Regional Land Use Plan
2. GSC in collaboration with Geoff Bradshaw completed a survey of the Flat River map area, south of the Cantung mine. This area has known high potential for tungsten and gold.

The results of both surveys will be released in early summer of 2006.

REGIONAL AEROMAGNETIC SURVEYS

Funding was awarded by DIAND under the Strategic Investments for Northern Economic Development Program (SINED) for Aeromagnetic surveys in the Wernecke/Mackenzie Mountains (1) and Eagle Plains area (2). The surveys are expected to be flown early in 2006.

MINERAL/OIL AND GAS ASSESSMENTS

Geoff Bradshaw and Lee Pigage are participating in regional land use planning for (1) North Yukon and (2) the Peel River watershed to address mineral and oil and gas potential, respectively. Geoff carried out regional mineral assessments that included field work in both areas to better understand mineral potential. Lee helped to interpret existing oil and gas assessments. The North Yukon Planning Commission is aiming for a draft plan by summer of 2006, whereas the Peel Planning Commission is in the early stage of collecting baseline data.

PROGRAMS

MINING AND PETROLEUM ENVIRONMENT RESEARCH GROUP (MPERG)*

In early 2005, the group expanded its mandate beyond mining to include environmental research in support of the petroleum industry and changed its name to reflect this partnership. Administration of the Mining and Petroleum Environmental Research Group (MPERG) is done by Karen Pelletier. Six studies were approved for funding for 2005/06. A Post-Fire Evaluation of the Bioengineering Trials at Noname Creek, previously funded by MPERG, was undertaken by Laberge Environmental Services. Following extensive local forest fires in 2004, increased surface runoff was anticipated on the permafrost slope which characterizes the area, providing opportunity to continue field monitoring of the erosion and to optimize the bioengineering applications already in place. Laberge Environmental Services also began a new bioengineering study on Gold Run Creek in the Klondike area. This study will examine bioengineering techniques that aim to mitigate large-magnitude disturbances in permafrost areas that are easily accessed by local miners, and prove that reclamation and erosion control can be accomplished using low-maintenance technology at relatively little expense. The Klondike Placer Miners' Association received

funding to develop a protocol for the identification of physical constraints of settling ponds in order to assist placer miners and regulators operating under the new placer regime. T. Lewkowicz from the University of Ottawa initiated a multi-faceted study on Permafrost distribution and dynamics in the Yukon, undertaken by a group of M.Sc. students. The study includes four projects that relate to the response of the permafrost landscape to climate change. These have applications in enhancing knowledge on the distribution of permafrost in the Yukon. This will be relevant to linear infrastructure development, such as the proposed Alaska Highway Gas Pipeline. A. Clark and T. Hutchinson of Trent University completed a three-year M.Sc. study, previously funded by MPERG, on Enhancing Natural Succession on Yukon Mine Tailings Sites and were awarded further funding to continue and expand the project. The study was initiated in 2003 at the Mount Skukum, United Keno Hill, and Wellgreen mine sites, with the overall objective to examine site-specific successional trajectories and to direct the succession pathways to obtain long-term, low-input solutions. Ducks Unlimited Canada received funding to study waterfowl moulting and fall staging in the Turner Lakes complex on the Peel Plateau. The objective is to gather information about the use of the Turner Lakes wetlands by moulting and staging water birds in the summer and fall. The information gathered will provide some environmental information for mitigating oil and gas activities during key water bird seasons, and will provide ecological values for developing a long-term management plan for the wetlands, as part of the Peel River watershed land-use planning.

YUKON MINING INCENTIVES PROGRAM (YMIP)

The Yukon Mining Incentives Program is currently administered by Steve Traynor. This year, funding was offered to 63 of 75 applications for a total of \$1,009,000. Twelve of the successful applications were in the Grassroots-Prospecting, 12 in the Focused Regional and 39 in the Target Evaluation modules. Eighty-four percent of these applicants were Yukon-based individuals or companies.

The continuing trend of increasing gold prices, combined with copper prices that have doubled in the past two years, has resulted in high levels of exploration targeting these two commodities. This trend mirrored the focus of 39 of the 54 exploration projects which preceded this year and included 10 applicants who explored for alluvial gold. Six projects explored for lead-zinc, three for molybdenum, three for silver and three for uranium and other commodities.

*Previously, Mining Environment Research Group (MERC)

LIAISON TO INDUSTRY, FIRST NATIONS AND THE PUBLIC

YGS recognizes the importance of effectively communicating information on the geology and mineral and energy resources of the Yukon to a broad audience that includes industry, resource managers, First Nations and the general public. We are continuing to focus more attention on developing strategies and products that meet these needs.

Mike Burke and Bill LeBarge, our main links to the exploration industry, continued to monitor Yukon hard-rock and placer mining and mineral exploration activity, visit active properties, review reports for assessment credit, and maintain the assessment report library.

Karen Pelletier, Charlie Roots and other YGS staff continue to make presentations in the schools and conduct field trips in the communities. New products developed this year to increase public awareness of the geology and mineral resources of the Yukon include an interpretive guide to the Whitehorse Copper Belt by Danièle Héon; a geological map and interpretive display of Tombstone Park by Charlie Roots; and a geological map of southwest Yukon with emphasis on the Kluane Ranges and Kluane Park in partnership with the Geological Survey of Canada.

Karen Pelletier continues to review Mining Land Use and Water License applications, and monitor reclaimed sites to document the effectiveness of mitigation practices. Karen also represents YGS on several committees which sponsor environmental research that involves geology. Karen has also been involved in developing a best practices guide for reclamation of placer mines.

INFORMATION MANAGEMENT AND DISTRIBUTION

With the increasing volume of information generated by YGS and others, and rapidly evolving digital technology, the Survey has placed considerable effort into making geological information more accessible. A large part of our effort has gone into developing and maintaining key databases and making all of our information internet-accessible. The extent of coverage of bedrock and surficial maps, regional geochemistry and geophysics are summarized in Figure 4. Ongoing activities include support for the H.S. Bostock Core Library (Range Road) and the Energy, Mines and Resources (EMR) library (Elijah Smith Building).

DATABASES

With new reporting requirements to securities regulators, widely recognized mineral deposit models are becoming increasingly important. In cooperation with the British Columbia Geological Survey, Anna Fonseca and Geoff Bradshaw have adapted the British Columbia Geological Survey Mineral Deposit profiles to the Yukon. These models are now incorporated into Yukon MINFILE and published separately as Open File 2005-5.

Yukon MINFILE, the Yukon's mineral occurrence database, is maintained by Robert Deklerk and Steve Traynor. An update was released in November, 2005. The database now contains 2612 records, of which more than 500 have been revised, and is complete to the end of 2004. All mineral occurrences are now assigned to a deposit model. Reserve tables have been completely revised and updated to match, as closely as possible, the Canadian Institute of Mining Standards for Reporting Mineral Resources and Reserves. All known assessment reports are now cited for each occurrence. In the past, some reports were not listed in an occurrence's reference field due to confidentiality rules in effect at that time.

The Yukon Placer Database, compiled under the direction of Bill LeBarge, was updated in May of 2005. The database is in Microsoft Access 2000 format and is a comprehensive record of the geology and history of Yukon placer mining. The database contains descriptions of 456 streams and rivers, and 1430 associated placer occurrences, of which 238 were updated for this version. It also includes location maps in Portable Document Format (PDF). A new release is planned for spring 2006 which will include detailed updated information from placer mining activity between 2003 and 2005.

The Yukon GEOPROCESS File, under the direction of Diane Emond, is an inventory of information on geological processes and terrain hazards. It includes 1:250 000-scale maps showing permafrost, landslides, recent volcanic rocks, structural geology, and seismic events, and also includes references and summaries of bedrock and surficial geology. The GEOPROCESS File is intended as a planning aid for development activities and is available for most areas south of 66° latitude. The maps are now standardized in colour, and available on a single compact disk. Maps with text are in AutoCAD 2000 and PDF formats.

The Yukon Digital Geology compilation was updated in 2003 by Steve Gordey and Andrew Makepeace of the Geological Survey of Canada, with funding from YGS. It

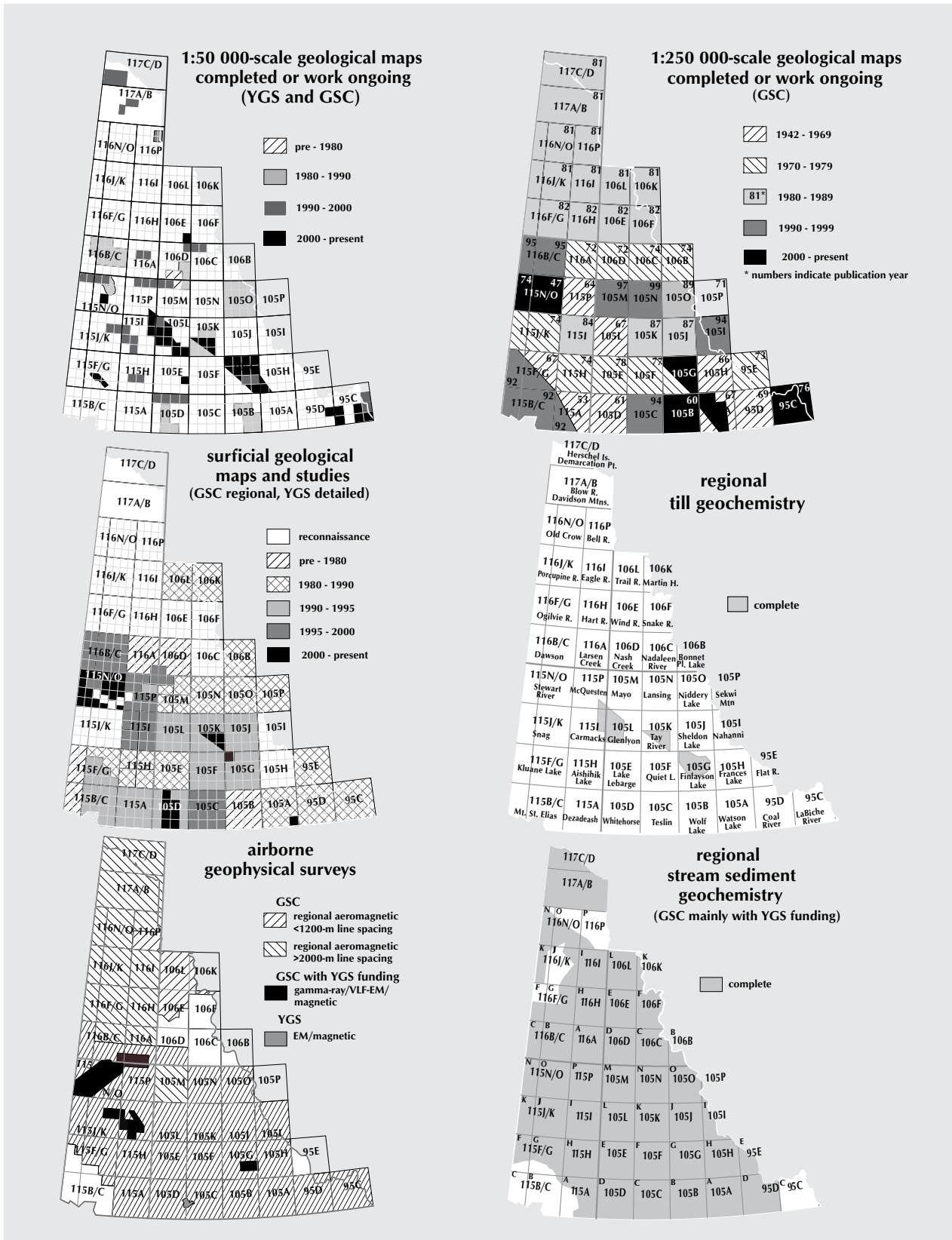


Figure 4. Summary of available geological maps, and regional geochemical and geophysical surveys in the Yukon.

includes syntheses of bedrock geology and glacial limits, compilations of geochronology, paleontology and mineral occurrences, and a compendium of aeromagnetic images, as well as an oil and gas well database. All are now available on CD-ROM. Bedrock geology and glacial limit paper maps are also available at 1:1 000 000 scale.

The Yukon Regional Geochemical Database 2003, compiled by Danièle Héon, contains all of the available digital data for regional stream sediment surveys that have been gathered in the Yukon under the Geological Survey of Canada's National Geochemical Reconnaissance Program. It is available on CD-ROM in Microsoft Excel 2000 format and in ESRI ArcView Shapefile format. The database has been enhanced this year through a contract with Georeference Online. Multi-element anomaly clusters were generated using Minematch software and matched with mineral deposit models. This exercise was essentially the same as one undertaken on the British Columbia stream geochemical database through the Rocks to Riches Program. Results are now available online through the YGS Map Gallery.

The YukonAge Database, compiled by Katrin Breitsprecher and Jim Mortensen at the University of British Columbia with funding from YGS, was updated in 2004. It can be viewed online at the YGS Map Gallery in a version modified by Mike Villeneuve and Linda Richard of the Geological Survey of Canada. The database now contains 1556 age determinations derived from 1166 rock samples from the Yukon Territory. It is available in both Microsoft Access 2000 format and as a flat file in Microsoft Excel 2000 format so that the data may be viewed without Microsoft Access.

The Yukon Geoscience Publications Database, originally compiled by Lara Lewis and Diane Emond, is current to 2005 and contains more than 5000 references to papers on Yukon geology and mineral deposits, including YGS publications. A completely up-to-date searchable version is now available on our website.

This year, YGS is continuing to digitize the backlog of assessment reports. By February 2006, the entire collection of more than 5000 reports will be in PDF format and accessible over the internet. In addition, we have acquired exploration records from the various companies that owned the Faro District. This acquisition includes both records of the Faro District, as well as outside projects. Most of the records are now available for viewing.

H. S. BOSTOCK CORE LIBRARY

Mike Burke and Ken Galambos maintain the H.S. Bostock Core Library. The facility contains about 128 000 m of diamond drill core from about 200 Yukon mineral occurrences. Confidentiality of material is determined on the same basis as mineral assessment reports. Confidential core can be viewed with a letter of release from the owner. Rock saws and other rock preparation equipment are available to the public.

EMR LIBRARY

The EMR library in the Elijah Smith Building is an invaluable resource that is available to the public, but often overlooked. It is Yukon's largest scientific library and includes collections that, prior to devolution, belonged to Indian and Northern Affairs Canada and the Department of Energy, Mines and Resources, Yukon Government. The library houses Yukon assessment reports, maps (including geological, topographical and aeromagnetic), and aerial photographs. It contains most geological journals and a good selection of references on general geology, Yukon geology and economic geology. The library is also the point of contact for access to Faro exploration records, which were recently acquired by YGS. In addition to geological information, the library also has books, reports and journals for the following subjects: oil and gas, forestry, agriculture and energy.

INFORMATION DISTRIBUTION

YGS distributes information in three formats: 1) paper maps and reports are sold and distributed through our Geoscience Information and Sales Office; 2) many recent publications and databases are available in digital format at much lower prices than for paper copies; and 3) most of our publications are available as PDF files on our website (www.geology.gov.yk.ca), free of charge. A catalogue of assessment reports is also available online (<http://www.emr.gov.yk.ca/library>).

We are pleased to make spatial data available through the Map Gallery interactive map server, which can be accessed through the YGS website. We are continuing to improve the Map Gallery. Users are encouraged to provide feedback and suggest improvements.

Hard copies of YGS publications are available at the following address:

Geoscience Information and Sales
c/o Whitehorse Mining Recorder
102-300 Main Street (Elijah Smith Building)
P.O. Box 2703 (K102)
Whitehorse, Yukon Y1A 2C6

Ph. (867) 667-5200
Fax (867) 667-5150
E-mail: geosales@gov.yk.ca

To access publications and to learn more about the Yukon Geological Survey visit our website at: <http://www.geology.gov.yk.ca> or contact us directly:

Grant Abbott, A/Director
Yukon Geological Survey
2099 Second Avenue
P.O. Box 2703 (K10)
Whitehorse, Yukon Y1A 2C6

Ph. (867) 667-3200
E-mail: grant.abbott@gov.yk.ca

Rod Hill, Manager
Yukon Geological Survey
2099 Second Avenue
P.O. Box 2703 (K10)
Whitehorse, Yukon Y1A 2C6

Ph. (867) 667-5384
E-mail: rod.hill@gov.yk.ca

To access the EMR Library:
Website: www.emr.gov.yk.ca/library
Ph.: (867) 667-3111
E-mail: emrlibrary@gov.yk.ca

or drop into Room 335-300 Main Street,
Elijah Smith Building, Whitehorse.

2005 PUBLICATIONS AND MAPS

YGS OPEN FILES

- Abbott, J.G. (ed.), 2005. Yukon Geoscience Needs: Results of the third Yukon Geoscience Planning Workshop. Yukon Geological Survey, Open File 2005-4, 55 p.
- Colpron, M., 2005. Geological map of Livingstone Creek area (NTS 105E/8), Yukon (1:50 000 scale). Yukon Geological Survey, Open File 2005-9.
- Fonseca, A. and Bradshaw, G., 2005. Yukon Mineral Deposit Profiles. Yukon Geological Survey, Open File 2005-5.
- Israel, S., Tizzard, A. and Major, J., 2005. Geological map of the Duke River area (parts of NTS 115G/2,3,5,6,7), Yukon (1:50 000 scale). Yukon Geological Survey, Open File 2005-11.
- Kennedy, K., 2005. Surficial Geology of Seagull Creek (Parts of NTS 105F/10 and 7), Yukon. Yukon Geological Survey, Open File 2005-1, 1:50 000 scale.
- Lipovsky, P.S. and McKenna, K., 2005. Local Scale Biophysical Mapping for Integrated Resource Management, Watson Lake (NTS 105A/2), Yukon. Yukon Geological Survey, Open File 2005-6 (includes report, 2 maps (Open Files 2005-7 and 8) and CD-ROM with digital files (Open File 2005-6(D))).
- Lipovsky, P.S., McKenna, K. and Huscroft, C.A., 2005. Surficial geology of Watson Lake (NTS 105A/2), Yukon (1:50 000 scale). Yukon Geological Survey, Open File 2005-7.
- McKenna, K., Lipovsky, P.S. and Huscroft, C.A., 2005. Preliminary biophysical map of Watson Lake area (NTS 105A/2), Yukon (1:50 000 scale). Yukon Geological Survey, Open File 2005-8.
- Mortensen, J.K. and Murphy, D.C. (compilers), 2005. Bedrock geological map of part of Watson Lake area (all or part of NTS 105A/2,3,5,6,7,10,11,12,13,14), southeastern Yukon (1:150 000 scale). Yukon Geological Survey, Open File 2005-10.
- Osadetz, K.G., Chen Z. and Bird T.D., 2005. Petroleum Resource Assessment, Eagle Plain Basin and Environs, Yukon Territory, Canada. Yukon Geological Survey, Open File 2005-2; Geological Survey of Canada, Open File 4922, 88 p.

Osadetz, K.G., MacLean B.C., Morrow D.W., Dixon J. and Hannigan P.K., 2005. Petroleum Resource Assessment, Peel Plateau and Plain, Yukon Territory, Canada. Yukon Geological Survey, Open File 2005-3; Geological Survey of Canada, Open File 4841, 76 p.

YGS GEOSCIENCE MAPS

Bond, J., Morison, S. and McKenna, K., 2005. Surficial Geology of Carcross (NTS 105D/2), Yukon (1:50 000 scale). Yukon Geological Survey, Geoscience Map 2005-2.

Bond, J., Morison, S. and McKenna, K., 2005. Surficial Geology of Fenwick Creek (NTS 105D/3), Yukon (1:50 000 scale). Yukon Geological Survey, Geoscience Map 2005-3.

Bond, J., Morison, S. and McKenna, K., 2005. Surficial Geology of Alligator Lake (NTS 105D/6), Yukon (1:50 000 scale). Yukon Geological Survey, Geoscience Map 2005-4.

Bond, J., Morison, S. and McKenna, K., 2005. Surficial Geology of Robinson (NTS 105D/7), Yukon (1:50 000 scale). Yukon Geological Survey, Geoscience Map 2005-5.

Bond, J., Morison, S. and McKenna, K., 2005. Surficial Geology of MacRae (NTS 105D/10), Yukon (1:50 000 scale). Yukon Geological Survey, Geoscience Map 2005-6.

Bond, J., Morison, S. and McKenna, K., 2005. Surficial Geology of Whitehorse (NTS 105D/11), Yukon (1:50 000 scale). Yukon Geological Survey, Geoscience Map 2005-7.

Bond, J., Morison, S. and McKenna, K., 2005. Surficial Geology of Upper Laberge (NTS 105D/14), Yukon (1:50 000 scale). Yukon Geological Survey, Geoscience Map 2005-8.

Devine, F., Murphy, D.C., Carr, S.D., Kennedy, R. and Tizzard, A., 2005. Geological Map of the southern Campbell Range (NTS 105H/3 SW), southeastern Yukon (1:20 000 scale). Yukon Geological Survey, Geoscience Map 2005-1.

YGS DATABASES

Deklerk, R. and Traynor, S. (compilers), 2005. Yukon MINFILE 2005 – A database of mineral occurrences. Yukon Geological Survey, CD-ROM.

LeBarge, W.P. and Coates J. (compilers), 2005. Yukon Placer Database 2005 – Geology and mining activity of placer occurrences. Yukon Geological Survey, CD-ROM.

ANNUAL REPORTS

Traynor, S. (compiler), 2005. Yukon Mineral Deposits 2005. Yukon Geological Survey, 16 p.

Traynor, S. (compiler), 2005. Yukon Mineral Property Update 2004. Yukon Geological Survey, 81 p.

YGS CONTRIBUTIONS TO OUTSIDE PUBLICATIONS

Colpron, M., Gladwin, K., Johnston, S.T., Mortensen, J.K. and Gehrels, G.E., 2005. Geology and juxtaposition history of Yukon-Tanana, Slide Mountain and Cassiar terranes in the Glenlyon area of central Yukon. *Canadian Journal of Earth Sciences*, vol. 42, p. 1431-1448.

Goldfarb, R.J., Baker, T., Dubé, B., Groves, D.I., **Hart, C.J.R.** and Gosselin, P., 2005. Distribution, Character, and Genesis of Gold Deposits in Metamorphic Terranes. *Economic Geology 100th Anniversary Volume*, J.W. Hedenquist, J.F.H. Thompson, R.J. Goldfarb and J.P. Richards (eds.).

Groat, L.A., **Hart, C.J.R.**, **Lewis, L.L.** and Neufeld, H., 2005. Emerald and Aquamarine Mineralization in Canada, *Geoscience Canada*, vol. 32, no. 2, p. 17-28.

Hart, C.J.R., Mair, J.L., Goldfarb, R.J. and Groves, D.I., 2005. Source and Redox Controls of Intrusion-Related Metallogeny, Tombstone-Tungsten Belt, Yukon, Canada. *Fifth Hutton Symposium Volume, Transactions of the Royal Society of Edinburgh, Earth Science*, vol. 95, p. 339-356. Also available as Geological Society of America Special Paper 389.

Hunt, J.A., Baker, T. and Thorkelson, D.J., 2005. Regional-scale Proterozoic IOCG-mineralised breccia systems: examples from the Wernecke Mountains, Yukon, Canada. *Mineralium Deposita*, vol. 40, no. 5, p. 492-514.

- Huscroft, C.** and **Lipovsky P.**, 2005. Changement de climat et glissements de terrain dans le corridor de la route de l'Alaska, au Yukon – Climate change and landslides in the Alaska Highway corridor, Yukon. *Meridian, Meridien Spring/Summer*, p. 14-18.
- Laughton, J.R., Thorkelson, D.J., Brideau, M., **Hunt, J.A.** and Marshall, D.D., 2005. Proterozoic orogeny and exhumation of Wernecke Supergroup revealed by vent facies of Wernecke Breccia, Yukon, Canada. *Canadian Journal of Earth Sciences, the Lithoprobe Slave - Northern Cordillera Lithospheric Evolution (SNORCLE) transect*, vol. 42, p. 1033-1044.
- Mao, J., Goldfarb R.J., Wang Y., **Hart, C.J.**, Wang Z. and Yang J., 2005. Late Paleozoic base and precious metal deposits, East Tianshan, Xin-jiang, China: Characteristics and geodynamic setting. *Episodes*, vol. 28, no. 1, p. 23-49.
- McCausland, P.J.A., Symons, D.T.A. and **Hart, C.J.R.**, 2005. Rethinking “Yellowstone in Yukon” and Baja British Columbia: Paleomagnetism of the Late Cretaceous Swede Dome stock, northern Canadian Cordillera. *Journal of Geophysical Research*, vol. 110, B12107, doi:10.1029/2005JB003742, 13 p., online.
- Piercey, S.J., **Murphy D.C.**, Mortensen, J.K. and Creaser R.A., 2004. Mid-Paleozoic initiation of the northern Cordilleran marginal backarc basin: Geologic, geochemical, and neodymium isotope evidence from the oldest mafic magmatic rocks in the Yukon-Tanana terrane, Finlayson Lake district, southeast Yukon, Canada. *Geological Society of America Bulletin*, vol. 116, no. 9, p. 1087–1106.
- Pigage, L.C.** and Mortensen J.K., 2004. Superimposed Neoproterozoic and Early Tertiary alkaline magmatism in the La Biche River area, southeast Yukon Territory. *Bulletin of Canadian Petroleum Geology*, vol. 52, p. 325-342.
- Symons, D.T.A., Harris, M.J., McCausland, P.J.A., Blackburn, W.H. and **Hart, C.J.R.**, 2005. Cenozoic paleomagnetism of the Intermontane and Yukon Tanana terranes, Canadian Cordillera. *Canadian Journal of Earth Sciences, the Lithoprobe Slave – Northern Cordillera Lithospheric Evolution (SNORCLE) transect*, vol. 42, p. 1163-1185.
- Symons, D.T.A., Harris, M.J., McCausland, P.J.A., Blackburn, W.H. and **Hart, C.J.R.**, 2005. Mesozoic-Cenozoic paleomagnetism of the Intermontane and Yukon-Tanana terranes, Canadian Cordillera. *Canadian Journal of Earth Sciences*, vol. 42, p. 1163-1185.
- Thorkelson, D.J., **Abbott, J.G.**, Mortensen, J.K., Creaser, R.A., Villeneuve, M.E., McNicoll, V.J. and Layer, P.W., 2005. Early and Middle Proterozoic evolution of Yukon Canada. *Canadian Journal of Earth Sciences, the Lithoprobe Slave - Northern Cordillera Lithospheric Evolution (SNORCLE) transect*, vol. 42, p. 1045-1071.

YGS ABSTRACTS

- Hart, C.J.R., 2005. Classifying, distinguishing and exploring for intrusion-related gold systems. *GAC-MAC-CSPG-CSSS Joint Meeting, Halifax, Nova Scotia, Abstracts* vol. 30, p. 81.
- Groves, D.I., Mair, J.L., Hart, C.J.R. and Vielreicher, N., 2005. The lithospheric settings of Carlin-type deposits: An important clue to their genetic associations. *Extended Abstract, Geological Society of Nevada*.
- Burke, M., Hart, C.J.R. and Lewis, L.L., 2005. Models for epigenetic gold exploration in the northern Cordilleran Orogen, Yukon, Canada. *In: Mineral Deposit Research, Meeting the Global Challenge*, J.W. Mao and F. Berliet (eds.), extended abstract, SGA Beijing Conference, Beijing, China, p. 525-528.
- Mueller, S.H., Goldfarb, R.J., Hart, C.J.R., Mair, J.L., Marsh, E.E. and Rombach, C.S., 2004. The Tintina Gold Province, Alaska and Yukon – New World-Class Gold Resources and Their Sustainable Development. *PACRIM 2004, AusIMM Conference Proceedings, Adelaide, Australia*, p. 189-198.
- Hart, C.J.R. and Goldfarb, R.J., 2005. Distinguishing intrusion-related from orogenic gold deposits. *2005 New Zealand Minerals Conference Proceedings, Auckland, New Zealand*, p. 125-133.
- Simard, R.-L., Dostal, J. and Colpron, M., 2005. The Little Salmon Formation, northern Canadian Cordillera, Magmatism in an intra-arc rift basin within a Mississippian continental arc system. *GAC-MAC-CSPG-CSSS Joint Meeting, Halifax, Nova Scotia, Abstracts*, vol. 30, p. 177
- Thorkelson, D.J., Abbott J.G., Mortensen, J.K., Creaser, R.A., Villeneuve, M.E., McNicoll, V.J. and Layer, P.W., 2005. Early and Middle Proterozoic evolution of northwestern Laurentia. *GAC-MAC-CSPG-CSSS Joint Meeting, Halifax, Nova Scotia, GAC Abstracts*, vol. 30, p. 193.

YUKON GEOLOGICAL PAPERS OF INTEREST

- Abraham, A.-C., Francis, D. and Polvé, M., 2005. Origin of recent alkaline lavas by lithospheric thinning beneath the northern Canadian Cordillera. *Canadian Journal of Earth Sciences, The Lithoprobe Slave - Northern Cordillera Lithospheric Evolution (SNORCLE) transect* vol. 42, p. 1073-1095.
- Carey, S.K. and Quinton, W.L., 2005. Evaluating runoff generation during summer using hydrometric, stable isotope and hydrochemical methods in a discontinuous permafrost alpine catchment. *Hydrological Processes*, January 2005, vol. 19, Issue 1, p. 95-114.
- Carey, S.K. and Woo, M., 2005. Freezing of subarctic hillslopes, Wolf Creek basin, Yukon, Canada. *Arctic, Antarctic, and Alpine Research*, vol. 37, p. 1-10.
- Cassidy, J.F. and Rogers, G.C., 2004. The M (sub w) 7.9 Denali Fault earthquake of 3 November 2002; felt reports and unusual effects across Western Canada. *Bulletin of the Seismological Society of America*, December 2004, vol. 94, issue 6, part B, p. 53-57.
- Cassidy, J.F., Rogers, G.C. and Ristau, J., 2005. Seismicity in the vicinity of the SNORCLE corridors of the northern Canadian Cordillera. *Canadian Journal of Earth Sciences, The Lithoprobe Slave - Northern Cordillera Lithospheric Evolution (SNORCLE) transect*, vol. 42, p. 1137-1148.
- Clowes, R.M., Hammer, P.T.C., Fernández-Viejo, G. and Welford, J.K., 2005. Lithospheric structure in northwestern Canada from Lithoprobe seismic refraction and related studies: A synthesis. *Canadian Journal of Earth Sciences, The Lithoprobe Slave - Northern Cordillera Lithospheric Evolution (SNORCLE) transect*, vol. 42, p. 1277-1293.
- Cook, F.A., Hall, K.W. and Lynn, C.W., 2005. The edge of northwestern North America at 1.8 Ga. *Canadian Journal of Earth Sciences, The Lithoprobe Slave - Northern Cordillera Lithospheric Evolution (SNORCLE) transect*, vol. 42, p. 983-997.
- Cook, F.A. and Erdmer, P., 2005. An 1800 km cross section of the lithosphere through the northwestern North American plate: lessons from 4.0 billion years of Earth's history. *Canadian Journal of Earth Sciences, The Lithoprobe Slave - Northern Cordillera Lithospheric Evolution (SNORCLE) transect*, vol. 42, p. 1295-1311.
- Creaser, B. and Spence, G., 2005. Crustal structure across the northern Cordillera, Yukon Territory, from seismic wide-angle studies: Omineca Belt to Intermontane Belt. *Canadian Journal of Earth Sciences, The Lithoprobe Slave - Northern Cordillera Lithospheric Evolution (SNORCLE) transect*, vol. 42, p. 1187-1203.
- Day, S.J. and Howell, R.J., 2005. Atypical and typical zinc geochemistry in a carbonate setting, Sä Dena Hes mine, Yukon Territory, Canada. *Geochemistry: Exploration, Environment, Analysis*, vol. 5, p. 255-266.
- Eberl, D.D., 2004. Quantitative mineralogy of the Yukon River system; changes with reach and season, and determining sediment provenance. *American Mineralogist*, December 2004, vol. 89, issue 11-12, p. 1784-1794.
- English, J.M., Johannson, G.G., Johnston, S.T., Mihalynuk, M.G., Fowler, M. and Wight, K.L., 2005. Structure, stratigraphy and petroleum resource potential of the Central Whitehorse Trough, Northern Canadian Cordillera. *Bulletin of Canadian Petroleum Geology*, vol. 53, p. 130-153.
- Hyndman, R.D., Flück, P., Mazzotti, S., Lewis, T.L., Ristau, J. and Leonard, L., 2005. Current tectonics of the northern Canadian Cordillera. *Canadian Journal of Earth Sciences, The Lithoprobe Slave - Northern Cordillera Lithospheric Evolution (SNORCLE) transect*, vol. 42, p. 1117-1136.
- Hynes, G.F. and Dixon, J.M., 2005. Geological mapping and analogue modeling of the Liard, Kotaneelee and Tlogotsho ranges, Northwest Territories. *Bulletin of Canadian Petroleum Geology*, vol. 53, p. 67-83.
- Jones, A.G., Ledo, J., Ferguson, I.J., Farquharson, C., Garcia, X., Grant, N., McNeice, G., Roberts, B., Spratt, J., Wennberg, G., Wolynec, L. and Wu, X., 2005. The electrical resistivity structure of Archean to Tertiary lithosphere along 3200 km of SNORCLE profiles, northwestern Canada. *Canadian Journal of Earth Sciences, The Lithoprobe Slave - Northern Cordillera Lithospheric Evolution (SNORCLE) transect*, vol. 42, p. 1257-1275.
- Jowett, D.M.S. and Schröder-Adams, C.J., 2005. Paleoenvironments and regional stratigraphic framework of the Middle–Upper Albian Lepine Formation in the Liard Basin, Northern Canada, *Bulletin of Canadian Petroleum Geology*, vol. 53, p. 25-50.

- Karunaratne, K.C. and Burn, C.R., 2004. Relations between air and surface temperature in discontinuous permafrost terrain near Mayo, Yukon Territory. *Canadian Journal of Earth Sciences*, vol. 41, p. 1437-1451.
- Kinnard, C. and Lewkowicz, A.G., 2005. Movement, moisture and thermal conditions at a turf-banked solifluction lobe, Kluane Range, Yukon Territory, Canada. *Permafrost and Periglacial Processes*, September 2005, vol. 16, issue 3, p. 261-275.
- Lane, L.S., 2005. Central Foreland NATMAP Project; stratigraphic and structural evolution of the Cordilleran foreland; Part 2. *Bulletin of Canadian Petroleum Geology*, vol. 53, p. 1-3.
- Lantuit, H. and Pollard, W.H., 2005. Temporal stereophotogrammetric analysis of retrogressive thaw slumps on Herschel Island, Yukon Territory. *Natural Hazards and Earth System Sciences NHESS*, vol. 5, issue 3, p. 413-423.
- Orberger, B., Gallien, J.P., Pinti, D.L., Fialin, M., Daudin, L., Grocke, D.R. and Pasava, J., 2005. Nitrogen and carbon partitioning in diagenetic and hydrothermal minerals from Paleozoic black shales, Selwyn Basin, Yukon Territory, Canada. *Chemical Geology*, vol. 218, p. 249-264.
- MacKenzie, J.M., Canil, D., Johnston, S.T., English, J., Mihalynuk, M.G. and Grant, B., 2005. First evidence for ultrahigh-pressure garnet peridotite in the North American Cordillera. *Geology*. February 2005, vol. 33, issue 2, p. 105-108.
- Sack, R.O., 2005. Internally consistent database for sulfides and sulfosalts in the system $\text{Ag}_2\text{S}-\text{Cu}_2\text{S}-\text{ZnS}-\text{FeS}-\text{Sb}_2\text{S}_3-\text{As}_2\text{S}_3$; update. *Geochimica et Cosmochimica Acta*, March 2005, vol. 69, issue 5, p. 1157-1164.
- Schiappa, T.A., Hemmesch, N.T., Spinosa, C. and Nassichuk, W.W., 2005. Cisuralian ammonoid genus *Uraloceras* in North America. *Journal of Paleontology*, March 2005, vol. 79, issue 2, p. 366-377.
- Shapiro, B., Drummond, A.J., Rambaut, A., Wilson, M.C., Sher, A., Pybus, O.G., Gilbert, T.P., Barnes, I., Binladen, J., Willerslev, E., Hansen, A.J., Baryshnikov, G.F., Burns, J.A., Davydov, S., Driver, J.C., Froese, D.G., Harington, C.R., Keddie, G., Kosintsev, P., Kunz, M.L., Martin, L.D., Stephenson, R.O., Storer, J., Tedford, R., Zimov, S. and Cooper, A., 2004. Rise and fall of the Beringian steppe bison. *Science*, vol. 306, p. 1561-1565.
- Snyder, D.B., Roberts, B.J. and Gordey, S.P., 2005. Contrasting seismic characteristics of three major faults in northwestern Canada. *Canadian Journal of Earth Sciences, The Lithoprobe Slave - Northern Cordillera Lithospheric Evolution (SNORCLE) transect*, vol. 42, p. 1223-1237.
- Utting, J., Zonneveld, J.P., MacNaughton, R.B. and Fallas, K.M., 2005. Palynostratigraphy, lithostratigraphy and thermal maturity of the Lower Triassic Toad and Grayling, and Montney formations of western Canada, and comparisons with coeval rocks of the Sverdrup Basin, Nunavut. *Bulletin of Canadian Petroleum Geology*, vol. 53, p. 5-24.
- Zazula, G.D., Froese, D.G., Westgate, J.A., La Farge, C. and Mathewes, R.W., 2005. Paleocology of Beringian "packrat" middens from central Yukon Territory, Canada. *Quaternary Research*, vol. 63, p. 189-198.
- Zhang, S., Pyle, L.J. and Barnes, C.R., 2005. Evolution of the early Paleozoic Cordilleran margin of Laurentia: Tectonic and eustatic events interpreted from sequence stratigraphy and conodont community patterns. *Canadian Journal of Earth Sciences, The Lithoprobe Slave - Northern Cordillera Lithospheric Evolution (SNORCLE) transect*, vol. 42, p. 999-1031.

GSC CONTRIBUTIONS TO YUKON GEOLOGY

- Fallas, K.M., Pigage, L.C. and Lane, L.S. (compilers), 2005. *Geology, La Biche River northwest (95 C/NW), Yukon and Northwest Territories*. Geological Survey of Canada, Open File 5018, 1:100 000-scale map.
- Froese, D.G., 2005. *Surficial geology, Medrick Creek, Yukon Territory (115O/16)*. Geological Survey of Canada, Open File 4593, 1:50 000-scale map.
- Jackson, L.E., Jr., 2005. *Surficial geology, Australia Mountain, Yukon Territory (115O/9)*. Geological Survey of Canada, Open File 4586, 1:50 000-scale map.

- Jackson, L.E., Jr., 2005. Surficial geology, Black Hills Creek, Yukon Territory (115O/7). Geological Survey of Canada, Open File 4584, 1:50 000-scale map.
- Jackson, L.E., Jr., 2005. Surficial geology, Borden Creek, Yukon Territory (115N/10). Geological Survey of Canada, Open File 4578, 1:50 000-scale map.
- Jackson, L.E., Jr., 2005. Surficial geology, Crag Mountain, Yukon Territory (115N/15). Geological Survey of Canada, Open File 4579, 1:50 000-scale map.
- Jackson, L.E., Jr., 2005. Surficial geology, Enchantment Creek, Yukon Territory (115N/16). Geological Survey of Canada, Open File 4580, 1:50 000-scale map.
- Jackson, L.E., Jr., 2005. Surficial geology, Excelsior Creek, Yukon Territory (115O/5). Geological Survey of Canada, Open File 4582, 1:50 000-scale map.
- Jackson, L.E., Jr., 2005. Surficial geology, Flat Creek, Yukon Territory (115O/15). Geological Survey of Canada, Open File 4592, 1:50 000-scale map.
- Jackson, L.E., Jr., 2005. Surficial geology, Garner Creek, Yukon Territory (115O/13). Geological Survey of Canada, Open File 4590, 1:50 000-scale map.
- Jackson, L.E., Jr., 2005. Surficial geology, Grand Forks, Yukon Territory (115O/14). Geological Survey of Canada, Open File 4591, 1:50 000-scale map.
- Jackson, L.E., Jr., 2005. Surficial geology, Granville, Yukon Territory (115O/10). Geological Survey of Canada, Open File 4587, 1:50 000-scale map.
- Jackson, L.E., Jr., 2005. Surficial geology, Ladue River, Yukon Territory (115N/2). Geological Survey of Canada, Open File 4574, 1:50 000-scale map.
- Jackson, L.E., Jr., 2005. Surficial geology, Los Angeles Creek, Yukon Territory (115O/4). Geological Survey of Canada, Open File 4581, 1:50 000-scale map.
- Jackson, L.E., Jr., 2005. Surficial geology, Marion Creek, Yukon Territory (115N/8). Geological Survey of Canada, Open File 4576, 1:50 000-scale map.
- Jackson, L.E., Jr., 2005. Surficial geology, Reindeer Mountain, Yukon Territory (115O/11). Geological Survey of Canada, Open File 4588, 1:50 000-scale map.
- Jackson, L.E., Jr., 2005. Surficial geology, Rice Creek, Yukon Territory (115N/7). Geological Survey of Canada, Open File 4588, 1:50 000-scale map.
- Jackson, L.E., Jr., 2005. Surficial geology, Rosebud Creek, Yukon Territory (115O/8). Geological Survey of Canada, Open File 4585, 1:50 000-scale map.
- Jackson, L.E., Jr., 2005. Surficial geology, Stewart River, Yukon Territory (115O/6). Geological Survey of Canada, Open File 4583, 1:50 000-scale map.
- Jackson, L.E., Jr., Morison, S.R. and Mougeot, C., 2005. Surficial geology, Matson Creek, Yukon Territory (115N/9). Geological Survey of Canada, Open File 4577, 1:50 000-scale map.
- Jackson, L.E., Jr., Morison, S.R. and Mougeot, C., 2005. Surficial geology, Ogilvie, Yukon Territory (115O/12). Geological Survey of Canada, Open File 4589, 1:50 000-scale map.
- Osadetz, K.G., Chen, Z. and Bird, T.D., 2005. Petroleum Resource Assessment, Eagle Plain Basin and Environs, Yukon Territory, Canada. Yukon Geological Survey, Open File 2005-2; Geological Survey of Canada, Open File 4922, 88 p.
- Osadetz, K.G., MacLean B.C., Morrow D.W., Dixon J. and Hannigan P.K., 2005. Petroleum Resource Assessment, Peel Plateau and Plain, Yukon Territory, Canada. Yukon Geological Survey, Open File 2005-3; Geological Survey of Canada, Open File 4841, 76 p.

YUKON THESES

- Hart, C.J.R., 2005. Mid-Cretaceous Magmatic Evolution and Intrusion-related Metallogeny of the Tintina Gold Province, Yukon and Alaska. Unpublished PhD thesis, The University of Western Australia, Perth, Australia, 198 p.
- Hunt, J., 2005. The geology and genesis of iron oxide-copper-gold mineralisation associated with Wernecke Breccia, Yukon, Canada. Unpublished PhD thesis, James Cook University, Australia, 120 p.
- Hynes, G.F., 2004. Geological field mapping and physical analogue modelling of the Liard, Kotaneelee, and Tlogotsho Ranges, southwest Northwest Territories, Canada. Unpublished M.Sc. thesis, Queen's University, Kingston, Ontario, 168 p.
- Livingston, J.M., 2004. Floodbed sedimentology: A new method to reconstruct paleo-ice-jam flood frequency. Unpublished M.Sc. thesis, University of Calgary, Calgary, Alberta, 2004, 159 p.

Ruks, T.W., 2005. Petrology and tectonic significance of potassic feldspar augen granitoids in the Yukon-Tanana Terrane, Stewart River, Yukon Territory. Unpublished M.Sc. thesis, Laurentian University, Sudbury, Ontario, 150 p.

YUKON GEOLOGICAL ABSTRACTS OF INTEREST

Duk-Rodkin, A., Barendregt, R.W. and Froese, D.G., 2005. Yukon and Mackenzie River systems: Glacially diverted drainages resulting from the first Cordilleran glaciation and the last continental ice sheet. GAC-MAC-CSPG-CSSS Joint Meeting, Halifax, Nova Scotia, GAC Abstracts vol. 30, p. 47.

Marsh, E.E., Allan, M.M., Goldfarb, R.J., Jensen, P., Mair, J.L. and Shepherd, T.J., 2005. LA-ICP-MS microanalysis of single fluid inclusions from intrusion-related gold deposits, Tintina gold province, Alaska and Yukon. Geological Society of America Abstracts with Programs, vol. 37, No. 7, p. 501.

Rasmussen, P.E., Edwards, G.C., Schroeder, W.W., Steffen, A., Ausma, S., Dias, G. and El Bilali, L., 2005. Atmospheric mercury fluxes from carbonaceous shales in Yukon Territory. GAC-MAC-CSPG-CSSS Joint Meeting, Halifax, Nova Scotia, GAC Abstracts, vol. 30, p. 163.

Westgate, J.A. and Peece, S.J.A., 2005. Cautionary tale of two tephras: the scientific method eking out errors in the late Cenozoic tephrochronological record of eastern Beringia. Geological Society of America, Abstracts with Programs, vol. 37, no. 7, p. 38.

La Commission géologique du Yukon

Grant Abbott¹ et Maurice Colpron²
Le Service de géologie du Yukon

Abbott, J.G. et Colpron, M., 2006. La Commission géologique du Yukon. *Dans : Yukon Exploration and Geology 2005*, D.S. Emond, G.D. Bradshaw, L.L. Lewis et L.H. Weston (réds.), la Commission géologique du Yukon, p. 67-70.

APERÇU

La commission géologique du Yukon (CGY; Figure 1, p. 51) a fait de grands progrès dans son évolution, lorsqu'en septembre de cette année elle est devenue une Direction au sein de la Division du pétrole, du gaz et des minéraux du ministère de l'Énergie, des Mines et des Ressources (MEMR). La CGY ne fait plus partie de la Division des ressources minérales. Son mandat est maintenant augmenté; elle fournit dorénavant de l'information en support des activités d'exploration, de développement et de gérance, non seulement des ressources minérales, mais aussi des ressources pétrolières et gazières, et de façons plus limitées, d'autres ressources telle que les forêts. La CGY est présentement en cours de réorganisation de façon à mieux répondre à son mandat élargi et à ses plus grandes responsabilités administratives. La CGY est maintenant sous-divisée entre quatre Services : soit les Services techniques, les Services minéraux, la Géologie régionale, et les Services d'évaluation du potentiel minéral et en hydrocarbures (Figure 2, p. 52). Durant cette période de transition, Don Murphy assumera le poste de gérant de la Géologie régionale, et Craig Hart celui de gérant des Services techniques et minéraux. Les autres Services se rapportent directement à Grant Abbott, qui fût nommé directeur intérimaire de la Commission géologique. Rod Hill demeure en charge de la gérance des opérations.

L'année passée fût aussi marquée par de nombreux changements au sein du personnel. La CGY est heureuse d'accueillir Tammy Allen et Tiffany Fraser à titre de géologue d'évaluation du potentiel pétrolier, deux positions contribuées par la Direction du pétrole et du gaz du MEMR. Ken Galambos est temporairement à l'emploi du ministère du Développement économique, jusqu'au 31 mars 2006. Steve Traynor le remplace à titre de coordonnateur du Programme d'encouragement des activités minières du Yukon, alors que Jo-Anne van Randen remplace Steve à titre de géologue économique. Amy Stuart est de retour parmi nous pour un contrat à court terme en tant que technicienne en système d'information géographique, et Monique Raitchey est temporairement à l'emploi d'un autre ministère jusqu'à l'automne 2006; elle est remplacée de façon experte par Kelly Coventry. John Mair, un associé post-doctoral de l'unité de recherche en gîtes minéraux de l'Université de Colombie-Britannique, fût aussi parmi nous pour une partie de l'année. Félicitations à Craig Hart pour avoir complété sa thèse de doctorat à l'Université d'Australie-occidentale de Perth et pour avoir reçu deux prix de l'Association géologique du Canada: le prix Julian Boldy pour une des trois meilleures présentations en géologie économique à la réunion annuelle de l'Association, et un autre prix pour ses années de services en tant qu'éditeur de GEOLOG, le périodique d'information de l'Association. Julie Hunt a elle aussi complétée sa thèse de doctorat à l'Université James Cook en Australie; nous la félicitons!

La CGY continue de recevoir un financement de base stable, quoiqu'un déficit de financement au niveau des salaires à l'échelle du ministère nous a forcé à éliminer une position vacante de

¹grant.abbott@gov.yk.ca

²maurice.colpron@gov.yk.ca

technicien en système d'information géographique. On espère pouvoir redistribuer nos ressources au cours de l'année à venir, afin de rétablir cette position. Nous avons aussi souffert une perte de financement à court terme avec la disparition des Fonds pour le savoir et l'innovation du ministère des Affaires indiennes et du Nord canadien (MAINC) et de l'initiative géoscientifique ciblée du ministère canadien des Ressources naturelles (RNCAN); financement qui fût amplement remplacé par les relevés géophysiques subventionnés par le nouveau programme de développement économique du Nord du MAINC. Bien que la troisième phase du programme d'initiative géoscientifique ciblée de RNCAN n'était pas offerte au Yukon, et que la stratégie de cartographie géologique coopérative de RNCAN n'a pas reçu de financement du gouvernement fédéral, on demeure toutefois optimistes que des nouveaux fonds seront disponibles soit par l'entremise du programme de développement économique du Nord du MAINC ou dans le cadre de la stratégie du Nord du gouvernement du Yukon et du MAINC.

Un comité de liaison technique à la CGY examine nos programmes deux fois par année. Nous remercions le président, Gerry Carlson, et les membres du comité pour leur précieux appui et les conseils constructifs qu'ils nous fournissent. Cette année, Moira Smith et Bernie Kreft ont quittés le comité; ils sont remplacés par Rob Carne et Shawn Ryan, qui sont deux des explorateurs les plus expérimentés au Yukon. Nous attendons avec plaisir leurs conseils experts. Les autres membres du comité sont Al Doherty, Jean Pautler, Forest Pearson, Jim Mortensen, Jim Christie et Greg Lynch.

TRAVAUX SUR LE TERRAIN

La CGY a connue cette année une autre campagne de travaux sur le terrain couronnée de succès avec 24 projets en cours, énumérés ci-dessous et indiqués en Figure 3. Nos travaux furent diversifiés de façon à mieux répondre à notre nouveau mandat de soutien à la mise en valeur des hydrocarbures et à la demande accrue pour les données de base à l'appui de la réglementation dans le domaine de l'environnement et de la gestion des terres, tout en continuant nos projets en support de l'industrie minière. Nos travaux cette année incluent quatre projets de cartographie géologique du substratum rocheux au 1 : 50 000, des études de gisements minéraux, des études et travaux de cartographie des formations superficielles, la géochimie régionale des cours d'eau et des études

géologiques détaillées. De plus, de nombreux projets de bureau avaient pour but l'amélioration de la base de données géoscientifiques du Yukon.

CARTOGRAPHIE DU SUBSTRATUM ROCHEUX

Lee Pigage a poursuivi sa cartographie de la région des lacs Toobally dans le sud-est du Yukon, alors que Don Murphy a étendu sa cartographie des roches du terrane de Yukon-Tanana, les roches hôtes des gisements de sulfures massifs de la région du lac Finlayson, vers le sud dans région du lac Watson. Pour sa part, Maurice Colpron a complété la carte du ruisseau Livingstone, où la source de l'or placérien demeure un mystère. Dans le sud-ouest, Steve Israel poursuit la cartographie des monts Kluane dans le but de mieux définir le mode d'emplacement des gisement de cuivre, nickel, et des éléments du groupe du platine, tel que Wellgreen.

ÉTUDES DE GISEMENTS MINÉRAUX

Craig Hart et Lara Lewis ont poursuivi leurs travaux sur le tungstène et le béryl; une étude de terrain dans la région de la rivière Hyland fût concentrée sur une minéralisation en or dont le contrôle semble être structural plutôt qu'intrusif. Jim Mortensen de l'Université de Colombie-Britannique a étudié en collaboration avec Bill LeBarge (CGY) les caractéristiques des éléments traces des gîtes d'or placériens afin d'identifier des populations distinctes et d'éventuelles sources d'or filonien. John Mair a entamé le développement d'une base de données sur les caractères lithologiques, géochimiques, et isotopiques des roches ignées d'âge Crétacé du Yukon. Julie Hunt poursuit ses travaux sur la géologie et le potentiel minéral des brèches de Wernecke, avec cette fois un focus sur l'uranium. Et Jake Hanley de l'Université de Toronto, avec le support de la CGY, en entrepris une étude sur l'origine et l'évolution des fluides magmatiques, et leurs relations avec la minéralisation aurifère.

PROJET DU BASSIN DE WHITEHORSE

Grant Lowey a continué ses études sédimentologiques et stratigraphiques du Groupe de Laberge et de la Formation de Tantalus, alors que Darrell Long de l'Université Laurentienne a poursuivi ses études du Groupe de Lewes River et de la Formation de Tantalus. Steve Piercey, lui aussi de l'Université Laurentienne, étudie pour sa part la géochimie des roches volcaniques du bassin de Whitehorse. Amy Tizzard de l'Université de Victoria aura bientôt complétée sa thèse de maîtrise portant sur l'évolution structurale de la marge occidentale du terrane

de Stikinia. La compilation des relevés sismiques à l'extrémité nord du bassin de Whitehorse, exécutés par la Commission géologique du Canada (CGC) en partenariat avec la CGY, est maintenant complétée; les résultats de cette étude seront publiés dans une série de rapports au cours de l'année à venir.

ÉTUDES DES FORMATIONS SUPERFICIELLES

Bill LeBarge a visité les opérations minières placériennes à travers le Yukon et a poursuivi ses études avec Mark Nowosad, des Services aux clients et d'inspection du MEMR, afin de mieux caractériser le contexte géologique et la relation entre la qualité des eaux et les effluents de sédiments des opérations de placers le long des rivières Klondike, Indian, McQuesten and Sixty Mile. Erin Troshim et Panya Lipovsky, en collaboration avec la CGC, ont entamées une compilation des informations de forages le long de la route de l'Alaska pour contribuer à la base de données nationale sur le pergélisol. Jeff Bond a débuté une étude sur la distribution des éléments dans le sol dans les terrains non-glaciaires du centre-ouest du Yukon, afin de développer une méthode d'interprétation des données géochimiques du sol dans ce type de terrain. Jeff a aussi étudié l'histoire glaciaire de la chaîne de Big Salmon. Brent Ward, de l'Université Simon Fraser, en collaboration avec Jeff Bond et John Gosse (Université de Dalhousie), a échantillonné des blocs dans la région du lac Aishihik pour de la datation cosmogénique afin d'établir l'âge de l'époque glaciaire de Reid. Panya Lipovsky a récemment complétée sa carte géologique des formations superficielles au 1 : 50 000 de la région de Watson Lake dans le cadre d'un projet de cartographie biophysique du sud-est du Yukon du ministère de l'Environnement du gouvernement du Yukon. Panya a aussi poursuivi la surveillance d'un glissement de terrain actif liés à la fonte du pergélisol près de Carmacks et a participé avec Antoni Lewkowicz de l'Université d'Ottawa à une étude des effets des récents feux de forêts sur la stabilité des terrains pergélisols. Docteur Lewkowicz étudie aussi l'origine et la dynamique des lacs thermokastiques et des palses dans le bassin du ruisseau Wolf, en plus de développer de nouvelles techniques pour la cartographie du pergélisol.

ÉTUDES DÉTAILLÉES

Dejan Milidragovic a débuté une étude pétrologique des dykes de lamprophyres des monts Wernecke sous la direction du Docteur Derek Thorkelson de l'Université Simon Fraser. Luke Beranek a pour sa part entamé une étude doctorale des roches sédimentaires triassiques du centre du Yukon sous la direction du Docteur Jim Mortensen de l'Université de Colombie-Britannique.

RELEVÉS GÉOCHIMIQUES

Des relevés géochimiques régionaux des cours d'eau furent complétés par la CGC en collaboration avec Geoff Bradshaw (CGY) à l'ouest du parc territorial de Fishing Branch dans le nord Yukon et dans la région de la rivière Flat, au sud de Cantung. Les résultats de ces relevés devrait être disponibles en début d'été 2006.

RELEVÉS GÉOPHYSIQUES

Deux relevés magnétiques aériens dans les monts Wernecke et Mackenzie et dans la région d'Eagle Plains sont financés par le MAINC dans le cadre de son programme d'investissements stratégiques dans le développement économique du Nord. L'acquisition des ces relevés est prévue pour le printemps 2006.

ÉVALUATIONS MINÉRALES ET EN HYDROCARBURES

Geoff Bradshaw et Lee Pigage sont tous deux impliqués dans les initiatives de planification de l'utilisation des terres pour le nord du Yukon et le bassin de la rivière Peel; Geoff agit en tant qu'évaluateur du potentiel minéral, alors que Lee est en charge de l'évaluation du potentiel en hydrocarbures.

DIFFUSION DE L'INFORMATION

La Commission géologique du Yukon diffuse de l'information en trois formats : 1) les cartes et rapports sur papier sont vendus par le Bureau d'information et des ventes en géoscience; 2) la plupart de nos publications et bases de données récentes sont disponibles en format numérique à prix réduit; et 3) plusieurs de nos publications sont disponibles sans frais sous format PDF sur notre site internet (<http://www.geology.gov.yk.ca>). La liste des rapports d'évaluation de propriétés minières disponibles en format numérique est maintenant aussi offerte par internet (<http://www.emr.gov.yk.ca/library>).

Nous sommes fier de diffuser de l'information géospatiale par l'entremise de notre service de carte interactive ('Map Gallery'), que l'on accède par le site internet de la CGY. Ce site de carte interactive est continuellement le sujet d'améliorations; nous apprécions les commentaires des usagers.

Les publications de la Commission géologique du Yukon sont diffusées par le Bureau d'information et des ventes en géoscience. Elles sont disponible à l'adresse suivante :

Bureau d'information et des ventes en géosciences
a/s Conservateur des registres miniers
le ministère de l'Énergie, des Mines et des Ressources
le gouvernement du Yukon

300, rue Main - bur. 102
C.P. 2703 (K102)
Whitehorse (Yukon) Y1A 2C6
Téléphone : (867) 667-5200
Télécopieur : (867) 667-5150
Courriel : geosales@gov.yk.ca

Pour en savoir plus sur la Commission géologique du Yukon, visitez notre page d'accueil à www.geology.gov.yk.ca ou communiquez directement avec :

Grant Abbott, Directeur
Commission géologique du Yukon
2099, 2ème Avenue
C.P. 2703 (K10)
Whitehorse (Yukon) Y1A 2C6
Téléphone : (867) 667-3200
Courriel : grant.abbott@gov.yk.ca

Rod Hill, Gestionnaire
Commission géologique du Yukon
2099, 2ème Avenue
C.P. 2703 (K10)
Whitehorse (Yukon) Y1A 2C6
Téléphone : (867) 667-5384
Courriel : rod.hill@gov.yk.ca

Robert E. Leckie Award for Outstanding Reclamation Practices

Judy St. Amand¹

Mining Lands, Energy Mines and Resources

St. Amand, J., 2006. Robert E. Leckie Awards for Outstanding Reclamation Practices. *In: Yukon Exploration and Geology 2005*, D.S. Emond, G.D. Bradshaw, L.L. Lewis and L.H. Weston (eds.), Yukon Geological Survey, p. 71-75.

QUARTZ RECLAMATION PRACTICES AWARD

EAGLE PLAINS RESOURCES LTD.

The Rusty Springs silver-lead-zinc property, located north of Dawson City, was first discovered in 1975 and was explored by several companies from 1975 through to 1986. A winter road and airstrip were constructed in 1978, and an all weather airstrip constructed in 1983.

In 1994, the property was transferred to Eagle Plains Resources. Eagle Plains conducted several exploration programs, which included diamond drilling and trenching. Each of these programs has included a major component of environmental clean-up and reclamation. The company, through good management practices, has steadily cleaned up the legacy of the 1975 through 1986 exploration.

In 2005, the company removed over 100 old fuel drums, and up to 2000 lbs of steel rods and various metal pieces, an old jeep, many plastic buckets and other debris from around drill sites. The crew cleaned up the old camp and burned the wood, tidied up the road and airstrip. They then cleaned up their drill sites and camp site. Every backhaul flight removed waste (Fig. 1). They also recovered a rod sloop and Longyear 38 Frame that had been abandoned for over 20 years.

Eagle Plains is a very worthy recipient of this award!



Figure 1. View of the airstrip at Rusty Springs post reclamation.

¹judy.stamand@gov.yk.ca

Honourable Mention: Strategic Metals Ltd.

Strategic Metals Ltd. is a Vancouver-based company doing grassroots exploration on the Logtung property, near Rancheria, in southeastern Yukon.

The site has seen activity since the 1970s, and the legacy of those years was apparent. Strategic Metals has been cleaning up the site for several years (Fig. 2). In 2004, they removed 300 45-gallon drums, part of a bulk sample left

on site. Many of these drums suffered water damage and were spilling their contents. They were stacked on pallets that were rotting. The drums, drum lids and metal bandings were crushed and removed to the Whitehorse landfill or recycled. The plastic liners were removed from site and the pallets burned.

Due to the efforts of the Strategic Metals crew, the site is now safer and far more pristine at no public cost.

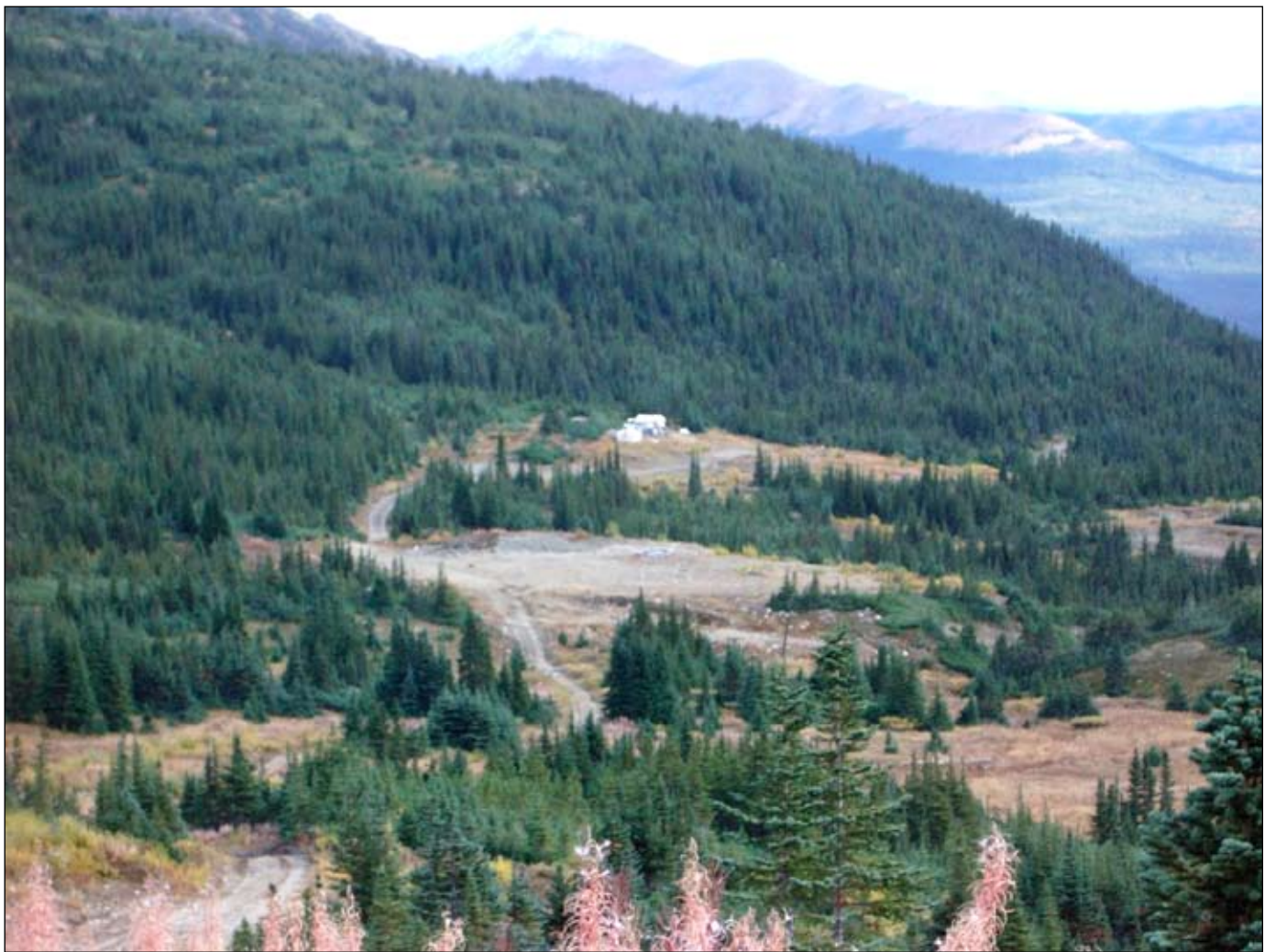


Figure 2. Logtung after years of cleanup by Strategic Metals.

PLACER RECLAMATION PRACTICES AWARD

GIMLEX ENTERPRISES LTD.

Dr. Jim Christie and family operated as **Gimlex Enterprises Ltd.** on Dominion Creek in the Klondike area from 1996 until 2004, mining a large portion of the wide valley bottom, a short distance upstream from the confluence with Sulphur Creek.

Old mine cuts have been sloped to shallow grades, creating natural looking ponds with vegetation growing right up to the water (Fig. 3). These ponds are already providing seasonal waterfowl habitat.

Tailing piles and other waste piles were contoured to low relief and stockpiled overburden was spread throughout

the area, which has resulted in rapid natural revegetation over wide areas.

In addition to the seasonal reclamation work done during the term of their water licence, a considerable amount of work was done to create a system of stable ditches. These provide ongoing control of surface drainage and prevent erosion of reclaimed areas.

Gimlex Enterprises is a great model for this industry and for ongoing reclamation.



Figure 3. View of Gimlex Enterprises' property on Dominion Creek. Notice the naturally revegetating ponds and contoured slopes.

Honourable Mention: 365334 Alberta Ltd.

Operator **Ross Edenoste of A-1 Cats**, has mined on Dominion Creek in the Dawson Mining district since 2002.

Since the start of operations, A-1 Cats management have worked to ensure that reclamation is addressed on an ongoing basis. Stripping and tailings piles are kept in low relief (Fig. 4). Organic overburden is stockpiled for spreading on contoured areas to facilitate rapid re-vegetation.

The camp was set up near mine cuts from a previous lessee of the property. These cuts had been reclaimed to the standard required prior to Mining Land Use.

A-1 Cats is reclaiming the property to present-day standards. Areas have been re-contoured, organic material has been spread and in some areas seeded, leaving an area of ponds with low-relief accesses that will facilitate their use by wildlife at cessation of mining. Areas that may never have re-vegetated are now flourishing.

The work A-1 Cats has done on the previously mined portion of the property has improved and accelerated the reclamation potential of this site.



Figure 4. Steep structures have been recontoured to low-relief angles, and vegetation is flourishing from the addition of overburden spread on the surface.

RÉSUMÉ

Le prix Robert E. Leckie pour des pratiques exemplaires en matière d'exploration du quartz et de restauration minière a été décerné en 2005 à Eagle Plains Resources Ltd. pour la remise en état de sa propriété de Rusty Springs, au nord de la ville de Dawson (Yukon). Découverte en 1975, la minéralisation de Rusty Springs a ensuite été explorée par plusieurs sociétés de 1975 à 1986. Une route d'hiver et une piste d'atterrissage ont été aménagées en 1978, de même qu'une piste d'atterrissage tous temps en 1983. La propriété a été cédée à Eagle Plains Resources en 1994 qui a mené plusieurs programmes d'exploration au cours des années suivantes, comprenant notamment des forages au diamant et l'excavation de tranchées. Chacun des programmes de la société comportait un important volet de dépollution environnementale et de remise en état, corrigeant une situation héritée des activités d'exploration menées de 1975 à 1986. En 2005, plus de 100 vieux barils de carburant et jusqu'à 2000 lbs (1000 kg) de tiges d'acier ainsi que diverses pièces de métal, une vieille jeep, de nombreux seaux de plastique et d'autres débris ont été retirés des sites de forage. Une équipe a nettoyé l'ancien camp, brûlé les débris de bois et remis en ordre la route et la piste d'atterrissage. Elle a ensuite nettoyé les sites de forage et le camp minier de la société. Des déchets étaient évacués lors de chaque vol de retour. La société a également récupéré un support de transport de tiges ainsi qu'un dispositif de forage Longyear 38 abandonné depuis plus de 20 ans. La société Eagle Plains Resources Ltd. mérite très certainement d'être récipiendaire de ce prix.

Le prix Robert E. Leckie pour des pratiques exemplaires en matière de restauration de placers a été décerné en 2005 à Gimlex Entreprises Ltd. pour la remise en état de son exploitation de placer, au sud de la ville de Dawson. M. Jim Christie (Ph. D.) et sa famille ont exploité sous le nom de Gimlex Entreprises Ltd., de 1996 à 2004, une grande partie du large fond de la vallée du ruisseau Dominion, à une courte distance vers l'amont de sa confluence avec le ruisseau Sulphur. Les pentes des anciennes tailles de l'exploitation minière ont été atténuées, créant des étangs d'apparence naturelle où la végétation atteint maintenant le bord de l'eau. Ces étangs constituent déjà des habitats saisonniers pour la sauvagine. On a réduit la hauteur des amas de stériles et d'autres déchets, et on a étendu les tas de morts-terrains sur l'ensemble de la zone, ce qui a permis une végétalisation naturelle et rapide sur de grandes superficies. En plus des travaux saisonniers de restauration exécutés pendant la durée du permis d'exploitation hydraulique, des travaux considérables ont été exécutés pour créer un réseau de fossés stables qui assurent un contrôle continu du drainage superficiel et préviennent l'érosion des zones remises en état. La société Gimlex Entreprises Ltd. représente un modèle à suivre pour l'industrie minière et pour la restauration permanente des sites.

GEOLOGICAL FIELDWORK

Triassic overlap assemblages in the northern Cordillera: Preliminary results from the type section of the Jones Lake Formation, Yukon and Northwest Territories (NTS 1051/13) L.P. Beranek and J.K. Mortensen.....	79
Geology and mineral potential of Yukon-Tanana Terrane in the Livingstone Creek area (NTS 105E/8), south-central Yukon M. Colpron.....	93
Gold mineralization in the upper Hyland River area: A non-magmatic origin C.J.R. Hart and L.L. Lewis.....	109
Unconformity-related uranium potential: Clues from Wernecke Breccia, Yukon J. Hunt, G. Abbott and D. Thorkelson	127
Bedrock geology of the Duke River area, parts of NTS 115G/2, 3, 4, 6 and 7, southwestern Yukon S. Israel, A. Tizzard and J. Major	139
Placer geology and prospective exploration targets of Sixtymile River area, west-central Yukon W. LeBarge.....	155
Active-layer detachments following the summer 2004 forest fires near Dawson City, Yukon P.S. Lipovsky, J. Coates, A.G. Lewkowicz and E. Trochim.....	175
Anatomy of a Late Jurassic Gilbert-type delta in basal strata of the Tantalus Formation, Whitehorse Trough, Yukon D.G.F. Long and G.M. Lowey.....	195
Summary of Rock-Eval data for the Whitehorse Trough, Yukon: Implications concerning the hydrocarbon potential of a frontier basin G.W. Lowey and D. Long	207
Geology of the Quartet Mountain lamprophyre suite, Wernecke Mountains, Yukon D. Milidragovic, D.J. Thorkelson and D.D. Marshall	231
Compositional studies of placer and lode gold from western Yukon: Implications for lode sources J.K. Mortensen, R. Chapman, W. LeBarge and E. Crawford.....	247
Uranium-lead ID-TIMS and LA-ICP-MS ages for the Cassiar and Seagull batholiths, Wolf Lake map area, southern Yukon J.K. Mortensen, C. Sluggett, T. Liverton and C.F. Roots.....	257
Stratigraphy Summary for southeast Yukon (NTS 95D/8 and 95C/5) L.C. Pigage	267
Geochronological and lithochemical studies of intrusive rocks in the Nahanni region, southwestern Northwest Territories and southeastern Yukon K.L. Rasmussen, J.K. Mortensen and H. Falck	287
Paleomagnetism of the ~91 Ma Deadman pluton: Post-mid-Cretaceous tectonic motion in central Yukon D.T.A. Symons, M.J. Harris, C.J.R. Hart and P.J.A. McCausland	299
Structural constraints for oil and gas assessment in the Whitehorse Trough: New results from seismic profiling D. White, M. Colpron, G. Buffett and B. Roberts.....	315

Triassic overlap assemblages in the northern Cordillera: Preliminary results from the type section of the Jones Lake Formation, Yukon and Northwest Territories (NTS 105I/13)

Luke P. Beranek and James K. Mortensen¹

Department of Earth and Ocean Sciences, University of British Columbia²

Beranek, L.P. and Mortensen, J.K., 2006. Triassic overlap assemblages in the northern Cordillera: Preliminary results from the type section of the Jones Lake Formation, Yukon and Northwest Territories (NTS 105I/13). *In: Yukon Exploration and Geology 2005*, D.S. Emond, G.D. Bradshaw, L.L. Lewis and L.H. Weston (eds.), Yukon Geological Survey, p. 79-91.

ABSTRACT

We present new field and whole-rock geochemical data from the type section of the Triassic Jones Lake Formation (JLF) located along the Yukon-Northwest Territories border in the Nahanni map area (NTS 105I/13). The type section is the first location of a regional-scale study that investigates the nature of Triassic siliciclastic rocks, and tests the presence of an overlap assemblage linking pericratonic terranes with North America by the Triassic, instead of Early to Middle Jurassic. The JLF is composed of carbonaceous shale and ripple cross-laminated calcareous sandstone thought to be associated with the Cordilleran miogeocline, and is devoid of sediment sourced from terranes to the west. Whole-rock shale geochemistry has provided evidence that the JLF is distinguishable from the underlying Mount Christie Formation and has trace and rare earth element concentrations that are most similar to old continental crust. However, the JLF does contain geochemical signatures suggestive of a minor mafic component.

RESUMÉ

Nous présentons ici de nouvelles données de terrain et de géochimie pour les roches du stratotype de la Formation de Jones Lake (FJL) du Trias le long de la limite entre le Yukon et les Territoires du Nord-Ouest dans la région de la rivière Nahanni sur la carte Mount Wilson (SNRC 105I/13). Le stratotype est le premier endroit visité dans le cadre d'une étude régionale sur la nature des roches siliciclastiques du Trias et don't le but est d'établir si ces roches représentent un assemblage liant les terranes péricratoniques à l'Amérique du Nord au Trias plutôt qu'au Jurassique précoce à moyen. La FJL se compose de shale carboné et de grès calcaire à stratification entrecroisée qui serait associé à la marge continentale de la Cordillère et dépourvu de sédiments provenant des terranes à l'ouest. La géochimie du shale a fourni des indications à l'effet que la FJL peut être distinguée de la sous-jacente Formation de Mount Christie et renferme des concentrations d'éléments traces et de terres rares des plus similaires à celles présentes dans la croûte continentale ancienne. Cependant, la FJL présente des signatures géochimiques suggérant l'existence d'une composante mafique mineure.

¹*jmortensen@eos.ubc.ca*

²*Vancouver, British Columbia, Canada V6T 1Z4*

INTRODUCTION

Triassic siliciclastic strata of the northern Canadian Cordillera are traditionally considered to be associated with the Western Canada Sedimentary Basin, a westward-thickening succession of sedimentary rocks deposited along the western edge of Laurentia (e.g., Gibson and Barclay, 1989). Sedimentary loading from the deposition of siliciclastic and carbonate strata, along with tectonic subsidence related to the adjacent Panthalassic ocean basin, provided accommodation space for sediments from the Late Proterozoic to middle Mesozoic. Siliciclastic sediments were derived from the Canadian Shield to the east, the Franklinian and Ellesmerian orogenic belts in Arctic Canada, local block uplifts to the west, and cannibalization of the miogeocline itself (Gordey and Anderson, 1993; Ross *et al.*, 1997; Patchett *et al.*, 1999).

Although the patterns of Phanerozoic sedimentation in Yukon appear similar to other locations in the northern Cordillera, the precise age, compositional variation, and relationship of Triassic siliciclastic rocks to pericratonic (margin-fringing) Yukon-Tanana Terrane (YTT), Slide Mountain Terrane (SMT), and autochthonous North America remain unresolved. Several characteristics of the Triassic rocks in Yukon are problematic and suggest that these strata may record a somewhat different depositional setting and provenance than age-equivalent formations in the Western Canada Sedimentary Basin: (1) coarse-grained siliciclastic sedimentary rocks containing late Paleozoic detrital zircon, along with metamorphic (serpentinite, garnet amphibolite, quartz-mica schist, phyllite, quartzite) and igneous (basalt, granitic gneiss) clasts, unconformably overlie YTT in several locations, suggesting western-derived sediment overlapped YTT and SMT by the early Mesozoic (Roots *et al.*, 2002; Pigage, 2004; Colpron *et al.*, 2005); (2) the Triassic basin architecture is unclear due to early(?) Mesozoic accretion of YTT and subsequent late Mesozoic contractional deformation, resulting in discontinuous outcrop exposure; (3) conodont biostratigraphic and early Mesozoic regional stratigraphic correlation is unresolved as the type Triassic section in the Selwyn Basin (Jones Lake Formation) has an Early Triassic age (Smithian; ~245 Ma) whereas Late Triassic ages (Carnian, Norian; ~220 Ma) dominate most other exposures in the YTT, SMT and Cassiar Platform.

In this study we are investigating the possibility that Triassic strata in Yukon comprise an overlap assemblage that links YTT and SMT with autochthonous North America. This would suggest that terrane accretion

in the northern Cordillera began by the Early Mesozoic, much earlier than has previously been believed (e.g., Gabrielse and Yorath, 1991) and would require substantial revisions to current models for the tectonic evolution of the Cordillera. This paper presents new data from fieldwork carried out in the summer of 2005 on the type sections of the Triassic Jones Lake Formation and immediately underlying Mississippian-Permian Mount Christie Formation, which were first described by Gordey and Anderson (1993). The goal of this study is to understand the age, stratigraphic position, and provenance of these units in order to test whether Triassic strata of westernmost North America received siliciclastic input from outboard YTT and SMT assemblages. Our approach was to investigate the lithologic and compositional characteristics of the Mount Christie and Jones Lake formations, noting any changes in time between them, and then compare those data to known rock units along the ancient Pacific margin.

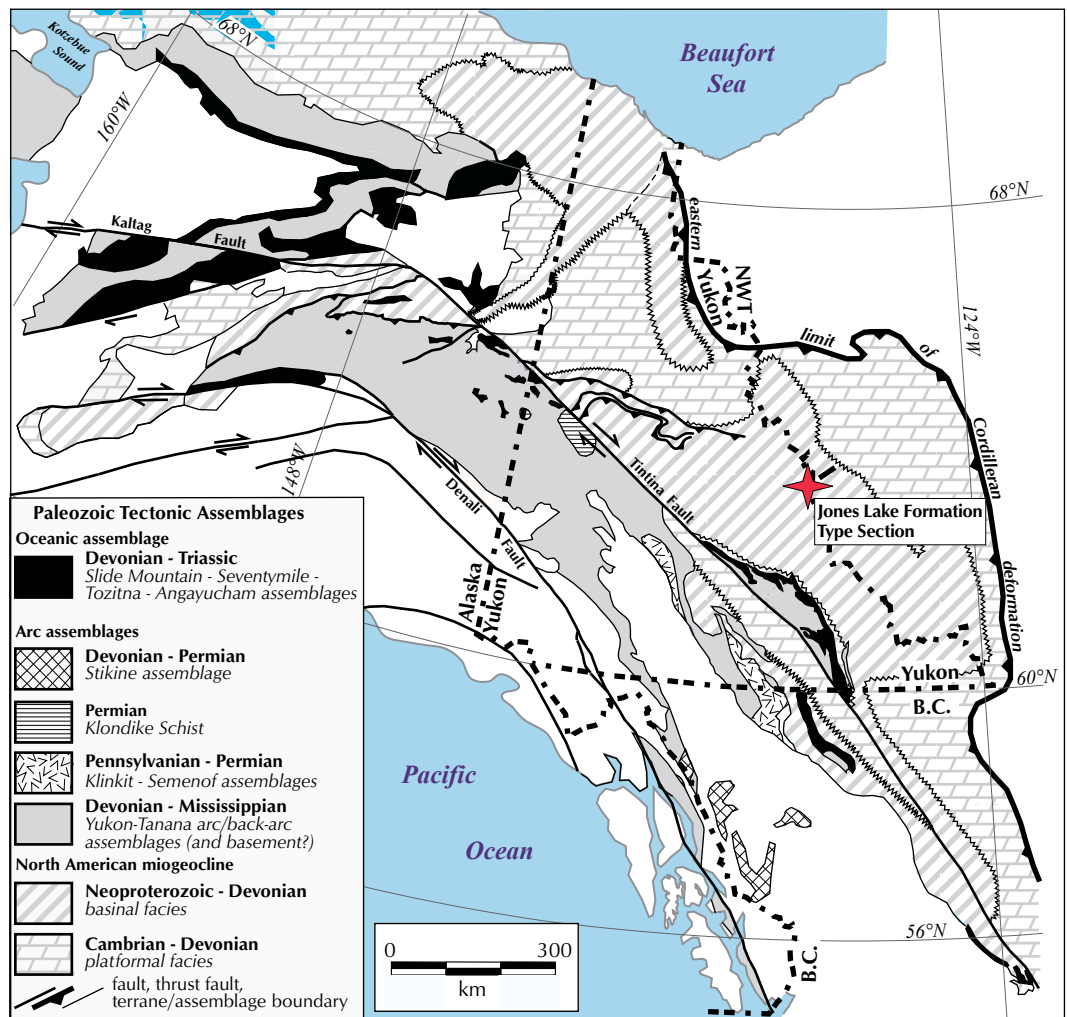
If the Jones Lake Formation is an overlap assemblage linking North America with YTT, rather than simply an offshore component of the North American miogeocline, this calls for dramatic revisions as to the timing and style of pericratonic terrane accretion in the northern Cordillera. Additionally, this would require that the basin in which the Jones Lake Formation was deposited was not simply part of the Cordilleran miogeocline, but rather was a flexural or foreland basin generated by the tectonic loading caused by accreting pericratonic terranes to the west.

PREVIOUS WORK

The type sections of the Mississippian-Permian Mount Christie Formation and Triassic Jones Lake Formation are exposed in the western limb of the Wilson Syncline, located along the Yukon-Northwest Territories border, approximately 9 km south of Mount Wilson in the Nahanni map area (NTS 1051/13) (Fig. 1). Gordey and Anderson (1993) measured, described, interpreted and obtained depositional ages for these two formations in the composite ~1500-m-thick section of dominantly fine-grained, offshore to shoreface siliciclastic sedimentary rocks. They were interpreted to be the youngest preserved strata of the Selwyn Basin.

The age of the Mount Christie Formation, which unconformably overlies the Mississippian Tsichu formation in its type section, is constrained by four conodont collections. The lower shale member of the

Figure 1. Regional view of northern Canadian Cordillera highlighting pericratonic terranes and adjacent facies belts of North America. Jones Lake Formation type section indicated by star symbol along Yukon-NWT border. Modified from Colpron et al. (2003).



Mount Christie Formation is thought to be Late Mississippian from a sample in the Niddy Lake map area (NTS 1050), whereas three conodont samples from the upper chert unit from the type section suggest an Early Permian (Late Wolfcampian to Leonardian) age (Gordey and Anderson, 1993). The Mount Christie Formation is thus thought to be age-equivalent to the Kindle and Fantasque formations of British Columbia and Alberta.

Gordey and Anderson (1993) suggested that the covered contact between the Mount Christie and Jones Lake formations in their type sections is unconformable, because the Triassic is observed to sit on lower portions of the Paleozoic section in other parts of the region. A single conodont collection from the type section approximately 300 m above the base of the Jones Lake Formation yielded a Smithian (Early Triassic) age (Gordey and Anderson, 1993). The age of the rest of the Jones Lake Formation in its type section is unconstrained. The

Jones Lake Formation is thought to be correlative with the Toad and Liard formations and Spray River Group to the south.

STRATIGRAPHIC COLUMN

During July, 2005, the type sections of the Mount Christie and Jones Lake formations were measured with a Jacob staff and sampled for palynomorph and conodont biochronology, detrital zircon and mica geochronology, and whole-rock geochemistry. Gordey and Anderson (1993) reported formation thicknesses and described lithofacies present in the section; however, we re-measured their type section in order to develop our own interpretations of sedimentary environments and lithofacies, and to apply a systematic sampling strategy that will be followed for the coming field seasons for all Triassic assemblages.

The stratigraphic column for the type sections are presented in Figure 2. A panoramic view of the composite column with highlighted features is shown in Figure 3.

Mount Christie Formation

The base of the Mount Christie Formation unconformably overlies the uppermost fine- to medium-grained, tan quartz arenite of the Tsuchi formation. This contact serves as our base datum (0 m) of the composite Mount Christie-Jones Lake section. We followed Gordey and Anderson (1993) in subdividing the Mount Christie Formation into two informal members, a lower shale member (550 m) and an upper chert and shale member (200 m).

The lower member comprises dark grey, greenish grey and reddish brown, thin- to wavy-laminated, cleaved, siliceous shale and siltstone which typically breaks into elongate pencil structures that commonly produce significant scree piles on the southwest-facing ridge (Fig. 4). Detrital mica appears variably along bedding planes in the lower shale member. At 400 m, near the top of the lower shale member, a resistant bed of very fine-grained sandstone contains nodules of barite. Barite nodules in the Mount Christie Formation vary from sand- to boulder-sized (Fig. 5). The origin of the locally abundant and characteristic barite nodules in the Mount Christie Formation is uncertain. Goodfellow *et al.* (1995) suggested that high barite concentrations in underlying middle Paleozoic units were ultimately derived from the reworking of lower Paleozoic alkalic and potassic volcanic rocks in the northern Cordilleran miogeocline.

Figure 2. Measured stratigraphic column of composite Mount Christie and Jones Lake type section. Unit thickness and sample locations above 1200 m are estimated.

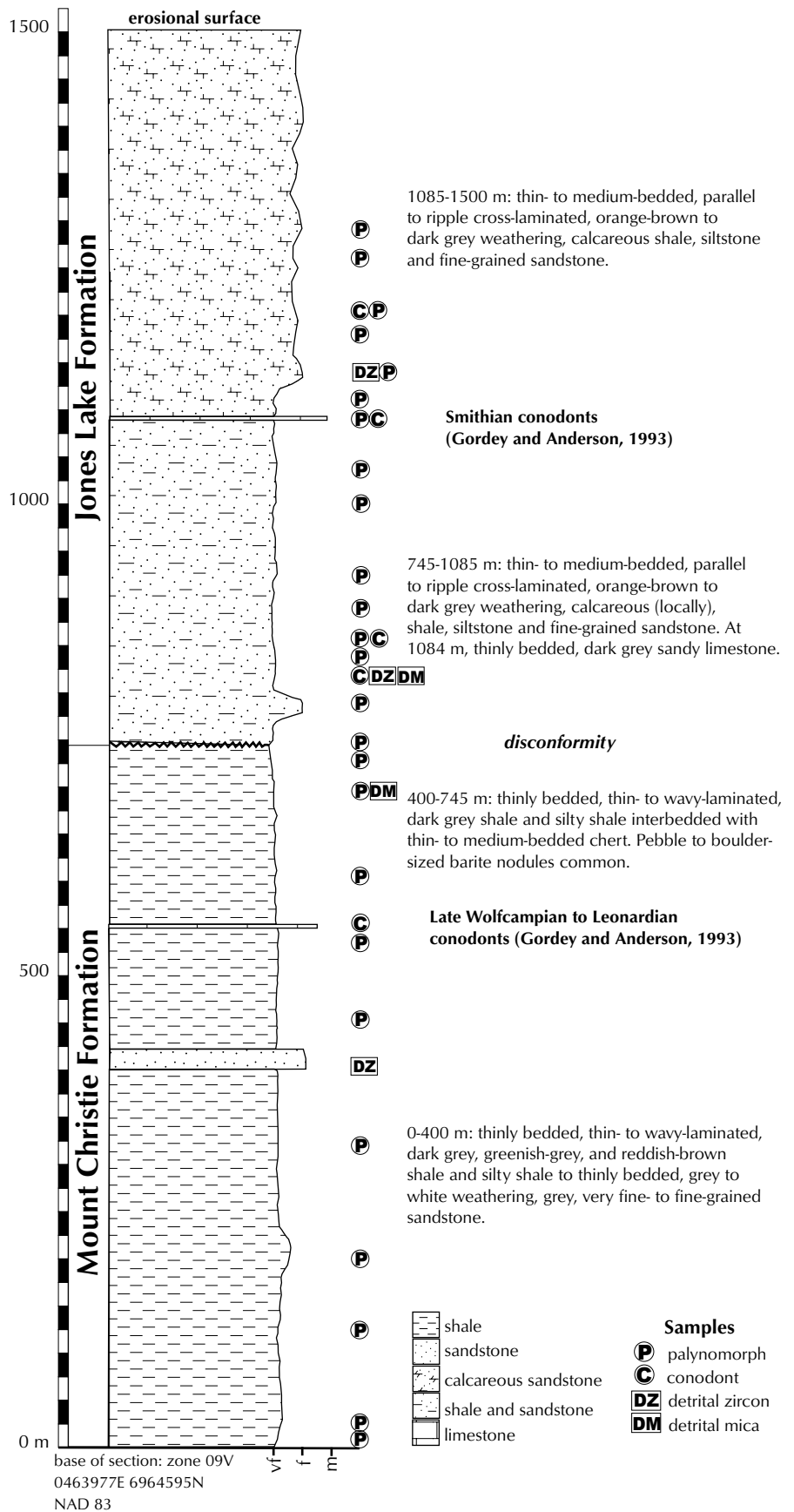




Figure 3. View to the northwest of composite Mount Christie-Jones Lake type section. M = Mississippian, P = Permian, Tr = Triassic, Fm = Formation

Separating the lower and upper members of the Mount Christie Formation is a discontinuous, red-weathering crystalline limestone that yielded a Late Wolfcampian to Leonardian (Early Permian) age (Gordey and Anderson, 1993).

The upper member of the Mount Christie Formation is characterized by dark grey splintery shale similar to that in the lower member, intercalated with thin- to medium-bedded grey and black chert. Local concentrations of barite nodules occur throughout the upper member. As with the lower member, detrital mica occurs locally in shaley and sandy horizons. The top of the upper member and base of the overlying Jones Lake Formation was chosen by Gordey and Anderson (1993) to be at the last

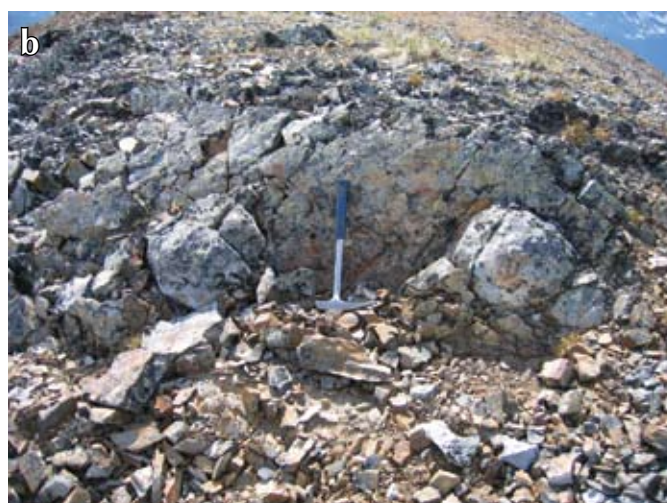


Figure 4. Typical splintery shale and siltstone of the Mount Christie Formation. Image is taken at the 223-m level in section.

Figure 5. Barite nodules from the upper Mount Christie Formation at 600 m. (a) Typical pebble to cobble-sized accumulations in siltstone. (b) Boulder-sized (up to 0.3 m in diameter) crystalline barite.

occurrence of chert. However, it is noteworthy that the lowermost Jones Lake Formation contains shale and siltstone that is lithologically similar to that of the uppermost Mount Christie Formation. The contact, presumed to be unconformable, is covered by vegetation and scree at this locality.

Considering the fine sediment size and cherty nature of these deposits, Gordey and Anderson (1993) interpreted the depositional environment for the Mount Christie Formation to be below wave-base, in an off-shelf setting. Sand and limestone occurrences within the section require sporadic clastic sediment inputs and regional shoaling events. Due to the fine-grained nature of these deposits and scree cover, no paleocurrent determinations were possible.

Jones Lake Formation

The core of the Wilson Syncline comprises distinctive orange-tan weathering shale, siltstone and sandstone of the Jones Lake Formation. Above the contact with the Mount Christie Formation, the Jones Lake Formation is typified by shale and siltstone to sandstone couplets of varying thicknesses, most commonly around 0.5 to 1 m. Contacts between lithofacies are commonly sharp and bedforms are planar to hummocky. Shale and siltstone beds commonly display 1-2 mm mud and silt laminations, and parallel to ripple cross-laminated fine quartzose sandstone is abundant. Paleocurrent indicators are not unidirectional but mainly indicate flow towards the

southeast (Fig. 6). Siltstones commonly show tangential, mud-draped, stoss-side laminae that locally grade into hummocky and swaley laminations (Fig. 6). Laminated siltstones in local float contain what is thought to be *Cruziana* ichnofacies (trace fossils). Detrital mica is present, especially along shaley bedding planes.

Approximately 130 m above the contact with the Mount Christie Formation, the Jones Lake beds display open to tight folding, which make our thickness measurements a maximum value. Triassic strata exposed on the ridge returns to the typical northeasterly dip above this narrow zone of minor folding. Approximately 200 m of dark grey splintery carbonaceous shale and tan-weathering, medium grey, wavy-laminated fine calcareous sandstone make up the majority of the section. A coarse sandy limestone unit that yielded a Smithian conodont age (Gordey and Anderson, 1993) is located at 1084 m. This age is crucial because this limy bed is 300 m above the contact with the underlying Mount Christie Formation. If the conodont elements are primary and not from a reworked source, the bulk of the Jones Lake Formation in its type section has a maximum age of Early Triassic and theoretically could extend down into the Permian.

Above the Smithian conodont locality, our measurement was discontinued due to steep exposures and locally pervasive deformation in the Jones Lake strata. We continued to sample and describe the sedimentary rocks in this upper section but have opted to use the stratigraphic thickness estimates of Gordey and Anderson



Figure 6. Images of Jones Lake Formation laminated siltstone to sandstone around 800 m. Both photos are taken towards east-northeast. **(a)** Ripple cross-laminated siltstone, with flow from left to right. Note concave-down laminae near top of image. **(b)** Cross-laminated siltstone that grades up into concave up and then concave-down laminae, consistent with hummocky and swaley geometry.

(1993) for the uppermost portions of the exposed Jones Lake Formation.

Gordey and Anderson (1993) interpreted that the ripple cross-laminated calcareous sandstone of the Jones Lake Formation indicates deposition in a shallow marine setting that was affected by both traction and suspension sedimentation. We agree with this interpretation and expand on it by noting shoreface ichnofacies and possible storm-induced features, indicated by Cruziana and hummocky bedform geometry. Gordey and Anderson (1993) did not report any paleocurrent information and assumed an easterly source for sediment. Our paleocurrent analyses from the Jones Lake Formation, and from other preliminary studies of Triassic sections in southeast Yukon, mainly indicate flow directions parallel to the North American margin (south-southeasterly).

CONODONT AND PALYNOMORPH BIOCHRONOLOGY

One main focus of this project is to tighten chrono-stratigraphic controls on Triassic sequences that appear to be spatially associated with pericratonic terranes in Yukon. To date, age determinations have been made using conodonts. Here, we apply the tool of palynomorph biochronology to the pre-existing conodont biostratigraphic framework for the Mount Christie-Jones Lake section. Palynomorphs can be recovered from calcareous and non-calcareous rocks and they may be particularly important in dating Triassic units, which are typically only weakly to moderately calcareous. As such, it is hoped that the biostratigraphic resolution afforded by conodonts can be enhanced by palynomorphs. The use of two independent biochronological methods will permit a greater chronostratigraphic resolution and, hopefully, more robust age determinations.

Twenty-five palynology and four conodont samples were collected from the composite Mount Christie and Jones Lake section (shown in Fig. 2). Fifteen palynology samples were processed during fall, 2005, and palynology slides were generated by Global Geolabs Ltd. These slides are currently being evaluated by J. Utting of the Geological Survey of Canada in Calgary. Preliminary results are mixed; initial examination indicates that palynomorphs are present but were highly altered during diagenesis. Palynomorphs from these samples are dark coloured, reflecting a high thermal maturity. This alteration is consistent with high conodont colour

alteration index (CAI) values of 4-5 for this region reported by Gordey and Anderson (1993). If palynomorphs are found to be a useful tool for the Jones Lake section, other samples collected from Triassic exposures in the MacNeil Lake, Frances Lake and Clinton Creek areas will be processed. New conodont samples from the Early Permian and Early Triassic localities in the section are currently being processed at the Geological Survey of Canada in Vancouver, along with two other new samples from the Jones Lake Formation (see Fig. 2). Age determinations on these samples are being carried out by M.J. Orchard.

WHOLE-ROCK GEOCHEMISTRY

Whole-rock geochemistry and isotopic data are useful for determining the bulk provenance of clastic sedimentary rocks, especially those containing monotonous, fine-grained siliciclastic sediments where ultimate source rock information is not available and petrographic methods (e.g., Gazzi-Dickinson) are not applicable (Heller and Frost, 1988; McLennan *et al.*, 1993). Specifically, trace elements such as high field strength (HFSE) and rare earth elements (REE) are not significantly diminished during weathering, transportation or diagenetic processes, and faithfully record their source rock composition (McLennan *et al.*, 1993).

We have obtained whole-rock major, trace and rare earth element data for 14 samples of shale and silty shale from the Mount Christie and Jones Lake type sections. Analyses were done by ALS Chemex in North Vancouver and consisted of XRF analyses of major elements and a combination of ICP-MS and ICP-AES analyses for minor and trace element concentrations. Our focus is to characterize the Mount Christie and Jones Lake sections independently and then document compositional changes or similarities between the two. We then compare our data to published data from other rock units and assemblages that could have been reservoirs that supplied sediment to Permian and Triassic depocentres.

MOUNT CHRISTIE FORMATION

Five shale to siltstone samples collected between 23 and 745 m in the Mount Christie type section yield similar whole-rock major and trace element signatures. Major element data will not be discussed in detail, however, it is noteworthy that SiO₂ values are elevated (68-78 wt.%) compared to the average for continental crust (Wedepohl, 1995) and continentally derived shale (Mason, 1982). In

the field, Mount Christie Formation shales appear to be highly siliceous, and this diagenetic or hydrothermal overprint may be responsible for the low quality of palynomorph preservation.

Chondrite-normalized REE and trace element data for the Mount Christie Formation samples are shown in Figures 7a and b. The Mount Christie Formation contains an enrichment of light rare earth elements (LREE) relative to a flat heavy rare earth element (HREE) pattern. This is shown by high (~7.0-8.5) La_N/Yb_N ratios, and Gd_N/Yb_N ratios from 1.0-1.5. LREE enrichment commonly occurs during igneous differentiation processes and is a feature observed in old upper continental crust (McLennan *et al.*, 1993). A significant negative Eu anomaly exists for the Mount Christie Formation, and Eu/Eu^* values range from 0.6-0.7, both suggesting derivation from evolved continental crust. First-cycle volcanic detritus, as would be associated in the outboard YTT and SMT assemblages, would not be expected to have a Eu anomaly because plagioclase would likely be present. Mount Christie Formation shales are enriched in Ba (up to 4900 ppm), presumably reflecting the presence of fine-grained disseminated barite. REE concentrations and trends in the Mount Christie Formation compare favourably with Cambrian-Devonian deposits of the northern miogeocline (Garzzone *et al.*, 1997; Patchett *et al.*, 1999).

Input from mafic and ultramafic sources associated with Slide Mountain Terrane do not appear to be present as our samples are low in Cr and Ni (Fig. 8a).

JONES LAKE FORMATION

Nine samples spanning the entire thickness of the Jones Lake Formation in its type section were analysed. Major element analyses show that the Jones Lake Formation is slightly different than the underlying Mount Christie Formation, and can be differentiated from it by alumina and titanium oxide contents (Fig. 9). The Jones Lake Formation contains less SiO_2 (48-68 wt.%) but more MgO (1-2.4 wt.%), and nearly double TiO_2 (avg. ~1 wt.%) and K_2O (average ~4 wt.%) than the Mount Christie Formation. A change up-section in these oxides may suggest a change in provenance but they appear to match the range of values observed in Paleozoic deposits of the northern miogeocline (e.g., Garzzone *et al.*, 1997).

Trace element patterns in the Jones Lake Formation are similar to the Mount Christie Formation, however, the former is commonly enriched relative to the latter (Fig. 7). Like the Mount Christie Formation, the Jones Lake Formation has high La_N/Yb_N ratios (average ~9.4), low Gd_N/Yb_N ratios (1.2-1.7), and a significant negative Eu anomaly, where Eu/Eu^* values are around 0.6. These data suggest that a significant source component feeding the Jones Lake basin was evolved and granitic in nature.

Although the Jones Lake Formation in its type section does not show an overwhelming signature consistent with a significant ultramafic or ophiolitic input, it does contain higher values of Cr and Ni than the Mount Christie Formation (Fig. 8a). Although used primarily for igneous rock classification, Figure 8b shows that the Jones Lake Formation samples plot largely within the mid-oceanic

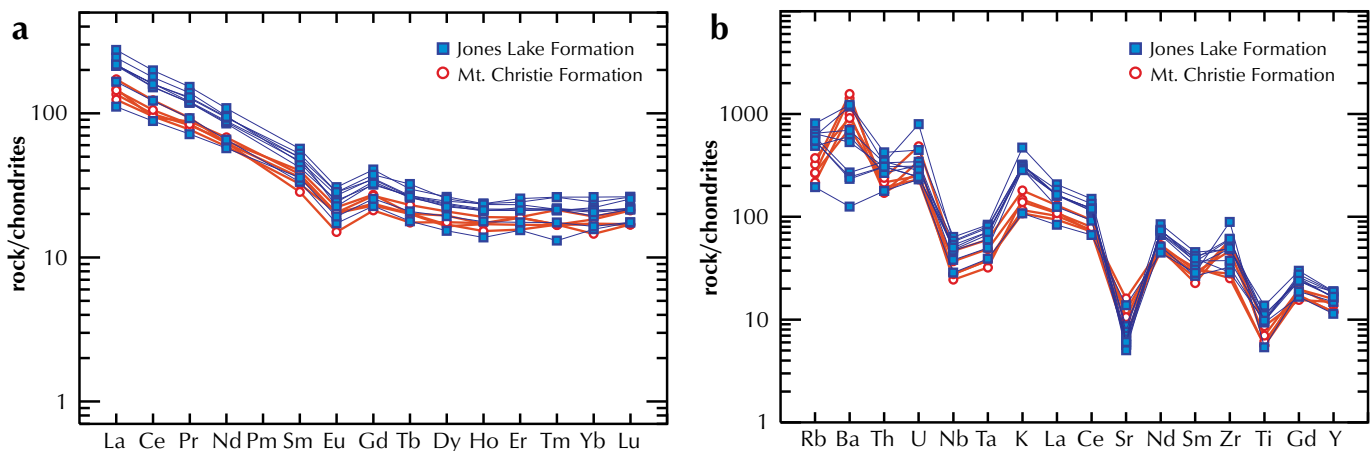


Figure 7. Multi-element plots of the Mount Christie and Jones Lake formations. (a) REE plot normalized to chondrite (Sun and McDonough, 1989). (b) Trace element plot normalized to chondrite (Sun, 1980). Calculated Eu/Eu^* , La_N/Yb_N and Gd_N/Yb_N determined from chondrite of Sun and McDonough (1995).

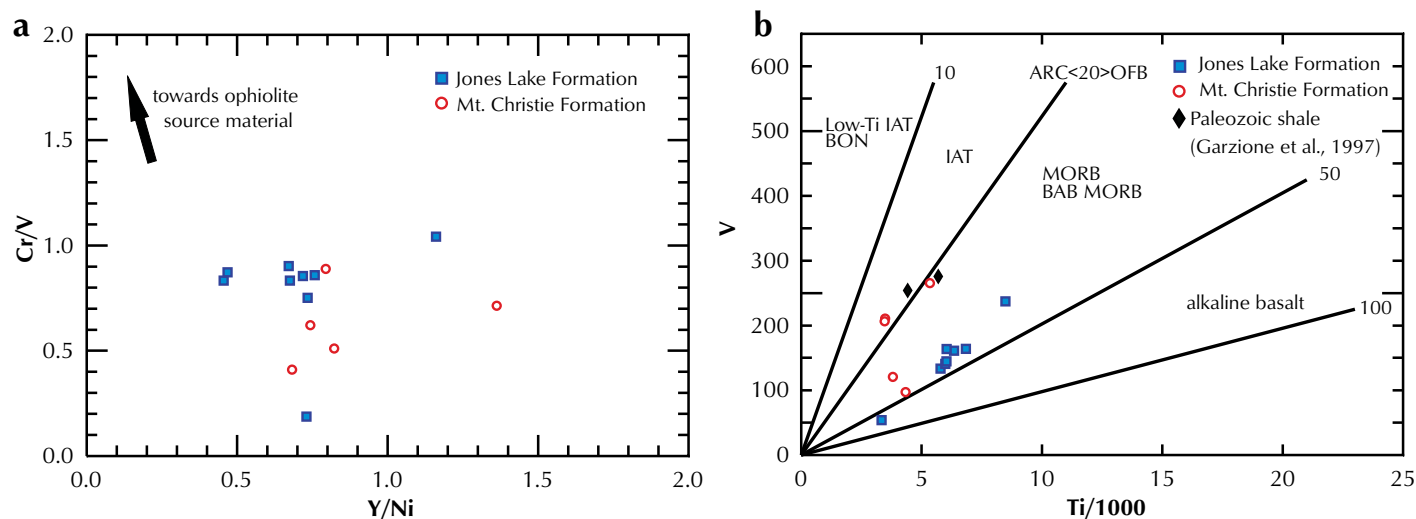


Figure 8. Bivariate diagrams that determine possible mafic input to the Mount Christie-Jones Lake section. **(a)** Cr/V versus Y/Ni plot after McLennan *et al.* (1993). **(b)** V versus Ti/1000 tectonomagmatic diagram after Shervais (1982). Paleozoic shale data from Garziona *et al.* (1997). BON = boninite, IAT = island-arc tholeiite, MORB = mid-oceanic ridge basalt, BAB = back-arc basin.

ridge basalt (MORB) field. This is quite different from the Mount Christie Formation and Paleozoic shale of the Cordilleran miogeocline of Garziona *et al.* (1997), which plot closer to, or in, the island-arc field (IAT). This could be consistent with the Mount Christie Formation being fed by the craton to east, which mainly comprises Proterozoic and Archean arc terranes, whereas detritus eroded from uplifted oceanic crust of the now-closed(?) marginal back-arc basin (Slide Mountain Ocean) could be present within the Jones Lake Formation.

It is noteworthy that the Ba enrichment that is so prevalent in the Mount Christie Formation persists in the Jones Lake Formation until 1114 m, which is 30 m above the Smithian conodont collection. From the base at 750 m to 1114 m, Ba values range from 1600-4000 ppm, while up-section of that they range from 390-870 ppm, which is possibly noting a change in local-scale provenance.

ND ISOTOPE GEOCHEMISTRY

Recent Sm-Nd isotopic studies of Paleozoic sedimentary strata within the northern Cordilleran miogeocline concluded that these units record an influx of juvenile material derived from early to middle Paleozoic rock units in Arctic Canada (Boghossian *et al.*, 1996; Garziona *et al.*, 1997; Patchett *et al.*, 1999). Although trace element concentrations showed relatively little variation amongst

the Paleozoic strata, the Nd isotopic signature was shown to display a significant shift from lower Paleozoic samples with continental affinity ($\epsilon_{Nd(T)}$ of -10 to -21) to middle Paleozoic and Mesozoic samples which yielded a mixture of continental values and a juvenile component with younger mantle extraction ages ($\epsilon_{Nd(T)}$ of -5 to -15).

Garziona *et al.* (1997) obtained an $\epsilon_{Nd(T)}$ value of -8.3 for a sample of the Mount Christie Formation collected along the Dempster Highway in northern Yukon. As no sources with that signature exist in western Canada, Garziona *et al.* (1997) suggested a mixture of evolved and juvenile sources. Patchett *et al.* (1999) traced the source of the juvenile signature to the Franklinian mobile belt of Arctic Canada. In addition, Boghossian *et al.* (1996) indicated Triassic Spray River Group shale and sandstone in southern Cordillera to have $\epsilon_{Nd(T)}$ of -9 to -10, Creaser and Harms (1998) received $\epsilon_{Nd(T)}$ values of -9 to -11 for Triassic rocks of the upper Klinkit assemblage in northern British Columbia (Teh clastic unit of Roots *et al.*, 2002), and Ross *et al.* (1997) reported $\epsilon_{Nd(T)}$ of -6 to -10 for the Triassic Toad and Liard formations in northern Alberta.

We plan to carry out Nd isotopic analyses for a suite of samples from the Mount Christie and Jones Lake type formations over the next several months. Although the Mount Christie and Jones Lake formations show mainly continental signatures in terms of their trace element concentrations, the more sensitive Sm-Nd system may reveal a juvenile component sourcing these sediments, as

Garzione *et al.* (1997) and Patchett *et al.* (1999) have shown. Interestingly, Piercey *et al.* (2004) noted that mafic assemblages of Yukon-Tanana and Slide Mountain terranes contain juvenile signatures similar to those coming from Arctic Canada, suggesting that a large portion of juvenile input to the miogeocline could be from proximal outboard terranes to the west.

DETRITAL ZIRCON AND MICA GEOCHRONOLOGY

We collected three detrital zircon samples from the Mount Christie and Jones Lake formations' type sections and two from the underlying Tschu formation. Detrital zircon geochronology has been widely employed in regional tectonic and sedimentary provenance studies in western North America. Previous investigations have documented age patterns for detrital zircons from various portions of the North American miogeocline and have identified significant latitudinal variations (e.g., Ross *et al.*, 1997; Gehrels and Ross, 1998; Gehrels, 2000; Stewart *et al.*, 2001; Ross *et al.*, 2005; Link *et al.*, 2005). Abundant U-Pb zircon geochronology that has been carried out in the pericratonic terranes in the Canadian Cordillera (e.g., Mortensen, 1992; Murphy *et al.*, in press; Colpron *et al.*, in press) will form the basis for recognition of any detrital zircon populations that might have been derived from those terranes. The new detrital zircon dating work will be done using laser ablation inductively coupled plasma mass spectrometer (LA-ICP-MS) methods at the University of British Columbia in Vancouver, BC.

Detrital zircons from the Triassic Liard and Whitehorse formations of Alberta, obtained using conventional thermal ionization mass spectrometry, have been reported by Ross *et al.* (1997). Their samples contained large Proterozoic (ca. 1000, 1800 Ma) and Archean (2800, 3500 Ma) populations, all of which are common in the Cordilleran passive margin. Interestingly, they document the presence of two lower Paleozoic grains with ages of 430 and 434 Ma. These ages are not common along the northern Cordilleran margin and were interpreted to have been recycled through early to middle Paleozoic clastic wedge deposits of the Innuitian orogenic belt of Arctic Canada (*cf.*, McNicoll *et al.*, 1995).

Detrital mica is commonly present in the Jones Lake Formation, and locally in the underlying Mount Christie Formation. The source of this mica is problematical, since no obvious source has been identified for many hundreds of kilometres to the east. Micaceous sedimentary rocks of the Mount Christie and Jones Lake formations were sampled for detrital mica geochronology (see Fig. 2). Individual mica grains will be analysed using the laser-equipped noble gas mass spectrometer at the University of British Columbia to constrain their possible provenance.

PRELIMINARY CONCLUSIONS

The Mississippian-Permian Mount Christie Formation and Triassic Jones Lake Formation have similar trace and rare-earth element concentrations, both suggestive of derivation from old continental crust. However, the formations can be differentiated by evaluating barium concentrations versus moderately immobile major

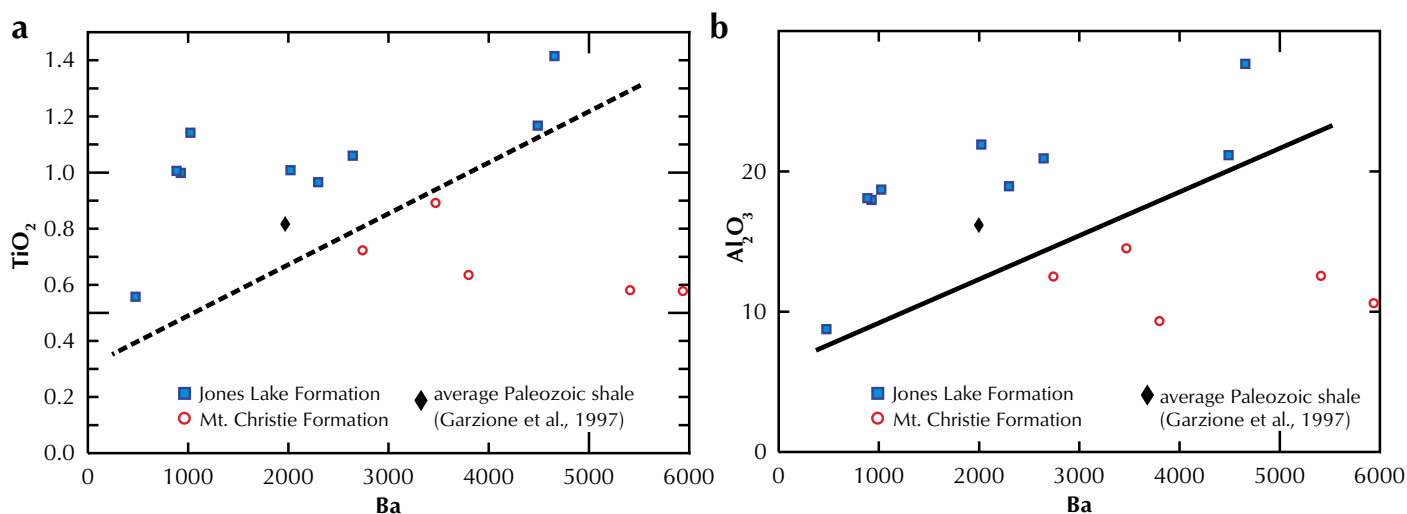


Figure 9. (a) TiO₂ versus Ba; and (b) Al₂O₃ versus Ba. Lines separate Mount Christie Formation samples from Jones Lake Formation samples. Paleozoic shale data from Garzione *et al.* (1997).

element oxides (Fig. 9). This tool could be used for future investigations where contact relationships between these two units are not clear.

The geochemistry of the Jones Lake Formation suggests that the source region included mafic or ultramafic rocks (Fig. 8). Future Nd isotopic analyses may yield more compelling data concerning the nature and possible identity of these juvenile sources.

Paleocurrent indicators in ripple cross-laminated siltstone of the Jones Lake Formation are inconclusive with respect to testing Triassic linkages between outboard pericratonic terranes and autochthonous North America. Paleocurrents predominantly trend to the south-southeast, probably reflecting margin-parallel currents in the distal shoreface.

Forthcoming detrital mineral geochronology and biochronology have a high potential to constrain the position of outboard terranes during the late Paleozoic to early Mesozoic.

ACKNOWLEDGEMENTS

Field work during summer 2005 was funded by the Yukon Geological Survey. Laboratory analyses were funded by a NSERC grant to J.K. Mortensen. We thank Stuart Sutherland for his comments on this manuscript.

REFERENCES

- Boghossian, N.D., Patchett, P.J., Ross, G.M. and Gehrels, G.E., 1996. Nd isotopes and the source of sediments in the miogeocline of the Canadian Cordillera. *Journal of Geology*, vol. 104, p. 259-277.
- Colpron, M., Murphy, D.C., Nelson, J.L., Roots, C.F., Gladwin, K., Gordey, S.P. and Abbott, J.G., 2003. Yukon Targeted Geoscience Initiative: Part 1. Results of accelerated bedrock mapping in Glenlyon (105L/1-7, 11-14) and northeast Carmacks (115I/9, 16) areas, central Yukon. *In: Yukon Exploration and Geology 2002*, D.S. Emond and L.L. Lewis (eds.), Exploration and Geological Services Division, Yukon Region, Indian and Northern Affairs Canada, p. 85-108.
- Colpron, M., Gladwin, K., Johnston, S.T., Mortensen, J.K. and Gehrels, G.E., 2005. Geology and juxtaposition history of the Yukon-Tanana, Slide Mountain, and Cassiar terranes in the Glenlyon area of central Yukon. *Canadian Journal of Earth Sciences*, vol. 42, p. 1431-1448.
- Colpron, M., Nelson, J.L. and Murphy, D.C. (in press). A tectonostratigraphic framework for the pericratonic terranes of the northern Canadian Cordillera. *In: Paleozoic Evolution and Metallogeny of Pericratonic Terranes at the Ancient Pacific Margin of North America*, M. Colpron, J.L. Nelson and R.I. Thompson (eds.), Canadian and Alaskan Cordillera, Geological Association of Canada Special Paper.
- Creaser, R.A. and Harms, T.A., 1998. Lithological, geochemical, and isotopic characterization of clastic units in the Klinkit and Swift River assemblages, northern British Columbia. SNORCLE and Cordilleran Tectonics Workshop, LITHOPROBE Report No. 69, p. 239-241.
- Gabrielse, H. and Yorath, C.J., 1991. Tectonic synthesis, Chapter 18. *In: Geology of the Cordilleran orogen in Canada*, H. Gabrielse and C.J. Yorath (eds.), Geological Survey of Canada, Geology of Canada, no. 4, p. 677-705.
- Garzzone, C.N., Patchett, J.P., Ross, G.M. and Nelson, J., 1997. Provenance of Paleozoic sedimentary rocks in the Canadian Cordilleran miogeocline: A Nd isotopic study. *Canadian Journal of Earth Sciences*, vol. 34, p. 1603-1618.
- Gehrels, G.E. and Ross, G.M., 1998. Detrital zircon geochronology of Neoproterozoic to Permian miogeoclinal strata in British Columbia and Alberta. *Canadian Journal of Earth Sciences*, vol. 35, p. 1380-1401.
- Gehrels, G.E., 2000. Introduction to detrital zircon studies of Paleozoic and Triassic strata in western Nevada and northern California. *In: Paleozoic and Triassic Paleogeography and Tectonics of Western Nevada and Northern California*, M.J. Soreghan and G.E. Gehrels (eds.), Geological Society of America Special Paper 347, p. 1-17.
- Gibson, D.W. and Barclay, J.E., 1989. Middle Absaroka Sequence – the Triassic stable craton. *In: Western Canada Sedimentary Basin - A case history*, B. Ricketts (ed.), Canadian Society of Petroleum Geologists, Special Publication No. 30, p. 219-233.

- Goodfellow, W.D., Cecile, M.P. and Leybourne, M.I., 1995. Geochemistry, petrogenesis, and tectonic setting of lower Paleozoic alkalic and potassic volcanic rocks, Northern Canadian Cordilleran Miogeocline. *Canadian Journal of Earth Sciences*, vol. 32, p. 1236-1254.
- Gordey, S.P. and Anderson, R.G., 1993. Evolution of the northern Cordilleran Miogeocline, Nahanni Map Area (1051), Yukon and Northwest Territories. Geological Survey of Canada, Memoir 428, 214 p.
- Heller, P.L. and Frost, C.D., 1988. Isotopic provenance of clastic deposits: Application of geochemistry to sedimentary provenance studies. *In: New perspectives in basin analysis*, K. Kleinspehn and C. Paola (eds.), Springer Verlag, New York, p. 23-42.
- Link, P.K., Fanning, C.M. and Beranek, L.P., 2005. Reliability and longitudinal change of detrital-zircon age spectra in the Snake River system, Idaho and Wyoming: An example of reproducing the bumpy barcode. *Sedimentary Geology*, vol. 118, p. 101-142.
- Mason, B., 1982. Principles of geochemistry. John Wiley and Sons Limited, New York, 329 p.
- McLennan, S.M., Hemming, S., McDaniel, K. and Hanson, G.N., 1993. Geochemical approaches to sedimentation, provenance, and tectonics. *In: Processes Controlling the Composition of Clastic Sediments*, M. Johnsson and A. Basu (eds.), Geological Society of America Special Paper 284, p. 21-40.
- McNicoll, V.J., Harrison, J.C., Trettin, H.P. and Thorsteinsson, R., 1995. Provenance of the Devonian clastic wedge of Arctic Canada: Evidence provided by detrital zircon ages. *In: Stratigraphic Evolution of Foreland Basins*, S.L. Dorobek and G.M. Ross (eds.), Society of Economic Paleontologists and Mineralogists, Special Publication 52, p. 77-93.
- Mortensen, J.K., 1992. Pre-mid-Mesozoic tectonic evolution of the Yukon-Tanana terrane, Yukon and Alaska. *Tectonics*, vol. 11, no. 4, p. 836-853.
- Murphy, D.C., Mortensen, J.K., Piercey, S.J., Orchard, M.J. and Gehrels, G.E. (in press). Mid-Paleozoic to Early Mesozoic tectonostratigraphic evolution of Yukon-Tanana and Slide Mountain terranes and affiliated overlap assemblages, Finlayson Lake massive sulphide district, southeastern Yukon. *In: Paleozoic Evolution and Metallogeny of Pericratonic Terranes at the Ancient Pacific Margin of North America*, M. Colpron, J.L. Nelson and R.I. Thompson (eds.), Canadian and Alaskan Cordillera, Geological Association of Canada Special Paper.
- Patchett, J.P., Roth, M.A., Canale, B.S., de Freitas, T.A., Harrison, J.C., Embry, A.F. and Ross, G.M., 1999. Nd isotopes, geochemistry, and constraints on sources of sediments in the Franklinian mobile belt, Arctic Canada. *Geological Society of America Bulletin*, vol. 111, no. 4, p. 578-589.
- Piercey, S.J., Murphy, D.C., Mortensen, J.K. and Creaser, R.A., 2004. Mid-Paleozoic initiation of the northern Cordilleran marginal backarc basin: Geologic, geochemical, and neodymium isotope evidence from the oldest mafic rocks in the Yukon-Tanana terrane, Finlayson Lake district, southeast Yukon, Canada. *Geological Society of America Bulletin*, vol. 116, no. 9/10, p. 1087-1106.
- Pigage, L.C., 2004. Bedrock geology compilation of the Anvil District (parts of NTS 105K/2, 3, 4, 5, 6, 7 and 11), central Yukon. Yukon Geological Survey, Bulletin 15, 103 p.
- Roots, C.F., Harms, T.A., Simard, R., Orchard, M.J. and Heaman, L., 2002. Constraints on the age of the Klinkit assemblage east of Teslin Lake, northern British Columbia. *Current Research, Part A, Geological Survey of Canada, Paper 2002- A7*, p. 1-11.
- Ross, G.M., Gehrels, G.E. and Patchett, J.P., 1997. Provenance of Triassic strata in the Cordilleran miogeocline, western Canada. *Bulletin of Canadian Petroleum Geology*, vol. 45, no. 4, p. 461-473.
- Ross, G.M., Patchett, P.J., Hamilton, M., Heaman, L., DeCelles, P.G., Rosenberg, E. and Giovanni, M.K., 2005. Evolution of the Cordilleran orogen (southwestern Alberta, Canada) inferred from detrital mineral geochronology, geochemistry, and Nd isotopes in the foreland basin. *Geological Society of America Bulletin*, vol. 117, no. 5/6, p. 747-763.

- Shervais, J.W., 1982. Ti-V plots and the petrogenesis of modern and ophiolitic lavas. *Earth and Planetary Science Letters*, vol. 59, p. 101-118.
- Stewart, J.H., Gehrels, G.E., Barth, A.P., Link, P.K., Christie-Blick, N. and Wrucke, C.T., 2001. Detrital zircon provenance of Mesoproterozoic to Cambrian arenites in the western United States and northwestern Mexico. *Geological Society of America Bulletin*, vol. 113, p. 1343-1356.
- Sun, S.S., 1980. Lead isotopic study of young volcanic rocks from mid-ocean ridges, ocean islands, and island arcs. *Philosophical Transactions of the Royal Society*, vol. A297, p. 409-445.
- Sun, S.S. and McDonough, W.F., 1989. Chemical and isotopic systematics of oceanic basalts: Implications for mantle composition and processes. *In: Magmatism in ocean basins*, A. Saunders and M. Norry (eds.), Geological Society of London Special Publication 42, p. 313-345.
- Sun, S.S. and McDonough, W.F., 1995. The composition of the Earth. *Chemical Geology*, vol. 120, p. 223-253.
- Wedepohl, K.H., 1995. The composition of the continental crust. *Geochimica et Cosmochimica Acta*, vol. 59, p. 1217-1232.

Geology and mineral potential of Yukon-Tanana Terrane in the Livingstone Creek area (NTS 105E/8), south-central Yukon

*Maurice Colpron*¹
Yukon Geological Survey

Colpron, M., 2006. Geology and mineral potential of Yukon-Tanana Terrane in the Livingstone Creek area (NTS 105E/8), south-central Yukon. *In: Yukon Exploration and Geology 2005*, D.S. Emond, G.D. Bradshaw, L.L. Lewis and L.H. Weston (eds.), Yukon Geological Survey, p. 93-107.

ABSTRACT

Yukon-Tanana Terrane in the Livingstone Creek area comprises five successions of metasedimentary and metavolcanic rocks which range in age from pre-Upper Devonian to Lower Mississippian. They are correlated with Lower Mississippian and older strata in the Glenlyon and Finlayson Lake areas. Yukon-Tanana rocks are intruded by at least five plutonic suites, ranging in age from Late Devonian to Late Cretaceous. The structural style of the area is dominated by a transposition foliation which is axial planar to isoclinal folds of an earlier foliation. The transposition foliation is itself folded by northeast-verging open folds. The d'Abbadie fault zone, a 1-km-wide zone of imbricate fault slices in the eastern part of the area, is characterized by multiple generations of ductile fabrics overprinted by younger cataclastic breccia zones. Deformation along d'Abbadie fault is in part constrained by syn-tectonic emplacement of a ca. 96 Ma granite pluton along the western margin of the fault zone. Two new showings are reported here: a Pb-Ag vein occurrence and a pyrrhotite skarn. In addition, anomalous Cu-Zn values in graphitic phyllite associated with chloritic schist suggest potential for volcanogenic massive sulphide- (VMS) or hybrid VMS-sedimentary-exhalative-style mineralization in the area.

RÉSUMÉ

Dans la région du ruisseau Livingstone, le terrane de Yukon-Tanana comprend cinq successions de roches méta-sédimentaires et méta-volcaniques dont les âges varient d'avant le Dévonien supérieur au Mississippien inférieur. Ces successions sont corrélées avec des strates d'âge mississippien et plus vieilles des régions de Glenlyon et du lac Finlayson. Les roches de Yukon-Tanana sont recoupées par au moins cinq cortèges plutoniques, dont les âges varient du Dévonien tardif au Crétacé tardif. Le style structural de la région est dominé par une foliation de transposition de plan axial à des plis isoclinaux d'une foliation antérieure. La zone faillée d'Abbadie correspond à une zone d'écaillés imbriquées de plus d'un kilomètre de large dans la partie orientale de la région. Elle est caractérisée par plusieurs générations de fabriques de déformation ductile recoupées par des brèches cataclastiques plus jeunes. La déformation le long de la faille d'Abbadie est en partie datée par la mise en place syn-tectonique d'un pluton de granite datant d'environ 96 million d'années le long de la marge occidentale de la zone faillée. Deux nouveaux indices minéraux sont signalés ici : une veine de quartz plombifère et argentifère, et un skarn à pyrrhotite. De plus, des concentrations anormales en cuivre et en zinc sont signalées dans un phyllade graphiteux associé à un schiste chloriteux, suggérant la possibilité d'une minéralisation en sulfures massifs volcanogènes (SMV) ou de type SMV-SEDEX (sédimentaire exhalatif) hybride dans la région.

¹maurice.colpron@gov.yk.ca

INTRODUCTION

The Livingstone Creek area, 80 km northeast of Whitehorse (Fig. 1), is a placer camp which has seen intermittent mining operations since the 1898 discovery of gold in the area (Bostock and Lees, 1938; Levson, 1992). A lode source for the placer gold remains, however, elusive. Published bedrock geology maps of the area are limited to reconnaissance-scale studies of Bostock and Lees (1938; 1:253 440) and Tempelman-Kluit (1984; 1:250 000 scale). Subsequent studies of the Livingstone Creek and surrounding areas provided more detailed descriptions of the bedrock geology. They primarily focused on the structural evolution of the region (e.g., Hansen, 1989; Harvey *et al.*, 1996; 1997; Gallagher *et al.*, 1998; de Keijzer *et al.*, 1999; Gallagher, 1999; de Keijzer, 2000). Detailed structural and geochronological studies in the Livingstone Creek area were most recently conducted by Harvey *et al.* (1996; 1997) and Gallagher (1999).

The Livingstone Creek area is underlain primarily by metasedimentary and meta-igneous rocks of Yukon-Tanana Terrane (YTT; Figs. 1 and 2). West of the South Big Salmon River, YTT is juxtaposed against late Paleozoic volcanic and sedimentary rocks of the Semenov Block along the Big Salmon fault (Simard, 2003; Simard and Devine, 2003). Interbedded meta-sandstone and meta-argillite of the Loon Lake succession (Barresi, 2004), which crops out southwest of the South Big Salmon River and south of Livingstone fault (Fig. 2), as well as sporadic outcrops of meta-argillite along the flanks of the South Big Salmon valley, are likely part of YTT as well. The eastern part of the Livingstone Creek area is dissected by the north-striking d'Abbadie fault zone (Fig. 2). Meta-sedimentary rocks in the east and northeast part of the area were previously assigned to Cassiar Terrane. For reasons outlined in this paper, I suggest that these rocks are also part of YTT.

Regional studies of YTT have shown that the terrane is composed of a series of mid- to late-Paleozoic arc and back-arc successions built upon a metasedimentary basement of continental margin affinity (Colpron *et al.*, 2006). In the Livingstone Creek area, YTT was previously considered to be only ~10-15 km wide and corresponded to the Teslin Suture Zone of Tempelman-Kluit (1979), a zone of highly strained rocks which were interpreted to have developed in a subduction zone setting during early Mesozoic convergence of Stikinia and North America (e.g., Tempelman-Kluit, 1979; Hansen, 1989; 1992). Subsequent studies of this portion of YTT have shown that ductile deformation features in the Teslin zone are the result of development of an early (late Paleozoic?) transposition foliation, superposed by younger (early Mesozoic?) northeast-verging folds (e.g., de Keijzer *et al.*, 1999; Gallagher, 1999).

Bedrock mapping of the Livingstone Creek area at 1:50 000 scale was undertaken by the Yukon Geological Survey in 2004-2005 to establish the stratigraphic framework of YTT in the area, and to place the Livingstone Creek area within the context of recent studies of YTT in the Finlayson Lake and Glenlyon areas of Yukon (e.g., Colpron *et al.*, 2006; Fig. 1). This study provides the basis for compiling earlier observations made by Gallagher (1999) and unpublished data collected by J.L. Harvey in 1995-1996. This report summarizes observations of YTT geology in the Livingstone Creek area made during the 2005 field season. It builds on preliminary observations reported by Colpron (2005a) and complements the 1:50 000-scale map of the area

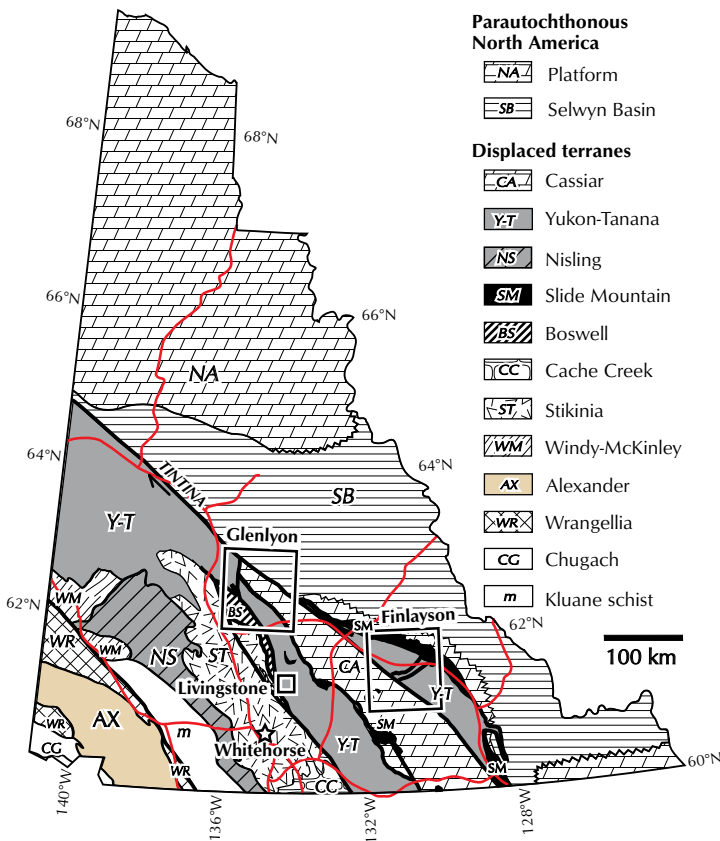


Figure 1. Terrane map of Yukon showing the location of the Livingstone Creek area with respect to the Glenlyon and Finlayson Lake areas (modified after Wheeler *et al.*, 1991).

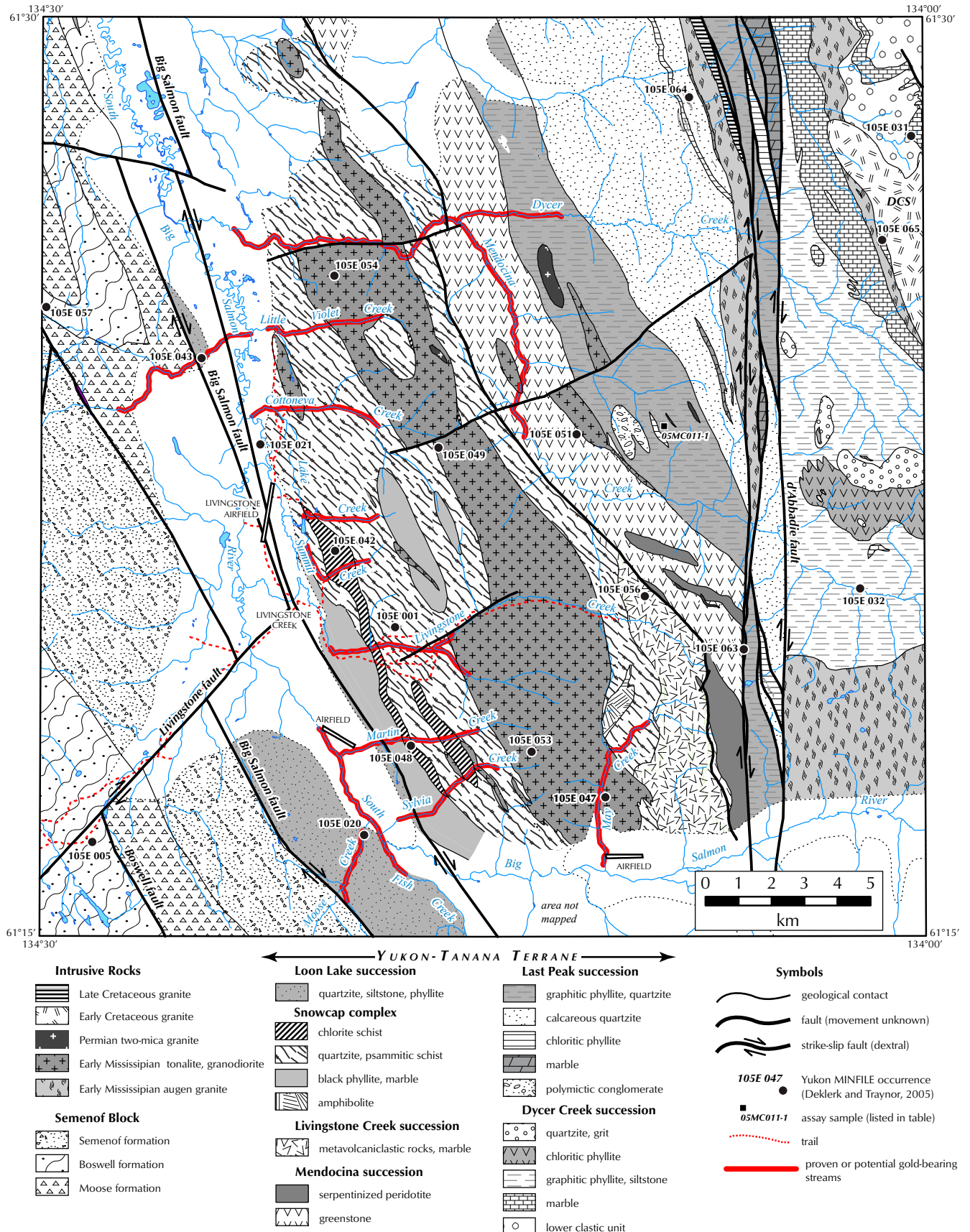


Figure 2. Bedrock geology map of the Livingstone Creek area (simplified from Colpron, 2005b). Placer potential from Lipovsky et al. (2001). DCS = Dycer Creek stock.

(Colpron, 2005b). The following observations are restricted to exposures of YTT to the east and north of the South Big Salmon River. Descriptions of the geology of the Semenof Block and the Loon Lake succession are presented in Simard and Devine (2003), and Barresi (2004), respectively.

YUKON-TANANA TERRANE

Yukon-Tanana Terrane east and north of the South Big Salmon River comprises five successions of metasedimentary and metavolcanic rocks: the Snowcap complex, and the Livingstone Creek, Mendocina, Last Peak and Dycer Creek successions (Fig. 2). These occur in two structural domains separated by d'Abbadie fault. The Dycer Creek succession occurs east of the fault; all other succession occur west of the fault.

SNOWCAP COMPLEX

The Snowcap complex (Colpron *et al.*, 2002, 2003) occupies a northwest-trending belt immediately east of the South Big Salmon River (Fig. 2). It consists predominantly of micaceous quartzite, quartzite and quartz-muscovite-biotite schist, with subordinate amounts of carbonaceous phyllite and schist, calcareous chloritic schist, marble and amphibolite. Carbonaceous phyllite is most abundant in the southwest part of the area, between Sylvia and Summit creeks, where it is locally calcareous; the most prominent marble band in the Snowcap complex occurs within carbonaceous phyllite between Martin and Livingstone creeks (Fig. 2). Carbonaceous phyllite along alpine ridges at the headwater of Lake and Summit creeks is more siliceous.

Chloritic schist of the Snowcap complex occurs along a narrow belt, structurally below the carbonaceous phyllite and extending more than 6 km between Sylvia and Lake creeks. A second, shorter band of chloritic schist is found at higher elevation between Sylvia and Livingstone creeks (Fig. 2). The chloritic schist is light to medium green, fine- to medium-grained and variably siliceous, suggesting a meta-volcaniclastic protolith for this rock. The chloritic schist is locally associated with dolomitic marble. Dark green to black, fine-grained amphibolite of the Snowcap complex is restricted to a few exposures north of May Creek (Fig. 2).

Rocks of the Snowcap complex are intruded by a large body of Early Mississippian tonalite gneiss. The Snowcap complex is therefore constrained to be

Lower Mississippian or older in the Livingstone Creek area. Regionally, the Snowcap complex is constrained to be of pre-Upper Devonian in age (Colpron *et al.*, 2006).

LIVINGSTONE CREEK SUCCESSION

The Livingstone Creek succession (Harvey *et al.*, 1997) is restricted to the southern part of the area, between Livingstone Creek and the South Big Salmon River (Fig. 2). It consists of light green to light grey quartzite, quartz-muscovite-plagioclase-chlorite schist, minor chlorite schist and dolomitic marble (Colpron, 2005a). No new observations of the Livingstone Creek succession were made in 2005. Colpron (2005a) suggested correlation of the Livingstone Creek succession with the Lower Mississippian Little Kalzas formation in the Glenlyon area to the north (Colpron *et al.*, 2002, 2003) on the basis of lithological similarities.

MENDOCINA SUCCESSION

Greenstone of the Mendocina succession (Harvey *et al.*, 1997) forms a 2- to 3-km-wide, northwest-trending belt which generally follows the Mendocina valley in the centre of the map area (Fig. 2). The greenstone is typically fine-grained and phyllitic, rarely massive. Patches of medium- to coarse-grained plagioclase-hornblende-rich greenstone occur sporadically in the finer grained rocks and likely represent dismembered gabbro dykes. Metagabbro is most common in proximity to, and within, the serpentinite bodies. Serpentinite occurs mainly at the southern end of the belt of Mendocina succession, near the d'Abbadie fault, the largest body forming a massif at the headwater of May Creek (Figs. 2 and 3). The rock is bottle-green in colour and soft, although silicification patches within the serpentinite are common. Coarse magnetite commonly occurs within the silicified ultramafic rock.

Marble occurs locally within greenstone of the Mendocina succession, the most prominent exposures being north of Mendocina Creek where marble is associated with calcareous and carbonaceous schist. Carbonaceous schist also occurs sporadically south of Mendocina Creek in proximity with serpentinite bodies.

In the northern part of the area, greenstone of the Mendocina succession is intercalated with a calcareous quartz-muscovite-chlorite-biotite schist of probable volcaniclastic origin. This rock resembles metavolcaniclastic rocks of the Livingstone Creek succession



Figure 3. Looking east at the serpentinite massif (DM_{Mu}) at the headwater of May Creek. Lower ridges in foreground are underlain by meta-volcaniclastic quartzite and phyllite of the Livingstone Creek succession (DM_{LCv}).

suggesting that the Livingstone Creek succession may be a lateral (distal?) facies of the Mendocina succession.

The contact relationships between the Mendocina succession and adjacent map units are difficult to assess due to poor exposures along contacts and the strong transposition fabric which characterizes the area (see Structure and Metamorphism below). Its southwestern contact with the Snowcap complex and Livingstone Creek succession is inferred to be a fault, because of apparent map truncation of these units along the contact (Fig. 2). However, this relationship may prove invalid if the Livingstone Creek succession is indeed a lateral volcanoclastic facies equivalent of the Mendocina greenstone. Between May Creek and the South Big Salmon River, the contact between serpentinite and greenstone of the Mendocina Creek succession and marble of the Livingstone Creek succession is marked by brecciated greenstone suggesting a brittle fault contact (Fig. 4). The northeastern contact with the Last Peak succession is intruded by meta-granodiorite of probable Early Mississippian age north of Mendocina Creek (Fig. 2).

The age of the Mendocina succession is not well constrained. It is apparently intruded by strongly foliated quartz diorite to granodiorite, inferred to be Early Mississippian in age. The felsic schist reported by Colpron (2005a) from the Mendocina succession is here reinterpreted as a dyke intruding the older greenstone; preliminary results of U/Pb analyses on zircon indicate a

Permian age for this rock (S.D. Carr, pers. comm., 2005). Colpron (2005a) suggested that the association of greenstone, meta-gabbro, serpentinite and minor carbonaceous phyllite resembles the Upper Devonian Fire Lake formation of the Finlayson Lake district (Murphy *et al.*, 2001, 2002).

LAST PEAK SUCCESSION

Rocks of the Last Peak succession (Harvey *et al.*, 1997) occupy a south-tapering wedge in the north-central part of the map area, bounded on the east by d'Abbadie fault and on the west by greenstone of the Mendocina succession (Fig. 2). The Last Peak succession consists primarily of two mappable units: (1) a graphitic phyllite and quartzite, which grades easterly into (2) a calcareous quartzite and schist unit. The graphitic phyllite is variably siliceous and locally intercalated with <2-m-thick buff-weathering, dolomitic marble. North of Mendocina Creek, chloritic phyllite is locally intercalated with the graphitic phyllite. Layer-parallel disseminated sulphide (mainly pyrite) horizons and pyrite-malachite veins locally occur in proximity to exposures of chloritic phyllite (see Mineral Potential below).

A distinctive, strongly foliated polymictic pebble metaconglomerate overlies the graphitic phyllite unit at one locality north of Mendocina Creek. The metaconglomerate is poorly sorted and contains clasts of white quartz, dark grey to black phyllite and quartzite, buff- to brown-



Figure 4. Looking south at contact between Mendocina serpentinite ($DMMu$) and greenstone ($DMMv$) and marble of the Livingstone Creek succession ($DMlCm$). Greenstone closest to the contact is brecciated.

weathering marble, and rare felsic metavolcanic rocks, supported by a matrix of arkosic meta-grit (Fig. 5a). Most of the clast compositions are consistent with local derivation for this meta-conglomerate.

Carbonaceous rocks of the Last Peak succession become more siliceous to the east where they pass progressively into a tan-weathering, micaceous and calcareous quartzite. The micaceous quartzite is typically strongly foliated and platy. It is locally intercalated with calcareous quartz-muscovite±chlorite schist, massive black, grey and white quartzite horizons (1-20 m), and minor tan-weathering marble. Thicker (10-30 m) white marble horizons define mappable units along the eastern part of the micaceous quartzite unit. A distinct, brown-weathering silicified grey marble occurs invariably at the contact between micaceous quartzite of the Last Peak succession and Early Mississippian augen granite to the east, wherever this contact has been observed. This unique marble is characterized by abundant dismembered boudins of quartzite which impart a “knobby” appearance to the rock (Fig. 5b).

Resistant, strongly foliated and lineated, siliceous chloritic phyllite defines a continuous band which extends more than 10 km from Dycer Creek northward to the Big Salmon River in the adjacent Teraktu Creek map area (NTS 105E/9; M. Colpron, unpublished map, 2005). The chloritic phyllite is characterized by well-developed, mm-thick laminations of quartzofeldspathic- and epidote-rich layers along the dominant foliation (Fig. 5c). Pyrrhotite and locally magnetite are common constituents of this rock.

The age of the Last Peak succession is only constrained by the Early Mississippian plutons that intrude it. Carbonaceous rocks of the Last Peak succession were originally considered to be part of Cassiar Terrane (Tempelman-Kluit, 1984; Gordey and Makepeace, 2000). They are here considered part of Yukon-Tanana Terrane because they are intruded by calc-alkaline Early Mississippian plutons characteristic of Yukon-Tanana, but unknown in Cassiar Terrane. Based on the abundance of carbonaceous lithologies, the Last Peak succession is most likely correlative with uppermost Devonian-Mississippian strata of Yukon-Tanana Terrane elsewhere in Yukon (e.g., Grass Lakes and Wolverine Lake groups in Finlayson district; Murphy *et al.*, 2006; Colpron *et al.*, 2006). Micaceous quartzite, graphitic phyllite, marble, and siliceous chloritic phyllite and meta-siltstone that occur in fault slivers within the d’Abbadie fault zone are tentatively assigned to the Last Peak succession.

DYCER CREEK SUCCESSION

The Dycer Creek succession (Gallagher, 1999) comprises all metasedimentary rock units east of d’Abbadie fault (Fig. 2). It includes a lower clastic unit in the northeast corner of the map area, overlain by marble, calcareous carbonaceous phyllite, chlorite schist and quartzite. The lower clastic unit comprises coarsely recrystallized pelitic, psammitic and calc-silicate schists, quartzite and marble. Pelitic and psammitic rocks commonly have coarse, post-tectonic andalusite and/or garnet (Fig. 5d), presumably as a result of contact metamorphism imposed by the Early Cretaceous Dycer Creek stock to the south. The



Figure 5. (a) Polymictic meta-conglomerate, Last Peak succession; (b) 'knobby' marble at contact between Last Peak succession and Early Mississippian augen meta-granite; (c) strongly foliated chlorite schist of the Last Peak succession; (d) coarse-grained, post-tectonic andalusite in psammitic schist of the lower clastic unit, Dycer Creek succession, northeast of Dycer Creek stock; (e) finely intercalated tan-weathering quartzite and green chlorite phyllite, Dycer Creek succession north of Mendocina Creek; (f) strongly foliated quartzite in upper part of Dycer Creek succession.

lower clastic unit is intruded by numerous 1- to 3-m-thick sills of augen meta-granite, similar to granite dated as Early Mississippian to the east (ca. 355 Ma; Hansen *et al.*, 1989; Gallagher, 1999). The contact between the lower clastic unit and the overlying marble is everywhere concealed by Early Mississippian and Early Cretaceous granite intrusions in the map area (Fig. 2).

Marble of the Dycer Creek succession forms a prominent marker with an apparent thickness of ~1 km in the northeast corner of the map area (Fig. 6), and also occurs as 1- to 10-m-thick horizons within the lower clastic unit. The marble is typically light grey to white, coarsely recrystallized and locally contains coarse garnet-diopside-epidote-tremolite and skarn-style mineralization (pyrite-pyrrhotite±scheelite) near the Early Cretaceous granite. The marble passes gradationally into black calcareous meta-siltstone and carbonaceous phyllite to the west (Fig. 6), the most extensive unit of the Dycer Creek succession.

A chlorite phyllite unit occurs within the carbonaceous phyllite of the Dycer Creek succession north of Mendocina Creek (Fig. 2). This greenstone unit was previously unrecognized in the area (Tempelman-Kluit, 1977, 1984). It commonly contains up to 2% magnetite octahedrons and corresponds to a magnetic high on the regional aeromagnetic survey (Lowe *et al.*, 1999). The chlorite phyllite is locally intercalated with mm- to cm-scale horizons of carbonaceous phyllite or tan-weathering quartzite (Fig. 5e). The chlorite phyllite is gradationally

overlain by quartzite, the structurally highest unit of the Dycer Creek succession.

Quartzite of the Dycer Creek succession is restricted to ridge-top exposures between Mendocina and Dycer creeks (Fig. 2). It is light greenish-grey, fine- to medium-grained, and typically displays mm- to cm-thick laminations parallel to an early foliation (Fig. 5f). The quartzite is locally gritty and arkosic, and interbedded with recessive grey phyllite.

Preliminary results of U/Pb isotopic analyses of detrital zircons from this unit suggests a primary derivation from a Late Devonian source and recycled Proterozoic and Archean cratonic sources (M. Colpron and G.E. Gehrels, unpublished data, 2005). This detrital zircon data, together with occurrences of ca. 355 Ma granite intruding the lower part of the succession, indicate a Lower Mississippian age for the Dycer Creek succession.

As is the case with the Last Peak succession, rocks of the Dycer Creek succession were previously assigned to Cassiar Terrane (with exception of the quartzite unit which was considered a klippe of Yukon-Tanana Terrane; Tempelman-Kluit, 1977, 1984; Gordey and Makepeace, 2000). These rocks are here re-assigned to Yukon-Tanana Terrane because (1) they are intruded by Early Mississippian granite; (2) they are in part derived from a Late Devonian arc source; and (3) all units have gradational contacts with adjacent units. Carbonaceous phyllite and quartzite of the Dycer Creek succession are probably correlative with similar rocks in the Last Peak



Figure 6. Looking northeast across Dycer Creek at marble (PDC_m) and black phyllite (PDC_p) of the Dycer Creek succession. High ridge in background is underlain by peraluminous Early Cretaceous granite of the Dycer Creek stock (EK_g) which intrudes the metasedimentary rocks and Early Mississippian meta-granite (DM_g).

succession west of d'Abbadie fault. The abundance of carbonaceous rocks and the Lower Mississippian age indicated for this sequence also suggest correlation of the Dycer Creek succession with either the Grass Lakes or the Wolverine Lake groups of the Finlayson Lake district (Murphy *et al.*, 2006; Colpron *et al.*, 2006).

INTRUSIVE ROCKS

At least five distinct suites of plutonic rocks intrude Yukon-Tanana Terrane in Livingstone Creek map area (Fig. 2). These are differentiated on the basis of composition, degree of deformation and age. They range in age from Late Devonian to Late Cretaceous.

The oldest suite includes Late Devonian to Early Mississippian augen meta-granite intruding rocks of the Last Peak and Dycer Creek successions. K-feldspar augen meta-granite, dated at ca. 358 Ma, forms an elongate body stretching more than 19 km along the western edge of d'Abbadie fault zone (Mendocina orthogneiss of Gallagher, 1999). This granite is generally coarse-grained, with K-feldspar augen up to 2 cm long, and is invariably strongly foliated and locally mylonitic (Fig. 7a). Biotite, muscovite, and locally garnet, occur as a metamorphic assemblage within the granite, presumably in part as the result of intrusion of a Late Cretaceous granite along d'Abbadie fault to the east (Last Peak granite of Gallagher, 1999). The western contact of the augen meta-granite with metasedimentary rocks of the Last Peak succession is typically transposed. Another similar augen meta-granite dated at ca. 355 Ma (Hansen *et al.*, 1989; and S.D. Carr, pers. comm., 2003) intrudes the lower clastic unit and marble of the Dycer Creek succession in the northeast corner of the map area. There, augen meta-granite occurs as a narrow tabular body which extends more than 10 km along the eastern contact of the marble unit (Little Lake granite of Gallagher, 1999) and as numerous 1- to 2-m-thick sills concordant with layering and the dominant foliation in the lower clastic unit (Fig. 7b).

Variably foliated K-feldspar porphyritic diorite to granodiorite is exposed in the southeast corner of the map area, between Mendocina Creek and the South Big Salmon River; the granodiorite yielded an imprecise U/Pb zircon age of ca. 369 Ma (Hansen *et al.*, 1989), and is likely, in part, from the same plutonic suite as Early Mississippian augen granites further north. However, as noted in Colpron (2005a), preliminary observations suggest that this body may consist of multiple intrusive

phases, some of which may be related to the Early Cretaceous Quiet Lake batholith.

The largest intrusive body in the Livingstone Creek area consists of strongly foliated and locally gneissic tonalite to granodiorite which intrudes metasedimentary rocks of the Snowcap complex (Fig. 2, Colpron, 2005a). The rock is generally fine-grained and light to medium grey. Hornblende and biotite are common constituents and are locally concentrated in melanocratic bands up to 10 cm wide. Preliminary results of U/Pb analyses on zircons indicate an Early Mississippian age for this body (S.D. Carr, pers. comm., 2005), confirming correlation with the 345-355 Ma Simpson Range plutonic suite (e.g., Mortensen and Jilson, 1985; Colpron, 2005a).

Weakly foliated two-mica granite of Permian age (S.D. Carr, pers. comm., 2005) is a volumetrically small but widespread intrusive suite in the Livingstone Creek area (see Colpron, 2005a). It intrudes meta-tonalite in the Snowcap complex, as well as rocks of the Mendocina and Last Peak successions. The rock is usually white, medium- to coarse-grained and locally pegmatitic. Dykes of two-mica granite are typically 10-20 cm wide (up to 40 cm locally) and concordant with the dominant foliation. The dykes are invariably weakly foliated and locally display pinch-and-swell structures suggesting that the granite was emplaced during development of the dominant foliation.

The Dycer Creek stock, along the northeastern edge of the map area (Fig. 2), consists of medium- to coarse-grained, equigranular two-mica granite dated at ca. 112 Ma (U/Pb zircon, Gallagher, 1999). This granite is undeformed, although a weak mica foliation of magmatic origin is locally developed. Small, euhedral garnet also occurs locally. A contact metamorphic aureole, caused by emplacement of the Dycer Creek stock, extends a few kilometres away from the intrusion. Along its western sides, contact metamorphism is most notable by development of coarse-grained garnet-diopside-epidote skarn mineralogy in marble near the intrusion. Farther west, contact metamorphism is more subtle and expressed by local talc-tremolite assemblage in the marble. Contact metamorphism is more obvious north of the pluton, where coarse-grained garnet-biotite-andalusite assemblage in pelite and psammite (Fig. 5d), and coarse garnet-diopside-epidote skarns in calc-silicate and marble are widespread.

The youngest dated intrusive suite is represented by the ca. 96 Ma granite body which occurs along the western edge of the d'Abbadie fault zone in the northern part of



Figure 7. (a) C-S fabrics and shear band in Early Mississippian augen granite indicate dextral ductile shear along d'Abbadie fault; (b) Early Mississippian augen granite intruding Dycer Creek succession in northeast corner of the map area; (c) Late Cretaceous porphyritic granite (LKg, right) near d'Abbadie fault is less penetratively deformed than Early Mississippian granite (DMg, left); (d) photomicrograph of cataclastic texture in Late Cretaceous granite along d'Abbadie fault. Plane-polarized light. The cataclastic fabric cuts across an earlier ductile foliation, shown along the upper and lower parts of the photo; (e) galena-bearing quartz vein at the RK showing (Yukon MINFILE 105E 064); (f) semi-massive to massive pyrrhotite horizon at the Dycer skarn showing (Yukon MINFILE 105E 065).

the map area (Fig. 2, Last Peak granite of Gallagher, 1999). This pluton extends from near Dycer Creek to north of the Big Salmon River in the adjacent Teraktu Creek map area (NTS 105E/9). It is composed of medium- to coarse-grained, leucocratic K-feldspar porphyritic granite. The rock is variably foliated and locally protomylonitic along its eastern margin. This Late Cretaceous granite clearly intrudes Early Mississippian augen meta-granite and metasedimentary rocks of the Last Peak succession to the west. These latter rocks are more strongly foliated than the ca. 96 Ma granite (Fig. 7c) indicating that the granite was emplaced after part of the ductile strain was acquired by the older rocks. The Late Cretaceous granite imposes a contact aureole (hornfels) which extends more than 1 km to the west. A quartz-plagioclase pegmatite dyke and associated north-northwest-trending quartz veins occur approximately 1 km west of the intrusive contact and are probably related to the Late Cretaceous granite. They are undeformed and cross-cut all fabrics in the country rocks.

Finally, undated monzonite dykes and a small andesite porphyry plug observed in 2004 south of Livingstone Creek are likely related to one of the two Cretaceous intrusive suites.

STRUCTURE AND METAMORPHISM

Rocks of Yukon-Tanana Terrane in the Livingstone Creek area are penetratively deformed by at least three generations of ductile fabrics. Outcrop-scale structures are typically characterized by a pervasive transposition foliation (e.g., Fig. 5c,f) which commonly contains a well-developed elongation lineation. The transposition foliation generally strikes to the northwest and dips moderately to steeply to the southwest or northeast. It is axial planar to tight or isoclinal folds of an earlier foliation or metamorphic layering (*cf.* Colpron, 2005a). These structures control the map pattern west of d'Abbadie fault where lithologic contacts parallel the dominant foliation. East of the fault zone, the map pattern is the result of interference of two phases of non-coaxial tight to isoclinal folds. In this region, primary layering is locally preserved. The dominant foliation is everywhere folded by northeast-verging open folds. Further details of structural styles and evolution of Yukon-Tanana Terrane in the region are presented in Gallagher (1999) and de Keijzer (2000).

Rocks of Yukon-Tanana Terrane in the area are generally metamorphosed to upper greenschist facies (biotite grade). Garnet-grade assemblages (amphibolite facies) are locally present in rocks of the Snowcap complex. In the

southern part of the area, garnet is syntectonic with respect to the transposition foliation and typically partially retrograded to chlorite. North of Mendocina Creek, garnet is post-tectonic, euhedral and fresh, suggesting that this part of the region was subjected to a later thermal event (concealed intrusion?). Garnet-grade assemblages are also developed in the contact aureole of the Cretaceous plutons.

D'ABBADIE FAULT

The north-trending d'Abbadie fault zone is the most striking structural feature in Livingstone Creek map area (Fig. 2). It is an approximately 1-km-wide zone of imbricate fault slices, which run the length of the map area near its eastern edge. It juxtaposes rocks of the Dycer Creek succession on the east against Mendocina and Last Peak successions to the west. The d'Abbadie fault zone is characterized by multiple generations of ductile fabrics and younger brittle structures, all of which are associated with shallow north-plunging stretching lineations (or slickenlines, on brittle fault planes). Ductile deformation along the fault was consistently dextral, as indicated by C-S fabrics (e.g., Fig. 7a), shear bands and rotated porphyroclasts. Mylonitic fabric is best developed in the Early Mississippian augen meta-granite which bounds the d'Abbadie fault zone to the west (Fig. 2). The mylonitic fabric in the augen meta-granite is locally cross-cut by lesser deformed Late Cretaceous granite, suggesting that ductile deformation along d'Abbadie fault began before 96 Ma (Fig. 7c). Development of a protomylonitic fabric along the eastern edge of the Late Cretaceous granite indicates that ductile deformation continued during and after emplacement of this granite. In addition, ductile strain extends more than 1.5 km in rocks west of the d'Abbadie fault zone along the northern half of the map area, where Late Cretaceous granite occurs along the fault; this suggests that heat from the granite facilitated development of ductile fabrics along the fault zone. Faulting continued after cooling of the Late Cretaceous granite as indicated by development of cataclastic breccia (Fig. 7d) and chlorite-coated brittle faults with dextral step-fibres.

Displacement along d'Abbadie fault is poorly constrained. Dextral displacement in the order of ~4 km has been suggested by Harvey *et al.* (1996) on the basis of offset of structural features.

MINERAL POTENTIAL

An estimated 50,000 ounces (1.6 million grams) of gold has been recovered from placers of the Livingstone Creek area since 1898 (W. LeBarge, pers. comm., 2004); however, its lode source remains elusive. The gold typically occurs as coarse (>1 cm) nuggets and is commonly associated with magnetite suggesting a nearby source and potentially a skarn style of mineralization. It is noteworthy that placer streams in the Livingstone camp generally occur around the large Early Mississippian meta-tonalite body that intrudes Snowcap complex in the western part of the area. Skarn-style mineralization associated with this intrusion may represent a lode source for the Livingstone gold. Evidence for skarn development near this intrusion was only locally noted during regional mapping.

Two new showings were discovered during regional mapping in 2005. The RK showing (105E 064, new showings listed here will be added to Yukon MINFILE, Deklerk and Traynor, 2005) consists of galena mineralization in a quartz vein (Fig. 7e). The galena occurs as fine- to medium-grained pods less than 2 cm-wide randomly distributed in the quartz vein. This vein forms part of a system of north-northwest-trending quartz veins that occurs approximately 1 km west of, and parallels, the western edge of d'Abbadie fault zone along the northern part of the area. These veins are typically 2-4 m wide, discontinuous and extend for some 7 km north into the Teraktu map area (NTS 105E/9). Assay results from three grab samples containing galena in quartz returned anomalous values in lead and silver (Table 1, 05MC085-1, -2, -3).

The Dycer showing (Yukon MINFILE 105E 065) corresponds to a 1-m-thick horizon of semi-massive to massive pyrrhotite, which occurs in association with skarn-style mineralogy (garnet-diopside-epidote) in marble of the Dycer Creek succession near the contact with the Early Cretaceous Dycer Creek stock (Fig. 7f). Assay results from four grab samples show anomalous values in copper and lead (Table 1, samples 05MC101-3, 05MC105-1, -2, -3).

Finally, a sample of pyrite-malachite vein (<1 cm wide) was collected near an occurrence of chlorite schist in graphitic phyllite of the Last Peak succession (sample 05MC011-1 on Fig. 2). The graphitic phyllite in the immediate area is commonly rusty weathering and contains disseminated pyrite-pyrrhotite. The assay analysis of this grab sample is anomalous in copper and zinc (Table 1, sample 05MC011-1). Occurrences of

disseminated sulphide minerals in graphitic phyllite near metavolcanic rocks suggest the potential for volcanogenic massive sulphide- (VMS) or hybrid VMS-sedimentary exhalative-style mineralization in the Last Peak succession. Possible correlation of these rocks with the Grass Lakes or Wolverine Lake groups of the Finlayson Lake district further enhances the mineral potential of this unit.

ACKNOWLEDGEMENTS

Reid Kennedy provided assistance in the field. His keen prospecting skills resulted in discovery of two new showings. Don Murphy, Steve Israel and Charlie Roots contributed valuable observations during visits to the area late in the season. Safe and reliable helicopter services were provided Heli Dynamics Ltd. Lee Pigage provided constructive comments on an earlier version of the manuscript.

Table 1. Selected assay results from the Livingstone Creek map area.

Element	05MC011-1 pyrite-malachite vein	05MC085-1 galena in quartz vein	05MC085-2 galena in quartz vein	05MC085-3 galena in quartz vein	05MC101-3 pyrrhotite skarn	05MC105-1 pyrrhotite skarn	05MC105-2 pyrrhotite skarn	05MC105-3 pyrrhotite skarn
Mo (ppm)	0.24	0.65	1.63	0.45	16.22	3.62	1.76	1.5
Cu (ppm)	998.31	35.03	120.53	21.5	1883.65	369.7	1081.17	964.71
Pb (ppm)	13.66	2.03%	7.78%	2.63%	594.64	400.06	68.87	30.22
Zn (ppm)	3132.2	5.8	42.8	3.5	324	40.9	92.9	115.8
Ag (ppb)	535	53 530	108 252	52 468	2912	1315	1586	1456
Ni (ppm)	8.9	5.2	6.5	2.8	7.8	61.5	31	28.9
Co (ppm)	27.1	1.3	2.6	0.6	57.5	92.7	60	48.4
Mn (ppm)	3257	24	812	32	1345	617	1163	1768
Fe (%)	4.83	0.7	1.64	0.6	34.84	36.82	19.33	20.9
As (ppm)	1.4	1.7	<.2	<.2	4.2	0.7	5.8	2
U (ppm)	<.1	0.1	0.6	<.1	1.3	4.2	8.2	3.9
Au (ppb)	15.7	<.100	<.100	<.100	<.100	<.100	<.100	<.100
Cd (ppm)	14.82	4.8	48.93	7.96	1.16	0.17	0.41	0.46
Sb (ppm)	0.07	4.04	10.08	4.56	0.19	0.09	0.11	0.06
Bi (ppm)	0.2	124.06	257.82	130.25	6.86	5.15	2.5	2.2
Cr (ppm)	5.4	6	24	18	8	16	21	11
W (ppm)	<.1	0.1	0.3	<.1	0.2	0.6	50.1	2.7
Zr (ppm)	0.8	2.1	7.6	2.5	3.1	7.7	22.2	11.4
Sn (ppm)	0.1	0.9	2.5	1	1.7	2.5	10.3	3.2
S (%)	0.14	0.48	1.38	0.63	>10	>10	7.86	>10
Y (ppm)	3.99	0.4	19.9	1	2.2	21.3	53.2	34
Ce (ppm)	3	1.13	9.65	0.26	18.66	62.8	97.77	81.36
Hf (ppm)	0.03	0.08	0.22	0.06	0.11	0.28	1	0.38
Li (ppm)	17.5	1.9	2.2	0.3	28	12.5	17.4	28.8
Easting	545490	546228	546228	546228	552213	552047	552047	552047
Northing	6806368	6816345	6816345	6816345	6812029	6812107	6812107	6812107
Yukon MINFILE (Deklerk and Traynor, 2005)		105E 064	105E 064	105E 064	105E 065	105E 065	105E 065	105E 065

Notes: Sample 05MC011-1 was analysed by ICP-MS (inductively coupled plasma mass spectrometry) on a 30-g split digested by aqua regia method; all other samples were analysed by ICP-MS on a 0.25-g split prepared by a 4-acid digestion method. Percent-level analyses for samples 05MC085-1, -2, -3 were analysed by ICP-ES on a 1-g split digested by aqua-regia method. All samples are grabs of mineralized material. All samples analysed at Acme Laboratories in Vancouver, B.C. Coordinates for all samples are given in Universal Transverse Mercator projection, Zone 8v, North American Datum 1983.

REFERENCES

- Barresi, T., 2004. Sedimentology, structure, and depositional setting of the Loon Lake sedimentary rock unit, southern Semenof Hills, central Yukon. Unpublished B.Sc. Honours thesis. Saint Mary's University, Halifax, Nova Scotia, 85 p.
- Bostock, H.S. and Lees, E.J., 1938. Laberge map-area, Yukon. Geological Survey of Canada, Geological map (105E), 1:253 440 scale, and report, 33 p.
- Colpron, M., 2005a. Preliminary investigation of the bedrock geology of the Livingstone Creek area (NTS 105E/8), south-central Yukon. In: Yukon Exploration and Geology 2004, D.S. Emond, L.L. Lewis and G.D. Bradshaw (eds.), Yukon Geological Survey, p. 95-107.
- Colpron, M., 2005b. Geological map of Livingstone Creek area (NTS 105E/8), Yukon (1:50 000 scale). Yukon Geological Survey, Open File 2005-9.
- Colpron, M., Nelson, J.L. and Murphy, D.C., 2006. A tectonostratigraphic framework for the pericratonic terranes of the northern Cordillera. In: Paleozoic Evolution and Metallogeny of Pericratonic Terranes at the Ancient Pacific Margin of North America, Canadian and Alaskan Cordillera, M. Colpron and J.L. Nelson (eds.), Geological Association of Canada, Special Paper 45, in press.
- Colpron, M., Murphy, D.C., Nelson, J.L., Roots, C.F., Gladwin, K., Gordey, S.P. and Abbott, J.G., 2003. Yukon Targeted Geoscience Initiative, Part 1: Results of accelerated bedrock mapping in Glenlyon (105L/1-7, 11-14) and northeast Carmacks (115I/9,16) areas, central Yukon. In: Yukon Exploration and Geology 2002, D.S. Emond and L.L. Lewis (eds.), Exploration and Geological Services Division, Yukon Region, Indian and Northern Affairs Canada, p. 85-108.
- Colpron, M., Murphy, D.C., Nelson, J.L., Roots, C.F., Gladwin, K., Gordey, S.P., Abbott, G. and Lipovsky, P.S., 2002. Preliminary geological map of Glenlyon (105L/1-7, 11-14) and northeast Carmacks (115I/9,16) areas, Yukon Territory (1:125 000 scale). Exploration and Geological Services Division, Yukon Region, Indian and Northern Affairs Canada, Open File 2002-9; also Geological Survey of Canada, Open File 1457.
- de Keijzer, M., Williams, P.F. and Brown, R.L., 1999. Kilometre-scale folding in the Teslin zone, northern Canadian Cordillera, and its tectonic implications for the accretion of the Yukon-Tanana terrane to North America. Canadian Journal of Earth Sciences, vol. 39, p. 479-494.
- de Keijzer, M., 2000. Tectonic evolution of the Teslin zone and the western Cassiar terrane, northern Canadian Cordillera. Unpublished Ph.D. thesis, University of New Brunswick, Fredericton, New Brunswick, 391 p.
- Gallagher, C., Brown, R.L. and Carr, S.D., 1998. Structural geometry of the Cassiar Platform and Teslin zone, Dycer Creek area, Yukon. In: Slave-Northern Cordillera Lithospheric Evolution (SNORCLE) Transect and Cordilleran Tectonic Workshop Meeting, F. Cook and P. Erdmer (eds.), Lithoprobe Report No. 64, p. 139-151.
- Gallagher, C.S., 1999. Regional-scale transposition and late large-scale folding in the Teslin Zone, Pelly Mountains, Yukon. Unpublished M.Sc. thesis, Carleton University, Ottawa, Ontario, 199 p.
- Gordey, S.P. and Makepeace, A.J., 2000. Bedrock geology, Yukon Territory. Exploration and Geological Services Division, Yukon Region, Indian and Northern Affairs Canada, Open File 2001-1; also known as Geological Survey of Canada, Open File 3754, 1:1 000 000 scale.
- Hansen, V.L., 1989. Structural and kinematic evolution of the Teslin suture zone, Yukon: Record of an ancient transpressional margin. Journal of Structural Geology, vol. 11, p. 717-733.
- Hansen, V.L., 1992. Backflow and margin-parallel shear within an ancient subduction complex. Geology, vol. 20, p. 71-74.
- Hansen, V.L., Mortensen, J.K. and Armstrong, R.L., 1989. U-Pb, Rb-Sr, and K-Ar isotopic constraints for ductile deformation and related metamorphism in the Teslin suture zone, Yukon-Tanana terrane, south-central Yukon. Canadian Journal of Earth Sciences, vol. 26, p. 2224-2235.
- Harvey, J.L., Brown, R.L. and Carr, S.D., 1996. Progress in structural mapping in the Teslin suture zone, Big Salmon Range, central Yukon Territory. In: Slave-Northern Cordillera Lithospheric Evolution (SNORCLE) Transect and Cordilleran Tectonic Workshop Meeting, F. Cook and P. Erdmer (eds.), Lithoprobe Report No. 50, p. 33-44.

- Harvey, J.L., Carr, S.D., Brown, R.L. and Gallagher, C., 1997. Deformation history and geochronology of plutonic rocks near the d'Abbadie fault, Big Salmon Range, Yukon. *In: Slave-Northern Cordillera Lithospheric Evolution (SNORCLE) Transect and Cordilleran Tectonic Workshop Meeting*, F. Cook and P. Erdmer (eds.), Lithoprobe Report No. 56, p. 103-114.
- Levson, V., 1992. The sedimentology of Pleistocene deposits associated with placer gold bearing gravels in the Livingstone Creek area, Yukon Territory. *In: Yukon Geology, Exploration and Geological Services Division, Yukon Region, Indian and Northern Affairs Canada, Volume 3*, p. 99-132.
- Lipovsky, P.S., LeBarge, W., Bond, J.D. and Lowey, G., 2001. Yukon placer activity map. Exploration and Geological Services Division, Yukon Region, Indian and Northern Affairs Canada, Open File 2001-30, 1:1 000 000 scale.
- Lowe, C., Kung, R. and Makepeace, A.J., 1999. Aeromagnetic data over Yukon Territory. *In: Yukon digital geology*, S.P. Gordey and A.J. Makepeace (eds.), Exploration and Geological Services Division, Yukon Region, Indian and Northern Affairs Canada, Open File 1999-1(D); also known as Geological Survey of Canada, Open File D3826.
- Mortensen, J.K. and Jilson, G.A., 1985. Evolution of the Yukon-Tanana terrane: evidence from southeastern Yukon Territory. *Geology*, vol. 13, p. 806-810.
- Murphy, D.C., Colpron, M., Roots, C.F., Gordey, S.P. and Abbott, J.G., 2002. Finlayson Lake Targeted Geoscience Initiative (southeastern Yukon), Part 1: Bedrock geology. *In: Yukon Exploration and Geology 2001*, D.S. Emond, L.H. Weston and L.L. Lewis (eds.), Exploration and Geological Services Division, Yukon Region, Indian and Northern Affairs Canada, p. 189-207.
- Murphy, D.C., Mortensen, J.K., Piercey, S.J., Orchard, M.J. and Gehrels, G.E., 2006. Mid-Paleozoic to Early Mesozoic tectonostratigraphic evolution of Yukon-Tanana and Slide Mountain terranes and affiliated overlap assemblages, Finlayson Lake massive sulphide district, southeastern Yukon. *In: Paleozoic Evolution and Metallogeny of Pericratonic terranes at the Ancient Pacific Margin of North America, Canadian and Alaskan Cordillera*, M. Colpron and J.L. Nelson (eds.), Geological Association of Canada, Special Paper 45, in press.
- Murphy, D.C., Colpron, M., Gordey, S.P., Roots, C.F., Abbott, G. and Lipovsky, P.S., 2001. Preliminary bedrock geological map of northern Finlayson Lake area (NTS 105G), Yukon Territory (1:100 000 scale). Exploration and Geological Services Division, Yukon Region, Indian and Northern Affairs Canada, Open File 2001-33.
- Simard, R.-L., 2003. Geological map of southern Semenof Hills (part of NTS 105E/1,7,8), south-central Yukon (1:50 000 scale). Yukon Geological Survey, Open File 2003-12.
- Simard, R.-L. and Devine, F., 2003. Preliminary geology of the southern Semenof Hills, central Yukon (105E/1,7,8). *In: Yukon Exploration and Geology 2002*, D.S. Emond and L.L. Lewis (eds.), Exploration and Geological Services Division, Yukon Region, Indian and Northern Affairs Canada, p. 213-222.
- Tempelman-Kluit, D.J., 1977. Quiet Lake (105F) and Finlayson Lake (105G) map areas, Yukon Territory. Geological Survey of Canada, Open File 486, 1:250 000.
- Tempelman-Kluit, D.J., 1979. Transported cataclasite, ophiolite and granodiorite in Yukon: evidence of arc-continent collision. *Geological Survey of Canada*, 27 p.
- Tempelman-Kluit, D.J., 1984. Geology, Laberge (105E) and Carmacks (105I), Yukon Territory. Geological Survey of Canada, Open File 1101, 1:250 000 scale.
- Wheeler, J.O., Brookfield, A.J., Gabrielse, H., Monger, J.W.H., Tipper, H.W. and Woodsworth, G.J., 1991. Terrane Map of the Canadian Cordillera. Geological Survey of Canada, Map 1713A, 1:2 000 000 scale.

Gold mineralization in the upper Hyland River area: A non-magmatic origin

Craig J.R. Hart¹ and Lara L. Lewis²

Yukon Geological Survey

Hart, C.J.R. and Lewis, L.L., 2006. Gold mineralization in the upper Hyland River area: A non-magmatic origin. *In: Yukon Exploration and Geology 2005*, D.S. Emond, G.D. Bradshaw, L.L. Lewis and L.H. Weston (eds.), Yukon Geological Survey, p. 109-125.

ABSTRACT

Gold occurrences in the upper Hyland River valley form a 50-km-long belt that is considered to be the easternmost portion of the Tombstone Gold Belt (TGB). Mineralization is thought to have a genetic association with nearby Cretaceous plutons, which were important in the formation of most mineralization in the TGB. However, an evaluation of the Hyland River occurrences indicates that evidence supporting an intrusion-related gold model is mostly lacking. Plutons and dykes do not occur in the vicinity of the gold occurrences; there are no obvious zones of hornfels; contact metamorphic minerals and skarns are mostly absent; there is no known mineral or metal zonation typical of intrusion-related systems; and aeromagnetic lows result from massive, variably altered quartz grit and conglomerate and not from unroofed 'low-mag' intrusions. Mineralization consists of four types: 1) disseminated pyrite and arsenopyrite in altered grit; 2) quartz-arsenopyrite veins; 3) quartz-pyrite-galena veins; and, 4) massive arsenopyrite veins. Auriferous quartz veins have characteristics similar to orogenic gold veins, and thus potentially relate to regional metamorphism and large structural features.

RÉSUMÉ

Les occurrences d'or dans la haute vallée de la rivière Hyland sont regroupées en une zone d'une longueur de 50 km que l'on estime être la partie la plus orientale de la ceinture aurifère de Tombstone (CAT). On estime qu'il y a association génétique entre la minéralisation et les plutons d'âge Crétacé adjacents qui ont été importants pour la plupart des minéralisations dans la CAT. Cependant, une évaluation des occurrences de la rivière Hyland révèle plutôt l'absence d'indications à l'appui d'un modèle de formation de l'or relié à l'intrusion. Les plutons et les filons intrusifs ne se trouvent pas à proximité des occurrences d'or; il n'existe aucune zone apparente de cornéennes; les minéraux et skarns du métamorphisme de contact sont principalement absents; il n'y a aucune zonation évidente des minéraux ou des métaux telle que celle qui pourrait exister aux environs d'un pluton; et les creux aéromagnétiques sont attribuables à des grès grossiers quartzeux et des conglomérats massifs diversement altérés plutôt qu'à des intrusions faiblement magnétisées exposées. On trouve quatre types de minéralisation : 1) pyrite et arsénopyrite disséminées dans le grès grossier altéré; 2) veines de quartz et arsénopyrite; 3) veines de quartz, pyrite et galène et 4) veines d'arsénopyrite massive. Les veines de quartz aurifère présentent des caractéristiques similaires à celles des veines d'or orogéniques et pourraient ainsi être reliées au métamorphisme régional et aux grandes entités structurales.

¹*craig.hart@gov.yk.ca*

²*lara.lewis@gov.yk.ca*

INTRODUCTION

Since the discovery of the intrusion-related Fort Knox gold deposit in Alaska in the early 1990s, gold exploration in Yukon has increasingly focused on plutons of mid-Cretaceous age. So prevalent is the association of gold mineralization with mid-Cretaceous intrusions of the Tombstone and Mayo plutonic suites, that it provided the foundation for an intrusion-related gold model that has gained widespread acceptance and application (e.g., Thompson *et al.*, 1999; Lang *et al.*, 2000; Goldfarb *et al.*, 2005). Intrusion-related gold mineralization in Yukon is preferentially concentrated in the Tombstone Gold Belt, which is part of the Tintina Gold Province (Hart *et al.*, 2002), and forms a 550-km-long belt across central Yukon (Fig. 1) that is coincident with the distribution of more than 100 reduced, 'low-mag' plutons. The gold occurrences at the eastern end of the belt are apparently less significant as they have attracted less exploration attention. Most intrusion-related mineralization in this region consists of tungsten skarns related to the Tungsten plutonic suite.

However, exploration, mostly in the late 1990s, resulted in the discovery of several gold occurrences and widespread soil anomalies that together form a 50-km-long, northwest-trending belt of gold occurrences in the upper Hyland River valley in northern NTS mapsheet 105H. Jones and Caulfield (2000) recognized a distinct style of gold mineralization on the Fer property that they interpreted

as a distal style of intrusion-related mineralization that formed 2-3 km above buried intrusions. Additionally, a pronounced, north-trending aeromagnetic low could be interpreted as an unroofed, low-mag, ilmenite-series, or reduced pluton, similar to those that characterize the Tombstone Gold Belt. These and other features have encouraged the use of an intrusion-related gold model as an exploration model for gold in the upper Hyland River valley.

Herein, we evaluate the role that granitoids play in generating gold mineralization in the upper Hyland River valley. In doing so, we also evaluate the regional geological setting of these occurrences and the geological controls on mineralization.

REGIONAL GEOLOGY AND STRATIGRAPHY

The regional geology of the upper Hyland River valley area is poorly understood, having received little attention since the mapping of the Frances Lake (105H) map area in the early 1960s (Blusson, 1966). However, information from more recent mapping to the north (Gordey and Anderson, 1993) and interpretations in Gordey and Makepeace (2003) have been used in conjunction with reconnaissance mapping to present the geological interpretation described below and illustrated in Figure 2. Aeromagnetic images indicate that the region has a moderate response with a distinctive large, south-trending low that is flanked by highs. This feature is discussed later.

Rock distribution is dominated by Neoproterozoic to Lower Cambrian clastic strata with lesser Paleozoic clastic and carbonate strata. Generalized stratigraphic relations between the main units are shown in Figure 3. The region west of the Little Hyland River is largely underlain by Neoproterozoic to lowest Cambrian Hyland Group clastic sedimentary rocks which are divisible into 1) coarse-clastic, quartz-rich grits, conglomerates and quartzites of the dominantly Neoproterozoic Yusezyu Formation, and 2) overlying maroon and green argillites, grey shales and lesser grits and sandstone, of the dominantly Lower Cambrian Narchilla Formation. The Yusezyu Formation is locally dominated by finer grained lithologies, but is characterized by the coarser grained ones. Thin discontinuous limestone horizons occur near the contact between the Yusezyu and Narchilla formations. East of the Hyland River, essentially coeval Neoproterozoic to Lower Cambrian brown and grey siltstone and shale with

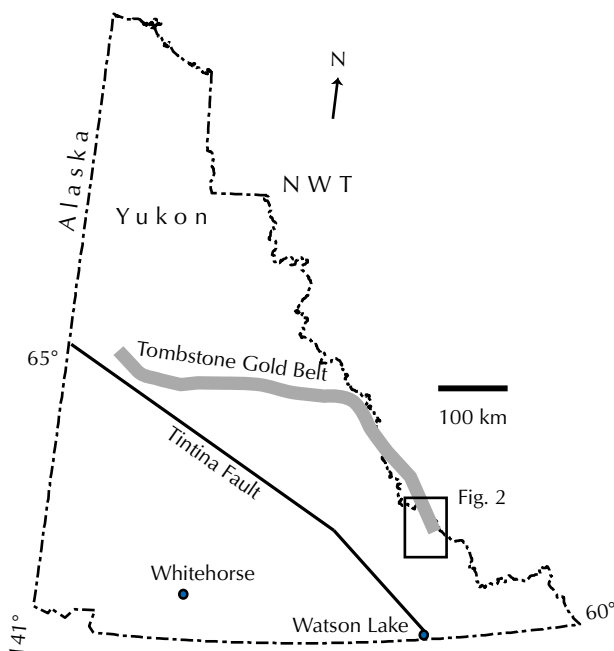


Figure 1. Regional location map of the upper Hyland River study area with respect to the Tombstone Gold Belt.

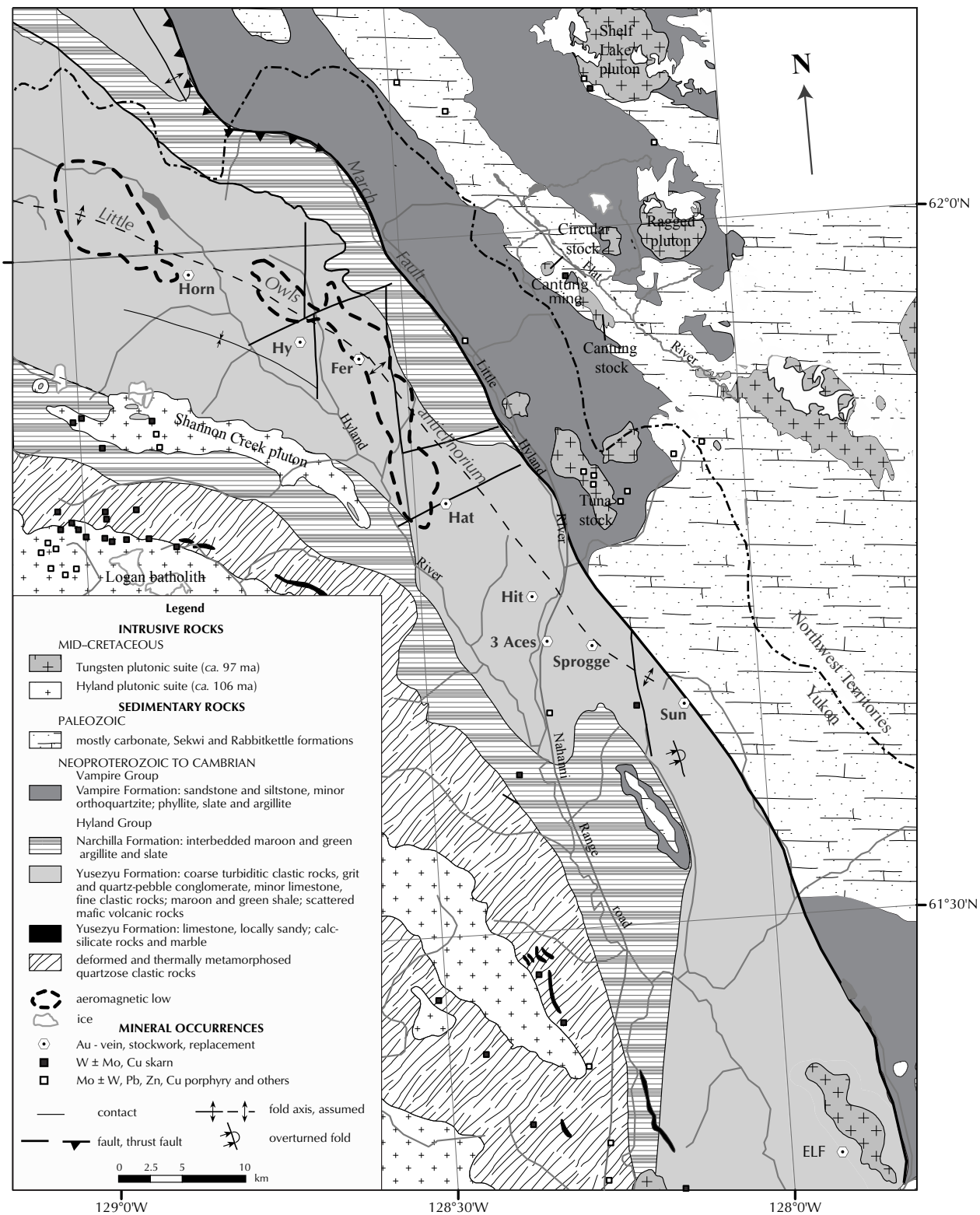


Figure 2. Regional geological and structural map for the upper Hyland River area showing gold properties and other mineral occurrences (after Gordey and Makepeace, 2003). Hyland plutonic suite plutons form a southwestern belt with a tungsten-molybdenum-copper-lead-zinc metal association. Tungsten plutonic suite plutons form an eastern belt with a tungsten-molybdenum-copper association. A central belt lacking intrusions has a gold-arsenic metal association.

fine-grained sandstone are assigned to the Vampire Formation.

Narchilla and Vampire formation strata are locally overlain by orange-brown weathering recessive shale of the Lower to Middle Cambrian, locally archaeocyath-bearing, Gull Lake Formation. Basal Gull Lake Formation limestone-conglomerate and limestone may be equivalent to off-shelf Lower Cambrian Sekwi Formation carbonate which is prevalent east of the Little Hyland River. Yusezyu, Vampire and Gull Lake formations are all unconformably overlain by Upper Cambrian to Lower Ordovician buff-weathering undulose-laminated and locally nodular limestone of the Rabbitkettle Formation. Rabbitkettle Formation is conformably overlain by undifferentiated Road River Group strata. Paleozoic rocks are rare except in the south of the study area and in the Flat River valley.

Significant within the region are the differences in the time-equivalent Neoproterozoic to Middle Cambrian stratigraphy on each side of the Little Hyland River valley (Figs. 2 and 3). Most distinctive are the lithological differences between the essentially time-equivalent Narchilla and Vampire formations, the largest difference being the presence of coarse-clastic strata in the Narchilla Formation. This lithological contrast continues into the Middle Cambrian with differences between the partly co-eval Sekwi and Gull Lake formations. The Sekwi Formation reflects platformal carbonate growth, whereas the Gull Lake Formation records dominantly slope to off-shelf clastic sedimentation. Paradoxically, the Vampire Formation represents a deeper water facies to the east of the contemporaneous Narchilla Formation, whereas Sekwi Formation represents shallow water compared to the Gull Lake Formation. The dramatic facies change across this boundary is best explained by an active structure, which is described later.

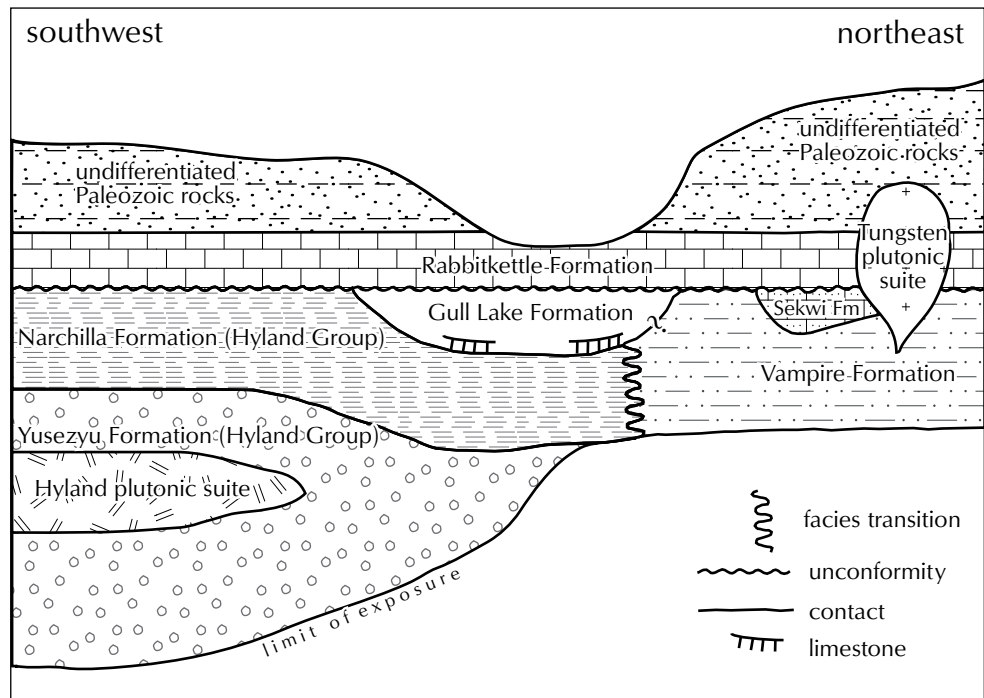


Figure 3. Generalized stratigraphic cross-section for the upper Hyland River area, modified from Gordey and Anderson (1993).

PLUTONIC ROCKS

Two suites of intrusive rocks are recognized in the study area: the Hyland and the Tungsten plutonic suites. The Hyland plutonic suite includes large heterolithic felsic batholiths, located in the southwest of the study area, that have contacts that are concordant with the fabric of the Hyland Group. These include the Logan Mountains and Shannon Creek batholiths (Figs. 2 and 4). The occurrence of the intrusions as thick flat concordant sheets suggests that they were emplaced at mid-crustal levels (~10-15 km). Hyland plutonic suite (introduced by Hart *et al.*, 2004a) includes part of the Anvil plutonic suite of Mortensen *et al.* (2000) and Heffernan *et al.* (2005). Tungsten plutonic suite intrusions include small to medium, circular to irregularly shaped, discordant bodies of generally homogeneous felsic compositions that occur east of the Little Hyland River. Associated plutons include Shelf Lake, Ragged and Tuna stock, as well as the Circular and Cantung stocks, which are associated with tungsten mineralization of the Cantung deposit. These plutons have steep sides and flat tops and were likely emplaced in the upper crustal levels (5-7 km). U-Pb isotopic dating indicates that the Hyland plutonic suite is approximately 106 Ma and the Tungsten plutonic suite is about 97 Ma (Hart *et al.*, 2004a,b, unpublished; Heffernan, 2004). Aeromagnetic imagery indicates moderate to moderately

high responses from Hyland suite plutons and moderate to moderately low responses from Tungsten suite plutons.

STRUCTURAL GEOLOGY

The study area is part of the Selwyn fold belt. Few faults and folds were indicated in previous mapping, and some features described below are newly interpreted from reconnaissance mapping, aeromagnetic data, maps available in assessment reports, or are newly extrapolated from those described to the north by Gordey and Anderson (1993). Regional structural features are shown in Figures 2 and 4.

Regional structural fabric

Most non-igneous rocks have a weak to moderate, northwest-trending, shallowly to moderately steep-dipping fabric. The fabric is defined by phyllitic partings with mica development on foliation surfaces. The intensity of phyllite development is highest in the southwest, proximal to Hyland plutonic suite intrusions, and diminishes to the northeast where slaty cleavage is mostly dominant. The fabric developed in response to deformation that transposed bedding through a series of northeast-verging overturned folds that are locally cut by thrust faults (Fig. 5). Quartz-rich beds of conglomerate, grit and quartzite are mostly undeformed, particularly where massive, but margins are mostly modified by minor faults.

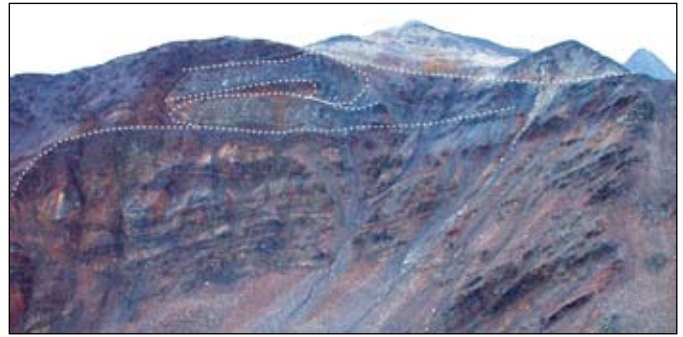


Figure 5. A north-facing ridge on the northern part of the Hy property, where Hyland Group is deformed into a series of moderately shallowly southwest-dipping overturned folds and thrusts, outlined in white.

Smaller units are ‘rolled’ among more ductile argillaceous host rocks. Lineations north of the map area plunge northwesterly (Gordey and Anderson, 1993), whereas those in the study area plunge shallowly to the south and southeast. The timing of fabric formation is uncertain but may be related to the emplacement of the mid-Cretaceous Hyland plutonic suite batholiths, which are similar in age to mid-Cretaceous deformation in the Tombstone strain zone near Mayo (Murphy, 1997; Mair, 2004). East of the Little Hyland River valley, the phyllitic sheen is rarely developed, but slaty cleavage is widely observed.

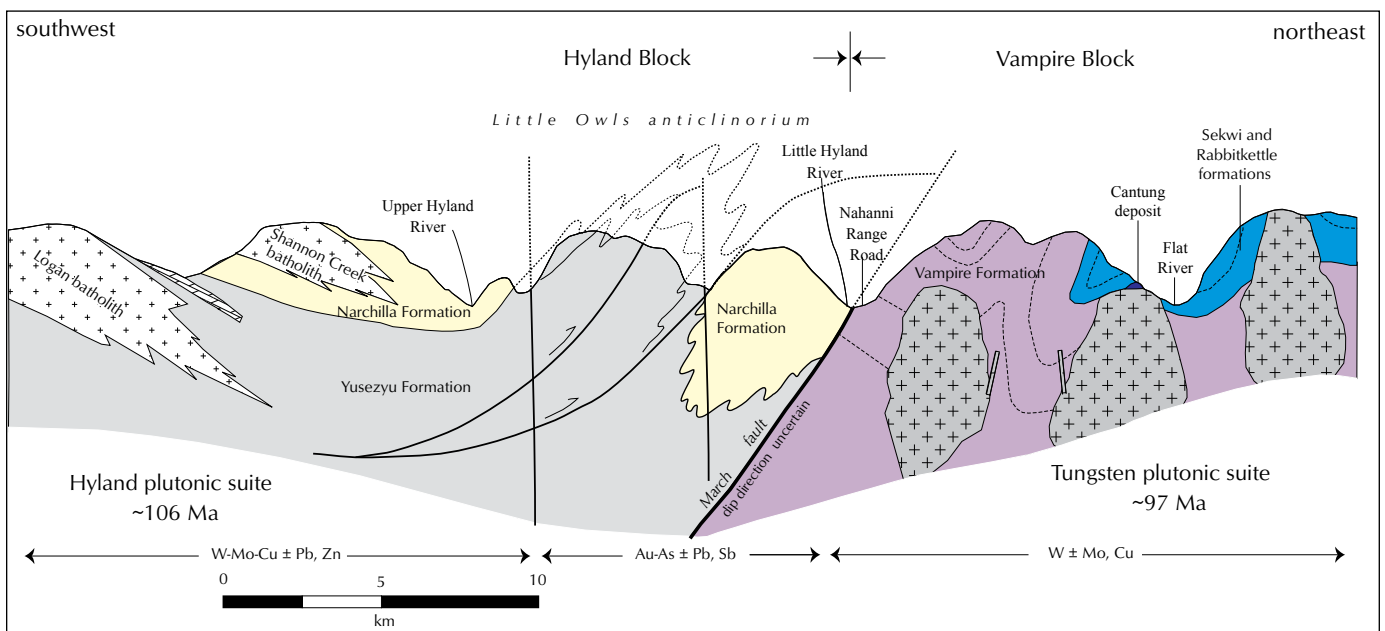


Figure 4. Schematic cross-section of the upper Hyland River valley area near the latitude of the Hy and Fer properties. Vertical scale is exaggerated such that dips are apparently steeper than actual. Late, steep northerly trending faults that cut the area are not shown.

Little Owls anticlinorium

Geological mapping in the upper Hyland River valley indicates that Yusezyu Formation strata, characterized by grits, conglomerates and sandstone, are flanked to the east by Narchilla Formation argillites and shales. Similarly, Narchilla Formation strata occur to the west, near and within the contact aureole of the Hyland plutonic suite. As such, a regional anticlinorium is recognized, and may be the southern extension of the Little Owls anticline (LOA) as defined by Gordey and Anderson (1993). The core of the LOA is mainly a structural culmination of overturned, south-dipping, northeast-verging folds. This feature is about 12 km wide and can be traced for about 70 km.

The structural geometry in this area is, however, complex and confusing. From southwest to northeast, near the latitude of the Hy and Fer occurrences, four structural domains are recognized: 1) a highly deformed package of Yusezyu and Narchilla formation strata proximal to the Hyland plutonic suite batholiths forms a northeast-dipping domain that includes many overturned folds and dips away from the uplifted batholiths; 2) east of the Hyland River valley is a less-deformed package of Yusezyu Formation that is southwest-dipping and also includes many overturned folds; 3) a south-dipping package of weakly deformed Narchilla Formation, with locally overturned beds; and, 4) east of the Little Hyland River valley are mainly northeast-dipping, weakly deformed Vampire Formation rocks.

The nature of the relations between the four domains is uncertain, but the style of deformation indicates that either overturned folds, thrust faults or a combination of both can accommodate the observed patterns. Overturned, potentially thrust anticlines likely generated a structural culmination that resulted in the anticlinorium. Similarly, overturned and thrust south-dipping Yusezyu coarse clastic rocks overlie Narchilla Formation strata and are likely in thrust-contact. A syncline is interpreted to reconcile the dip differences between the first and second domains; however, the northerly dips on the south limb may result from later uplift of the batholiths and not directly relate to fabric development. A syn-deformation backthrust may also accommodate this relationship (A. Fonseca, pers. comm., 2005).

March fault

We propose that a fault underlies the 40-km-long, linear, north-northwest Little Hyland River valley where it juxtaposes purplish and grey (lower?) Narchilla Formation strata with dark brown slates of the (upper?) Vampire Formation. As well, parallel structures are mapped immediately east of the Little Hyland River valley (Blusson, 1968). Differences in the contemporaneous Gull Lake (west) and Sekwi (east) formations also exist across this feature. The present-day, long-linear nature of the feature is characteristic of a large strike-slip fault, but the Neoproterozoic and Cambrian facies variations indicate ancient vertical motion. To the north, in the Nahanni map-area, this fault is mapped as a northeast-vergent thrust that is moderately southwest- to near-vertical-dipping. It places Hyland Group over Cambro-Ordovician Rabbitkettle Formation and Ordovician-Silurian Road River Group, and is termed the March fault (Gordey and Anderson, 1993). In the southern part of the study area, the steeply east-dipping fault is observed east of the Sun property, where Hyland Group strata are juxtaposed with Rabbitkettle and younger carbonate units to the east. In addition, there are differences in the styles of emplacement of nearly coeval plutonic rocks on each side of this feature (see Plutonic Rocks, above), which suggests west-side up displacement. These three apparently different types of offset likely reflect movement on, and reactivation of, the same fault.

We interpret this fault to represent a Neoproterozoic structure that caused the Neoproterozoic and Cambrian facies variations now observed as stratigraphic differences between Hyland Group and Vampire Formation. As well, neither Gull Lake nor Sekwi formations were deposited across this fault, which indicates that it was a facies-controlling structure that was active in the mid-Cambrian (noted by Gordey and Anderson, 1993). Additionally, west-side-up movement along this fault likely resulted from Cretaceous reactivation due to northeast-directed thrusting, as observed to the north and south of the study area (described above). As well, there are different styles and intensities of deformation and fabric development across this structure, which also indicates syn- to post-mid-Cretaceous displacement.

North-trending faults

Numerous small north- and northwest-trending faults cut deformed Hyland Group strata, particularly within rocks of the LOA. As a result, several straight, north-trending valleys are also interpreted to be larger north-trending

faults that have been preferentially downcut by erosion. The nature of the offset is not well known, but is likely normal motion with displacements of less than one kilometre. North-trending structures are also indicated by north-trending veins, north-trending geochemical anomalies, and north-trending lineations. This series of faults cut deformation, but are, in turn, cut by northeast-trending faults.

Northeast-trending faults

The youngest structural elements are northeast- to east-northeast-trending faults. These faults are easily recognized cutting north-trending ridges, and are a dominant control on the orientation of secondary drainages. They offset the general northwest trend of the other geological features, as well as the north-trending structures, which show an apparent dextral offset. To the north, Gordey and Anderson (1993) show similar faults with normal, north-side-down displacements. Offset on these faults is typically less than 1 km.

METALLOGENY

As indicated by Jones and Caulfield (2000), the following three different, intrusion-related metallogenic associations are present in the upper Hyland River valley: (1) a tungsten-molybdenum-copper \pm lead, zinc signature associated with skarns in Hyland Group carbonate rocks adjacent to Hyland plutonic suite batholiths in the western part of the study area; (2) a tungsten \pm molybdenum, copper signature associated with skarns and lesser porphyry-style occurrences in Cambrian calcareous strata near Tungsten plutonic suite plutons in the eastern part of the study area; and (3) a central gold zone with a gold-arsenic \pm lead, antimony metallogenic signature that has no known igneous association.

REGIONAL GEOCHEMISTRY

Regional geochemical stream silt data indicate that the central zone hosts several gold and numerous and widespread arsenic anomalies, but is not particularly well endowed in other metals (Fig. 6; Hornbrook and Friske, 1989). Widespread, moderate tungsten anomalies, weak antimony anomalies, and moderate lead anomalies occur in the south. Gold values in stream silts of >46 ppb are considered highly anomalous (>98 th percentile), although the exploration significance of values 18-46 ppb should not be overlooked, particularly if associated with elevated arsenic. Many of the properties discovered to date have

resulted from follow-up and detailed silt sampling programs that targeted areas identified by the government regional stream sampling program (Hornbrook and Friske, 1989).

HYLAND RIVER GOLD OCCURRENCES

There are six properties within the central Hyland River gold belt that have significant gold values. From north to south, they are the Horn, Hy, Fer, 3 Aces, Sprogge and Sun (Fig. 2). All properties are still in the grassroots exploration stage, with most efforts directed towards prospecting, surface sampling and mapping. The entire belt has seen only 15 diamond drill holes divided among 4 of the properties.

All properties are underlain by uppermost Yusezyu Formation quartz-rich grits, phyllites and shales, locally with thin beds of limestone, and Narchilla Formation phyllite, slate, argillite, wacke and shale with Yusezyu-like grit beds. Locally, the grits are altered and gossanous. Barren quartz veins are abundant throughout the region, occur mainly in extensional zones in brittle quartzose rocks, and were emplaced during regional deformation at some time prior to intrusion of the Hyland plutonic suite intrusions. Mineralization post-dates deformation such that barren quartz veins are overprinted by mineralized ones.

Property descriptions below are compiled from a variety of sources including Yukon MINFILE¹ Yukon mineral assessment reports, press releases and company websites.

Horn

The Horn property was staked following a 1996 stream-silt geochemical sampling program that outlined gold anomalies. A follow-up soil survey on the northern part of the property revealed three apparently north-trending >20 ppb gold-in-soil anomalies that are >200 m long (Buchanan 1999a). One anomaly consists of four samples with values of 141 to 340 ppb Au and up to 300 ppm As. This anomaly is likely continuous with samples from 200 m to the south with values of 390 and 60 ppb Au. The most significant anomaly in the southwestern part of the grid may be >600 m long, is open to the south and west, and has gold values up to 650 ppb, with many >50 ppb, and arsenic values >300 ppm. Bismuth values are all very low (<2 ppm) and have no association with gold.

¹All references to Yukon MINFILE are from Deklerk and Traynor (2005).

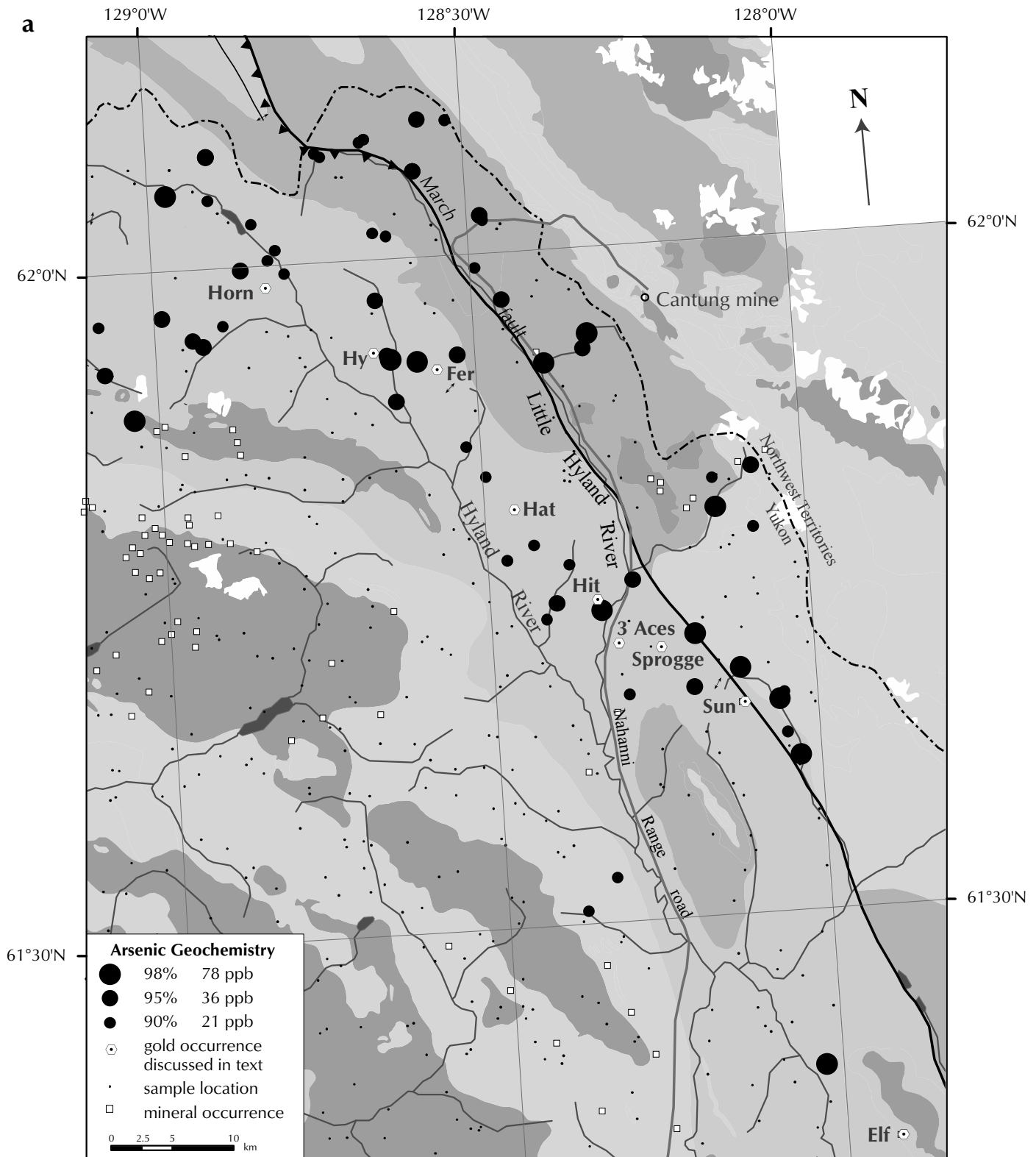


Figure 6. Regional silt stream geochemistry for (a) arsenic and (b) gold for the upper Hyland River valley area. Two separate surveys provide coverage for the area. North of 62° (NTS 105I), samples were analysed using instrumental neutron activation (INA), whereas south of 62° (NTS 105H), samples were analysed using fire assay-neutron activation (FA-NA). The second numbers for percentile cut-offs (46 ppb, 18 ppb and 9 ppb) are those samples analysed by FA-NA. Data north of 62° from Friske et al. (2001) and data south of 62° from Hornbrook and Friske (1989). Geology in background is as in Figure 2.

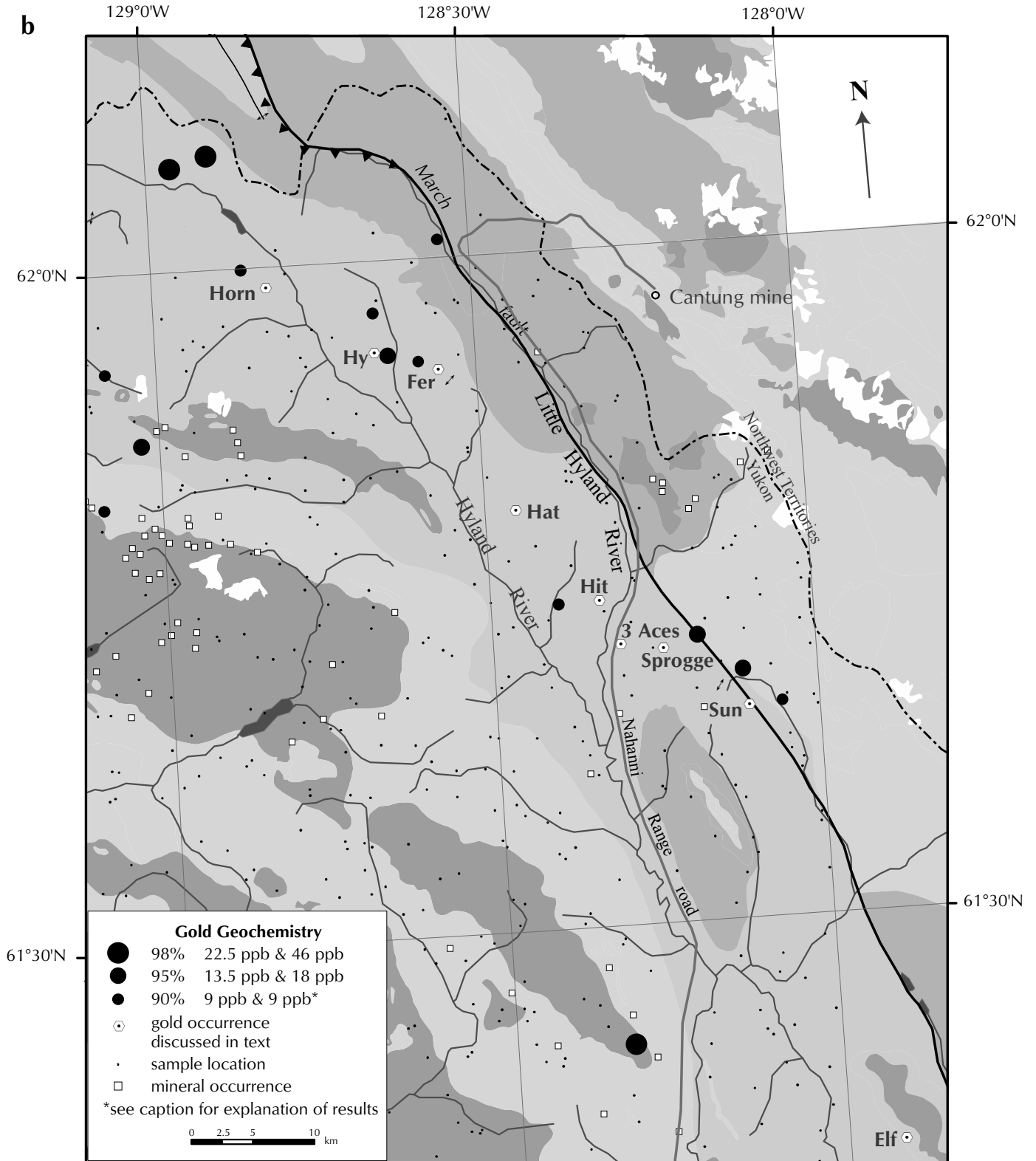


Figure 6. continued, caption on facing page.

Hy (Yukon MINFILE 105H 102 (Fer))

Highly anomalous gold, arsenic and antimony in stream silt samples collected in 1996 encouraged exploration on the Hy property. Three areas contained high-grade gold mineralization associated with strongly anomalous (>50 ppb) gold-arsenic-antimony soil geochemistry (Fox, 1998; Harris, 2000). The 1400 x 100 m West Zone has anomalies in soils up to 909 ppb Au and up to 253 ppm As. Rock samples assayed up to 144.2 g/t Au. Approximately 800 m away, the East Zone is 900 x 350 m and has soil values of up to 1259 ppb Au and 1783 ppm As, and up to 37.6 g/t Au in rock samples from talus. A chip sample of a quartz vein in phyllite obtained from the northeast part of the claims contained 23.05 g/t Au.

Gold mineralization is controlled by north- to northwest-trending, steep westerly dipping faults (Fig. 7). The most important type of mineralization consists of quartz-arsenopyrite veins and stockwork cutting quartzite. Galena and pyrite are common, and visible gold has been observed in a talus sample. Sulphide content generally ranges from a few percent up to 10%; however, higher gold values tend to be associated with higher sulphide contents, particularly arsenopyrite. The quartz veins range from 0.2 cm to 40 cm thick and occur in swarms of up to 5 to 10 veins per metre. Veins are white to grey-blue, massive to ribbon-banded and locally vuggy or with wallrock fragments (Fig. 8). Ribbon-banded veins indicate formation from numerous seismic events and are characteristic of orogenic gold vein deposits (Sibson *et al.*, 1988). Such veins are generally considered to form from metamorphogenic fluids (Groves *et al.*, 2003; Goldfarb



Figure 7. Looking northeast towards the eastern shoulder of the Hy property, where a diamond drill is targeting a north-trending, southwest-dipping structure (dashed line). Note resistant conglomerate (cg). Auriferous soil and rock samples are associated with this structure.

et al., 2005). Muscovite is a sparse but characteristic alteration mineral. Other types of mineralization include quartz veins within shaly horizons, quartz breccias and 'replacement-style' disseminated mineralization within quartzite, and less commonly phyllite, layers.

Fer (Yukon MINFILE 105H 102)

The Fer property was staked in 1996 to cover a cluster of strong stream-silt anomalies. Three mineralized zones were recognized from soil surveys and prospecting, as indicated by Jones and Caulfield (2000). Gold-in-soil anomalies correlate with elevated arsenic and lead; bismuth values are uniformly low. The gold anomalies are primarily associated with thick quartz-rich clastic units and faults. The Southern Grid anomaly is 2 km long and thickens where cut by north-trending faults. Gold-in-soil values are up to 1870 ppb, with three consecutive grid samples averaging 1590 ppb Au; arsenic values are up to 5430 ppm. The 500 x 200 m Northeast Grid soil anomaly is up to 665 ppb Au and overlies mineralization in quartz-rich clastic units near an east-trending fault. Similar but spotty soil anomalies occur in the Camp Cirque area, but the region has heavy talus cover and yields locally exceptional values such as a composite chip sample of bedrock that contains 1970 ppb Au over 8 m (Jones, 1997).

There are widespread indications of mineralization throughout the Fer property, such as large gossanous conglomerate outcrops, alteration of conglomerate, ferricrete gossans, and boxwork after pyrite (Fig. 9). Mineralization consists of stockwork to wide-spaced veins



Figure 8. Ribbon-banded quartz veins separated by graphitic septa. Galena (gn) occurs along some of the septa. The rock is approximately 12 cm across.



Figure 9. Resistant, but altered and limonitic, quartz-grit and conglomerate, with ferricrete and limonitic sludge forming in creek (foreground). Note backpack in the mid-distance for scale, circled.

and fractures that occur in zones with disseminated mineralization and pervasive silicification (Fig. 10). Some linear zones strike 110° . Stockwork with pervasive silicification preferentially forms at contacts between upper conglomerate and phyllite, and between upper conglomerate and limestone (Jones and Caulfield, 2000). Sulphide minerals are widespread but in low concentrations and dominated by disseminated pyrite. Local arsenopyrite and rare galena are observed, but are more common in late quartz veins. Locally, pyrite occurs as bleb-like replacements of up to 10% of rock volume.

Hit (Yukon MINFILE 105H 036 (Road))

Very little public information is available for this property that straddles the Hyland River. Most exploration occurred on the west side of the river, where eight significant >50 ppm gold-in-soil anomalies up to 1500 m long cover areas more than 500×500 m (Buchanan,

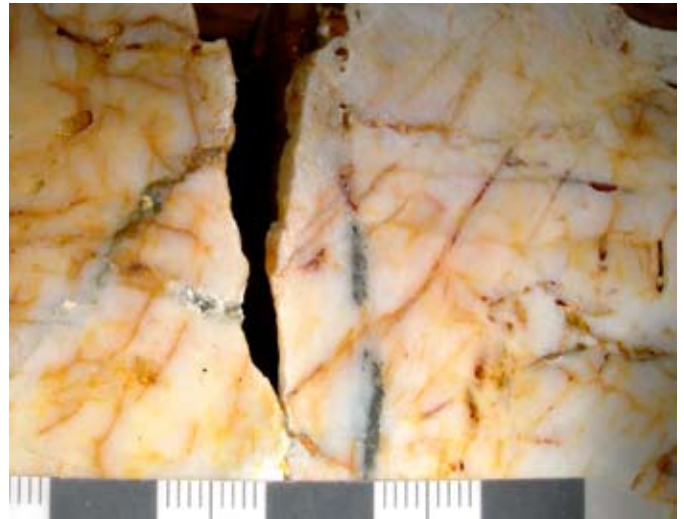


Figure 10. Early white and waxy barren quartz vein cut by later fractures, including a vertical fracture that hosts sulphide minerals (dark grey). Scale is in centimetres.

1999b). Many of the samples are >100 ppb Au, several values are >1000 ppb Au, and one soil value is 5810 ppb Au. The soil anomalies largely correlate with the location of quartzite and grit units. There is no record of rock sampling or geological mapping, but a four-hole diamond drill program (660 m) followed up the soil survey and intersected significant gold mineralization in one hole. Intersections included 4505 ppb Au over 1.5 m, 723 ppb Au over 4.5 m, and 275 ppb Au and 358 ppm As over 44.5 m within arkosic wacke (Buchanan, 2000).

3 Aces (Yukon MINFILE 105H 036 (Road))

This property is contiguous with the Hit property and straddles the Little Hyland River. Two >20 ppb gold-in-soil anomalies, each covering more than 200×200 m, have been outlined to the west of the river (Buchanan 1999c). Samples contained >200 ppb Au, >500 ppm As and anomalous lead. Outcrops hosting mineralization have

been discovered in two locations. One is located near the soil anomalies about 2 km west of the highway. A sample containing visible gold in conglomerate outcrops yielded an assay value reportedly as high as 5400 g/t Au (A. McMillan, pers. comm., 2004). A second zone of mineralization also contained visible gold. Quartz veins have been discovered in the Little Hyland River valley, adjacent to the highway and the river. In particular, north-trending gold veins have been discovered, and exposed beneath overburden, for approximately 6 m in a ditch parallel to the road (A. McMillan, pers. comm., 2004). The host rocks are Hyland Group quartz grits and conglomerates that contain disseminated arsenopyrite. Assay values of up to 30 g/t Au have been reported by the prospector Alex McMillan (pers. comm., 2004).

Sprogge (Yukon MINFILE 105H 103)

The Sprogge property includes the Sugar Bowl prospects, which were discovered following up 1996 regional geochemical stream silt anomalies. The Sugar Bowl consists of numerous mineralized zones within a >2 x 2 km northwest-trending area of gold, arsenic and trace metal values mainly related to quartz-arsenopyrite veins and disseminated quartz and arsenopyrite in altered and gossanous quartz-rich conglomerate and grits (Fig. 11; Scott, 1999). A 1200 x 600 m main area of >200 ppb gold-in-soil values assayed up to 10.3 g/t Au. Additionally, over 50 of the rock chip samples taken along the 2.5-km-long ridge gave multi-gram gold values. Most notably, the Ridge zone hosts the Matilda vein, a 0.4-m-wide variably



Figure 11. Siliciclastic Hyland Group grit from the Sprogge property with disseminated blebs of pyrite and arsenopyrite (dark grey) in the matrix.

oxidized arsenopyrite-in-quartz vein that returned values up to 32.9 g/t Au. The Sheila/KD zone yielded 1.83 g/t Au over a 2-m arsenopyrite-bearing monzonite dyke, but the zone also hosts stockwork or fracture-controlled veining. A 4-km-long northwest-trending gold-in-soil anomaly, with values between 30 and 875 ppb, links the Dayo Creek and Swagman zones. Most of these zones are characterized by high arsenic values. Bismuth is typically low except in highly mineralized samples.

Mineralization is in variably altered and locally quartz-veined coarse clastic grits, siltstone, shale and silty limestone along the hinge of a broad anticline that is cut by east- and northerly trending faults. Four diamond drill holes (762 m) tested a small portion of the lower Sugar Bowl anomaly in late 2000 and, except for a single sample of 705 ppb Au over 0.3 m of brecciated quartz with pyrite and arsenopyrite, failed to intersect values similar to surface samples.

Sun (Yukon MINFILE 105H 015)

This property is the only gold property in the Hyland area recognized prior to 1995. It was discovered in 1964 and drilled in 1988 (four holes for 389 m). Also known as Rain, Snow and Justin, the Sun prospects are at the southern end of the Sprogge property, 9 km from the Sugar Bowl, and consist of a 3000 x 700 m Au-Cu-Bi-As soil and rock anomaly that defines the Main, Confluence and Kangas zones. These showings are described in a Novagold News Release³ and on the Eagle Plains website⁴. The Main Zone consists of a 600 x 250 m area underlain by gently southeast-dipping calc-silicate skarn pods and brecciated phyllite that is proximal to a monzonite dyke. Mineralization consists of abundant pyrrhotite and pyrite that replaces host rocks and chalcopyrite- and arsenopyrite-bearing veins. Chip samples yielded 2.38 g/t Au over 22.5 m and 4.24 g/t Au over 4.5 m. The Confluence Zone consists of 500 m of silicified, limonitic and clay-altered, locally brecciated coarse clastic strata with arsenopyrite and 'chalcedonic-looking' veinlets that returned values of 4.2 g/t Au over 4.5 m in bedrock. Other rock samples assayed up to 15.8 g/t Au. The 400 x 75 m Kangas Zone includes skarn and replacement-style mineralization in calcareous siltstone and widespread anomalous gold including 1375 ppb over 3.5 m and grab samples of up to 3460 ppb. Most high values in the zone are from north-trending fractures and

³Sept. 14, 2000, <http://www2.cdn-news.com/scripts/ccn-release.pl?enews/2000/09/14/45325.html>.

⁴<http://www.eagleplains.ca/yt/sprogge.html>.

shears, and have elevated arsenic and bismuth. Gold-in-soil values on the property correlate best with copper, bismuth and arsenic, but in skarned rocks, gold correlates best with antimony, silver, cadmium and zinc (Scott, 1999).

All zones include calc-silicate skarn pods and andalusite hornfels, and are cut by north-trending monzonite dykes. These features indicate a proximal intrusion; however, it is uncertain if the auriferous mineralization is related to the skarning or to later quartz veins (Scott, 1999). Unlike other properties described herein, the Sun locally hosts significant base-metal mineralization, and samples have returned values of ~0.3% Cu, 0.1% WO₃, 3.1% Pb, 178 g/t Ag and anomalous bismuth.

SUMMARY OF CHARACTERISTICS

Gold-associated mineralization in the upper Hyland River valley is diverse but divisible into a few main types:

- Disseminated pyrite and arsenopyrite in conglomerate;
- Sulphidized 'sheeted' fractures in brittle quartzose sedimentary units and early quartz veins;
- Bleb-like (1-5 cm) sulphide replacement minerals within conglomerate;
- Stockwork quartz veining with a minor sulphide mineral component, in quartzose units;
- Solitary, or widely spaced, quartz-sulphide (either arsenopyrite or pyrite-galena) veins.

Skarn and calc-silicate with sulphide mineral replacement or cross-cutting quartz veining is a feature of the Rain prospects, but is not found elsewhere.

Prominent features typically associated with the first three styles of mineralization include extensive limonitic, and locally jarositic, gossans that are well developed in the resistant conglomerate units. These regions are also typically highlighted by the presence of ferricrete gossans in the valleys and creeks that drain from the conglomerate. Examination of the conglomerate typically indicates boxwork development after pyrite, or limonitic fractures that previously hosted sulphide minerals. Alteration within these conglomerates is widespread. Feldspar clasts are clay-altered and the matrix is altered to fine-grained sericitic fuzzi, probably illite. Quartz-vein-style mineralization is characterized by silicification and local muscovite development.

Weathering of the altered and weakly mineralized conglomerates also generates broad low to moderate (Au >25 ppb) gold and arsenic geochemical anomalies in soil. Quartz-vein-style mineralization yields long, narrow, continuous and high (Au >60 ppb) geochemical anomalies. In addition to arsenic, lead and antimony may be pathfinders to mineralized regions. Bismuth does not correlate with gold, and is typically below 2 ppm.

Three main geological characteristics of this region are responsible for focusing hydrothermal fluids and for precipitating sulphide minerals: (1) the high permeability of coarse-grained clastic sedimentary rocks promotes fluid flow and precipitation of sulphide minerals within these lithologies; (2) the presence of limestone, conglomerate with a dominantly calcareous matrix, and other calcareous sedimentary rocks, which are preferentially reactive lithologies that are susceptible to sulphide mineral replacement and silicification; and (3) the presence of faults that act as conduits for mineralizing fluids. Additionally, deformation preferentially fractures the brittle quartzose conglomerate, grit and quartzite units, and thus further enhances the permeability of these lithologies.

Therefore, three types of potentially economic gold deposits exist: bulk-tonnage low-grade deposits in clastic-sedimentary rocks; high-grade quartz-sulphide veins; and auriferous sulphide replacement deposits in calcareous lithologies. Exploration for large low-grade resources should focus on thick packages of quartzose conglomerate, grit and quartzite. Emphasis should be directed towards high intensity of alteration or high fracture density that may be associated with faulted or fractured margins. Surface exposures underlying gold-in-soil anomalies may appear unmineralized or fail to return anomalous results due to intense weathering and leaching of sulphide minerals. These highly altered quartz-rich conglomerate units may be the cause of the south-trending magnetic lows near the Hy and Fer properties.

Exploration for high-grade quartz sulphide veins should focus on north-trending faults or fractures, particularly where they cut brittle units. The few available observations indicate that these are steep west-dipping features. Consequently, soil or geophysical survey lines, or wildcat drilling, may be most effective in an easterly direction. Locally, very high gold values in soil and rock samples, and the recognition of visible gold, indicates that metallic-type analyses may be required to obtain accurate values for samples with coarse and nuggety gold. East-trending faults are also common features in the region,

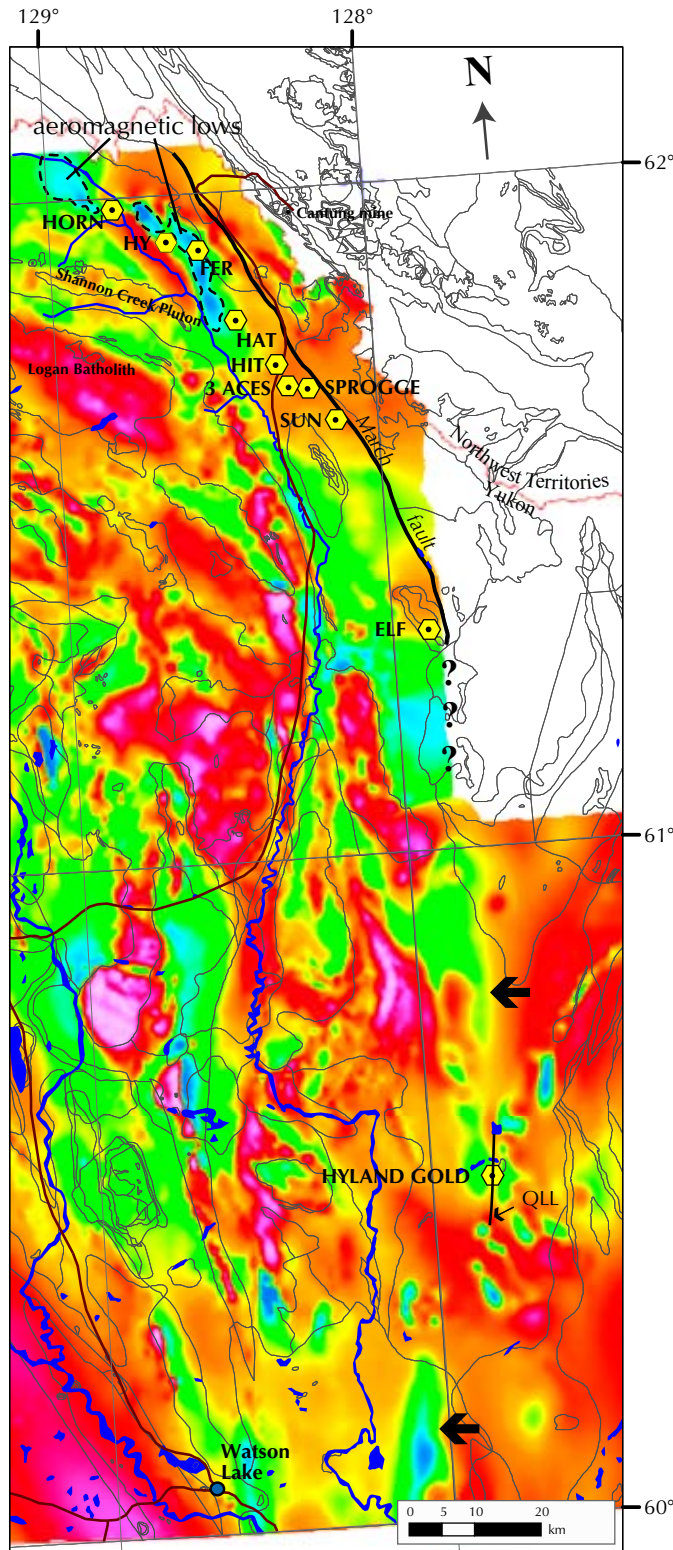


Figure 12. Regional aeromagnetic image⁵ of the Hyland River area with outline of major geological elements and distribution of gold occurrences and deposits. Note the north-trending linear magnetic breaks (shown with arrows) that may be the southerly continuation of the March fault. QLL=Quartz Lake lineament.

and although they appear to cut the north-trending structures, they may also be targets.

Regional mapping indicates that calcareous units occur at the top of the Yusezyu Formation and at the base of the Gull Lake Formation above the Narchilla Formation, and that these horizons should be targeted. However, structural complexities have hindered mapping at more detailed scales, and maps at an optimal scale for exploration are not available. In places where property scale geology maps are available, these calcareous horizons, particularly where underlain by fractured conglomerate, are favourable sites for mineralization.

Igneous rocks, hornfels and calc-silicate rocks were not observed on most properties, and are exposed only west of the Hyland River and east of the March fault, leaving the central gold belt mostly barren of igneous activity. The Hit property has numerous mafic dykes on both sides of the highway (A. Fonseca, pers. comm., 2005), but their association with mineralization is unknown. Felsic dykes, mostly north-trending, are prominent features at only the south end of the Sprogge property (i.e., Sun), where skarn and base metals (copper, tungsten, lead, bismuth, antimony) are present. This is likely the only location within the central gold zone where an unroofed intrusion may exist.

REGIONAL CONSIDERATIONS

The distribution of gold prospects form a northwest-trending belt that is proximal to, parallel to, and always to the west of the dominant structural feature in the area: the March fault. This structure is recognized as locally displaying thrust, normal and strike-slip characteristics, and has been active during Neoproterozoic and Cretaceous times. It appears to be of crustal scale and should have continuity to the north and south. To the north it is beneath Earn Group strata, indicating that most of its activity was pre-Upper Devonian (G. Abbott, pers. comm., 2005). To the south, its distribution is not apparent; however, several features assist in indicating its presence.

The distributions of Hyland Group and Vampire Formation strata as compiled by Gordey and Makepeace (2003) are such that a north-trending contact could separate the two units. As well, there is a prominent, 60-km-long, north-trending linear aeromagnetic break (Fig. 12) that is

⁵<http://www.mapsyukon.gov.yk.ca/webmaps/geoscience/bedrockgeology>. See also http://gdr.agg.nrcan.gc.ca/wms/index_e.html (Canada Geophysical Data Repository, Survey 25902, 25903).

interpreted to continue another 60 km to the Yukon-British Columbia border. Along this southerly anomaly is the Hyland gold deposit, which is a significant pyrite and arsenopyrite mineralized gold system that hosts a near-surface oxide resource of 3.1 Mt of 1.1 g/t Au (Stratagold website⁶, 2005). The deposit is located on the north-trending Quartz Lake lineament. Regional gold- and arsenic-in-silt geochemical data define an approximately 20-km-long, north-trending region of anomalous values (Hornbrook and Friske, 1989) south of the Hyland gold deposit. These observations indicate that not only is there likely a crustal-scale structure along this trend continuous with the March fault, but that it is locally mineralized, and may play a role in controlling the distribution of gold mineralization throughout the region.

EXPLORATION MODEL

Proximity of gold mineralization to a felsic intrusion is a powerful and compelling feature that encourages explorationists to focus on them as exploration targets, and indeed, such is the focus of the intrusion-related gold model that was developed in the Tombstone Gold Belt of the Tintina Gold Province (Lang *et al.*, 2000; Hart *et al.*, 2002). In the absence of an observable intrusion, distal plutonic features such as dykes, hornfels, skarning, contact metamorphic minerals and element zonation can be called upon to support a plutonic association; however, such features are missing from the Horn, Hy, Fer and Hit prospects. Those features are recognized at the Sprogge, and more fully at the Sun, suggesting a proximal pluton, but the role of the magma in forming gold mineralization is not confidently known. In addition, none of the mineralization herein described, except at Sun, is similar to that typically related to the intrusion-related gold model (Lang *et al.*, 2000; Hart *et al.*, 2000, 2002).

Jones and Caulfield (2000) recognized gold mineralization in the Hyland River area as distinct and lacking associated intrusive rocks and hornfels. They interpreted the Fer to represent mineralization that formed distal (4-6 km) to a related intrusion, potentially similar to an origin ascribed to the Telfer deposit in Australia (Rowins *et al.*, 1997). Like Telfer, mineralization at Fer is focused in structural zones in axial planar regions of folds, and preferentially hosted by quartz-rich lithologies.

The lack of evidence for plutonic activity at most of the Hyland River gold prospects makes an intrusion-related model unlikely. The association of mineralization with

north-trending structures, the proximity to a large crustal-scale structure, and the orogenic characteristic of some veins support a non-magmatic origin. Mineralization may instead be related to metamorphogenic fluids focused by the March fault and distributed along second-order, north-trending faults. Such fluids may have been generated in response to regional deformation, prograde metamorphism and generation of melts that formed the Hyland plutonic suite intrusions.

ACKNOWLEDGEMENTS

Conversations with Anna Fonseca about the regional geology and mineralization have been enlightening and informative. Access to the Hy property and discussions with Al Doherty are appreciated. Thanks to Geoff Bradshaw for reviews and critical comments.

REFERENCES

- Blusson, S.L., 1966. Geology, Frances Lake, Yukon Territory and District of Mackenzie. Geological Survey of Canada, Preliminary Map 6-1966, 1:253 440 scale.
- Blusson, S.L., 1968. Geology and tungsten deposits near the headwaters of Flat River, Yukon, and southwest District of Mackenzie, Canada. Geological Survey of Canada, Paper 67-22, 77 p.
- Buchanan, M., 1999a. Assessment Report. Geochemical Survey. Horn Property. Energy, Mines and Resources, Government of Yukon, Assessment Report #094116.
- Buchanan, M., 1999b. Assessment Report, Geochemical Survey of the Hit Property. Energy, Mines and Resources, Government of Yukon, Assessment Report #093975.
- Buchanan, M., 1999c. Assessment Report on Geochemical Survey. 3 Ace Property, Yukon. Energy, Mines and Resources, Government of Yukon, Assessment Report #094077.
- Buchanan, M., 2000. Assessment Report Diamond Drilling Hit Property. Energy, Mines and Resources, Government of Yukon, Assessment Report #094112.
- Deklerk, R. and Traynor, S. (compilers), 2005. Yukon MINFILE 2005. Yukon Geological Survey, CD-ROM.

⁶<http://www.stratagold.com/s/Hyland.asp>

- Fox, P., 1998. Geological and Geochemical report on the Hy group of mineral claims. Energy, Mines and Resources, Government of Yukon, Assessment Report #093913.
- Friske, P.W.B., McCurdy, M.W. and Day, S.J.A., 2001. Regional stream sediment and water geochemical data, eastern Yukon and western Northwest Territories. Geological Survey of Canada, Open File 4016; Exploration and Geological Services Division, Yukon Region, Indian and Northern Affairs Canada, Open File 2001-12(D), CD-ROM.
- Goldfarb, R.J., Baker, T., Dubé, B., Groves, D.I., Hart, C.J.R. and Gosselin, P., 2005. Distribution, Character, and Genesis of Gold Deposits in Metamorphic Terranes. *In: Economic Geology 100th Anniversary Volume.* J.W. Hedenquist, J.F.H. Thompson, R.J. Goldfarb and J.P. Richards (eds.), p. 407-450.
- Gordey, S.P. and Anderson, R.G., 1993. Evolution of the Northern Cordilleran Miogeocline, Nahanni map area (1051), Yukon and Northwest Territories. Geological Survey of Canada, Ottawa, GSC Memoir 428, 214 p.
- Gordey, S.P. and Makepeace, A.J. (compilers), 2003. Yukon Digital Geology (version 2). Yukon Geological Survey, Open File 2003-9(D); also known as Geological Survey of Canada Open File 1749, 2 CD-ROMs.
- Groves, D.I., Goldfarb, R.J., Robert, F. and Hart, C.J.R., 2003. Gold Deposits in Metamorphic Belts: Overview of Current Understanding, Outstanding Problems, Future Research, and Exploration Significance. *Economic Geology*, vol. 98, no. 1, p. 1-29.
- Harris, S., 2000. Geological mapping, prospecting, and soil sampling program on the Hy property. Prepared for Athlone Minerals Ltd. Energy, Mines and Resources, Government of Yukon, Mineral Assessment Report #094146.
- Hart, C.J.R., Baker, T. and Burke, M., 2000. New exploration concepts for country-rock hosted, Intrusion-Related Gold Systems: Tintina Gold Belt in Yukon. *In: The Tintina Gold Belt: Concepts, Exploration and Discoveries*, British Columbia and Yukon Chamber of Mines, Special Volume 2, p. 145-172.
- Hart, C.J.R., McCoy, D.T., Goldfarb, R.J., Smith, M., Roberts, P., Hulstein, R., Bakke, A.A. and Bundtzen, T.K., 2002. Geology, exploration and discovery in the Tintina Gold Province, Alaska and Yukon. *In: Global Exploration 2002: Integrated Methods for Discovery*, E.E. Marsh, R.J. Goldfarb and W.C. Day (eds.), Society of Economic Geologists, p. 25-26.
- Hart, C.J.R., Goldfarb, R.J., Lewis, L.L. and Mair, J.L., 2004a. The Northern Cordillera Mid-Cretaceous Plutonic Province: Ilmenite/Magnetite-Series Granitoids and Intrusion-Related Mineralisation. *Resource Geology*, vol. 54, no. 3, p. 253-280.
- Hart, C.J.R., Villeneuve, M.E., Mair, J.L., Goldfarb, R.J., Selby, D., Creaser R.A. and Wijns, C., 2004b. Comparative U-Pb, Re-Os and Ar-Ar geochronology of mineralizing plutons in Yukon and Alaska. *In: SEG 2004 Predictive Mineral Discovery Under Cover, Extended Abstracts*, J. Muhling et al. (eds.), Perth, Australia, p. 347-349.
- Heffernan, R.S., 2004. Temporal, geochemical, isotopic and metallogenic studies of mid-Cretaceous magmatism in the Tintina Gold Province, southeastern Yukon and southwestern Northwest Territories, Canada. Unpublished MSc thesis, The University of British Columbia, Vancouver, BC, 83 p.
- Heffernan, R.S., Mortensen, J.K., Gabites, J.E. and Sterenberg, V., 2005. Lead isotope signatures of Tintina Gold Province intrusions and associated mineral deposits from southeastern Yukon and southwestern Northwest Territories: Implications for exploration in the southeastern Tintina Gold Province. *In: Yukon Exploration and Geology 2004*, D.S. Emond, L.L. Lewis and G.D. Bradshaw (eds.), Yukon Geological Survey, p. 121-128.
- Hornbrook, E.H.W. and Friske, P.W.B., 1989. Regional stream and water geochemical data, southeast Yukon, Map 105H. Geological Survey of Canada, Open File 1649, 1:500 000 scale.
- Jones, M.I., 1997. Fer Property. 1996 Assessment report, FER 1 to 76 mineral claims, geological mapping and soil sampling surveys, NTS 105H/15. Energy, Mines and Resources, Government of Yukon, Assessment Report 093628.

- Jones, M. and Caulfield, D., 2000. The Fer property: A plutonic-related gold property in southeastern Yukon. *In: Yukon Exploration and Geology 1999*, D.S. Emond and L.H. Weston (eds.), Exploration and Geological Services Division, Yukon Region, Indian and Northern Affairs Canada, p. 229-236.
- Lang, J.R., Baker, T., Hart, C.J.R. and Mortensen, J.K., 2000. An exploration model for intrusion-related gold systems. *Society of Economic Geology Newsletter*, no. 40, p. 1, 6-15.
- Mair, J., 2004. Geology and metallogenic signature of gold occurrences at Scheelite Dome, Tombstone gold belt, Yukon. Unpublished PhD thesis, University of Western Australia, Perth, 197 p., plus appendices.
- Mortensen, J.K., Hart, C.J.R., Murphy, D.C., and Heffernan, S., 2000. Temporal evolution of Early and mid-Cretaceous magmatism in the Tintina Gold Belt. *In: The Tintina Gold Belt: Concepts, Exploration and Discoveries*, British Columbia and Yukon Chamber of Mines, Special Volume 2, p. 49-58.
- Murphy, D.C., 1997. Geology of the McQuesten River Region, Northern McQuesten and Mayo Map Areas, Yukon Territory (115P/14, 15, 16; 105M/13, 14). Exploration and Geological Services Division, Yukon Region, Indian and Northern Affairs Canada, Bulletin 6, 95 p., five 1:50 000-scale maps.
- Rowins, S.M., Groves, D.I., McNaughton, N.J., Palmer, M.R. and Eldridge, C.S., 1997. A re-interpretation of the role of granitoids in the genesis of Neoproterozoic gold mineralization in the Telfer Dome, Western Australia. *Economic Geology*, vol. 92, p. 133-160.
- Scott, E., 1999. 1998 Geological and Geochemical Assessment Report on the Sprogge Project. Prepared for Viceroy Exploration (Canada) Ltd., Energy, Mines and Resources, Government of Yukon, Assessment Report #093959.
- Sibson, R.H., Robert, F. and Poulsen, K.H., 1988. High-angle reverse faults, fluid-pressure cycling, and mesothermal gold-quartz deposits. *Geology*, vol. 16, p. 551 - 555.
- Thompson, J.F.H, Sillitoe, R.H., Baker, T., Lang, J.R. and Mortensen, J.K., 1999. Intrusion-related gold deposits associated with tungsten-tin provinces. *Mineralium Deposita*, vol. 34, p. 323-334.

Unconformity-related uranium potential: Clues from Wernecke Breccia, Yukon

Julie Hunt¹ and Grant Abbott

Yukon Geological Survey

Derek Thorkelson

Simon Fraser University

Hunt, J.A., Abbott, J.G. and Thorkelson, D.J., 2006. Unconformity-related uranium potential: Clues from Wernecke Breccia, Yukon. *In: Yukon Exploration and Geology 2005*, D.S. Emond, G.D. Bradshaw, L.L. Lewis and L.H. Weston (eds.), Yukon Geological Survey, p. 127-137.

ABSTRACT

Unconformity-related uranium deposits are best known from the Athabasca Basin, Canada and the Pine Creek area of Australia. In both regions, fault-controlled mineralization is associated with a regional unconformity between Paleo- to Mesoproterozoic clastic rocks and locally carbonaceous Paleoproterozoic metasedimentary rocks. A similar scenario exists in the Wernecke and Ogilvie mountains of the Yukon where Mesoproterozoic Pinguicula Group strata unconformably overlie Paleoproterozoic Wernecke Supergroup metasedimentary rocks. Uranium occurs in veins that cut Wernecke Supergroup rocks, most notably in association with Wernecke Breccia – a large-scale Paleo- to Mesoproterozoic breccia system. Ages returned by uranium minerals are significantly younger than the ages of the host strata and may be reflecting mobilization of uranium during later tectonic and/or thermal events. The possibility that uranium occurrences in the Wernecke and Ogilvie mountains fit the unconformity model needs to be verified with further study, but is intriguing and raises the possibility that significant deposits may be found.

RÉSUMÉ

Les gisements d'uranium associés à des discordances qui sont les mieux connus sont ceux du bassin d'Athabasca au Canada et de la région de Pine Creek en Australie. Dans ces deux régions, la minéralisation déterminée par les failles est associée à une discordance régionale entre les roches clastiques du Mésoprotérozoïque et les roches métasédimentaires du Paléoprotérozoïque par endroits carbonées. On observe un scénario similaire dans les monts Wernecke-Ogilvie au Yukon où les strates du Groupe de Pinguicula du Mésoprotérozoïque reposent en discordance sur les roches métasédimentaires du Supergroupe de Wernecke (SGW) du Paléoprotérozoïque. L'uranium est présent dans des veines recoupant les roches du SGW et il est des plus remarquablement associé à la brèche de Wernecke – un grand réseau bréchique paléo- à mésoprotérozoïque. Les âges révélés par les minéraux uranifères sont significativement moindres que ceux des strates hôtes et pourraient refléter une mobilisation de l'uranium lors d'événements tectoniques et/ou thermiques ultérieurs. Des études plus poussées sont nécessaires pour vérifier la possibilité d'existence dans les monts Wernecke-Ogilvie d'occurrences d'uranium conformes au modèle de la discordance, mais elle est intrigante et évoque la possibilité de découverte de gisements importants.

¹julie.hunt@gov.yk.ca

INTRODUCTION

Unconformity-type uranium deposits are the highest grade, lowest cost uranium resource in the world (e.g., Jefferson *et al.*, 2003). They are best known from the Athabasca Basin, Canada and the Pine Creek area, Australia (Fig. 1; e.g., Ruzicka, 1995). The mineralization is spatially related to regional tectonic discontinuities and occurs at, or below, a regional unconformity between late Paleoproterozoic to Mesoproterozoic clastic rocks and underlying, locally carbonaceous, Paleoproterozoic metasedimentary rocks (e.g., Ruzicka, 1995; Tourigny *et al.*, 2001). In a generally accepted model, uranium deposition results from the mixing of saline, oxidized, uranium-bearing basinal brines with basement-derived reduced fluid at, or near, the intersection of fault zone(s) with the unconformity (Fig. 1; e.g., Kotzer and Kyser, 1995; Ruzicka, 1995; Fayek and Kyser, 1997).

In the Wernecke and Ogilvie mountains of the Yukon, uranium is hosted by Paleoproterozoic Wernecke Supergroup metasedimentary rocks and ?Paleo- to Mesoproterozoic Wernecke Breccia that are unconformably overlain by Mesoproterozoic Pinguicula Group sedimentary rocks; the Richardson fault array, a long-lived, regional-scale fault system, is located just east of the Wernecke Mountains (Fig. 2; e.g., Abbott, 1997; Thorkelson, 2000). Brannerite and pitchblende in veins and fractures returned U-Pb ages considerably younger than those of the host strata and may be reflecting uranium mobilization during tectonic and/or thermal events (e.g., Archer *et al.*, 1986). This, in turn, suggests that uranium mineralization in the Wernecke and Ogilvie mountains may fit an unconformity-type model, thereby raising the possibility that major deposits may exist in the area.

WERNECKE-OGILVIE MOUNTAINS, YUKON

GEOLOGIC SETTING

The Wernecke and Ogilvie mountains are largely underlain by Paleoproterozoic (>ca. 1710 Ma) rocks of the Wernecke Supergroup (e.g., Delaney, 1985; Abbott, 1997; Thorkelson, 2000). The base of the Supergroup is not exposed but is interpreted to sit on ≥ 1.84 Ga crystalline basement that is the westward continuation of the Canadian shield (e.g., Norris, 1997; Thorkelson, 2000; Thorkelson *et al.*, 2005). A regional-scale breccia system known as Wernecke Breccia cuts the Wernecke Supergroup and hosts iron oxide-copper-gold \pm uranium \pm cobalt (IOCG) mineralization (e.g., Thorkelson, 2000;

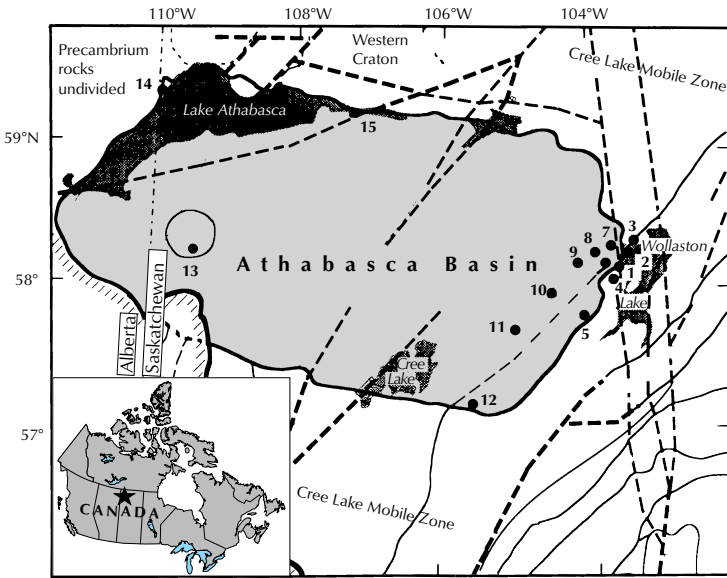
Hunt *et al.*, 2005). Mesoproterozoic strata of the Pinguicula Group unconformably overlie Wernecke Supergroup and Wernecke Breccia (e.g., Abbott, 1997; Thorkelson, 2000).

WERNECKE SUPERGROUP

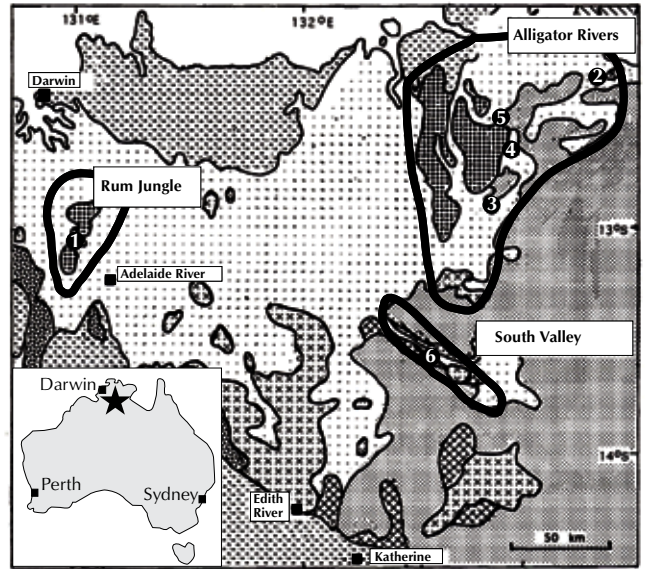
Wernecke Supergroup is approximately 13 km thick, and is made up of the Fairchild Lake, Quartet and Gillespie Lake groups (e.g., Gabrielse, 1967; Delaney, 1981; Bell, 1986a; Thorkelson, 2000). The Fairchild Lake Group forms the basal part of the Wernecke Supergroup and consists of at least a 4-km thickness of siltstone, mudstone, claystone and fine-grained sandstone, plus minor carbonate rocks and evaporites. The Quartet Group gradationally overlies the Fairchild Lake Group, is at least 5 km thick, and consists of basal black carbonaceous shale and conformably overlying, coarsening-upwards, interlayered shale, siltstone and sandstone (Delaney, 1978, 1981). The Gillespie Lake Group gradationally overlies the Quartet Group and forms the upper part of the Wernecke Supergroup. It consists dominantly of locally stromatolitic dolostone and limestone, with lesser claystone, mudstone and sandstone, and is at least 4 km thick. The Wernecke Supergroup was metamorphosed to greenschist facies and multiply deformed during the Paleoproterozoic Racklan Orogeny (e.g., Thorkelson, 2000; Brideau *et al.*, 2002).

Figure 1. (facing page) Location of unconformity-type uranium deposits in the Athabasca Basin and Pine Creek areas plus genetic models for each region. Deposits in the Athabasca Basin include: 1) Rabbit Lake, 2) Collins Bay, 3) Eagle Point, 4) Horseshoe and Raven, 5) West Bear, 6) McClean-Sue, 7) JEB, 8) Dawn Lake, 9) Midwest, 10) Cigar Lake, 11) P2 North, 12) Key Lake, 13) Cluff, Dominique-Janine and Claude, 14) Maurice Bay and 15) Fond du Lac. In the Athabasca Basin, mineralization occurs above, at, and below the regional unconformity. Deposits occur in three areas in the Pine Creek region: Alligator Rivers, South Valley and Rum Jungle; deposits include: 1) Rum Jungle Creek South, 2) Nabarlek, 3) Koongarra, 4) Ranger 1, 5) Jabiluka and 6) Coronation Hill. Mineralization is hosted in rocks below the unconformity. Modified from Ruzicka (1995).

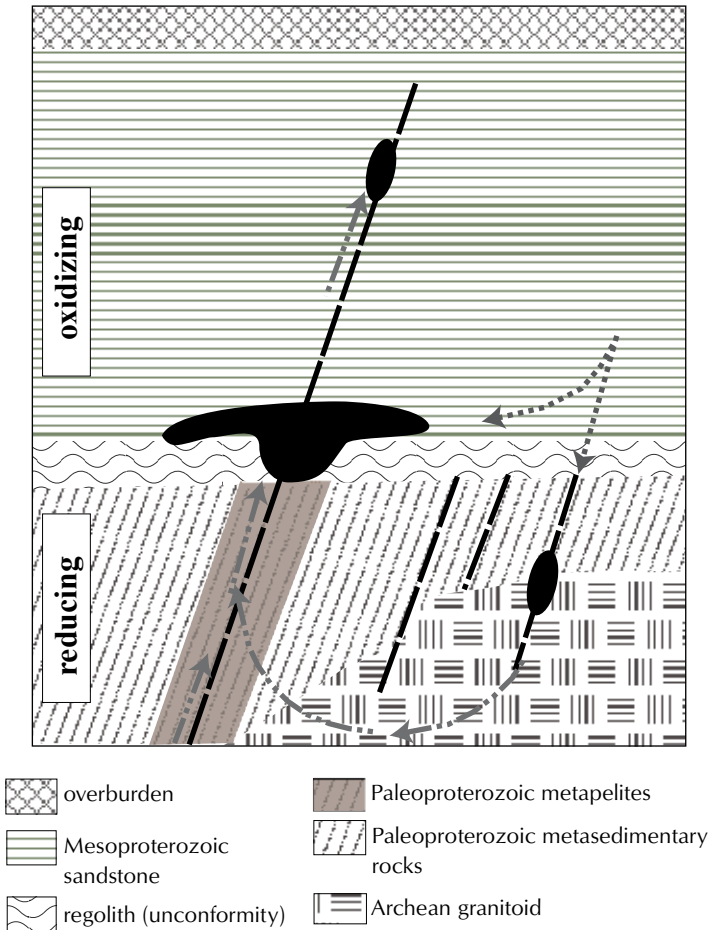
Athabasca Basin



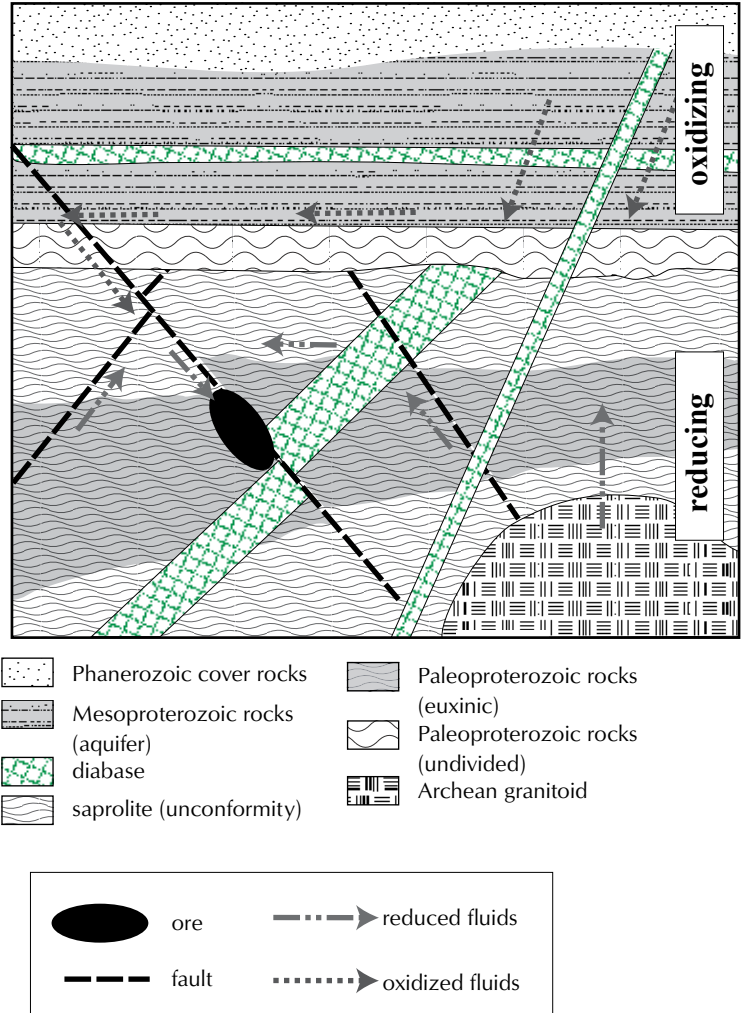
Pine Creek area, Australia



Genetic Model – Athabasca Basin



Genetic Model – Pine Creek area



- overburden
- Mesoproterozoic sandstone
- regolith (unconformity)
- Paleoproterozoic metapelites
- Paleoproterozoic metasedimentary rocks
- Archean granitoid

- Phanerozoic cover rocks
- Mesoproterozoic rocks (aquifer)
- diabase
- saprolite (unconformity)
- Paleoproterozoic rocks (euxinic)
- Paleoproterozoic rocks (undivided)
- Archean granitoid

- ore
- reduced fluids
- oxidized fluids
- fault

Figure 1. (caption on facing page)

WERNECKE BRECCIA

At least 65 bodies of Wernecke Breccia cross-cut the Wernecke Supergroup and are made up largely of clasts of the Supergroup in a matrix of rock flour and hydrothermal precipitates (dominantly quartz, feldspar, carbonate, hematite and magnetite; e.g., Thorkelson 2000; Hunt *et al.*, 2005). The breccias are spatially associated with regional-scale faults and formed in weak and/or permeable zones such as faults, fold axes and lithological contacts during the expansion of over-pressured fluids (e.g., Bell, 1978, 1986a,b; Bell and Delaney, 1977; Thorkelson, 2000; Hunt *et al.*, 2005). Iron oxide-copper (\pm uranium \pm gold \pm cobalt) minerals are

disseminated and occur as veins within the breccia and surrounding Wernecke Supergroup rocks; cross-cutting relationships indicate multiple phases of brecciation and mineralization (e.g., Brookes *et al.*, 2002; Hunt *et al.*, 2002, 2005; Thorkelson *et al.*, 2003; Yukon MINFILE²).

PINGUICULA GROUP

The Pinguicula Group unconformably overlies Wernecke Supergroup and Wernecke Breccia, is about 3500 m thick, and has been divided from base to top into units A, B and C (e.g., Abbott, 1997; Thorkelson, 2000). Conglomerate and locally pyritic sandstone occur at the base of unit A and are overlain by shale and siltstone. The basal

²All Yukon MINFILE references are found in Deklerk and Traynor (2005).

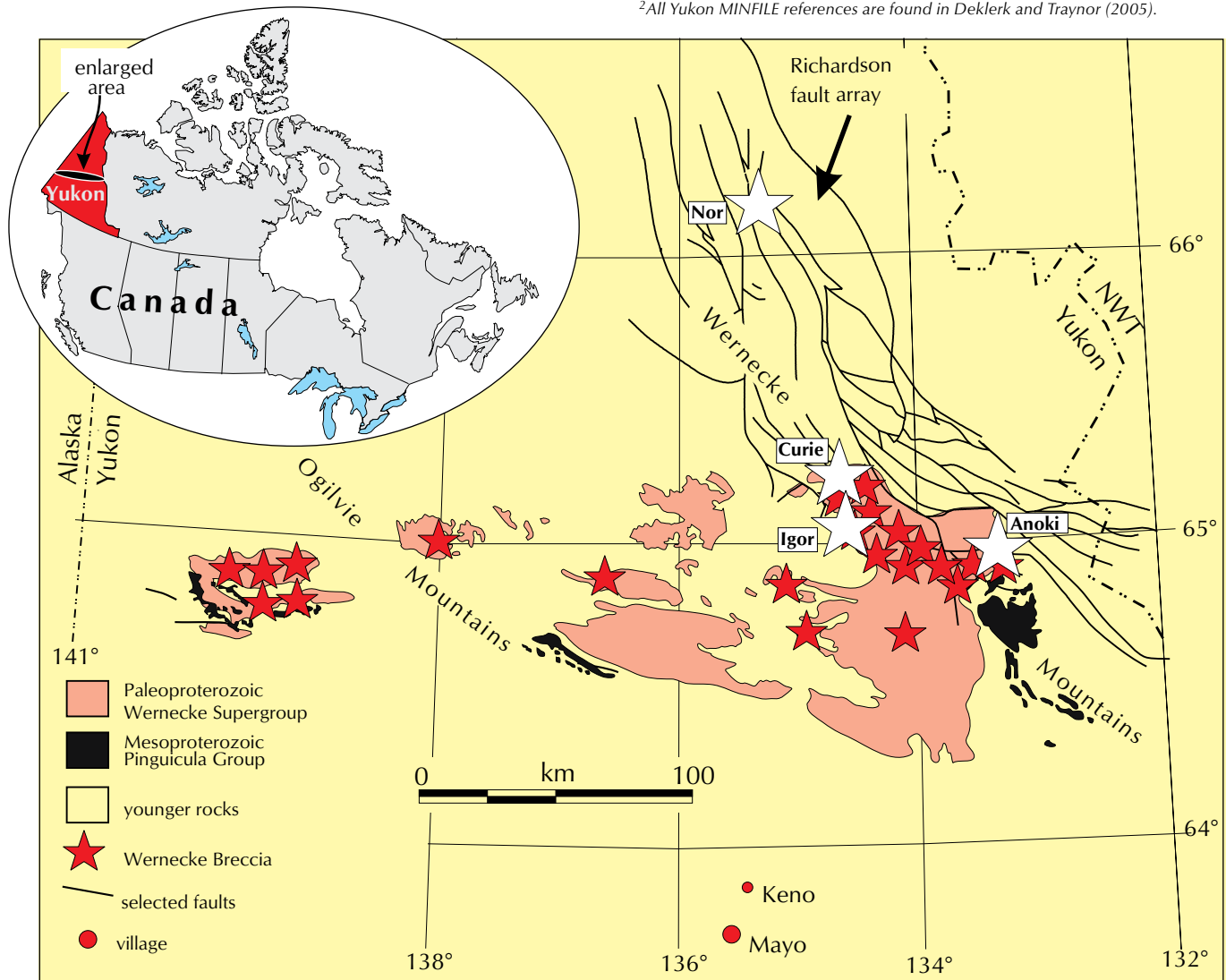


Figure 2. Location of the Wernecke and Ogilvie mountains and the distribution of Wernecke Supergroup, Wernecke Breccia and Pinguicula Group rocks, plus the locations of the Nor, Igor and Anoki mineral occurrences (Yukon MINFILE, Deklerk and Traynor, 2005) and the Curie mineralized area.

conglomerate is dominated by clasts of siltstone, likely derived from Wernecke Supergroup. Clasts of Wernecke Breccia are locally present. Unit B gradationally overlies Unit A and is made up of dolostone, limestone and minor siltstone. Limestone and dolostone of Unit C abruptly to gradationally overlie Unit B.

URANIUM MINERALIZATION

Uranium minerals occur in two distinct styles in the Wernecke and Ogilvie mountains: 1) disseminated in Wernecke Breccia and proximal Wernecke Supergroup strata, and 2) in veins and fractures that cut breccia and the Wernecke Supergroup (e.g., Yukon MINFILE 2005). The disseminated mineralization is likely part of the IOCG mineralizing event that is associated with the formation of Wernecke Breccia. However, the occurrence of mineralization in veins that cross-cut breccia and Wernecke Supergroup, and ages of uranium minerals that are significantly younger than the host strata, suggest later uranium mineralizing events. The ages approximately correspond to those of regional tectonic and/or thermal pulses, indicating uranium may have been mobilized by fluid flow driven by these events (Table 1). The age determinations were derived from pitchblende and brannerite, and it is possible that the U-Pb systematics have been disturbed, and therefore the resulting ages may not represent the timing of uranium mineralization. However, similar minerals were dated in the Athabasca Basin and their ages are interpreted to correspond to three main hydrothermal events, ca. 1500, 950 and 300 Ma, that were identified from clay and other mineral parageneses (e.g., Kotzer and Kyser, 1995; Fayek and Kyser, 1997). Transport of uranium and deposition of ore occurred during the first event. Alteration and remobilization of uranium took place during the second event. Remobilization of uranium, alteration of existing ore, and possible deposition of new ore occurred during the youngest event (e.g., Fayek and Kyser, 1997).

SOURCES OF URANIUM

Sources of uranium that could potentially be mobilized by later fluids occur in Wernecke Supergroup and in Wernecke Breccia. Elevated levels of uranium occur in some Wernecke Supergroup strata, particularly phyllite and siltstone layers in the Fairchild Lake (≤ 40 ppm U) and Quartet (≤ 18 ppm U) groups (Fig. 3; Goodfellow, 1979; Delaney, 1985). Disseminated uranium minerals occur in the matrix of Wernecke Breccia in association with IOCG mineralization (e.g., Bell and Delaney, 1977; Yukon

MINFILE). Additional uranium sources could potentially be present in crystalline basement, however it is not exposed in the region, and the nature and composition of rocks underlying the Wernecke Supergroup remain unknown. Erosion of the above rocks may have contributed uranium to younger sedimentary successions; for example, clasts of Wernecke Supergroup and Wernecke Breccia occur in basal Pinguicula Group conglomerate (Thorkelson, 2000).

YUKON EXAMPLES

Wernecke Supergroup and Wernecke Breccia in the Anoki area (106C 086³) are unconformably overlain by basal Pinguicula Group (Fig. 2; Fig. 32 in Thorkelson, 2000). Results from rock samples collected at varying distances from the contact demonstrate that uranium is concentrated at the unconformity, i.e., U=25.7 ppm 0.2 m above and 0.3 m below the unconformity, and decreases to 4.0 ppm at 3 m below, and to 1.6 ppm at 7 m below the unconformity (Fig. 4). This pattern of enrichment suggests that uranium may have been deposited by fluid flow along the unconformity. Fracture zones from this area also contain uranium, and samples returned up to 0.6% U₃O₈ over 1 m (Stammers and Ikona, 1977). At the nearby Pterd occurrence (106C 069) pitchblende occurs in fractured Quartet Group; samples returned up to 7.67% U₃O₈ and gave ²⁰⁷Pb/²⁰⁶Pb ages of 521-469 Ma (Table 1; Archer *et al.*, 1986; Cash Minerals, 2005⁴).

The Curie area, largely underlain by Quartet Group strata and Wernecke Breccia, covers several MINFILE occurrences (106E 005, 006, 011, 028-031) that consist of disseminated and vein-style uranium mineralization (Fig. 2). Regional geochemical silt (RGS) samples from creeks draining this area returned elevated levels of uranium and rare earth elements (REE) ± silver, gold, cobalt, copper, nickel, tungsten, manganese, arsenic (Table 2; Hornbrook *et al.*, 1990) — a similar suite of elements to those enriched in unconformity-type deposits in the Athabasca Basin and Pine Creek region (e.g., Ruzicka, 1995). A boulder collected recently from a trench in the Curie area (Fig. 2) contained 54.3% U₃O₈ (Signet Minerals Inc., 2005⁵). Samples of brannerite

³Numbers in brackets refer to Yukon MINFILE. See Yukon Geological Survey website <http://www.geology.gov.yk.ca/minfile/index.html> for on-line access to occurrence descriptions or Deklerk and Traynor (2005) for a published version.

⁴For results from Lumina (Pterd) and Igor, see Cash Minerals website <http://www.cashminerals.com/s/Uranium.asp?ReportID=103562>.

⁵Signet Minerals Inc. News release 2005-10-26 "Signet Minerals finds 54.3% U₃O₈ in Curie grab sample."

Table 1. Comparison of age dates with tectonic and thermal events and suggested correlation of Proterozoic successions in the Wernecke, Ogilvie and Mackenzie mountains, and the western Arctic. Modified from Thorkelson (2000). Data in the age date column is from Archer et al. (1986). Fm = formation, Gp = Group, S.Gp = Supergroup.

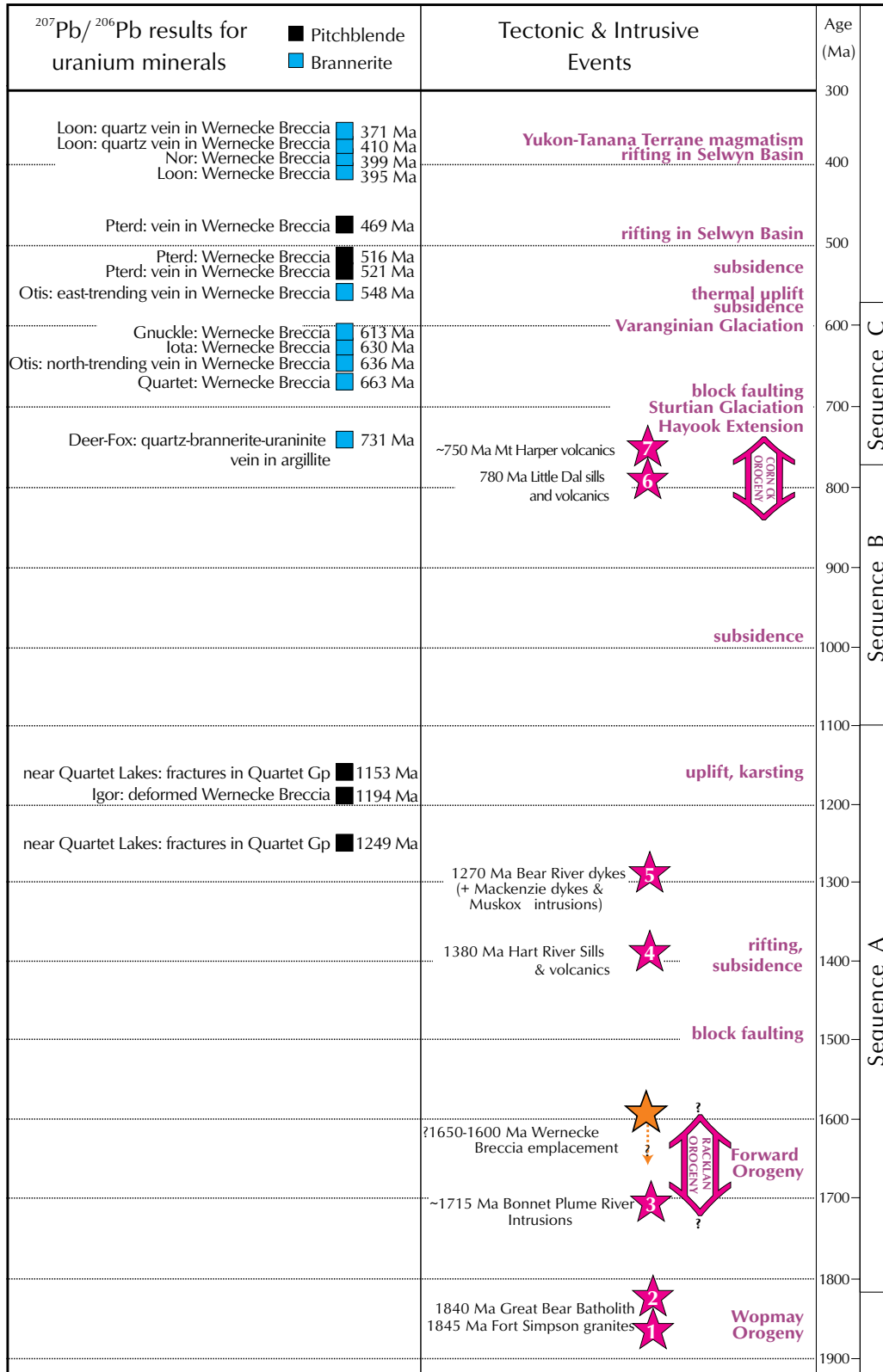
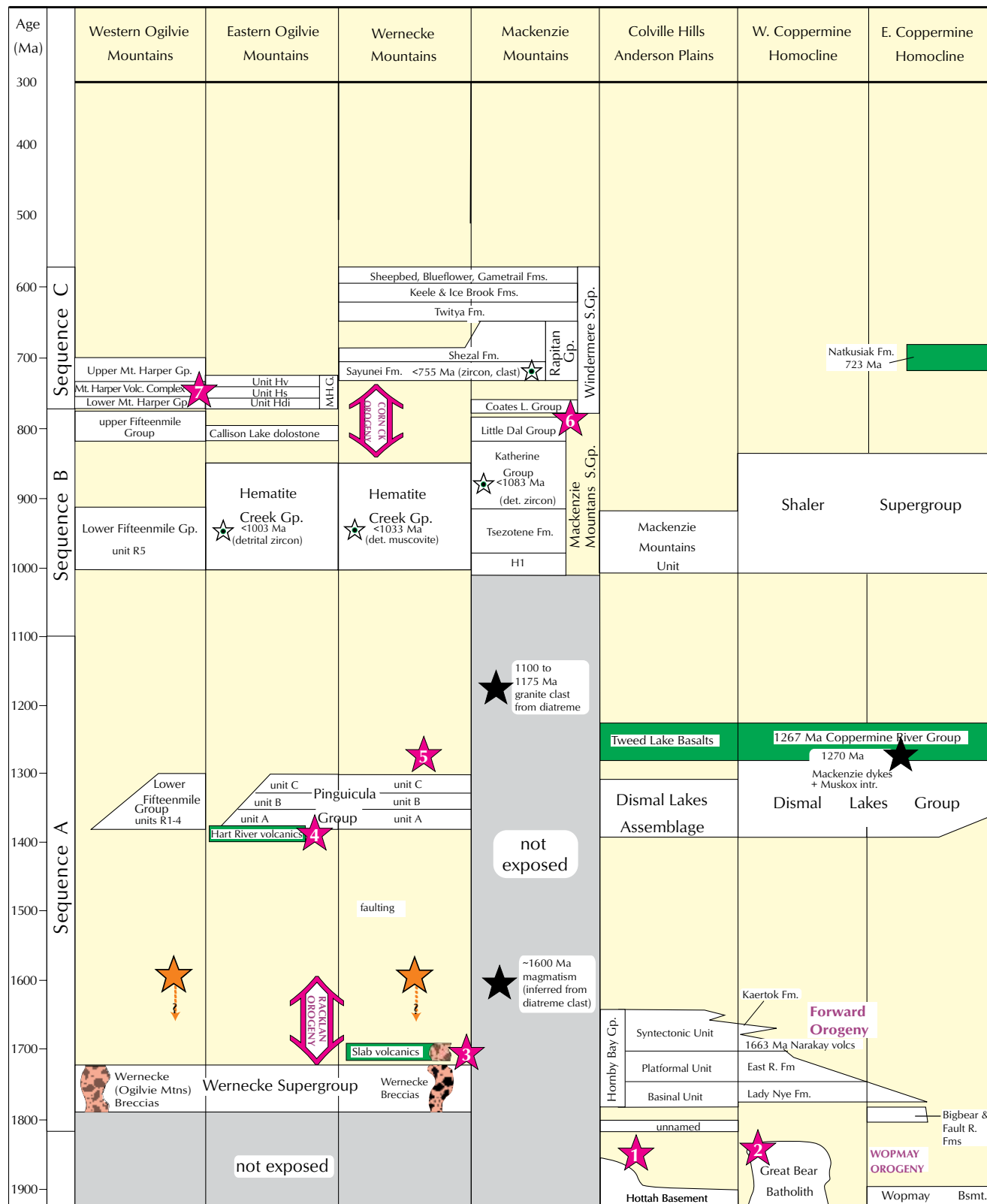


Table 1. (continued)



returned $^{207}\text{Pb}/^{206}\text{Pb}$ ages of 410-371 Ma (Table 1 – Loon; Archer *et al.*, 1986). Disseminated and vein-style uranium mineralization also occurs in Wernecke Breccia and proximal Quartet Group on the Igor prospect (106E 009). RGS samples returned elevated levels of uranium and REE \pm barium, cobalt, copper, arsenic. Significant results include 0.4% U_3O_8 and 6.62% Cu over 4.32 m in drill core (Cash Minerals, 2005⁵). Pitchblende from Igor returned a $^{207}\text{Pb}/^{206}\text{Pb}$ age of 1194 Ma (Table 1; Archer *et al.*, 1986). Uranium mineralization at the Nor prospect (106L 061), which occurs about 120 km north of the main Wernecke Breccia belt, is hosted by Fairchild Lake Group and Wernecke Breccia (Fig. 2). Monazite at the Nor was dated by U-Pb at approximately 1270 Ma, whereas brannerite from the same area returned a $^{207}\text{Pb}/^{206}\text{Pb}$ age of 399 Ma (Table 1; Archer *et al.*, 1986; Parrish and Bell, 1987).

SUMMARY

Information on uranium mineralization in the Wernecke and Ogilvie mountains is not abundant, however, the available data provides tantalizing clues that suggest the mineralization may fit an unconformity-type model. The overall general geological setting is similar to that in areas (Athabasca Basin, Pine Creek region) that are known to host unconformity-associated deposits: Paleoproterozoic, locally carbonaceous, metasedimentary rocks are unconformably overlain by Mesoproterozoic clastic rocks, and the unconformity is intersected by regional-scale faults that could have acted as fluid conduits. In the Athabasca Basin, intense hydrothermal alteration is present around deposits and consists largely of clay minerals and local enrichments of potassium, magnesium, calcium, boron, uranium, nickel, cobalt, arsenic, copper and iron (e.g., Kotzer and Kyser, 1995; Fayek and Kyser, 1997). Chlorite is the dominant alteration mineral in the Pine Creek area deposits (e.g., Ruzicka, 1995). Possible unconformity-related uranium mineralization in the Wernecke and Ogilvie mountains generally occurs in, or near, bodies of Wernecke Breccia, which themselves contain IOCG (\pm U \pm Co) mineralization and are associated with extensive potassic, sodic and carbonate

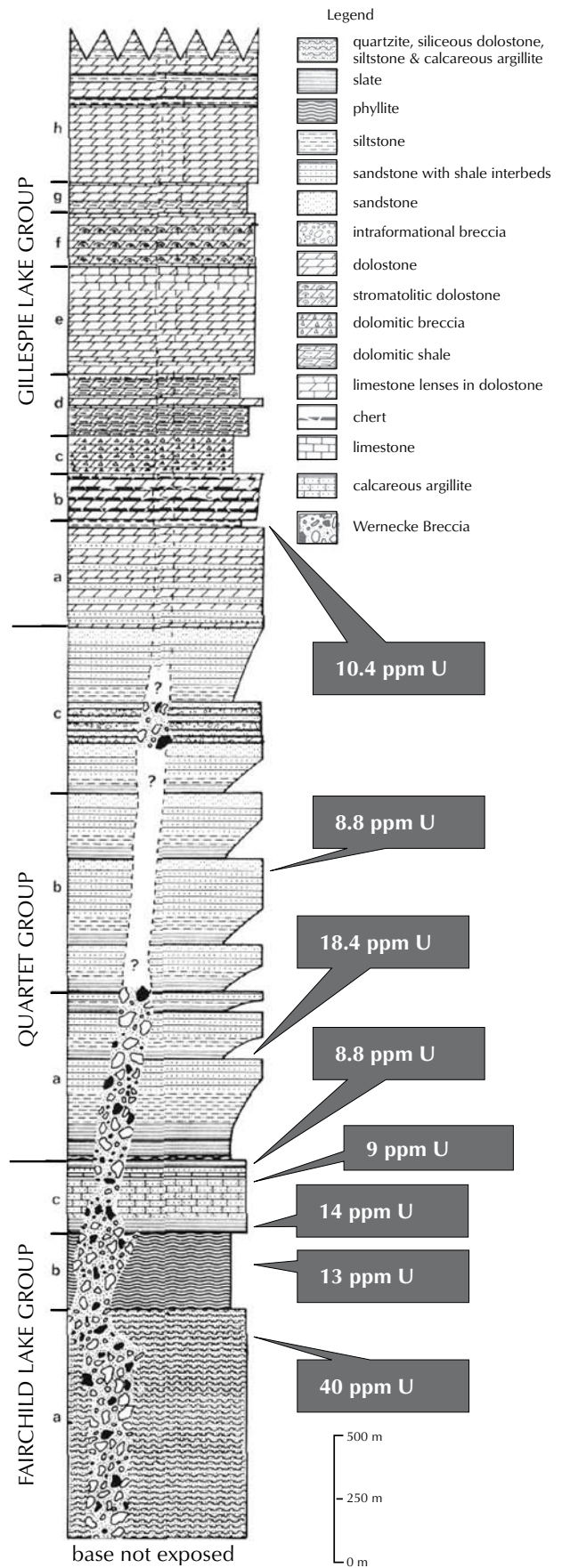
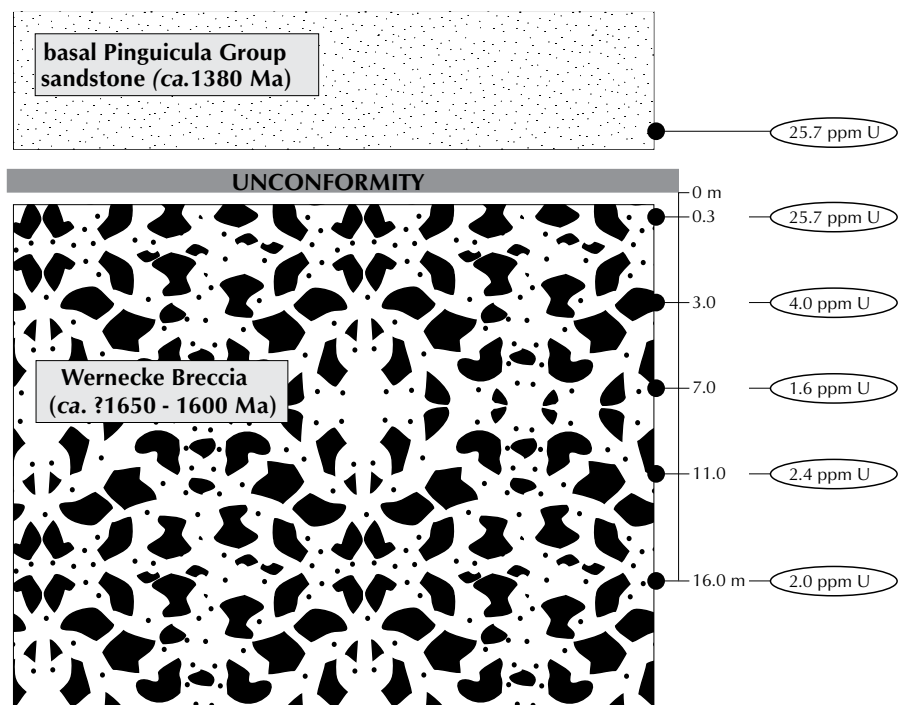


Figure 3. Elevated levels of uranium occur in some Wernecke Supergroup strata. Unmineralized samples were analysed; figure modified from Goodfellow (1979). Results are presented in Goodfellow (1979) and Delaney (1985). Samples are described in Bell and Delaney (1977).

Figure 4. Elevated levels of uranium occur in rocks collected proximal to the regional unconformity between Wernecke Supergroup – Wernecke Breccia and Pinguicula Group. Results are reported in Thorkelson (2000).



alteration. The presence of the breccia-related alteration may make recognition of alteration related to unconformity-type uranium mineralization difficult. However, there are some hints of post-breccia alteration: for example, abundant sericite occurs at least locally at the Igor prospect and appears to overprint breccia-related alteration; at the Nor prospect, clay-altered uranium-bearing rocks were exposed in a trench at the contact between Fairchild Lake Group rocks and Wernecke Breccia.

The verification of an unconformity-type model for uranium mineralization in the Wernecke and Ogilvie mountains would be aided by geochronological studies

that focused on the identification of regional fluid flow events. Regional alteration studies that examine the unconformity and basal Pinguicula Group would also be helpful. Airborne and ground geophysical surveys, particularly gamma-ray radiometrics, have been important prospecting tools in the search for uranium in the Athabasca Basin and Pine Creek region and have led to the discovery of several deposits (e.g., Ruzicka, 1995). There is limited airborne geophysical coverage of the Ogilvie Mountains and none over the Wernecke Mountains: an airborne geophysical survey that included radiometrics could be very helpful in identifying prospective areas.

Table 2. Selected regional geochemical survey sample results from the Curie area compared to values for the North American shelf. Data is from Hornbrook et al. (1990). All values in ppm, except Au = ppb. Analysis by INA except Cu by AAS.

#	Au	Ce	Co	Cu	Eu	Lu	Rb	Sm	Ta	Th	U	W	Yb	As
761407	6	99.0	15	72	0.5	0.8	160	10.0	1.4	19.0	31	3.0	2	27.0
761409	11	15.5	16	153	2.0	2.0	77	15.4	0.3	9.1	224	0.5	6	14.0
763342	11	150.0	69	182	2.0	1.5	130	11.0	2.4	27.3	17	4.0	5	101.0
763347	14	130.0	35	116	2.0	1.4	130	10.1	2.1	22.7	17	3.0	4	64.9
763348	1	110.0	33	98	1.0	1.4	120	8.4	1.6	21.9	19	5.0	4	56.8
Percentile for North American Shelf														
95th	8	120	30	76	2	0.8	150	9	1.7	17	8	2	4	26
99th	20	180	56	134	3	1.2	190	14	2.8	24	16	4	5	45

ACKNOWLEDGEMENTS

International KRL Resources Corp., Shawn Ryan, Archer, Cathro and Associates (1981) Ltd., Cash Minerals Ltd., Aurora Geosciences and Signet Minerals Inc. kindly provided access to confidential data and/or properties. International KRL Resources Corp. and Archer, Cathro and Associates (1981) Ltd. also provided wonderful hospitality and logistical help.

REFERENCES

- Abbott, G., 1997. Geology of the upper Hart River area, eastern Ogilvie Mountains, Yukon Territory. Exploration and Geological Services Division, Yukon Region, Indian and Northern Affairs Canada, Bulletin 9, 92 p.
- Archer, A., Bell, R.T. and Thorpe, R.I., 1986. Age relationships from U-Th-Pb isotope studies of uranium mineralization in Wernecke Breccias, Yukon Territory. *In: Current Research, Part A, Geological Survey of Canada, Paper 86-1A, p. 385-391.*
- Bell, R.T., 1986a. Geological map of north-eastern Wernecke Mountains, Yukon Territory. Geological Survey of Canada, Open File 1027.
- Bell, R.T., 1986b. Megabreccias in northeastern Wernecke Mountains, Yukon Territory. *Current Research, Part A, Geological Survey of Canada, Paper 86-1A, p. 375-384.*
- Bell, R.T., 1978. Breccias and uranium mineralization in the Wernecke Mountains, Yukon Territory – a progress report. *Current Research, Part A, Geological Survey of Canada, Paper 78-1A, p. 317-322.*
- Bell, R.T. and Delaney, G.D., 1977. Geology of some uranium occurrences in Yukon Territory. *In: Report of Activities, Part A, Geological Survey of Canada, Paper 77-1A, p. 33-37.*
- Brideau, M-A., Thorkelson, D.J., Godin, L. and Laughton, J.R., 2002. Paleoproterozoic deformation of the Racklan Orogeny, Slats Creek (106D/16) and Fairchild Lake (106C/13) map areas, Wernecke Mountains, Yukon. *In: Yukon Exploration and Geology 2001, D.S. Emond, L.H. Weston and L.L. Lewis (eds.), Exploration and Geological Services Division, Yukon Region, Indian and Northern Affairs Canada, p. 65-72.*
- Brookes, M., Baker, T. and Hunt, J., 2002. Alteration zonation, veining and mineralization associated with the Wernecke Breccias at Slab creek, Yukon Territory, Canada. *In: Yukon Exploration and Geology 2001, D.S. Emond, L.H. Weston and L.L. Lewis (eds.), Exploration and Geological Services Division, Yukon Region, Indian and Northern Affairs Canada, p. 249-258.*
- Deklerk, R. and Traynor, S. (compilers), 2005. Yukon MINFILE – a database of mineral occurrences. Yukon Geological Survey, CD-ROM.
- Delaney, G.D., 1978. A progress report on stratigraphic investigations of the lowermost succession of Proterozoic rocks, northern Wernecke Mountains, Yukon Territory. Exploration and Geological Services Division, Yukon Region, Indian and Northern Affairs Canada, Open File Report EGS 1978-10, 12 p.
- Delaney, G.D., 1981. The Mid-Proterozoic Wernecke Supergroup, Wernecke Mountains, Yukon Territory. *In: Proterozoic Basins of Canada, Geological Survey of Canada, Paper 81-10, p. 1-23.*
- Delaney, G.D., 1985. The middle Proterozoic Wernecke Supergroup, Wernecke Mountains, Yukon Territory. PhD Thesis, University of Western Ontario, London, Ontario, Canada., 373 p.
- Fayek, M. and Kyser, T.K., 1997. Characterization of multiple fluid-flow events and REE mobility associated with formation of unconformity-type uranium deposits in the Athabasca Basin, Saskatchewan. *Canadian Mineralogist, vol. 35, p. 627-658.*
- Gabrielse, H., 1967. Tectonic evolution of the northern Canadian Cordillera. *Canadian Journal of Earth Sciences, vol. 4, p. 271-298.*
- Goodfellow, W.D., 1979. Geochemistry of copper, lead, and zinc mineralization in Proterozoic rocks near Gillespie Lake, Yukon. *In: Current Research, Part A, Geological Survey of Canada, Paper 79-1A, p. 333-348.*
- Hornbrook, E.H.W., Friske, P.W.B., Lynch, J.J., McCurdy, M.W., Gross, H., Galletta, A.C. and Durham, C.C., 1990. Regional Stream Sediment and Water Geochemical Reconnaissance Data (NTS 106D; Parts of 106C, 106E and 106F). Geological Survey of Canada, Open File 2175, 1:250 000 scale.

- Hunt, J.A., Laughton, J.R., Brideau, M-A., Thorkelson, D.J., Brookes, M.L. and Baker, T., 2002. New mapping around the Slab iron oxide-copper-gold occurrence, Wernecke Mountains. *In: Yukon Exploration and Geology 2001*, D.S. Emond, L.H. Weston and L.L. Lewis (eds.), Exploration and Geological Services Division, Yukon Region, Indian and Northern Affairs Canada, p. 125-138.
- Hunt, J.A., Baker, T. and Thorkelson, D.J., 2005. Regional-scale Proterozoic IOCG-mineralised breccia systems: examples from the Wernecke Mountains, Yukon, Canada. *Mineralium Deposita*, vol. 40, no. 5, p. 492-514.
- Jefferson, C.W., Delaney, G. and Olson, R.A., 2003. EXTECH IV Athabasca uranium multidisciplinary study of northern Saskatchewan and Alberta, Part 1: Overview and impact. Geological Survey of Canada, Current Research 2003-C18, 10 p.
- Kotzer, T.G. and Kyser, T.K., 1995. Petrogenesis of the Proterozoic Athabasca Basin, northern Saskatchewan, Canada and its relation to diagenesis, hydrothermal uranium mineralization and paleohydrogeology. *Chemical Geology*, vol. 120, p. 45-89.
- Norris, D.K., 1997. Geology and mineral and hydrocarbon potential of northern Yukon Territory and northwestern district of Mackenzie. Geological Survey of Canada, Bulletin 422, 401 p.
- Parrish, R.R., and Bell, R.T., 1987. Age of the NOR breccia pipe, Wernecke Supergroup, Yukon Territory. *In: Radiogenic age and isotopic studies*, Report 1, Geological Survey of Canada, Paper 87-2, p. 39-42.
- Ruzicka, V., 1995. Unconformity-type uranium deposits. *In: Mineral Deposit Modelling*, R.V. Kirkham, W.D. Sinclair, R.I. Thorpe and J.M. Duke (eds.), Geological Association of Canada, Special Paper 40, p. 125-149.
- Stammers, M.A. and Ikona, C., 1977. Geologic report on the Ram 1-48 mineral claims. Energy Mines and Resources, Yukon Government, Assessment Report #090284.
- Thorkelson, D.J., 2000. Geology and mineral occurrences of the Slats Creek, Fairchild Lake and "Dolores Creek" areas, Wernecke Mountains, Yukon Territory. Exploration and Geological Services Division, Yukon Region, Indian and Northern Affairs Canada, Bulletin 10, 73 p.
- Thorkelson, D.J., Laughton, J.R., Hunt, J.A. and Baker, T., 2003. Geology and mineral occurrences of the Quartet Lakes map area (NTS 106E/1), Wernecke and Mackenzie mountains, Yukon. *In: Yukon Exploration and Geology 2002*, D.S. Emond, L.H. Weston and L.L. Lewis (eds.), Exploration and Geological Services Division, Yukon Region, Indian and Northern Affairs Canada, p. 223-239.

Bedrock geology of the Duke River area, parts of NTS 115G/2, 3, 4, 6 and 7, southwestern Yukon

Steve Israel¹

Yukon Geological Survey

Amy Tizzard

University of Victoria

Jeremy Major

Simon Fraser University

Israel, S., Tizzard, A. and Major, J., 2006. Bedrock geology of the Duke River area, parts of NTS 115G/2, 3, 4, 6 and 7, southwestern Yukon. *In: Yukon Exploration and Geology 2005*, D.S. Emond, G.D. Bradshaw, L.L. Lewis and L.H. Weston (eds.), Yukon Geological Survey, p. 139-154.

ABSTRACT

The Duke River area comprises Late Paleozoic arc volcanic and sedimentary rocks, Triassic basalts, carbonate and sedimentary rocks, overlain by Tertiary terrestrial sedimentary and volcanic deposits. These rocks are intruded by Upper Triassic to Miocene plutons, sills and dykes. Post-late Paleozoic uplift and erosion are suggested by the lack of Early Triassic rocks, as well as a higher degree of folding exhibited by the older stratigraphy. A subsequent, compressional episode thrust Paleozoic rocks over Triassic rocks and folded the strata into upright, to overturned, tight folds. This event is younger than the Upper Triassic to Cretaceous Tatamagouche succession, but older than mid-Cretaceous plutons. Post-Cretaceous, steeply dipping strike-slip faults dissect the area and include both extensional and compressional components. A recent compressional event is exhibited by Triassic rocks thrust over folded Tertiary strata. The structural complexity of the area is significant, as it affects exploration targeted at mineralized Upper Triassic ultramafic intrusions.

RÉSUMÉ

Dans la région de la rivière Duke reposent des roches sédimentaires et d'arc volcanique du Paléozoïque tardif ainsi que des basaltes, des roches sédimentaires et des roches carbonatées du Trias recouverts par des dépôts sédimentaires et volcaniques d'origine terrestre du Tertiaire. Ces roches sont pénétrées par des plutons, des filons-couches et des dykes datant du Trias supérieur au Miocène. L'absence de roches du Trias précoce ainsi que le plissement plus intense des strates plus anciennes suggèrent qu'il y a eu soulèvement et érosion après le Paléozoïque tardif. Un ultérieur épisode de compression a poussé les roches du Paléozoïque sur les roches du Trias et plissé les strates en plis serrés droits à déversés. Cet épisode est plus récent que la succession de Tatamagouche datant du Trias supérieur au Crétacé, mais plus ancien que les plutons du Crétacé moyen. Des failles décrochantes post-crétacé fortement inclinées dissèquent la région et présentent des composantes d'extension et de compression. Les roches du Trias poussées sur les strates plissées du Tertiaire témoignent d'un événement de compression récent. La région est d'une grande complexité structurale, ce dont doit tenir compte l'exploration ciblant les intrusions ultramafiques minéralisée du Trias supérieur.

¹steve.israel@gov.yk.ca

INTRODUCTION

The Kluane Ranges project was initiated in 2004. Bedrock mapping was carried out at 1:50 000 scale in an effort to increase geologic knowledge of southwest Yukon. The project focuses on the Paleozoic and Mesozoic volcanic, sedimentary and intrusive rocks of Wrangellia Terrane, and Mesozoic to Cenozoic overlap assemblages that occur in a southeastward-tapering wedge between the St. Elias Mountains and the Denali Fault (Fig. 1). The area includes several styles of mineralization including significant deposits related to Upper Triassic mafic-ultramafic intrusions. Mapping in the Kluane Ranges emphasizes the resolution of the complex stratigraphic and structural relationships found within the area, to better constrain the overall tectonic and geologic understanding.

Mapping in 2004 centred on the Quill Creek area, between the Donjek River and the Alaska Highway and is summarized by Israel and van Zeyl (2005). Fieldwork conducted between June and August, 2005 centred on the Duke River area, extending the 2004 map area to the

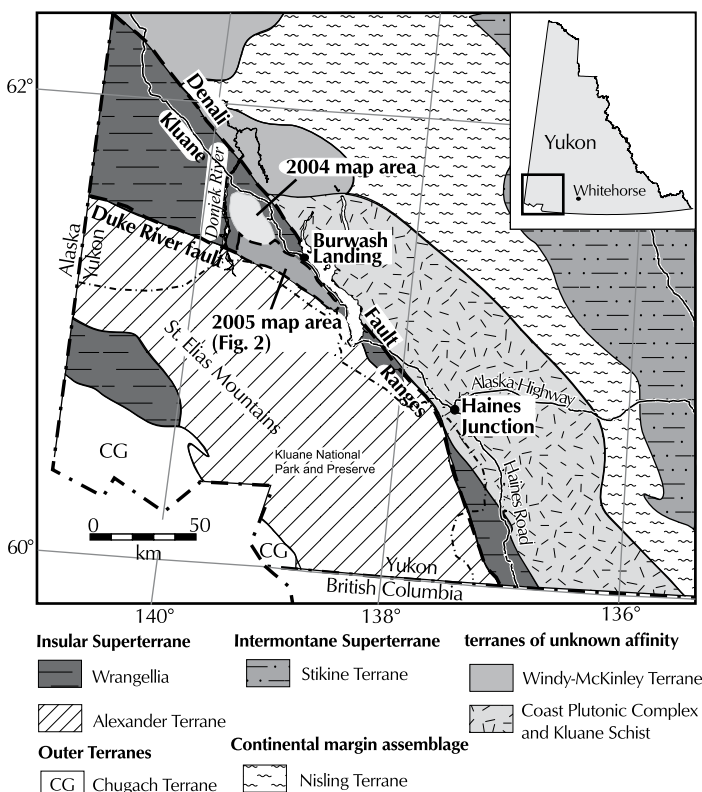


Figure 1. Terrane map of southwest Yukon, displaying the distribution of the Wrangellia Terrane (after Wheeler *et al.*, 1991). The location of Figure 2 is highlighted.

southeast to cover the region between Kluane National Park and Reserve and the Alaska Highway (Fig. 1; Israel *et al.*, 2005).

The Duke River area encompasses the range of mountains between the Shakwak Valley and the Duke River. It includes the Burwash Uplands and continues southeast to Congdon Creek (Fig. 2). Geologic mapping by Muller (1967), Read and Monger (1976), Dodds and Campbell (1992) and T. Bremner (unpublished data) have aided in the preliminary interpretations presented in this report.

REGIONAL GEOLOGY

The Kluane Ranges are almost entirely underlain by the Wrangellia Terrane. Wrangellia Terrane is exposed in the Yukon in two fault-bounded tectonic blocks separated by the Alexander Terrane (Fig. 1). The Alexander Terrane at this latitude is composed of Cambrian to Devonian meta-sedimentary and meta-volcanic rocks intruded by Pennsylvanian to Early Permian plutons. A Pennsylvanian pluton cross-cuts Wrangellia and Alexander terranes in Alaska, suggesting the two terranes were together as one tectonic element by late Paleozoic time (Gardner *et al.*, 1988). Together with the Peninsular Terrane, they form the Insular Superterrane and were accreted to the western margin of the Intermontane Superterrane by at least Middle Jurassic (van der Heyden, 1992; Monger and Nokleberg, 1996; Gehrels, 2001). Jura-Cretaceous sedimentary and volcanic rocks of the Gravina-Nutzotin belt overlap Wrangellia and Alexander terranes throughout the Yukon and Alaska. Northeast of the Kluane Ranges, metamorphic and igneous rocks of the Nisling and Windy-McKinley terranes and the Kluane schist and Coast Plutonic Complex are juxtaposed next to Wrangellia Terrane across the Denali Fault (Fig. 1). The Nisling Terrane is a metamorphosed continental assemblage of late Proterozoic and lower Paleozoic schists, quartzites, marbles and meta-basites that are believed to be associated with the Yukon-Tanana Terrane (Gehrels, 2002). The Windy-McKinley Terrane is an enigmatic assemblage of Paleozoic to Mesozoic oceanic sedimentary and volcanic rocks that are apparently thrust onto rocks of the Nisling Terrane (Gordey and Makepeace, 2001).

Wrangellia Terrane, within the Yukon and adjacent Alaska, is composed of Late Paleozoic arc volcanic and sedimentary rocks of the Skolai Group, unconformably overlain by sparse outcrops of Middle Triassic marine sedimentary rocks, Upper Triassic oceanic flood basalts of

the Nikolai formation, and shallow marine carbonates and mudstones of the Chitstone limestone and McCarthy Formation (Muller, 1967; MacKevett, 1971; Read and Monger, 1976; Israel and van Zeyl, 2005). The Skolai Group is divided into a Pennsylvanian (?) to Early Permian, lower volcanic unit known as the Station Creek Formation, and an upper sedimentary unit known as the Hasen Creek Formation (MacKevett, 1971; Read and Monger, 1976). The Station Creek Formation represents a Late Pennsylvanian to Permian volcanic arc that was overlain by marine sedimentary deposits of the Hasen Creek Formation during arc subsidence. Middle to Upper Triassic igneous bodies of the Kluane mafic-ultramafic complex intrude into the Skolai Group and are thought to be feeders to the overlying flood basalts of the Nikolai formation. These flood basalts are believed to be part of a large oceanic plateau that includes the Karmutsen Formation on Vancouver Island. The flood basalts are considered the hallmark of Wrangellia Terrane from southern British Columbia to central Alaska (Hulbert, 1997; Greene *et al.*, 2005).

Jura-Cretaceous sedimentary basins overlap onto Wrangellia Terrane from south-central to central Alaska, and include the Dezadeash Formation, a thick sequence of marine turbidites found within the Kluane Ranges (Eisbacher, 1976; Ridgway *et al.*, 2002). Diorite and gabbro of the mid-Cretaceous Kluane Ranges suite intrude Wrangellia Terrane as part of the Chisana magmatic arc that formed during resurgence in north-dipping subduction (Plafker and Berg, 1994). Volcanic material related to the Chisana arc is not present within the Kluane Ranges and likely reflects a more distal position for the Dezadeash Formation.

Tertiary strike-slip faulting in a transpressional environment led to the formation of the Denali and Duke River faults and subsequent formation of pull-apart and compressional basins into which the Amphitheatre Formation terrestrial sediments were deposited (Read and Monger, 1976; Dodds and Campbell, 1992; Ridgway *et al.*, 1992; Trop *et al.*, 2002). Local extension within the Kluane Ranges allowed for eruption of the Wrangell Lavas that overly much of the Amphitheatre Formation.

GEOLOGY OF THE DUKE RIVER AREA

The following briefly describes the stratigraphy of the Duke River area with emphasis on the upper Mesozoic and Tertiary strata. For a more comprehensive description of the Paleozoic and early Mesozoic stratigraphy of the area, see Israel and van Zeyl (2005).

ALEXANDER TERRANE

Only a very small component of the Alexander Terrane outcrops in the Duke River map area and it was not mapped in great detail. Included in the Alexander Terrane are meta-sedimentary rocks that outcrop in the west-central portion of the Duke River map area on the south side of the Duke River fault (Fig. 2). This unit consists of phyllites, marbles and meta-sandstones, which are all highly deformed. Intruding these rocks is the Mount Hoge pluton, a partially deformed and metamorphosed, coarse- to medium-grained hornblende biotite-granite. The Mount Hoge pluton is part of the Pennsylvanian to Permian Icefield suite that intrudes much of the Alexander Terrane in southwest Yukon (Read and Monger, 1976; Dodds and Campbell, 1988).

WRANGELLIA TERRANE

Skolai Group

The Skolai Group is the basal unit of the Wrangell Terrane in southwest Yukon and Alaska. The base of the group is either not exposed, or faulted. The Skolai Group is divided into two formations: the lower Station Creek Formation, which is dominated by volcanic rocks, and the upper Hasen Creek Formation, which is dominated by sedimentary rocks (Smith and MacKevett, 1970, MacKevett, 1971; Read and Monger, 1976; Israel and van Zeyl, 2005).

- Station Creek Formation

The Station Creek Formation outcrops extensively in the Duke River area (Fig. 2). Thickness of the unit is difficult to ascertain as the base is nowhere exposed, but it is at least several hundred metres thick. The formation is dominated by volcanic rocks that include breccias, crystalline tuffs, tuffaceous siltstone and flows. Breccias are composed of sub-rounded to angular clasts, up to 50 cm in diameter in a matrix of fine-grained material of the same composition (Fig. 3). They form beds several metres thick and locally several tens of metres thick. The breccias commonly grade up into pale green to beige tuffaceous

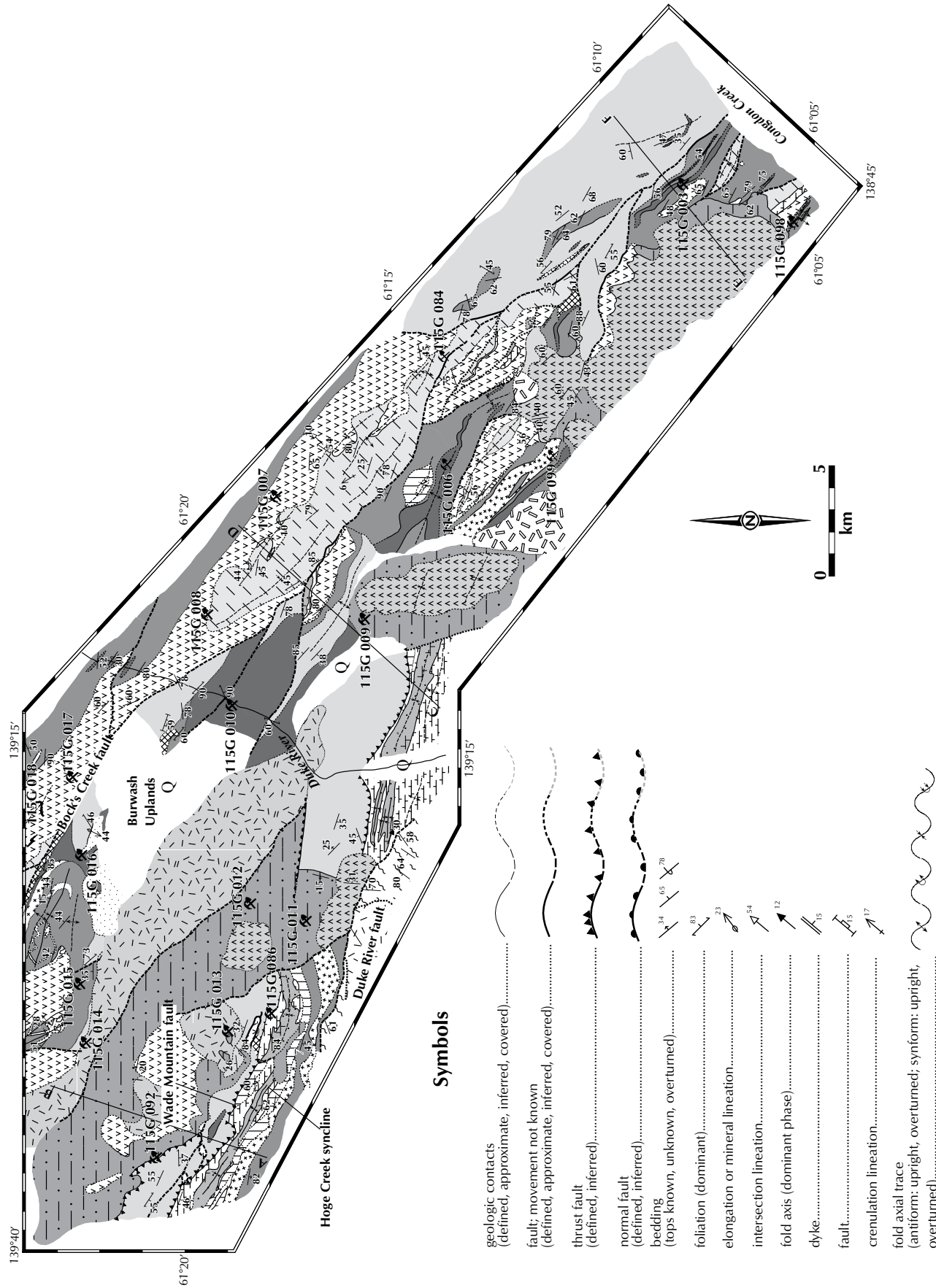


Figure 2. Generalized geological map of the Duke River area.

LEGEND

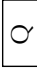


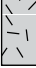
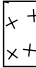


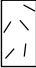



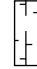


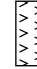
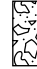






QUATERNARY		unconsolidated alluvium, colluvium and glacial deposits
MIOCENE	<i>Wrangell Suite</i>	 fine- to medium-grained, hornblende ± biotite granodiorite and medium-grained biotite diorite and pyroxene gabbro
OLIGOCENE	<i>Tkope suite</i>	 fine- to medium-grained, equigranular hornblende ± biotite quartz-feldspar porphyry
CRETACEOUS	<i>Kluane Ranges suite</i>	 fine- to medium-grained, equigranular hornblende ± pyroxene diorite and gabbro
TRIASSIC	<i>Maple Creek gabbro</i>	 fine- to coarse-grained diabase, and gabbro sills and dykes, locally abundant epidote and chlorite alteration; locally, columnar-jointed
	<i>Kluane mafic-ultramafic complex</i>	 coarse-grained to pegmatitic gabbro
		 peridotite, dunite and clinopyroxenite, layered intrusions
PENNSYLVANIAN to PERMIAN (?)	<i>Mt. Hoge pluton</i>	 coarse- to medium-grained, hornblende-biotite granite and granodiorite
LAYERED ROCKS		
PALEOGENE TO NEOGENE	<i>Wrangell Lava</i>	 rusty red, brown, phyrlic and non-phyric basalt and andesite flows, interbedded with felsic tuff, volcanic sandstone and conglomerate
	<i>Amphitheatre Formation</i>	 yellow-buff to grey-buff sandstone, pebbly sandstone, polymictic conglomerate, siltstone and mudstone; minor brown-grey carbonaceous shale and coal
TRIASSIC TO CRETACEOUS	<i>Tatamagouche succession</i>	 dark to light grey phyllite, medium- to coarse-grained sandstone, minor greywacke and pebble to cobble conglomerate; may include upper parts of McCarthy Formation
UPPER TRIASSIC	<i>Chitstone Limestone</i>	 light grey to beige, massive to thickly bedded limestone, limestone breccia, and rare, thinly bedded limy mudstone; includes white to pale grey gypsum
	<i>McCarthy Formation</i>	 light to dark grey shale and argillite interbedded with buff-coloured limestone
	<i>Nikolai formation</i>	 thinly bedded, grey limestone and minor maroon to olive-green argillite
		 dark green to maroon amygdaloidal basalt and basaltic andesite flows, locally pyroxene and plagioclase-phyric; developed pillows; rare olivine crystals
		 light to dark green volcanic breccia; angular clasts of amygdaloidal basalt and dark grey argillite in a fine-grained matrix
MIDDLE (?) TRIASSIC	<i>Hoge Creek succession</i>	 dark grey phyllite, locally limy, thin, grey limestone
PENNSYLVANIAN (?) AND PERMIAN	<i>Hasen Creek Formation</i>	 light to dark grey limestone, fossiliferous and frequently pebbly, commonly graded and cross-bedded
		 light-grey to white bioclastic limestone, local cherty interbeds
		 dark to light grey-brown siltstone turbidites, siliceous argillite, chert and minor volcanoclastic sandstone and tuffs
	<i>Station Creek Formation</i>	 dark to light green volcanic breccia, crystal tuff and tuffaceous sandstone; breccia clasts consist of augite-phyric basalt within tuffaceous matrix; augite-phyric basalt flows locally amygdaloidal
UPPER PALEOZOIC/PERMIAN (?)	<i>Alexander Terrane</i>	 grey and brown phyllite, metasandstone, unfossiliferous carbonate



Figure 3. Station Creek Formation volcanic breccia located at the headwaters of Bock's Creek.

sandstones and crystal-lithic tuffs. Sandstones are fine-grained and well bedded with individual beds ranging from less than 1 cm to 10 cm thick. Crystal tuffs are pale green with fragments of basalt (up to 1 cm) and 1-2 mm crystals of pyroxene; these tuffs are commonly interbedded with medium- to fine-grained tuffaceous sandstone. Some outcrops of these crystal tuffs are difficult to distinguish from gabbro sills and dykes that are found throughout the Skolai Group. Pale-green-weathering, pyroxene-phyric basalt flows are found throughout the Station Creek Formation. They are up to several metres thick and locally amygdaloidal; amygdules are filled with quartz, epidote and chlorite. In several localities, flows are pillowed, and in one case, exhibit columnar jointing (Fig. 4). Beds of black to dark-brown, fine-grained argillite and mudstone occur locally within the Station Creek Formation and are more prevalent at stratigraphically higher positions in the section.

The age of the Station Creek Formation is not well constrained, however, fossils found within the upper portions of the unit, as well as its gradational relationship with the Hasen Creek Formation, suggest a Pennsylvanian to Permian age (Nokleberg *et al.*, 1994).

- Hasen Creek Formation

The Hasen Creek Formation is found throughout the Duke River area, but is more extensive in the northwest portion of the map area and into the Quill Creek map area; it appears to lose much of its thickness in the southeast (Fig. 2; Israel and van Zeyl, 2005). It



Figure 4. Columnar-jointed basalt flows within the Station Creek Formation located near the headwaters of Bock's Creek.

gradationally overlies the Station Creek Formation with the base of the formation typically placed at the cessation of volcanic material. Campbell (1981) describes the gradational contact between the two formations as a "transition zone" that records the decreasing amount of volcanic deposition and the increasing sediment input. It is at this transition zone that Hulbert (1997) suggests many of the ultramafic bodies intrude. The Hasen Creek Formation is unconformably overlain by Middle Triassic sedimentary rocks of the Hoge Creek succession and volcanic rocks of the Nikolai formation (Fig. 2).

The Hasen Creek Formation is dominated by marine clastic sedimentary rocks, carbonates, chert and conglomerates. Rare basaltic flows and volcanic breccia occur near the middle of the unit. In the Duke River area, the conglomerate, chert and carbonate units are rare and the formation is mainly composed of fossiliferous siltstone, turbidites, mudstones and fine-grained sandstones.

The age of the Hasen Creek Formation is Early Permian, based upon numerous fossil controls (MacKevett, 1971; Read and Monger, 1976; Dodds *et al.*, 1993).

Hoge Creek succession

An enigmatic package of rocks, informally named here as the Hoge Creek succession, outcrops in the westernmost, and central portions of the Duke River map area (Fig. 2). No noticeable break separates the Hoge Creek succession from the underlying Hasen Creek Formation, and only through the identification of fossils collected from the Hoge Creek succession can it be distinguished

from the older sedimentary package (Muller, 1967; Read and Monger, 1976). The Hoge Creek succession is overlain by rocks of the Nikolai formation, and where the Nikolai formation is absent, the Hoge Creek succession is overlain by Chitistone Limestone and McCarthy Formation (Fig. 2). The thickness of the succession is unknown as it is restricted to slivers and discontinuous lenses.

The Hoge Creek succession consists of dark-grey argillite, beige- to brown-weathering calcareous siltstone, fine- to medium-grained sandstone, and rare beige to grey limestone. Near Hoge Creek, the succession is well bedded with alternating beds of siltstone and sandstone (Fig. 5). The age of the Hoge Creek succession is Middle Triassic (Ladinian), based upon fossils collected by Muller (1967) and Read and Monger (1976). There has been no other mention of Middle Triassic units from northern Wrangellia Terrane, however, on Vancouver Island, there is a similar package of Middle Triassic fossil-bearing strata (Carlisle and Suzuki, 1974).

Nikolai formation

The Nikolai formation is an informally named package that consists of thick accumulations of subaerial basalt flows. It outcrops throughout the Duke River map area where it unconformably overlies the Skolai Group and conformably overlies the Hoge Creek succession. It is overlain by the Chitistone Limestone, McCarthy Formation and the Tatamagouche succession (Fig. 2). Thickness of the Nikolai formation is not well constrained in the Duke River map area, but elsewhere in the Klauane

Ranges, it can be up to ~1000 m thick. In the Hoge Creek area, the Nikolai formation is more or less absent, with only a thin sliver of basalt outcropping between the Hoge Creek succession and the Chitistone Limestone. The Nikolai formation consists of a sporadically formed basal breccia, a thick sequence of highly amygdaloidal basalt flows, and thin interbeds of calcareous argillite and limestone near the top of the flows. Hulbert (1997) suggests that the amount of amygdaloidal and vesicular flows within the formation demonstrate that the majority of the Nikolai formation erupted subaerially. However, rare pillows found near the base of the formation, and thin carbonate horizons near the top, indicate that at least parts of the formation erupted subaqueously (Fig. 6).

The age of the Nikolai formation is likely Late Triassic (Norian), based upon conodonts collected from the interbedded limestone. The base of the formation may be as old as Middle Triassic as it apparently conformably overlies the Hoge Creek succession.

Chitistone Limestone

The Chitistone Limestone outcrops extensively in the Duke River map area (Fig. 2). It conformably overlies the Nikolai formation, and at one locality near Bock's Creek, appears to be interbedded with the underlying basalts. Where the Nikolai formation is absent, the Chitistone Limestone unconformably overlies the Hoge Creek succession. The Chitistone Limestone is conformably overlain by the McCarthy Formation, and locally, by the Tatamagouche succession. It forms the footwall of the Wade Mountain fault, while volcanic rocks of the Station



Figure 5. Well bedded siltstone and fine-grained sandstone of the Hoge Creek succession.



Figure 6. Rare pillowed flows found at the base of the Nikolai formation; outcrop located north of Hoge Creek.

Creek Formation form the hanging wall. Thickness of the Chitistone Limestone is highly variable and can form thick packages several hundred metres thick, or thin discontinuous lenses.

The Chitistone Limestone is characterized by massive, white- to beige-weathering limestone that usually forms resistant, craggy outcrops that stand out from the surrounding rock (Fig. 7). Limestone breccia forms thick portions of the Chitistone Limestone unit and consists of blocks of white and grey limestone fragments hosted within a similar fine-grained matrix. Included within the Chitistone Limestone are deposits of white-weathering gypsum. Within the Duke River map area, gypsum outcrops north and south of Bock's Creek. A large deposit of gypsum, up to 1 km thick and 7 km in length, outcrops outside of the Duke River map area to the southeast. The Chitistone Limestone is rarely fossiliferous, but has abundant micro-fossils that yield an Late Triassic (Norian) age.

McCarthy Formation

The McCarthy Formation mainly outcrops in the western and central portion of the map area and is most obvious in the core of the Hoge Creek syncline (Fig. 2). It conformably overlies the Chitistone Limestone and grades indiscernibly into the overlying Tatamagouche succession. Thickness of the unit is impossible to determine because of the nature of folding found ubiquitously throughout the area (Fig. 8). In Alaska, MacKevett (1971) divides the McCarthy Formation into a lower member defined by shale, chert and impure limestone, and an upper member



Figure 7. Resistant-weathering outcrops of Chitistone Limestone; photo was taken looking east into the Duke River.

characterized by calcareous chert, spiculite, impure limestone and rare shale; together the lower and upper members have a combined thickness of over 1000 m. In the Duke River map area, both members described by MacKevett are present; however, the upper member likely includes some rocks mapped as the Tatamagouche succession since the two of these units are difficult to distinguish. The McCarthy Formation mainly outcrops as well bedded, alternating dark grey calcareous siltstone and light grey limestone. This gives the rocks a distinctive striped appearance that is easily recognizable from a distance. However, in the Hoge Creek area, rocks of the Hoge Creek succession have a similar appearance in outcrop and can easily be mistaken for the McCarthy Formation. The McCarthy Formation is locally very fossiliferous with thick death bed deposits of the bivalve *Monotis subcircularis* Gabb.

Fossils collected from the McCarthy Formation in the Duke River map area and the neighbouring Quill Creek map area are Late Triassic (Norian) in age (Israel and van Zeyl, 2005). MacKevett (1971) reports an Early Jurassic (Pliensbachian) age for fossils from the upper McCarthy Formation, suggesting an age range of Triassic to Early Jurassic for the formation.

OVERLAP ASSEMBLAGES

Tatamagouche succession

The Tatamagouche succession is a package of marine, clastic sedimentary rocks that is poorly defined within the Kluane Ranges. It has uncertain relationships with the

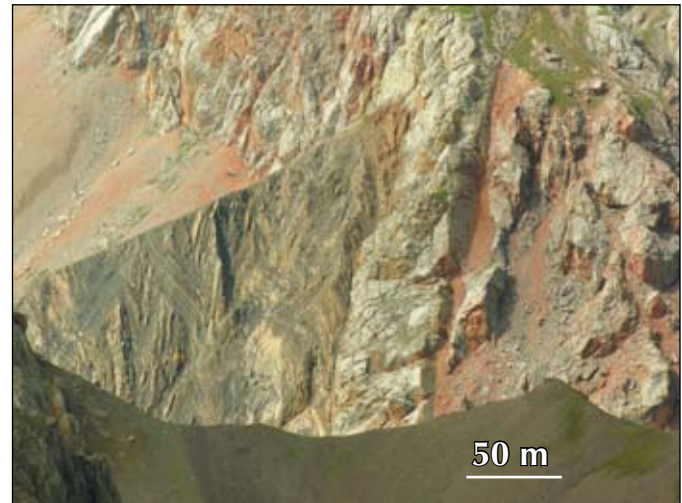


Figure 8. Chevron folds typical of the McCarthy Formation; photo was taken looking west into the Hoge Creek syncline.



Figure 9. Strongly deformed conglomerate found within the Tatamagouche succession.

older strata and is unconformably overlain by Tertiary sedimentary and volcanic deposits. It likely unconformably overlies the Nikolai formation and the Chitistone Limestone and probably includes the upper portion of the McCarthy Formation in its lower sections. The Jurassic to Cretaceous portions of the succession may be, in part, equivalent to the Dezadeash Formation found to the southeast of the Duke River map area. For this reason, the Tatamagouche succession could be considered part of the Wrangellia Terrane, or as an overlap assemblage. The difficulty in separating the Tatamagouche succession from underlying rocks led Read and Monger (1976) to group together a package of rocks that ranged from Late Triassic to Early Cretaceous in age; that same division is used for this study.

The Tatamagouche succession outcrops extensively in the Duke River map area, but is more prevalent in the central and southeast portion of the study area (Fig. 2). It mainly overlies the Nikolai formation and cores large synclines, but locally overlies the Chitistone Limestone, and is in fault contact with both the Station Creek and Hasen Creek formations. The Tatamagouche succession is characterized by dark-grey argillite, fine- to medium-grained sandstone and greywacke, pebble to cobble conglomerate and calcareous siltstone. The conglomerate is composed of well rounded clasts of siltstone, limestone and granitic material, within a muddy, dark-grey matrix (Fig. 9). Locally, a brick-red conglomerate with similar clast lithologies is interbedded with greywacke and siltstone. The Tatamagouche succession is ubiquitously strongly deformed and exhibits evidence suggesting



Figure 10. Poorly sorted, terrestrially deposited conglomerate of the Amphitheatre Formation.

several phases of deformation. The age of the Tatamagouche succession is problematic since the unit is not well defined. Fossils range in age from Late Triassic to Early Cretaceous (Muller, 1967; MacKevett, 1971; Read and Monger, 1976; Dodds and Campbell, 1993).

Amphitheatre Formation

The Amphitheatre Formation outcrops throughout the Duke River map area with the most extensive deposit located near the Burwash Uplands in the northwest portion of the map area (Fig. 2). It typically has an unconformable lower contact with nearly all the older strata, but locally the contacts are defined by faults that were likely basin-bounding structures. Thickness of the Amphitheatre Formation ranges from 350 m to 1100 m and it is unconformably overlain by the Wrangell Lavas. It is composed of terrestrial sediments that consist of conglomerates, fine- to coarse-grained sandstones, as well as coal deposited in structurally controlled basins related to the Denali fault system (Ridgway, 1992). The conglomerates are poorly sorted with sub-rounded to well rounded clasts of quartz, dark-grey siltstone, porphyritic volcanic rocks, plutonic rocks and metamorphic rocks (Fig. 10). Discontinuous coal seams are found throughout the formation and can be up to several tens of metres in thickness. Deposition of the Amphitheatre Formation occurred in strike-slip, pull-apart basins related to movement along the Denali and Duke River fault systems (Ridgway *et al.*, 1992). Material filling the basins was derived from rocks of the Wrangellia Terrane and the Kluane Schist (Ridgway *et al.*, 1992). The age of the

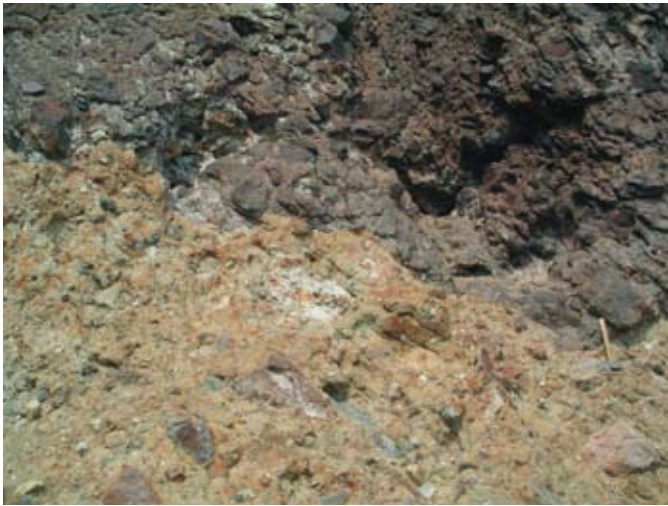


Figure 11. Wrangell Lava basal volcanic breccia overlying the Amphitheatre Formation

Amphitheatre Formation is Eocene to Oligocene, based on palynological studies (Ridgway *et al.*, 1992).

Wrangell Lavas

The Wrangell Lavas are the youngest rocks in the Duke River map area and outcrop extensively along the western boundary of the study area along the Duke River fault. They lie unconformably on top of the Amphitheatre Formation and, locally, have been deposited on the Skolai Group, the Nikolai formation and the Chitistone Limestone (Fig. 2). The Wrangell Lavas in the Duke River map area are a combination of volcanic rocks that include basaltic flows, andesitic flows, rare rhyolitic flows, volcanic breccias, air fall tuffs and volcanoclastic sandstones (Skulski, 1988). The upper sections of the Wrangell Lavas were not examined in this study, however, all basal contacts observed in the Duke River map area consist of flow breccia and rare pillowed flows of plagioclase-phyric basalt (Fig. 11).

INTRUSIVE ROCKS

The Duke River area is intruded by several different plutonic bodies that are variable in both composition and age (Fig. 2).

Maple Creek gabbro

The Maple Creek gabbro outcrops mainly in the northwestern portion of the Duke River map area. At this location, it occurs as sill-like bodies that intrude into the Hasen Creek Formation and along the contact between

the Hasen Creek Formation and the Hoge Creek succession. It is a fine- to medium-grained, pyroxene gabbro that is believed to be coeval with the Kluane mafic-ultramafic complex and acts as a feeder to the Nikolai formation (Hulbert, 1997). It is distinguished from other gabbro sills and dykes by the less prevalent alteration and 'salt and pepper' appearance (see next section). The age of the Maple Creek gabbro is 232 ± 1 Ma defined by U-Pb analyses of zircon (Mortensen and Hulbert, 1991).

Kluane mafic-ultramafic complex

The Kluane mafic-ultramafic complex (Hulbert, 1997) comprises sills and dykes that intrude the Paleozoic stratigraphy throughout the Duke River map area (Fig. 2). Individual bodies are exposed for up to several kilometres, but thicknesses are poorly defined in the Duke River area. The largest of these intrusions, the Tatamagouche complex, is found along the Duke River, and geophysical data suggests that it underlies much of the Burwash Uplands. As the name implies, the Kluane mafic-ultramafic complex consists of both mafic and ultramafic components. Hulbert (1997) studied the complex in great detail and has described many of the bodies as being zoned with a marginal gabbro rimming phase, a peridotite/pyroxenite zone and a dunite core. The majority of ultramafic rocks examined in the Duke River area are peridotites, with varying amounts of pyroxenite. The gabbro phase associated with the ultramafic rocks tends to be coarse- to medium-grained and ubiquitously altered. This phase of gabbro is similar to sills and dykes found throughout the Duke River map area that intrude rocks of the Skolai Group. A preliminary U-Pb age of 219 Ma (J. Mortensen, pers. comm.) was obtained from one of these gabbroic bodies found along Burwash Creek. This age is significantly younger than the Maple Creek gabbro and suggests that multiple phases of Triassic gabbro exist in the study area. This may have exploration significance as mineralization associated with the Kluane mafic-ultramafic complex is commonly found within the gabbro phase; however, the age differences between the Maple Creek gabbro and other gabbros in the area raises the question of which gabbro phase should be targeted for exploration, and moreover, the actual age of ultramafic intrusions.

Kluane Ranges suite

The Kluane Ranges suite is restricted to the northern portion of the Duke River map area, where it intrudes the

Paleozoic and Mesozoic stratigraphy, and is in fault contact and is unconformably overlain by the Amphitheatre Formation (Fig. 2). It is characterized by fine- to medium-grained, hornblende \pm biotite, quartz-diorite, diorite and gabbro. Copper, molybdenum and gold mineralization is associated with the Kluane Ranges suite along Burwash Creek (Fig. 2). K-Ar ages on hornblende from the main intrusive body near Burwash Creek have yielded ages of 117 Ma to 115 Ma (Christopher *et al.*, 1972) and a preliminary U-Pb zircon age of 122 Ma (J. Mortensen, pers comm.); together, these dates indicate an Early Cretaceous age for the Kluane Ranges suite.

Tkope suite

The Tkope suite outcrops exclusively along Burwash Creek, intruding the Hasen Creek and Station Creek formations, the Kluane mafic-ultramafic complex and the Kluane Ranges suite (Fig. 2). The suite is composed of white- to pale-yellow-weathering hornblende \pm biotite, quartz-feldspar porphyry. Preliminary U-Pb analyses of this mafic body suggest an Oligocene age for the suite.

Wrangell suite

The Wrangell suite outcrops as two small intrusive bodies in the southeastern portion of the Duke River map area (Fig. 2). Both bodies intrude Paleozoic and Mesozoic rocks and Tertiary Amphitheatre Formation and Wrangell Lavas, making these the youngest rocks in the map area. The Wrangell suite in the Duke River map area is characterized by medium-grained, equigranular hornblende \pm biotite granodiorite to diorite. The westernmost intrusion, near the Duke River, yields a U-Pb age of \sim 14 Ma (Dodds and Campbell, 1988).

STRUCTURE

The Duke River area is characterized by northwest-southeast structural trends resulting from several generations of deformation (Fig. 2). Three generalized phases of deformation can be separated, based upon field observations: 1) an enigmatic pre-Middle Triassic compressional event; 2) a post-Triassic, pre-mid-Cretaceous contractional event; and 3) a post-Cretaceous strike-slip faulting event. Figure 12 illustrates the general structural features observed in the Duke River map area.

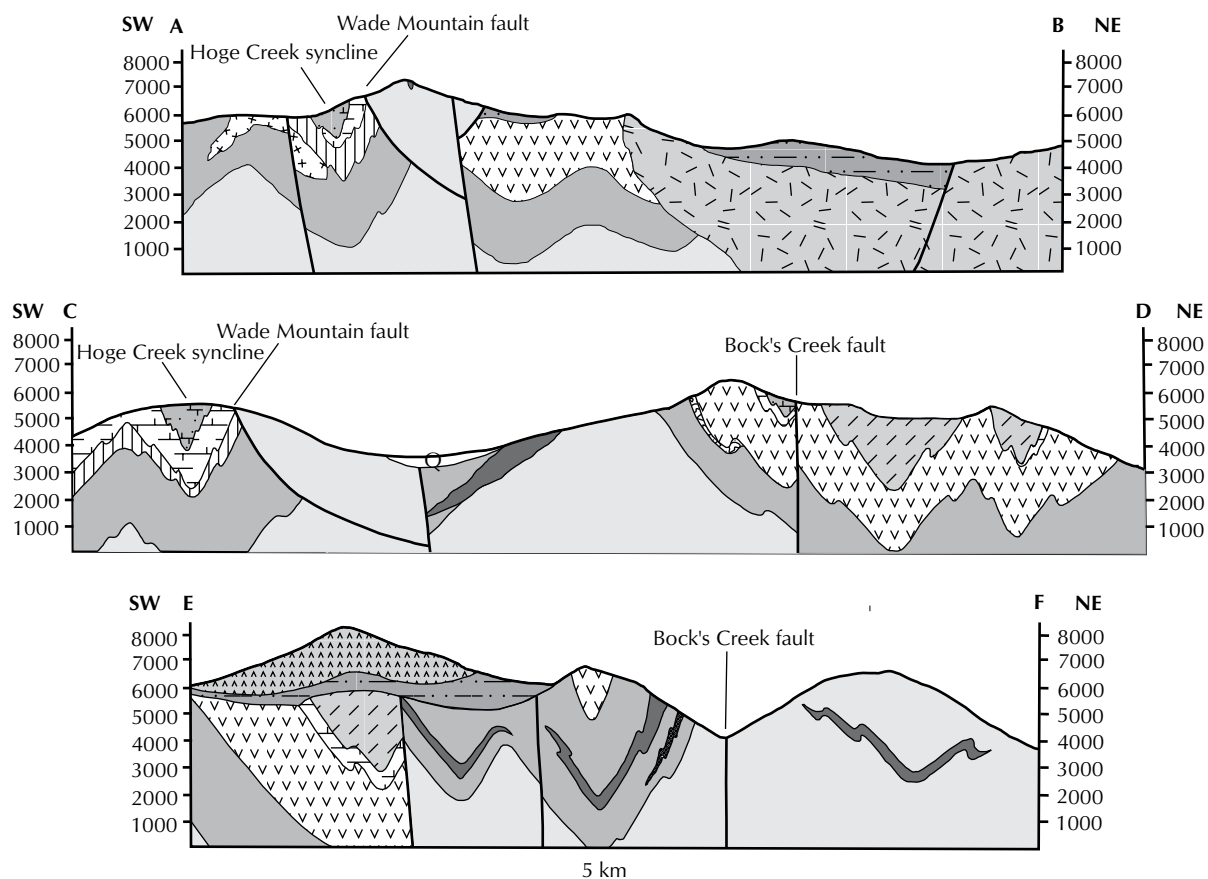


Figure 12. Schematic geologic cross-sections from the Duke River map area. (Locations of sections and pattern fills are shown in Figure 2.)

Pre-Middle Triassic

There is evidence for Pre-Middle Triassic contraction throughout the Duke River map area, but it is difficult to fully decipher because of intense, younger overprinting structures. Stratigraphic relationships reveal some indication that deformation involving uplift of the Paleozoic units occurred prior to deposition of the Triassic strata.

Read and Monger (1976) describe an unconformable contact between the Hasen Creek Formation and a gabbro body just west of the Duke River map area. At every other location where the base of the Hasen Creek Formation is exposed, outside of faulted contacts, the Station Creek Formation is preserved underlying the sedimentary unit. The lack of any Station Creek Formation below the Hasen Creek Formation may suggest local uplift and erosion of the Station Creek Formation prior to, or during, deposition of the Hasen Creek Formation.

To date, no Early Triassic stratigraphy has been identified anywhere within the Kluane Ranges. The absence of stratigraphy of this age could be the result of uplift and erosion that may have taken place prior to deposition of the Hoge Creek succession.

Finally, at two localities in the adjacent Quill Creek map area, tightly folded Hasen Creek sedimentary strata appear to be unconformably overlain by Nikolai formation volcanic rocks (Israel and van Zeyl, 2004).

Post-Triassic pre-mid-Cretaceous

Deformation during the post-Triassic to pre-mid-Cretaceous time appears to represent the main contractional event to affect the Kluane Ranges. Effects of this event can be observed throughout the Duke River map area and are characterized by northwest-southeast-trending, upright to locally overturned, tight to isoclinal folds and southwest-directed thrust faults. The Wade Mountain fault is a major southwest-directed thrust/reverse fault that places rocks of the Station Creek Formation over Mesozoic strata (Figs. 12, 13). The footwall is tightly folded to form the Hoge Creek syncline with tight chevron folds developed within the McCarthy Formation. Movement along the Bock's Creek fault is not well constrained; tightly folded Tatamagouche succession and Nikolai formation may indicate at least some contractional deformation (Fig. 2, 12). The Duke River fault appears to place metamorphic rocks of the Alexander Terrane over the relatively unmetamorphosed rocks of Wrangellia Terrane. Little information on the

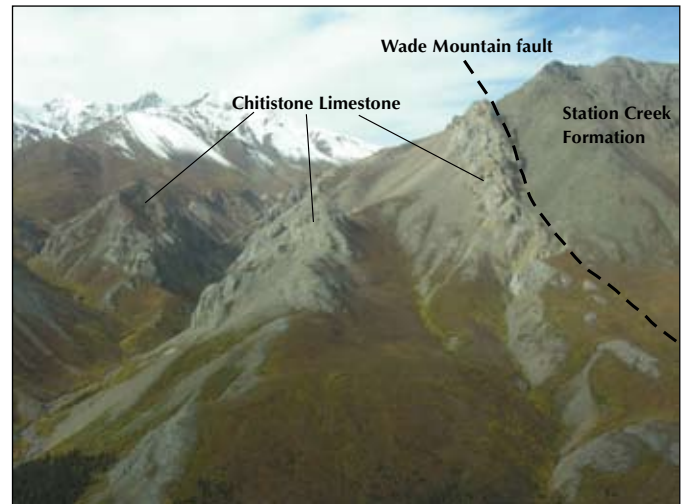


Figure 13. Aerial view looking west towards the Wade Mountain fault.

kinematics along the Duke River fault exists outside of recognizing strike-slip related lineations along the fault surface (Read and Monger, 1976). Read and Monger (1976) speculate that K-Ar dates in the eastern Alexander Terrane do not reflect large vertical movement of the terrane. It should be noted that some of the folds in the Quill Creek area, and locally, within the Hoge Creek syncline, are overturned to the northeast, and large northeast-directed thrust faults are also present to the northeast of the Duke River map area (Israel and van Zeyl, 2004). Timing of the contractional event is poorly constrained; it must be older than the Kluane Ranges suite, as these intrusions apparently do not show effects of this deformation; and must be at least as young as the Tatamagouche succession, as it exhibits evidence for the deformation, and may be as young as Hauterivian (Read and Monger, 1976). As with earlier deformation, many of the faults and folds that can be attributed to this event have been reactivated or overprinted by younger deformation.

Post-mid-Cretaceous

The two largest structures in the immediate vicinity of the Duke River area are the Denali and Duke River faults (Fig. 1). The Denali Fault occupies the Shakwak valley, immediately northeast of the Duke River area and is believed to have accommodated ~370 km of right-lateral displacement some time between mid-Cretaceous and the present (Lowey, 1998). The fault extends from northwestern British Columbia, through the Yukon Territory and into central Alaska. It is a major terrane-bounding, presently active, structure, which separates

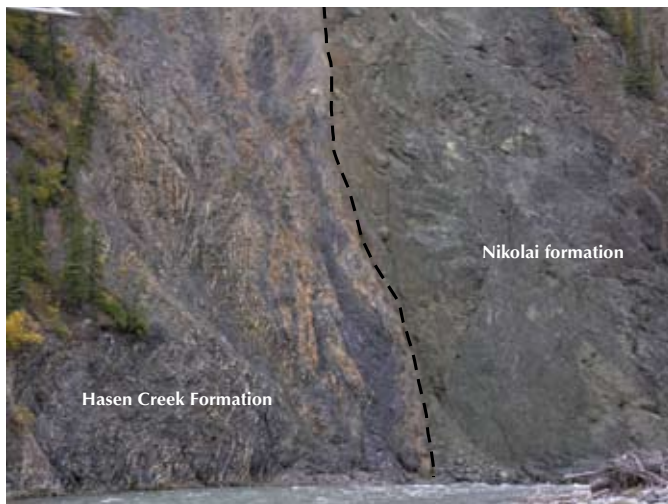


Figure 14. Steeply dipping fault placing Hasen Creek Formation next to the Nikolai formation.

Wrangellia Terrane from the Windy-McKinley and Nisling terranes, and the Coast Plutonic Complex (Fig. 1).

Only small segments of the Duke River fault outcrop in the map area (Fig. 2). The Duke River fault is the bounding fault between Wrangellia and Alexander terranes. It cuts through the entire southwest Yukon and continues into Alaska as the Totschunda Fault, an active splay off the Denali Fault. The fault has been described as a thrust fault that places rocks of the Alexander Terrane over Wrangellia (Muller, 1967), or alternatively, as a remnant of a megathrust that transported Wrangellia to the east overtop of the Alexander Terrane (MacKevett and Jones, 1975). Regardless of the earlier history of the Duke River fault, it has certainly been active as a late-Mesozoic through Cenozoic strike-slip fault (Read and Monger, 1976; Trop *et al.*, 2004). It deforms rocks as young as Miocene age, and earthquakes along the northwesternmost portion of the fault attests to its current active state.

Numerous, steeply dipping faults that are related to movement along the Denali and Duke River faults dissect the map area into northwest-trending fault blocks (Figs. 12, 14). Bock's Creek fault is a map-scale structure that runs the length of the Duke River map area, offsetting Paleozoic and Mesozoic stratigraphy. It cross-cuts many older, steeply dipping faults and has several smaller splays along its length. Gouge and breccia define many of the fault zones, indicating that the deformation at the level exposed was brittle. Large thrust/reverse faults have all been reactivated to some degree, exhibiting nearly

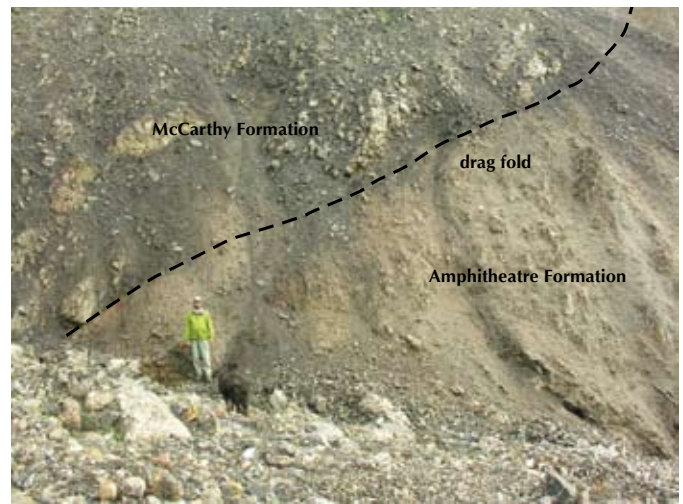


Figure 15. Tertiary contractional fault represented by Triassic McCarthy Formation thrust over the Amphitheatre Formation. Note drag folds in the Amphitheatre Formation.

horizontal stretching lineations and slickenside fibres. Fault-bound basins that are the sites of deposition of the Amphitheatre Formation are interpreted as either pull-apart or compressional basins caused by the partitioning of strain between the Denali and Duke River faults (Ridgway and DeCelles, 1993). Thrust faults, associated with deformation along the Denali and Duke River faults, place McCarthy Formation over top of the Amphitheatre Formation and folds the Wrangell Lavas (Fig. 15).

MINERALIZATION

Several mineral occurrences are found within the Duke River area and are associated with many different deposit types (Fig. 2, Table 1). Exploration in the area began in the mid-1950s after completion of the Alaska Highway. Since that time, the majority of exploration has centred on nickel-copper-platinum group element (PGE) mineralization hosted in intrusive bodies of the Kluane mafic-ultramafic complex. In 1994, Inco Limited staked the area located between Copper Joe Creek (called Halfbreed Creek on many maps) and Congdon Creek in the southeast portion of the Duke River area. For the next three years, Inco Limited completed mapping programs, lithogeochemical and silt sampling, and geophysical surveys. Massive sulphide showings were found over an area of ~3.6 km at the base of the Spy Sill (Yukon MINFILE 115G 003, Deklerk and Traynor, 2005²). Grab samples collected from the contact between the ultramafic body and the Hasen Creek Formation assayed up to 3.1% Ni,

²All Yukon MINFILE occurrences are from Deklerk and Traynor (2005).

Table 1. Yukon MINFILE occurrences within the Duke River area (Deklerk and Traynor, 2005).

Yukon MINFILE number	Name	Status	Commodity
115G 003	Congdon	showing	Cu-Ni
115G 005	Dickson	prospect	gabbroid Cu-Ni
115G 006	Destruction	prospect	gabbroid Cu-Ni
115G 007	Halfbreed	unknown	gabbroid Cu-Ni
115G 008	Squirrel	unknown	gabbroid Cu-Ni
115G 009	Windgap	prospect	coal
115G 010	Duke	showing	Asbestos
115G 011	Hoge	prospect	coal
115G 012	Amphitheatre	showing	coal
115G 013	Wade	showing	gabbroid Cu-Ni
115G 014	Amp	anomaly	porphyry Cu-Mo-Au
115G 015	Cork	drilled prospect	porphyry Cu-Mo-Au
115G 016	Glen	drilled prospect	gabbroid Cu-Ni
115G 017	Burwash	drilled prospect	Besshi MS Cu (Zn)
115G 018	Nelms	unknown	unknown
115G 084	Bock	showing	gabbroid Cu-Ni
115G 086	Gypsum	showing	gypsum
115G 092	Biczok	anomaly	paleoplacer
115G 098	Tony	showing	gabbroid Cu-Ni
115G 099	Kluane, Duke S	showing	gabbroid Cu-Ni

2.8% Cu, 0.2% Co, 3.1 g/t Pt, 1.4 g/t Pd and 1.0 g/t Au (Yukon MINFILE 115G 003). Several other ultramafic bodies are present in the Duke River area, with the largest being the Tatamagouche complex which outcrops along the Duke River. After extensive study of the entire Kluane mafic-ultramafic complex, Hulbert (1997) considered the Tatamagouche complex to have great potential for significant Ni-Cu-PGE mineralization.

Copper, molybdenum and gold mineralization is associated with the Kluane Ranges suite and the Tkope suite near Burwash Creek (Yukon MINFILE 115G 014 and 115G 015, respectively; Table 1). Drilling on the property (Yukon MINFILE 115G 015) by a syndicate of several companies in 1970, returned low values of copper and molybdenum.

Coal is found at several localities within the Amphitheatre Formation (Yukon MINFILE 115G 009, 115G 011 and 115G 012). At each locality, coal seams up to several metres thick occur in tightly folded sediments. Coal from

Yukon MINFILE 115G 012 occurrence was reportedly mined very briefly in 1950. In 1985, Noranda Inc. investigated anomalous gold values in silt at the Biczok property (Yukon MINFILE 115G 092) and concluded that the Amphitheatre Formation is likely a paleoplacer deposit.

ACKNOWLEDGEMENTS

Trans North Helicopters provided safe and reliable access to the Kluane Ranges. Thanks to Northern Platinum Ltd. and Coronation Minerals Inc. for access to the Wellgreen property. Discussion with Bill Wengzynowski and Rob Carne of Archer Cathro and Associates (1981) Ltd. were much appreciated. Critical review and editing of the manuscript was completed by Lori Kennedy, and editing by Leyla Weston and Diane Emond.

REFERENCES

- Campbell, S.W., 1981. Geology and genesis of copper deposits and associated host rocks in and near the Quill Creek area, southwestern Yukon. Unpublished Ph.D. thesis, University of British Columbia, Vancouver, British Columbia, 215 p.
- Carlisle, D. and Suzuki, T., 1974. Emergent basalt and submergent carbonate-clastic sequences including the Upper Triassic Dilleri and Welleri zones on Vancouver Island. Canadian Journal of Earth Sciences, vol. 11, p. 254-279.
- Christopher, P.A., White, W.H. and Harakal, J.E., 1972. K-Ar dating of the 'Cork' (Burwash Creek) Cu-Mo prospect, Burwash Landing area, Yukon Territory, Canada. Canadian Journal of Earth Science, vol. 9, p. 918-921.
- Deklerk, R. and Traynor, S. (compilers), 2005. Yukon MINFILE - A database of mineral occurrences. Yukon Geological Survey, CD-ROM.
- Dodds, C.J. and Campbell, R.B., 1988. Potassium-argon ages of mainly intrusive rocks in the Saint Elias Mountains, Yukon and British Columbia. Geological Survey of Canada, Paper 87-16, 43 p.

- Dodds, C.J. and Campbell, R.B., 1992. Overview, legend and mineral deposit tabulations for: Geological Survey of Canada Open File 2188, Geology of SW Kluane Lake map area (115G and F[East half]), Yukon Territory; Open File 2189, Geology of Mount St. Elias map area (115B and C[East half]), Yukon Territory; Open File 2190, Geology of SW Dezadeash map area (115A), Yukon Territory; Open File 2191, Geology of NE Yakutat (114O) and Tatshenshini River (114P) map areas, British Columbia. Geological Survey of Canada, summary report, 85 p.
- Dodds, C.J., Campbell, R.B., Read, P.B., Orchard, M.J., Tozer, E.T., Bamber, E.W., Pedder, A.E.H., Norford, B.S., McLaren, D.J., Harker, P., McIver, E., Norris, A.W., Ross, C.A., Chatterton, B.D.E., Cooper, G.A., Flower, R.H., Haggart, J.W., Uyeno, T.T. and Irwin, S.E.B., 1993. Macrofossil and conodont data from: SW Kluane Lake (115G and F [East half]), Mount St. Elias (115B and C [East half]), SW Dezedeash (115A), NE Yakutat (114O) and Tatshenshini River (114P) map areas, southwestern Yukon and northwestern British Columbia. Geological Survey of Canada, Open File 2731, 137 p.
- Eisbacher, G.H., 1976. Sedimentology of the Dezadeash flysch and its implications for strike-slip faulting along the Denali Fault, Yukon Territory and Alaska. *Canadian Journal of Earth Sciences*, vol. 13, no. 11, p. 1495-1512.
- Gardner, M.C., Bergman, S.C., Cushing, G.W., MacKevett, E.M., Jr., Plafker, G., Campbell, R.B., Dodds, C.J., McClelland, W.C. and Mueller, P.A., 1988. Pennsylvanian pluton stitching of Wrangellia and the Alexander terrane, Wrangell Mountains, Alaska. *Geology*, vol. 16, p. 967-971.
- Gehrels, G., 2001. Geology of the Chatham Sound region, southeast Alaska and Coastal British Columbia. *Canadian Journal of Earth Science*, vol. 38, p. 1579-1599.
- Gehrels, G., 2002. Detrital zircon geochronology of the Taku terrane, southeast Alaska. *Canadian Journal of Earth Science*, vol. 39, p. 921-931.
- Gordey, S.P. and Makepeace, A.J. (compilers), 2001. Bedrock geology, Yukon Territory. *In: Geological Survey of Canada, Open File 3754; also known as Exploration and Geological Services Division, Yukon Region, Indian and Northern Affairs Canada, Open File 2001-1, 1:1 000 000 scale.*
- Greene, A.R., Scoates, J.S., Weiss, D. and Israel, S., 2005. Flood basalts of the Wrangellia Terrane, southwest Yukon: Implications for the formation of oceanic plateaus, continental crust and Ni-Cu-PGE mineralization. *In: Yukon Exploration and Geology 2004*, D.S. Emond, L.L. Lewis and G.D. Bradshaw (eds.), Yukon Geological Survey, p. 109-120.
- Hulbert, L., 1997. Geology and metallogeny of the Kluane mafic-ultramafic belt, Yukon Territory, Canada: Eastern Wrangellia - A new Ni-Cu-PGE metallogenic terrane. Geological Survey of Canada, Bulletin 506, 265 p.
- Israel, S. and Van Zeyl, D., 2004. Preliminary geological map of the Quill Creek area, (parts of NTS 115G/5,6,12), southwest Yukon (1:50,000 scale). Yukon Geological Survey, Open File 2004-20.
- Israel, S. and Van Zeyl, D., 2005. Preliminary geology of the Quill Creek map area, southwest Yukon parts of NTS 115G/5,6,12. *In: Yukon Exploration and Geology 2004*, D.S. Emond, L.L. Lewis and G.D. Bradshaw (eds.), Yukon Geological Survey, p. 129-126.
- Israel, S., Tizzard, A. and Major, J., 2005. Geological map of the Duke River area (parts of NTS 115G/2,3,5,6,7) Yukon (1:50 000 scale). Yukon Geological Survey, Open File 2005-11.
- Lowey, G., 1998. A new estimate of the amount of displacement on the Denali Fault system based on the occurrence of carbonate megaboulders in the Dezadeash formation (Jura-Cretaceous), Yukon, and the Nutzotin Mountains sequence (Jura-Cretaceous), Alaska. *Bulletin of Canadian Petroleum Geology*, vol. 46, no. 3, p. 379-386.
- MacKevett, E.M., Jr., 1971. Stratigraphy and general geology of the McCarthy C-5 Quadrangle, Alaska. United States Geological Survey, Bulletin 1321, 35 p.
- MacKevett, E.M., Jr. and Jones, D.L., 1975. Relations between Alexander and Taku-Skolai terranes in the McCarthy quadrangle. *In: Geological Survey Research 1975*, USGS, Professional Paper 975, 69 p.
- Mortensen, J.K. and Hulbert, L.J., 1991. A U-Pb zircon age for a Maple Creek gabbro sill, Tatamagouche Creek area, southwest Yukon Territory. *In: Radiogenic age and isotopic studies: Report 5*, Geological Survey of Canada, paper 91-2, p. 175-179.

- Monger, J.W.H. and Nokleberg, W.J., 1996. Evolution of the northern North American Cordillera: generation, fragmentation, displacement and accretion of successive North American plate-margin arcs. *In: Geology and Ore Deposits of the American Cordillera*, A.R. Coyner and P.L. Fahey (eds.), Geological Society of Nevada Symposium Proceedings, Reno/Sparks, Nevada, p. 1133-1152.
- Muller, J.E., 1967. Kluane Lake map-area, Yukon Territory. Canadian Geological Survey, Memoir 340, 137 p.
- Nokleberg, W.J., Plafker, G. and Wilson, F.H., 1994. Geology of south-central Alaska. *In: The geology of Alaska: Geological Society of America*, G. Plafker and H.C. Berg (eds.), *Geology of North America*, vol. G-1, p. 311-366.
- Plafker, G. and Berg, H.C., 1994. Overview of the geology and tectonic evolution of Alaska. *In: The geology of Alaska: Geological Society of America*, G. Plafker and H.C. Berg (eds.), *Geology of North America*, vol. G-1, p. 989-1021.
- Read, P.B. and Monger, J.W.H., 1976. Pre-Cenozoic volcanic assemblages of the Kluane and Alsek Ranges, southwestern Yukon Territory. Geological Survey of Canada, Open File 381, 96 p.
- Ridgway, K.D., 1992. Cenozoic tectonics of the Denali fault system, Saint Elias Mountains, Yukon Territory: Synorogenic sedimentation, basin development, and deformation along a transform fault system. Unpublished Ph.D. thesis, University of Rochester, Rochester, New York, 506 p.
- Ridgway, K.D. and De Celles, P.G., 1993. Stream-dominated alluvial-fan and lacustrine depositional systems in Cenozoic strike-slip basins, Denali Fault system, Yukon Territory, Canada. *Sedimentology*, vol. 40, p. 645-666.
- Ridgway, K.D., De Celles, P.G., Cameron, A.R. and Sweet, A.R., 1992. Cenozoic syntectonic sedimentation and strike-slip basin development along the Denali Fault system, Yukon Territory. *In: Yukon Geology Volume 3*, T.J. Bremner (ed.), Exploration and Geological Services Division, Yukon Region, Indian and Northern Affairs Canada, p. 1-26.
- Ridgway, K.D., Trop, J.M., Nokleberg, W.J., Davidson, C.M. and Eastham, K.R., 2002. Mesozoic and Cenozoic tectonics of the eastern and central Alaska Range: Progressive basin development and deformation in a suture zone. *Geological Society of America Bulletin* 114, no. 12, p. 1480-1504.
- Skulski, T., 1988. The origin and setting of anomalous arc magmatism in the Wrangell volcanic belt, southwest Yukon. *In: Yukon Geology Volume 2*, J.G. Abbott (ed.), Exploration and Geological Services Division, Yukon Region, Indian and Northern Affairs Canada, vol. 2, p. 88-89.
- Smith, J.G. and MacKevett, E.M., Jr., 1970. The Skolai Group in the McCarthy B-4, C-4 and C-5 quadrangles, Wrangell Mountains, Alaska. *United States Geological Survey, Bulletin* 1274-Q, 26 p.
- Trop, J.M., Ridgway, K.D., Manuszak, J.D. and Layer, P., 2002. Mesozoic sedimentary basin development on the allochthonous Wrangellia composite terrane, Wrangell Mountains basin, Alaska: A long-term record of terrane migration and arc construction. *Geological Survey of America, Bulletin*, vol. 114, no. 6, p. 693-717.
- Trop, J.M., Ridgway, K.D. and Sweet, A.R., 2004. Stratigraphy, palynology, and provenance of the Colorado Creek basin, Alaska, USA: Oligocene transpressional tectonics along the central Denali fault system. *Canadian Journal of Earth Sciences*, vol. 41, p. 457-480.
- van der Heyden, P., 1992. A Middle Jurassic to early Tertiary Andean-Sierran arc model for the Coast belt of British Columbia. *Tectonics*, vol. 11, p. 82-97.
- Wheeler, J.O., Brookfield, A.J., Gabrielse, H., Monger, J.W., Tipper, H.W. and Woodsworth, G.J., 1991. Terrane map of the Canadian Cordillera. Geological Survey of Canada, Map 1713A.

Placer geology and prospective exploration targets of Sixtymile River area, west-central Yukon

William LeBarge¹
Yukon Geological Survey

LeBarge, W., 2006. Placer geology and prospective exploration targets of Sixtymile River area, west-central Yukon. *In: Yukon Exploration and Geology 2005*, D.S. Emond, G.D. Bradshaw, L.L. Lewis and L.H. Weston (eds.), Yukon Geological Survey, p. 155-174.

ABSTRACT

Sixtymile River alluvial deposits can be subdivided into four main types, on the basis of age and physiographic setting. These are pre-Reid and older; interglacial (prior to the McConnell glacial episode); modern (Holocene); and technogenic. All deposit types are placer-gold-bearing, and historically the most placer gold has been produced from modern (Holocene) deposits, followed by pre-Reid and older, interglacial, and finally, technogenic deposits.

Prospective placer gold exploration targets still exist and include 1) pre-Reid and older buried abandoned channels; 2) interglacial buried and/or abandoned alluvial terraces; 3) modern (Holocene) alluvial channels and gulches; and 4) technogenic deposits. Various exploration techniques can be used to evaluate these targets including airphoto interpretation, seismic and ground-penetrating radar surveys, electrical resistivity and magnetometer surveys, auger and reverse circulation drilling, and bulk sampling.

RÉSUMÉ

Les dépôts alluviaux de la région de Sixtymile se répartissent selon l'âge et le cadre physiographique en quatre grands groupes principaux. Ceux-ci sont d'âge pré-Reid et plus anciennes; des dépôts alluviaux interglaciaires (antérieur à l'époque glaciaire de McConnell); des dépôts alluviaux contemporains (Holocène); et des dépôts résultant du développement technologique. Tous ces types de dépôts contiennent de l'or placerien, et historiquement la plupart de l'or placerien était produit des dépôts contemporains (Holocène), suivit par les dépôts pré-Reid, et plus anciennes, les dépôts interglaciaires, et finalement, ceux résultant du développement technologique.

Plusieurs prometteuses cibles d'exploration à la recherche de placers peuvent être identifiées dans le bassin de la rivière Sixtymile et regroupées en quatre principaux cadres de dépôt : 1) chenaux abandonnés enfouis pré-Reid et plus anciennes; 2) terrasses alluviales enfouies et abandonnées; 3) chenaux et ravins alluviaux contemporains; et 4) dépôts résultant du développement technologique. Diverses méthodes d'exploration de ces cibles peuvent être utilisées dont l'interprétation de photographies aériennes, les levés sismiques et au géoradar, les levés de résistivité électrique et magnétométriques ainsi que le forage à la tarière suivi d'un échantillonnage en vrac.

¹bill.lebarge@gov.yk.ca

RATIONALE OF STUDY

The Sixtymile River and several of its tributaries have been the focus of placer gold mining since 1892, pre-dating the Klondike Gold Rush which began with the discovery of gold on Bonanza (then Rabbit) Creek in August, 1896. Active mining in the area has been more or less continuous since then, and several of the creeks have been mined up to four times, with increasingly larger and more efficient equipment.

This study builds upon the work of previous researchers and is intended to fulfill two purposes: to supplement previous understanding of the paleogeography and Quaternary history of the Sixtymile River area; and to focus on the detailed placer geology for the purposes of broadening placer gold exploration and current placer mining efforts.

LOCATION

The Sixtymile River is located in the unglaciated, west-central Yukon, and it is one of the major left limit tributaries of the Yukon River (Fig. 1, see facing page). Its headwaters are located in Alaska, and from there it flows east-northeast and finally southeasterly to join the Yukon River at the abandoned site of Ogilvie. Placer mining has mainly been confined to the Canadian side of the Sixtymile River, which includes major tributaries: Bedrock Creek, Miller Creek, Glacier Creek, Big Gold Creek, Little Gold Creek, California Creek, Fifty Mile Creek, Matson Creek and Ten Mile Creek.

PREVIOUS WORK

The glacial limits in this area were first mapped by O.L. Hughes (1968), later compiled by Hughes *et al.* (1969) and subsequently re-mapped by Duk-Rodkin (1996).

A 1:250 000-scale surficial map of the northern parts (NTS 116B/C) of the drainage was completed by Duk-Rodkin (1999), and the surficial geology of the southern part of the study area was mapped at 1:50 000 scale by Jackson (2005).

R.L. Hughes studied the evolution and origin of the placer-gold-bearing gravel of the Miller Creek and Sixtymile River drainages (Hughes, 1986; Hughes *et al.*, 1986). More recently, the placer geology of the drainage was studied by Lowey (2000, 2004).

FIELD AND LABORATORY METHODOLOGY

Twenty-five sections were visited and described within the study area between 2000 and 2003. Mining operations provided excellent exposures of pay gravel and overburden, which enabled the stratigraphic relationships between different units to be ascertained. Sections were described with emphasis on physical sedimentary features, including grain size, bed thickness, gravel fabric, primary sedimentary structures, lithology and rounding of clasts. Cryogenic features such as ice-wedge casts and cryoturbation of sediments were also noted and described when present. Samples were collected for grain-size, heavy mineral and radiocarbon analyses.

Forty-five bulk sediment samples of between 3 and 4 kg each were collected. Selected samples were panned on site to document any presence of gold, while most samples were collected for grain-size and heavy mineral analysis following the methodology of Folk (1974). Grain-size samples were dried, split and sieved through #4, #10, #18, #35, #60, #120 and #230 US Standard mesh screens. Each fraction was collected and weighed (Fig. 2), and the minus #230 mesh screen material was then analysed by hydrometer for the sand, silt and clay ratio.

Hand-panned concentrates of the heavy minerals from several samples were derived from the combined #18 to #120 mesh fractions. Gold, when present, was separated from the other heavy minerals and both fractions were air-dried. Selected gold and other heavy mineral grains were analysed by PetraScience Consultants Inc. (Vancouver, BC) using a scanning electron microscope (SEM) and electron microprobe.



Figure 2. Gravel samples were dried and sieved through a series of US Standard mesh screens to determine matrix grain-size distribution.

Six organic samples were collected for ^{14}C dating. Wood was sampled wherever possible to avoid any root contamination, which may occur while bulk-sampling organic-rich soil samples. Since some samples were likely

to be close to, or beyond the age of radiocarbon-dating methods, Accelerated Mass Spectrometer (AMS) analyses were completed.

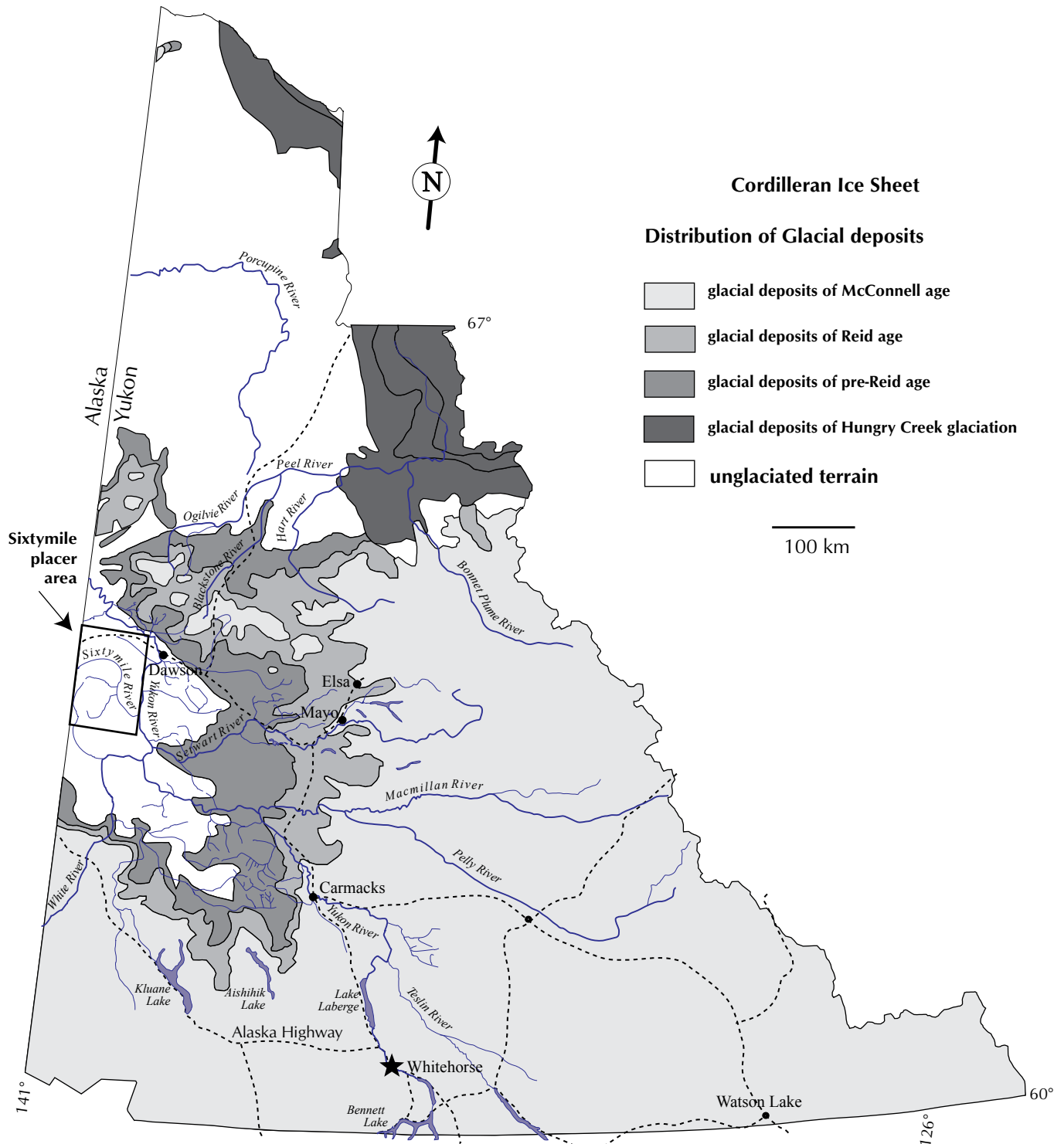


Figure 1. Glacial limits in Yukon showing location of Sixtymile placer area (glacial limits after Duk-Rodkin, 1999).

MINING HISTORY

The Sixtymile River area has been mined for placer gold since well before the discovery of gold in the Klondike in 1896. In 1877, while prospecting along the Yukon River, Arthur Harper and Jack McQuesten reported 'good prospects' on bars of the lower Sixtymile River (Wright, 1976). McQuesten himself reportedly made \$6 to \$8 per day on several bars (at \$20.65/ounce). These bars were worked to a small extent by members of the Schwatka expedition in 1883 (Wright, 1976).

Glacier creek was extensively hand-mined for years following the discovery of gold on it in 1883. Prospecting first occurred on Miller Creek in 1887, but no significant activity was recorded until 1892, when considerable mining was reported on Glacier, Miller, and to a lesser extent on Bedrock and Big Gold creeks. By 1895, 350 miners were reportedly working in the Sixtymile area (Wright, 1976). Activity temporarily dwindled when gold was discovered on Bonanza Creek in 1896.

Beginning in 1912, the Northern American Transportation and Trading Company dredged for a few years on Miller Creek. The dredge was subsequently acquired by Holbrook Dredging Company in 1929, and in 1937 was converted from steam to diesel power, operating until 1941 on the Sixtymile River (Debicki, 1983).

In the late 1930s, prospect drilling was conducted by North American Mines, Inc. on the ground at the mouth of Glacier Creek and at the confluence of Big Gold Creek and Sixtymile River. From 1949 to 1959, Yukon Placer Mining Company was operating on Yukon Exploration Company's property on Big Gold, at the mouth of Glacier Creek. They used a 3.5-cubic-foot (0.099 m³) bucket-line diesel-electric dredge (built by Yukon Exploration Company in 1947) and an open-cut bulldozer-slucing plant (Debicki, 1983).

In the 1950s and 1960s, several small operators including James Lynch, Miller Creek Placers and Glacier Creek Placers mined on Miller, Glacier, Bedrock and Big Gold creeks as well as the left limit of Sixtymile River (LeBarge and Coates, 2005).

Companies and individuals active in the 1970s and 1980s included Sixtymile Enterprises, Brisebois Brothers Construction Ltd., Cogasa Mining Corporation, Fell Hawk Placers, W. Hakonson, Chuck and Lynn McDougall, Territorial Gold Placers, Oak Bay Manor, Granges Exploration and Tri-Kay Placers. In the 1980s, underground mining was conducted on Miller Creek by

Chumar Placers, Dublin Gulch Mining and Klondike Underground Mining Ltd. (LeBarge and Coates, 2005).

In the 1990s, active operators included K-1 Mining & Services, Fell-Hawk Mining, D & P Mining Exploration Ltd., S. Prohaszka, Coulee Resources Ltd., Eldorado Placers Ltd., Aardvark Placers, 6077 Yukon Ltd., Graham Ventures, Walter Yaremcio, Brisbois Brothers Construction Ltd., Hawker/Tri-Kay Properties, Goldmark Minerals, No Name Resources, G. Fowler, M. Orbanski and J.M. Mining Ltd. (Mining Inspection Division, 2003).

Since 2000, mining has been conducted by F. and K. Hawker, J.M. Mining, W. Yaremcio, Gordon Hagen, Tim Coles, Northway Mining, Brisbois Brothers Construction Ltd., Dredgemaster Gold, Maurice Alexander, S. Prohaszka, Midas Rex Mining, Powers and Long, J. Ganter, K-1 Mining and Eldorado Placers (LeBarge and Coates, 2005).

MINING VOLUMES

Between 1998 and 2002, 13 placer mining operations (Fig. 3) were active on the Sixtymile River and its tributaries (Mining Inspection Division, 2003). Although data is incomplete, Table 1 is a compilation of available information of the amount of sediment stripped and sluiced during that period.

PLACER GOLD PRODUCTION

Table 2 shows the recorded placer gold production from available sources. This production can be considered minimum amounts, as gold is sometimes not reported in royalties and pre-1978 information is anecdotal in nature.



Figure 3. Frank and Karen Hawker's placer mine in the Sixtymile River valley, 2001.

Table 1. Minimum amount of material stripped and sluiced, Sixtymile area, 1998-2002.

Drainage	Stripped, cubic yards (m ³)	Sluiced, cubic yards (m ³)
Sixtymile	2,706,614 (2 069 355)	949,551 (725 983)
Miller	130,926 (100 100)	63,773 (48 758)
Big Gold	356,793 (272 787)	52,768 (40 344)
Glacier	468,519 (358 208)	137,378 (105 033)
Little Gold	12,460 (9526)	3327 (2543)
Totals	3,675,311 (2 809 977)	1,206,796 (922 661)

GENERAL SETTING

BEDROCK GEOLOGY

Figure 4 is a generalized map of the bedrock geology of the study area, which was mapped by Mortensen (1988, 1990, 1996). The area is underlain by Proterozoic to Mississippian metamorphic rocks of the Yukon-Tanana Terrane; this, in turn, is overlain by mainly flat-lying Cretaceous Tantalus Formation sandstone and pebble conglomerate, and Late Cretaceous Carmacks Group andesitic flows and breccias.

Structurally, the Sixtymile River flows along an asymmetric graben structure which progressively down-drops flat-lying panels of Tantalus Formation and Carmacks Group volcanic rocks to the level of the valley bottom on the north side of the Sixtymile river valley. A set of major northeast-trending faults generally separates this package from dominantly metamorphic rocks of Yukon-Tanana Terrane to the south.

MINERAL DEPOSITS

Several mineral deposits of various types occur in the Sixtymile area (Fig. 4 and Table 3). As documented in the Yukon MINFILE database (Deklerk and Traynor, 2005), veins are the main occurrence type. The veins cut both Tantalus Formation and Carmacks Group rocks and the metamorphic basement rocks; many of them are thought

Table 2. Recorded placer gold production, Sixtymile area.

Creek	Tributary of	Recorded production, crude ounces (g)		
		1892-1977	1978-2005	1892-2005
Sixtymile	Yukon	8152 (253 556)	227,964 (7 090 478)	236,116 (7 344 034)
Miller	Sixtymile	47,525 (1 478 194)	49,876 (1 551 318)	97,401 (3 029 512)
Glacier	Big Gold	34,365 (1 068 872)	16,462 (512 026)	50,827 (1 580 897)
Big Gold	Sixtymile	31,098 (967 257)	2637 (82 020)	33,735 (1 049 277)
Little Gold	Big Gold	3775 (117 416)	5066 (157 570)	8841 (274 986)
Bedrock	Sixtymile	4393 (136 638)	3796 (118 067)	8189 (254 706)
Fifty Mile	Sixtymile	0	105 (3266)	105 (3266)
Matson		0	24,385 (758 459)	24,385 (758 459)
Ten Mile		0	30,261 (941 223)	30,261 (941 223)
Totals		129,308 (4 021 931)	360,554 (11 214 491)	489,862 (15 236 422)

to be epithermal in nature (Glasmacher, 1985, Glasmacher and Friedrich, 1999). Studies of gold compositions in the Sixtymile District by Mortensen *et al.* (2006) suggest that these epithermal veins may not be the main contributors to placer gold in the Sixtymile River and its tributaries. Significant lode gold sources may remain to be discovered in the Sixtymile River area.

QUATERNARY HISTORY AND REGIONAL SURFICIAL GEOLOGY

The Sixtymile River is situated in the dominantly unglaciated western part of the Yukon Plateau (Fig. 1). Previous researchers (Bostock, 1966; Hughes, 1968) had considered the drainage to be unglaciated, however, Duk-Rodkin (1999) described part of the Sixtymile river valley as glaciated during one of the pre-Reid (780K to 2.5 Ma B.P.) glacial events, with a corresponding glacial moraine terminating between left limit tributaries, Twelve Mile Creek and California Creek. Lowey (2004) shows the Sixtymile river drainage to be unglaciated, while Jackson (2005) mapped several glaciofluvial terraces along the Sixtymile river valley, upstream of Bedrock Creek, and on the left limit of Mosquito Creek. Fifty Mile Creek is also mapped with a right-limit glaciofluvial terrace. These are

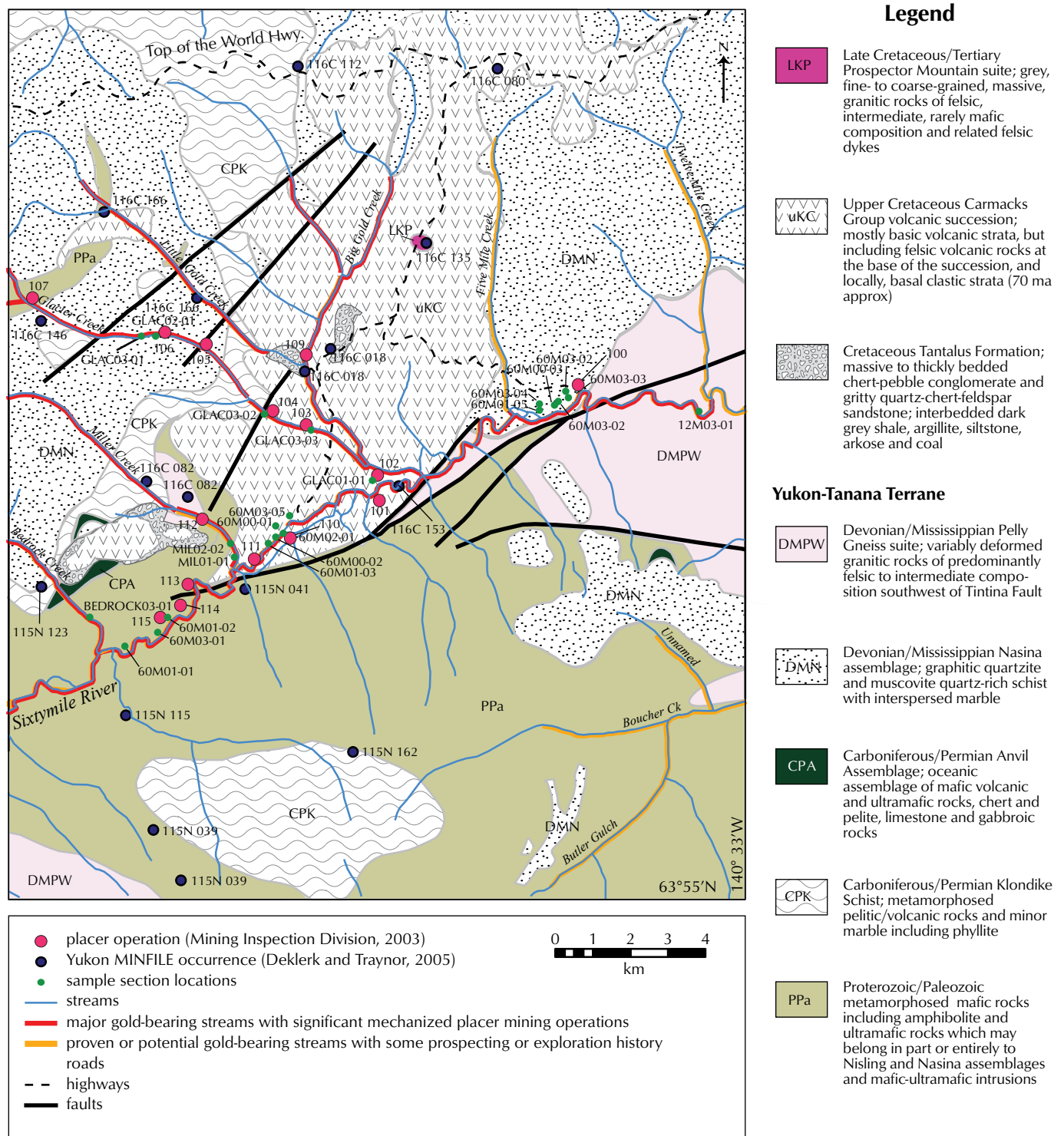


Table 3. Mineral deposits, Sixtymile River area.

MINFILE number	Name	Status	Class	Commodity
115N 039	Golden Crag; Judy; Lerner	open pit past producer	vein	lead; silver, gold
115N 040	Connaught; Mosquito Creek	open pit past producer	vein	lead; silver, gold
115N 041	Per	drilled prospect	disseminated; stockwork; vein	gold; lead; silver; zinc
115N 115	The	unknown	unknown	unknown
115N 123	Bedrock	showing	igneous-contact; vein	silver, copper, gold
115N 162	Peak	showing	syngenetic	unknown
116C 018	Hungry; Kostem; Lgc; Pine; Rod	drilled prospect	coal	gold
116C 019	Boundary Lake; Devils Canyon; Gold Flake	showing	vein	lead; silver; zinc
116C 020	Alaska	anomaly	unknown	unknown
116C 080	Hamburger; Tony	unknown	unknown	unknown
116C 082	Elsie; Klonx; Marv	anomaly	unknown	mercury; tungsten
116C 112	Pub	showing	sedimentary; stratiform	zinc, copper, lead
116C 133	Baldy	showing	unknown	copper; lead; silver; zinc
116C 135	Be; Cholach; Guch; Jem	showing	vein	lead; silver
116C 146	Birch; Cedar	anomaly	unknown	gold; zinc
116C 153	Glasmacher; Lcg	showing	epithermal; replacement	gold
116C 158	Big Gold; Chels	unknown	breccia; vein	unknown
116C 166	Little Gold	anomaly	vein	unknown

interpreted by Jackson (2005), and Nelson and Jackson (2002) to be related to local pre-Reid alpine glaciations.

The subsequent Reid (311±32 ka to ca. 80 ka; Alloway *et al.*, 2005) Cordilleran ice sheet did not advance into the region, but was likely contemporaneous with local alpine glaciation, as documented by geomorphic features described in the Fifty Mile Creek drainage by Lowey (2000, 2004). Periglacial weathering and increasing base-levels caused aggradation in the period leading up to the maximum glacial extent, and later, incision with decreasing base-levels during glacial retreat.

The McConnell (27-10 ka; Mathews *et al.*, 1990) glaciation brought wind-blown silt (loess) into the area on katabatic winds. This blanketed existing sediments and bedrock surfaces, and through erosion, accumulated into the lower parts of the Sixtymile River valley.

STRATIGRAPHY AND SEDIMENTOLOGY

Table 4 displays the location and elevation of stratigraphic sections measured and sampled in the Sixtymile area drainages.

DESCRIPTION AND INTERPRETATION OF STRATIGRAPHIC SECTIONS

Although some evidence exists for glaciofluvial sediment in the Sixtymile drainage basin (Jackson, 2005), all stratigraphic sections examined in this study are interpreted to be fluvial in origin. On the basis of age and physiographic setting, four types of alluvium can be described: modern (Holocene); interglacial (prior to the McConnell glacial episode); pre-Reid and older; and technogenic deposits. Although all of these types of alluvium are placer-gold bearing, there are broad differences between them in size and grade. Radiocarbon dates are shown in Table 5.

Table 4. Stratigraphic sections from Sixtymile River area (plotted on Figure 4).

Section	Creek	Latitude			Longitude			Elevation	
		°	min	sec	°	min	sec	feet	metres
60M00-01	Sixtymile River	64	0	6	140	46	16	2262	689
60M00-02	Sixtymile River	63	59	53	140	45	59	2224	678
60M00-03	Sixtymile River	64	2	21.1	140	38	2.5	2100	640
60M01-01	Sixtymile River	63	57	51	140	51	33.7	2335	712
60M01-02	Sixtymile River	63	58	31.8	140	49	22.4	2322	708
60M01-03	Sixtymile River	63	59	42.2	140	46	35.3	2270	692
60M01-04	Sixtymile River	64	2	11.6	140	39	57.7	2100	640
GLAC01-01	Glacier Creek	64	1	13.2	140	44	29.6	2279	695
MIL01-01	Miller Creek	63	59	30	140	47	48	2290	698
60M02-01	Sixtymile River	63	59	57	140	46	25.8	2270	692
60M02-02	Sixtymile River	64	2	19.8	140	38	33	2130	649
GLAC02-01	Glacier Creek	64	2	34.2	140	51	26.6	2753	839
MIL02-01	Miller Creek	63	59	38.5	140	47	48.7	2287	697
MIL02-02	Miller Creek	63	59	48.7	140	48	13.2	2334	711
10M03-01	10 Mile Creek	63	30	51	140	0	38	1750	533
12M03-01	12 Mile Creek	64	2	37.5	140	33	12.3	2080	634
BEDROCK03-01	Bedrock Creek	63	58	38	140	52	56.1	2446	746
GLAC03-01	Glacier Creek	64	2	24.9	140	51	59.1	2763	842
GLAC03-02	Glacier Creek	64	1	45.3	140	47	45.6	2418	737
GLAC03-03	Glacier Creek	64	1	34.5	140	45	29.2	2330	710
60M03-01	Sixtymile River	63	58	28.4	140	49	13.8	2314	705
60M03-02	Sixtymile River	64	2	28.5	140	37	20.4	2063	629
60M03-03	Sixtymile River	64	2	31.3	140	37	29.7	2148	655
60M03-04	Sixtymile River	64	2	9	140	39	47	2096	639
60M03-05	Sixtymile River	64	0	6.2	140	45	44.4	2557	779

Table 5. Radiocarbon dates for Sixtymile area drainages.

Original sample number	Beta sample number	Section - unit	Drainage	14C date in years (AMS)	Mining operation
60M003-04	Beta 165202	60M00-03-04	Sixtymile	4520 ± 40 BP	Hakonson
60M00-1	Beta 165203	60M00-01-02	Sixtymile	45 420 ± 1100 BP	Hawker bench
60M01-04	Beta 165204	60M01-04-01	Sixtymile	9380 ± 40 BP	Hakonson
60M01-02-05	Beta 165205	60M01-02-05	Sixtymile	1290 ± 40 BP	Sandberg
WL03-76	Beta 189861	60M03-04-04	Sixtymile	2430 ± 40 BP	Hakonson peat
WL03-80-2	Beta 189862	60M03-05-02	Sixtymile	>50 030 BP	Hawker bench

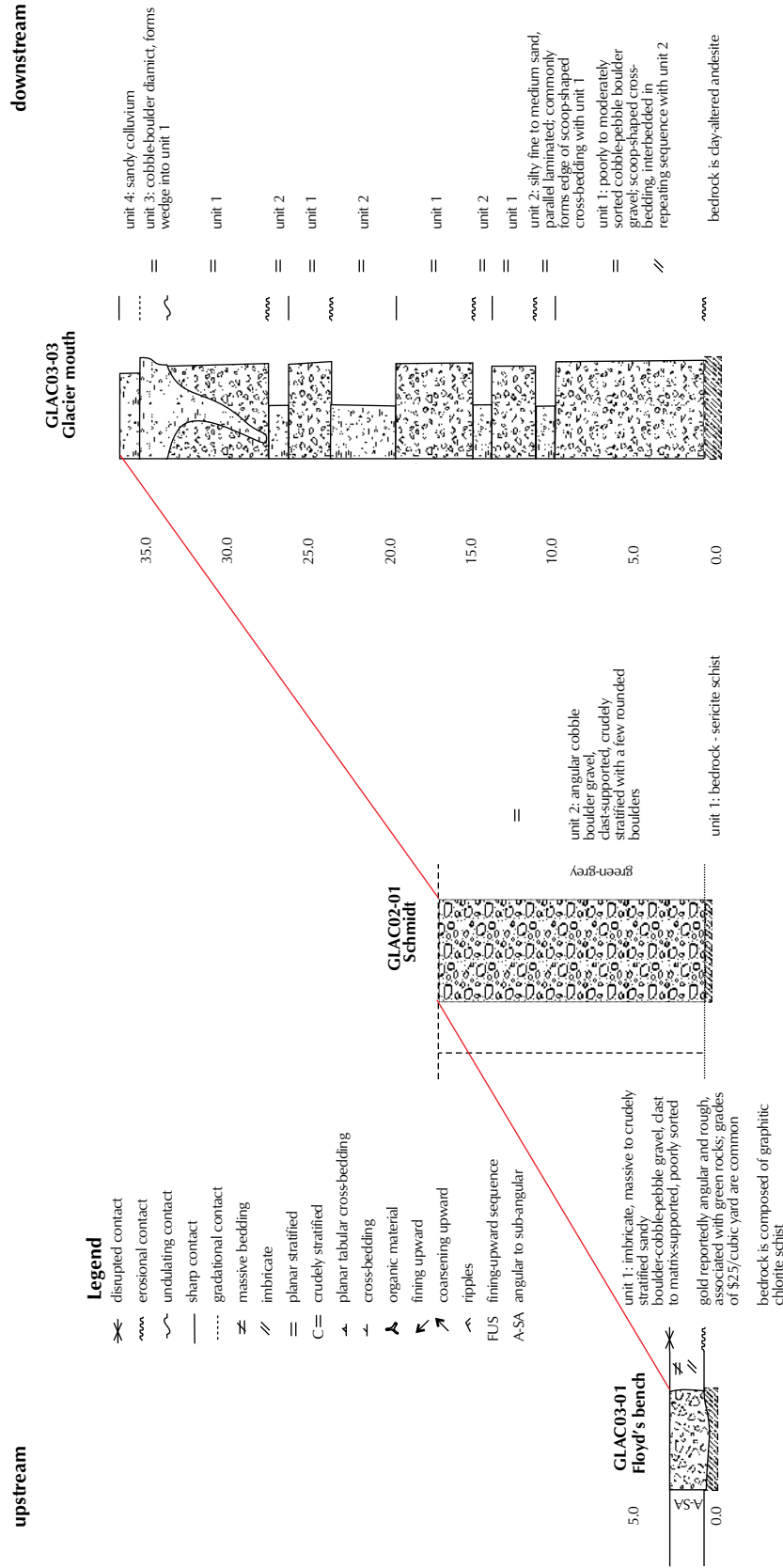


Figure 5. Pre-Reid and older correlation, Glacier Creek valley.

PRE-REID AND OLDER DEPOSITS

Pre-Reid and older deposits are represented by intermediate- to high-level terrace gravels exposed along the lower reaches of Glacier and Miller creeks. In upstream reaches, these terraces form incised abandoned channels, which run parallel to the modern channel. Figure 5 displays the stratigraphic correlation of measured sections GLAC03-01, GLAC02-01 and GLAC03-03. Sediments in these sections consist mainly of poorly sorted, angular, massive to crudely stratified, cobble-boulder gravel, which is interbedded with planar-laminated fine to medium sand (Fig. 6). This sequence represents a period of alluvial fan deposition under periglacial climatic conditions, which would be consistent with the onset of one of the pre-Reid glacial events. Further evidence of a periglacial environment is provided by the presence of a large ice-cast sand/gravel wedge at the top of measured section GLAC03-03 (Fig. 5), as well as the absence of any organic material.

These abandoned channels contain significant placer gold and have been mined extensively, including underground mining which was conducted on the left limit of Miller Creek. The highest gold grades are found at the gravel/bedrock contact and this deposit type ranks second (to modern or Holocene deposits) in the amount of placer gold produced in the Sixtymile River drainage.

INTERGLACIAL (PRE-MCCONNELL) DEPOSITS

Interglacial alluvial deposits in the Sixtymile River drainage are found on left-limit, low- to intermediate-level terraces. They consist mainly of massive to crudely stratified, quartz-rich, cobble-pebble gravel, overlain in



Figure 6. Periglacial pre-Reid and older age gravel, at the mouth of Glacier Creek, measured section GLAC03-03, approximately 30 m in height.

varying combinations by rusty planar-stratified pebble-cobble gravel, and ice-rich to ice-poor silt and macro-organic materials (Figs. 7 and 8). The crudely stratified gravel represents a time of braided river sedimentation in the Sixtymile River drainage, while the planar-stratified gravel represents a transition to a wandering gravel-bed river system. Silt represents abandonment of the channel, and subsequent growth of macro-organic materials, which were further buried by aeolian sediments and infiltrated by permafrost ground ice.



Figure 7. Interglacial alluvial terrace gravel, measured section 60M00-01, at Frank and Karen Hawker's placer mine. Note in-situ tree stump (AMS radiocarbon dated at $45\,420 \pm 1100$ years B.P. – Beta 165203).



Figure 8. Interglacial alluvial terrace, measured section 60M03-05. Note ice-cast sand/gravel wedge at the contact between massive gravel and well stratified gravel units (adjacent to shovel). This is coincident with the transition from a braided to a wandering gravel-bed stream environment.

Radiocarbon dates of $45\,420 \pm 1100$ BP (Beta 165203) from section 60M00-01, and $>50\,030$ BP (Beta 189862) from section 60M03-05 (Table 5) indicate that these deposits are at least as old as the pre-McConnell interglacial.

Figure 9 shows stratigraphic correlations of measured sections in these deposits, which include 60M00-01, 60M03-05, GLAC01-01, 60M03-03 and 12M03-01.

These deposits have been mined on the left limit of Sixtymile River between Glacier and Miller creeks. Placer gold grades are highest at the gravel/bedrock contact, although this deposit type ranks lowest in the relative amount of placer gold historically produced.

MODERN (HOLOCENE) ALLUVIAL DEPOSITS

Modern (Holocene) alluvial deposits in the Sixtymile River drainage basin occur along the present flood plain, on low terraces and within gulches. In the main valley of Sixtymile River, deposits consist of varying combinations of massive to crudely stratified pebble-cobble gravel, planar-, cross- and epsilon-stratified pebble-cobble gravel, medium to fine sand, and silt. Crudely stratified and massive gravel represent fluvial channel lag deposits, while the planar-, cross- and epsilon-stratified gravel represent point bar and channel bar sequences. Sand is typically deposited on bar tops and silt is the result of overbank flood deposition. These are fining-upward sequences characteristic of a meandering river system. Contemporaneous gulch deposits of Sixtymile River tributaries are represented by poorly sorted, locally-derived angular gravel.

Figure 10 displays the stratigraphic correlations of Sixtymile River upstream of Glacier Creek, and includes measured sections 60M01-01, 60M01-02 (Fig. 11) and 60M03-01. A modern (Holocene) age is indicated by a radiocarbon date of 1290 years B.P. (Beta 165205).

Figure 12 displays the stratigraphic correlations of Sixtymile River downstream of Five Mile Creek, and includes measured sections 60M01-04, 60M03-04, 60M02-02, 60M00-03 and 60M03-02. Three radiocarbon dates (Beta 165204 – 9350 years B.P.; Beta 189861 – 2420 years B.P.; and Beta 165202 – 4520 years B.P.) indicate that this sequence is also Holocene in age. Measured sections from Sixtymile River tributaries Ten Mile, Miller and Bedrock creeks (10M03-01, MIL01-01, MIL02-02 and BEDROCK03-01; W. LeBarge, unpublished data) have similar stratigraphy and are also interpreted to be Holocene in age.



Figure 11. Measured section 60M01-02, modern (Holocene) alluvial gravel and silt on Sixtymile River, Don Sandberg's placer mine.

Placer gold occurs in all modern (Holocene) alluvial deposits studied but has mainly been mined in the valleys of Glacier, Miller, Big Gold, Little Gold and Bedrock creeks and Sixtymile River, making this deposit type the highest placer-gold producer. Gold grades are generally highest at the gravel/bedrock contact, but economic values commonly extend a metre or more into bedrock.

TECHNOGENIC DEPOSITS

Technogenic deposits can be described as alluvial deposits which have been subjected to some component of human disturbance, and include both actual tailings from previous mining activity, and remnant undisturbed placer-gold-bearing sediments which have been buried by tailings, or



Figure 13. Technogenic deposit, measured section 60M01-03. Typical dredge tailings with planar-tabular stratified sandy gravel over mud and bedrock. Fractured bedrock here contains economic gold values.

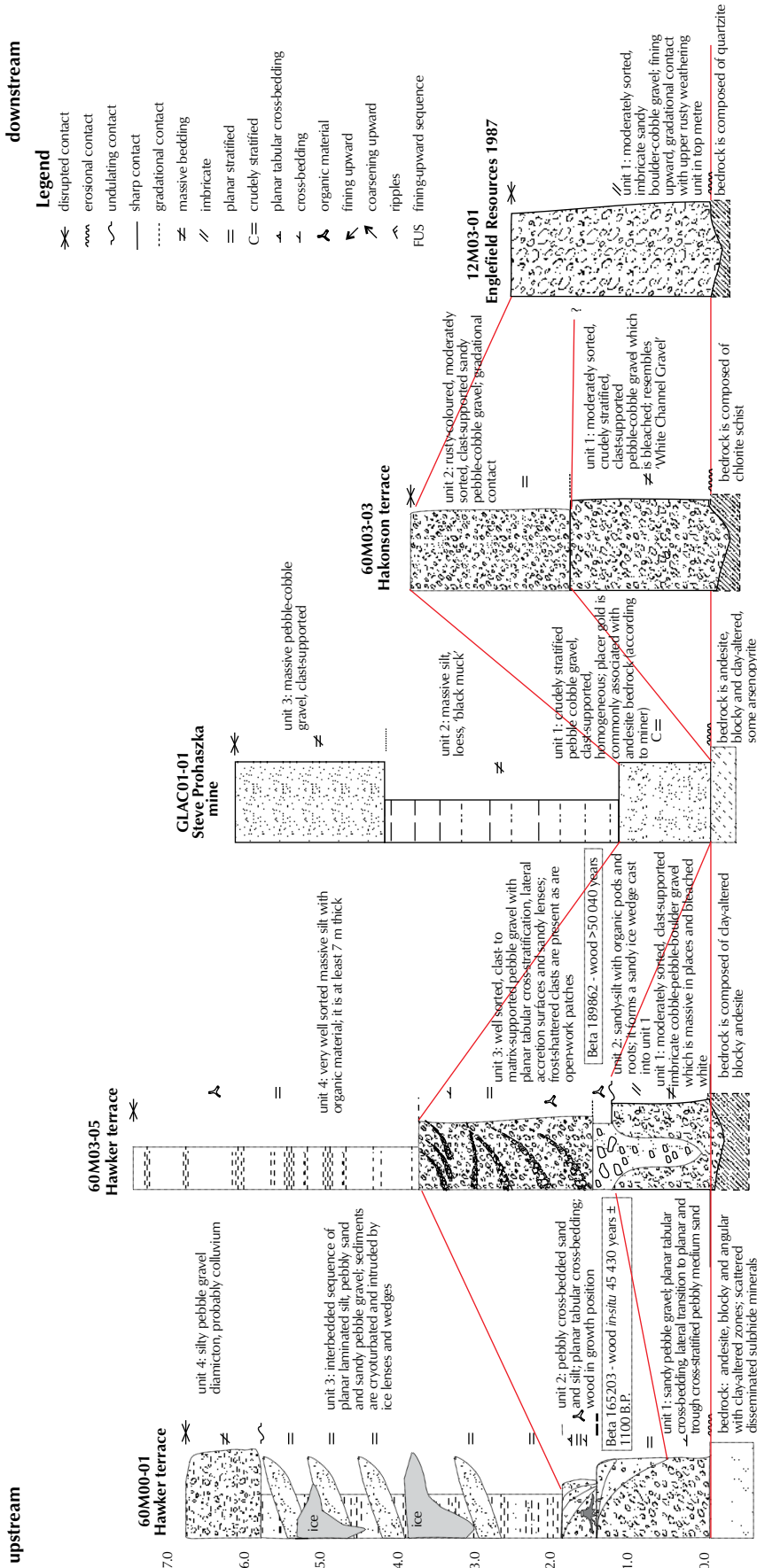


Figure 9. Interglacial (pre-McConnell) correlation Sixtymile river valley.

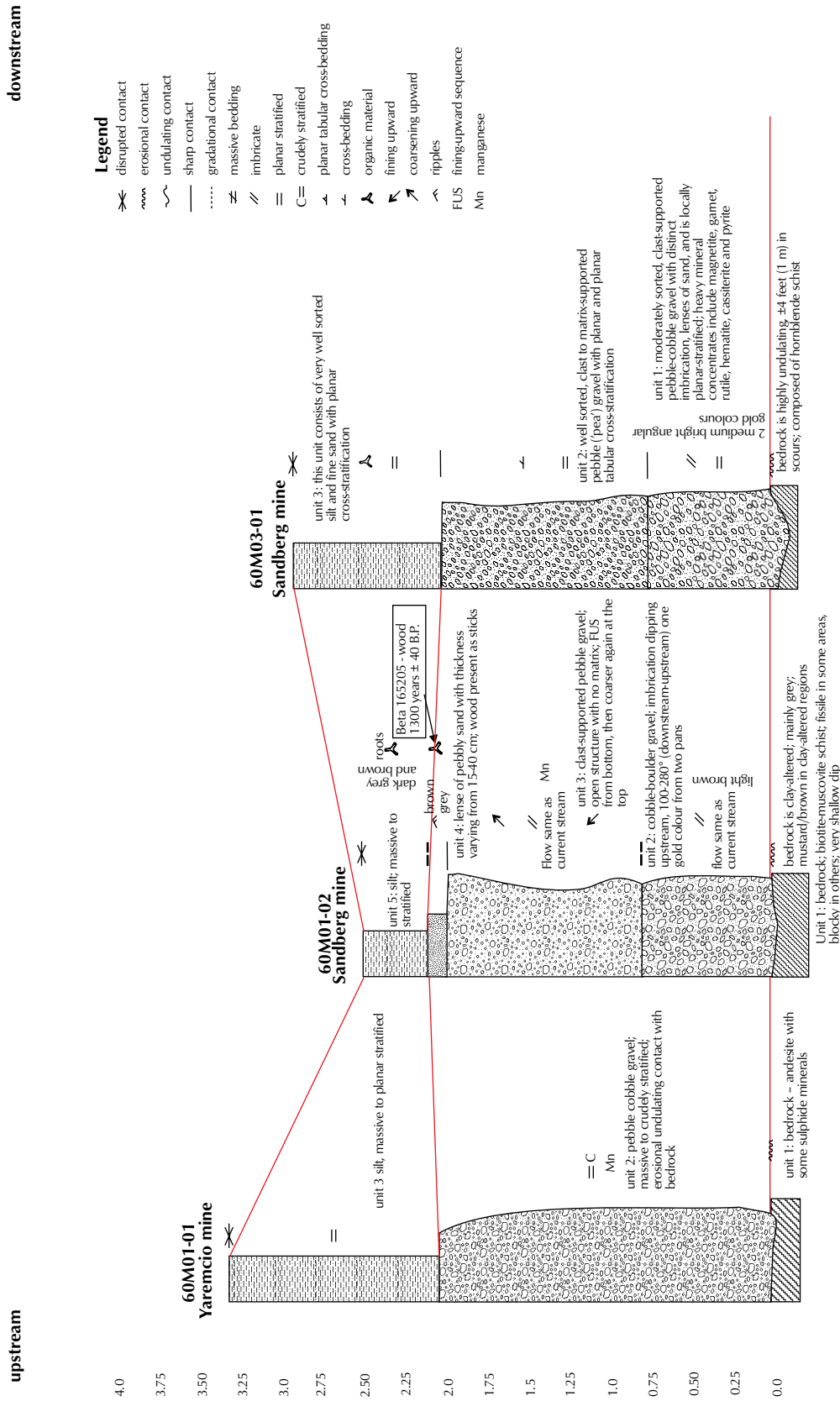


Figure 10. Modern (Holocene) correlation Sixtymile River upstream of Glacier Creek.

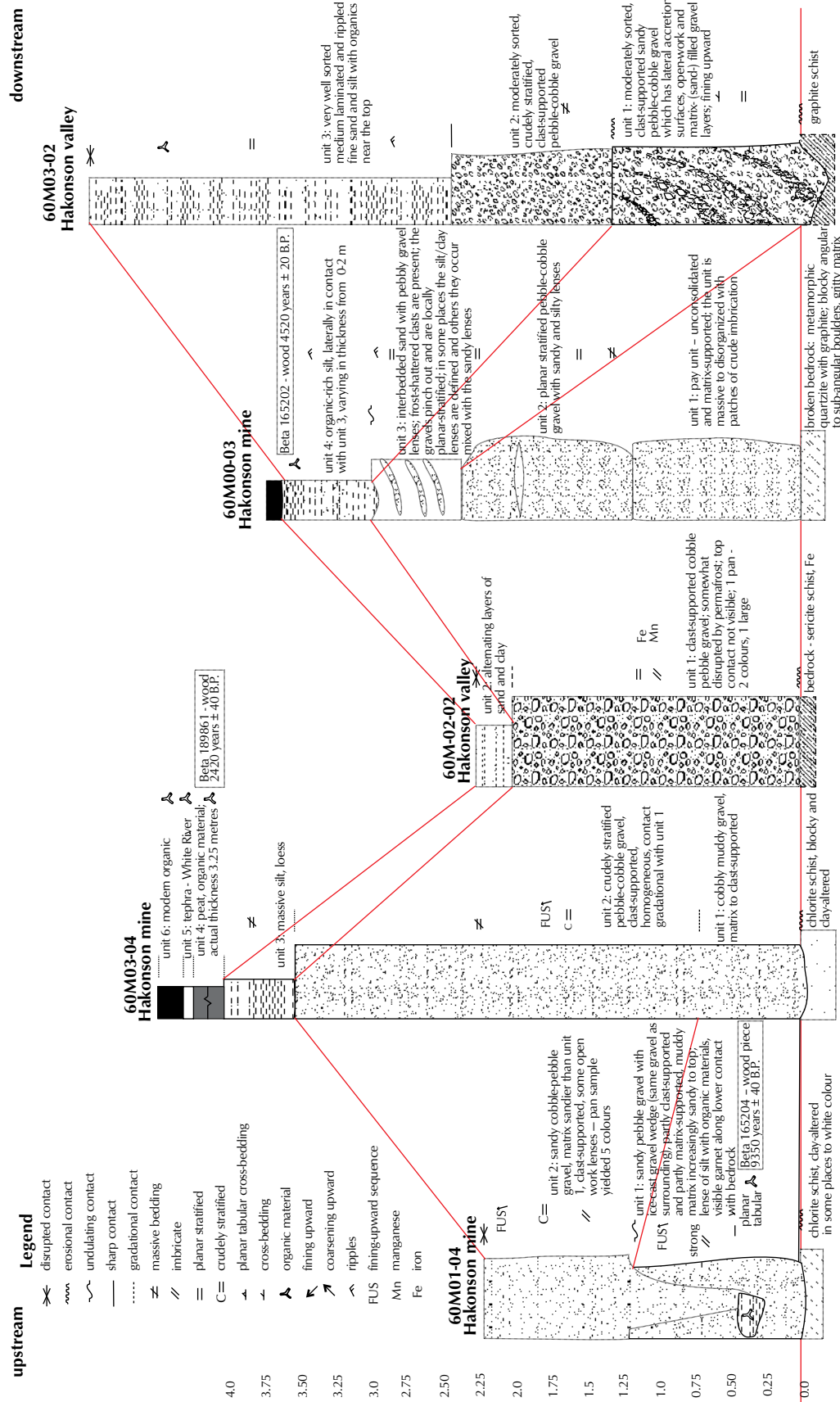


Figure 12. Modern (Holocene) correlation, Sixtymile River downstream of Five Mile Creek.

covered by man-made structures or objects. Such deposits mainly lie within the confines of the modern floodplains of Sixtymile River and its tributaries. Sediments generally consist of various combinations of fractured bedrock with localized pockets and reefs of crudely to well stratified pebble-cobble gravel (virgin gravel), overlain by well sorted clay and silt (fine tailings), and well sorted planar-tabular-stratified pebbly gravel and sand (coarse tailings). These sediments are found in measured sections 60M01-03 (Fig. 13), 60M00-02, 60M02-01, MIL02-01 and GLAC03-02.

These deposits commonly contain rich values of placer gold but are generally small in extent, with the best gold grades found in berms and pockets of virgin gravel, and the lowest gold grades found in dredge tailings. Fractured bedrock commonly contains economic values of placer gold extending one or more metres from the former gravel contact. This deposit type ranks third highest in the amount of gold produced relative to the other deposit types described in this study.

DISCUSSION AND INTERPRETATION OF PALEOGEOGRAPHIC HISTORY

Based on the stratigraphic sections studied and the regional surficial geology, a paleogeographic history of the Sixtymile drainage basin can be reconstructed.

Prior to the onset of Pleistocene glaciations, the Sixtymile River area was a stable plateau which was subjected to a long period of slow erosion, which formed pediment surfaces on the upper slopes. Jackson (2005) mapped these as P^T.

The onset of the first of the pre-Reid glaciations resulted in an increase in physical weathering and erosion of bedrock, and a dramatic increase in stream base-levels. In drainage basins which lacked local alpine ice, periglacial conditions during maximum glacial time nonetheless triggered downstream aggradation of gravel in a braided stream depositional environment. As the pre-Reid glaciation waned, the stream channels of Miller, Glacier, and possibly other Sixtymile tributary streams, shifted southwest, resulted in downcutting into bedrock, and abandonment of the former stream deposits as high-level terraces. Ice-cast sand and gravel wedges formed on those surfaces under diminishing periglacial conditions. The end result was the formation of the pre-Reid and older terraces, which are mapped by Jackson (2005) as unit At^T. In drainage basins subjected to pre-Reid alpine

glaciations, glaciofluvial deposits formed downstream, mapped by Jackson (2005) as units Gt^{PR} and Cx/Gt^{PR}.

Interglacial (pre-McConnell) intermediate-level fluvial gravel terraces aggraded during increased base-levels, caused by either a subsequent pre-Reid glaciation or the later Reid glaciation. Braided stream deposits formed during a period of high sediment availability and stream flow. As stream flow and deposition waned, ice-cast sand and gravel wedges formed on the abandoned gravel surfaces. Better sorting and stable channels developed as the stream morphology evolved from a braided to a wandering gravel bed stream depositional environment. Downcutting of these terraces ensued as the interglacial period progressed. These terraces are mapped by Jackson (2005) as units At^P and Af/At^P, along with contemporaneous tributary valley alluvial deposits mapped as ACx^P.

The McConnell glaciation was likely not proximal enough to affect base-levels, however, it did result in the deposition of loess on slopes and abandoned intermediate-level terraces. As the McConnell glaciation ended, the Klondike plateau was uplifted differentially, resulting in the incision of Sixtymile River into bedrock and the formation of gravel-covered bedrock terraces, which progressively increase in elevation above the modern river level towards the confluence with Yukon River. Stable reworking and slow deposition of alluvial sediments evolved the Sixtymile River into a meandering stream system, resulting in the modern (Holocene) sediments which currently lie within the valley bottom of the Sixtymile River and its tributaries. These are mapped by Jackson (2005) as units Ap, Af and Ax.

Technogenic deposits are human-made deposits formed by mining activity, and these lie mainly within the valley of Sixtymile River in modern-age sediments. Most of them are the result of dredging activity which took place between 1912 and 1959, although some were the result of mechanical mining in subsequent years. These are mapped by Jackson (2005) as unit m.

GOLD AND HEAVY MINERAL CHARACTERISTICS

In the main Sixtymile River valley, placer gold is generally fine-grained and flat, although angular coarse gold and wire gold have also been found. The average size is between 10 mesh and 40 mesh US Standard screen size (2 mm to 0.425 mm). Some of the gold is manganese-

stained, and the fineness (purity out of a possible maximum value of 1000) varies between 810 and 840.

Gold from Miller Creek is reported to have a fineness of 827 to 857, and is commonly rough or angular, and iron and manganese-stained. It generally varies in size between 10 mesh and 60 mesh (2 mm to 0.250 mm).

In Glacier Creek, gold is approximately 20 mesh (0.850 mm) in size, with some fine and granular grains, and some nuggets with dark staining. Gold recovered from the bench gravel is generally coarser grained than that in the creek gravel. Fineness of the gold, based on bulk bullion assays, ranges from 830-860. Recent mining has encountered mercury amalgam along with the gold, presumably from old-timers' tailings (LeBarge and Coates, 2005).

Gold from Little Gold Creek has a fineness of around 850, and has included some nuggets which were described as smooth and spongy with quartz attached, and weighing 2-3 pennyweights (3 g to 4.6 g).

Big Gold Creek gold is generally fine-grained and flat with few nuggets, and has a fineness between 820-840.

Table 6 is compiled from an unpublished report by PetraScience Consultants Inc., and contains scanning electron microscope analyses (SEM) of selected gold grains and other heavy minerals from throughout the Sixtymile River area. All grains of gold were somewhat flat with smooth edges, and some grains contained minor amounts of silver, but most had high gold/silver ratios.

Heavy minerals found throughout the Sixtymile River area include magnetite, hematite, garnet, pyrite, arsenopyrite, galena, barite and scheelite. In addition, cinnabar is found in Miller Creek in the vicinity of Wy gulch. This is one of only two reported occurrences of placer cinnabar in Yukon. Scanning-electron microscope (SEM) analyses also identified zircon and chromite in heavy mineral samples.

FUTURE PLACER GOLD POTENTIAL

Potential placer gold exploration targets ranging from pre-Reid to modern (Holocene) age exist in several stratigraphic settings in the Sixtymile River area. Figure 14 is a schematic cross-valley profile, which illustrates generalized overall stratigraphy and potential placer gold targets. These targets include: 1) pre-Reid and older buried abandoned channels; 2) interglacial (pre-McConnell) buried and/or abandoned alluvial terraces; 3) modern (Holocene) alluvial channels and gulches; and 4) technogenic deposits.

PRE-REID AND OLDER BURIED ABANDONED CHANNELS

This setting is illustrated as exploration target number 1 in Figure 14. Left-limit abandoned channels on both Glacier (measured sections GLAC03-01, GLAC02-01 and GLAC03-03; Figs. 5 and 6) and Miller creeks demonstrate the potential for buried abandoned channels in other drainages such as Bedrock and Little Gold creeks. The left limit of such creeks should be targeted for exploration by

Table 6. Summary of SEM analyses of gold and heavy minerals in Sixtymile area.

Sample number	Location	Section number	Observations (SEM)
GLAC99-1	Glacier Creek	GLAC 99-1 McDougall	pure gold, several small grains
2001 Hawker	Sixtymile River	60M01-03 Hawker valley	pure gold, clay in holes
WL03-62	Sixtymile River	60M03-02 Hakonson	dominantly high gold, minor silver (single nugget)
60M mouth	Sixtymile River	60M mouth	dominantly gold, minor mixed gold-silver
SixtyM 002 unit 2	Sixtymile River	60M00-02 Hawker valley	pure gold (no silver observed)
SixtyM 002 unit 3	Sixtymile River	60M00-02 Hawker valley	dominantly gold, trace silver; quartz
SixtyM 003 bedrock	Sixtymile River	60M00-03 Hakonson	dominantly gold, trace silver
SixtyM 003 unit 1	Sixtymile River	60M00-03 Hakonson	gold, other phases – magnetite, barite, pyrite, ?chromite, ?garnet (CaFeAlSi)
SixtyM 003 unit 2A	Sixtymile River	60M00-03 Hakonson	pure gold; barite, zircon, garnet (CaFeAlSiMn)
SixtyM 003 unit 2B	Sixtymile River	60M00-03 Hakonson	gold with trace silver; garnet (FeMnAlSi)
WL03-50	Sixtymile River	60M03-01 Sandberg	gold with trace silver, trace clay

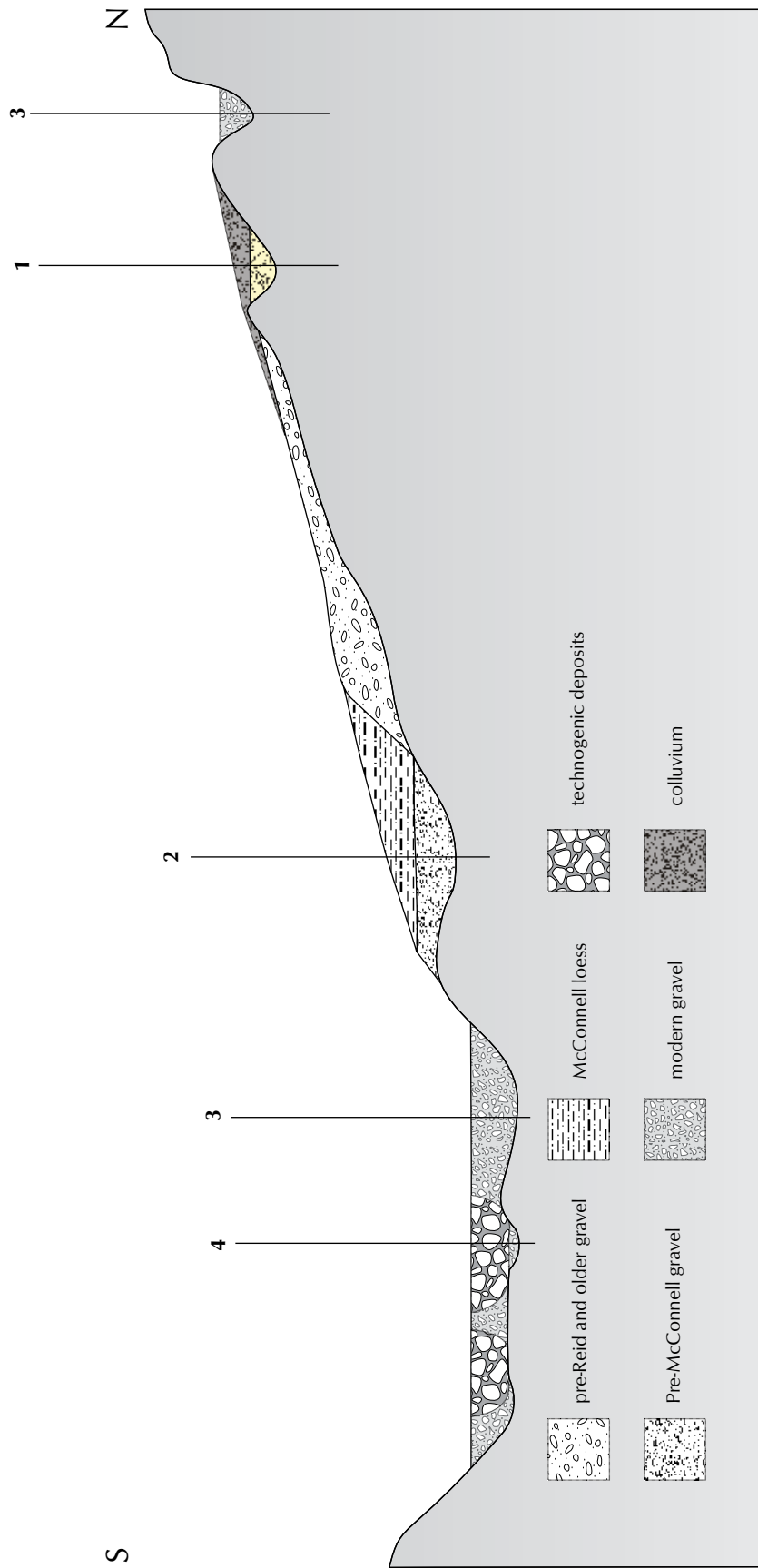


Figure 14. Schematic cross-valley profile of Sixtymile River, illustrating generalized stratigraphic relationships and exploration targets: 1) pre-Reid buried abandoned channels; 2) interglacial (pre-McConnell) buried and/or abandoned alluvial terraces; 3) modern alluvial channels and gulches; and 4) technogenic deposits.

methods such as ground-penetrating radar or seismic surveys, followed by test-pitting or drilling.

INTERGLACIAL (PRE-MCCONNELL) BURIED AND/OR ABANDONED ALLUVIAL TERRACES

This setting presents several exploration targets, mainly on the left limit of Sixtymile River, although a similar stratigraphic setting may exist on the right limit of Sixtymile River as well. Measured sections 60M00-01 (Fig. 7) and 60M03-05 (Fig. 8) best illustrate this setting, displayed in Figure 14 as target number 2. These terraces are most obvious towards the mouth of Sixtymile River, otherwise airphoto interpretation, followed by test pitting or drilling, will confirm their presence further upstream.

MODERN (HOLOCENE) ALLUVIAL CHANNELS AND GULCHES

Along the main valley of Sixtymile River, and in many tributary gulches, lie numerous unexplored potential placer targets. These are illustrated in Figure 14 as target number 3. Measured sections describing this type of deposit include 60M01-01, 60M01-02, 60M03-01, 60M01-04, 60M03-04, 60M02-02, 60M00-03 and 60M03-02 (Figs. 10, 11 and 12). The potential of these deposits can be explored by geophysical methods such as ground-penetrating radar or seismic surveys to determine the bedrock profile, and test-pitting or drilling to determine grade and volume.

TECHNOGENIC DEPOSITS

These have been described in measured sections 60M01-03 (Fig. 13), 60M00-02, 60M02-01, MIL02-01 and GLAC03-02. These deposits are shown as target number 4 in Figure 14. Exploration for these types of deposits would involve airphoto interpretation and literature research to determine areas of previous mining activity; and test-pitting or drilling to determine grade and volume of potential remnant placer-gold-bearing zones. Seismic and ground-penetrating radar surveys may help to determine thawed (mined) versus frozen (unmined) ground and the thickness of deposits.

RECOMMENDATIONS FOR FURTHER WORK

A program of detailed (1:25 000-scale or greater) surficial mapping, which includes ground-truthing and sampling of gravel deposits for gold content, is recommended. In addition, the development of a longitudinal profile of Sixtymile River bedrock terraces would be useful in correlating gravel deposits and helping to further reconstruct the paleogeographic history, as well as identifying additional prospective areas for placer gold deposits.

Detailed study of gold particles from known lode sources, as well as from placer deposits, may help us to reconstruct the sedimentary and geological history of Sixtymile River area. By using a combination of SEM, electron microprobe and laser-ablation ICP-MS methods to analyse the shape and composition of gold particles, it may be possible to trace the history of gold particles from lode sources, through intermediate hosts in bedrock and unconsolidated gravel, to present hosts in modern gravels. It may also be possible to use this method to determine the presence of possible undiscovered lode gold sources in the Sixtymile area.

ACKNOWLEDGMENTS

Enthusiastic assistance in the field was provided by Julianne Madsen, Cheryl Peters, Alexandra Shaw, Kerri Heft, Nicola Struyk, Catherine Craig and Angela Johnson. Much of the digital bedrock map compilation was completed by James Coates.

Much appreciation goes to the placer miners who generously gave their time, as well as donated pay samples, including Mike McDougall, Frank and Karen Hawker, Jayce Murtagh, Stuart Schmidt, Don Sandberg, Walter Yaremcio, Steve Prohaszka and Greg Hakonson.

Enlightening discussions in the field were provided by Dr. Jim Mortensen and Rob Chapman, and this paper was improved by reviews by Jeff Bond and Jim Mortensen.

REFERENCES

- Alloway, B.V., Froese, D.G. and Westgate, J.A. (eds.), 2005. Proceedings of the International Field Conference and Workshop on Tephrochronology and Volcanism: Dawson City, Yukon Territory, Canada, July 31–August 8, 2005. Institute of Geological & Nuclear Sciences, Science Report 2005/22, 64 p.
- Bostock, H.S., 1966. Notes on glaciation in central Yukon Territory. Geological Survey of Canada, Paper 65-36, 19 p.
- Debicki, R.L., 1983. Yukon Mineral Industry, 1941 to 1959. Indian and Northern Affairs Canada, Whitehorse, Yukon, 136 p.
- Deklerk, R. and Traynor, S., (compilers) 2005. Yukon MINFILE - A database of Yukon mineral occurrences. Yukon Geological Survey, CD-ROM.
- Duk-Rodkin, A., 1996. Surficial geology, Dawson, Yukon Territory. Geological Survey of Canada, Open File 3288 (1:250 000-scale map with marginal notes).
- Duk-Rodkin, A., 1999. Glacial limits of Yukon Territory, Northwest Canada (abstract). *In: CANQUA – CGRC 1999, Canadian Quaternary Association - Canadian Geomorphology Research Group, Program and Abstracts, August 23-27, 1999, University of Calgary, Calgary, Canada, p. 20.*
- Folk, R.I., 1974. Petrology of sedimentary rocks. Hemphill, Austin, Texas, 182 p.
- Glasmacher, U., 1985. Geology, petrography and mineralization in the Sixtymile River area, Yukon Territory, Canada. Unpublished M.Sc. thesis, Institute of Mineralogy and Economic Geology, Aachen, Germany, 205 p.
- Glasmacher, U. and Friedrich, G., 1999. Volcanic-hosted epithermal gold-sulphide mineralization and associated enrichment processes, Sixtymile River area, Yukon Territory, Canada. Yukon Geology, Volume 3, T.J. Bremner (ed.), Exploration and Geological Services Division, Yukon Region, Indian and Northern Affairs Canada, p. 271-291.
- Gordey, S.P. and Makepeace, A.J. (compilers), 2003. Yukon digital geology, version 2. Yukon Geological Survey, Open File 2003-9(D); also known as Geological Survey of Canada, Open File 1749, 2 CD-ROMs.
- Hughes, O.L., 1968. Glacial map of Yukon Territory (1:1 000 000). Geological Survey of Canada, Map 6-1968, Paper 1968-34.
- Hughes, O.L., Campbell, R.B., Muller, J.E. and Wheeler, J.O., 1969. Glacial limits and flow patterns, Yukon Territory, south of 65 degrees North Latitude. Geological Survey of Canada, Paper 68-34, 9 p.
- Hughes, R.L., 1986. Sedimentology of the Sixtymile River placer gravels, Yukon Territory. Unpublished M.Sc. thesis, Department of Geology, University of Alberta, Edmonton, Alberta, 210 p.
- Hughes, R.L., Morison, S.R. and Hein, F.J., 1986. Placer gravels of Miller Creek, Sixty Mile River area, 116B,C. *In: Yukon Geology Volume 1, Exploration and Geological Services Division, Yukon Region, Indian and Northern Affairs Canada, p. 50-55.*
- Jackson, L.E., Jr., 2005. Surficial geology, Ogilvie, Yukon Territory, 115 O/12. Geological Survey of Canada, Open File 4589, 1:50 000 scale.
- LeBarge, W.P. and Coates, J. (compilers), 2005. Yukon Placer Database 2005 - Geology and mining activity of placer occurrences. Yukon Geological Survey, CD-ROM.
- Lowey, G.W. 2000. Glaciation, gravel and gold in the Fifty Mile Creek area, west-central Yukon. *In: Yukon Exploration and Geology 1999, D.S. Emond and L.H. Weston (eds.), Exploration and Geological Services Division, Yukon Region, Indian and Northern Affairs Canada, p. 199-209.*
- Lowey, G.W., 2004. Placer Geology of the Stewart River (115N&O) and part of the Dawson (116B&C) map areas, west-central Yukon, Canada. Yukon Geological Survey, Bulletin 14, 275 p.
- Mathews, J.V., Jr., Schweger, C.E. and Hughes, O.L., 1990. Plant and insect fossils from the Mayo Indian Village Section (central Yukon); new data on middle Wisconsinan environments and glaciation; *Geographie Physique et Quaternaire*, vol. 44, p. 15-26.
- Mining Inspection Division, 2003. Yukon Placer Mining Industry 1998-2002. Indian and Northern Affairs Canada, Whitehorse, Yukon.
- Mortensen, J.K., 1988. Geology of southwestern Dawson map area (NTS 116 B, C). Geological Survey of Canada, Open File 1927, 1: 250 000 scale.

- Mortensen, J.K., 1990. Geology and U-Pb chronology of the Klondike District, west-central Yukon Territory. *Canadian Journal of Earth Sciences*, vol. 27, p. 903-914.
- Mortensen, J.K., 1996. Geological compilation maps of the northern Stewart River map area, Klondike and Sixtymile Districts (115N/15, 16; 115O/13, 14; and parts of 115O/15, 16). Exploration and Geological Services Division, Yukon Region, Indian and Northern Affairs Canada, Open File 1996-1 (G), 43 p.
- Mortensen, J.K., Chapman, R., LeBarge, W. and Crawford, E., 2006 (this volume). Compositional studies of placer and lode gold from western Yukon: Implications for lode sources. *In: Yukon Exploration and Geology 2005*, D.S. Emond, G.D. Bradshaw, L.L. Lewis and L.H. Weston (eds.), Yukon Geological Survey, p. 247-255.
- Wright, A.A., 1976. *Prelude to Bonanza, the discovery and exploration of the Yukon*. Grays Publishing Limited, Whitehorse, Yukon, 321 p.

Active-layer detachments following the summer 2004 forest fires near Dawson City, Yukon

Panya S. Lipovsky¹
Yukon Geological Survey

Jim Coates and Antoni G. Lewkowicz
Department of Geography, University of Ottawa²

Erin Trochim
Yukon Geological Survey

Lipovsky, P.S., Coates, J., Lewkowicz, A.G. and Trochim, E., 2006. Active-layer detachments following the summer 2004 forest fires near Dawson City, Yukon. *In: Yukon Exploration and Geology 2005*, D.S. Emond, G.D. Bradshaw, L.L. Lewis and L.H. Weston (eds.), Yukon Geological Survey, p. 175-194.

ABSTRACT

Numerous active-layer detachments occurred in watersheds surrounding Dawson City following forest fires that burned the area during the summer of 2004. The distribution of these shallow landslides was mapped in the Mickey Creek, Steele Creek and Fifty Mile Creek watersheds. Selected slope failures were surveyed in detail to describe their geometry and geomorphological settings in order to investigate the mechanisms of failure, and to assess the effects of the forest fires on local permafrost conditions. The failures generally initiated on moderate convex slopes at shallow depths (< 65 cm) in silty colluvium; frost tables were close to 1 m in depth. Most active-layer detachments were on the order of 5-20 m wide and 10-100 m long and occurred on slopes with a variety of aspects; however, the detachments occurred only where permafrost was present. In some cases, they developed on gentle slopes (as low as 10°) and traveled several hundred metres, depositing sediment directly into creeks, or across access trails. Their cumulative effects may significantly impact sediment transport within the watersheds. Potential concerns for fish habitat and implications for placer mining water quality regulations have consequently been raised.

RÉSUMÉ

Des décollements répandus de la couche active se sont produits dans un grand nombre de bassins versants des environs de Dawson City suite aux incendies forestiers qui ont ravagé la région pendant l'été de 2004. Plusieurs décollements dans les bassins versants des ruisseaux Mickey, Steele et Fifty Mile ont été étudiés afin d'en décrire la géométrie et les cadres morphologiques, pour déterminer les mécanismes de glissement et pour évaluer les effets des incendies forestiers sur l'état du pergélisol local. Les glissements s'amorcent généralement à des faibles profondeurs (< 65 cm) sur des talus convexes dans des colluvions limoneuses; la limite du pergélisol se trouvait à une profondeur d'environ 1 m. La plupart des décollements présentaient une largeur de 5 à 20 m sur une longueur de 10 à 100 m et étaient développés sur des pentes d'orientations variables. Cependant, les décollements se retrouvent seulement là où l'on a identifié du pergélisol. Dans certains cas, les décollements se sont produits sur des pentes très douces (d'aussi peu que 10°) et il y a eu glissement sur plusieurs centaines de mètres tel que des sédiments se sont déposés directement dans les ruisseaux et en travers des sentiers d'accès. Leurs effets cumulés pourraient avoir une incidence importante sur le transport de sédiments dans les bassins versants. Des préoccupations pour l'habitat du poisson et les incidences possibles en matière de réglementation de la qualité de l'eau destinée à l'exploitation minière des placers ont en conséquence été soulevées.

¹panya.lipovsky@gov.yk.ca

²Simard Hall, Room 047, 60 University Avenue, Ottawa, Ontario, Canada K1N 6N5

INTRODUCTION

BACKGROUND AND PURPOSE

Extensive forest fires burned in the Dawson City area from late-June to mid-September, 2004 (Fig. 1). Numerous active-layer detachment failures subsequently developed in the burnt areas during the summers of 2004 and 2005. Investigations in three watersheds near Dawson City revealed that more than 70 detachments occurred on slopes and tributaries adjacent to a 10-km-reach of Mickey Creek, 40 detachments on slopes adjacent to a 4-km reach of Steele Creek, and a further 28 detachments in the lower 12 km of the Fifty Mile Creek watershed.

Active-layer detachments are defined as slope failures “in which the thawed or thawing portion of the active layer detaches from the underlying frozen material” (van Everdingen, 1998). They are shallow landslides which generally involve an initial sliding movement that may be transformed into, or followed by, flow of the thawed debris. Events which cause rapid thickening of the active

layer, such as forest fires and hot and/or wet weather, commonly trigger active-layer detachments (Dyke, 2004; Lewkowicz, 1992; Lewkowicz and Harris, 2005a). Many factors influence the occurrence of detachment failures, including depth of the active layer, meteorological conditions, soil moisture conditions, slope form and steepness, aspect, surficial materials and vegetation cover.

Active-layer detachments have been well documented in the Mackenzie Valley, Northwest Territories (e.g., McRoberts and Morgenstern, 1974; Aylsworth *et al.*, 2000; Dyke, 2004; Lewkowicz and Harris, 2005b), in southwest Yukon (e.g., Hugenholtz, 2000; Huscroft *et al.*, 2004) and in the Canadian Arctic Archipelago (e.g., Stangl *et al.*, 1982; Lewkowicz, 1992; Lewkowicz and Harris, 2005b), but never in unglaciated subarctic regions of Canada. Investigations were therefore conducted in the Mickey Creek, Steele Creek and Fifty Mile Creek watersheds to document the geomorphological controls on the detachments, in order to elucidate active-layer detachment failure mechanisms. The immediate effects of

forest fires on local permafrost conditions were assessed, and the role of forest fires in initiating landslides was also examined in this study. In addition, potential environmental and economic implications were identified.

Different methodologies were followed while assessing each of the watersheds. Studies at Mickey and Fifty Mile creeks were reconnaissance in nature, and were undertaken over a nine-day period in July, 2005 by the Yukon Geological Survey (P. Lipovsky and E. Trochim). Studies at Steele Creek were more comprehensive and were undertaken over numerous months by J. Coates and A. Lewkowicz as the basis of a Master of Science thesis (initiated in the fall of 2004); the results from Steele Creek presented in this paper are preliminary.

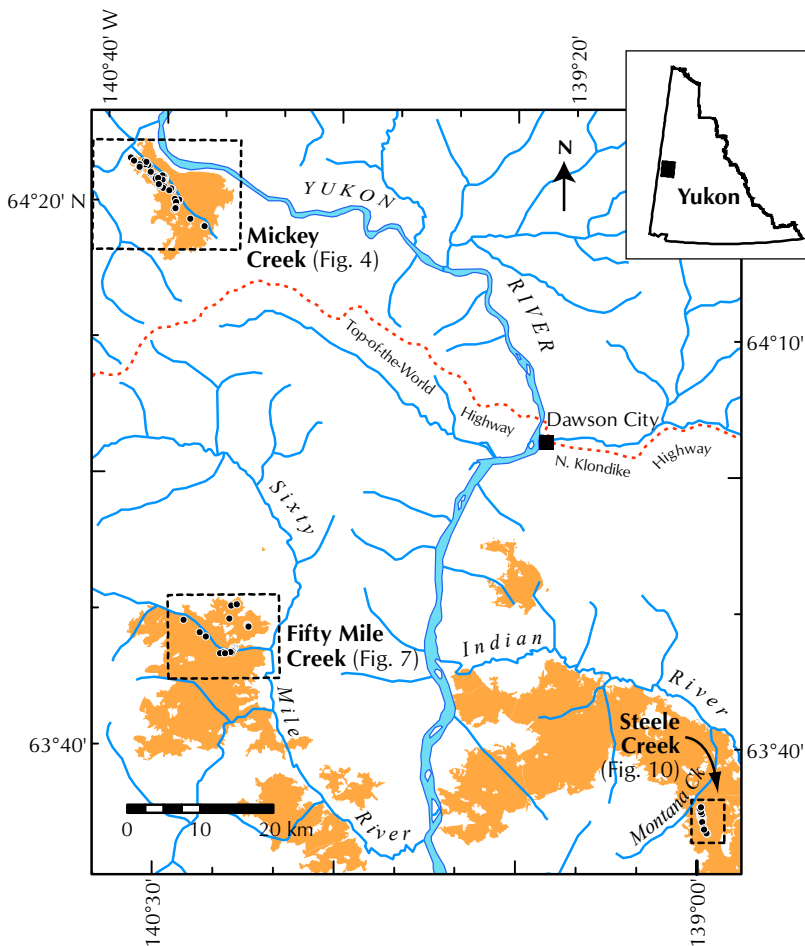
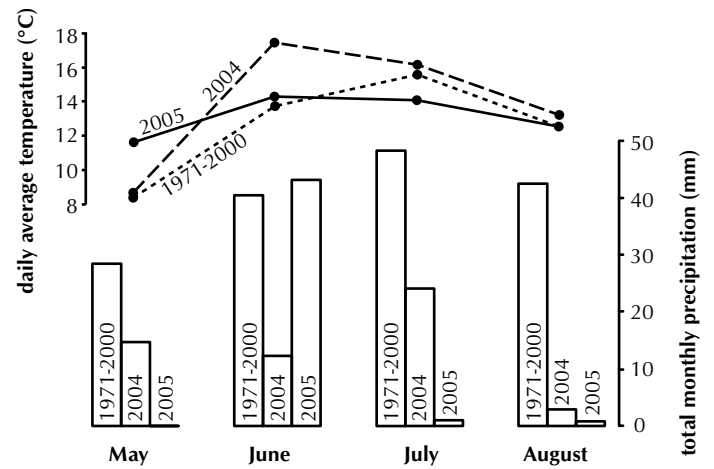


Figure 1. Index map of Dawson area, displaying the locations of Mickey Creek, Fifty Mile Creek and Steele Creek watersheds. Dots represent locations of active-layer detachments. Shaded areas represent those regions burned by forest fires in 2004. Inset map shows location of study area within Yukon.

REGIONAL SETTING

Most of the study area remained unglaciated during the Quaternary period. V-shaped valleys of the rolling Klondike Plateau are dissected by dendritic drainages. Slopes are generally convex in shape and mantled with colluvium derived from local, weathered, Paleozoic quartzite and schist (Duk-Rodkin, 1996; Jackson, 2005). Soils are shallow and are generally capped by deposits of loess.

The Dawson area experiences a subarctic continental climate with long cold winters and short warm summers. Mean annual temperature is -5°C, and mean annual precipitation is 300-500 mm (Smith *et al.*, 2004). Environment Canada (Dawson weather station) daily temperature and precipitation data from May 2004 to November 2005 are shown in Figure 2; climate normals for the summer months are compared with 2004 and 2005 records in Figure 3. Comparison of this data with limited climatic data collected from Steele Creek during the 2004 and 2005 summer months suggests that the Dawson weather station may not necessarily be



representative of the surrounding areas. Climatic data

Figure 3. 2004 and 2005 daily average temperature and total monthly precipitation for the months of May to August, compared to 1971-2000 climate normals. (Data from Environment Canada Dawson weather station, 64°3'N, 139°7'W, elevation 370 m.)

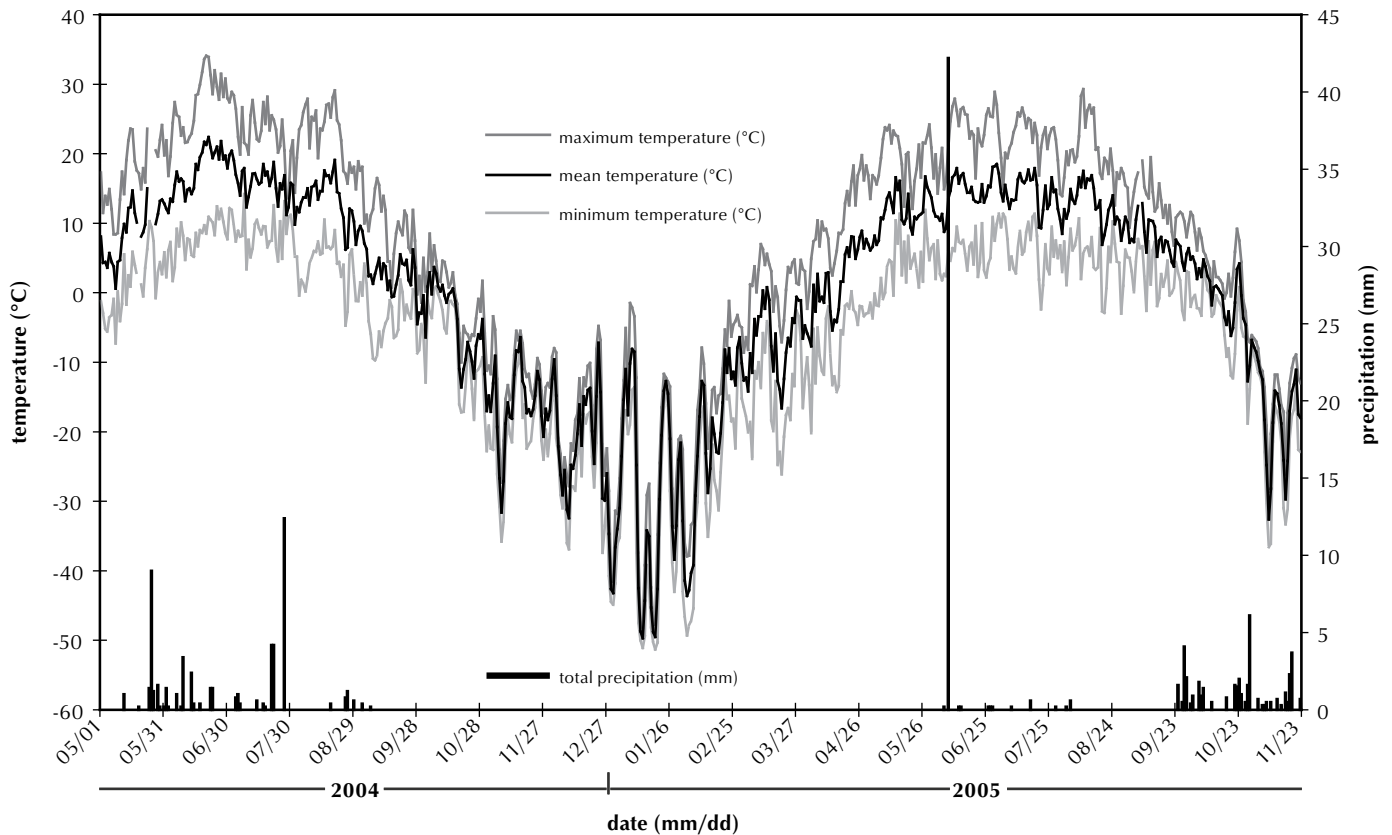


Figure 2. Daily temperatures (mean, maximum and minimum) and total daily precipitation at Dawson weather station (64°3'N, 139°7'W, elevation 370 m; data from Environment Canada).

obtained from Steele Creek have shown temperatures to be slightly colder in summer, and precipitation patterns may be entirely different. (Further discussion on Steele Creek climatic data is presented below.)

North-facing slopes in the area are dominated by stands of black spruce, shrubs and thick sphagnum and feather moss. South-facing slopes generally consist of mixed trembling aspen, balsam poplar and paper birch forests (Smith *et al.*, 2004).

The study area is within the extensive discontinuous permafrost zone (Heginbottom *et al.*, 1995). Burn (in Smith *et al.*, 2004) reports permafrost thicknesses of 20-60 m in valley bottoms near Dawson.

North-facing slopes and upland plateaus are perennially frozen, although permafrost can be absent on well drained, south-facing slopes (EBA Engineering Consultants Ltd., 1989a). Massive ice beds and ice wedges are found in valley bottom settings and within loess-rich soil horizons (Smith *et al.*, 2004). Active layers are generally near, or less than, 1 m thick (this study), but can be up to 1.5 m thick in alluvial sediments (EBA Engineering Consultants Ltd., 1983, 1989b).

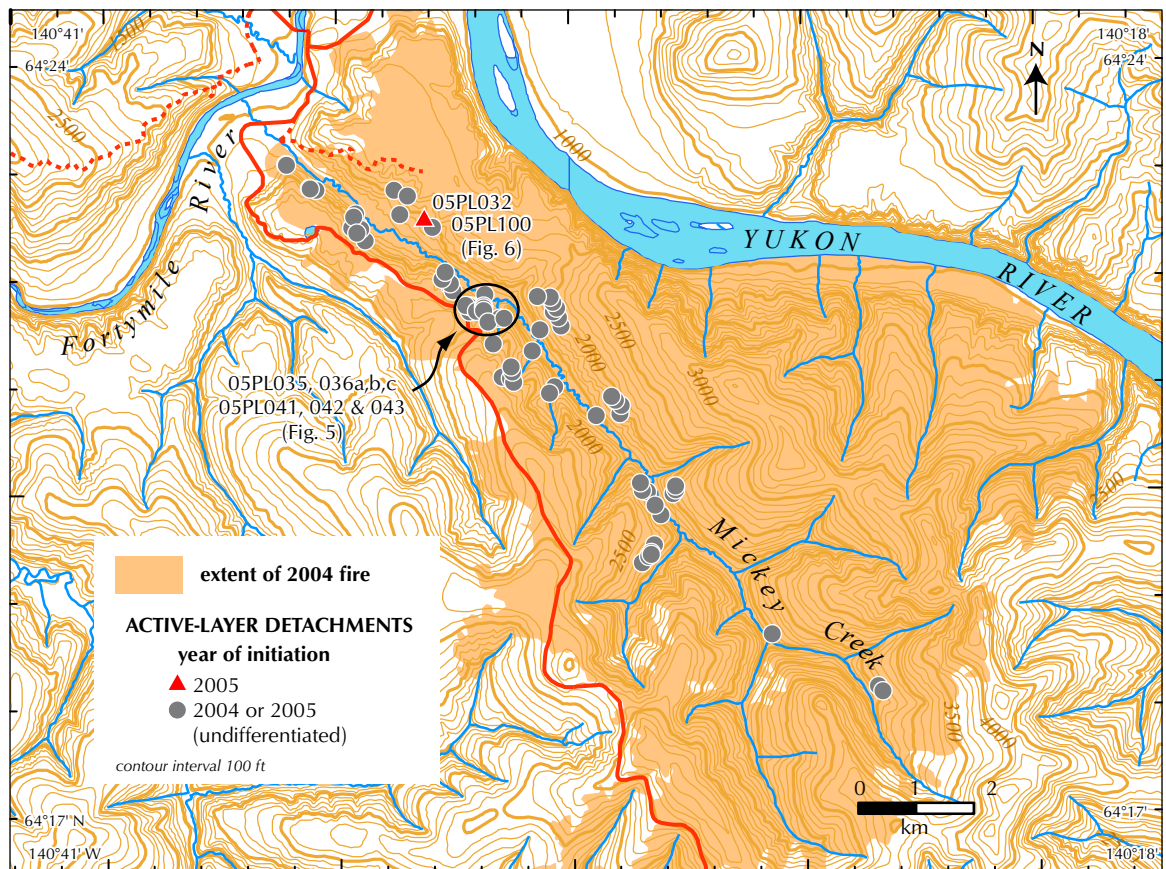
FIELD OBSERVATIONS

MICKEY CREEK

• Setting

The valley of Mickey Creek is located at approximately 64°21'N and 140°30'W (60 km northwest of Dawson City) and spans elevations of 300-1300 m above sea level (asl) (Fig. 4). Mickey Creek is a small, northwesterly flowing tributary that enters the Fortymile River about 6 km upstream from its confluence with the Yukon River. Active placer claims exist along the lower part of the creek, but no commercial mining has been undertaken in the watershed. Steep slopes, averaging between 19° and 27°, flank the southwest side of the valley along the entire 18 km length of the creek. Slopes on the northeast side of the creek are gentler, generally ranging between 11° and 18°. The slopes are blanketed by colluvial deposits, commonly consisting of grey phyllitic bedrock fragments in a matrix of silty loess. On the gentler slopes, surface soil horizons generally contain a higher percentage of loess. In the lower reaches of the creek, Pre-Reid glaciofluvial terraces are found on the upper slopes (Duk-Rodkin, 1996). Probing in mid-July

Figure 4. Location map displaying the extent of burned areas, as well as locations of active-layer detachments surveyed in Mickey Creek watershed.



revealed frost tables at depths of 57-125 cm at all burned sites visited; on one unburned southwest-facing slope, the frost table was at 75 cm depth.

The forest fire which burned the area was moderately severe. Trees remaining in the area have few branches and little bark left on the trunks, while some trees were charred through. Most of the burned trees are still standing, but some have fallen as blowdown. From 5 to 10% bare mineral soil was exposed at the sites visited, particularly around the base of trees, and in many places at least half of the surface organic mat was removed.

Fires were detected throughout the watershed by MODIS satellite instruments between June 24 and July 17, 2004 (USDA Forest Service, 2005). The fires began burning in the southern portion of the watershed and remained on the upper slopes until June 29. The most extensive amount of burning occurred between June 30 and July 3, during which time the fire spread nearly to the mouth of the creek. After July 4, scattered fires continued to burn until July 17.

Concerns regarding sediment loads in the creek prompted the Department of Fisheries and Oceans to visit the site in 2004; fish surveys were conducted during the summer of 2005. Immediately after the forest fire, they reported that streamflows in Mickey Creek had increased while flows in adjacent unburned watersheds remained very low (A. von Finster, pers. comm., 2005). Periodic water sampling near the mouth of the creek was carried out in an attempt to observe the stream's sediment regime. The results were highly variable and sediment concentrations ranged from clear to very turbid, depending on antecedent weather conditions, time of day and season. Suspended sediment values were only elevated when high streamflows occurred in early summer. Large numbers of juvenile Chinook salmon and slimy sculpin were found near the mouth of the creek, possibly having been displaced from upstream areas by high streamflows and increased sediment loads transported in suspension, or as sand-sized bedload (A. von Finster, pers. comm., 2005). Small numbers of Arctic grayling were also found near the mouth of the creek.

• Field survey methodology

On July 20, 2005, seventy-four slope failures were located in the watershed by hovering above each detachment with a helicopter and recording GPS waypoints. Fifteen of the detachments were visited on the ground on July 13, 20 and 21 (Figure 4).

Reconnaissance-level surveys were conducted at these sites in order to characterize slope steepness, aspect, surficial material type, and basic morphology. At selected failures, a Laser Technology Impulse laser range finder and stadia rod were used to survey slope profiles (accuracy $\pm 0.1^\circ$), detachment shape and failure dimensions (accuracy ± 1 cm). Soil profiles were examined in natural exposures, or pits dug near the headscarps of the detachments, and selected materials were sampled for grain-size analysis. Frost table depths were determined by frost probing. Burn severity was described in the vicinity of the landslide, and digital photographs were taken to document various features of the failures and their surrounding environment.

• Failure settings and morphologies

Approximately two-thirds of all the failures in Mickey Creek occurred on moderately steep, north- to east-facing slopes, in mid- to upper-slope positions. Nearly one-quarter of the detachments reached tributary valley floors, or the main valley floor, thus contributing sediment directly into the watershed's drainage network. In general, the failures occurred in three geomorphological settings, as listed below:

1) *high-level glaciofluvial terraces, on moderately steep, northeast-facing slopes*

Seventeen of the surveyed detachments initiated at, or near the edge of, a narrow (~20-m-wide) Pre-Reid distal glaciofluvial terrace. The terrace is located on the upper, moderately steep, northeast-facing slopes in the lower portion of the watershed. The failures exposed light-coloured gravel which contrasted well with the burned surface and readily defined the existence of the terrace, which was otherwise difficult to detect (Fig. 5).

The surficial materials typically consist of loose, slightly silty, medium to coarse, sandy pebble gravel (50-60% coarse fragments), overlain by a thin (2-3 cm), severely burnt, organic mat. Detachments occurred at depths of 50-65 cm. The top of the terrace had a gentle to moderate slope, ranging between 15° and 26° , while the side of the terrace steepened up to 31° . The frost table within the terrace was found between 57 cm and 125 cm. Grey phyllite bedrock was found at, or close to, the surface near many of the sites visited.

2) *shallow bedrock, on moderately steep, northeast-facing slopes*

Dark-grey phyllite is found at shallow depths on most of the slopes throughout the lower portion of the watershed.

The phyllite weathers readily and has covered the steep slopes with a colluvial veneer composed of coarse, dark-grey, silty sand (composing 60% of the soil by volume where sampled), as well as granules and flat angular clasts (composing 40% of the soil by volume where sampled). In some cases, the clasts were imbricated parallel to slope, possibly providing a natural sliding plane.

Twenty of the surveyed failures occurred in this setting, as determined by helicopter surveys. At the one detachment visited on the ground, the sliding plane was 26°, the slope directly above the headscarp was 21°, the sliding depth was 40-45 cm, and the frost table was 43-74 cm below the ground surface.



Figure 5. Oblique aerial photograph of numerous failures originating along the scarp of a Pre-Reid glaciofluvial terrace (see dotted lines) on upper, northeast-facing slopes. View is to the southwest. Numbers represent active-layer detachments surveyed near Mickey Creek.

3) loess-rich colluvium, on gentle south to west-facing slopes

Southwest-facing slopes in the watershed are veneered by a silty surface layer. At these locations, loess deposits have been mixed into colluviated regolith deposits by the process of colluviation and cryoturbation. The loess-rich horizon is commonly 20-30 cm thick, but can be as thick as 2 m. When saturated, these soils can flow on very gentle slopes, as low as 10°. Nineteen failures were recorded in this setting.

A fresh detachment (05PL032) was observed on July 20, with material still actively flowing (Fig. 6). The detachment was not visible in photographs taken 7 days earlier and it is likely that the detachment occurred within a day or two of the field visit. The failure began with a small slide in a 20-m-wide headscarp bowl, on a southwest-facing, gentle (13°), lower slope. The initial sliding depth was between 10 cm and 50 cm, just below the bulk of the root mat. The organic mat had collapsed along the edge of the headscarp, indicating that it had greater strength than the underlying soil. Probing revealed a frost table at 104 cm beneath a fresh sliding plane, and 88-99 cm behind the headscarp. Above the headscarp, water was ponded around many tree wells. Roots were outstretched in the direction of extension (Fig. 6b) and fresh sliding plane surfaces were exposed between tension cracks above the headscarp, and along the flow path margins where intact blocks of forest floor had been torn away (Fig. 6c).

Following the initial slide, secondary debris flows traveled more than 200 m to the valley floor, down slopes of less than 10°, to form a large shallow debris fan adjacent to the creek. Active debris flows moved at rates of approximately 0.5 m/min, carrying cobbles up to 10 cm in clast diameter (at location S2 in Figure 6a). The flowing material was very viscous, had a moisture content of 10% by weight, and was composed of 70% sticky, sandy loam (54% sand, 37% silt and 9% clay) with 30% clasts (mostly flat fragments of phyllite).



Figure 6. (a) Oblique aerial view of two detachments (05PL032 and 05PL100) that occurred on a gentle south- to southwest-facing slope. The larger failure is over 200 m long and initiated only a few days prior to these photos being taken on July 20, 2005. (b) Detachment of organic mat exposed in tension cracks above the headscarp (location S1 in Figure 6a). Roots are stretched in the direction of sliding. (c) Deformed organic mat (location S3 in Figure 6a), marginal to flow path (heavy arrow). The mat was initially compressed (direction D1) to form folded compression ridges (small dotted lines). It was then torn away from the surrounding mat (direction D2).

FIFTY MILE CREEK

• **Setting**

The valley of Fifty Mile Creek is located at approximately 63°48'N and 140°20'W (50 km southwest of Dawson City) and spans elevations of 450-1500 m asl (Fig. 7). The Fifty Mile Creek valley is approximately 40 km long from its headwaters to its confluence with Sixtymile River. Field surveys were conducted only in the lower half of the watershed. The unglaciated, subdued slopes are generally mantled by colluvium and veneered by loess up to 1 m thick (Jackson, 2005). Paleozoic Klondike Schist (Mortensen, 1996) outcrops along the creek and comprises the vast majority of clasts in the colluvium. Organic materials, loess and colluvium have commonly been reworked by fluvial and colluvial processes to produce accumulations of muck deposits in lower slope and valley-bottom positions (Fraser, 1995).

Pre-Reid glaciofluvial terraces form valley-bottom benches along the creek (Jackson, 2005) and some placer potential exists within them (Lowey, 2000). Limited exploration has occurred within the benches, and while active placer claims exist along parts of Fifty Mile Creek, no commercial mining has been undertaken. Watershed-

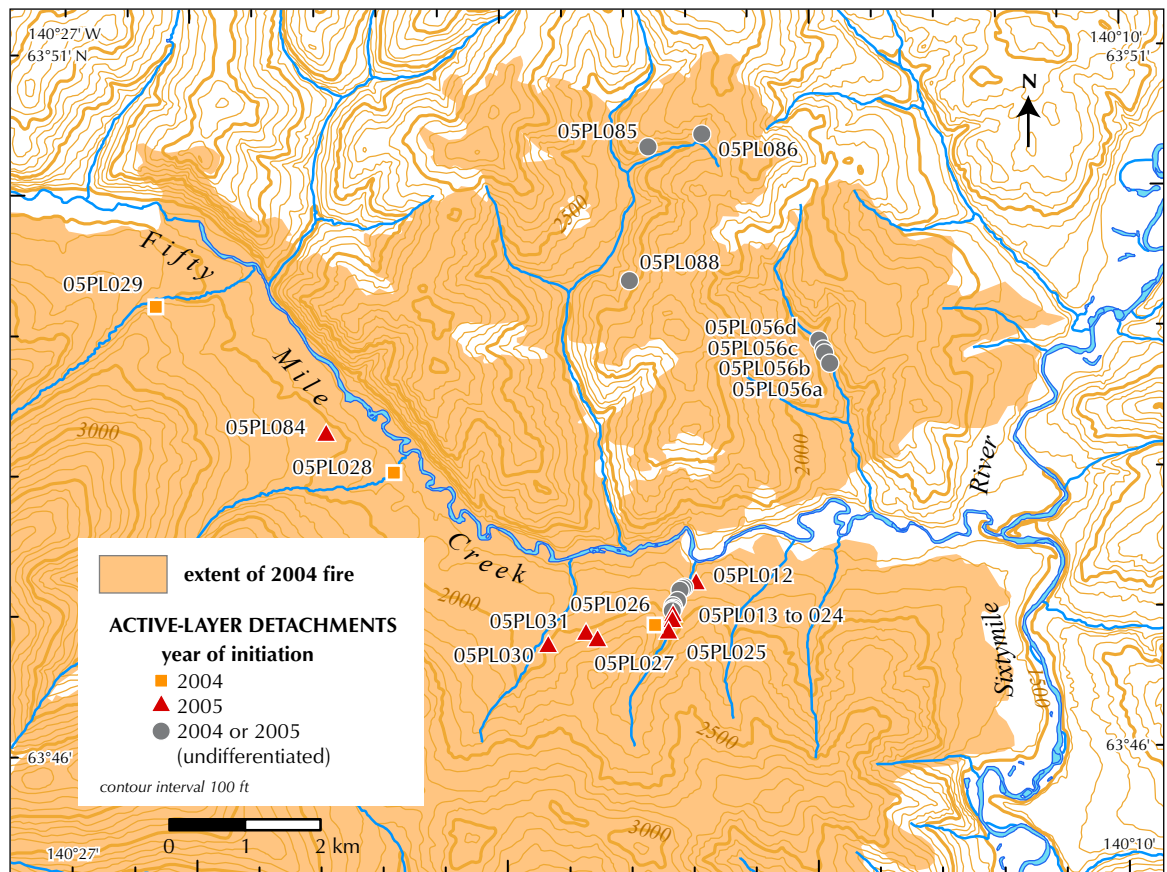
scale monitoring of hydrological and biological parameters has been ongoing by various agencies (Department of Fisheries and Oceans; Yukon Environment; Yukon Energy Mines and Resources, Client Services and Inspections) as part of an environmental baseline study to characterize the impacts of placer mining and exploration on watershed systems.

The lower half of the watershed was burned in the 2004 fires (Fig. 7). Fires were detected by MODIS satellite instruments in the watershed between June 25 and July 13, 2004 (USDA Forest Service, 2005). The fires started on the upper slopes, south of Fifty Mile Creek, about a third of the way up the valley. They burned most extensively near the subsequent detachments on June 29 and 30. Between July 1 and 11, only scattered hotspots were detected. On July 12, the entire lower portion of the watershed burnt extensively both north and south of the creek.

• **Field survey methodology**

Twenty-eight slope failures were located in the watershed using GPS waypoints recorded while hovering above each detachment with a helicopter; this data was gathered on July 16 and 19, 2005 (Fig. 7). Twenty of the failures were

Figure 7. Location map displaying the extent of burned areas, as well as locations of active-layer detachments surveyed in the lower part of the Fifty Mile Creek watershed.



visited on the ground between July 16 and 19. The same site survey methods were employed at Fifty Mile Creek as were used in the Mickey Creek watershed.

• **Failure settings and morphologies**

Active-layer detachments occurred mainly along the upper portions of convex tributary valley slopes in the Fifty Mile Creek watershed. The morphology of a typical elongate-shaped detachment is shown in Figure 8. Slope angles in the initiation zones ranged between 11° and 25°. Failures occurred on all aspects, but were most common on north- and east-facing slopes. The highest density of failures occurred along one tributary valley, where 15 detachments have occurred within 1 km (05PL012 to 05PL027). Failures were very shallow, ranging between 15 cm and 50 cm. They were generally up to 60 m long and up to 25 m wide, although a few failures traveled several hundred metres downslope. Surficial materials in the initiation zones of the failures consisted of brown, silt-rich (up to 37-60% silt) colluvium, with 20-50% angular to sub-angular schistose clasts.

Sediment-laden artesian springs (sediment plumes) were noted in proximity to many initiation zones (Fig. 9), indicating extremely high pore water pressures. Frost probing in mid July located the frost table between 44 cm



Figure 9. Surface sediment plume created by artesian groundwater flow. These commonly occurred on saturated slopes and near the initiation zones of recent failures.

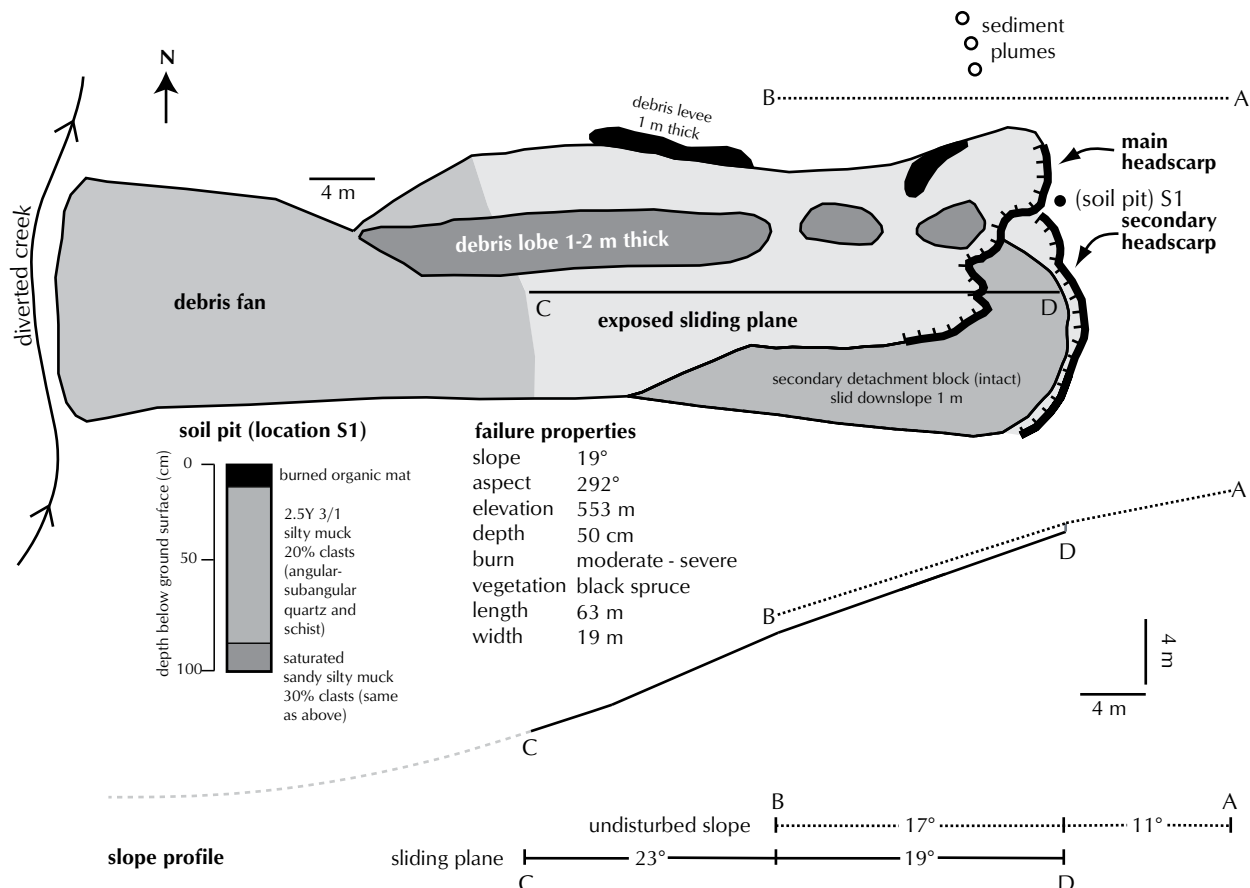


Figure 8. Morphology and slope profile of typical elongate detachment (05PL012) in Fifty Mile Creek watershed; drawn to scale.

and 106 cm below the ground surface adjacent to the initiation zones. Three of the failures (05PL024, 05PL027 and 05PL084) appeared to have been triggered within days of the field investigations, as indicated by the highly saturated flow materials, live vegetation in the debris, and the presence of very fine outstretched live roots along the headscarp sliding planes.

STEELE CREEK

• Setting

The valley of Steele Creek is located at approximately 63°35'N and 138°59'W (55 km south-southeast of Dawson City) and spans elevations of 580-1000 m asl (Fig. 10). The watercourse is 8 km long and drains north from the Black Hills into Montana Creek, which is a tributary of the Indian River. The terrain in the area is characterized by V-shaped valleys and rolling hills with rounded summits. Hillslopes are blanketed in colluvium derived from the underlying Nasina assemblage graphitic

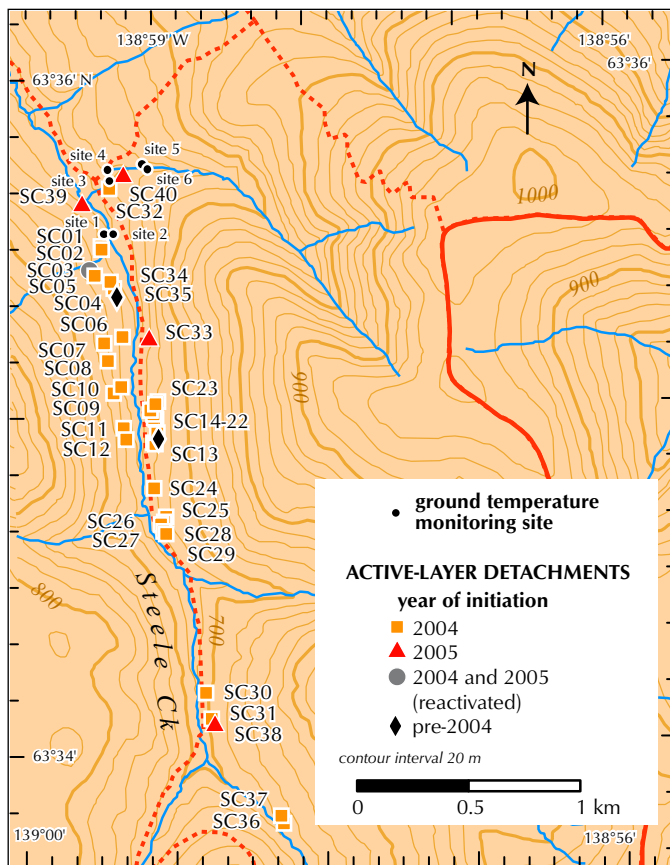


Figure 10. Map displaying burned area and locations of active-layer detachments surveyed in Steele Creek watershed. The entire area was burned during the summer of 2004.

quartzite and muscovite-quartz schist (Gordey and Makepeace, 2003). Field observations confirmed that only well drained, south-facing slopes are permafrost-free. Where permafrost is present, field measurements showed extremely variable active layer depths, ranging from 30-150 cm, depending on vegetation cover and aspect.

MODIS satellite instruments detected fires in the valley of Steele Creek from June 30-July 4, 2004. The fires started in the upper reaches of the watershed on June 30. The majority of the fires were detected between July 1 and July 3 during which time they spread most of the way down the watershed. Scattered hotspots were detected near the mouth of the creek on July 4.

The valley was selected for study based on aerial photographs (taken August 26, 2004 by Jim Leary of Yukon Energy, Mines and Resources, Client Services and Inspections) which revealed the large number of detachment failures that had taken place within weeks of the forest fire. The site is accessible by mining roads, which allowed monitoring of freeze-up processes in the fall of 2004 and observation of additional detachment failures in the summer of 2005.

There are currently no placer mining operations on Steele Creek, but mineral prospecting and active claims exist. Evidence of historical placer works was found, and was likely associated with the old Dawson-to-Whitehorse winter stagecoach trail located along the length of the valley bottom.

• Field survey methodology

In the fall of 2004, preliminary observations of active-layer detachments and ground thermal conditions were made. Forty-metre transects were laid out across the boundary between burned and unburned forest at six sites encompassing different aspects and terrain types. Probing to the frost table was conducted at one-metre intervals along each transect, approximately every two weeks, from mid-September to early December. At the end of each transect, as well as at the centre point, boreholes were drilled to depths of 1-2 m below the permafrost table and pipes were inserted into them. On the same dates as the frost-probing transects were performed, thermistors were inserted down the borehole pipes at 20 cm intervals to measure ground temperatures. Observations of vegetation, degree of burn and snow depth were also made.

All existing detachment failures were photographed from the air on May 18, 2005. Since this was immediately after

snowmelt, and thaw depths were less than 35 cm, this inventory represented landslides that had occurred in the summer of 2004 immediately following the fires. The inventory revealed that thirty-five detachment failures had occurred in 2004 along a 3.7-km-long section of the main valley and on slopes within its tributaries (Fig. 10). In 2005, an additional five new slides developed by mid-August and several old slides from 2004 were also reactivated.

Representative detachment failures from both years were mapped in detail, and soil pits were excavated in order to examine soil stratigraphy (Fig. 11). Probing was conducted

throughout the summer to determine the depth of the frost table.

In May 2005, two-channel Onset Hobo Pro temperature loggers (accuracy $\pm 0.2^{\circ}\text{C}$) were set up on burnt slopes which approximately faced the four cardinal directions (Table 1). These temperature loggers measured screen-height air temperatures (external thermistor) and surface ground temperatures (internal thermistor) at hourly intervals. Two more loggers of the same type were installed on unburnt north- and south-facing slopes in mid-June. Four-channel Onset Hobo 8 temperature loggers were also installed at the same sites and their external

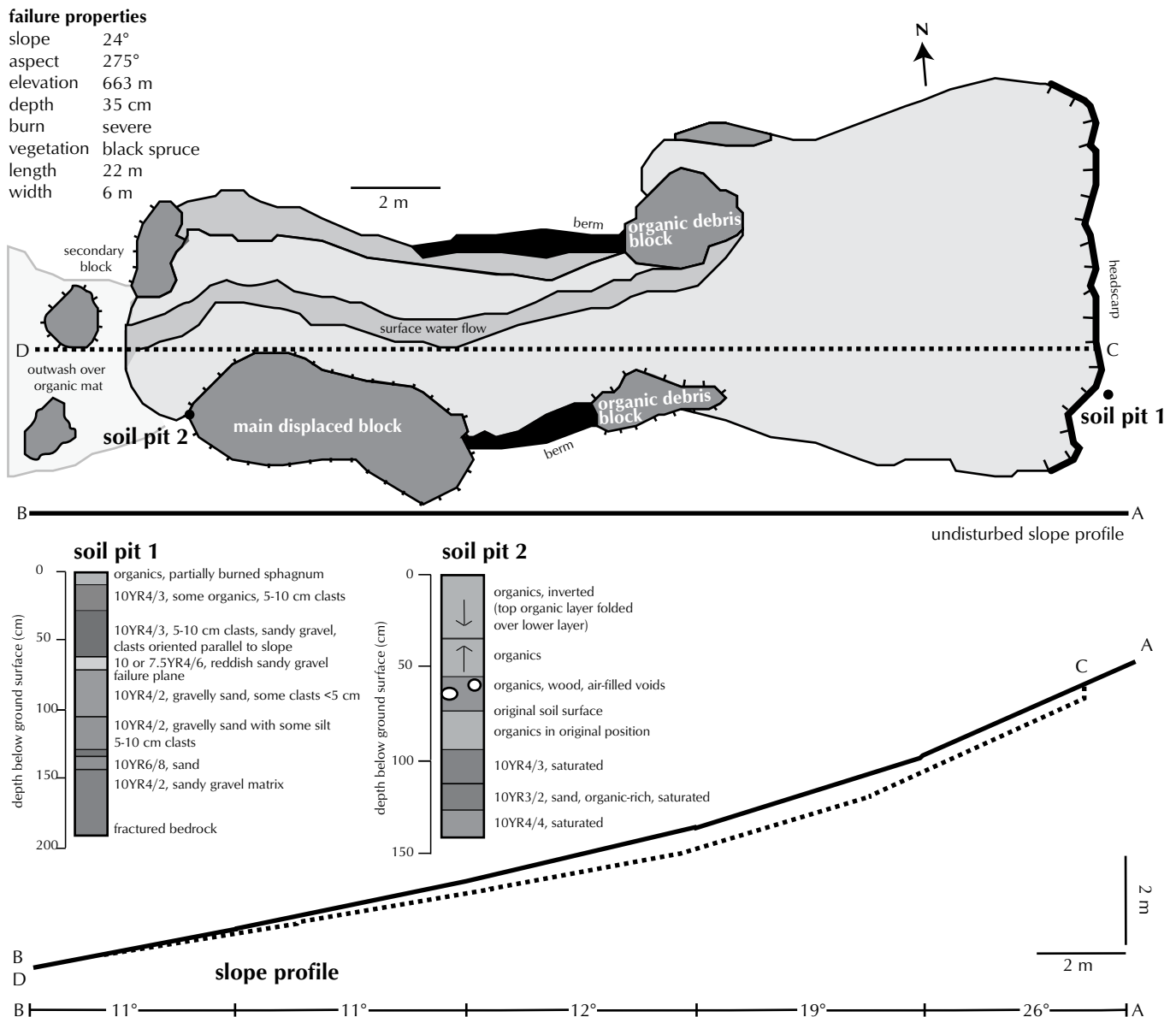


Figure 11. Morphology and slope profile of typical elongate detachment (SC13) in Steele Creek watershed; drawn to scale.

Table 1. Summary characteristics at temperature monitoring sites, Steele Creek, summer 2005.

Site	1	2	3	4	5	6
Aspect	east	west	northwest	south-southeast	south	north
Burn condition	burnt	burnt	burnt	burnt	unburnt	unburnt
Permafrost	present	present	present	absent	absent	present
Vegetation type	burnt spruce forest	burnt spruce forest	burnt spruce forest	burnt aspen and birch forest	mixed spruce and aspen forest	open spruce forest with thick moss
Depth of ground sensors and period of data collection ¹	0 cm: May 19, 2005 25 cm: May 19, 2005 50 cm: May 19, 2005 60 cm: May 19, 2005 - July 11, 2005 70 cm: May 19, 2005 100 cm: July 11, 2005			0 cm: May 19, 2005 25 cm: May 19, 2005 50 cm: May 19, 2005 70 cm: May 19, 2005 100 cm: May 19, 2005		0 cm: June 12, 2005 10 cm: June 12, 2005 - June 21, 2005 20 cm: June 12, 2005 - June 21, 2005 25 cm: June 21, 2005 30 cm: June 12, 2005 - June 21, 2005 50 cm: June 21, 2005 60 cm: June 21, 2005 - July 11, 2005 70 cm: July 11, 2005 100 cm: July 11, 2005
Mean July air temperature (°C)	13.2	13.2	13.7	13.7	12.9	13.1
Mean July ground surface temperature (°C)	11.5	12.7	13.7	14.6	11.7	10.7
Calculated frost table depth on August 12, 2005 ²	158 cm	81 cm	89 cm	unfrozen	unfrozen	80 cm

¹Data-collection is ongoing where no end-date is indicated; last download was on 13/8/2005.

²Frost table depths were calculated using a second-order polynomial fit to measured ground temperatures.

thermistors (accuracy $\pm 0.5^\circ\text{C}$) were inserted in the ground at a variety of depths. As the frost table fell during the summer, the thermistors were moved deeper into the ground in order to track the frost table position (see Table 1). A tipping-bucket rain-gauge was also installed in the valley from the end of July to mid-August.

Preliminary analysis of measured summer air temperatures, which are relevant to active layer development, suggest that values are about 1°C colder than those at Dawson, due to the 200-300 m higher elevation difference. The July average temperature at Dawson was 14.2°C , while the average of the two unburnt sites in Steele Creek was 13.0°C (Table 1). Precipitation amounts, however, differed

greatly from those at Dawson. Severe thunderstorms were observed frequently at Steele Creek in June and July 2005 and almost 50 mm of rain was recorded between July 27 and August 5. Dawson recorded less than 2 mm of precipitation in these two months.

• Failure settings and morphologies

Both bell-shaped and elongated detachment failures (Lewkowicz and Harris, 2005b) were present (Fig. 12). They developed on hillslopes with a variety of aspects. All failures occurred on slopes underlain by permafrost; no detachments were observed on south-facing slopes that were permafrost-free. Most failures initiated on slopes of $19\text{-}24^\circ$, often proximal to a convex break in slope (Fig. 13).

Active-layer detachments were 50-80 cm in depth, ranged in length from tens to hundreds of metres, and were 1 m to 20 m wide. The morphology and slope profile of a typical elongate detachment failure (SC013) is shown in Figure 11. Several of the failures deposited sediment and debris directly into Steele Creek (Fig. 14). One detachment failure partially blocked the creek, creating a small pond upstream.

Based on observations of failure morphology and stratigraphy, most failure histories appear to have involved a combination of slide and flow. As in the other two watersheds, the failure surface for almost all the detachment failures that occurred in 2005 was between the ground surface and the frost table. By mid-August, the frost table varied between 81 cm and 169 cm below the ground surface at the burnt sites underlain by permafrost

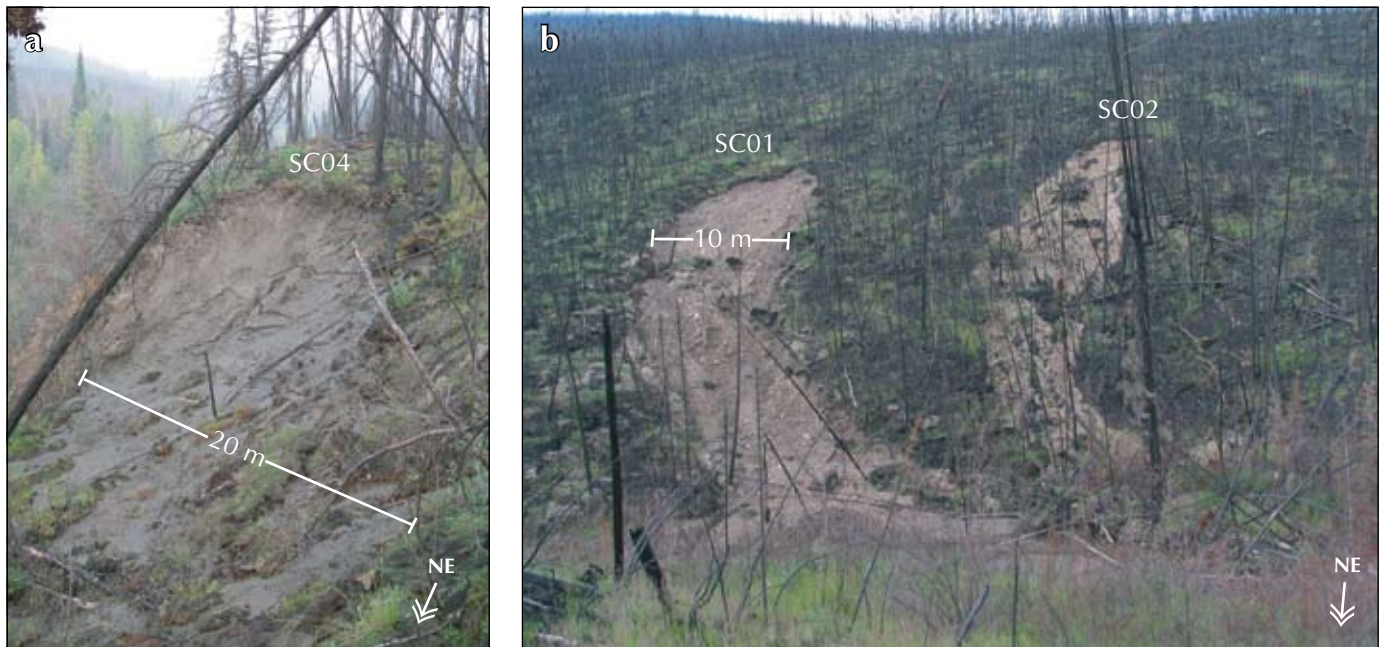


Figure 12. Typical bell-shaped (a) and elongate (b) detachment failures on northeast-facing slopes in the Steele Creek watershed.

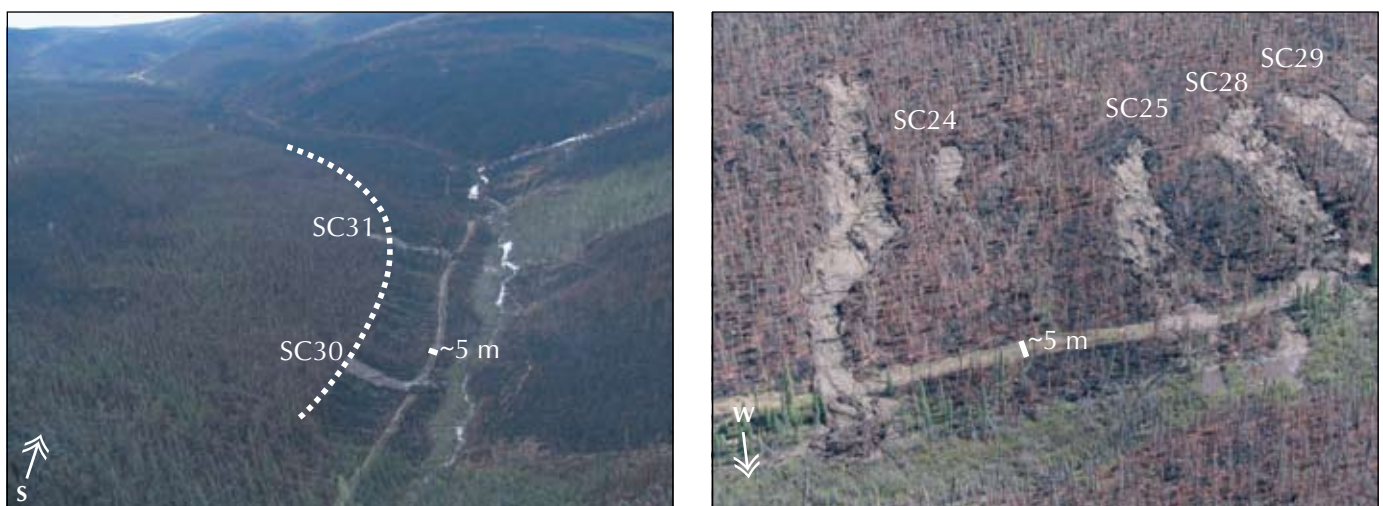


Figure 13. Oblique aerial photograph of active-layer detachments in Steele Creek, which initiated from a prominent convex break in slope (shown by dotted line).

Figure 14. Oblique aerial photograph of multiple active-layer detachments on a west-facing slope. The failures crossed local access trails and deposited material directly into Steele Creek.

(see Table 1). Although the failure depths observed for the 2004 detachments did not appear to be different from those in 2005, it is not known whether movements took place along the frost table (which would likely have been higher than in 2005), or within unfrozen soil layers. The location of the 2005 failure surfaces above the frost table distinguishes these active-layer detachments from those observed elsewhere following fire or other disturbance on permafrost slopes (e.g., Lewkowicz and Harris, 2005a, 2005b).

Most of the reactivations involved relatively small movements at the headscarp and shallow minor mudflows in the floors, but in some cases, major blocks of material moved downslope. As in the other watersheds, there was evidence of high pore water pressures within the slopes in 2005, with sediment plumes emerging onto the burnt organic mat, particularly near failure headscarps. Water under artesian pressure was also observed bubbling to the surface in the floor of one of the detachment failures.

DISCUSSION

IMPACTS OF FOREST FIRE ON SLOPE STABILITY

Forest fires impact numerous aspects of the thermal, hydrological and geotechnical conditions of slopes underlain by permafrost. A conceptual framework for these direct and indirect factors is shown in Figure 15. The relative significance of each of these controls on overall slope stability is difficult to assess, and merits future study.

Fire alters slope thermal conditions by burning the vegetation canopy and ground cover, thereby reducing shading. Simultaneously, charring of the surface organic mat decreases the albedo. The result of these two changes is an increase in the solar radiation absorbed at the ground surface. As a consequence, the mean July ground surface temperatures on burnt north-facing and south-facing slopes in Steele Creek were about 3°C warmer than comparable unburnt slopes (see Table 1). The destruction of live vegetation may also reduce evapotranspiration so that less of the heat available at the ground surface is lost by latent heat transfer to the atmosphere. Finally, a reduction in the thickness of the insulating surface organic mat allows heat to be transmitted downwards more easily. All of these impacts cumulatively lead to enhanced summer ground heat flux

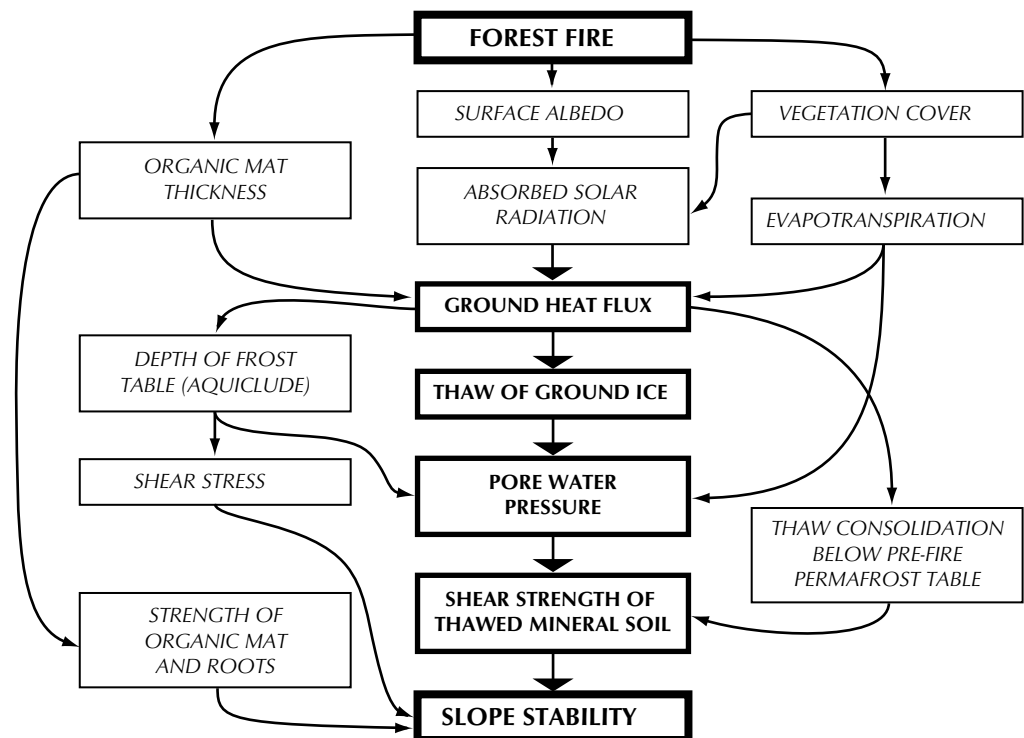


Figure 15. Conceptual framework for the impacts of forest fire on the stability of slopes underlain by permafrost. Note: for clarity, factors that are unaffected by fire (e.g., topography, precipitation) are not shown.

downwards towards the frost/permafrost table (Yoshikawa *et al.*, 2002; Ping *et al.* 2005).

The increased downward ground heat flux can be expected to cause deeper thaw than in the pre-fire period, both in the year of the fire and in subsequent years. Data from both pairs of comparable burned and unburned temperature monitoring sites (north-facing sites 2 and 6 and south-facing sites 4 and 5 in Table 1 and Fig. 16) suggest this effect, but the observations are too limited spatially to be regarded as conclusive. Where the upper layers of permafrost contain excess ice, their thaw may result in increased porewater pressure (McRoberts and Morgenstern, 1974; Dyke, 2000; Harris and Lewkowicz, 2000). Porewater pressures may also be affected by the reduction in surface evapotranspiration and subsequent increase in overland flow. Maximum porewater values may additionally be influenced by the increased depth of the thaw plane.

Other geotechnical changes relate to burning of the organic mat and tree roots, as their contribution to slope shear strength can be significantly reduced following forest fires. Organic mats were shown to have greater strength than the underlying soil, even in burned areas, as they were commonly observed draped over the edges of detachment failures. Thaw settlement of the thawing permafrost material may contribute to breaking the bond between the organic mat and the underlying soil, as suggested by the presence of gaps between dried rigid organic mats and the underlying mineral soil at the edge of some failures. At the advancing thaw plane, the faster the release of water and the slower the consolidation, the lower the shear strength will be (McRoberts and Morgenstern, 1974).

Although not shown in Figure 15, which focuses only on changes following forest fire, topography and precipitation are also very important factors for slope

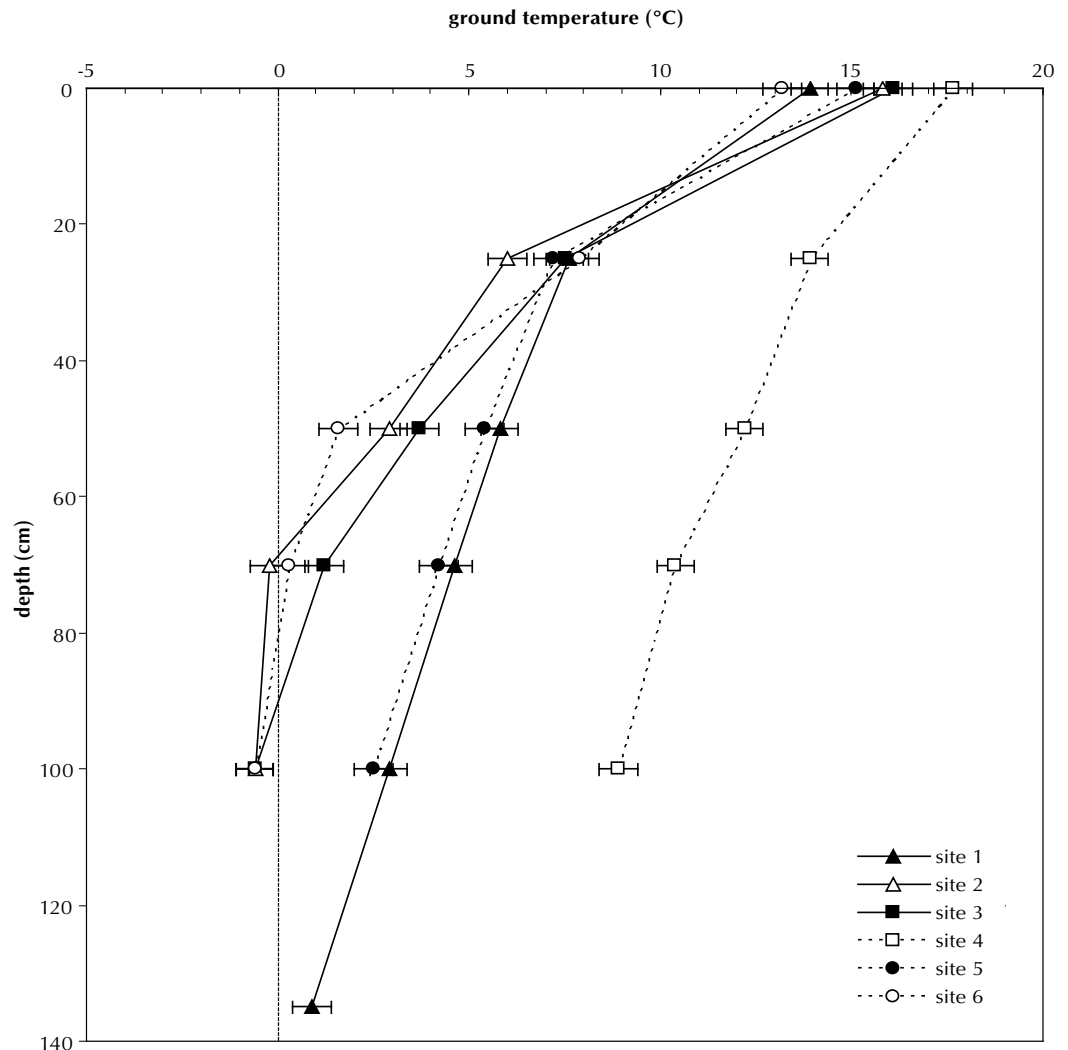


Figure 16. Average ground temperature profiles on August 12, 2005 at the Steele Creek monitoring sites. Values shown are 24-hour averages. A sensor accuracy of $\pm 0.5^{\circ}\text{C}$ is shown by error bars at respective measurement depths.

stability. Topography (slope steepness) directly affects shear stress, while precipitation acts to alter slope stability through its effect on shear stress, cohesion and porewater pressure. The numerous heavy precipitation events observed over the summer of 2005 in Steele Creek likely contributed to slope instability in the watershed.

The relative severity of the 2004 fires within the three watersheds was examined using 30-m resolution Landsat 7 Thematic Mapper (TM) satellite imagery taken at approximately the same time of year before and after the forest fires. TM Band 4 (near infrared) is sensitive to live vegetation, while Band 7 (middle infrared) is sensitive to ash, char and mineral soil. A Normalized Burn Ratio (NBR) was calculated ($NBR = (Band\ 4 - Band\ 7) / (Band\ 4 + Band\ 7)$) for all pixels in the pre-fire scene (September 2001) and the post-fire scene (September 2004). The difference in the pre-fire NBR and the post-fire NBR is referred to as the Differenced Normalized Burn Ratio (DNBR), which has been shown by field testing to be a reliable indicator of burn severity (Cocke *et al.*, 2005). Preliminary analyses of the data (Fig. 17) suggest that detachment failures in all three watersheds occurred in areas where the relative burn severity (with respect to each watershed) was moderate to severe. This indicates that significant burning promotes detachment failures in the watersheds. Not all significantly burned slopes fail, however, since numerous other factors (as described above) affect their stability.

DETACHMENT FAILURE FREQUENCY AND CLIMATE CHANGE IMPLICATIONS

The long-term frequency of fire-related active-layer detachments depends on the frequency of fires and on the recovery time for degraded icy permafrost (Lewkowitz and Harris, 2005a). Minimum return intervals for fire frequency are limited by the recovery of vegetation and the redevelopment of sufficient fuel. Estimates of current fire frequency in the northern boreal forest range between 30 to 500 years, but are typically about 100-200 years (Johnson, 1992; Yoshikawa *et al.*, 2002; Hinzman *et al.*, 2003).

The time needed for permafrost to become stable following a fire depends on the ground thermal regime. In the southern Yukon, where ground temperatures at the top of undisturbed permafrost are $\geq 1^{\circ}\text{C}$, the permafrost table was still falling slowly, 40 years after a forest fire (Burn, 1998). However, in interior Alaska where conditions are similar to those at Dawson, it was estimated that it would take 25-50 years for the

permafrost table to return to its original depth, following re-establishment of spruce and feathermoss as part of post-fire succession (Viereck, 1982; Van Cleve and Viereck, 1983). Consequently, it appears that at present, detachment failure recurrence around Dawson is limited by vegetation recovery and the frequency of forest fire, and not by geocryological conditions.

There appear to be broad links between climate change and fire frequency in the northern boreal forest. While the climate has warmed, the annual burn area in Canadian boreal forests has doubled in the past 20 years (Kasischke and Stocks, 2000; Stocks *et al.*, 2002) because of increased aridity, drier fuel and more frequent convective storm activity. Attempts at modeling future changes in Canadian forest fire activity project increases of 40% in size and 46% in severity, for a doubling of carbon-dioxide levels (Van Wagner, 1988; Flannigan and Van Wagner, 1991). In central Yukon (including Dawson), the number of fires are projected to increase by up to two-thirds, while the area burned is projected to increase by up to 300% by 2069, based on general circulation models and regional climate scenarios (McCoy and Burn, 2005). If this occurs, there should be a concomitant increase in the frequency of detachment failure activity for the same period, given the current state of permafrost thermal conditions in the area.

ENVIRONMENTAL AND ECONOMIC IMPLICATIONS

The impacts of active-layer detachments on watershed-scale sedimentation processes in the Dawson area may be significant, particularly if their frequency increases in the future. Aside from the obvious risks to infrastructure and local access roads, fisheries stocks, as well as placer mining could be affected. The active-layer detachments could also provide new prospecting opportunities by exposing fresh colluvial materials at the surface.

Following the forest fires in Mickey Creek, increased stream sedimentation into summer-rearing habitat was reported as having the potential to displace juvenile Chinook salmon (A. von Finster, pers. comm., 2005). This was of concern as Yukon River Chinook salmon support commercial, subsistence and aboriginal fisheries in Canada and Alaska. Settleable solids, and in particular, sand-sized particles, can clog spawning gravel and abrade algae beds. Suspended solids reduce visibility for capturing prey, and limit the productivity of algae and invertebrates, thereby reducing fish food sources. In some places along Mickey Creek, the landslides blocked the

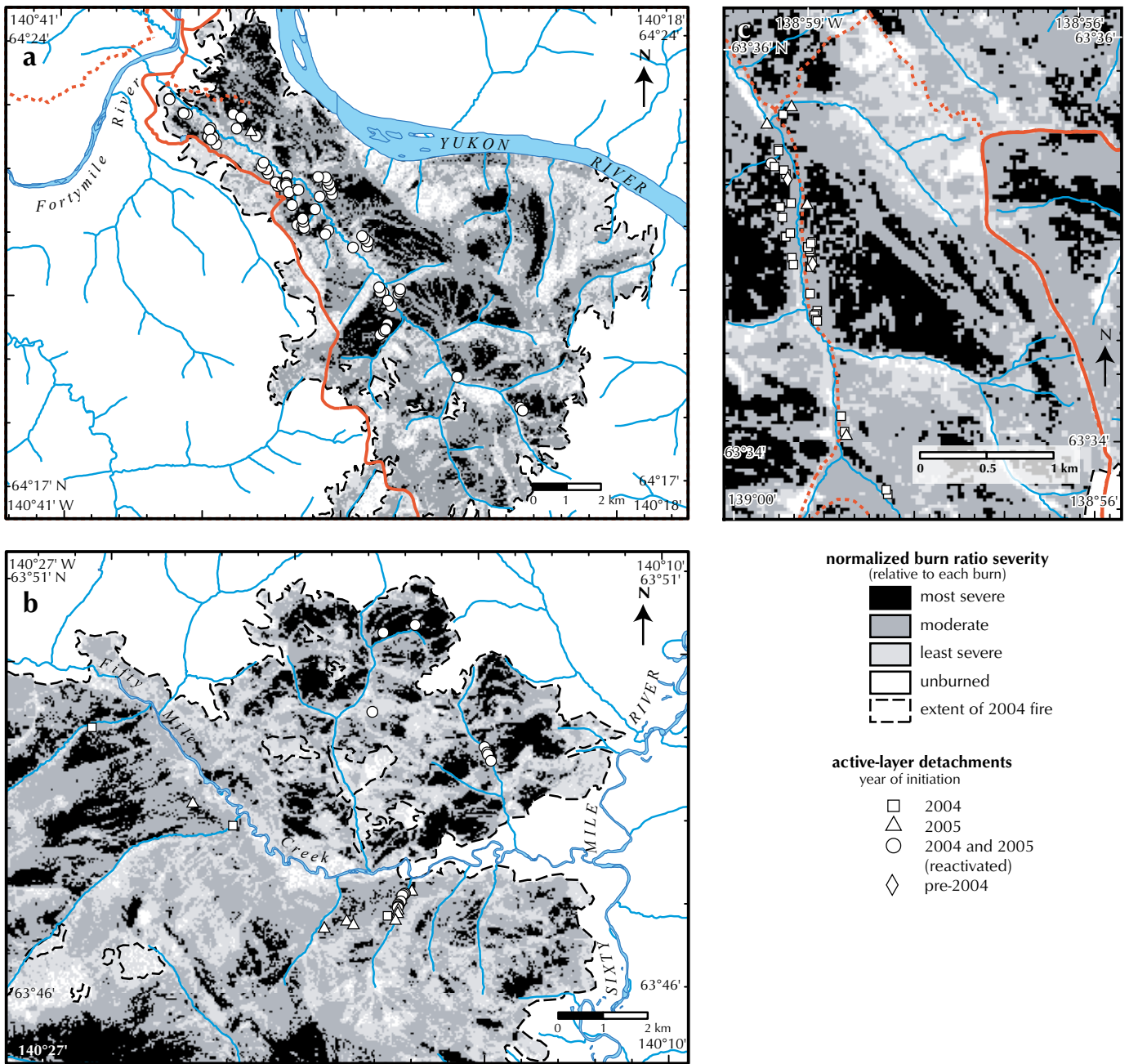


Figure 17. Example of relative burn severity evaluation performed in the (a) Mickey Creek, (b) Fifty Mile Creek and (c) Steele Creek watersheds. Differenced Normalized Burn Ratio (DNBR) analysis is based on differences in ground cover reflected in Landsat 7 TM Bands 4 and 7 (30 m resolution) before (September, 2001) and after (September, 2004) the forest fire. White outlined shapes represent active-layer detachments as shown on Figures 4, 7 and 10.

stream channel, and destroyed natural cover and shading. However, detachment failures may also introduce nutrients into the stream system and create new habitat.

Understanding the degree to which active-layer detachments contribute to sedimentation in the drainage network is critical at the present time, as the Department of Fisheries and Oceans (DFO) transitions into a new placer mining regulatory framework for the Yukon by 2007. The new regulatory regime proposes to consider natural sediment contributions and incorporate local watershed health monitoring strategies in determining the water quality objectives that are appropriate to individual watersheds. The limited amount of data collected by DFO in the summers of 2004 and 2005 demonstrate that natural turbidity levels in burned watersheds can be highly variable throughout the day and season. It will be important that the proposed adaptive management strategy reflects potential sediment contributions that will occur from active-layer detachments after forest fires. More detailed water quality monitoring will be needed in the future to quantify the amount of these sediment contributions.

CONCLUSIONS

Nearly one hundred and fifty active-layer detachments developed in three catchments in the Dawson region following the 2004 forest fires. While field measurements and data analyses are continuing in 2006, the following preliminary conclusions could be reached:

1. The majority of detachment failures initiated in the summer months immediately following the fires; a minority of the landslides developed in 2005.
2. Active-layer detachments developed on moderate to steep slopes of all aspects, provided permafrost was present. Aspect may influence the distribution of these landslides where surficial materials vary widely with orientation. No failures were observed on south-facing permafrost-free slopes. Relative burn severity at most failure sites, established from satellite imagery, was moderate or high.
3. The location of the failure plane in the majority of the landslides in the Dawson area appears to have been within the thawed surficial materials of the active layer and not at the frost table. This differs from those reported in the literature from the Mackenzie Valley and Canadian Arctic Archipelago.
4. The number and size of the active-layer detachments appears to have been sufficient to affect stream sediment loadings.

ACKNOWLEDGEMENTS

Funding for the Steele Creek investigations was generously provided to A. Lewkowicz by a Yukon Geological Survey contribution agreement, NSERC and the University of Ottawa. Winter accommodation and assistance was donated by the Indian River Farm.

Field assistance was ably given by Martina Knopp (Steele Creek) and Erin Trochim (Mickey Creek and Fifty Mile Creek). Lorraine Millar generously performed initial helicopter surveys in the Fifty Mile Creek watershed and supplied digital photos for preliminary inventories. Jason Adams, Amy Stuart and Brian Sorbel assisted with the burn severity analysis, and Al von Finster provided invaluable fisheries information. The authors are also grateful to Jeff Bond and Leyla Weston for improvements to the paper.

REFERENCES

- Aylsworth, J.M., Duk-Rodkin, A., Robertson, T. and Traynor, J.A., 2000. Landslides of the Mackenzie Valley and adjacent mountainous and coastal regions. *In: The Physical Environment of the Mackenzie Valley, Northwest Territories: A Base Line for the Assessment of Environmental Change*, L.D. Dyke and G.R. Brooks (eds.), Geological Survey of Canada, Bulletin 547, p. 167-176.
- Burn, C.R., 1998. The response (1958-1997) of permafrost and near-surface ground temperatures to forest fire, Takhini River valley, southern Yukon Territory. *Canadian Journal of Earth Sciences*, vol. 35, no. 2, p. 184-199.
- Cocke, A.E., Fulé, P.Z. and Crouse, J.E., 2005. Comparison of burn severity assessments using Differenced Normalized Burn Ratio and ground data. *International Journal of Wildland Fire*, vol. 14, p. 189-198.
- Duk-Rodkin, A., 1996. Surficial geology, Dawson, Yukon Territory. Geological Survey of Canada, Open File 3288, 1:250 000 scale.

- Dyke, L.D., 2000. Stability of permafrost slopes in the Mackenzie Valley. *In: The Physical Environment of the Mackenzie Valley, Northwest Territories: A Base Line for the Assessment of Environmental Change*, L.D. Dyke and G.R. Brooks (eds.), Geological Survey of Canada, Bulletin 547, p. 177-186.
- Dyke, L., 2004. Stability of frozen and thawing slopes in the Mackenzie Valley, Northwest Territories. *Géo Quebec 2004, 57th Canadian Geotechnical Society Conference*, p. 31-38.
- EBA Engineering Consultants Ltd., 1983. Geothermal performance of a buried utility system in permafrost, Dawson, Yukon. Report to National Research Council of Canada, 52 p.
- EBA Engineering Consultants Ltd., 1989a. Geotechnical evaluation, C-2 Land Claim area, Dawson City, Yukon. Report to Department of Community and Transportation Services, Yukon Territorial Government, Whitehorse, Yukon.
- EBA Engineering Consultants Ltd., 1989b. Geotechnical evaluation, proposed West Dawson rural residential subdivision near Dawson City, Yukon. Report to Department of Community and Transportation Services, Yukon Territorial Government, 17 p.
- Flannigan, M.D. and Van Wagner, C.E., 1991. Climate change and wildfire in Canada. *Canadian Journal of Forest Research*, vol. 21, p. 66-72.
- Fraser, T., 1995. On the nature and origin of muck deposits, Klondike District, Yukon Territory. M.A. thesis, Carleton University, Ottawa, Canada, 203 p.
- Gordey, S.P. and Makepeace, A.J., 2003. Yukon digital geology, Version 2.0. Geological Survey of Canada Open File 1749 and Yukon Geological Survey Open File 2003-9(D), 2 CD-ROMS.
- Harris, C. and Lewkowicz, A.G., 2000. An analysis of the stability of thawing slopes, Ellesmere Island, Nunavut, Canada. *Canadian Geotechnical Journal*, vol. 37, p. 449-462.
- Heginbottom, J.A., Dubreuil, M.A. and Harker, P.T., 1995. National Atlas of Canada (5th edition), Canada. Permafrost, Plate 2.1, (MCR 4177), 1:7 500 000 scale.
- Hinzman, L.D., Fukuda, M., Sandberg, D.V., Chapin III, F.S. and Dash, D., 2003. FROSTFIRE: An experimental approach to predicting the climate feedbacks from the changing boreal fire regime. *Journal of Geophysical Research*, vol. 108, D1, 8153, p. 6.
- Hugenholtz, C.H., 2000. Active-layer detachment slides on an alpine plateau, Kluane Lake, Yukon Territory. Sixth National Student Conference on Northern Studies, Université de Laval, p. 35-41.
- Huscroft, C.A., Lipovsky, P.S. and Bond, J.D., 2004. A regional characterization of landslides in the Alaska Highway corridor, Yukon. Yukon Geological Survey, Open File 2004-18, 65 p., report and CD-ROM.
- Jackson, L.E., Jr., 2005. Surficial geology, Enchantment Creek, Yukon Territory. Geological Survey of Canada, Open File 4580, 1:50 000 scale.
- Johnson, E.A. 1992. Fire and vegetation dynamics: studies from the North American boreal forest. Cambridge University Press, Cambridge, 129 p.
- Kasischke, E.S. and Stocks, B.J., 2000. Fire, climate change, and carbon cycling in the boreal forest. *Ecological Studies Series*, Springer-Verlag, New York, 461 p.
- Lewkowicz, A.G., 1992. Factors influencing the distribution and initiation of active-layer detachment slides on Ellesmere Island, Arctic Canada. *Periglacial Geomorphology*, John Wiley and Sons (eds.), p. 223-250.
- Lewkowicz, A.G. and Harris, C., 2005a. Frequency and magnitude of active-layer detachment failures in discontinuous and continuous permafrost, northern Canada. *Permafrost and Periglacial Processes*, vol. 16, p. 115-130.
- Lewkowicz, A.G. and Harris, C., 2005b. Morphology and geotechnique of active-layer detachment failures in discontinuous and continuous permafrost, northern Canada. *Geomorphology*, vol. 69, p. 275-297.
- Lowey, G.W., 2000. Glaciation, gravel and gold in the Fifty Mile Creek area, west-central Yukon. *In: Yukon Exploration and Geology 1999*, D.S. Emond and L.H. Weston (eds.), Exploration and Geological Services Division, Yukon, Indian and Northern Affairs Canada, p. 199-209.

- McCoy, V.M. and Burn, C.R., 2005. Potential alteration by climate change of the forest-fire regime in the boreal forest of central Yukon Territory. *Arctic*, vol. 58, p. 276-285.
- McRoberts, E.C. and Morgenstern, N.R., 1974. Stability of slopes in frozen soil, Mackenzie Valley, N.W.T. *Canadian Geotechnical Journal*, vol. 11, p. 554-573.
- Mortensen, J.K., 1996. Geological compilation maps of the northern Stewart River map area, Klondike and Sixtymile districts (115N/15, 16; 115O/13, 14 and parts of 115O/15, 16). Exploration and Geological Services, Yukon Region, Indian and Northern Affairs Canada, Open File 1996-1(G), 43 p., 1:50 000 scale.
- Ping, C.L., Michaelson, G.J., Packee, E.C., Stiles, C.A., Swanson, D.K. and Yoshikawa, K., 2005. Soil catena sequences and fire ecology in the boreal forest of Alaska. *Soil Science Society of America Journal*, vol. 69, p. 1761-1772.
- Smith, C.A.S., Meikle, J.C. and Roots, C.F. (eds.), 2004. Ecoregions of the Yukon Territory: Biophysical properties of Yukon landscapes. Agriculture and Agri-Food Canada, PARC Technical Bulletin No. 04-01, 313 p.
- Stangl, K.O., Roggensack, W.D. and Hayley, D.W., 1982. Engineering geology of surficial soils, eastern Melville Island. *In: The Roger J.E. Brown Memorial Volume*, H.M. French (ed.), Proceedings Fourth Canadian Permafrost Conference. National Research Council of Canada, Ottawa, p. 136-147.
- Stocks, B.J., Mason, J.A., Todd, J.B., Bosch, E.M., Wotton, B.M., Amiro, B.D., Flannigan, M.D., Hirsch, K.G., Logan, K.A., Martell, D.L. and Skinner, W.R., 2002. Large forest fires in Canada, 1959-1997. *Journal of Geophysical Research*, vol. 108, no. D1, p. 13.
- USDA Forest Service, 2005. USDA Forest Service MODIS Active Fire Mapping Program, USDA Forest Service Remote Sensing Application Center. GIS data available online at <http://activefiremaps.fs.fed.us/canada>.
- Van Cleve, K. and Viereck, L.A., 1983. A comparison of successional sequences following fire in permafrost-dominated and permafrost-free sites in interior Alaska. *In: Permafrost, Fourth International Conference, Proceedings, Fairbanks, Alaska*. National Academy Press, Washington, D.C., p. 1286-1291.
- van Everdingen, R. (ed.), 1998 (revised January, 2002). Multilanguage glossary of permafrost and related ground-ice terms. International Permafrost Association Terminology Working Group, Boulder, CO: National Snow and Ice Data Centre/World Data Centre for Glaciology, 88 p.
- Van Wagner, C.E., 1988. The historical pattern of annual burned area in Canada. *The Forestry Chronicle*, vol. 64, p. 182-185.
- Viereck, L.A., 1982. Effects of fire and firelines on active layer thickness and soil temperature in interior Alaska. *In: The Roger J.E. Brown Memorial Volume, Proceedings, H.M. French (ed.), Fourth Canadian Permafrost Conference, National Research Council of Canada, Ottawa*, p. 123-135.
- Yoshikawa, K., Bolton, W.R., Romanovsky, V.E., Fukuda, M. and Hinzman, L.D., 2002. Impacts of wildfire on the permafrost in the boreal forests of Interior Alaska. *Journal of Geophysical Research*, vol. 108, no. D1-8148, p. 14.

Anatomy of a Late Jurassic Gilbert-type delta in basal strata of the Tantalus Formation, Whitehorse Trough, Yukon

Darrel G.F. Long

Department of Earth Sciences, Laurentian University¹

Grant M. Lowey

Yukon Geological Survey²

Long, D.G.F. and Lowey, G.M., 2006. Anatomy of a Late Jurassic Gilbert-type delta in basal strata of the Tantalus Formation, Whitehorse Trough, Yukon. *In: Yukon Exploration and Geology 2005*, D.S. Emond, G.D. Bradshaw, L.L. Lewis and L.H. Weston (eds.), Yukon Geological Survey, p. 195-205.

ABSTRACT

Most chert-pebble conglomerate units within the Late Jurassic to mid-Cretaceous Tantalus Formation were deposited in shallow, deep and meandering gravel-bed rivers. However, the presence of large-scale angle of repose foresets of large- to small-pebble conglomerate, with distinct down-slope termination in laminated mudrocks, indicates that at least some >5 m foresets were formed by episodic flood-controlled progradation of a small river-dominated lobate delta. Architectural analysis of exposures at the Whitehorse Coal deposit, 26 km south-southwest of Whitehorse, indicates periodic rapid progradation into a small lake that was at least 6 m deep. Thinning and downlap of some foreset units indicate shifting location of topset distributary channels. Down-slope transition of gravel foresets into thin sub-horizontal beds of massive and graded sandstone and pebbly sandstone suggests that the foresets were inertia-dominated. Deformation of bottomset beds is directly related to foreset progradation over under-compacted lacustrine clays.

RÉSUMÉ

La plupart des unités de conglomérat avec cailloux de chert comprises dans la Formation de Tantalus du Jurassique tardif au Crétacé moyen ont été déposées dans les lits de gravier de cours d'eau à méandre peu profonds ou profonds. Cependant, la présence de lits frontaux très inclinés de conglomérats avec gros à petits cailloux et distinctes terminaisons aval dans des argiles laminaires indique qu'au moins certains des lits frontaux de plus de 5 m ont été formés par progradation épisodique déterminée par les crues dans un delta dominé de petits cours d'eau. L'analyse architecturale d'affleurements au gisement de charbon de Whitehorse, situé à 26 km au sud-sud-ouest de Whitehorse, révèle une progradation périodique rapide dans un petit lac dont la profondeur était d'au moins 6 m. L'amincissement et la surface basale de certaines des unités de lits frontaux indiquent un déplacement des défluent ayant déposé les lits sommitaux. Vers l'aval une transition des lits frontaux de gravier vers de minces couches sub-horizontales de grès massif et granoclassé et de grès caillouteux indique que l'inertie dominait les lits frontaux. La déformation des lits de fond est directement reliée à la progradation des lits frontaux sur des argiles lacustres sous-compactées.

¹Sudbury, Ontario, Canada P3E 2C6, dlong@laurentian.ca

²Box 2703 (K10), Whitehorse, Yukon, Canada Y1A 2C6, grant.lowey@gov.yk.ca

INTRODUCTION

The stratigraphy and sedimentology of the Tantalus Formation is being examined as part of a larger program to evaluate the hydrocarbon potential of the Whitehorse Trough (Long, 2005; Lowey, 2004, 2005; Lowey and Long, this volume). Sections were measured and samples collected in 2005 and 2006 for petrographic and geochemical analysis to determine the stratigraphic framework, geotectonic significance, sedimentology, age and provenance of the formation.

This paper deals specifically with exposures of the Tantalus Formation at the Whitehorse Coal deposit (McConnell, 1901; Cairnes, 1908; Cockfield and Bell, 1926, 1944; Fyles, 1950; Wheeler, 1961; Hart and Pelletier, 1989; Bremner, 1988; Hart and Radloff, 1990; Hunt, 1994; Hunt and Hart, 1994; Hart, 1997; Cameron and Beaton, 2000), located on the southern flank of Mount Granger, 26 km south-southwest of the city of Whitehorse (Fig. 1). Goodarzi and Jerzykiewicz (1989) indicate that the coals within this deposit have been subject to both regional and contact metamorphism. They recorded reflectance values

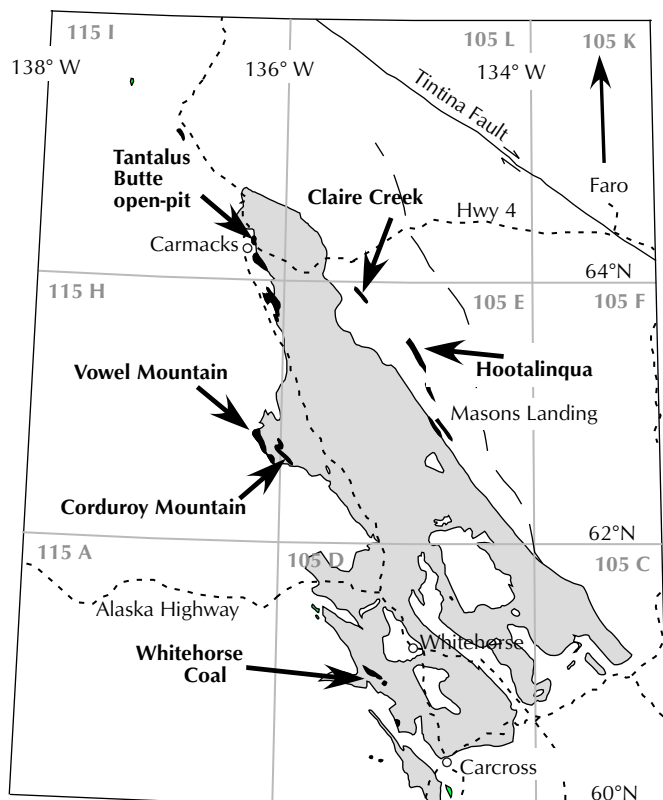


Figure 1. Distribution of the Late Jurassic to mid-Cretaceous Tantalus Formation (black) within the Whitehorse Trough. Strata of the underlying Lewes River and Laberge groups are shown in grey.



Figure 2. Peperite (white and grey flecks, top right) and natural coke (black) produced by intrusion of a felsic porphyry dyke (left and lower right) into water-saturated medium- to low-volatile bituminous coal, Mount Granger, Whitehorse. Age of the dyke is not known.

of up to 3.81 in samples adjacent to felsic dykes, and suggested that this indicates that a medium- to low-volatile bituminous coal had been coked at a temperature of around 600°C. Later studies by Beaton *et al.* (1992), Hunt and Hart (1994), and Cameron and Beaton (2000), found that the coal is typically anthracite, or meta-anthracite, with maximum vitrinite reflectance of 1.65 to 5.62. Intrusion of felsic dykes into exposures at Mount Granger led to the local development of natural coke and peperite, with fluidized magma invading the coal (Fig. 2).

SEDIMENTOLOGY OF THE TANTALUS FORMATION

The Tantalus Formation represents the youngest unit within the Whitehorse Trough (Tempelman-Kluit 1984; Hart, 1997; Lowey, 2004). It is dominated by chert-pebble conglomerate, with minor sandstone, mudstone and coal. Past investigations demonstrate that most of the conglomerates were deposited in shallow (<3 m) and deep (>3 m) gravel-bed braided rivers, with some thicker composite sets representing deposits of meandering gravel-bed rivers (Long, 1986, 2005; Lowey, 1984).

Deep (>3 m) gravel-bed river deposits have been identified at Hootalinqua and Corduroy Mountain (Fig. 1),

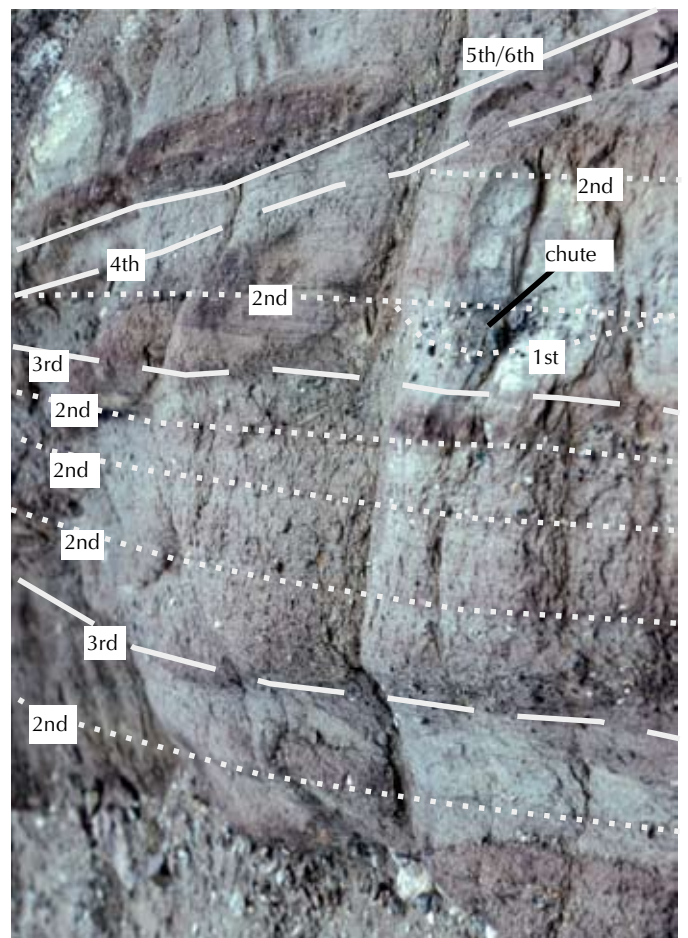


Figure 3. Thickness of gravel foresets (formed as DA elements) provides minimum depth estimates of 3 m for some rivers at Tantalus Butte (left; staff is 1.5 m long) and >4 m for rivers at Hootalinqua (right).

where channels may have been several kilometres wide (Long, 2005). In many cases, the minimum depth of these rivers can be estimated from the maximum size of planar cross-stratification formed by avalanching at the downstream end of compound braid bars (DA element of Miall, 1985). As bar tops are typically eroded by later fluvial action, the preserved thickness of these downstream accretionary elements underestimates true maximum flow depth (Fig. 3).

Twelve-metre-thick lateral accretion (LA) sets in exposures at Claire Creek indicate deposition in meandering gravel-bed rivers (Fig. 3; Long 1986, 2005). The composite nature of lateral accretion sets is confirmed by the presence of isolated packages of cross-stratified sandstone and lenticular gravel units in which paleoflow indicators are at a high angle to the slope of the set boundaries (Fig. 4).

Figure 4. Composite gravel and gravelly sandstone units forming lateral accretion (LA) elements in a large-scale gravel-dominated point-bar in the Tantalus Formation at Claire Creek. Note limited preservation of overbank elements and preservation of isolated lenses of gravel oriented at right angles to the slope of the bar-form (chute deposits).



Fine-grained, massive to weakly laminated mudstones, and organic-rich mudstones with abundant slickensides were deposited in overbank and floodplain settings. The high ash content of many of the associated coals (16-76%: Cameron and Beaton, 2000) suggests that these were also deposited in a floodplain, or floodplain swamp environment, subject to frequent clay input during floods. Thin, stacked sandstone sheets in this setting represent both levee and splay deposits (Fig. 5a,b). Channel-fill sandstone units are rare, and represent deposits of small high-constructive anastomosed and single-channel

streams. Composite macroforms, with inclined sheets of mudstone and sandstone, exposed in the lower part of the test-pit at the Whitehorse Coal site, were deposited in mixed, sandy-muddy, meandering streams (Fig. 5c).

Given the preponderance of fluvial deposits within the formation, it is tempting to interpret all large-scale gravel foresets as either accretionary sets, formed at the downstream end of longitudinal braid bars (DA elements of Miall, 1985), or if gently inclined, lateral accretion elements from the margins of braid bars, side-bars or

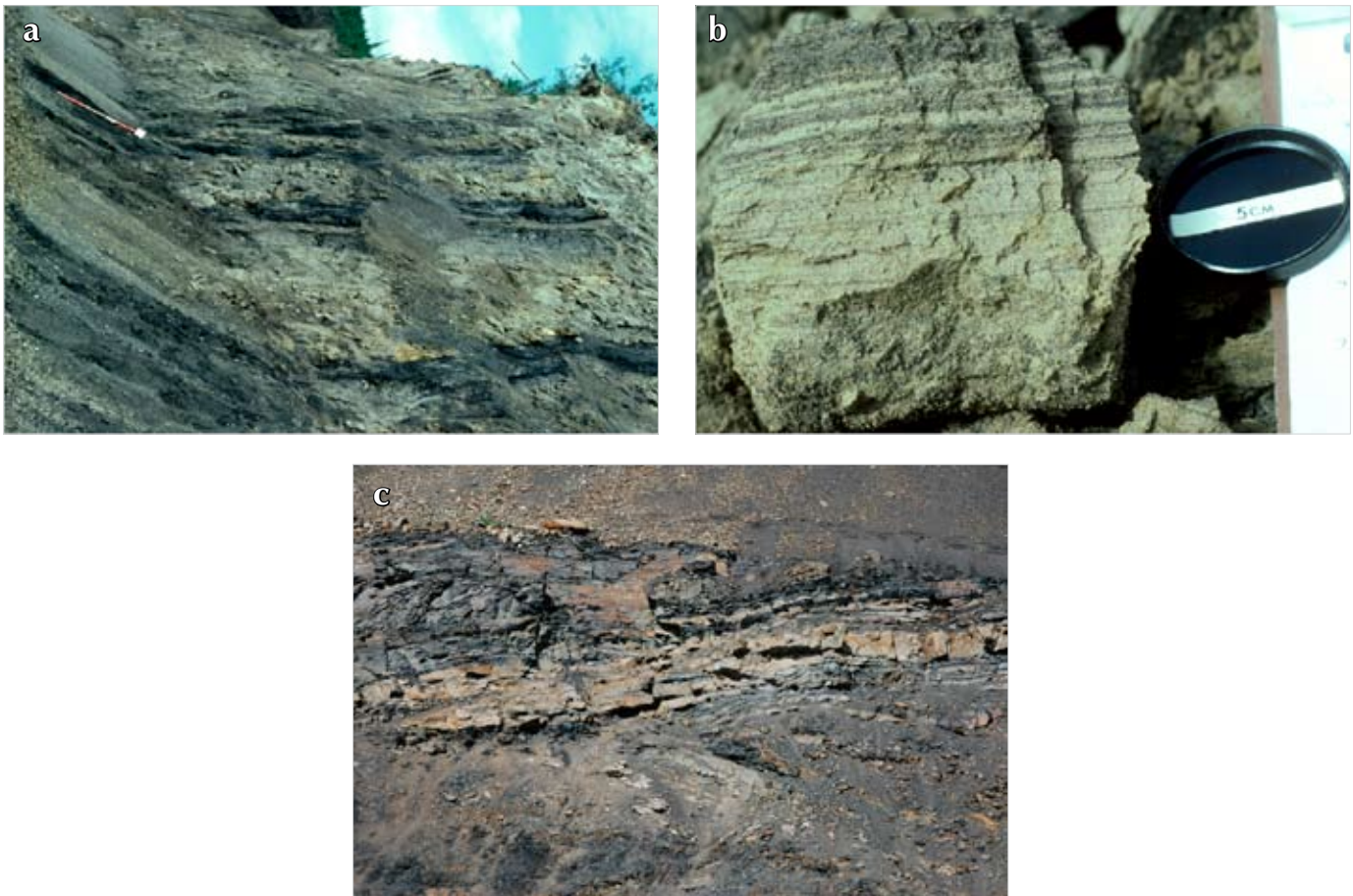


Figure 5. (a) Overbank levee (dark) and splay (light) deposits in the Tantalus Formation at Tantalus Butte open pit, Carmacks. Staff is 1.5 m long. (b) Detail of splay deposit in the Tantalus Formation at the Tantalus Butte open pit. Note abundance of reworked organic detritus in the upper part of the sample. These 'coffee-grounds' reflect reworking of woody organic debris from levee deposits during flood events in both meandering and high-constructive fluvial systems. (c) Exposure of a fine-grained meandering stream channel deposit (inclined strata in lower part of photograph) in the test-pit at Whitehorse Coal, near Mount Granger. LA surfaces consist of alternating flat- and ripple-laminated sandstone, and silty, organic-rich mudstone. Prominent semi-continuous sandstone units (with mudstone partings) above the channel represent splay deposits; massive to weakly bedded organic-rich mudstones (with abundant slickensides) above and below the sandstone units represent overbank floodplain deposits. Main coal seam at this location is immediately below this photograph. Width of photograph is about 10 m.

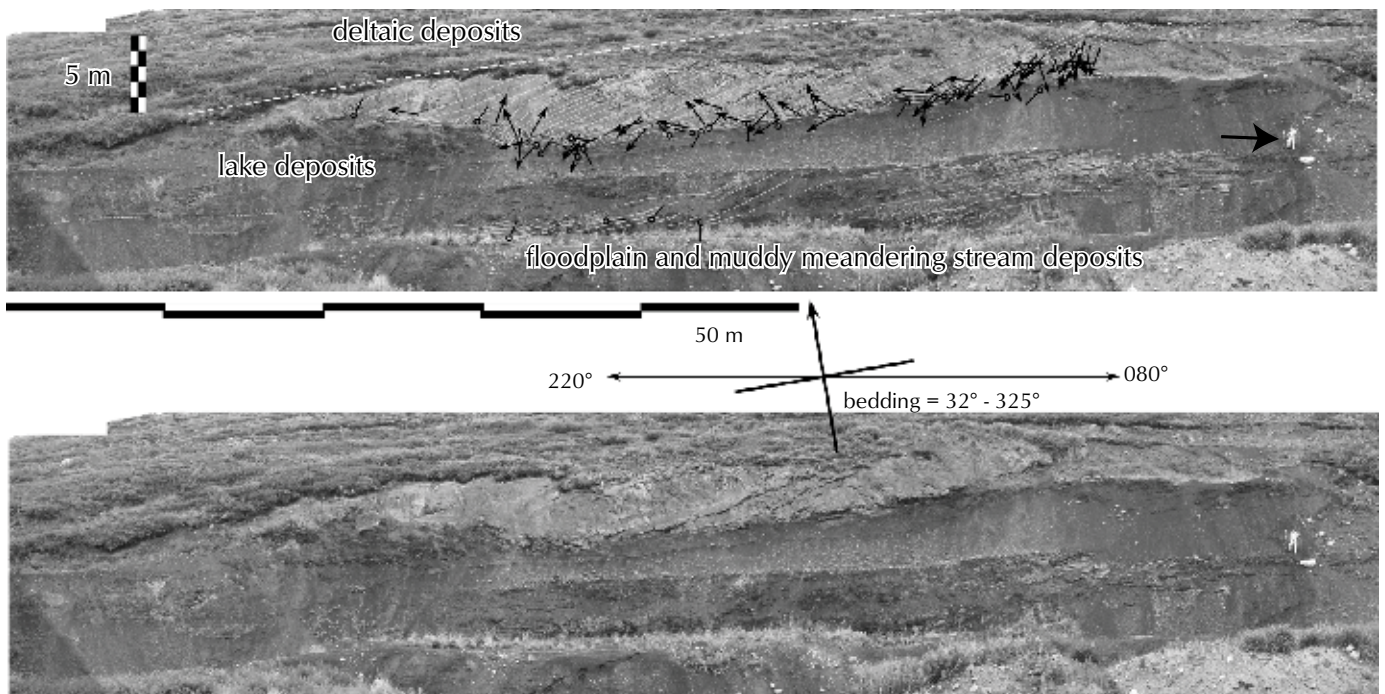


Figure 6. Large-scale gravel foresets exposed in the test pit at the Whitehorse Coal site near Mount Granger. Upper diagram shows main surfaces bounding depositional elements. Person on right for scale.

meander-bends (LA elements). This would be a mistake as large-scale foresets exposed at the Whitehorse Coal deposit, behind Mount Granger, were formed as foresets of a Gilbert-type delta which prograded into a small fresh-water lake.

Architectural analysis of the exposure in the coal pit (Fig. 6) indicates that the delta was lobate, with minor shifts in the distributary mouth position, indicated by downlap of some foreset laminae. In this diagram, primary orientation data has been corrected for structural dip of the outcrop, and presented so that arrows (foresets) and pins (bed surfaces) pointing away from the observer are up, and those pointing down indicate slopes (flow) towards the observer (cf. Long et al., 2000).

The average inclination of 52 (dip-corrected) foreset elements is 27° (Fig. 7a), with dip decreasing slightly from crest to toe. Mean paleoflow direction was to the southwest (Fig. 7b). Foreset elements are typically 20 to 170 cm thick (average 70 cm), and tend to thin and fine slightly down-dip. Amalgamated foreset packages are 1 to 1.7 m thick. Within these packages, sub-elements typically consist of clast-supported medium-pebble conglomerate (granule to large pebble), with lesser amounts of large

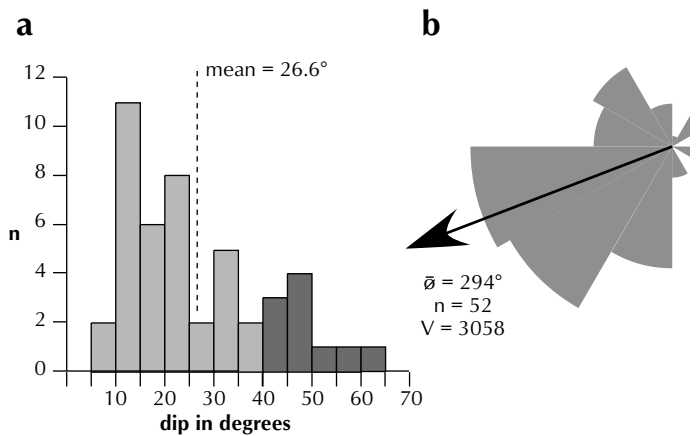


Figure 7. (a) Histogram of foreset dips. Values over 40° exceed the angle of repose for medium gravel. (b) Rose diagram of foreset dip directions. $\bar{\theta}$ = vector mean; n = number of observations; V = variance.

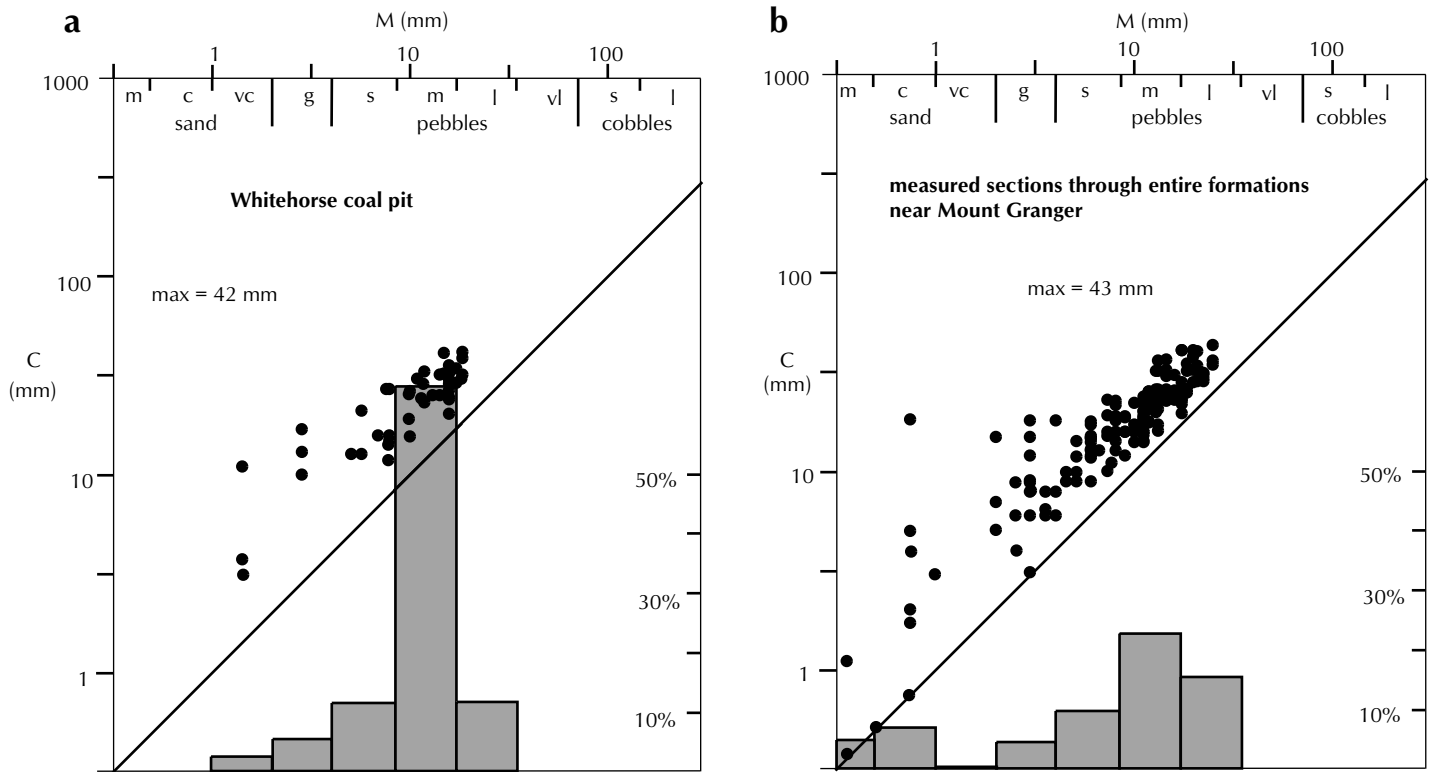


Figure 8. Comparison of maximum (C) and medium (M) grain-size in delta foreset units in (a) the Whitehorse Coal pit and (b) in measured sections in the same area, indicating strong overlap of populations. Histograms show volumetric percentages of conglomerate grades recorded in each of these sections. Sandstone component of the deltaic section may be underestimated.

pebble, small pebble and granule conglomerate (Fig. 8a). The size distribution is remarkably similar to the values obtained from measured sections through the whole formation near Mount Granger (Fig. 8b) suggesting that these are genetically linked. Maximum grain size in both data sets is 42 to 43 mm (large pebble grade).

Lower ends of foresets either terminate abruptly against bottomset mudstones (Fig. 9a,b), or prograde a few decimetres to metres into pro-delta mudstones (Fig. 9c,d,e) with rounded or snub-nosed terminations (Fig. 9f). Soles of some units have distinct grooves (Fig. 9d). Some of the grainflow units show evidence of gravitational sinking into underlying bottomset muds, and are in places deformed by overlying foreset gravels (Fig. 10).

INTERPRETATION

Large-scale gravel foresets exposed in the Whitehorse Coal pit are best interpreted as deposits of a classic steep-sloped Gilbert-type delta, which prograded into a shallow fresh-water lake in an intermontane basin setting. The similarity of grain-size distributions in the foresets and associated fluvial strata (Fig. 8) indicates that the deposit reflects progradation of a large-scale fluvial system into a small lake, and is not a local high-gradient fan-delta with a point-sourced fluvial system. The delta appears to more closely resemble the deeper water, inertia-dominated, type B model of Postma (1990), with shifting or multiple distributaries. Gravel-dominated Gilbert-type deltas typically have foreset slopes over 20° (Gilbert, 1885, 1890; Postma *et al.*, 1988; Sohn *et al.*, 1997). The dip of foresets in sand-dominated Gilbert-type deltas may be as high as 24 to 27°, and in gravel-dominated systems can be 30-35° (Nemec, 1990). The average 27° dip recorded in this study (Fig. 7) falls between these two extremes. A



Figure 9. (a) Central part of exposure showing grouped (0.7-1.7 m thick) packages of gravel foresets, separated by sandy layers (third-order surfaces), that probably mark individual flood seasons (width of view = 8.5 m). (b) Detail of foreset toes, showing three packages related to seasonal flood events. (c) Detail of sand beds at base of foresets that are tangential to underlying bottomsets. This indicates these units were deposited from grainflows, initiated by oversteepening of upper foreset slopes by grain-fall processes. (d) Linear grooves (sole marks) at base of large pebble grainflow on foreset bed (width of view = 80 cm). (e) Snub-nosed bed of medium pebble conglomerate emplaced at toe of foreset, overlain by massive sandstones of similar grainflow origin. (f) Isolated large pebble in sparsely pebbly sandstone of grainflow origin.



Figure 10. (a) Load cast and tool marks at base of sandstone grainflow. (b) Multiple sandstone grainflow units interbedded with bottomset mudstones and deformed beneath a gravel lobe at the base of a later grainflow unit. (c) Large-scale deformation of bottomset beds beneath prograding gravel foresets. (d) Graded granular sandstone unit interbedded with bottomset mudstones, showing load and flame structures.

total of 21% of the dips recorded are greater than 40°, which is close to or above the static angle of repose for gravel in water, and so the slopes may have been over-steepened by later gravitational processes.

In coarse-grained Gilbert-type deltas, the character of foresets is directly influenced by flow inertia, and the relative density of the sediment-laden river water compared with lake water (Orton and Reading, 1993). In friction-dominated distributaries of gravel-bed systems, where the river-water density is similar (homopycnal) to that of the lake water, the flow will expand and coarse material will accumulate rapidly from turbulent suspension immediately below the brink-point by grain-fall processes (Kleinbans, 2005). If the river water is buoyant (hypopycnal), coarser material is expected to fall out close to the brink-point, with progressively finer material

accumulating further from the distributary mouth. This would produce low-gradient foresets, with tangential lower contacts and a marked coarsening-upwards tendency, not seen in these deposits. Tangential lower contacts would also be expected if river waters were denser than lake waters (hyperpycnal flows). In this case cold-water underflows or sediment-laden flash-flood waters would flow down the foreset slope as dilute-sediment gravity flows, to produce abundant normally and/or inverse-graded units (Postma and Roep 1985; Nemec, 1990; Postma, 2001).

In friction-dominated homopycnal systems, inertial forces may propel individual pebbles over the brink-point, so that they roll down the foreset under the influence of gravity. Collision with other grains during down-slope transport can transfer kinetic energy and trigger

avalanching of other grains. In most cases, rapid sedimentation by grain-fall processes on the upper part of the foreset will cause this to rapidly become over-steepened, fail and cause a grainflow (Kleinhans, 2005). Kinetic sieving, where coarser material overrides finer material during grainflow, should result in inverse coarse-tail grading. This is not readily apparent in foresets in the Whitehorse Coal pit. This may be due to the uniformity of gravel populations delivered to the delta front, and a general deficiency of sand-sized material in the rivers that form the Tantalus Formation. Alternatively, the absence of marked inverse coarse-tail grading in the foresets may be related to the scale of individual grainflow events. Kleinhans (2005) found that in flume experiments small-scale grainflows initiated on the upper part of foreset slopes exhibit inverse coarse-tail grading, but did not travel to the toe of the slope. He found that, in thicker flows, friction at the base of the larger grainflow dragged the top of the underlying deposit down-slope, and flows continued to the base of the slope. For small-sized (sand and granule) material, this could lead to concentration of coarser material at the base of the slope.

Post-depositional slope failure does not appear to be an important process on the delta deposit studied. In deep-water Gilbert-type deltas, load-induced slope failure can cause remobilization of foreset material in the form of sediment gravity flows (Postma 1990; Nemec, 1990; Orton and Reading, 1993; Postma and Roep 1985; Sohn *et al.*, 1997). This should produce tangential toe-set beds, with graded and ungraded turbidite and debris-flow-like beds prograding over bottomset beds. Most foreset beds in the Whitehorse Coal pit exposures come to an abrupt stop at the base of the slope, or prograde only a short distance over bottomset beds, consistent with deposition as grainflows (Fig. 9, 10). Only one graded, granular sandstone unit of possible low-density turbidite origin was observed (Fig. 10d). Down-slope sediment failure should also produce slump-scars and syn-sedimentary faults on, and in the upper parts, of foresets (Nemec, 1990). These are not present in the deposits studied.

Deformation of bottomset mudstones beneath gravel foresets was caused by sediment loading (Fig. 10a,d), and not by shallow rotational sliding of delta front sediments, as suggested by Postma *et al.* (1988). Minor mudstone laminae on foresets are too discontinuous to represent significant permeability barriers.

Sand- and granule-dominated foresets tend to be isolated from gravel foresets and may indicate minor floods, or falling-stage flood conditions near third-order surfaces

(Fig. 9a,b). The 0.7-1.7-m thick sinusoidal packages between third-order surfaces probably represent individual flood events or amalgamated products of seasonal floods (Mastalerz, 1990). This might indicate that strata exposed in the pit (Fig. 6) accumulated over at least 20 to 25 years. The presence of downlapping packages of laminae within these foreset elements suggest that the position of distributary channels shifted from time to time.

CONCLUSIONS

The presence of large-scale, steeply dipping foresets, above and grading laterally into mudrocks in the Tantalus Formation at the Whitehorse Coal site are best interpreted as a product of shoal-water Gilbert-type deltas that were fed by a fluvial distributary system with closely spaced, highly mobile bed-load channels feeding the delta as a line source (Type B – deeper water Gilbert-type model of Postma, 1990). Progradation of the delta-front took place over a number of flood seasons, each of which produced downlapping packages of foreset strata, and are capped by finer material near the delta toe. There is no evidence for flash-flood induced progradation, such as marked inverse grading of foresets (Postma *et al.*, 1988; Postma, 2001); hence distributary channels were probably characterized by flood events with moderate discharge (Postma, 2001).

ACKNOWLEDGEMENTS

We thank the Yukon Geological Survey, Indian and Northern Affairs Canada, Northern Science Training Program and the NSERC Discovery Grants program for funding parts of this study. Jeremie Caza and Julie Fillmore provided able assistance in the field in 2004 and 2005. We thank Steve Piercey of Laurentian University for critically reviewing an earlier version of this paper.

REFERENCES

- Beaton, A.P., Cameron, A.R. and Goodarzi, F., 1992. Characterization of Yukon coals. Proceedings of the Canadian Coal and Coalbed Methane Geoscience Forum, British Columbia Geological Survey Branch, Alberta Geological Survey, Geological Survey of Canada, p. 245-264.
- Bremner, T., 1988. Geology of the Whitehorse Coal Deposit. *In: Yukon Geology Volume 2*, G. Abbott (ed.), Exploration and Geological Services Division, Yukon Region, Indian and Northern Affairs Canada, p. 1-7.
- Cairnes, D.D., 1908. Report on a portion of the Conrad and Whitehorse Mining District, Yukon, Canada. Department of Mines, Geological Survey Branch, Publication 982, 38 p.
- Cameron, A.R. and Beaton, A.P., 2000. Coal resources of Northern Canada with emphasis on Whitehorse Trough, Bonnet Plume Basin and Brackett Basin. *International Journal of Coal Geology*, vol. 43, no. 1-4, p. 187-210.
- Cockfield, W.E. and Bell, A.H., 1926. Whitehorse District, Yukon. Geological Survey of Canada, Memoir 150, 63 p.
- Cockfield, W.E. and Bell, A.H., 1944. Whitehorse District, Yukon. Geological Survey of Canada, Paper 44-14, 22 p.
- Fyles, J.G., 1950. Geology of the northwest quarter of Whitehorse map-area, Yukon and studies of weathered granitic rocks near Whitehorse. Unpublished M.Sc. thesis, University of British Columbia, Vancouver, BC.
- Gilbert, G.K., 1885. The topographic features of lake shores. *United States Geological Survey, Annual Report*, vol. 5, p. 69-123.
- Gilbert, G.K., 1990. Lake Bonneville. *United States Geological Survey, Monograph 1*, 438 p.
- Goodarzi, F. and Jerzykiewicz, T., 1989. The nature of thermally altered coal from Mount Granger, Whitehorse area, Yukon Territory. *In: Contributions to Canadian Coal Geoscience*, Geological Survey of Canada, Paper 89-8, p. 104-107.
- Hart, C.J.R., 1997. A transect across Northern Stikinia: geology of the northern Whitehorse Map area, southern Yukon Territory (105D/13-16). Exploration and Geological Services Division, Yukon Region, Indian and Northern Affairs Canada, Bulletin 8, 112 p.
- Hart, C.J.R. and Pelletier, K.S., 1989. Geology of the Whitehorse (105D/11) map area. Exploration and Geological Services Division, Yukon Region, Indian and Northern Affairs Canada, Open File 1989-2, 1:50 000 scale.
- Hart, C.J.R. and Radloff, J.K., 1990. Geology of the Whitehorse, Alligator Lake, Fenwick Creek, Carcross and part of Robinson map areas (105D/11,6,3,2 and 7). Exploration and Geological Services Division, Yukon Region, Indian and Northern Affairs, Open File 1990-4, 113 p.
- Hunt, J.A., 1994. Yukon coal inventory 1994. Report prepared for Energy and Minerals Branch, Economic Development, Yukon Territorial Government, 169 p.
- Hunt, J.A. and Hart, C.J., 1994. Thermal maturation and hydrocarbon source rock potential of Tantalus Formation coals in the Whitehorse area, Yukon Territory. *In: Yukon Exploration and Geology 1993*, Exploration and Geological Services Division, Yukon Region, Indian and Northern Affairs Canada, p. 67-77.
- Kleinhans, M.G., 2005. Grain-size sorting in grainflows at the lee side of deltas. *Sedimentology*, vol. 52, p. 291-311.
- Long, D.G.F., 1986. Coal in Yukon. *In: Mineral deposits of the northern Cordillera*, J.A. Morin (ed.), Canadian Institute of Mining and Metallurgy, Special Volume 37, p. 311-318.
- Long, D.G.F., 2005. Sedimentology and hydrocarbon potential of fluvial strata in the Tantalus and Aksala formations, northern Whitehorse Trough, Yukon. *In: Yukon Exploration and Geology 2004*, D.S. Emond, L.L. Lewis and G.D. Bradshaw (eds.), p. 165-174.
- Long, D.G.F., Lowey, G. and Sweet, A.R., 2000. Age and setting of dinosaur track-ways, Ross River, Yukon Territory (NTS 105F/15). *In: Yukon Exploration and Geology 2000*, D.S. Emond and L.H. Weston (eds.), Exploration and Geological Services Division, Yukon Region, Indian and Northern Affairs Canada, p. 181-198.
- Lowey, G.W., 1984. The stratigraphy and sedimentology of siliciclastic rocks, west-central Yukon, and their tectonic implications. Unpublished PhD thesis, University of Calgary, Calgary, Alberta, 602 p.

- Lowey, G.W., 2004. Preliminary lithostratigraphy of the Laberge Group (Jurassic), south-central Yukon: implications concerning the petroleum potential of the Whitehorse Trough. *In: Yukon Exploration and Geology 2003*, D.S. Emond and L.L. Lewis (eds.), Yukon Geological Survey, p. 129-142.
- Lowey, G.W., 2005. Sedimentology, stratigraphy and source rock potential of the Richthofen formation (Jurassic), northern Whitehorse Trough, Yukon. *In: Yukon Exploration and Geology 2004*, D.S. Emond, L.L. Lewis and G.D. Bradshaw (eds.), Yukon Geological Survey, p. 177-191.
- Mastalerz, K., 1990. Diurnally and seasonally controlled sedimentation on a glaciolacustrine foreset slope: an example from the Pleistocene of eastern Poland. *In: Coarse-grained Deltas*, A. Colella and D.B. Prior (eds.), International Association of Sedimentologists, Special Publication 10, p. 297-309.
- McConnell, R.G., 1901. Exploration of the Stewart River from its mouth to Fraser Falls, the Yukon between Stewart and Cliff Creek, and the Whitehorse Copper Deposits, Yukon. Geological Survey of Canada, Summary Report 1900.
- Miall, A.D., 1985. Architectural-element analysis: a new method of facies analysis applied to fluvial deposits. *Earth Science Reviews*, vol. 22, p. 261-308.
- Nemec, W., 1990. Aspects of sediment movement on steeper delta slopes. *In: Coarse-grained Deltas*, A. Colella and D.B. Prior (eds.), International Association of Sedimentologists, Special Publication 10, p. 29-73.
- Orton, G.J. and Reading, H.G., 1993. Variability of deltaic processes in terms of sediment supply, with particular emphasis on grain size. *Sedimentology*, vol. 40, p. 475-512.
- Postma, G., 1990. Depositional architecture and facies of river and fan deltas: a synthesis. *In: Coarse-grained Deltas*, A. Colella and D.B. Prior (eds.), International Association of Sedimentologists, Special Publication 10, p. 13-27.
- Postma, G., 2001. Physical climate signatures in shallow- and deep-water deltas. *Global and Planetary Change*, vol. 28, p. 93-106.
- Postma, G., Babic, L., Zupanic, J. and Røe, S.L., 1988. Delta-front failure and associated bottomset deformation in a marine, gravelly Gilbert-type fan delta. *In: Fan Deltas: sedimentology and tectonic settings*, W. Nemec and R.J. Steel (eds.), Blackie, Glasgow and London, UK., p. 91-102.
- Postma, G. and Roep, T.B., 1985. Resedimented conglomerates in the bottomsets of Gilbert-type gravel deltas. *Journal of Sedimentary Petrology*, vol. 55, p. 874-885.
- Sohn, Y.K., Kim, S.B., Hwang, I.G., Bahk, J.J., Choe, M.Y. and Chough, S.K., 1997. Characteristics and depositional processes of large-scale gravelly Gilbert-type foresets in the Miocene Doumsan fan delta, Pohang basin, SE Korea. *Journal of Sedimentary Research*, vol. 67, p. 130-141.
- Tempelman-Kluit, D.J., 1984. Geology, Laberge (105E) and Carmacks (115I), Yukon Territory. Geological Survey of Canada, Open File 1101, 1:250 000 scale.
- Wheeler, J.O., 1961. Whitehorse map-area, Yukon Territory, 105D. Geological Survey of Canada, Memoir 312, 156 p.

Summary of Rock-Eval data for the Whitehorse Trough, Yukon: Implications concerning the hydrocarbon potential of a frontier basin

Grant W. Lowey¹

Yukon Geological Survey

Darrel Long

Laurentian University

Lowey, G.W. and Long, D., 2006. Summary of Rock-Eval data for the Whitehorse Trough, Yukon: Implications concerning the hydrocarbon potential of a frontier basin. *In: Yukon Exploration and Geology 2005*, D.S. Emond, G.D. Bradshaw, L.L. Lewis and L.H. Weston (eds.), Yukon Geological Survey, p. 207-230.

ABSTRACT

Whitehorse Trough is a frontier basin in south-central Yukon that is thought to contain gas and possibly oil. Over 400 samples from the Whitehorse Trough have been analysed by programmed pyrolysis and combustion, which together with coal rank, vitrinite reflectance, and the colour of microfossils indicate the following: the Povoas formation has no source rock potential; the Aksala formation is a poor source rock, probably gas-prone and postmature; the Richthofen formation is a poor to fair source rock, gas-prone and postmature; the Nordenskiöld formation has no source rock potential; and the Tanglefoot and Tantalus formations are potentially good to very good source rocks, mainly gas-prone with a possibility of oil and mature. The Aksala and Richthofen formations are interpreted as spent source rocks, whereas the Tanglefoot and Tantalus formations are interpreted as potential source rocks and possibly effective source rocks. The most prospective areas for hydrocarbon exploration are Division Mountain, Tantalus Butte and Five Finger Rapids.

RÉSUMÉ

Le bassin de Whitehorse est un bassin de région pionnière dans la partie centrale sud du Yukon qui renfermerait du gaz et peut-être du pétrole. Pour plus de 400 échantillons provenant du bassin de Whitehorse, analysés par pyrolyse et combustion programmées, on a déterminé le classement du charbon, la réflectance de la vitrinite et la couleur des microfossiles; les résultats sont exposés ci-après. La Formation de Povoas ne présente aucun potentiel comme roche mère; la Formation d'Aksala constitue une mauvaise roche mère, probablement favorable à la présence de gaz et post-mature; la formation de Nordenskiöld ne présente aucun potentiel comme roche mère; et les formations de Tanglefoot et de Tantalus pourraient être de bonnes à très bonnes roches mères, principalement favorables à la présence de gaz, renfermant peut-être du pétrole et parvenues à maturité. Les formations d'Aksala et de Richthofen sont interprétées comme étant des roches mères épuisées alors que les formations de Tanglefoot et de Tantalus pourraient constituer des roches mères et peut-être même des roches mères efficaces. Les régions les plus prometteuses pour l'exploration à la recherche d'hydrocarbures sont celles des monts Division et Tantalus ainsi que celle des rapides Five Finger.

¹grant.lowey@gov.yk.ca

INTRODUCTION

Whitehorse Trough is one of eight oil and gas basins in the Yukon (Fig. 1). It occurs in southern Yukon and extends from just north of Carmacks, 650 km southwards, past Whitehorse and the Yukon-British Columbia border, into northern British Columbia. As a 'frontier' basin, interest in the Whitehorse Trough is based on its similarity to other Interior Cordilleran basins, such as the Bowser and Nechako basins in British Columbia, which all have a similar sedimentary history and tectonic evolution, and hence, corresponding oil and gas potential (Teitz and Young, 1982). In addition, there have been rumours of 'fire balls' and oil seeps in the Whitehorse area; Koch (1973) reported dry gas in samples from the Trough; and based on the volume and type of sedimentary rock preserved, it is estimated that the predicted potential mean oil content of the Whitehorse Trough is $\sim 15 \times 10^6 \text{ m}^3$, and the expected mean gas volume is $\sim 136 \times 10^6 \text{ m}^3$ (Osadetz, pers. comm., 2004)². Given that the proposed

²Whitehorse Trough new gas-oil potential. E-mail, Wednesday, November 3, 2004.

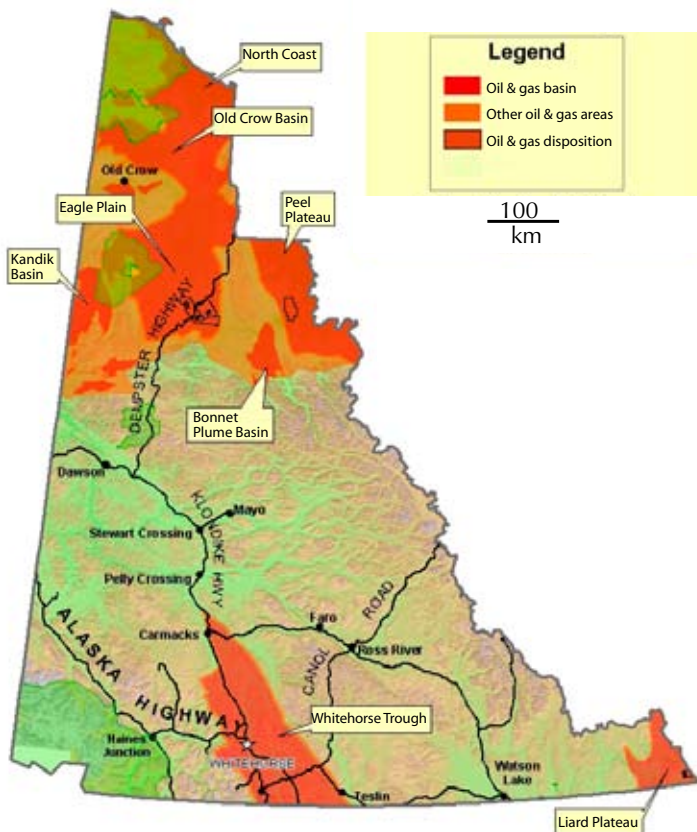


Figure 1. Oil and gas basins in the Yukon showing the location of the Whitehorse Trough (Energy, Mines and Resources).

Alaska Highway pipeline would run through the centre of the Trough, any oil and gas discoveries in the area would have a greater chance of being economically viable.

The National Energy Board (2001) describes the Whitehorse Trough as an 'immature, mainly gas-prone' basin and identified potential source rocks (i.e., Triassic carbonates, Jurassic mudstones and Cretaceous mudstones), reservoirs (i.e., Triassic carbonates, and Jurassic and Cretaceous sandstones), seals (i.e., Jurassic mudstones and volcanoclastic rocks) and traps (i.e., anticlines and pinch-outs). A possible 'oil shale' in Jurassic rocks north of Whitehorse was described by Koch (1973), and Petro-Canada concluded that Jurassic rocks throughout the Whitehorse Trough have the potential to generate gas and possibly oil, whereas Cretaceous rocks have the potential to generate gas (Gilmore, 1985; Gunther, 1985). In addition, Beaton *et al.* (1992a) determined that coal seams from the Whitehorse Trough have a low potential to generate oil and gas, and Allen (2000) suggested that Jurassic rocks northwest of Whitehorse have the potential to generate gas and possibly oil. The purpose of this paper is to present the results of Rock-Eval analysis. This is a temperature-programmed geochemical whole-rock technique used to evaluate the petroleum source rock potential of the Whitehorse Trough strata in Yukon. Results of Rock-Eval analyses are supplemented with coal rank, vitrinite reflectance, conodont alteration index, and spore and pollen thermal alteration index data.

TECTONIC AND STRATIGRAPHIC SETTING

Whitehorse Trough is located in the Intermontane belt of the Canadian Cordillera. It forms part of Stikine Terrane, which is flanked to the west and east by Yukon-Tanana Terrane, and is bordered on the south by Cache Creek Terrane (Wheeler and McFeely, 1991). Whitehorse Trough is thought to have originated in Middle to Late Triassic time, and has been variably interpreted as a back-arc basin (Tempelman-Kluit, 1978; Monger and Price, 1979; Bultman, 1979), a fore-arc basin (Tempelman-Kluit, 1979, 1980; Dickie and Hein, 1995; Johannson *et al.*, 1997), a simple marginal basin (Eisbacher, 1981), or part of a complex of inter-arc basins (Monger *et al.*, 1991) and small ocean basins (Souther, 1991). Lowey and Hills (1988) demonstrated that sandstone compositions from the Whitehorse Trough indicate sedimentation in two discrete basins: sandstones from Triassic and Jurassic rocks reflect

an undissected through to dissected magmatic arc provenance, compatible with a back-arc or fore-arc basin, whereas sandstones from Jura-Cretaceous rocks reflect a lithic and transitional orogenic provenance, compatible with an intra-suture embayment basin.

Wheeler (1961) introduced the term 'Whitehorse Trough' and recognized three stratigraphic units (i.e., the Lewes River and Laberge groups, and the Tantalus Formation). The Lewes River Group (Upper Triassic) was informally subdivided by Tempelman-Kluit (1984) into the lowermost Povoas formation, consisting of basalt, tuff and agglomerate, and interpreted as subaqueous lava flows, and the uppermost Aksala formation, consisting of sandstone, mudstone, conglomerate and limestone, and interpreted as deep-marine, reef, beach and tidal flat deposits (Tempelman-Kluit, 1978, 1980, 1984). The Laberge Group (Lower-Middle Jurassic) was informally subdivided by Tempelman-Kluit (1984) into four units, which from the base upwards, includes the Richthofen (i.e., thin- to medium-bedded turbidites), Conglomerate (i.e., framework-supported conglomerate), Nordenskiöld (i.e., dacite tuff) and Tanglefoot (i.e., coal-bearing sandstone, mudstone and conglomerate) formations. Lowey (2004, 2005) demonstrated that the 'Conglomerate formation' is not a stratigraphic unit and these rocks can be assigned to other formations (i.e., the Richthofen and Tanglefoot formations). The Richthofen, Nordenskiöld and Tanglefoot formations are interpreted as submarine fan, subaqueous pyroclastic and delta deposits, respectively (Cairnes, 1910; Lees, 1934; Bostock and Lees, 1938; Lowey, 2004). The Tantalus Formation (Upper Jurassic-Lower Cretaceous) consists of fluvial and paralic sandstone, mudstone, conglomerate and coal (Long, 1986; Lowey and Hills, 1988).

METHODS

Rock-Eval analysis is a standard screening technique used for evaluating the source rock potential of a sedimentary basin (Lafargue *et al.*, 1998). Rock-Eval 6, the latest version of the apparatus, consists of a computer-controlled, temperature-programmed pyrolysis oven and oxidation oven (Behar *et al.*, 2001; Lafargue *et al.*, 1998). An approximately 70 mg sample of pulverized whole rock is placed in the pyrolysis oven, which has a nitrogen atmosphere and is at a temperature of 300°C; after two minutes the temperature is increased to 650°C at a rate of 25°C/min (Behar *et al.*, 2001; Lafargue *et al.*, 1998; Fowler *et al.*, 2005). A flame ionization detector records the

amount of hydrocarbons distilled from the sample, referred to as 'free hydrocarbons', or 'S1' in mg HC/g rock, and hydrocarbons pyrolysed from the sample, referred to as 'potential hydrocarbons', or 'S2' in mg HC/g rock; whereas an infrared cell records the amount of CO and CO₂ in the sample, referred to as 'S3' and 'S4', respectively (Behar *et al.*, 2001; Lafargue *et al.*, 1998; Fowler *et al.*, 2005). The residual sample is then cooled to 300°C, placed in the oxidation oven, and the temperature is increased to 850°C at a rate of 20°C/min (Behar *et al.*, 2001; Lafargue *et al.*, 1998). A second infrared cell records the amount of additional CO and CO₂ in the sample, which are also referred to as 'S3' and 'S4', respectively (Behar *et al.*, 2001; Lafargue *et al.*, 1998; Fowler *et al.*, 2005). The four 'acquisition parameters' (i.e., S1, S2, S3 and S4) are used to generate several 'calculated parameters', including: T_{max}, the temperature of the maximum production of pyrolysed hydrocarbons; TOC, the percent of total organic carbon (basically a sum of the acquisition parameters); OI, the oxygen index (OI=S3x100/TOC); HI, the hydrogen index (HI=S2x100/TOC); and PI, the production index (PI=S1/(S1+S2)).

Three main factors are considered in determining the potential of a rock for generating oil and gas: 1) quantity, or generative potential, based on TOC, S1 and S2; 2) quality, or type of hydrocarbon generated, based on HI and the S2/S3 ratio; and 3) maturation, or level of thermal alteration of the rock with respect to oil generation, based on PI and T_{max} (Peters, 1986; Peters and Cassa, 1994). Guidelines published by Peters (1986), Peters and Moldowan (1993), and Peters and Cassa (1994) were used for evaluating the source rock potential based on the results of the Rock-Eval analysis (see Table 1). Note that Behar *et al.* (2001), Lafargue *et al.* (1998) and Peters (1986) all advise that results of programmed pyrolysis from outcrop samples be interpreted with caution (i.e., organic matter may have been oxidized, resulting in low S1 and S2 values and high T_{max} values) and supported by other analyses (i.e., vitrinite reflectance). T_{max} is also affected by the type of organic matter and minerals in the matrix of the sample (Peters, 1986). In addition, Peters (1986) cautions that samples with S2 values <0.2 mg HC/g rock are commonly inaccurate and should be rejected, whereas Natural Resources Canada (2004)³ suggests that if TOC ≤0.3%, all parameters have questionable significance; if TOC ≤0.5%, OI has questionable significance; and if S1 and S2 ≤0.2 mg HC/g rock, T_{max}

³www.em.gov.bc.ca/dl/oilgas/cog/geofile200301/doc/html/rockeval.htm

and PI have questionable significance. In addition, Waples (1985) notes that results of Rock-Eval analysis provides information only on the present-day hydrocarbon generative capacity of kerogen in the rock, that is, mature to overmature rocks may have generated hydrocarbons previously.

Previous Rock-Eval analyses for the Yukon portion of the Whitehorse Trough (i.e., 124 samples) were presented by Gilmore (1985), Gunther (1985), Beaton *et al.* (1992a) and Allen (2000). This paper presents the results of 443 samples that were collected from outcrop and drill core of limestone, sandstone-mudstone couplets and mudstone throughout the Whitehorse Trough in Yukon (and includes Rock-Eval results for the Richthofen formation that were previously reported by Lowey, 2005). The analyses were performed on a Rock-Eval 6 'Turbo' apparatus by the Geological Survey of Canada at Calgary, Alberta (Appendix 1).

Table 1. Programmed pyrolysis and oxidation guidelines describing source rock quantity, quality and maturation parameters (Peters and Cassa, 1994).

Quantity	TOC (wt.%)	S ₁ (mg HC/g rock)	S ₂ (mg HC/g rock)	
Poor	0-0.5	0-0.5	0-2.5	
Fair	0.5-1	0.5-1	2.5-5	
Good	1-2	1-2	5-10	
Very good	2-4	2-4	10-20	
Excellent	>4	>4	>20	
Quality	HI (mg HC/g TOC)	S ₂ /S ₃	Kerogen type	
None	<50	<1	IV	
Gas	50-200	1-5	III	
Gas and oil	200-300	5-10	II/III	
Oil	300-600	10-15	II	
Oil	>600	>15	I	
Maturation	R _o (%)	T _{max} (°C)	TAI	
Immature	0.2-0.6	<435	1.5-2.6	
	Early	0.6-0.65	435-445	2.6-2.6
Mature	Peak	0.65-0.9	445-450	2.7-2.9
	Late	0.9-1.35	450-470	2.9-3.3
Postmature	>1.35	>470	>3.3	

RESULTS

Lewes River Group

The Povoas formation consists of volcanic rocks and no samples were analysed by Rock-Eval. The Aksala formation does not contain abundant transported organic material (Long, 2005), but mudstone is present, and the National Energy Board (2001) suggested that a 'fetid limestone' was a possible source rock. Hence, only a few samples were analysed by Rock-Eval, and these results show that both the fetid limestone (i.e., samples GL03-6A, GL04-39A and GL04-97A) and mudstone (i.e., samples GL04-67B and GL04-68A) contain very small amounts of TOC, S₁ and S₂ (Fig. 2), indicating that, in terms of quantity, it is a poor source rock. Due to the low values of these parameters, determining the petroleum quality of the rock is not very accurate; hence, HI should be ignored, although the S₂/S₃ ratio is valid and indicates that only gas would be expected (Fig. 3). The thermal maturation of the samples cannot be determined because of the low values for TOC, S₁ and S₂.

Laberge Group

Koch (1973) and the National Energy Board (2001) suggested that thin-bedded sandstone-mudstone couplets in the Richthofen formation resemble an 'oil shale' and are a potential source rock. However, Rock-Eval analysis of 70 samples shows that this unit contains only small amounts of TOC, S₁ and S₂ (Fig. 4), indicating that in terms of quantity, it is a poor and possibly a fair source rock. In terms of quality, only gas would be expected (Fig. 5). Due to the low values for S₁ and S₂, determining the thermal maturation of the samples is not very accurate, hence PI should be ignored, but two values for T_{max} are valid and these indicate the unit is postmature (Fig. 6).

The Nordenskiöld formation consists mostly of dacite tuff; it is not considered a source rock and no samples were analysed by Rock-Eval.

The Tanglefoot formation was not considered by the National Energy Board (2001) as a potential source rock. However, Rock-Eval analysis of 182 samples shows that this unit contains large amounts of TOC, small amounts of S₁ and moderate amounts of S₂ (Fig. 7), indicating that in terms of quantity, it is a good to very good source rock. In terms of quality, mainly gas would be present, but there is also the possibility of oil (Fig. 8). Also, the thermal maturation of the samples appear to be late immature

according to PI, and early mature according to T_{max} (Fig. 9).

Prospective areas for gas and oil generation are Division Mountain (located approximately half-way between Whitehorse and Carmacks), Tantalus Butte (located at Carmacks) and Five Finger Rapids (located north of Carmacks). At all of the localities, hydrocarbon fluid inclusions were observed in the macerals (V. Stasiuk, per. comm., 2005)⁴.

⁴Vitrinite reflectance data, Whitehorse Trough. E-mail, Wednesday, November 6, 2005.

Tantalus Formation

The National Energy Board (2001) described the Tantalus Formation as a potential source rock. Rock-Eval analysis of 186 samples shows that this unit contains moderate amounts of TOC, small amounts of S1 and moderate amounts of S2 (Fig. 10), indicating that in terms of quantity, it is a good to very good source rock. In terms of quality, mainly gas would be present, but there is also the possibility of oil (Fig. 11). Also, the thermal maturation of the samples appears to be late immature according to PI, and early mature according to T_{max} (Fig. 12). Hydrocarbon fluid inclusions were observed in the macerals at Tantalus Butte (V. Stasiuk, personal communication, 2005), which is the only prospective area for gas and oil generation in the Tantalus Formation.

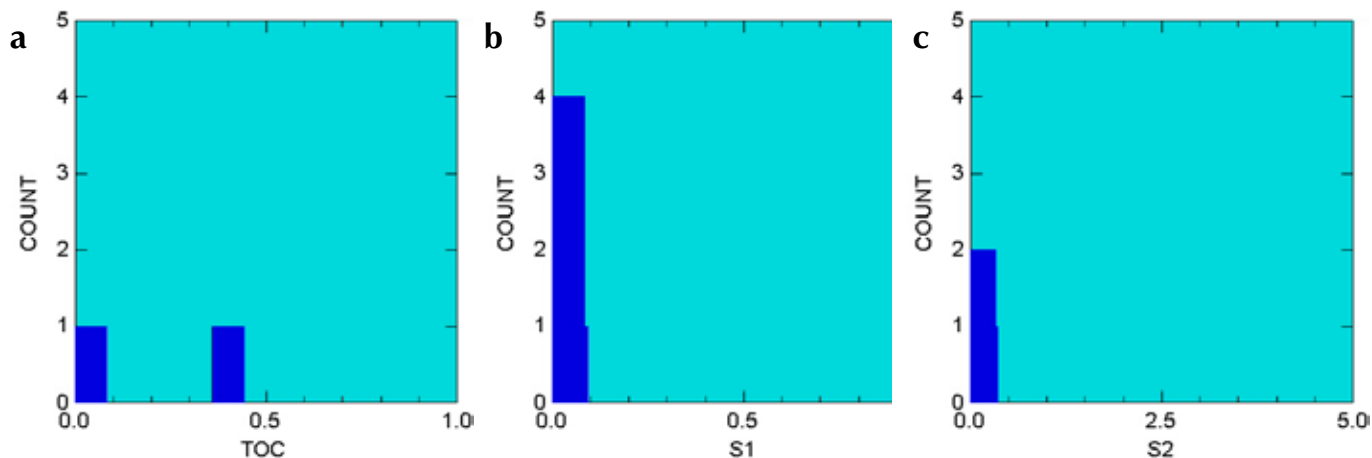


Figure 2. Rock-Eval quantity parameters, Aksala formation.

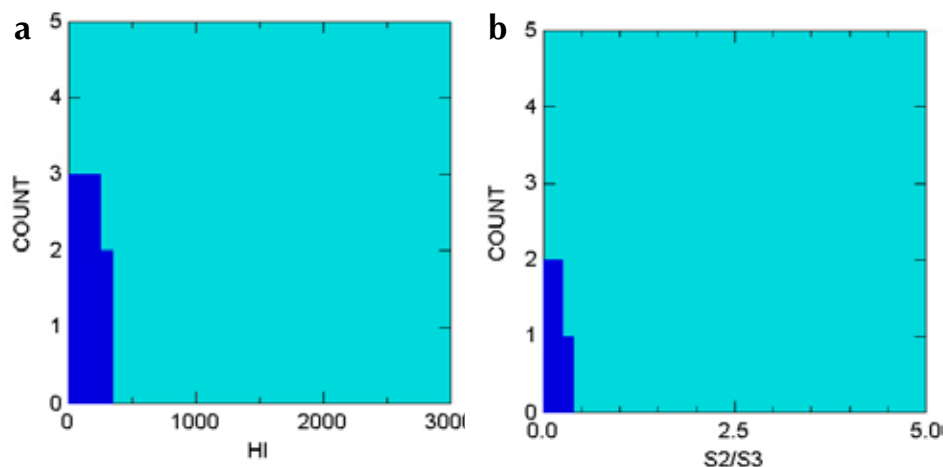


Figure 3. Rock-Eval quality parameters, Aksala formation.

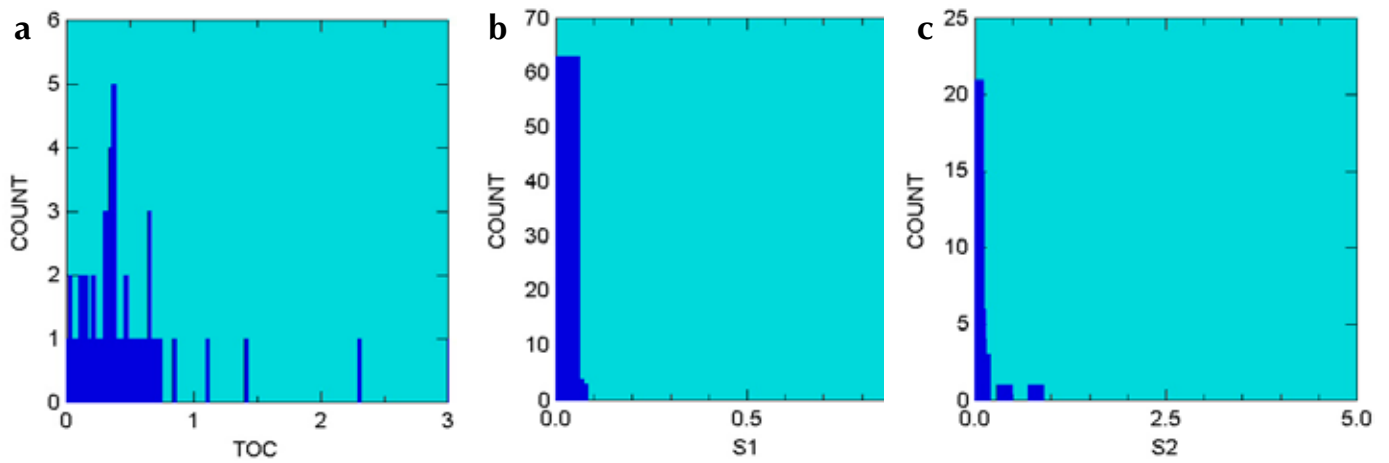


Figure 4. Rock-Eval quantity parameters, Richthofen formation.

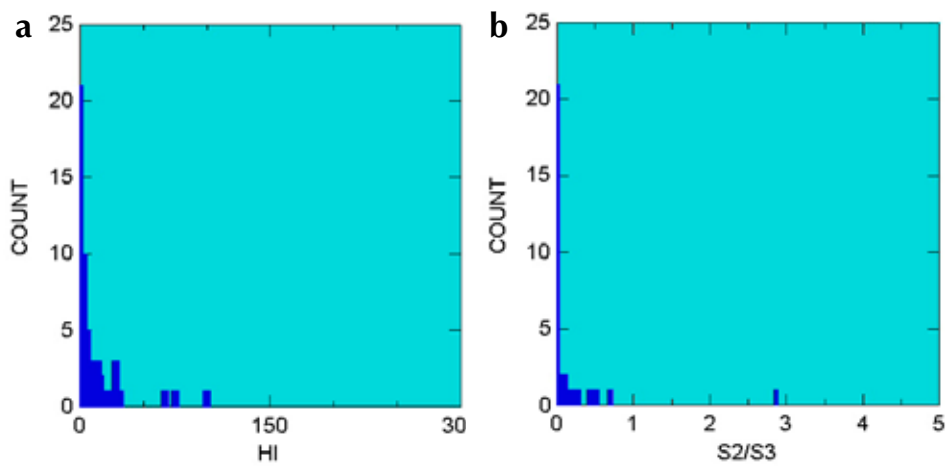


Figure 5. Rock-Eval quality parameters, Richthofen formation.

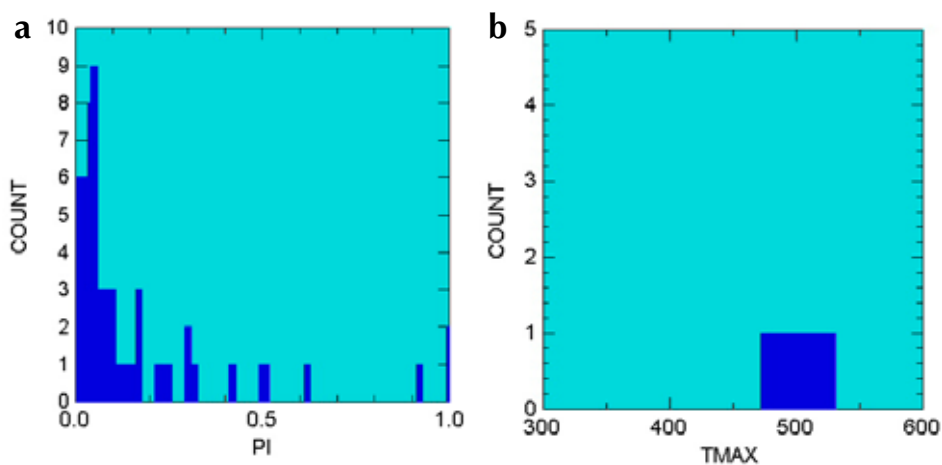


Figure 6. Rock-Eval maturation parameters, Richthofen formation.

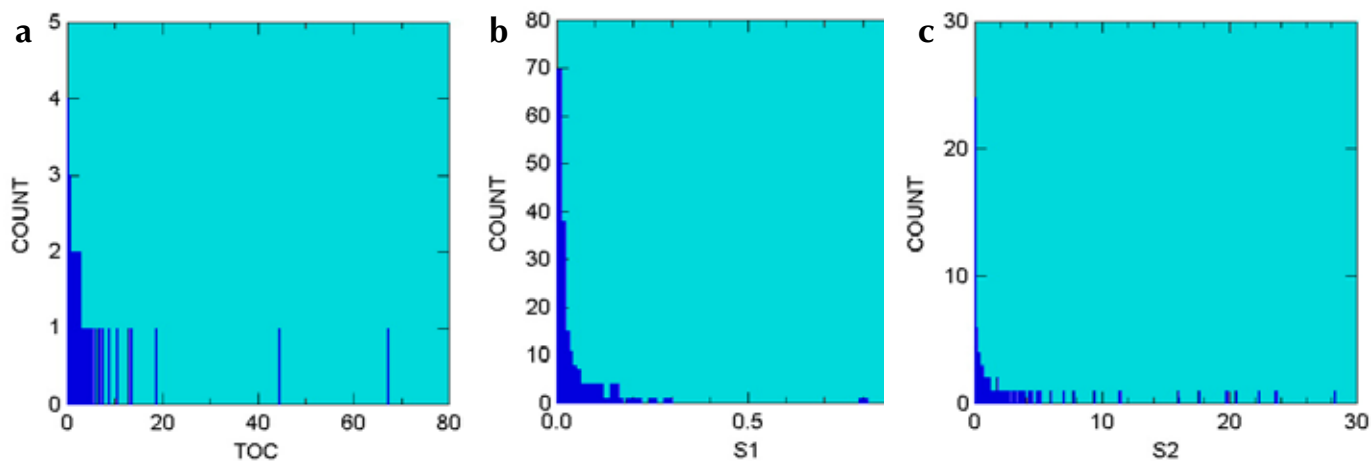


Figure 7. Rock-Eval quantity parameters, Tanglefoot formation.

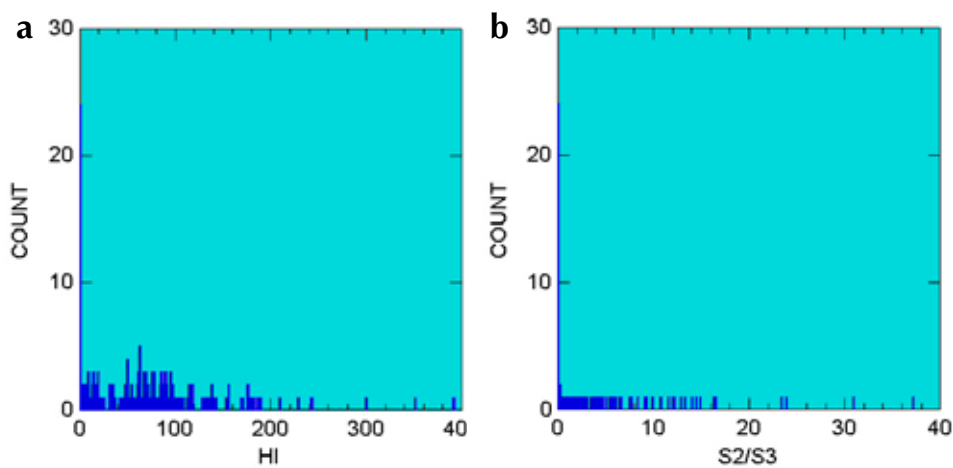


Figure 8. Rock-Eval quality parameters, Tanglefoot formation.

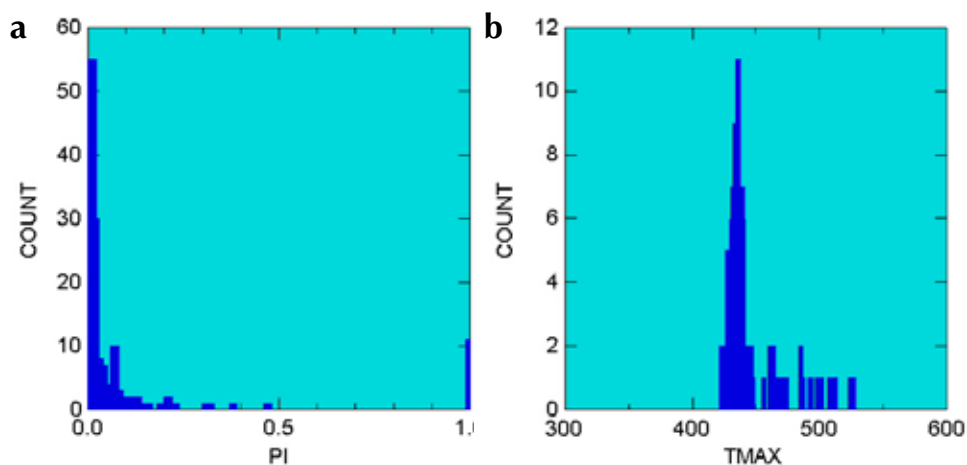


Figure 9. Rock-Eval maturation parameters, Tanglefoot formation.

DISCUSSION AND CONCLUSIONS

The Povoas formation is not considered a source rock based on its lithology. The Aksala formation is a poor source rock and gas-prone. The thermal maturation of the unit could not be determined by Rock-Eval analysis. However, over 40 samples have been analysed for conodonts, and these indicate a conodont alteration index (CAI) of 5 in the Whitehorse area, and 2 to 4 in the Carmacks area (England, 1980; Hart, 1997;

Tempelman-Kluit, 1980). Note that the 'oil window' occurs between a CAI of 1.5 and 2 (Fowler *et al.*, 2005). Also, Tempelman-Kluit (1978) reported that pyrobitumen (i.e., thermally altered solidified bitumen) occurs locally in fractures and cavities in limestone. Hence, the Aksala formation is probably postmature and is interpreted as a 'spent' source rock, implying that it has reached the postmature stage and is incapable of further oil generation, but it still may be able to generate wet and dry gas (Peters and Cassa, 1994).

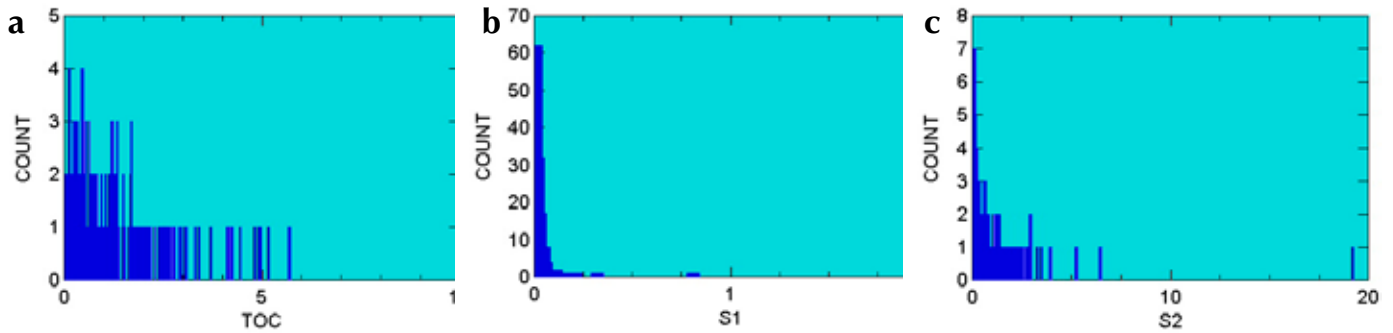


Figure 10. Rock-Eval quantity parameters, Tantalus Formation.

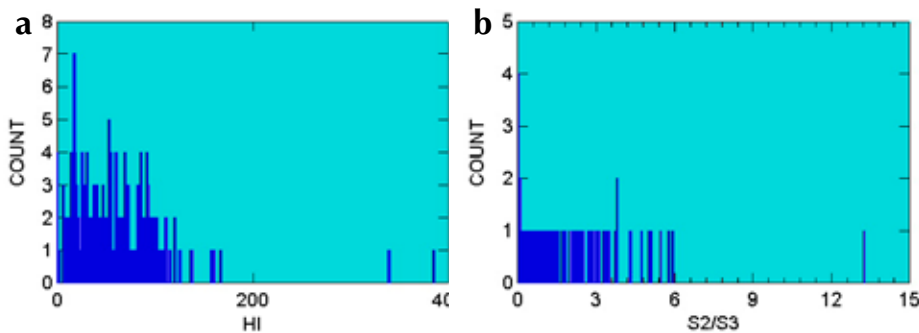


Figure 11. Rock-Eval quality parameters, Tantalus Formation.

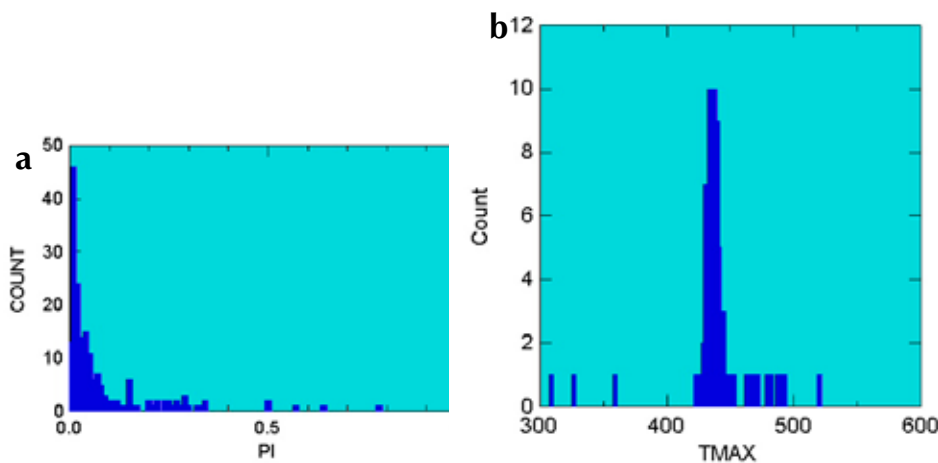


Figure 12. Rock-Eval maturation parameters, Tantalus Formation.

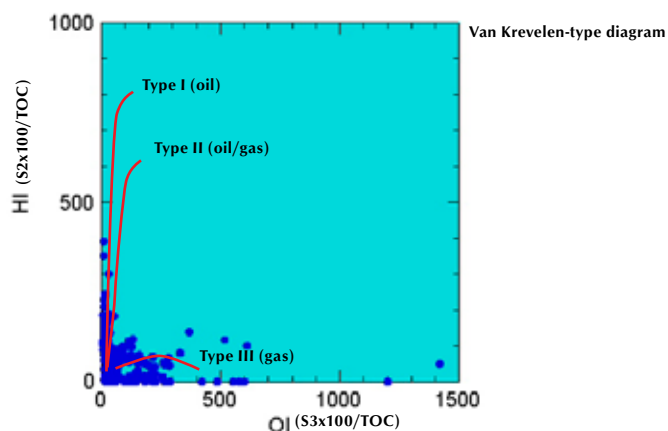


Figure 13. Ol-HI diagram, Tanglefoot Formation.

The Richthofen formation is a poor to fair source rock, gas-prone and postmature. English *et al.* (2005) reached a similar conclusion for the correlative Inklin Formation in the Whitehorse Trough in northern British Columbia. The Nordenskiöld formation is not considered a source rock based on its lithology. The Tanglefoot formation is a good to very good source rock, and mainly gas-prone with a possibility of oil. The possibility of oil generation is supported by the OI-HI Van Krevelen-type diagram (Fig. 13). Although most samples plot along the Type III axis (i.e., gas-prone kerogen from terrestrial plants), several samples have HI values greater than 200 and plot along the Type I and Type II kerogen axes (i.e., lacustrine and marine kerogen, respectively). HI values greater than 200 and Type I and Type II macerals are conducive to oil generation (Peters and Cassa, 1994; Tissot and Welte, 1984). Oil generation is marginally supported by the composition of coal in the Tanglefoot formation. Beaton *et al.* (1992b) determined that the coal contains 13% liptinite (basically amorphous or structureless organic matter). According to Peters and Cassa (1994), 15-20% liptinite is required for coal to generate oil. The Rock-Eval PI indicates that the Tanglefoot formation is late immature, whereas T_{max} indicates it is early mature. Coal rank in the Tanglefoot formation is high-volatile C to B bituminous (Cameron and Beaton, 2000; Beaton *et al.*, 1992b), corresponding to the beginning half of the oil window (Fowler *et al.*, 2005). According to Stack *et al.* (1982), economic accumulations of petroleum occur where the coal is less than or equal to high-volatile bituminous rank. Also, random vitrinite reflectance values for the Tanglefoot formation range from 0.48-0.61% (Cameron and Beaton, 2000; Beaton *et al.*, 1992a,b; Russell, 1978; V. Stasiuk,

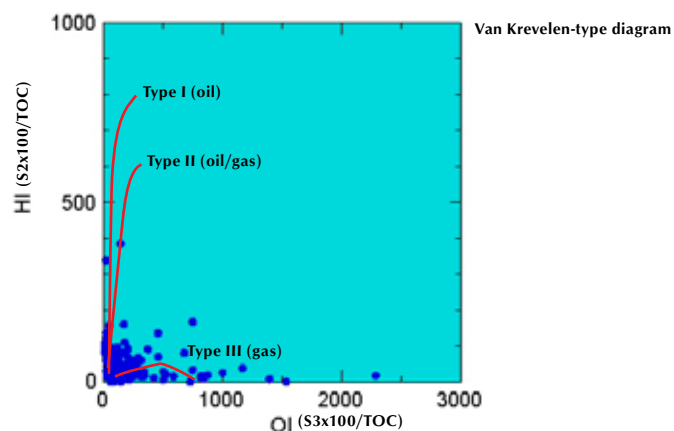


Figure 14. Ol-HI diagram, Tantalus Formation.

personal communication, 2005), averaging ~0.58% (Beaton *et al.*, 1992b), corresponding also to the beginning half of the oil window. In addition, spore and pollen from this unit are brown-black to brown in colour (Sweet, 2004), indicating a thermal alteration index (TAI) of 3 to 4; the oil window occurs between a TAI of ~2-3.5 (Fowler *et al.*, 2005). Hence, the Tanglefoot formation is probably early mature and is interpreted as a 'potential' source rock (i.e., the rock contains adequate quantities of organic matter to generate petroleum; Peters and Cassa, 1994), and possibly an 'effective' source rock (i.e., the rock is, or has, generated and expelled petroleum; Peters and Cassa, 1994). Three potentially petroliferous source-rock pods in the Tanglefoot formation are identified in the northern portion of the Whitehorse Trough at Division Mountain, Tantalus Butte and Five Finger Rapids.

The Tantalus Formation is a good to very good source rock and mainly gas-prone with a possibility of oil.

The possibility of oil generation is supported by the OI-HI Van Krevelen-type diagram (Fig. 14). Although most samples plot along the Type III axis (i.e., gas-prone terrestrial kerogen), several samples have HI values greater than 200 and plot along the Type I and Type II kerogen axes (i.e., oil-prone lacustrine and marine kerogen). However, oil generation is not supported by the composition of coal in the Tantalus Formation: Beaton *et al.* (1992b) determined that the coal contains only 2-7% liptinite. The Rock-Eval PI indicates that the Tantalus Formation is late immature, whereas T_{max} indicates it is early mature. Coal rank in the Tantalus Formation is high-volatile B to A bituminous (Cameron and Beaton, 2000; Beaton *et al.*, 1992a,b; Swartzman, 1948), corresponding

to the middle of the oil window (Fowler *et al.*, 2005). Also, random vitrinite reflectance values for the Tantalus Formation range from 0.61-1.09% (Cameron and Beaton, 2000; Hacquebard, 1972; Russell, 1978; V. Stasiuk, personal communication, 2005), corresponding to the middle of the oil window, although Hunt and Hart (1994) reported values of 1.68-3.45%, but the latter are due to intrusion of rhyolite sills. In addition, spore and pollen from this unit are brown-black to brown (Sweet, 2004), indicating a thermal alteration index (TAI) of 3 to 4. Hence, the Tanglefoot formation is probably early to peak mature, and is interpreted as a potential source rock, and possibly an effective source rock. One potentially petroliferous source rock pod in the Tantalus Formation is identified in the northern portion of the Whitehorse Trough at Tantalus Butte.

ACKNOWLEDGEMENTS

We thank Greg McAllister, Thierry Bruand and Karl Ziehe for their expert helicopter flying and Andrew Cook for his help as a summer fieldwork assistant. The Rock-Eval analyses and comments by Martin Fowler and Vern Stasiuk are gratefully appreciated. Discussions with Steve Piercey, Maurice Colpron and Lee Pigage concerning the Whitehorse Trough were also appreciated.

REFERENCES

- Allen, T., 2000. An evaluation of coal-bearing strata at Division Mountain (115H/8 east-half, 105E/5 west-half), south-central Yukon. *In: Yukon Exploration and Geology 1999*, D.S. Emond and L.H. Weston (eds.), Exploration and Geological Services Division, Yukon Region, Indian and Northern Affairs Canada, p. 177-198.
- Beaton, A.P., Cameron, A.R. and Goodarzi, F., 1992a. Petrography, geochemistry and utilization potential of the Division Mountain coal occurrences, Yukon Territory. *In: Current Research, Part E*, Geological Survey of Canada, Paper 92-1E, p. 23-32.
- Beaton, A.P., Cameron, A.R. and Goodarzi, F., 1992b. Characterization of coals from the Whitehorse Trough, Yukon Territory. *In: The Canadian Coal and Coalbed Methane Geoscience Forum*. B.C. Geological Survey Branch, Alberta Geological Survey and Geological Survey of Canada, Parksville, B.C., February 2-5, 1992.
- Behar, F., Beaumont, V. and Penteadó, H.L. De B., 2001. Rock-Eval 6 technology: performances and developments. *Oil & Gas Science and Technology*, vol. 56, p. 111-134.
- Bostock, H.S. and Lees, E.J., 1938. Laberge map-area, Yukon. Geological Survey of Canada, Memoir 217, 32 p.
- Bultman, T.R., 1979. Geology and tectonic history of the Whitehorse Trough west of Atlin, British Columbia. Unpublished Ph.D. thesis, Yale University, New Haven, Connecticut, U.S.A., 284 p.
- Cairnes, D.D., 1910. Preliminary memoir on the Lewes and Nordenskiöld rivers coal district, Yukon Territory. Geological Survey of Canada, Memoir 5, 70 p.
- Cameron, A.R. and Beaton, A.P., 2000. Coal resources of Northern Canada with emphasis on Whitehorse Trough, Bonnet Plume Basin and Brackett Basin. *International Journal of Coal Geology*, vol. 43, p. 187-210.
- Dickie, J.R. and Hein, F.J., 1995. Conglomeratic fan deltas and submarine fans of the Jurassic Laberge Group, Whitehorse Trough, Yukon Territory, Canada: Fore-arc sedimentation and unroofing of a volcanic arc complex. *Sedimentary Geology*, vol. 98, p. 263-292.
- Eisbacher, G.H., 1981. Late Mesozoic-Paleogene Bowser Basin molasses and cordilleran tectonics. *In: Sedimentation and Tectonics in Alluvial Basins*, A.D. Miall (ed.), Geological Association of Canada, Special Paper 23, p. 125-151.
- England, T.D.J., 1980. A Study of Upper Triassic Conodonts of the Intermontane Belt, Yukon Territory. Unpublished B.Sc. thesis, Department of Geological Sciences, University of British Columbia, Vancouver, BC, 70 p.
- English, J.M., Johannson, G.G., Johnston, S.T., Mialynuk, M.G., Fowler, M. and Wight, K.L., 2005. Structure, stratigraphy and petroleum potential of the central Whitehorse Trough, Northern Canadian Cordillera. *Bulletin of Canadian Petroleum Geology*, vol. 53, p. 130-153.
- Fowler, M., Snowdon, L. and Stasiuk, V., 2005. Applying petroleum geochemistry to hydrocarbon exploration and exploitation. AAPG Short Course Notes, June 18-19, 2005, Calgary, Alberta.
- Gilmore, R.G., 1985. Whitehorse field party. Unpublished Report, Petro-Canada, 16 p. (plus photographs)

- Gunther, P.R., 1985. Geochemical evaluation of Whitehorse field party samples. Unpublished Report, Petro-Canada, 19 p. plus appendices.
- Hacquebard, P.A., 1972. Petrographic correlation of the Tantalus and Tantalus Butte coal seams at Carmacks, Yukon Territory. Geological Survey of Canada Technical Report No. 115 1/1-3.
- Hart, C.J.R., 1997. A transect across northern Stikinia: geology of the northern Whitehorse map area, southern Yukon Territory (105D/13-16). Exploration and Geological Services Division, Yukon Region, Indian and Northern Affairs Canada, Bulletin 8, 112 p.
- Hunt, J.A. and Hart, C.J.R., 1994. Thermal Maturation and Hydrocarbon Source Rock Potential of Tantalus Formation Coals in the Whitehorse Area, Yukon Territory. *In: Yukon Exploration and Geology 1993*, Exploration and Geological Services Division, Yukon Region, Indian and Northern Affairs Canada, p. 67-77.
- Johannson, G.G., Smith, P.L. and Gordey, S.P., 1997. Early Jurassic evolution of the northern Stikinian arc: evidence from the Laberge Group, northwestern British Columbia. *Canadian Journal of Earth Science*, vol. 34, p. 1030-1057.
- Koch, G., 1973. The Central Cordilleran Region. *In: The Future Petroleum Provinces of Canada*, R.G. McCrossan (ed.), Canadian Society of Petroleum Geologists, Memoir 1, p. 37-71.
- Lafargue, E., Marquis, F. and Pillot, D., 1998. Rock-Eval 6 applications in hydrocarbon exploration, production, and soil contamination studies. *Oil & Gas Science and Technologies*, vol. 53, p. 421-437.
- Lees, E.J., 1934. Geology of the Laberge area, Yukon. *Transactions of the Royal Canadian Institute*, no. 43, vol. 20, part 1, 48 p.
- Long, D.G.F., 1986. Coal in Yukon. *In: Mineral Deposits of the Northern Cordillera*, J.A. Morin (ed.), Canadian Institute of Mining and Metallurgy, Special Volume 37, p. 311-318.
- Long, D.G.F., 2005. Sedimentology and hydrocarbon potential of fluvial strata in the Tantalus and Aksala formations, northern Whitehorse Trough, Yukon. *In: Yukon Exploration and Geology 2004*, D.S. Emond, L.L. Lewis and G.D. Bradshaw (eds.), Yukon Geological Survey, p. 167-176.
- Lowey, G.W., 2004. Preliminary lithostratigraphy of the Laberge Group (Jurassic), south-central Yukon: Implications concerning the petroleum potential of the Whitehorse Trough. *In: Yukon Exploration and Geology 2003*, D.S. Emond and L.L. Lewis (eds.), Yukon Geological Survey, p. 129-142.
- Lowey, G.W., 2005. Sedimentology, stratigraphy and source rock potential of the Richthofen formation (Jurassic), northern Whitehorse Trough, Yukon. *In: Yukon Exploration and Geology 2004*, D.S. Emond, L.L. Lewis and G.D. Bradshaw (eds.), Yukon Geological Survey, p. 177-191.
- Lowey, G.W., and Hills, L.V., 1988. Lithofacies, petrography and environments of deposition, Tantalus Formation (Lower Cretaceous) Indian River area, west-central Yukon. *Bulletin of Canadian Petroleum Geology*, vol. 36, p. 296-310.
- Monger, J.W.H. and Price, R.A., 1979. Geodynamic evolution of the Canadian Cordillera, progress and problems. *Canadian Journal of Earth Sciences*, vol. 16, p. 770-791.
- Monger, J.W.H., Wheeler, J.O., Tipper, H.W., Gabrielse, H., Harms, T., Struik, L.C., Campbell, R.B., Dodds, G.E., Geherels, G.E. and O'Brien, J., 1991. Part B, Cordilleran terranes. *In: Upper Devonian to Middle Jurassic Assemblages*, Chapter 8, *Geology of the Canadian Orogen in Canada*, H. Gabrielse and C. Yorath (eds.), Geological Survey of Canada, *Geology of Canada*, vol. 4, p. 281-327.
- National Energy Board, 2001. Petroleum resource assessment of the Whitehorse Trough, Yukon Territory, Canada. Oil and Gas Resource Branch. Department of Economic Development, Government of the Yukon, 59 p.
- Peters, K.E., 1986. Guidelines for evaluating petroleum source rock using programmed pyrolysis. *The American Association of Petroleum Geologists Bulletin*, vol. 70, p. 318-329.
- Peters, K.E. and Cassa, M.R., 1994. Applied source rock geochemistry. *In: The petroleum system – from source to trap*, L.B. Magoon and W.G. Dows (eds.), AAPG Memoir 60, p. 93-117.
- Peters, K.E. and Moldowan, J.M., 1993. *The Biomarker Guide*. Prentice Hall, Englewood Cliffs, New Jersey, 363 p.

- Russell, N.J., 1978. Coal petrography of twelve coal samples from the Yukon Territory, Canada. Minerals Research Laboratories, Fuel Geoscience Unit, Restricted Investigation Report 924R.
- Souther, J.G., 1991. Volcanic regimes, Chapter 14. *In: Geology of the Cordilleran Orogen in Canada*, H. Gabrielse and C. Yorath (eds.), Geological Survey of Canada, Geology of Canada, vol. 4, p. 457-490.
- Stack, E., Mackowsky, M.Th., Teichmuller, M., Taylor, G.H., Chandra, D. and Teichmuller, R., 1982. Stack's textbook of coal petrology, Third Revised Edition. Gerbruder Borntraeger, Berlin, Stuttgart, Germany.
- Swartzman, E., 1948. Study of coal from Tantalus Butte Mine, Yukon Territory. Department of Mines and Resources, Physical and Chemical Survey Report No. 137.
- Sweet, A.R., 2004. Applied Research Report on 37 Samples From the Laberge Group, Whitehorse Trough, Yukon Territory. Paleontological Report 6-ARS-2004, Geological Survey of Canada
- Teitz, H.H. and Young, F.G., 1982. Canadian hydrocarbon resource development up to the year 2000. *Journal of Petroleum Geology*, vol. 4, p. 347-375.
- Tempelman-Kluit, D.J., 1978. Reconnaissance geology, Laberge map-area, Yukon. *In: Current Research, Part A*, Geological Survey of Canada, Paper 78-1A, p. 61-66.
- Tempelman-Kluit, D.J., 1979. Transported cataclastite, ophiolite and granodiorite in Yukon: evidence of arc-continent collision. Geological Survey of Canada, Paper 79-14, 27 p.
- Tempelman-Kluit, D.J., 1980. Highlights of field work in Laberge and Carmacks map areas, Yukon Territory. *In: Current Research, Part A*, Geological Survey of Canada, Paper 80-1A, p. 357-362.
- Tempelman-Kluit, D.J., 1984. Geology, Laberge (105E) and Carmacks (115I), Yukon Territory. Geological Survey of Canada, Open File 1101, 1:250 000 scale.
- Tissot, B.P. and Welte, D.H., 1984. Petroleum formation and occurrence. Springer-Verlag, New York, New York, 699 p.
- Waples, D.W., 1985. Geochemistry in petroleum exploration. International Hyman Resources Development Corporation, Boston, Massachusetts, 232 p.
- Wheeler, J.O., 1961. Whitehorse map-area, Yukon Territory. Geological Survey of Canada, Memoir 312, 156 p.
- Wheeler, J.O. and McFeely, P., 1991. Tectonic assemblage map of the Canadian Cordillera. Geological Survey of Canada, Map 1712A, 1:1 000 000 scale.
- White, D., Buffet, G., Roberts, B., Colpron, M. and Abbott, G., 2004. Seismic images from an inverted sedimentary basin: The Whitehorse Trough, Yukon, Canada. Abstract submitted to the American Association of Petroleum Geologists Annual Meeting, June, 2005, Calgary, Alberta.

APPENDIX 1: RESULTS OF ROCK-EVAL 6 ANALYSIS

For explanation of abbreviations of headings, see description in text in section on Methods.

Aksala Formation

Sample	Easting	Northing	T _{max}	S1	S2	S3	PI	S2/S3	TOC	HI	OI
GL03-6A	426085	6915152	-40	0.00	0.00	0.68	1.00	0.00	0.40	0	170
GL04-39A	491169	6775460	439	0.01	0.04	0.27	0.19	0.15	0.04	100	675
GL04-67B	485092	6717134	402	0.00	0.01	0.30	0.02	0.03	0.01	100	3000
GL04-68A	485164	6716803	400	0.00	0.01	0.26	0.00	0.04	0.00	0	0
GL04-97A	507428	6765766	459	0.00	0.00	0.20	0.19	0.00	0.02	0	1000

Richthofen Formation

Sample	Easting	Northing	T _{max}	S1	S2	S3	PI	S2/S3	TOC	HI	OI
GL03-90A	489245	6772712	-40	0.00	0.00	0.16	1.00	0.00	0.85	0	19
GL03-90B	489245	6772712	-40	0.00	0.00	0.29	0.00	0.00	0.37	0	78
GL03-81R	489919	6770781	411	0.00	0.02	0.45	0.04	0.04	0.43	5	105
GL04-01A	482978	6802442	494	0.00	0.09	0.99	0.01	0.09	0.32	28	309
GL04-02A	482393	6803720	497	0.02	0.38	0.55	0.04	0.69	1.41	28	39
GL04-03A	482168	6804552	491	0.01	0.10	0.24	0.06	0.42	0.37	27	65
GL04-05A	482623	6799519	508	0.00	0.03	0.93	0.05	0.03	0.21	14	443
GL04-08A	480760	6799644	496	0.00	0.10	0.19	0.03	0.53	0.48	21	40
GL04-08B	480760	6799644	506	0.02	0.80	0.28	0.02	2.86	3.02	28	9
GL04-10A	482916	6796053	506	0.00	0.09	0.19	0.03	0.47	0.58	16	33
GL04-16A	485588	6792821	511	0.00	0.04	0.16	0.02	0.25	0.39	10	41
GL04-16B	485588	6792821	490	0.00	0.00	0.18	0.09	0.00	0.09	0	200
GL04-16C	485588	6792821	519	0.00	0.10	0.20	0.01	0.50	1.11	9	18
GL04-17A	487670	6784498	414	0.00	0.04	0.53	0.01	0.08	0.52	8	102
GL04-18A	487314	6784785	406	0.00	0.04	0.41	0.04	0.10	0.74	5	55
GL04-19A	487296	6785151	395	0.00	0.02	0.30	0.08	0.07	0.33	6	91
GL04-20A	487103	6785663	419	0.00	0.01	0.20	0.11	0.05	0.14	7	143
GL04-22A	486673	6786747	417	0.00	0.00	0.32	0.10	0.00	0.16	0	200
GL04-23A	486360	6788169	404	0.00	0.00	0.23	0.09	0.00	0.17	0	135
GL04-24A	489553	6778917	427	0.00	0.00	0.39	0.15	0.00	0.32	0	122
GL04-26A	489406	6778202	415	0.00	0.01	0.25	0.08	0.04	0.35	3	71
GL04-27A	489383	6779415	372	0.01	0.01	0.30	0.51	0.03	0.30	3	100
GL04-28A	489268	6780112	390	0.00	0.00	0.10	0.00	0.00	0.11	0	91
GL04-29A	489175	6780655	363	0.00	0.00	0.18	0.01	0.00	0.03	0	600
GL04-30A	489037	6781689	427	0.00	0.04	0.25	0.05	0.16	0.13	31	192
GL04-31A	488848	6782553	425	0.00	0.01	0.14	0.07	0.07	0.36	3	39
GL04-32A	488094	6783424	400	0.00	0.01	0.28	0.01	0.04	0.15	7	187
GL04-33A	491444	6771562	443	0.00	0.01	0.36	0.02	0.03	0.11	9	327

Richthofen formation (continued)

Sample	Easting	Northing	T _{max}	S1	S2	S3	PI	S2/S3	TOC	HI	OI
GL04-34A	491725	6771506	412	0.00	0.01	0.24	0.04	0.04	0.01	100	2400
GL04-36A	492078	6772503	394	0.00	0.00	0.27	0.32	0.00	0.51	0	53
GL04-38A	491169	6775360	380	0.00	0.01	0.28	0.03	0.04	0.31	3	90
GL04-41A	489115	6773985	410	0.00	0.00	0.25	0.14	0.00	0.61	0	41
GL04-42A	489883	6775821	418	0.00	0.02	0.66	0.10	0.03	0.03	67	2200
GL04-43A	490070	6775227	379	0.00	0.03	0.27	0.02	0.11	0.04	75	675
GL04-44A	490421	6773773	406	0.00	0.01	0.19	0.10	0.05	0.05	20	380
GL04-45A	490594	6768588	425	0.00	0.05	0.39	0.05	0.13	0.36	14	108
GL04-47A	488682	6795733	591	0.00	0.01	0.23	0.02	0.04	0.67	1	34
GL04-48A	488298	6794223	568	0.00	0.01	0.85	0.25	0.01	0.32	3	266
GL04-48B	488298	6794223	538	0.00	0.02	0.43	0.17	0.05	0.65	3	66
GL04-48C	488298	6794223	418	0.00	0.00	0.31	0.42	0.00	0.37	0	84
GL04-49A	489163	6793656	439	0.00	0.08	0.55	0.05	0.15	0.31	26	177
GL04-50A	488339	6791663	544	0.00	0.00	0.16	0.05	0.00	0.13	0	123
GL04-52A	489026	6789126	569	0.00	0.02	0.19	0.04	0.11	0.37	5	51
GL04-53A	489319	6788320	552	0.00	0.02	0.19	0.01	0.11	0.65	3	29
GL04-55A	494422	6776779	493	0.02	0.05	0.11	0.24	0.45	0.21	24	52
GL04-56A	495108	6775504	496	0.01	0.03	0.13	0.13	0.23	0.19	16	68
GL04-57A	495525	6774105	511	0.01	0.05	0.18	0.17	0.28	0.35	14	51
GL04-59A	493297	6763660	417	0.00	0.09	0.50	0.05	0.18	0.49	18	102
GL04-59B	493297	6763660	410	0.00	0.02	0.18	0.05	0.11	0.31	6	58
GL04-60A	491993	6766061	394	0.00	0.00	0.12	0.22	0.00	0.18	0	67
GL04-60B	491993	6766061	425	0.00	0.03	0.57	0.00	0.05	0.25	12	228
GL04-61A	491415	6766150	402	0.00	0.02	0.36	0.04	0.06	0.26	8	138
GL04-63A	492320	6765079	419	0.00	0.08	1.29	0.03	0.06	2.30	3	56
GL04-65A	474962	6788368	452	0.00	0.01	0.59	0.07	0.02	0.40	3	148
GL04-69A	542111	6689770	422	0.00	0.03	0.56	0.04	0.05	0.65	5	86
GL04-72A	538399	6697887	328	0.00	0.00	0.71	0.30	0.00	0.45	0	158
GL04-74A	490495	6760518	598	0.00	0.00	0.24	0.92	0.00	0.55	0	44
GL04-76A	545510	6682568	387	0.00	0.01	0.25	0.09	0.04	0.37	3	68
GL04-78B	517479	6671919	374	0.00	0.00	0.16	0.50	0.00	0.70	0	23
GL04-79A	501900	6651051	392	0.00	0.00	0.17	0.12	0.00	0.62	0	27
GL04-83A	491538	6763490	431	0.00	0.02	0.40	0.02	0.05	0.35	6	114
GL04-85B	491119	6763203	438	0.00	0.01	0.34	0.03	0.03	0.28	4	121
GL04-86A	491441	6763165	431	0.00	0.01	0.48	0.05	0.02	0.68	1	71
GL04-92A	489819	6759345	416	0.00	0.02	0.44	0.07	0.05	0.42	5	105
GL04-92C	489819	6759345	410	0.00	0.03	0.54	0.05	0.06	0.35	9	154
GL04-93A	490232	6759119	319	0.00	0.00	0.50	0.30	0.00	0.47	0	106
GL04-93C	490232	6759119	316	0.00	0.00	0.25	0.62	0.00	0.63	0	40
GL04-94B	492711	6760581	-40	0.00	0.00	0.35	1.00	0.00	0.47	0	74
GL04-95A	492000	6761523	433	0.00	0.05	0.46	0.04	0.11	0.29	17	159
GL04-101B	506577	6765794	443	0.00	0.00	0.33	0.17	0.00	0.16	0	206

Tanglefoot Formation

Sample	Easting	Northing	T _{max}	S1	S2	S3	PI	S2/S3	TOC	HI	OI
C-76-01-015	434000	6889070	440	0.00	0.52	3.23	0.00	0.16	1.53	35	211
C-76-01-032	434000	6889070	456	0.00	0.04	0.66	0.05	0.06	0.32	13	206
C-76-01-042	434000	6889070	435	0.09	15.90	4.73	0.01	3.36	8.78	182	54
C-76-01-043	434000	6889070	431	0.04	0.57	1.20	0.07	0.48	1.04	56	115
C-76-01-046	434000	6889070	437	0.00	0.10	1.06	0.02	0.09	0.47	21	226
C-76-03-320	433900	6889920	501	0.09	30.03	13.91	0.00	2.16	67.18	46	21
C-76-03-364	433900	6889920	440	0.00	0.04	0.40	0.02	0.10	0.22	18	182
C-76-03-384	433900	6889920	429	0.01	1.44	0.39	0.01	3.69	1.52	95	26
C-76-03-444	433900	6889920	436	0.08	23.61	1.01	0.00	23.38	10.40	229	10
C-76-03-483	433900	6889920	428	0.02	2.49	0.50	0.01	4.98	1.89	132	26
C-76-03-540	433900	6889920	438	0.02	3.79	0.90	0.01	4.21	3.57	108	25
C-76-03-555	433900	6889920	438	0.04	11.42	0.99	0.00	11.54	7.41	156	13
C-76-03-595	433900	6889920	429	0.03	2.45	0.62	0.01	3.95	2.15	114	29
C-76-03-625	433900	6889920	439	0.05	3.19	0.53	0.02	6.02	2.31	139	23
C-76-03-637	433900	6889920	435	0.01	1.15	0.28	0.01	4.11	1.24	94	23
C-76-03-638	433900	6889920	436	0.01	0.99	0.39	0.01	2.54	1.26	79	31
C-76-03-639	433900	6889920	432	0.01	1.17	0.52	0.01	2.25	1.35	87	39
C-76-03-656	433900	6889920	436	0.00	0.50	0.46	0.00	1.09	0.80	63	58
C-76-03-730	433900	6889920	437	0.01	0.82	0.99	0.01	0.83	1.07	78	93
C-76-03-761	433900	6889920	436	0.01	0.58	0.30	0.01	1.93	0.71	82	42
C-76-03-762	433900	6889920	434	0.00	0.58	0.32	0.01	1.81	0.76	76	42
C-76-03-786	433900	6889920	437	0.07	19.77	1.33	0.00	14.86	12.80	156	10
C-76-03-796	433900	6889920	431	0.01	0.62	1.83	0.02	0.34	1.03	60	178
C-76-03-799	433900	6889920	443	0.03	4.34	0.47	0.01	9.23	2.48	176	19
C-76-04-312	434600	6884035	524	0.02	0.81	0.55	0.02	1.47	2.55	33	22
C-76-04-483	434600	6884035	436	0.00	0.00	0.52	0.02	0.00	0.09	0	578
C-76-04-503	434600	6884035	498	0.08	0.32	0.52	0.19	0.62	0.72	44	72
C-76-05-413	433900	6889920	446	0.03	4.87	1.70	0.01	2.86	5.70	87	30
C-76-05-460	433900	6889920	436	0.05	4.99	0.65	0.01	7.68	2.86	176	23
C-76-05-465	433900	6889920	433	0.04	3.87	0.83	0.01	4.66	2.76	141	30
C-76-05-468	433900	6889920	434	0.09	4.35	1.14	0.02	3.82	3.18	138	36
C-76-05-498	433900	6889920	434	0.01	1.68	1.09	0.01	1.54	2.00	85	55
C-76-05-499	433900	6889920	433	0.01	1.74	1.30	0.00	1.34	2.07	85	63
C-76-05-537	433900	6889920	439	0.02	4.42	0.98	0.00	4.51	4.96	90	20
C-76-05-538	433900	6889920	432	0.02	1.07	0.62	0.01	1.73	1.20	89	52
C-76-06-252	434760	6883730	461	0.00	0.03	0.36	0.02	0.08	0.21	14	171
C-76-06-345	434760	6883730	462	0.05	3.41	0.28	0.01	12.18	2.65	131	11
C-76-06-362	434760	6883730	471	0.01	0.47	0.25	0.02	1.88	0.96	50	26
C-76-06-408	434760	6883730	485	0.01	0.90	0.33	0.01	2.73	2.72	35	12
C-76-06-412	434760	6883730	515	0.00	0.19	0.17	0.00	1.12	0.98	19	17
C-76-06-516	434760	6883730	493	0.01	0.23	0.39	0.03	0.59	0.37	65	105
C-76-07-573	434655	6884080	476	0.00	0.01	0.18	0.00	0.06	0.07	14	257

Tanglefoot formation (continued)

Sample	Easting	Northing	T _{max}	S1	S2	S3	PI	S2/S3	TOC	HI	OI
C-76-07-598	434655	6884080	511	0.00	0.00	0.16	0.14	0.00	0.06	0	267
C-76-07-750	434655	6884080	440	0.00	1.02	0.38	0.00	2.68	1.15	90	33
C-76-08-030	434080	6890040	433	0.01	0.94	0.73	0.01	1.29	1.04	91	70
C-76-08-040	434080	6890040	440	0.00	0.08	0.88	0.02	0.09	0.43	19	205
C-76-08-049	434080	6890040	435	0.01	1.14	0.73	0.01	1.56	1.26	91	58
C-76-08-054	434080	6890040	433	0.00	0.17	0.96	0.02	0.18	0.67	25	143
C-76-08-060	434080	6890040	442	0.01	1.02	0.37	0.01	2.76	1.35	77	27
C-76-08-075	434080	6890040	438	0.06	11.32	0.76	0.01	14.89	6.46	177	12
C-76-08-142	434080	6890040	437	0.00	0.32	0.32	0.01	1.00	0.28	114	114
C-76-08-164	434080	6890040	438	0.00	0.64	0.71	0.00	0.90	0.67	97	106
C-76-08-168	434080	6890040	433	0.03	3.92	0.42	0.01	9.33	1.31	300	32
C-76-08-183	434080	6890040	441	0.00	0.31	0.44	0.01	0.70	0.45	69	98
C-76-08-184	434080	6890040	437	0.01	1.54	0.28	0.01	5.50	1.16	134	24
C-76-08-206	434080	6890040	433	0.00	0.66	0.54	0.01	1.22	0.86	78	63
C-76-08-215	434080	6890040	439	0.01	0.41	0.31	0.02	1.32	0.65	63	48
C-76-08-219	434080	6890040	436	0.01	1.23	0.40	0.01	3.08	1.58	78	25
C-76-08-220	434080	6890040	436	0.01	0.67	0.47	0.02	1.43	1.02	67	46
C-76-08-254	434080	6890040	432	0.00	0.34	0.32	0.01	1.06	0.60	57	53
C-76-08-270	434080	6890040	434	0.00	0.21	0.35	0.01	0.60	0.28	75	125
C-76-08-386	434080	6890040	440	0.00	0.61	0.37	0.00	1.65	1.00	62	37
C-76-08-390	434080	6890040	432	0.00	0.35	0.41	0.00	0.85	0.51	69	80
C-76-08-394	434080	6890040	438	0.01	0.82	0.46	0.01	1.78	1.20	69	38
C-76-08-411	434080	6890040	431	0.00	0.19	0.23	0.00	0.83	0.40	48	58
C-76-08-415	434080	6890040	439	0.00	0.34	0.67	0.01	0.51	0.54	63	124
C-76-08-435	434080	6890040	428	0.00	0.08	0.34	0.00	0.24	0.12	67	283
C-76-08-450	434080	6890040	432	0.00	0.07	0.31	0.01	0.23	0.06	117	517
C-76-09-094	434050	6890100	432	0.00	0.12	0.39	0.00	0.31	0.18	67	217
C-76-09-113	434050	6890100	438	0.00	0.30	0.40	0.02	0.75	0.31	97	129
C-76-09-114	434050	6890100	436	0.01	0.77	0.31	0.01	2.48	1.07	73	29
C-76-09-121	434050	6890100	431	0.00	0.50	0.49	0.01	1.02	0.58	86	84
C-76-09-132	434050	6890100	431	0.01	1.30	0.52	0.01	2.50	1.34	98	39
C-76-09-148	434050	6890100	433	0.01	0.14	0.47	0.04	0.30	0.26	54	181
C-76-09-149	434050	6890100	441	0.00	0.29	0.88	0.00	0.33	0.41	71	215
C-76-09-159	434050	6890100	431	0.01	0.27	0.57	0.02	0.47	0.36	75	158
C-76-10-645	434785	6883720	485	0.15	20.49	1.46	0.01	14.03	18.62	112	8
C-76-10-654	434785	6883720	465	0.01	0.54	0.43	0.02	1.26	1.10	50	39
C-76-12-170	434980	6883475	489	0.01	0.13	0.25	0.06	0.52	0.19	68	132
C-76-12-261	434980	6883475	470	0.04	0.92	0.61	0.04	1.51	1.27	74	48
C-76-12-264	434980	6883475	468	0.04	1.16	0.25	0.04	4.64	1.99	60	13
C-76-12-376	434980	6883475	498	0.01	0.08	0.43	0.15	0.19	0.19	42	226
C-76-12-402	434980	6883475	452	0.01	0.08	0.33	0.07	0.24	0.10	80	330
C-76-12-412	434980	6883475	498	0.01	0.09	0.55	0.08	0.16	0.09	100	611

Tanglefoot formation (continued)

Sample	Easting	Northing	T _{max}	S1	S2	S3	PI	S2/S3	TOC	HI	OI
C-76-12-441	434980	6883475	440	0.00	0.00	0.36	0.02	0.00	0.06	0	600
C-76-12-509	434980	6883475	342	0.00	0.00	0.36	0.00	0.00	0.03	0	1200
C-76-12-756	434980	6883475	436	0.01	0.57	0.39	0.01	1.46	0.67	85	58
C-76-14-057	433950	6889920	431	0.01	0.18	0.48	0.07	0.38	0.13	138	369
C-76-14-066	433950	6889920	434	0.03	0.39	1.53	0.07	0.25	0.82	48	187
C-76-14-077	433950	6889920	429	0.03	0.36	1.50	0.07	0.24	0.76	47	197
C-76-14-080	433950	6889920	437	0.02	0.32	2.03	0.06	0.16	0.71	45	286
C-76-14-090	433950	6889920	431	0.02	0.30	1.71	0.07	0.18	0.64	47	267
C-76-14-097	433950	6889920	435	0.02	0.28	1.35	0.07	0.21	0.52	54	260
C-76-14-105	433950	6889920	436	0.08	2.66	2.45	0.03	1.09	2.71	99	90
C-76-14-111	433950	6889920	437	0.05	0.57	1.81	0.08	0.31	1.16	50	156
C-76-14-124	433950	6889920	430	0.05	0.62	0.92	0.08	0.67	1.19	52	77
C-76-14-132	433950	6889920	435	0.07	1.85	1.88	0.04	0.98	2.25	84	84
C-76-14-143	433950	6889920	440	0.15	9.37	1.13	0.02	8.29	6.63	143	17
C-76-14-146	433950	6889920	428	0.29	28.25	1.73	0.01	16.33	13.54	209	13
C-76-14-154	433950	6889920	440	0.02	0.75	1.62	0.03	0.46	1.08	70	150
C-76-14-156	433950	6889920	439	0.03	0.68	1.54	0.04	0.44	1.11	62	139
C-76-14-162	433950	6889920	429	0.06	1.95	0.54	0.03	3.61	2.07	95	26
C-76-14-174	433950	6889920	440	0.11	1.00	1.76	0.10	0.57	1.60	63	110
C-76-14-175	433950	6889920	434	0.06	1.05	1.61	0.05	0.65	1.66	63	97
C-76-14-185	433950	6889920	423	0.07	0.52	0.58	0.12	0.90	0.44	118	132
C-76-16-150	434265	6184310	487	0.14	1.88	0.67	0.07	2.81	3.07	62	22
C-76-16-177	434265	6184310	463	0.11	2.04	0.32	0.05	6.38	2.79	75	11
GL03-2A	429657	6904616	447	0.15	0.78	1.72	0.16	0.45	2.44	32	70
GL03-3B	429524	6904655	461	0.03	0.48	0.69	0.06	0.70	1.32	37	52
GL03-5A	429668	6904864	442	0.19	1.74	0.94	0.10	1.85	2.47	71	38
GL03-5C	429668	6904864	439	0.21	4.96	1.32	0.04	3.76	3.70	135	36
GL03-5D	429668	6904864	439	0.80	22.30	0.60	0.03	37.17	5.71	391	11
GL03-9A	429948	6905297	489	0.02	0.15	0.90	0.13	0.17	0.64	23	141
GL03-10C	428392	6912139	-40	0.00	0.00	2.01	0.00	0.00	1.82	0	110
GL03-13D	460022	6893977	-40	0.00	0.00	1.12	1.00	0.00	0.92	0	122
GL03-17B	455988	6877573	513	0.00	0.00	0.83	0.38	0.00	0.38	0	218
GL03-18B	455718	6877707	501	0.00	0.06	0.84	0.01	0.07	0.74	8	114
GL03-20B	441298	6886202	535	0.00	0.18	0.98	0.01	0.18	2.71	7	36
GL03-20D	441298	6886202	545	0.00	0.14	1.39	0.02	0.10	2.66	6	52
GL03-22A	441748	6885861	549	0.00	0.11	0.52	0.03	0.21	1.79	7	29
GL03-22C	441748	6885861	526	0.01	0.21	0.40	0.03	0.53	2.65	9	15
GL03-22E	441748	6885861	524	0.00	0.01	1.12	0.21	0.01	0.82	1	137
GL03-22J	441748	6885861	537	0.00	0.08	2.06	0.04	0.04	2.05	4	100
GL03-23A	436456	6888383	508	0.00	0.10	0.96	0.00	0.10	1.10	9	87
GL03-23D	436456	6888383	512	0.00	0.26	1.36	0.00	0.19	1.92	14	71
GL03-23F	436456	6888383	508	0.00	0.32	1.27	0.00	0.25	1.84	17	69

Tanglefoot formation (continued)

Sample	Easting	Northing	T _{max}	S1	S2	S3	PI	S2/S3	TOC	HI	OI
GL03-24E	434006	6890664	443	0.01	2.12	3.52	0.00	0.60	3.54	61	99
GL03-30C	431042	6908305	-40	0.00	0.00	0.76	1.00	0.00	0.41	0	185
GL03-30D	431042	6908305	-40	0.00	0.00	0.85	1.00	0.00	0.38	0	224
GL03-30E	431042	6908305	-40	0.00	0.00	0.77	1.00	0.00	0.52	0	148
GL03-39A	436777	6908818	-40	0.00	0.00	1.39	0.00	0.00	0.61	0	228
GL03-44B	441092	6861315	605	0.00	0.93	12.63	0.00	0.07	44.46	3	28
GL03-44C	441092	6861315	-40	0.00	0.00	0.96	0.00	0.00	0.52	0	185
GL03-45A	439319	6865677	474	0.00	0.38	1.90	0.00	0.20	1.25	31	152
GL03-45E	439319	6865677	463	0.01	0.27	0.48	0.02	0.56	0.91	31	53
GL03-68B	455245	6877903	465	0.00	0.07	0.52	0.00	0.13	0.44	16	118
GL03-69A	466405	6809300	508	0.03	0.04	0.29	0.47	0.14	0.98	4	30
GL03-69E	466405	6809300	513	0.00	0.12	0.60	0.01	0.20	1.02	13	59
GL03-69EE	466405	6809300	510	0.01	0.42	0.91	0.02	0.46	2.75	16	33
GL03-70A	466134	6809925	500	0.00	0.01	0.11	0.07	0.09	0.33	3	33
GL03-70B	466134	6809925	507	0.01	0.07	0.24	0.07	0.29	0.84	8	29
GL03-70C	466134	6809925	509	0.00	0.09	0.14	0.02	0.64	0.85	11	16
GL03-73A	442488	6860181	-40	0.00	0.00	0.03	1.00	0.00	0.05	0	60
GL03-73B	442488	6860181	-40	0.00	0.00	0.03	1.00	0.00	0.13	0	23
GL03-75A	442204	6801621	444	0.00	0.12	0.18	0.00	0.67	0.64	19	28
GL03-75C	442204	6801621	437	0.00	0.03	0.49	0.02	0.06	0.35	9	140
GL03-78C	454918	6829145	-40	0.00	0.00	0.26	1.00	0.00	0.09	0	289
GL03-91G	464396	6803479	-40	0.00	0.00	0.50	1.00	0.00	0.51	0	98
GL03-95B	463534	6806068	-40	0.00	0.00	1.16	1.00	0.00	0.21	0	552
GL03-97B	463713	6805770	-40	0.00	0.00	1.13	1.00	0.00	0.42	0	269
GL03-97C	463713	6805770	-40	0.00	0.00	1.14	1.00	0.00	0.27	0	422
GL03-99B	470476	6797182	-40	0.00	0.00	0.64	0.00	0.00	0.50	0	128
GL03-100A	475575	6790537	456	0.10	6.98	0.65	0.01	10.74	6.86	103	9
GL03-100C	475575	6790537	469	0.03	0.18	0.88	0.13	0.20	0.57	32	154
GL03-102B	481339	6777628	-40	0.00	0.00	0.31	0.00	0.00	0.49	0	63
GL03-103A	481560	6777390	548	0.00	0.00	0.17	0.00	0.00	0.79	0	22
GL04-64B	463503	6802692	407	0.00	0.00	0.34	0.01	0.00	0.07	0	486
GL04-102B	513914	6790104	606	0.01	0.01	0.53	0.31	0.02	1.76	1	30
GL04-102D	513914	6790104	598	0.00	0.00	0.27	0.05	0.00	0.69	0	39
GL04-102E	513914	6790104	606	0.02	0.04	0.40	0.32	0.10	2.69	2	15
GL04-103B	513341	6789935	553	0.02	0.10	0.40	0.12	0.25	2.11	5	19
94-25-20	441900	6801798	432	0.02	1.50	0.40	0.01	3.75	1.66	92	24
94-25-163	441900	6801798	428	0.02	1.63	0.28	0.01	5.82	1.39	118	20
94-38-28	444410	6799580	434	0.00	1.16	0.20	0.00	5.80	1.23	95	16
94-38-69	444410	6799580	446	0.09	3.59	0.27	0.03	13.30	3.16	115	9
94-38-150	444410	6799580	430	0.11	4.25	0.43	0.02	9.88	4.76	90	9
94-38-154	444410	6799580	427	0.12	5.13	0.40	0.02	12.83	4.01	128	10
94-38-161	444410	6799580	428	0.08	3.84	0.32	0.02	12.00	3.37	115	9

Tanglefoot formation (continued)

Sample	Easting	Northing	T _{max}	S1	S2	S3	PI	S2/S3	TOC	HI	OI
94-38-172	444410	6799580	425	0.16	9.33	0.39	0.02	23.92	5.02	186	8
94-40-262	444409	6799579	424	0.25	17.59	0.57	0.01	30.86	5.01	351	11
94-40-267	444409	6799579	429	0.15	5.94	0.41	0.02	14.49	3.49	170	12
94-42-253	444189	6799726	423	0.04	3.74	0.64	0.01	5.84	1.98	189	32
94-42-259	444189	6799726	426	0.05	4.23	0.33	0.01	12.82	3.02	140	11
94-47-98	442860	6801040	432	0.02	1.90	0.29	0.01	6.55	1.25	153	23
94-47-175	442860	6801040	605	0.03	0.08	0.21	0.23	0.38	1.81	5	12
94-47-199	442860	6801040	436	0.04	2.48	0.47	0.01	5.28	1.47	169	32
94-47-218	442860	6801040	426	0.13	9.36	0.63	0.01	14.86	3.86	243	16
94-47-219	442860	6801040	432	0.06	2.97	0.40	0.02	7.43	3.58	84	11
97-61-79	444703	6797233	434	0.05	2.33	0.31	0.02	7.52	2.21	106	14
97-61-207	444703	6797233	434	0.04	3.00	0.33	0.01	9.09	2.21	137	15
97-61-229	444703	6797233	409	0.01	0.03	0.85	0.21	0.04	0.06	50	1417
97-63-83	445122	6796798	428	0.11	7.75	0.47	0.01	16.49	4.35	180	11

Tantalus Formation

Sample	Easting	Northing	T _{max}	S1	S2	S3	PI	S2/S3	TOC	HI	OI
C-76-01-108	434000	6889070	435	0.04	2.93	1.90	0.01	1.54	4.44	67	43
C-76-01-126	434000	6889070	427	0.01	0.14	1.08	0.04	0.13	0.51	27	212
C-76-01-127	434000	6889070	443	0.01	0.03	1.49	0.25	0.02	0.17	18	876
C-76-01-132	434000	6889070	425	0.01	0.23	1.63	0.04	0.14	0.76	30	214
C-76-01-139	434000	6889070	441	0.01	0.04	0.52	0.17	0.08	0.23	17	226
C-76-01-197	434000	6889070	432	0.01	0.34	2.03	0.03	0.17	0.71	48	286
C-76-01-327	434000	6889070	449	0.00	0.06	1.07	0.04	0.06	0.45	13	238
C-76-01-331	434000	6889070	431	0.00	0.09	1.08	0.04	0.08	0.48	19	225
C-76-01-339	434000	6889070	440	0.01	0.06	1.57	0.15	0.04	0.30	20	523
C-76-01-404	434000	6889070	435	0.01	0.14	0.87	0.07	0.16	0.41	34	212
C-76-01-405	434000	6889070	437	0.00	0.01	1.37	0.20	0.01	0.06	17	2283
C-76-01-614	434000	6889070	433	0.02	1.90	0.76	0.01	2.50	1.88	102	40
C-76-01-620	434000	6889070	434	0.02	0.26	1.11	0.06	0.23	0.38	68	292
C-76-01-668	434000	6889070	437	0.00	0.68	0.86	0.01	0.79	0.94	73	91
C-76-01-685	434000	6889070	472	0.00	0.02	0.32	0.05	0.06	0.12	17	267
C-76-01-690	434000	6889070	446	0.00	0.02	0.37	0.00	0.05	0.19	11	195
C-76-01-751	434000	6889070	434	0.01	1.13	0.62	0.01	1.82	1.34	85	46
C-76-01-754	434000	6889070	440	0.00	0.12	0.42	0.01	0.29	0.26	46	162
C-76-01-761	434000	6889070	436	0.01	1.61	0.43	0.01	3.74	1.71	95	25
C-76-01-774	434000	6889070	433	0.00	0.34	0.36	0.01	0.94	0.45	76	80
C-76-01-793	434000	6889070	435	0.00	0.61	0.44	0.01	1.39	1.19	52	37
C-76-01-796	434000	6889070	437	0.01	0.44	0.36	0.02	1.22	0.48	92	75
C-76-01-810	434000	6889070	439	0.01	1.37	0.81	0.01	1.69	2.65	53	31
C-76-02-001	434000	6889070	439	0.02	1.02	1.53	0.02	0.67	1.50	69	102
C-76-02-050	434000	6889070	433	0.06	3.94	1.13	0.02	3.49	3.30	120	34
C-76-02-059	434000	6889070	441	0.01	0.15	0.63	0.04	0.24	0.31	48	203
C-76-02-060	434000	6889070	434	0.00	0.19	0.54	0.02	0.35	0.54	35	100
C-76-02-114	434000	6889070	438	0.02	1.75	0.73	0.01	2.40	1.95	91	37
C-76-02-143	434000	6889070	429	0.01	0.81	2.39	0.02	0.34	2.18	38	110
C-76-02-171	434000	6889070	456	0.00	0.04	1.59	0.05	0.03	0.27	15	589
C-76-02-174	434000	6889070	432	0.02	1.19	0.98	0.01	1.21	1.67	72	59
C-76-02-189	434000	6889070	436	0.00	0.09	0.99	0.05	0.09	0.42	21	236
C-76-02-205	434000	6889070	434	0.01	1.37	0.48	0.01	2.85	1.69	82	28
C-76-02-207	434000	6889070	440	0.02	2.70	1.73	0.01	1.56	4.23	65	41
C-76-02-215	434000	6889070	444	0.01	0.11	1.26	0.05	0.09	0.43	26	293
C-76-02-221	434000	6889070	434	0.00	0.11	0.39	0.02	0.28	0.30	37	130
C-76-02-277	434000	6889070	449	0.03	1.22	2.54	0.03	0.48	2.08	60	122
C-76-02-279	434000	6889070	438	0.01	0.74	1.07	0.01	0.69	1.36	55	79
C-76-02-421	434000	6889070	435	0.02	3.27	0.57	0.01	5.74	3.39	97	17
C-76-02-632	434000	6889070	442	0.03	5.21	1.02	0.01	5.11	4.96	107	21
C-76-02-660	434000	6889070	431	0.02	1.73	0.56	0.01	3.09	2.05	85	27
C-76-02-768	434000	6889070	437	0.03	2.31	0.40	0.01	5.78	1.70	137	24

Tantalus formation (continued)

Sample	Easting	Northing	T _{max}	S1	S2	S3	PI	S2/S3	TOC	HI	OI
C-76-02-814	434000	6889070	434	0.02	2.19	0.37	0.01	5.92	2.04	108	18
C-76-03-043	433900	6889920	441	0.01	0.63	2.01	0.01	0.31	1.76	37	114
C-76-03-045	433900	6889920	432	0.01	0.37	2.02	0.02	0.18	1.10	34	184
C-76-03-263	433900	6889920	445	0.02	0.63	2.38	0.03	0.26	1.77	36	134
C-76-03-273	433900	6889920	441	0.02	1.18	2.54	0.01	0.46	1.96	61	130
C-76-05-060	433900	6889920	438	0.00	0.15	1.16	0.03	0.13	0.71	21	163
C-76-05-065	433900	6889920	429	0.00	0.05	0.71	0.08	0.07	0.30	17	237
C-76-05-077	433900	6889920	441	0.00	0.39	1.90	0.01	0.21	1.34	30	142
C-76-05-078	433900	6889920	445	0.00	0.09	1.35	0.05	0.07	0.53	17	255
C-76-05-090	433900	6889920	441	0.01	0.10	0.47	0.07	0.21	0.34	29	138
C-76-05-093	433900	6889920	445	0.00	0.02	1.56	0.08	0.01	0.31	6	503
C-76-05-101	433900	6889920	490	0.00	0.00	1.68	0.00	0.00	0.23	0	730
C-76-05-104	433900	6889920	446	0.00	0.01	1.81	0.29	0.01	0.13	8	1392
C-76-05-107	433900	6889920	444	0.01	0.04	1.48	0.24	0.03	0.35	11	423
C-76-05-652	433900	6889920	438	0.01	0.40	0.45	0.01	0.89	0.69	58	65
C-76-05-750	433900	6889920	431	0.01	1.23	0.57	0.01	2.16	1.35	91	42
C-76-05-855	433900	6889920	440	0.01	1.92	0.38	0.00	5.05	1.69	115	22
C-76-05-858	433900	6889920	435	0.01	2.52	0.75	0.00	3.36	2.39	106	31
C-76-05-878	433900	6889920	440	0.01	2.04	0.54	0.01	3.78	2.02	102	27
C-76-05-883	433900	6889920	438	0.01	1.74	0.47	0.01	3.70	1.93	91	24
C-76-05-916	433900	6889920	423	0.00	0.30	0.33	0.01	0.91	1.00	30	33
C-76-05-942	433900	6889920	437	0.01	1.59	0.53	0.01	3.00	1.68	96	32
C-76-08-488	434080	6890040	430	0.02	1.22	0.58	0.01	2.10	1.30	95	45
C-76-08-500	434080	6890040	428	0.01	0.21	0.34	0.03	0.62	0.19	111	179
C-76-10-212	434785	6883720	470	0.01	0.33	2.57	0.04	0.13	1.30	26	198
C-76-10-529	434785	6883720	446	0.01	0.14	1.86	0.06	0.08	0.61	23	305
C-76-10-666	434785	6883720	468	0.02	0.31	0.44	0.05	0.70	1.28	25	34
C-76-10-747	434785	6883720	437	0.05	1.85	4.82	0.03	0.38	5.16	37	93
C-76-10-786	434785	6883720	453	0.01	1.53	0.67	0.01	2.28	2.62	60	26
C-76-10-801	434785	6883720	463	0.03	1.65	1.12	0.02	1.47	2.55	66	44
C-76-10-861	434785	6883720	479	0.00	0.69	0.51	0.01	1.35	1.28	55	40
C-76-11-087	434120	6888920	433	0.01	0.56	2.44	0.02	0.23	1.33	43	183
C-76-11-099	434120	6888920	454	0.00	0.01	1.25	0.30	0.01	0.04	25	3125
C-76-11-106	434120	6888920	444	0.00	0.07	1.32	0.01	0.05	0.38	18	347
C-76-11-108	434120	6888920	445	0.00	0.04	0.46	0.02	0.09	0.24	17	192
C-76-11-163	434120	6888920	437	0.03	1.55	0.56	0.02	2.77	1.49	105	38
C-76-11-210	434120	6888920	444	0.01	0.51	1.46	0.03	0.35	1.21	43	121
C-76-11-242	434120	6888920	442	0.00	0.05	1.21	0.09	0.04	0.37	14	327
C-76-11-261	434120	6888920	445	0.01	0.26	1.36	0.04	0.19	0.80	33	170
C-76-11-274	434120	6888920	435	0.01	0.08	1.25	0.10	0.06	0.45	18	278
C-76-11-278	434120	6888920	435	0.01	0.19	1.03	0.07	0.18	0.49	39	210
C-76-11-284	434120	6888920	434	0.01	0.21	1.17	0.02	0.18	0.53	40	221

Tantalus formation (continued)

Sample	Easting	Northing	T _{max}	S1	S2	S3	PI	S2/S3	TOC	HI	OI
C-76-11-445	434120	6888920	434	0.01	0.48	0.68	0.01	0.71	0.54	89	126
C-76-11-470	434120	6888920	445	0.07	1.83	1.59	0.04	1.15	2.94	64	54
C-76-11-490	434120	6888920	435	0.03	0.45	0.34	0.07	1.32	0.73	63	47
C-76-11-496	434120	6888920	435	0.02	2.45	0.49	0.01	5.00	2.50	99	20
C-76-11-512	434120	6888920	439	0.03	1.62	0.73	0.02	2.22	1.75	94	42
C-76-11-519	434120	6888920	435	0.05	0.35	0.77	0.13	0.45	0.63	56	122
C-76-11-520	434120	6888920	436	0.00	0.10	0.83	0.03	0.12	0.40	25	208
C-76-11-524	434120	6888920	438	0.01	0.09	1.61	0.11	0.06	0.32	28	503
C-76-11-528	434120	6888920	434	0.00	0.23	0.79	0.02	0.29	0.51	45	155
C-76-11-586	434120	6888920	437	0.03	2.76	0.55	0.01	5.02	2.77	101	20
C-76-11-649	434120	6888920	434	0.01	1.25	0.53	0.01	2.36	1.37	92	39
C-76-11-650	434120	6888920	439	0.01	0.99	0.87	0.01	1.14	1.23	81	71
C-76-11-653	434120	6888920	434	0.03	1.47	0.64	0.02	2.30	1.69	88	38
C-76-11-666	434120	6888920	443	0.00	0.04	0.46	0.03	0.09	0.28	14	164
C-76-11-675	434120	6888920	441	0.01	0.51	0.29	0.02	1.76	0.61	85	48
C-76-11-680	434120	6888920	434	0.00	0.77	0.31	0.00	2.48	0.82	94	38
C-76-11-699	434120	6888920	438	0.02	3.93	0.72	0.00	5.46	4.80	83	15
C-76-11-707	434120	6888920	440	0.00	0.43	0.33	0.01	1.30	0.85	52	39
C-76-11-709	434120	6888920	430	0.00	0.21	0.50	0.01	0.42	0.52	40	96
C-76-11-744	434120	6888920	437	0.00	0.63	0.45	0.00	1.40	0.87	74	52
C-76-11-773	434120	6888920	433	0.01	0.46	0.25	0.03	1.84	0.67	69	37
C-76-11-817	434120	6888920	439	0.01	0.55	0.30	0.01	1.83	0.76	72	39
C-76-11-821	434120	6888920	439	0.01	1.02	0.27	0.01	3.78	1.21	85	22
C-76-11-827	434120	6888920	434	0.00	0.08	0.20	0.01	0.40	0.15	53	133
C-76-13-068	434445	6884315	525	0.01	0.01	0.92	0.64	0.01	0.11	9	836
C-76-13-402	434445	6884315	471	0.01	0.03	0.38	0.15	0.08	0.11	27	345
C-76-13-487	434445	6884315	471	0.01	0.24	0.44	0.04	0.55	0.45	53	98
C-76-13-544	434445	6884315	465	0.02	0.25	0.40	0.06	0.63	0.39	64	103
C-76-13-609	434445	6884315	459	0.01	0.08	0.35	0.09	0.23	0.13	62	269
C-76-14-235	433950	6889920	436	0.03	0.40	2.09	0.07	0.19	1.15	36	182
C-76-14-247	433950	6889920	430	0.18	6.44	1.94	0.03	3.32	4.12	157	47
C-76-14-256	433950	6889920	440	0.21	19.18	1.45	0.01	13.23	5.68	339	26
C-76-14-260	433950	6889920	432	0.06	0.57	0.71	0.09	0.80	0.65	88	109
C-76-14-270	433950	6889920	431	0.06	1.09	0.52	0.05	2.10	1.12	98	46
C-76-14-273	433950	6889920	436	0.02	0.14	0.92	0.12	0.15	0.20	70	460
C-76-14-429	433950	6889920	438	0.02	0.50	1.02	0.03	0.49	0.61	82	167
C-76-14-430	433950	6889920	441	0.02	0.81	1.37	0.02	0.59	1.15	71	119
C-76-14-452	433950	6889920	435	0.03	1.24	0.36	0.02	3.44	1.04	120	35
C-76-14-455	433950	6889920	432	0.04	1.93	0.77	0.02	2.51	1.94	101	40
C-76-14-466	433950	6889920	438	0.01	0.28	0.62	0.04	0.45	0.34	82	182
C-76-14-502	433950	6889920	432	0.01	0.09	0.27	0.11	0.33	0.13	69	208
C-76-14-504	433950	6889920	429	0.02	0.28	0.33	0.05	0.85	0.40	70	83

Tantalus formation (continued)

Sample	Easting	Northing	T _{max}	S1	S2	S3	PI	S2/S3	TOC	HI	OI
C-76-14-510	433950	6889920	440	0.01	0.43	1.56	0.02	0.28	0.93	47	168
C-76-14-523	433950	6889920	430	0.02	0.57	0.29	0.04	1.97	0.90	63	32
C-76-14-589	433950	6889920	434	0.02	0.11	0.25	0.12	0.44	0.12	92	208
C-76-14-600	433950	6889920	432	0.02	0.84	0.34	0.03	2.47	1.21	69	28
C-76-14-601	433950	6889920	448	0.03	2.88	0.67	0.01	4.30	3.70	79	18
C-76-15-106	434070	6888500	430	0.05	1.00	2.24	0.05	0.45	1.92	53	117
C-76-15-111	434070	6888500	440	0.03	0.73	2.17	0.04	0.34	1.49	50	146
C-76-15-253	434070	6888500	434	0.07	2.93	1.02	0.02	2.87	3.07	96	33
C-76-15-257	434070	6888500	466	0.02	0.38	0.67	0.05	0.57	1.34	29	50
C-76-15-282	434070	6888500	437	0.03	1.56	0.33	0.02	4.73	1.26	125	26
T1-7 14.0	450400	6798400	452	0.01	0.08	2.45	0.15	0.03	0.21	38	1167
T9-5 192.3	439400	6703200	449	0.00	0.01	0.65	0.34	0.02	0.08	13	813
T9-9 452.0	439400	6703200	431	0.00	0.01	0.40	0.10	0.03	0.04	25	1000
T9-10 467.7	439400	6703200	402	0.03	0.10	0.45	0.25	0.22	0.06	167	750
T9-11 486.0	439400	6703200	436	0.01	0.04	0.90	0.22	0.04	0.12	33	750
T9-28 1179.2	439400	6703200	430	0.10	1.03	1.28	0.08	0.80	1.06	97	121
T9-30 1280.0	439400	6703200	437	0.03	1.12	2.20	0.02	0.51	1.68	67	131
T11-7 63.9	480600	6867600	458	0.01	0.15	0.65	0.07	0.23	0.54	28	120
T11-8 72.7	480600	6867600	487	0.02	0.22	0.89	0.07	0.25	0.62	35	144
T11-11 157.0	480600	6867600	339	0.02	0.02	0.99	0.50	0.02	0.12	17	825
T12-4	480500	6867500	344	0.02	0.06	0.32	0.29	0.19	0.10	60	320
T12-41	480500	6867500	577	0.02	0.03	0.27	0.33	0.11	0.39	8	69
T12-43	480500	6867500	520	0.01	0.29	1.29	0.04	0.22	1.12	26	115
T12-46	480500	6867500	482	0.04	0.41	0.39	0.08	1.05	0.94	46	41
T12-50	480500	6867500	368	0.02	0.05	0.29	0.34	0.17	0.11	45	264
T13-2 1.0	434300	6890300	443	0.02	0.35	0.69	0.05	0.51	0.80	44	86
T13-3 3.7	434300	6890300	438	0.05	3.48	3.36	0.01	1.04	4.89	72	69
T13-6 7.1	434300	6890300	435	0.05	1.57	2.42	0.03	0.65	2.91	55	83
T13-11 9.8	434300	6890300	424	0.13	0.34	1.15	0.27	0.30	0.25	136	460
T13-12 10.1	434300	6890300	436	0.04	0.57	1.31	0.06	0.44	1.13	51	116
T13-13 10.5	434300	6890300	435	0.06	1.36	1.26	0.04	1.08	2.27	61	56
T13-22 16.3	434300	6890300	436	0.04	0.64	0.83	0.06	0.77	1.22	53	68
T17-1 0.0	433800	6885200	309	0.32	0.24	0.26	0.57	0.92	0.15	160	173
T17-4 1.5	433800	6885200	359	0.04	0.10	0.41	0.26	0.24	0.11	91	373
T17-10 75.3	433800	6885200	327	0.81	2.12	0.79	0.28	2.68	0.55	385	144
T17-12 181.5	433800	6885200	452	0.11	0.70	2.77	0.14	0.25	1.29	55	215
T17-32 297.7	433800	6885200	441	0.05	0.14	1.25	0.29	0.11	0.49	29	255
T18-6 32.0	432900	6883400	335	0.03	0.07	0.27	0.32	0.26	0.13	54	208
T19-4 10.0	484700	6706900	515	0.00	0.02	0.73	0.15	0.03	0.34	6	215
T19-13 65.0	484700	6706900	336	0.01	0.03	0.51	0.22	0.06	0.21	14	243
T19-46 123.5	484700	6706900	521	0.01	0.05	2.12	0.20	0.02	2.12	2	100
T19-60 224.0	484700	6706900	334	0.00	0.00	0.46	0.50	0.00	0.03	0	1533

Tantalus formation (continued)

Sample	Easting	Northing	T _{max}	S1	S2	S3	PI	S2/S3	TOC	HI	OI
T20-7 3.0	485800	6705900	348	0.01	0.04	0.34	0.21	0.12	0.05	80	680
T22-22	495700	6686100	497	0.00	0.00	0.38	0.78	0.00	0.25	0	152
GL03-24A	434006	6890664	437	0.01	0.96	1.18	0.01	0.81	1.63	60	72
GL03-24B	434006	6890664	447	0.00	0.73	2.22	0.00	0.33	1.83	40	121
GL03-24C	434006	6890664	440	0.00	1.86	2.58	0.00	0.72	3.03	62	85
GL03-46E	438192	6867931	473	0.00	0.00	0.16	0.02	0.00	0.25	0	64
GL03-58B	455535	6802395	513	0.00	0.09	1.67	0.00	0.05	1.32	7	127
GL03-59C	455484	6803101	491	0.01	0.21	1.40	0.06	0.15	1.13	19	124
GL03-60B	454797	6804082	492	0.05	0.27	1.31	0.15	0.21	1.48	19	89
GL03-60C	454797	6804082	509	0.01	0.03	0.78	0.27	0.04	0.47	6	166
GL03-63B	457911	6803958	508	0.00	0.08	0.52	0.00	0.15	0.57	14	91
GL03-64B	457738	6804139	491	0.02	0.13	0.42	0.16	0.31	0.84	15	50
GL03-64D	457738	6804139	488	0.02	0.09	0.18	0.15	0.50	0.58	16	31
GL03-65A	457985	6803864	491	0.04	0.12	0.32	0.24	0.38	0.65	18	49
GL03-67C	438047	6814323	444	0.11	1.20	1.29	0.08	0.93	2.66	46	48
GL03-67D	438047	6814323	440	0.00	0.24	1.33	0.00	0.18	2.44	10	55
GL03-67F	438047	6814323	426	0.00	0.76	0.70	0.00	1.09	2.61	30	27
97-63-28	445122	6796798	430	0.05	1.14	0.35	0.04	3.26	1.04	111	34

Geology of the Quartet Mountain lamprophyre suite, Wernecke Mountains, Yukon

Dejan Milidragovic

Simon Fraser University¹, Yukon Geological Survey

Derek J. Thorkelson² and Daniel D. Marshall

Simon Fraser University¹

Milidragovic, D., Thorkelson, D.J. and Marshall, D.D., 2006. Geology of the Quartet Mountain lamprophyre suite, Wernecke Mountains, Yukon. *In: Yukon Exploration and Geology 2005*, D.S. Emond, G.D. Bradshaw, L.L. Lewis and L.H. Weston (eds.), Yukon Geological Survey, p. 231-245.

ABSTRACT

The Early Cambrian Quartet Mountain lamprophyres are volatile-rich ultramafic alkaline dykes that cross-cut the Wernecke and Mackenzie mountains supergroups in the Wernecke Mountains of northern Yukon. Their emplacement may have been triggered by Early Paleozoic extension of the Cordilleran miogeocline. Numerous small-volume alkalic igneous rocks that range in age from Cambrian to Devonian occur elsewhere in the miogeocline and may reflect a similar tectonic setting. The Quartet Mountain lamprophyres contain phenocrysts of phlogopite \pm diopside \pm olivine within a dark-grey aphanitic groundmass and were likely generated by low-percentage melting of mantle at depths >90 km. One of the lamprophyres contains abundant pseudomorphed olivine xenocrysts and xenoliths of inferred crustal and mantle affinities. Although this dyke resembles kimberlite because of its abundance of mantle xenoliths and xenocrysts and its ultramafic composition, it differs from kimberlite in its abundance of phlogopite phenocrysts. It is best described as an ultramafic lamprophyre with kimberlitic affinity. The lamprophyres have modest potential to host diamonds.

RÉSUMÉ

Les lamprophyres de Quartet Mountain du Cambrien précoce sont organisés en filons intrusifs alcalins ultrabasiques riches en composants volatils recoupant les supergroupes de Wernecke et de Mackenzie Mountains dans les monts Wernecke du Yukon septentrional. Leur mise en place fut possiblement déclenché lors de l'extension du miogéocline de la Cordillère au Paléozoïque précoce. Un grand nombre de masses de roches ignées alcalines de petit volume et d'âges s'étendant du Cambrien au Dévonien se retrouvent aussi ailleurs dans le miogéocline, ce qui peut refléter un environnement tectonique similaire. Les lamprophyres de Quartet Mountain sont gris-sombre, à matrice aphanitique avec cristaux dispersés de phlogopite \pm diopside \pm olivine et ont vraisemblablement été générés par fonte d'une faible proportion du manteau à des profondeurs excédant 90 km. Un des lamprophyres contient d'abondants xénocristaux d'olivine pseudomorphe et des xénolites présumés d'origines crustales et mantelliques. Malgré que ce filon, de par son abondance en xénolites et xénocristaux mantelliques et sa composition ultrabasique, ressemble aux kimberlites, son abondance en phénocristaux de phlogopite le distingue de celles-ci. On le dénommera ainsi lamprophyre ultrabasique à affinités kimberlitiques. Les lamprophyres ont un potentiel diamantifère limité.

¹Earth Sciences, Simon Fraser University, Burnaby, British Columbia, Canada V5A 1S6

²dthorkel@sfu.ca

INTRODUCTION

Early to Middle Paleozoic alkalic igneous rocks have been reported from numerous localities in the northern Cordilleran miogeocline from Alaska to southwestern Alberta (Cecile, 1982; Godwin and Price, 1986; Roots, 1988; Cecile and Norsford, 1992; Goodfellow *et al.*, 1995; Abbott, 1997). The igneous rocks consist of spatially restricted volcanic successions and small intrusions of alkalic to ultrapotassic composition and are interpreted to represent continental rift magmatism (Roots, 1988; Goodfellow *et al.*, 1995). Mid-Paleozoic mafic to ultramafic diatremes, at least one of which was interpreted to be a kimberlite, occur in the Mackenzie Mountains of western Northwest Territories (Godwin and Price, 1986). Late Ordovician to Mississippian, mafic, alkaline intrusions, including carbonatites, lamprophyres, lamproites and kimberlites, occur in a narrow, north-west trending belt that straddles the boundary of the Omineca and Foreland belts, along the length of British Columbia (Pell, 1994; Simandl, 2004). Kimberlites of Cambrian and Siluro-Ordovician ages are exposed to the east of the miogeocline in the Slave province of Northwest Territories (Heaman *et al.*, 2004) but are not demonstrably related to extension.

This paper provides new information on the Quartet Mountain lamprophyres (Thorkelson *et al.*, 2003), a set of ultramafic alkaline volatile-rich intrusions that cross-cut the Wernecke and Mackenzie mountains supergroups in the Wernecke Mountains of northern Yukon. They are exposed in a region between Fairchild Lake and Kiwi Lake, herein called the study area (Fig. 1). At least three members of the suite host abundant xenoliths of apparent mantle and crustal affinity. The lamprophyres and their xenoliths have potential to provide new and important information on the mantle and crustal conditions of northern Yukon at the time of their emplacement. Two preliminary ^{40}Ar - ^{39}Ar biotite and phlogopite dates indicate that the lamprophyres are early Cambrian (Fig. 1). One of the dates (ca. 522 Ma) was reported by Thorkelson (2000; see clarification in Thorkelson *et al.*, 2003) and the other (ca. 532 Ma) was recently obtained from the Pacific Centre for Geochemical and Isotopic Research (T. Ullrich, pers. comm., 2005). Two previous K-Ar dates of 552 ± 13 Ma and 613 ± 15 Ma (Delaney, 1981) suggest that the lamprophyres could be as old as Neoproterozoic. However, these ages are considered to be less accurate than the ^{40}Ar - ^{39}Ar ages and for that reason we interpret the lamprophyres as early Cambrian. Additional

geochronology is underway to more thoroughly address the age-range of the lamprophyres.

GEOLOGICAL SETTING

Emplacement of the Quartet Mountain lamprophyres took place during early development of the Paleozoic miogeocline of ancestral North America (Laurentia). The crustal architecture of the northern part of this miogeocline was largely inherited from Neoproterozoic rifting and concurrent deposition of the Windermere Supergroup. Several discrete episodes of rifting began at ca. 780 Ma and may have separated Laurentia from another continent (Ross, 1991; Colpron *et al.*, 2002; Harlan *et al.*, 2003). Along the northern proto-Pacific margin, extension and associated magmatism primarily occurred early in the history of Windermere deposition (Armstrong *et al.*, 1982; Roots and Parrish, 1988; Jefferson and Parrish, 1989; Heaman *et al.*, 1992; Dudas and Lustwerk, 1997). The basal Coates Lake and Rapitan groups were deposited in fault-bounded basins and embayments (Eisbacher, 1977; Jefferson, 1978) and were overlain by strata which record a transition from rift to continental shelf on a prograding passive margin (MacNaughton *et al.*, 2000). In the Early Cambrian, renewed extension led to further rifting of western Laurentia and division of the continental margin into deep clastic basins flanked by shallow carbonate platforms. The Quartet Mountain lamprophyres were emplaced into one of these shallower-water regions known as the Mackenzie Platform (Lenz, 1972). Extensional faulting continued sporadically until the Middle-Jurassic, when terrane collision led to imbrication and folding the miogeoclinal succession (Gordey and Anderson, 1993). Paleozoic magmatic activity, which occurred episodically from Cambrian until Late Devonian (Goodfellow *et al.*, 1995), is apparently related to the extension.

The northern Cordilleran miogeocline hosts minor Cambrian to Devonian alkaline to ultrapotassic igneous rocks that form thin, laterally restricted volcanic piles and intrusions along most of its strike length. In addition to the Quartet Mountain lamprophyres, known Paleozoic igneous rocks in the Mackenzie-Ogilvie platform are the Silurian Mountain, Bear and Stib diatremes (Godwin and Price, 1986) and the poorly studied Nash, Tuk and Silurian volcanics (unit Sv of Abbott, 1997). Godwin and Price (1986) proposed that the Mountain diatreme is a kimberlite, based on mineral chemistry and diagnostic indicator minerals, including micro-diamonds. The

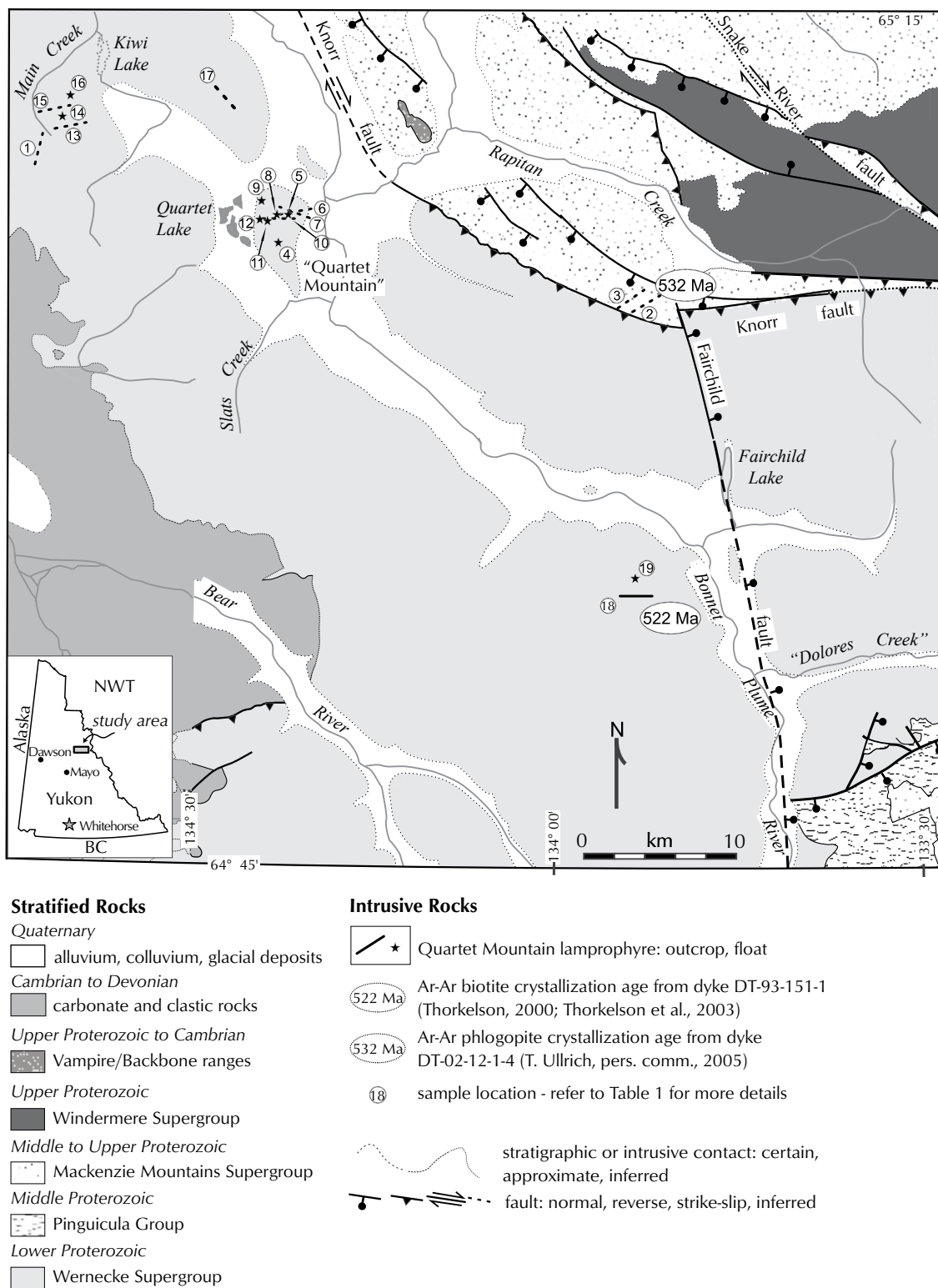


Figure 1. Geological map of the study area showing locations of the Quartet Mountain lamprophyres; modified from Gordey and Makepeace (2003), Schwab and Thorkelson (2000) and Thorkelson et al. (2005).

mineralogical and textural characteristics of the diatreme, however, are different from most kimberlites. Abundant volcanic rocks are exposed in the Selwyn Basin, a major paleogeographic element which lies to the southwest of the Mackenzie Platform. Geochemical data from these rocks are consistent with paleotectonic models of the Selwyn Basin that characterize it as a passive continental rift that underwent episodic reactivation from the Cambrian to Late Devonian (Cecile, 1982; Gordey and Anderson, 1993; Goodfellow *et al.*, 1995). Major volcanic episodes occurred in the Selwyn Basin in the Cambrian, Early to Middle Ordovician and Middle to Late Devonian (Goodfellow *et al.*, 1995). In British Columbia, temporal distribution of alkaline diatremes that include carbonatites, kimberlites, lamproites, lamprophyres and nepheline syenites indicate that they formed during three major periods of rifting in the Late Ordovician to Silurian, Early Devonian and Late Devonian (Pell, 1994).

QUARTET MOUNTAIN LAMPROPHYRE LOCATIONS AND FIELD RELATIONS

PREVIOUS WORK

Lamprophyres in the Wernecke Mountains were documented by several workers but have not been studied in detail. Locations and ages of the confirmed Quartet Mountain lamprophyres are provided in Table 1. Delaney (1981) first reported lamprophyres in the Wernecke Mountains in the vicinity of Kiwi Lake (Fig. 1). Hulstein (1994) mapped lamprophyres near the Gremlin and Chloe mineral occurrences in the same area. A few kilometres to the southeast, Laznicka and Gaboury (1988) recorded fine-grained grey weathering, tan to light-brown, olivine-biotite lamprophyres on the western and northern slopes of Quartet Mountain, a prominent and informally named feature west of the Bonnet Plume River (Fig. 1). They reported perovskite phenocrysts up to 1 cm long, but this finding has not yet been verified. Thorkelson and Wallace (1994) reported two biotite-phyric andesite dykes approximately 7 and 10 km southwest of Fairchild Lake (Fig. 1). Subsequently, Thorkelson *et al.* (2003) noted

Table 1. Locations of Quartet Mountain lamprophyres and available field measurements.

Sample	Lamprophyre field number	Location		1:50 000 NTS map sheet	Orientation (degrees)	Width (m)
		Easting	Northing			
1	DM-05-01-1-2	514617	7226946	106E/2	015/80	1.5
2	DT-02-12-1-4	546987	7219808	106F/4	240/85	0.15
3	DM-05-03-2-3	546610	7219902	106E/1	232/60	0.8
4	DM-05-04-1-1	528748	7222915	106E/1	float on top of ridge	-
5	DM-05-04-2-1	528950	7223483	106E/1	toppled	0.85
6	DT-02-7-1-1	529033	7223487	106E/1	290/80	2
7	DT-02-7-3-1	529033	7223487	106E/1	080/70	1.75
8	RBI-05-01-1-1	528607	7223554	106E/1	talus	-
9	DM-05-05-1-1	528037	7223962	106E/1	talus	-
10	DM-05-06-2-1	528632	7223374	106E/1	090/89	0.8
11	DM-05-06-3-1	528478	7223438	106E/1	float on top of ridge	-
12	DM-05-06-4-1	528273	7223543	106E/1	float on top of ridge	-
13	DM-05-07-1-1	516530	7227670	106E/2	260/89	1.2
14	DM-05-07-2-1	516037	7228640	106E/2	-	-
15	DM-05-07-4-1	515768	7229922	106E/2	steeply dipping at 255	1.5
16	TOA-96-8-1	516399	7230074	106E/2	float on top of ridge	-
17	DT-02-9-4-1	524225	7231523	106E/1	140/80	1-2
18	DT-93-151-1	553466	7197871	106C/13	270/90	-
19	-	-	-	106C/13	-	-

several dykes on and near Quartet Mountain and described them as brown-weathering, mafic, clinopyroxene- and phlogopite-phyric lamprophyres. Thorkelson *et al.* (2003) also noted a xenolith-rich lamprophyre dyke approximately 7 km south of Rapitan Creek, east of the Bonnet Plume River (Fig. 1). Thorkelson *et al.* (2003) assigned all the dykes mentioned above to a single igneous suite named the Quartet Mountain lamprophyres. We retain this name and extend it to additional lamprophyre localities described below.

RECENTLY DISCOVERED LOCALITIES

In July 2005, eleven new lamprophyres were discovered in a mountainous area southwest of Kiwi Lake and on the northern and western slopes of Quartet Mountain. In addition, two xenolith-rich lamprophyres south of Rapitan Creek previously identified by Thorkelson *et al.* (2003), were examined and sampled. Overall, approximately 200 kg of rock were collected for petrographic, geochemical, isotopic, and geochronological studies.

FIELD RELATIONS

The field information for all of the known Quartet Mountain lamprophyres is summarized in Table 1. North of Knorr fault (Fig. 1), the lamprophyres cross-cut the carbonate rocks of Mesoproterozoic to Neoproterozoic Mackenzie Mountains Supergroup. South of the Knorr fault the lamprophyres cross-cut the Paleoproterozoic metasedimentary rocks of the Wernecke Supergroup.

The lamprophyres are steeply dipping, range in width from 15 cm to 2 m (Fig. 2), and strike in a general east or southeast direction. The contact between the dykes and their host rocks ranges from sharp and regular to poorly defined and irregular. Intrusion of the dykes was partly controlled by pre-existing foliations or fractures in the host rock. Four of the eleven newly discovered dykes were observed in outcrop, whereas the other seven were observed as float. The lamprophyres are more prone to weathering and erosion than their host rocks, and commonly form trains of float on steep mountain sides. Abundant lamprophyre talus on the northern and western slopes of Quartet Mountain suggests that numerous dykes were emplaced in this area and lie beneath shallow talus and felsenmeer.



Figure 2. Sharp contact between steeply dipping lamprophyre DT-02-7-1-1 and laminated Quartet Group metasedimentary rocks.

LAMPROPHYRE PETROGRAPHY

Petrographic analysis of the Quartet Mountain lamprophyres was carried out using a combination of hand-sample analysis, conventional petrographic microscopy, and scanning electron microscopy (SEM). To date, only samples 2, 6, 7, 16, 17 and 18 have been petrographically characterized (Table 1). Sample 2 is texturally and mineralogically distinct from the rest of the suite and has some features that are characteristic of kimberlite. This sample is discussed in a separate section below.

The Quartet Mountain lamprophyres are light to dark grey, brown weathering, and porphyritic. In rare instances they contain abundant mafic xenoliths up to 4 cm in diameter (Fig. 3). The phenocrysts range from euhedral to anhedral,



Figure 3. Steeply dipping lamprophyre DM-05-03-2-3 hosting abundant mafic xenoliths. The xenoliths are concentrated near the centre of the dyke. Carbonate vein cuts the dyke (arrow).

vary in abundance, and include phlogopite, bladed diopside and equant pseudomorphed olivine. Apatite and unidentified opaque phenocrysts vary in abundance. Some samples contain abundant 0.2- to 3-mm-diameter amygdules that are filled with sparry carbonate and opaque minerals. Groundmass is pervasively altered to chlorite, clay and carbonate. Phlogopite and minor opaque minerals are the only primary groundmass minerals. It is unclear whether carbonate minerals in the groundmass are of primary or secondary origin.

The modal phlogopite abundance in the suite varies from 10-35%. The phlogopite phenocrysts are up to 3 mm long, are anhedral to euhedral, and commonly enclose diopside or opaque mineral inclusions. Phlogopite is variably altered to chlorite and a bright red mineral, possibly

hematite, and is commonly embayed. Modal diopside abundance ranges from 7-32%. The diopside grains are euhedral and commonly form radial aggregates. Chlorite alteration of diopside is common, but generally confined to crystal edges. Pseudomorphed olivine is an important phenocrystic and xenocrystic phase in most Quartet Mountain lamprophyres. No relict olivine was recorded in any of the samples, as it has been completely replaced by chlorite, carbonate and various opaque minerals. Distinction between xenocrystic and phenocrystic olivine was made on the basis of crystal size and shape. Olivine interpreted as xenocrysts is generally rounded to sub-rounded, whereas olivine interpreted as phenocrysts is euhedral. Diopside overgrowths occur on some olivine xenocrysts. With the exception of sample 2, the modal amount of pseudomorphed olivine ranges from 0 to 8%. The opaque phases include Ti-rich magnetite, pyrite, rutile and spinel and occur as both primary and secondary groundmass and phenocryst grains. They typically comprise a minor component of the rock mass. Apatite is euhedral, up to 0.5 mm long, and ranges in modal abundance from 1-2.5%.

Chemical compositions of major mineral phases of the Quartet Mountain lamprophyre suite were qualitatively determined using the energy dispersive analysis x-ray (EDAX) method at Simon Fraser University. Phlogopite in sample 6 was nearly pure phlogopite with sub-equal amounts of Fe and Ti substituting for approximately 5% of Mg.

The approximate formula of $\text{Ca}_{12}\text{Mg}_{0.6}\text{Fe}_{0.2}\text{Si}_2\text{O}_6$ for diopside was determined using EDAX.

Groundmass typically makes up approximately 30 to 40% of the whole rock mode in the Quartet Mountain lamprophyres. The pervasive replacement of groundmass minerals makes the Quartet Mountain lamprophyres impossible to classify according to the petrographic criteria of Rock (1987, 1991) or the International Union of Geological Sciences (Le Maitre, 2002), which require knowledge of both phenocryst and groundmass mineralogy. Consequently, the lamprophyres were classified on the basis of chemical composition in the geochemistry section below.

LAMPROPHYRE SAMPLE 2

Sample 2 (Table 1) differs from other samples of Quartet Mountain lamprophyre by its strong textural and mineralogical similarities to kimberlite, most notably the inequigranular texture and abundance of anhedral

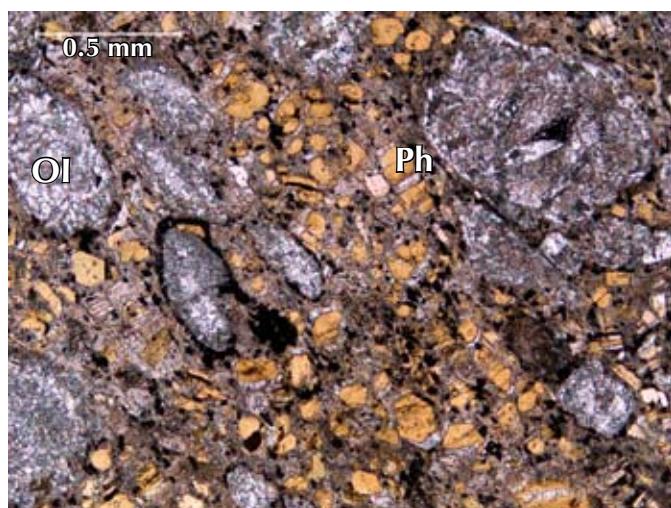


Figure 4. Pseudomorphed olivine macrocrysts (Ol) in fine groundmass composed of euhedral phlogopite (Ph), clay and carbonate (sample 2). Euhedral phlogopite groundmass crystals are uncommon in type I kimberlites.

xenocrystic olivine (Fig. 4). The three main petrographic components of this sample are xenoliths, large mineral grains (>0.5 mm) collectively termed macrocrysts, and groundmass.

The xenoliths are variably distributed in sample 2 and tend to occur in clusters. Three general types of xenoliths were identified. These are angular to sub-angular carbonate xenoliths of the Mackenzie Mountains Supergroup, crustal xenoliths of high metamorphic grade and mantle xenoliths. The latter two are discussed in greater detail in subsequent sections.

The macrocryst assemblage is composed of carbonate and chlorite pseudomorphs after olivine, phlogopite, and minor opaque minerals that include chromian spinel and rutile. The pseudomorphed olivine macrocrysts are inferred to be xenocrysts derived from disaggregation of peridotite xenoliths. The olivine macrocrysts show mesh texture that suggests serpentinization preceded carbonate replacement. Phlogopite grains are commonly euhedral and are therefore thought to be phenocrysts that were in equilibrium with the melt. Bent and kinked phlogopite grains, showing visible parting along the cleavage planes, are scattered throughout the rock and are probably xenocrysts. One phlogopite grain has oscillatory zoning, with an inner rim enriched in Mg and an outer rim and core depleted in Fe and Ti. EDAX shows that chromium content decreases outward toward the rim and that the inner rim is compositionally most similar to the phlogopite

from sample 6. The EDAX-estimated chemical formula of a chromian spinel macrocryst from sample 2 is $Mg_{0.67}Fe_{0.33}AlCrO_4$. The groundmass mineral assemblage consists of euhedral phlogopite, anhedral to euhedral opaque minerals, chlorite, clay and carbonate. Olivine and diopside are notably absent from groundmass.

The most striking characteristic of sample 2 is the presence of rounded anhedral olivine macrocrysts of variable size set in a fine-grained matrix. This texture is characteristic of kimberlites (Mitchell, 1986). Despite this similarity, other textural features and some important mineralogical characteristics of sample 2 differ from those of kimberlites. Specifically, the high abundance of cognate phlogopite and the apparent lack of microphenocrystic and groundmass olivine are inconsistent with type I kimberlites (Mitchell, 1986, 1995). The absence of groundmass or microphenocrystic diopside is atypical of type II kimberlites (Mitchell, 1995). We classify sample 2 as an ultramafic lamprophyre with kimberlitic affinity.

PETROGRAPHIC CHARACTERISTICS OF MANTLE XENOLITHS

The mantle xenoliths are well-rounded, grey-green to black, commonly elongated mafic inclusions up to 5 cm long (Fig. 5). An accurate mineral mode for the xenoliths could not be established, because alteration and replacement of primary minerals by serpentine, clay and carbonate minerals is near-complete. The xenoliths were most likely dominated by olivine, a conclusion supported in part by the ubiquitous pseudomorphed olivine xenocrysts. Minor, relict orthopyroxene grains, up to 3 mm in diameter stand out in serpentinized inclusions. EDAX indicates that the composition of these grains is



Figure 5. Dark green, ovoid, serpentinized mantle xenolith (circled) from sample 2.

approximately En_{95} . Most grains are partly altered to sericite and are unusually rich in potassium. Trace relict clinopyroxene was identified in one xenolith. Another xenolith contains abundant garnet. Opaque minerals that include pyrite and hematite account for approximately 20% of the mantle xenolith mode. Growth of secondary phlogopite near the xenolith margins is a consequence of reaction between the lamprophyre melt and the entrained inclusions. On the basis of observed mineralogy, the Early Cambrian upper mantle in this region was composed of, at least in part, garnet-peridotite.

PETROGRAPHIC CHARACTERISTICS OF CRUSTAL XENOLITHS

The crustal xenoliths are less abundant than the mantle xenoliths, but are generally better preserved, allowing for more accurate characterization. They occur as rounded inclusions of garnet-sillimanite-quartz gneiss (Fig. 6), garnet-quartz gneiss, and foliated plagioclase-rich metamorphic rock.

The garnet-sillimanite-quartz gneiss contains thin bands (<2 mm) of fine-grained, quartz crystals. The quartz grains are locally separated by a thin hematite film. Within the quartz bands, small (20 μm -120 μm), well-rounded, isolated grains of zircon occur. Individual quartz bands are separated by equally thin discontinuous bands of garnet and sillimanite. The garnet grains are irregularly shaped and heavily fractured. Chlorite and iron-oxide lines the fractures. Garnet composition was estimated, using EDAX, as 60% pyrope and 40% almandine with minor Ca. Garnet forms bands on its own, or in association with sillimanite. Sillimanite grains are irregular, approximately 0.05 mm in diameter and set in a potassium feldspar groundmass. Monazite, rutile and zircon occur as isolated grains within the garnet grains, or

as isolated interstitial minerals in association with both garnet and sillimanite.

The gneissic xenoliths are pervasively altered along their margins, where a combination of calcite, phlogopite, hematite, clay and/or sericite replaced all minerals except quartz. The gneiss is cut by calcite veinlets that are truncated at the xenolith margins, indicating that the veining predated the incorporation of xenoliths into the lamprophyre magma.

A single feldspathic xenolith was identified in sample 2. The feldspathic xenolith is composed of sub-parallel laminae of polygonal to irregular-shaped feldspar grains, thin carbonate laminae and minor, very thin, opaque laminae. The feldspar layers are compact, 0.5-2 mm wide, and contain a few percent interstitial opaque minerals. The feldspar is dominantly plagioclase, and grains range in size from 0.1- 0.9 mm. The carbonate laminae are approximately 0.2 mm thick.

GEOCHEMISTRY

Geochemical data exist for five of the eighteen known Quartet Mountain lamprophyres (Table 2; Thorkelson, 2000; Milidragovic, 2005). The major element contents that are discussed in this and the following sections have been normalized to a volatile-free basis (data are not normalized in Table 2, but values discussed in text are normalized).

MAJOR ELEMENT GEOCHEMISTRY

The Quartet Mountain lamprophyres are characterized by high volatile contents that range between 4.7 and 24.8%. Volatile content of samples 6, 7, 16 and 18 is probably dominated by H_2O , as carbonate alteration is minor, and hydrous minerals such as chlorite and phlogopite are

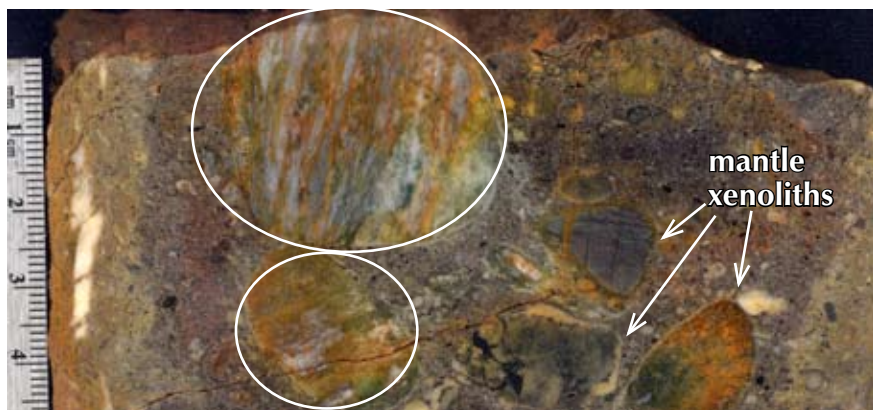


Figure 6. Finely banded, garnet-sillimanite-quartz gneiss xenolith (circled) in sample 2. Darker, serpentinized mantle xenoliths are located in the right half of the photograph.

abundant. The higher volatile content of sample 2 is likely a result of the greater abundance of xenoliths and xenocrysts, most of which are rich in carbonate and/or hydrous minerals, and thus probably contain significant H₂O and CO₂. Whole rock Mg numbers, defined as atomic Mg / (Mg + Fe)*100, of the Quartet Mountain

lamprophyre suite range from 63 to 86. The suite is silica-undersaturated, and has SiO₂ contents that vary from 32.3% to 43.4%, and normative nepheline contents that range from 0.37 to 5.28 wt.%. The high P₂O₅ concentration in sample 16 is consistent with its high apatite content. The suite plots in the alkaline field on the

Table 2. Major and trace element data from the Quartet Mountain lamprophyres. Data have not been normalized to a volatile-free basis. Data for sample 18 is from Thorkelson (2000). Data for samples 2, 6, 7 and 16 is from Milidragovic (2005).

	Sample number				
	2	6	7	16	18
Major oxides (wt%)					
SiO ₂	23.78	39.63	40.19	31.03	37.40
TiO ₂	1.420	3.259	3.287	3.760	3.500
Al ₂ O ₃	2.83	7.8	8.34	6.33	6.62
FeO					6.8
Fe ₂ O ₃	7.56	13.00	13.19	13.47	14.10
MnO	0.12	0.19	0.26	0.31	0.44
MgO	19.43	15.38	14.73	14.18	16.00
CaO	16.29	11.50	11.39	14.82	9.20
Na ₂ O	0.06	1.07	0.87	0.18	0.46
K ₂ O	1.89	1.37	1.03	2.60	1.01
P ₂ O ₅	1.01	0.63	0.69	1.95	0.86
LOI	24.80	4.71	4.95	10.20	7.25
Trace elements (ppm) NOTE: * - ppb ** - wt.%					
Cs	3.47	2.74	3.65	3.33	3.12
Tl	0.34	0.15	0.14	0.12	0.15
Rb	86.2	43.62	31.96	91.74	38.31
Ba	1204	983	543	2160	4263
W	6	-1	2	1.82	
Th	29.47	6.91	7.16	23.17	8.74
U	4.69	1.73	1.75	3.85	2.42
Nb	168.59	84.41	89.31	157.29	122.42
Ta	7.86	5.02	5.27	8.12	5.94
La	194.44	56.02	59.42	194.54	66.78
Ce	360.11	111.31	118.65	380.45	134.02
Pb	13.52	11.45	9.42	-5	6.38
Pr	39.06	12.96	13.75	37.33	16.21
Sr	1544	432	388	950.9	845.83
Nd	138.54	51.9	54.0	157.25	64.24
Sm	20.30	10.85	11.57	26.29	12.12
Zr	258.41	259.96	268.49	354.39	317.77
Hf	6.47	6.64	6.53	8.82	7.59
Eu	4.90	3.01	3.25	6.44	3.58

	Sample number				
	2	6	7	16	18
Major oxides (wt%)					
Sn	1.66	2.44	3.59	2.00	3.14
Sb	0.9	0.8	0.9	0.71	1.61
Gd	11.84	8.24	8.56	18.6	11.11
Tb	1.46	1.18	1.22	2.25	1.23
Dy	5.59	5.09	5.32	9.56	6.53
Y	20	21	22	41.5	24.64
Ho	0.79	0.78	0.81	1.4	1.03
Er	1.82	1.86	2.06	3.44	2.26
Tm	0.21	0.23	0.25	0.305	0.30
Yb	1.23	1.37	1.45	1.87	1.44
Lu	0.13	0.17	0.17	0.259	0.19
Zn	80.27	106.53	109.09	302	408.04
V	100	248	250	220	321.7
Sc	20.1	27.5	24.1		23.84
Co	74.2	84.1	86.1	97.1	84
Cu	18.92	67.16	63.69	-5	19.37
Cr	1220	734	736	364	851
Ni	744	457	458	412	591
Ag	-0.3	0.6	0.4	-0.5	
Cd	-0.3	-0.3	-0.3		
Au*	3	-1	6		
As	8	3	4	8	
Br	-0.5	-0.5	-0.5		
Hg	-1	-1	-1		
Ir*	-1	-1	-1		
Mo	-2	-2	2	1.5	
Se	-0.5	-0.5	-0.5		
Ga	9.1	19.4	20.9	19	
Ge	2.8	1.4	1.4	1.4	
In	-0.1	-0.1	-0.1	0.1	
Sn	1.658	2.438	3.595	2	
S**	0.093	0.124	0.284		

total alkali vs. silica diagram (Irvine and Baragar, 1971). Xenolith-poor samples 6, 7, 16 and 18 show positive correlation between Al_2O_3 , Na_2O and SiO_2 , and negative correlation between SiO_2 , TiO_2 and K_2O .

The ultramafic character and presence of normative nepheline precludes the Quartet Mountain lamprophyres from being classified as calc-alkaline lamprophyres of Rock (1987, 1991). This is further supported by the positive Ta-Nb ± Ti anomaly (see trace element geochemistry section below) that is characteristic of the suite, but highly uncharacteristic of calc-alkaline lamprophyres. The metaluminous composition of the Quartet Mountain lamprophyres is inconsistent with the characteristically peralkaline composition of lamproites. The Quartet Mountain lamprophyres are best classified as ultramafic lamprophyres rather than alkaline lamprophyres (Fig. 7). None of the Quartet Mountain lamprophyres plot in the kimberlite field of Figure 8.

TRACE ELEMENT GEOCHEMISTRY

The Quartet Mountain lamprophyres are enriched in all trace elements (Fig. 9) relative to the primitive mantle values of Sun and McDonough (1989). Although the enrichment factors within the suite vary by as much as 10 times for the most incompatible elements (e.g., Ba), the overall trace element patterns throughout the suite are very similar. The concentrations of the highly mobile, large ion lithophile elements likely reflect post-emplacment processes, which are evidenced by pervasive groundmass alteration; hence, their

concentrations likely do not have major genetic implications. The lamprophyres are characterized by a positive Ta-Nb ± Ti anomaly. Like many of the rocks hosted by the northern Cordilleran miogeocline, the Quartet Mountain lamprophyres show $Nb/Y > 1$ (Fig. 10), $Zr/Nb < 6$ and $Ce/Y > 2$. The Neoproterozoic volcanic rocks of Yukon are characterized by distinctly lower high field strength element abundances and have significantly lower Nb/Y, Zr/Y, Nb/Zr and Ce/Y ratios. Ni and Cr concentrations of 774 and 1220 ppm, respectively, in sample 2 probably reflect the abundance of mantle xenoliths in this sample. The xenolith-free samples have Ni and Cr concentrations between 412 and 591 ppm and 364 and 851 ppm, respectively.

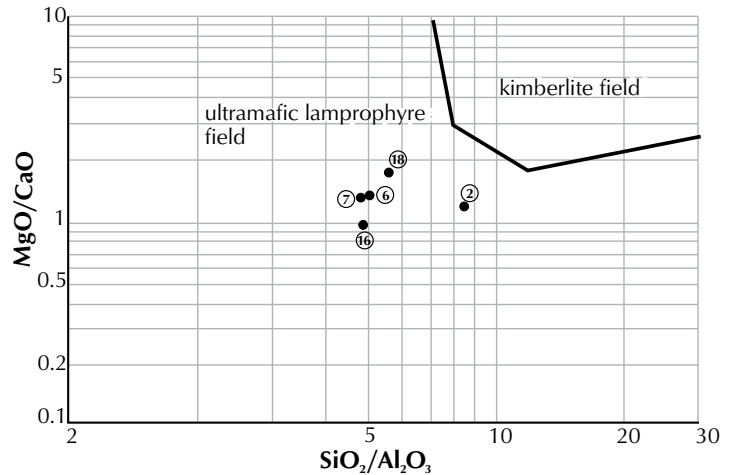


Figure 8. Classification diagram for ultramafic lamprophyres and kimberlites. Quartet Mountain lamprophyres plot in the ultramafic lamprophyre field. Modified from Rock (1991).

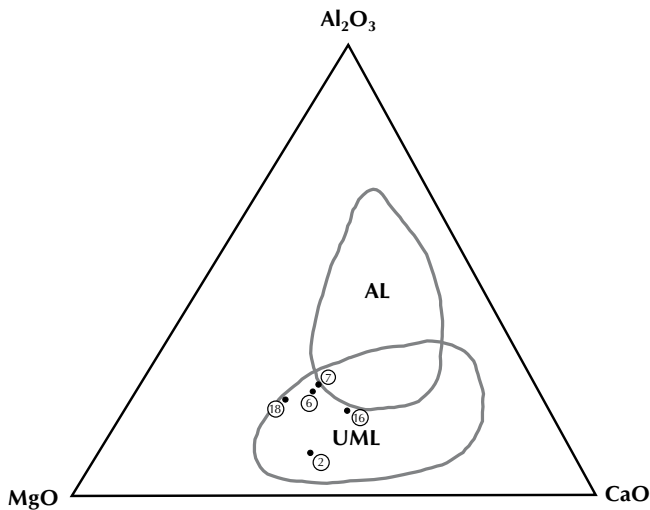


Figure 7. Classification diagram for ultramafic (UML) and alkaline (AL) lamprophyre types showing ultramafic composition of Quartet Mountain lamprophyres (from Rock, 1987).

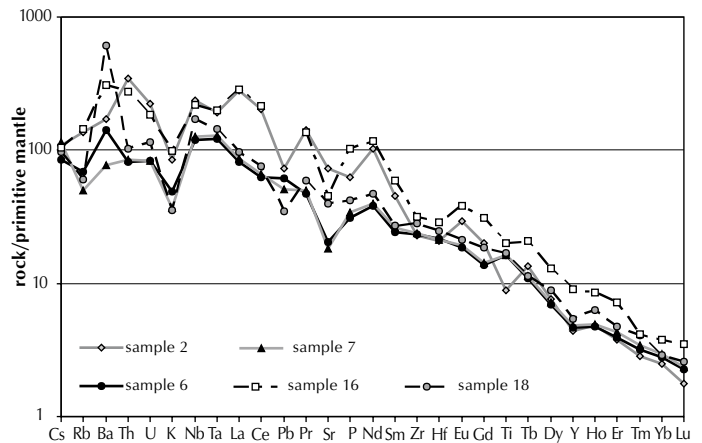


Figure 9. Trace element profiles of Quartet Mountain lamprophyres, normalized to primitive mantle values of Sun and McDonough (1989).

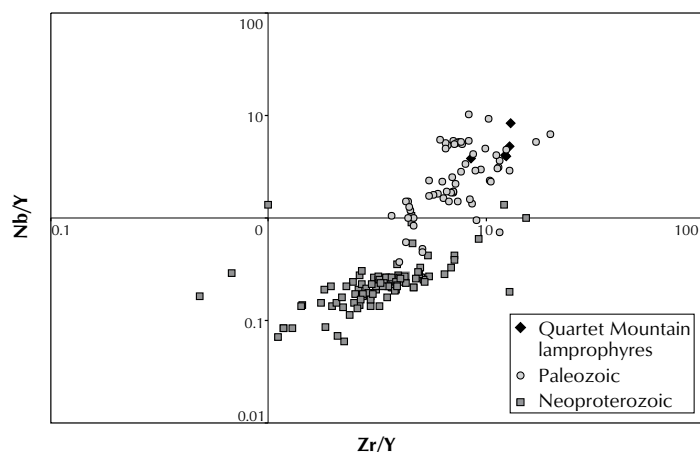


Figure 10. Nb/Y vs. Zr/Y diagram comparing Neoproterozoic and Paleozoic igneous rocks in Mackenzie Platform and Selwyn Basin. Data is from Godwin and Price, 1986; Roots, 1988; Goodfellow et al., 1995; Abbott, 1997; Dudas and Lustwerk, 1997; Mustard and Roots, 1997.

Rare earth element (REE) concentrations suggest the lamprophyres are strongly fractionated (Fig. 9). Chondrite-normalized (Sun and McDonough, 1989) La values range from 236-821 and Lu values range from 5.2-10.2, suggesting an origin as low-degree partial melts. Sample 2 has the highest LREE and the lowest HREE concentrations, and the most fractionated pattern. Samples 6, 7 and 18 show nearly identical REE patterns and very similar overall trace element distributions. Sample 16 shows a significant LREE enrichment relative to samples 6, 7, and 18. Although it is probable that some of the trace element differences are due to variable post-emplacment processes, it is possible that samples 2 and 16 represent smaller degree partial melts derived from the same source as samples 6, 7, and 18. Alternatively, these samples may have originated as partial melts from a different mantle source.

GEOLOGICAL SIGNIFICANCE

The preliminary Ar-Ar phlogopite dates of ca. 522 Ma (Thorkelson, 2000; Thorkelson et al., 2003) and ca. 532 Ma (Ullrich, pers. comm.) suggest an Early Cambrian emplacement age for the Quartet Mountain ultramafic lamprophyres. Ultramafic lamprophyres are typically emplaced in divergent margin and intraplate tectonic settings (Rock, 1991), and hence fit the general tectonic model of passive margin subsidence punctuated by episodic extensional events for the

northern Cordilleran miogeocline (Gordey and Anderson, 1993; Goodfellow et al., 1995). Numerous, small volume, alkalic, volcanic rocks that have been interpreted as extension related (Roots, 1988; Pell, 1994; Goodfellow et al., 1995) occur along the length of the miogeocline, ranging in age from Cambrian to Devonian. Their alkaline character, timing of emplacement and immobile element ratios are broadly similar to those of the Quartet Mountain lamprophyres, although a petrogenetic link has not been established. Paleozoic kimberlite magmatism in the Slave craton includes the 523-535 Ma Snap Lake dyke (Heaman et al., 2004), which is coeval with the Quartet Mountain lamprophyres. Geological controls on the emplacement of the Slave kimberlites are poorly understood, but they are not thought to be related to the extensional tectonism that affected the northern Cordilleran miogeocline.

The mantle origin of the Quartet Mountain lamprophyres, their ultramafic character, the kimberlitic affinity of sample 2, and the proximity of the Quartet Mountain lamprophyres to the microdiamond-bearing Mountain diatreme command the assessment of the lamprophyres' diamond potential. Diamond-bearing occurrences of ultramafic lamprophyres exist in Canada (e.g., Ile Bizard, Torngat; Rock, 1991; Kjarsgaard and Levinson, 2002) but, together with Type II kimberlites and lamproites, they account for only a small percentage (~8%) of the world's total diamond production. Type I kimberlites, and marine and alluvial sediments are the dominant sources of world's diamond supply (Willmott, 2004). For the lamprophyres to be diamondiferous they must have been generated at depths of at least 140 km from a Cambrian lithospheric mantle root under appropriate physical and geochemical conditions. The garnet-bearing mantle xenoliths in sample 2 constrain the depth of origin of that lamprophyre to at least 90 km (Fig. 11). Factors influencing the suitability of the mantle root include its age, composition, thickness, oxygen fugacity, geothermal gradient and metasomatic history (Haggerty, 1986; Helmstaedt and Gurney, 1995). These factors are presently undetermined for the mantle beneath Yukon in the Cambrian. Based on the interpreted tectonic history of the region, the likelihood of diamondiferous mantle beneath northern Yukon during the Cambrian is modest. Neoproterozoic to Cambrian rifting is likely to have modified the existing mantle root, making it thinner, warmer and less likely to retain a keel of diamond-bearing peridotite and eclogite. Further work is required to more closely ascertain the diamond potential of the lamprophyres.

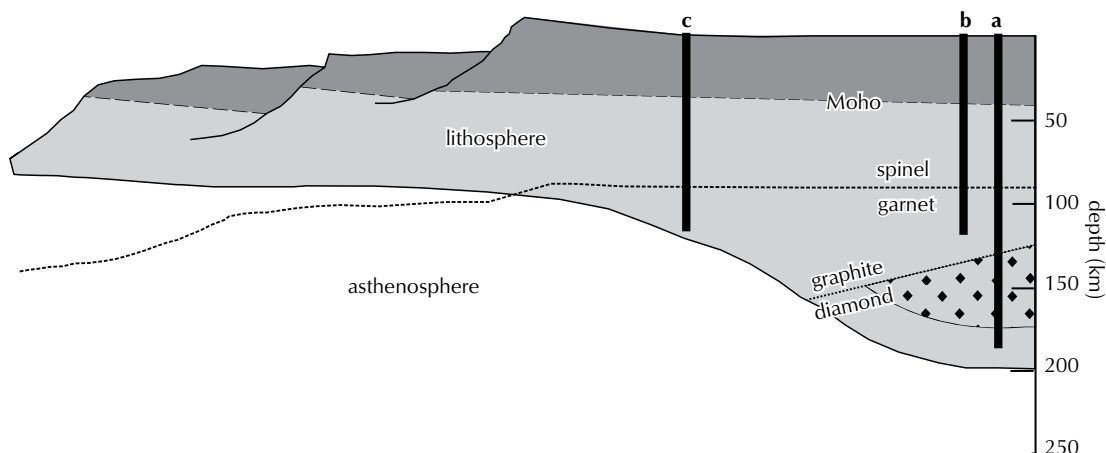


Figure 11. A conceptual cross-section of the crust and upper mantle across the northwestern margin of Early Paleozoic North America. The “diamond window” is illustrated by black diamonds and indicates the area of lithosphere in which diamonds are stable (below approximately 140 km and between 900-1200°C). Conduit **a** illustrates the generation depth and tectonic setting that favours diamond entrainment. Conduit **b** illustrates the source region in a favourable setting, but at a depth that is too shallow for diamond entrainment. The source region of conduit **c** illustrates an unfavourable tectonic setting in which attenuation of the continental lithosphere caused complete disappearance of the potentially diamondiferous mantle root. Which conduit most accurately represents the Quartet Mountain lamprophyres is uncertain.

CONCLUSIONS

The Quartet Mountain lamprophyres in the study area are phlogopite- ± diopside- ± olivine-phyric dykes that are exposed over a 40 km by 35 km area in the Wernecke Mountains. The lamprophyres crosscut the Paleoproterozoic and Mesoproterozoic strata of the Wernecke and Mackenzie mountains supergroups. Preliminary Ar-Ar dates from phlogopite of ca. 522 Ma (Thorkelson *et al.*, 2003) and ca. 532 Ma (T. Ullrich, pers. comm.) suggest an Early Cambrian age.

Trace element compositions suggest that the lamprophyres were derived by small degrees of partial melting of a parent mantle source. Major and trace element geochemistry, in addition to the limited petrographic information, is consistent with the classification of the Quartet Mountain lamprophyres as ultramafic lamprophyres.

Sample 2 contains mantle and crustal xenoliths, large anhedral to euhedral minerals collectively termed macrocrysts and groundmass. The inequigranular texture of sample 2 is similar to that of kimberlite, but this rock is best classified as ultramafic lamprophyre, based on petrographic and geochemical criteria. A detailed study of the xenoliths is in progress and may yield important

information about the lithospheric architecture of Early Cambrian northwestern North America.

The diamond potential of the Quartet Mountain lamprophyres is modest. The current models for the Early Paleozoic evolution of North America do not favour the presence of a widespread “diamond window” in the lithospheric mantle beneath the Cordillera. However, the nature of the mantle beneath the Mackenzie platform, which hosts the lamprophyres and has undergone less extension than neighbouring regions such as the Selwyn Basin, has not been thoroughly investigated.

ACKNOWLEDGMENTS

Funding was provided by the Yukon Geological Survey, an NSERC grant to D. Thorkelson, and a Northern Studies Training Program grant to D. Milidragovic. We thank Tom Ullrich from the Pacific Centre for Geochemical and Isotopic Research for the preliminary Ar-Ar phlogopite date from lamprophyre DT-02-12-1-4, Maya Kopylova for allowing access to her kimberlite and lamprophyre collection, and Ryan Ickert for field assistance. Comments by critical readers Dan Gibson and Geoff Bradshaw led to significant improvements.

REFERENCES

- Abbott, G., 1997. Geology of the Upper Hart River area, Eastern Ogilvie Mountains, Yukon Territory (116A/10, 116A/11). Exploration and Geological Services Division, Yukon, Indian and Northern Affairs Canada, Bulletin 9, 76 p.
- Armstrong, R.L., Eisbacher, G.H. and Evans, P.D., 1982. Age and stratigraphic-tectonic significance of Proterozoic diabase sheets, Mackenzie Mountains, northwestern Canada. *Canadian Journal of Earth Sciences*, vol. 19, p. 316-323.
- Cecile, M.P., 1982. The Lower Paleozoic Misty Creek embayment, Selwyn Basin, Yukon and Northwest territories. *Bulletin, Geological Survey of Canada*, vol. 335, 78 p.
- Cecile, M.P. and Norford, B.S., 1992. Enriched: Cambrian to Middle Devonian assemblages; Ordovician and Silurian assemblages. *In: Geology of the Cordilleran Orogen in Canada*, H. Gabrielse and C.J. Yorath (eds.). Geological Survey of Canada.
- Colpron, M., Logan, J.M. and Mortensen, J.K., 2002. U-Pb zircon age constraint for Late Neoproterozoic rifting and initiation of the Lower Paleozoic passive margin of western Laurentia. *Canadian Journal of Earth Science*, vol. 39, p. 133-136.
- Delaney, G.D., 1981. The Mid-Proterozoic Wernecke Supergroup, Wernecke Mountains, Yukon Territory. *In: Proterozoic basins of Canada*, Halifax, Nova Scotia, p. 1-23.
- Dudas, F.O. and Lustwerk, R.L., 1997. Geochemistry of the Little Dal basalts; continental tholeiites from the Mackenzie Mountains, Northwest Territories, Canada. *Canadian Journal of Earth Sciences*, vol. 34, p. 50-58.
- Eisbacher, G.H., 1977. Tectono-stratigraphic framework of the Redstone copper belt, district of Mackenzie. Geological Survey of Canada, Paper 77-1A, p. 229-234.
- Godwin, C.I. and Price, B.J., 1986. Geology of the Mountain Diatreme kimberlite, north-central Mackenzie Mountains, District of Mackenzie, Northwest Territories. *In: Mineral deposits of Northern Cordillera symposium*, Whitehorse, Yukon, vol. 37, p. 298-310.
- Goodfellow, W.D., Cecile, M.P., and Leybourne, M.I., 1995. Geochemistry, petrogenesis, and tectonic setting of Lower Paleozoic alkalic and potassic volcanic rocks, Northern Canadian Cordilleran Miogeocline. *Canadian Journal of Earth Sciences*, vol. 32, p. 1236-1254.
- Gordey, S.P. and Anderson, R.G., 1993. Evolution of the Northern Cordilleran Miogeocline, Nahanni map area (1051), Yukon and Northwest Territories, Geological Survey of Canada, Memoir 428, 214 p.
- Gordey, S.P. and Makepeace, A.J. (compilers), 2003. Yukon Digital Geology (version 2). Yukon Geological Survey, Open File 2003-9(D); also known as Geological Survey of Canada Open File 1749, 2 CD-ROMs.
- Haggerty, S.E., 1986. Diamond genesis in a multiply-constrained model. *Nature (London)*, vol. 320, p. 34-38.
- Harlan, S.S., Heaman, L., LeCheminant, A.N. and Premo, W.R., 2003. Gunbarrel mafic magmatic event: A key 780 Ma time marker for Rodinia plate reconstructions. *Geology*, vol. 31, p. 1053-1056.
- Heaman, L.M., LeCheminant, A.N. and Rainbird, R.H., 1992. Nature and timing of Franklin igneous events, Canada: Implications for a Late Proterozoic mantle plume and the break-up of Laurentia. *Earth and Planetary Science Letters*, vol. 109, p. 117-131.
- Heaman, L.M., Kjarsgaard, B.A. and Creaser, R.A., 2004. The temporal evolution of North American kimberlites. *Lithos*, vol. 76, p. 377-397.
- Helmstaedt, H.H. and Gurney, J.J., 1995. Geotectonic controls of primary diamond deposits; implications for area selection. *Journal of Geochemical Exploration*, vol. 53, p. 125-144.
- Hulstein, R., 1994. Assessment Report on the 1993 geological and geochemical investigation of the Kiwi Property, Kennecott Canada Inc., Mayo Mining District, Yukon Territory, NTS map area 106E/2. Energy, Mines and Resources, Government of Yukon, Assessment Report, 23 p.
- Irvine, T.N. and Baragar, W.R.A., 1971. A guide to the chemical classification of the common volcanic rocks. *Canadian Journal of Earth Sciences*, vol. 8, p. 523-548.

- Jefferson, C.W., 1978. Stratigraphy and sedimentology, Upper Proterozoic Redstone Copper Belt, Mackenzie Mountains, Northwest Territories: A preliminary report. *In: Mineral industry report for 1975, Northwest Territories; Department of Indian Affairs and Northern Development, Exploration and Geological Services Unit, Yellowknife, Northwest Territories, Report EGS 1978-5, p. 157-169.*
- Jefferson, C.W. and Parrish, R.R., 1989. Late Proterozoic stratigraphy, U-Pb zircon ages, and rift tectonics, Mackenzie Mountains, northwestern Canada. *Canadian Journal of Earth Sciences*, vol. 26, p. 1784-1801.
- Kjarsgaard, B.A. and Levinson, A.A., 2002. Diamonds in Canada. *Gems and Gemology*, vol. 38, p. 208-238.
- Laznicka, P. and Gaboury, D., 1988. Wernecke breccias and Fe, Cu, U mineralization: Quartet Mountain-Igor area (NTS 106E). *In: Yukon Geology, Volume 2, J.G. Abbott (ed.), Exploration and Geological Services Division, Yukon Region, Indian and Northern Affairs Canada, p. 42-50.*
- Le Maitre, R.W. (ed.), 2002. *Igneous rocks; a classification and glossary of terms; recommendations of the International Union of Geological Sciences Subcommission on the systematics of igneous rocks.* Cambridge, Cambridge University Press, United Kingdom, 236 p.
- Lenz, A.C., 1972. Ordovician to Devonian history of northern Yukon and adjacent District of Mackenzie. *Bulletin of Canadian Petroleum Geology*, vol. 20, p. 321-359.
- MacNaughton, R.B., Narbonne, G.M., and Dalrymple, R.W., 2000. Neoproterozoic slope deposits, Mackenzie mountains, northwestern Canada: Implications for passive-margin development and ediacaran faunal ecology. *Canadian Journal of Earth Sciences*, vol. 37, p. 997-1020.
- Milidragovic, D., 2005. Petrography and geochemistry of the Quartet lamprophyres, Unpublished B.Sc. thesis, Simon Fraser University, 38 p.
- Mitchell, R.H., 1986. Kimberlites; mineralogy, geochemistry, and petrology. Plenum Press, New York, 442 p.
- Mitchell, R.H., 1995. Kimberlites, orangeites, and related rocks. Plenum Press, New York, 410 p.
- Mustard, P.S. and Roots, C.F., 1997. Rift-related volcanism, sedimentation, and tectonic setting of the Mount Harper Group, Ogilvie Mountains, Yukon Territory. *Geological Survey of Canada, Bulletin 492, 92 p.*
- Pell, J., 1994. Carbonatites, nepheline syenites, kimberlites and related rocks in British Columbia. *British Columbia Ministry of Energy, Mines and Petroleum Resources, Bulletin 88, 133 p.*
- Rock, N.M.S., 1987. The nature and origin of lamprophyres; an overview. *In: Alkaline igneous rocks, J. Fitton and B. Upton (eds.), Geological Society of London, Special Publication, vol. 30, p. 191-226.*
- Rock, N.M.S., 1991. *Lamprophyres.* Blackie & Son, Glasgow, United Kingdom, 285 p.
- Roots, C.F., 1988. Cambro-Ordovician volcanic rocks in eastern Dawson map-area, Ogilvie Mountains, Yukon. *In: Yukon Geology, Volume 2, Exploration and Geological Services Division, Yukon Region, Indian and Northern Affairs Canada, p. 81-87*
- Roots, C.F. and Parrish, R.R., 1988. Age of the Mount Harper volcanic complex, southern Ogilvie Mountains, Yukon. *Radiogenic Age and Isotope Studies: Report 2, Geological Survey of Canada, Paper 88-2, p. 29-35.*
- Ross, G.M., 1991. Tectonic setting of the Windermere Supergroup revisited. *Geology*, vol. 19, p. 1125-1128.
- Schwab, D.L., Thorkelson, D.J., 2000. Geology and alteration signature of a Middle Proterozoic Bear River dyke in the Slats Creek map area, Wernecke Mountains, Yukon (106D/16). *In: Yukon Exploration and Geology 2001, D.S. Emond and L.H. Weston (eds.), Exploration and Geological Services Division, Yukon Region, Indian and Northern Affairs Canada, p. 257-266.*
- Simandl, G.J., 2004. Concepts for diamond exploration in "on/off craton" areas; British Columbia, Canada. *Lithos*, vol. 77, p. 749-764.
- Sun, S.S. and McDonough, W.F., 1989. Chemical and isotopic systematics of oceanic basalts; implications for mantle composition and processes. *In: Magmatism in the ocean basins, Geological Society of London, Special Publication, vol. 42, p. 313-345.*

- Thorkelson, D.J., 2000. Geology and mineral occurrences of the Slats Creek, Fairchild Lake and “Dolores Creek” areas, Wernecke Mountains, Yukon (106D/16, 106C/13, 106C/14). Exploration and Geological Services Division, Yukon Region, Indian and Northern Affairs Canada, Bulletin 10, 73 p.
- Thorkelson, D.J. and Wallace, C.A., 1994. Geological setting of mineral occurrences in Fairchild Lake map area (106C/13), Wernecke Mountains, Yukon. *In: Yukon Exploration and Geology 1993*, Exploration and Geological Services Division, Yukon Region, Indian and Northern Affairs Canada, p. 79-92.
- Thorkelson, D.J., Laughton, J.R., Hunt, J.A. and Baker, T., 2003. Geology and mineral occurrences of the Quartet Lakes map area (NTS 106E/1), Wernecke and Mackenzie mountains, Yukon. *In: Yukon Exploration and Geology 2002*, D.S. Emond and L.L. Lewis (eds.), Exploration and Geological Services Division, Yukon Region, Indian and Northern Affairs Canada, p. 223-239.
- Thorkelson, D.J., Abbott, J.G., Mortensen, J.K., Creaser, R.A., Villeneuve, M.E., McNicoll, V.J. and Layer, P.W., 2005. Early and Middle Proterozoic evolution of Yukon, Canada, *Canadian Journal of Earth Sciences*, vol. 42, p. 1045-1071.
- Willmott, E., 2004. World diamond production. *Rough Diamond Review*, December, 2004.

Compositional studies of placer and lode gold from western Yukon: Implications for lode sources

Jim K. Mortensen

Earth and Ocean Sciences, University of British Columbia¹

Rob Chapman

School of Earth Sciences, University of Leeds²

William LeBarge

Yukon Geological Survey³

Evan Crawford

Earth and Ocean Sciences, University of British Columbia¹

Mortensen, J.K., Chapman, R., LeBarge, W. and Crawford, E., 2006. Compositional studies of placer and lode gold from western Yukon: Implications for lode sources. *In: Yukon Exploration and Geology 2005*, D.S. Emond, G.D. Bradshaw, L.L. Lewis and L.H. Weston (eds.), Yukon Geological Survey, p. 247-255.

ABSTRACT

On-going compositional studies of gold from placer and lode deposits and occurrences in western Yukon provide new insights into their nature and origin. Two main compositional populations are present in placer and lode deposits in the Klondike District. The dominant population has high fineness and low mercury content, and appears to be mainly derived from lode sources in the Lone Star, King Solomon Dome and lower Gold Run Creek areas. A second population of low fineness, high-mercury-content gold is derived from lode sources on the left limit of Eldorado Creek and in the headwaters of Bear and Last Chance creeks. Placer gold in the Sixtymile District was not derived from epithermal vein occurrences like those in the Sixtymile River valley but rather has compositions more similar to Klondike-type metamorphogenic veins. Placer gold in Scroggie Creek in southern Stewart River map area appears to be derived from intrusion-related vein occurrences.

RÉSUMÉ

Des études en cours sur la composition de l'or provenant de gisements placériens et filoniens ainsi que d'occurrences dans l'ouest du Yukon apportent un nouvel éclairage sur leur nature et leur origine. Deux principales populations statistiques de la composition sont présentes dans les gisements placériens et filoniens dans le district de Klondike. La population dominante, présentant un titre élevé et une faible teneur en mercure, semble dériver principalement de sources filoniennes dans les régions de la mine Lone Star, du dôme King Solomon et du cours inférieur du ruisseau Gold Run. Une deuxième population, à titre faible et à teneur élevée en mercure, est dérivée de sources filoniennes à la limite gauche du ruisseau Eldorado et dans le cours supérieur des ruisseaux Bear et Last Chance. L'or placérien du district de Sixtymile ne provient pas d'occurrences filoniennes épithermales comme celles de la vallée de la rivière Sixtymile, mais présente plutôt des compositions qui s'apparentent davantage à celles des filons métamorphogéniques de type Klondike. L'or placérien du ruisseau Scroggie dans le sud de la région de la carte Stewart River semble provenir d'occurrences filoniennes apparentées à des intrusions.

¹6339 Stores Road, Vancouver, British Columbia, Canada V6T 1Z4, jmortensen@eos.ubc.ca

²United Kingdom, aedrjc@earth.leeds.ac.uk

³Whitehorse, Yukon, bill.lebarge@gov.yk.ca

INTRODUCTION

We are continuing our study of the composition and shape evolution of placer and lode gold in various localities in western Yukon. We aim to investigate the nature and evolution of placer gold and specifically the relationship between placer gold and potential lode sources. In this contribution, we report new analytical results from the Klondike and Sixtymile districts as well as Scroggie and Matson creeks (Fig. 1). These creeks contain smaller and poorly understood placer gold deposits for which no lode sources have yet been identified. Yukon MINFILE occurrences cited in this document refer to Deklerk and Traynor (2005).

ANALYTICAL METHODS

Placer gold samples were either donated by individual placer miners or obtained by the authors by panning and/or sluicing. Placer gold grains were mounted in epoxy, ground down approximately half-way through the grain such that the interior of the grain was exposed, and then brought to a high polish. The grains were first examined using a scanning electron microscope to establish the assemblages of inclusion species and to determine the nature and thickness of leached high fineness rims. Compositions of cores were determined using an electron microprobe at The University of Leeds, United Kingdom. Individual spots were analysed for gold, silver, iron, mercury and copper.

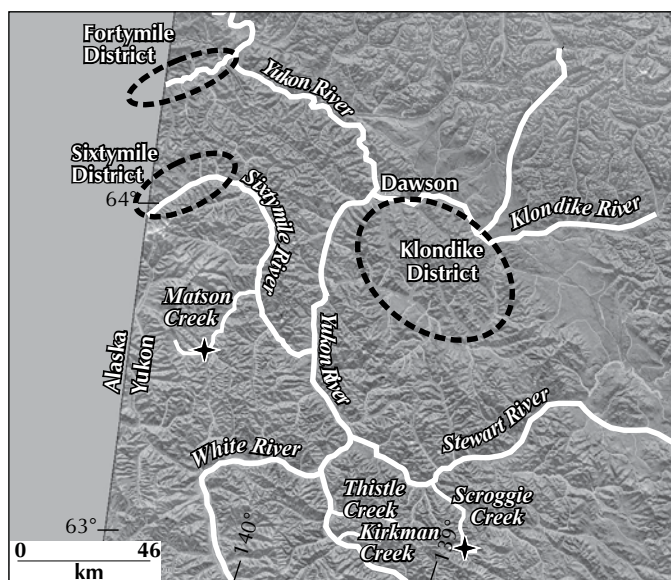


Figure 1. Location map of western Yukon showing major placer districts and specific placer streams that are discussed in the paper.

KLONDIKE DISTRICT

Previous studies of compositions and shapes of gold from placer deposits and lode occurrences in the Klondike District (Knight *et al.*, 1999a,b; Mortensen *et al.*, 2005) led to the following main conclusions:

- Preliminary shape studies of placer gold grains from the main drainages in the Klondike indicate that most gold appears to have originated from four main source areas; these are the King Solomon Dome area, the Lone Star mine area between Eldorado and upper Bonanza creeks, lower Gold Run Creek and middle and upper Bear and Last Chance creeks (Fig. 2)
- Two main compositional populations are represented in Klondike placer gold. The first and most widespread yields fineness values (purity out of a possible maximum value of 1000) in the range of ~700-850 with negligible to low mercury contents and rare trace amounts of copper, whereas the subordinate population is typified by lower fineness (~550-700) and up to 5 wt.% Hg.
- The high-fineness gold population contains nearly all gold from Dominion, Sulphur, Quartz, Eldorado and upper Bonanza creeks, as well as upper and middle Hunker Creek; it also comprises most of the placer gold on lower Bonanza Creek. Gold from lode occurrences in the King Solomon Dome area, Lone Star mine area and lower Gold Run Creek area show the same compositions as placer gold in streams draining those areas.

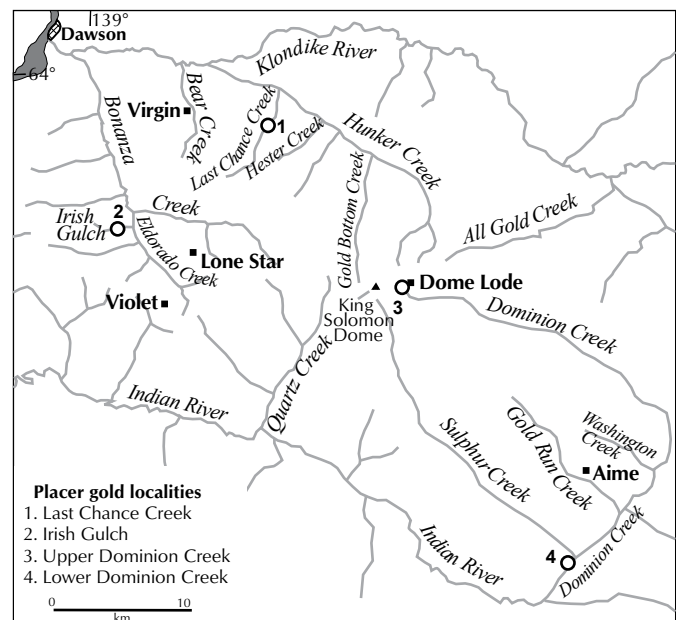


Figure 2. Location map of the Klondike District showing the main placer streams and locations of specific placer gold samples (○) and lode gold (■) occurrences.

- The low-fineness gold population is mainly restricted to north-draining streams in the northern part of the Klondike, including Bear, Last Chance and Hester creeks. Gold of this same composition is present at the Virgin lode occurrence on middle Bear Creek and at the Violet occurrence on the left limit of Eldorado Creek.

We have obtained and determined compositions for placer gold from four additional sites in the Klondike; these are Irish Gulch, uppermost Dominion Creek, lower Dominion Creek and middle Last Chance Creek (Fig. 2). We also analysed additional gold grains from the Aime lode occurrence on lower Gold Run Creek (Fig. 2) for comparison with placer gold in lower Dominion Creek. Compositions for gold from these localities are shown graphically, together with previously determined compositional data, in the form of cumulative frequency plots for silver and a plot of % Ag vs. % Hg for selected data sets in Figure 3. Mineral inclusions are very uncommon in placer gold grains from the Klondike, and there is currently insufficient data to facilitate analysis of placer populations using this criteria.

Placer gold recovered from an operation at the very head of Dominion Creek (Fig. 2) is rough and angular, with abundant attached quartz. Compositions are identical to gold from the Dome Lode occurrence on the ridge immediately to the east (Fig. 2), supporting the argument that the placer gold was derived from the Dome Lode veins or similar vein systems in the immediate King Solomon Dome area.

The main Dominion Creek paystreak begins at the head of the drainage but has largely disappeared by the mouth of Washington Creek (Fig. 2). A separate paystreak picks up at the mouth of Gold Run Creek and continues southwest past the mouth of Sulphur Creek to the junction with the Indian River. The placer paystreak on lower Dominion Creek extends several kilometres up lower Gold Run Creek, suggesting that a major lode gold source existed in this area. Preliminary analyses of rough to highly flattened gold grains from a placer operation on lower Dominion Creek near the mouth of Sulphur Creek (Fig. 2) shows the same general compositional range as gold from upper Dominion Creek and lode occurrences in that vicinity. Although it is unclear how much of the gold from the lower Dominion Creek locality was derived from Sulphur Creek, we note that gold derived from quartz veins at the Aime lode occurrence on the left limit of lower Gold Run Creek is identical in composition to the lower Dominion Creek gold. Additional samples are currently being analysed from Gold Run Creek itself to

help evaluate how much of the lower Dominion Creek gold derived from Gold Run Creek rather than Sulphur Creek.

Placer gold from middle Last Chance Creek (Fig. 2) is mainly moderately flattened. Compositional studies indicate relatively low fineness (most silver contents in the range of 26 to 40 wt.% and low to moderate mercury contents (up to 0.9 wt.%). These compositions are similar to those previously reported from Bear Creek and from the Virgin lode occurrence on middle Bear Creek (Fig. 2).

Placer gold from Irish Gulch (Fig. 2) is typically very crystalline in character (B. and R. Johnson, pers. comm., 2005). A sample of gold from the middle portion of this short, steep drainage shows very low fineness values (most grains with silver contents of 26 to 46 wt.%) and moderate to very high mercury contents (up to 4.6 wt.%). Mercury contents in some of the Irish Gulch gold are so high that caution should be exercised by anyone melting this gold to make jewelry. In general, compositions of the Irish Gulch gold are similar to that from the Violet lode occurrence on the ridge southwest of Eldorado Creek, approximately 6.5 km southeast of Irish Gulch (Fig. 2). Our data suggests that the Irish Gulch placer gold was likely derived from Violet-like quartz veins that presumably occur for a considerable distance from the Violet occurrence along the ridge to the northwest. Interestingly, this low-fineness, high-mercury gold population appears to represent only a minor component of placer gold in Eldorado and lower Bonanza creeks (based on data reported by Knight *et al.* 1999a), suggesting that the lode sources on the left limits of these drainages were not significant contributors to the placer gold deposits.

SIXTYMILE DISTRICT

The Sixtymile District (Figs. 1, 4) is underlain by metamorphic rocks of the Yukon-Tanana Terrane that are overlain by mainly flat-lying Cretaceous sandstone and pebble conglomerate of the Tantalus Formation and subsequently by andesitic flows and breccias of the Late Cretaceous Carmacks Group (Mortensen, 1988; Fig. 4). Small high-level intrusions that represent subvolcanic feeders to the Carmacks volcanic rocks are also locally present. The structure of the Sixtymile District is dominated by a set of northeast-trending normal faults. Most of these structures are southeast-side down; however, a major fault along the southern side of the Sixtymile River valley is northwest side down (Fig. 4).

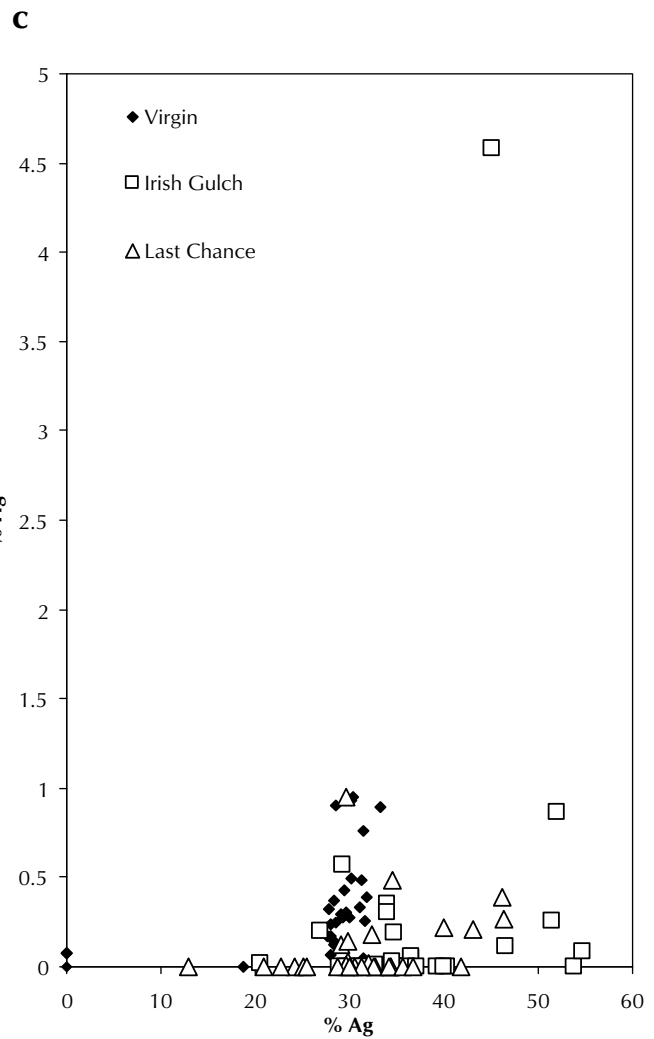
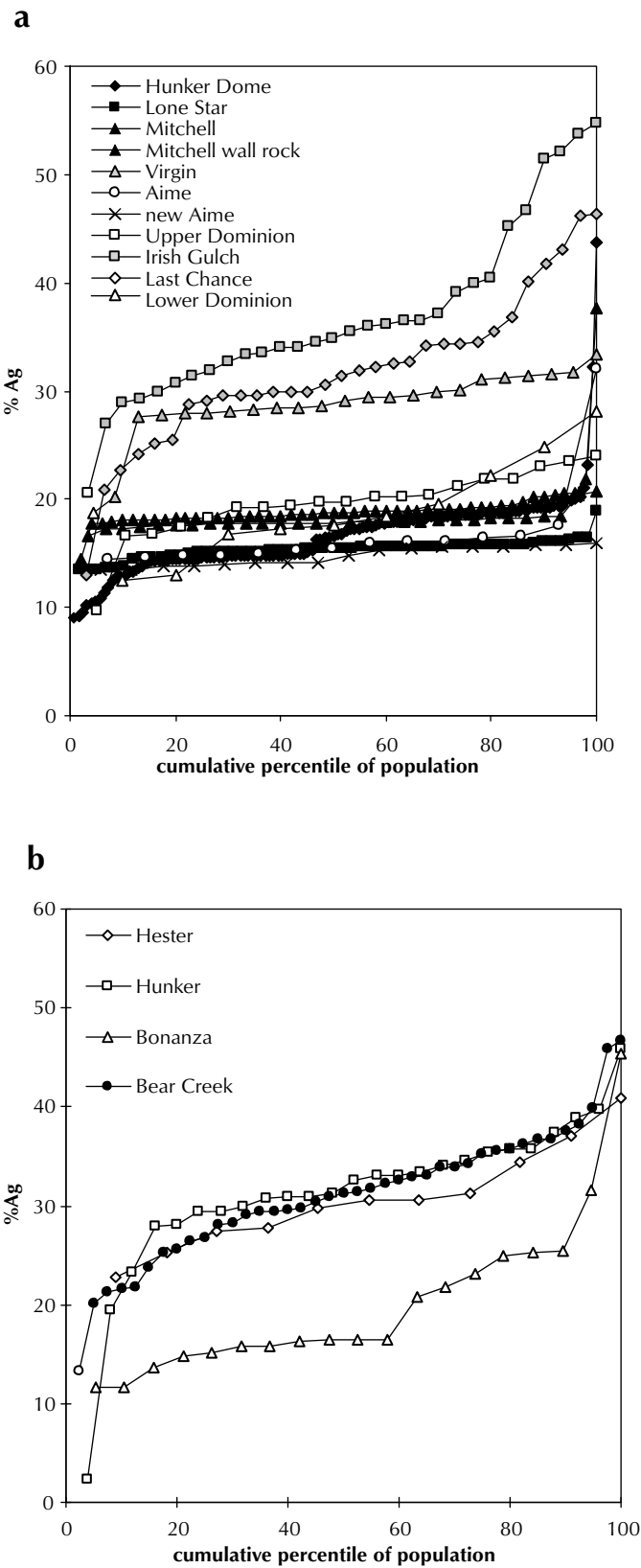


Figure 3. Cumulative frequency plots for Ag, and Ag vs. Hg plots for placer and lode gold from the Klondike District. The Hunker Dome, Lone Star, Mitchell, Mitchell wall rock, Virgin, Aime and new Aime samples in Figure 3a and the Virgin sample in Figure 3c are all lode occurrences; the remaining samples are from placer occurrences.

Thus, the Sixtymile River in the Sixtymile District flows along an asymmetric graben structure that progressively down-drops flat-lying panels of Tantalus Formation and Carmacks Group volcanic rocks to the level of the valley bottom. Numerous veins cut the Tantalus Formation, Carmacks Group and the metamorphic basement rocks. These veins commonly show crustiform banding and cockade textures, and fluid inclusion studies by Glasmacher and Friedrich (1992a) indicate that the veins are epithermal in nature. Only minor gold has been recognized within these veins; however, veins of this type are widespread in the Sixtymile River valley. This observation, together with the occurrence of abundant cinnabar in placer deposits on lower Miller Creek (Fig. 3),

has led many workers to suggest that most of the placer gold in the Sixtymile District was derived from epithermal veins.

We have studied three samples of placer gold from the Sixtymile District. A large sample of gold from lower Miller Creek was donated by Jayce Murtagh; another sample from the Sixtymile River valley below the mouth of Little Gold Creek was donated by Greg Hakonson; and a final sample was obtained by panning from the middle reaches of Glacier Creek (Fig. 4). An additional small sample was panned from the headwaters of Moose Creek, which is a small stream that drains north from the Top-of-the-World Highway near the Yukon-Alaska border (Fig. 4), approximately 15 km north of the mouth of

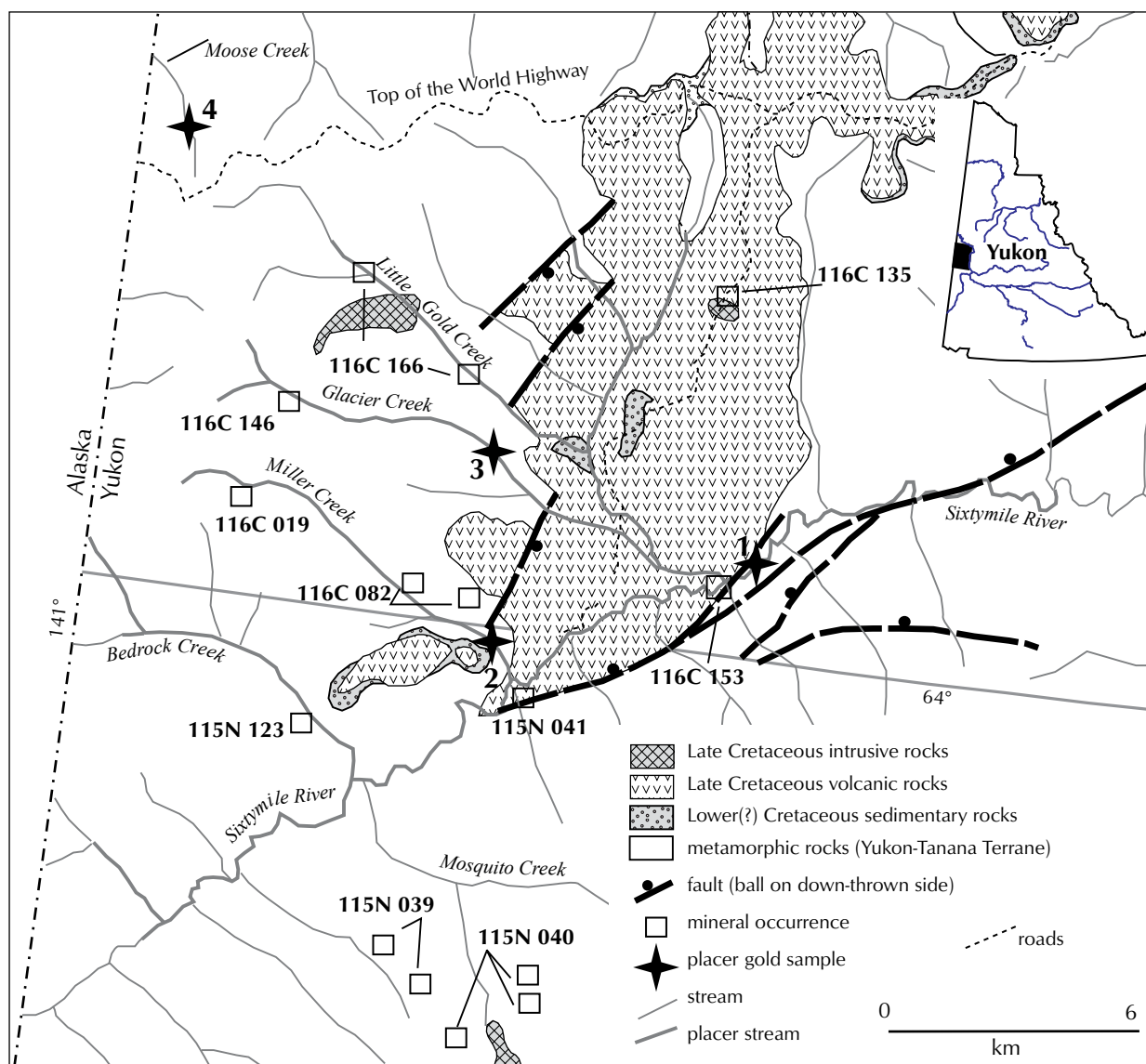


Figure 4. Simplified geology map of the Sixtymile District (simplified from Mortensen, 1988, and unpublished mapping) showing locations of known vein occurrences and placer gold samples discussed in the paper.

Miller Creek. Analytical data from the Sixtymile District placer gold are shown graphically as cumulative frequency plots for silver in Figure 5.

The lower Miller Creek sample mainly consisted of blocky to tabular grains with a few thin flakes; out of the 99 grains analysed from this sample, >90% of the grains contained 10-24 wt.% Ag. Only three grains contained mercury contents above detection limit on the microprobe; these grains had 1.3-4.0 wt.% Hg. A small number of gold grains were recovered by panning on Glacier Creek and nine grains were analysed. Silver contents range from 12.6-44 wt.% and none of the grains

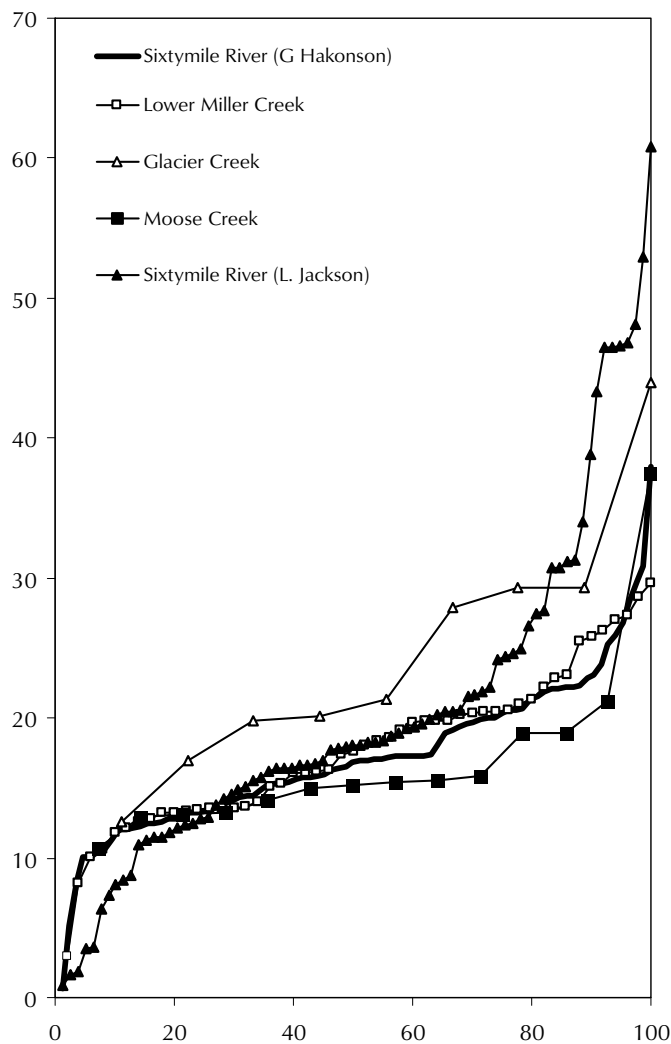


Figure 5. Cumulative frequency plot for silver for placer gold from the Sixtymile District and Moose Creek. Additional data previously determined from a separate sample of placer gold from the Sixtymile River (exact location is uncertain) is shown for comparison and is labelled as "Sixtymile River (L. Jackson)".

contained measurable mercury. Placer grains from the Sixtymile River sample (Fig. 4) range from rough and irregular to rounded to strongly flattened. Since this sample should be reasonably representative of all the placer gold in the Sixtymile District, we analysed a large number of grains. Measured compositions are very similar to gold from lower Miller Creek, with >90% of the grains yielding 10-24 wt.% silver and mercury mostly below detection limit (only two grains from the Sixtymile sample contain measurable mercury). Compositional data from another sample of placer gold, collected by L. Jackson from the Sixtymile River in approximately the same location as our sample, are shown on Figure 5 for comparison; data from the two samples are in very close agreement. A small number of placer grains analysed from near the head of Moose Creek, immediately north of the Sixtymile District, yielded compositions similar to the Miller Creek and Sixtymile River samples (silver-contents of 10-19 wt.% and trace amounts of mercury). Opaque mineral inclusions are uncommon in these samples; however, the sulphide-sulpharsenide assemblage observed in some of the grains was atypical of an epithermal signature (Chapman and Mortensen, in press).

The results of our study of Sixtymile District placer gold are somewhat surprising. In general, gold from epithermal veins commonly displays a wide range of silver contents and includes relatively high silver values (typically >25 wt.%, or fineness <750) and measurable to high mercury-contents (e.g., mean values of around 0.5%, with maximum values of about 10%; Chapman and Mortensen, submitted). Most of the gold from the lower Miller Creek and Sixtymile River samples has silver- and mercury-contents that are lower than those expected from epithermal vein sources. Glasmacher and Friedrich (1992a) described the mineralogy, mineral chemistry and fluid chemistry for several veins that are interpreted to be epithermal in origin in the Sixtymile District. For example, the Glasmacher occurrence (Yukon MINFILE⁴ 116C 153), located in the bed of the Sixtymile River near the mouth of Little Gold Creek, contained trace amounts of gold. Analyses of gold formed during three interpreted stages of deposition yielded 4.8 wt.%, 24.6 wt.% and 19.8 wt.% Ag. The gold contained trace levels of tellurium and bismuth, but no detectable mercury. These silver-contents are on the low end of the compositional range normally associated with epithermal veins; however, fluid inclusion data reported for the vein by Glasmacher and Friedrich

⁴Yukon MINFILE mineral occurrences listed in this report are from Deklerk and Traynor, 2005.

(1992a) are fairly typical of epithermal veins. Only a single vein occurrence was studied, however, and it is unclear how representative these measured values are of gold in epithermal veins in the Sixtymile District. Other vein occurrences in the Sixtymile District that are thought to be epithermal in nature include the Per (Yukon MINFILE 115N 041), hosted by Carmacks Group volcanic rocks south of the Sixtymile River and the Guch (Yukon MINFILE 116 135), which is hosted by a small Late Cretaceous stock (Fig. 4).

There are two possible explanations for our gold compositional data for the Sixtymile District samples. Either the gold was derived from epithermal veins that represent an unusual end-member of the epithermal style (perhaps formed at relatively deep levels in an epithermal system), or the gold was mainly derived from an entirely different style of vein. Other styles of quartz veins have been recognized in the Sixtymile District, and some of these contain precious metals (mainly silver). Arsenopyrite-rich quartz-sulphide veins are widespread along and north of the ridge crest on the right limit of Sixtymile River (e.g., the Lerner occurrence – Yukon MINFILE 115N 039, and the Connaught occurrence – Yukon MINFILE 115N 040; Glasmacher and Friedrich, 1992b). These veins are relatively high in silver but are typically low in gold. Very little gold has been recovered from streams that drain this area (e.g., Mosquito Creek), suggesting that this set of veins do not represent a viable source of placer gold. A separate set of quartz-sulphide (\pm carbonate) veins cut metamorphic rocks on lower Bedrock Creek and on the middle and upper portions of Miller, Glacier and Little Gold creeks (e.g., the Bedrock occurrence – Yukon MINFILE 115N 123, the Yaremico 116C 082, the Miller 116C 019, the Cedar 116C 146, and the Little Gold 116C 166). These veins yield temperatures and salinities that are considerably higher than those typical of epithermal veins (temperatures of 320-350°C and salinities >18 wt.% NaCl equivalent). They are mineralogically and texturally very different from the epithermal-style veins that cut the overlying Tantulus Formation sedimentary rocks and Carmacks Group volcanic rocks (Glasmacher and Friedrich, 1992a,b). Lead isotopic studies of the two different styles of veining (Mortensen, unpublished data) also suggest that the vein systems are unrelated. The veins cutting metamorphic bedrock are weakly anomalous in gold, and locally, contain minor scheelite (U. Glasmacher, pers. comm., 1995), and therefore are the likely source of barite, scheelite, wolframite and possibly placer gold that occur in the placer deposits on lower Miller Creek. The veins

within the metamorphic bedrock in the Sixtymile District are somewhat similar to gold-bearing orogenic quartz veins in the Klondike District.

SCROGGIE AND MATSON CREEKS

We have investigated gold compositions from samples of placer gold from Scroggie and Matson creeks (Fig. 1), for which no lode source has ever been identified. The drainage basins for both of these streams are underlain mainly by metamorphic rocks of the Yukon-Tanana Terrane; however, exposure is very limited in both areas and the geology of the local bedrock is poorly understood. The placers on Scroggie Creek have yielded considerable relatively coarse gold and gold nuggets. The gold that we analysed from this locality was finer grained and moderately to highly flattened. Gold analysed from Matson Creek mainly consisted of thin to thick tabular morphologies. Analytical data are shown graphically in the form of cumulative frequency plots for silver in Figure 6. Also shown for comparison in Figure 6 are silver contents for gold from Thistle, Kirkman and Blueberry creeks, which are located west of Scroggie Creek. These data are from samples previously studied by Dumula and Mortensen (2002).

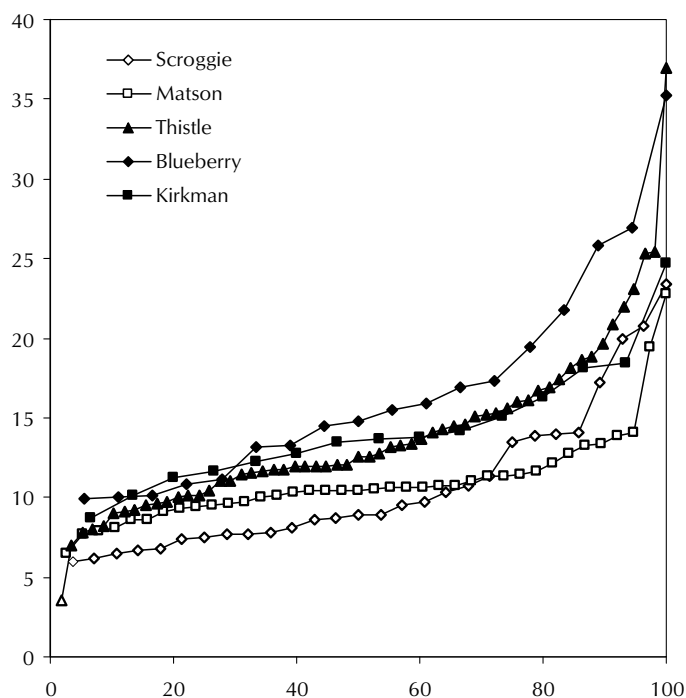


Figure 6. Cumulative frequency plot for silver from Scroggie, Matson, Thistle and Kirkman creeks in southern Stewart River area.

Gold compositions from Scroggie and Matson creeks are generally similar, with silver contents ranging from 5-13 wt.% (corresponding to fineness of 870-950). Gold from Thistle, Kirkman and Blueberry creeks gives slightly higher silver contents (8-20 wt.% Ag, corresponding to fineness of 800-920). Scroggie and Matson gold has mercury contents at or below detection limits and copper contents below detection limits. The similarity in gold compositions from these various creeks suggests a common source, and the low silver content is consistent with this being an intrusion-related source. Two tellurium-bearing inclusions were detected in gold grains from Scroggie Creek, which is suggestive of a magmatic component to the mineralizing fluids, and sets this gold apart from Klondike-style lode sources. Late- and post-tectonic intrusions of several ages (Early Jurassic, Early Cretaceous and Late Cretaceous) are present within the drainage basins of these placer streams and it is likely that the gold was derived from vein systems related to some of these bodies. The generally poor exposure in the Stewart River map area has made prospecting difficult; however, several mineral occurrences are known in the Scroggie and Thistle creek drainages and could have contributed gold to the placer deposits. The Mariposa occurrence (Yukon MINFILE 115O 075) on Mariposa Creek, a tributary of upper Scroggie Creek, is characterized by well developed gold-in-soil anomalies and some minor quartz-pyrite veining with anomalous gold values, although a substantial vein system has yet to be identified. The Black Fox and Hakonson occurrences (Yukon MINFILE 115O 014 and 106), on Lulu and Blueberry creeks, respectively (both tributaries of the upper Thistle Creek), are quartz-sulphide veins with negligible to moderately anomalous gold, and could be representative of the style of lode source from which the placer gold was derived. There are no gold-bearing occurrences known in the vicinity of the Matson Creek placer deposits and the ultimate source of the gold is uncertain. Porphyry-style molybdenum-copper (\pm gold) mineralization, thought to be associated with Late Cretaceous or Early Tertiary intrusions, occurs in the general vicinity. These occurrences include the Ladue (Yukon MINFILE 115N 026, located ~25 km southwest of the placer deposits) and the Pax (Yukon MINFILE 115N 029, in the Dawson Creek drainage ~10 km upstream from the placers). This style of lode occurrence may have been the ultimate source of the placer gold on Matson Creek.

ON-GOING RESEARCH

We continue to work on these and a large number of additional samples of placer and lode gold from western Yukon. We are focusing particularly on using laser ablation ICP-MS methods to more completely characterize the geochemical 'fingerprint' of the gold by expanding it to include a large number of trace elements. We are also developing a systematic, semi-automated image analysis procedure for quantifying the shapes of placer gold grains. This latter development will make it possible to apply a statistical approach to evaluating the evolution of the shape of placer gold grains during transport and construct better constrained correlation curves for grain shape vs. transport distance.

ACKNOWLEDGMENTS

We thank the many Yukon placer miners who have generously donated samples of their increasingly valuable gold or have given us permission to pan for our own samples for this study. In particular, we thank Jayce Murtagh, Mike McDougall, Lisle Gatenby, John Alton, Tim Coles, Bernie and Ron Johnson, Greg Hakonson, Zdenek and Michal Bidrman, Stuart Schmidt, Daniel Jones, Grant Klein and Alan Radford.

REFERENCES

- Chapman R. and Mortensen, J.K., in press. Application of microchemical characterization of placer gold grains to exploration for epithermal gold mineralization in regions of poor exposure. *Journal of Geochemical Exploration*, submitted.
- Deklerk, R. and Traynor, S., 2005. Yukon MINFILE – A database of mineral occurrences. Yukon Geological Survey, CD-ROM.
- Dumula, M.R. and Mortensen, J.K., 2002. Composition of placer and lode gold as an exploration tool in the Stewart River map area, western Yukon. *In: Yukon Exploration and Geology 2001*, D.S. Emond, L.H. Weston and L.L. Lewis (eds.), Exploration and Geological Services Division, Yukon Region, Indian and Northern Affairs Canada, 2000, p. 1-16.

- Glasmacher, U. and Friedrich, G., 1999a. Volcanic-hosted epithermal gold-sulphide mineralization and associated enrichment processes, Sixtymile River area, Yukon Territory, Canada. Yukon Geology, Volume 3, T.J. Bremner (ed.), Exploration and Geological Services Division, Yukon Region, Indian and Northern Affairs Canada, p. 271-291.
- Glasmacher, U. and Friedrich, G., 1999b. Gold-sulphide enrichment processes in mesothermal veins of the Sixtymile River area, Yukon Territory, Canada. Yukon Geology, Volume 3, T.J. Bremner (ed.), Exploration and Geological Services Division, Yukon Region, Indian and Northern Affairs Canada, p. 292-311.
- Knight, J.B., Mortensen, J.K. and Morison, S.R., 1999a. Lode and placer gold compositions from the Klondike District, Yukon Territory, Canada: Its implications for the nature and genesis of Klondike placer and lode gold deposits. *Economic Geology*, vol. 94, p. 649-664.
- Knight, J.B., Morison, S.R. and Mortensen, J.K., 1999b. The relationship between placer gold particle shape, rimming and distance of fluvial transport; as exemplified by gold from the Klondike District, Yukon Territory, Canada. *Economic Geology*, vol. 94, p. 635-648.
- Mortensen, J.K., 1988. Geology of southwestern Dawson map area (NTS 116 B, C). Geological Survey of Canada, Open File 1927.
- Mortensen, J.K., Chapman, R., LeBarge, W. and Jackson, L., 2005. Application of placer and lode gold geochemistry to gold exploration in western Yukon. *In: Yukon Exploration and Geology 2004*, D.S. Emond, L.L. Lewis and G.D. Bradshaw (eds.), Yukon Geological Survey, p. 205-212.
- Ryan, J.J. and Gordey, S.P. 2002. Bedrock geology of Yukon-Tanana terrane in southern Stewart River map area, Yukon Territory. Geological Survey of Canada, Current Research 2002-A1, 11 p.
- Ryan, J.J., Gordey, S.P., Glombick, P., Piercey, S.J. and Villeneuve, M.E., 2003. Update on bedrock geological mapping of the Yukon-Tanana terrane, southern Stewart River map area, Yukon Territory. Geological Survey of Canada. Current Research 2003-A9, 7 p.

Uranium-lead ID-TIMS and LA-ICP-MS ages for the Cassiar and Seagull batholiths, Wolf Lake map area, southern Yukon

Jim K. Mortensen¹ and Christa Sluggett

Pacific Centre for Isotopic and Geochemical Research, University of British Columbia²

Tim Liverton

Rhyoflow Inc.³

Charlie F. Roots

Geological Survey of Canada⁴

Mortensen, J.K., Sluggett, C., Liverton, T. and Roots, C.F., 2006. U-Pb zircon and monazite ages for the Seagull and Cassiar batholiths, Wolf Lake map area, southern Yukon. *In: Yukon Exploration and Geology 2005*, D.S. Emond, G.D. Bradshaw, L.L. Lewis and L.H. Weston (eds.), Yukon Geological Survey, p. 257-266.

ABSTRACT

The Cassiar and Seagull batholiths are mainly post-tectonic felsic intrusions emplaced into the North American miogeocline and Yukon-Tanana Terrane, respectively, near the British Columbia-Yukon boundary. The two bodies range in composition from granodiorite and quartz monzonite to granite. Previous studies reported K-Ar and Rb-Sr dates of ~100 Ma for Seagull batholith and about 110 Ma for Cassiar batholith. Two samples of massive quartz monzonite from the interior of the Cassiar batholith, and a strongly foliated and lineated augen gneiss within a ductile shear zone near the western margin of the batholith, yield overlapping U-Pb monazite and/or zircon ages of 112.3 ± 2.0 Ma, 113.2 ± 2.2 Ma, and 110.2 ± 1.0 Ma respectively, by ID-TIMS methods. Samples of aplitic biotite granite and megacrystic biotite granite from the Seagull batholith give distinctly younger U-Pb zircon ages of 99.3 ± 2.2 Ma and 95.7 ± 2.1 Ma, respectively, using LA-ICP-MS methods.

RÉSUMÉ

Les batholites de Cassiar et de Seagull sont principalement des intrusions felsiques post-tectoniques mises en place respectivement dans le miogéocline nord-américain et dans le terrane de Yukon-Tanana, près de la limite entre la Colombie-Britannique et le Yukon. La composition des deux masses varie de la granodiorite et de la monzonite quartzifère au granite. Des études antérieures ont établi par des méthodes de datation aux K-Ar et aux Rb-Sr des âges d'environ 100 Ma pour le batholite de Seagull et d'environ 110 Ma pour le batholite de Cassiar. Deux échantillons de monzonite quartzifère massive, prélevés près de la limite ouest du batholite de Cassiar, ainsi qu'un gneiss oeilé à structure fortement foliée et linéations marquées à l'intérieur d'une zone de cisaillement ductile près de la limite occidentale du batholite, indiquent un chevauchement des datations aux U-Pb de la monazite et/ou des zircons de $112,3 \pm 2,0$ Ma, $113,2 \pm 2,2$ Ma et $110,2 \pm 1,0$ Ma, respectivement, d'après des méthodes ID-TIMS. Des échantillons de granite aplitique à biotite et de granite mégacristallin à biotite provenant du batholite de Seagull livrent des âges U-Pb des zircons nettement plus récents de $99,3 \pm 2,2$ Ma et de $95,7 \pm 1,7$ Ma, respectivement, d'après des méthodes LA-ICP-MS.

¹*jmortensen@eos.ubc.ca*

²*6339 Stores Road, Vancouver, British Columbia, Canada V6B 1Z4*

³*Box 393, Watson Lake, Yukon, Canada Y0A 1C0*

⁴*Box 2703, K-10, Whitehorse, Yukon, Canada Y1A 2C6*

INTRODUCTION

Plutonic rocks are widespread in the Wolf Lake map area (NTS 105B) in southern Yukon (Fig. 1), where they intrude pericratonic terranes including displaced strata of the North American miogeocline (Cassiar Platform) on the east, and metamorphosed continental and arc rocks of the Yukon-Tanana Terrane on the west. Previous geochronology of plutons in this portion of the Cordillera have shown that most are Early Cretaceous in age, although Permian and Early Jurassic plutonic rocks are also present within the Yukon-Tanana Terrane, and scattered Late Cretaceous bodies have also been identified. All Early Cretaceous intrusions in the Cassiar Platform adjacent Yukon-Tanana Terrane southwest of the Tintina Fault in southern Yukon have mainly been assigned to the Cassiar plutonic suite (e.g., Mortensen *et al.*, 2000). This is based on scarce isotopic age information as well as overall lithology and geochemistry. Significant silver, tin and tungsten

occurrences are thought to be temporally and genetically associated with the Cassiar suite intrusions in this area.

A detailed geochemical and isotopic study along the length of the Cassiar batholith constituted a M.Sc. thesis (Driver *et al.*, 2000). The nature of the Seagull batholith and intrusions to the northwest is discussed by Liverton and Alderton (1994), Liverton and Botelho (2001) and Liverton *et al.* (2001). Despite the metallogenic significance of the Early Cretaceous plutonism, available geochronological data consist mainly of K-Ar and Rb-Sr age determinations. In this paper, we report U-Pb zircon and monazite ages for three samples from the Cassiar batholith and two from the Seagull batholith. The 10- to 15-m.y. separation in age of these two batholiths warrants more complete distinction within the Cassiar suite. Forthcoming publications will address more fully the geological, tectonic and metallogenic significance of the new results.

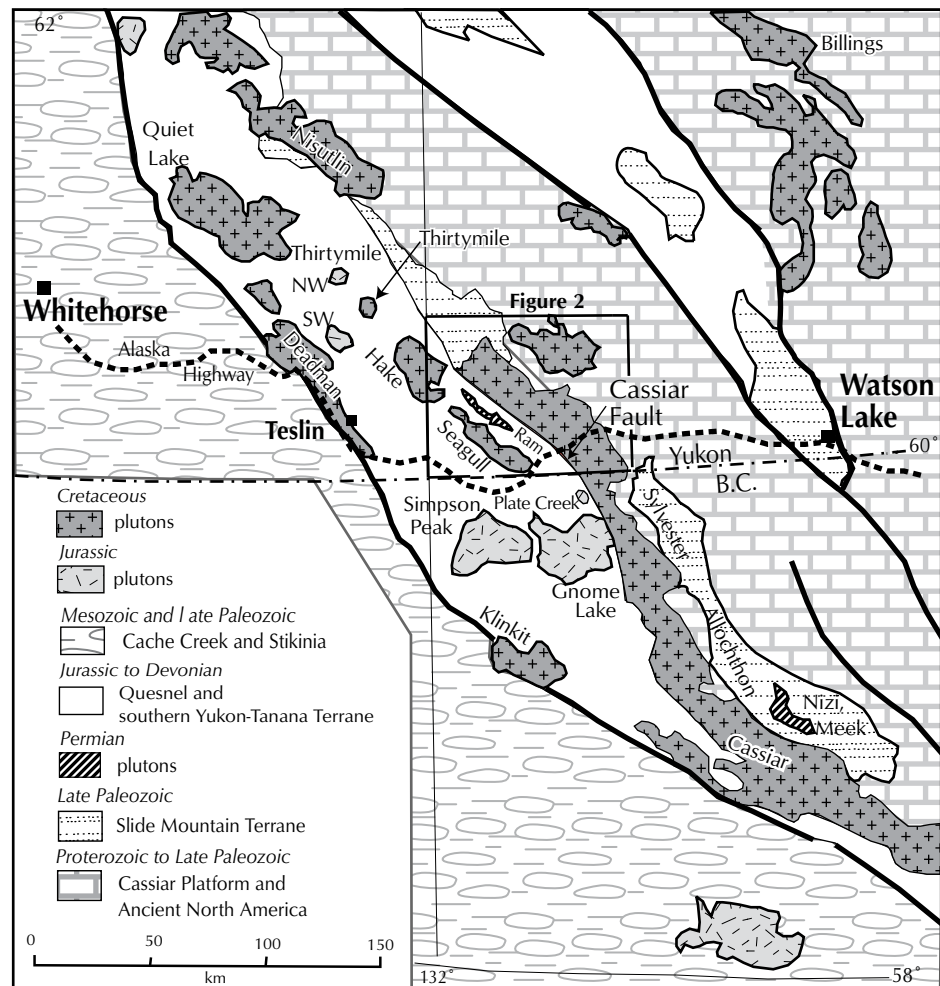


Figure 1. Simplified geology of southern Yukon and northern British Columbia, with major plutons labelled. Box shows location of Figure 2.

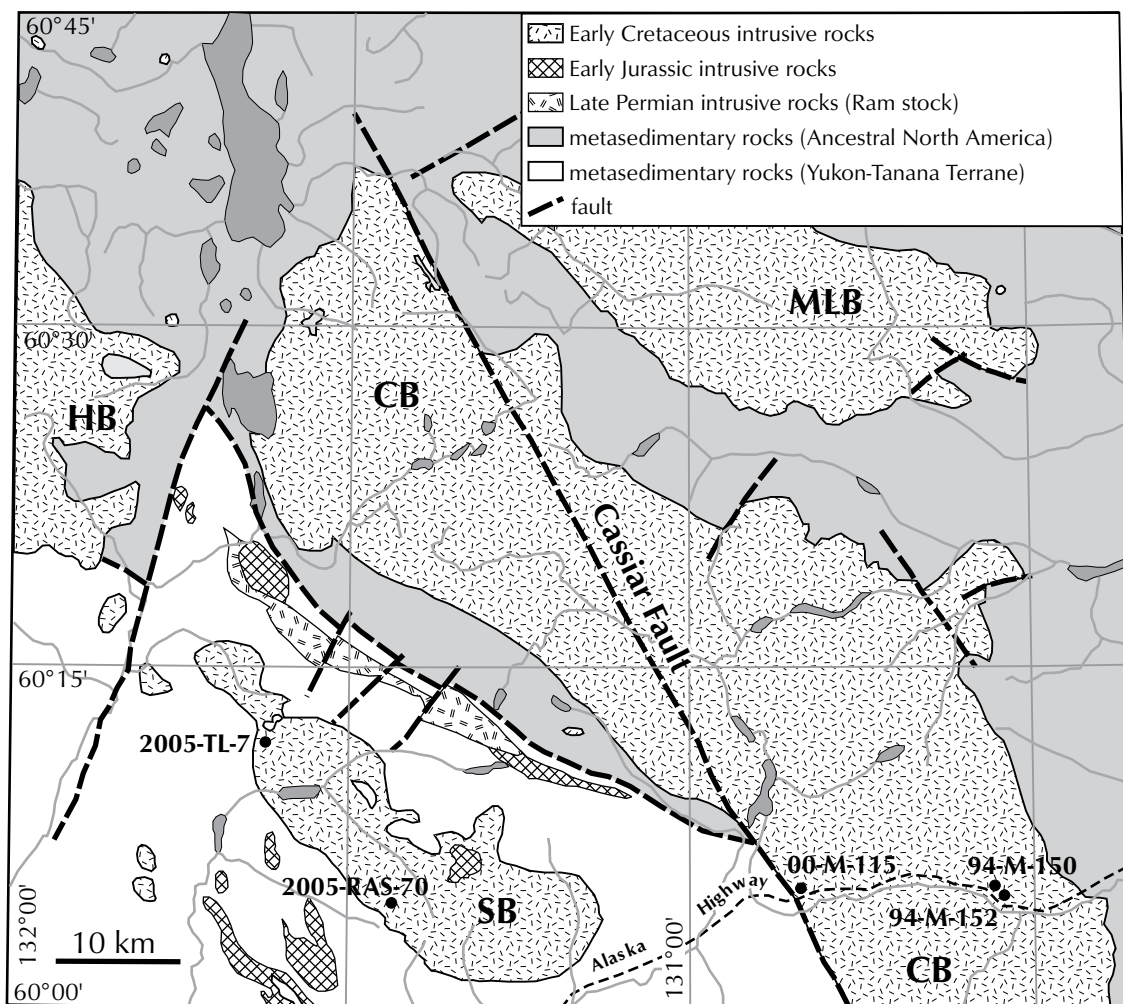
CASSIAR BATHOLITH

The Cassiar batholith is a northwest-trending, elongate body, approximately 350 km in length and from 5 to 40 km wide, that intruded the western shelf edge of Ancestral North America (Figs. 1 and 2). It is mainly felsic, comprising biotite ± muscovite quartz monzonite and granite with less abundant biotite ± hornblende granodiorite and monzodiorite. Geochemical and isotopic studies by Driver *et al.* (2000) indicate that the various phases in the batholith are subalkaline and typically weakly to moderately peraluminous, with evolved isotopic signatures (initial Sr ratios = 0.706 to 0.734; $\epsilon_{\text{ND}} = -2.7$ to -17.1). Driver *et al.* (2000) concluded that magmas that formed the Cassiar batholith represent partial melts of two distinct sources: one likely derived from Proterozoic metasedimentary and/or basement rocks of Ancestral North America; the other was a mafic source of uncertain age and origin.

Where the Alaska Highway crosses Cassiar batholith in southern Yukon, the western contact of the batholith is the Cassiar Fault, a northwest-trending dextral shear (Fig. 1). Roadcuts show that the degree of mylonitization decreases eastward over about 5 km (Poole *et al.*, 1960; Gabrielse, 1969); farther south, where the fault crosses ridge spurs in northern BC, it is only tens of metres wide. Although brittle deformation clearly occurred after the Cassiar batholith had cooled, the elongated shape of the pluton suggests it intruded along a pre-existing zone of crustal weakness.

Previous age information for the Cassiar batholith consists of two K-Ar biotite ages of 103 ± 10 Ma and 101 ± 8 Ma for samples of massive granite (Baadsgaard *et al.*, 1961; Lowdon, 1961), a single K-Ar age of 89 ± 4 Ma for muscovite from “cataclastic granite” near the western margin of the body (Wanless *et al.*, 1972), and a Rb-Sr whole-rock isochron age of 112 ± 4 Ma for various fine-grained phases of the Cassiar batholith in southeastern Wolf Lake map area (G. Medford and R.L. Armstrong, unpublished data).

Figure 2. Geology of southwestern Wolf Lake map area showing locations of geochronological samples. Plutons labeled as follows: CB = Cassiar batholith, SB = Seagull batholith, HB = Hake batholith, MLB = Marker Lake batholith.



SEAGULL BATHOLITH

The Seagull and Hake batholiths (possibly joined beneath a 7-km-wide septum of metasedimentary host rock) are distinct one-mica granites with enriched biotite (Liverton *et al.*, 2005). Northwest of Hake batholith are the Thirtymile and Ork stocks which contain some of the most evolved lithofacies reported in the northern Cordillera. These include zinnwaldite-topaz leucogranites with extreme Rb/Sr ratios, and range from metaluminous to peraluminous in composition. Trace element contents fall within the fields of within-plate ('anorogenic'), rather than arc-related granitoids. These plutons have a distinct metallogenic signature comprising pronounced Sn-B-F enrichments. The granites had previously been interpreted to represent a single intrusive suite on the basis of chemistry and metallogeny (Liverton and Alderton, 1994; Liverton and Botelho, 2001). The whole-rock chemical data for these intrusions, and their very Fe-rich mica chemistry, are consistent with being late-orogenic magmas derived from the middle crust. The Thirtymile, Hake and Seagull plutons were emplaced at a sufficiently shallow level in the crust to have allowed 'ultrafractionation'. This happens when the presence of fluorine facilitates fractionation by inhibiting nucleation in the magma chamber, depolymerizing silicates and depressing the solidus so that elements such as lithium and boron can move upward in the magma (C. Hart, pers. comm., 2003).

Isotopic studies yielded Rb-Sr ages of 101 ± 5.3 Ma for the Thirtymile stock, and an interpreted cooling age of 98.3 ± 2.9 Ma for the marginal phase of the Hake batholith (Liverton *et al.*, 2001). Seven K-Ar biotite ages from various samples of the Seagull batholith itself range from 94 ± 4 Ma to 102.8 ± 1.1 Ma, and a single Rb-Sr whole-rock isochron age of 100.3 ± 2.8 Ma was reported for the Seagull batholith by Mato *et al.* (1983).

U-PB GEOCHRONOLOGY

In this study, we determined U-Pb crystallization ages for three samples from the Cassiar batholith and two samples from the Seagull batholith. Conventional thermal ionization mass spectrometry (TIMS) methods were employed to date zircons and monazites from the Cassiar batholith samples, and laser ablation inductively coupled plasma mass spectrometry (LA-ICP-MS) methods were used to date zircons from the Seagull batholith. All of the analytical work was done at the Pacific Centre for Isotopic

and Geochemical Research (PCIGR) at the University of British Columbia.

METHODOLOGY

The methodology used for TIMS analyses at the PCIGR is as described by Mortensen *et al.* (1995). LA-ICP-MS dating has recently been established as a routine procedure at the PCIGR. Zircons are separated from their host rocks using conventional mineral separation methods. Approximately 25 of the coarsest, clearest, most inclusion-free grains are selected from each sample, mounted in an epoxy puck along with several grains of internationally accepted standard zircon (in this case we used FC-1, a ~1100 Ma zircon standard), and brought to a very high polish. The grains are examined using a stage-mounted cathodoluminescence unit, which makes it possible to detect the presence of altered zones or older inherited cores within the zircon. High-quality portions of each grain, free of alteration, inclusion, or cores, are selected for analysis. The surface of the mount is then washed for ~10 minutes with dilute nitric acid and rinsed in high purity water. Analyses are carried out using a New Wave 213 nm Nd-YAG laser coupled to a Thermo Finnigan Element2 high-resolution ICP-MS. Ablation takes place within a New Wave "Supercell" ablation chamber which is designed to achieve very high efficiency entrainment of aerosols into the carrier gas. Helium is used as the carrier gas for all experiments and gas flow rates, together with other parameters such as torch position, are optimized prior to beginning a series of analyses. A 25 micron spot with 40% laser power is used, making line scans rather than spot analyses in order to avoid within-run elemental fractions. Each analysis consists of a 7-second background measurement (laser off) followed by a ~28-second data acquisition period with the laser firing. A typical analytical session consists of four analyses of the standard zircon, followed by four analyses of unknown zircons, two standard analyses, four unknown analyses, etc., and finally four standard analyses. Data are reduced using the GLITTER software marketed by the GEMOC group at Macquarrie University in Sydney, Australia, which automatically subtracts background measurements, propagates all analytical errors, and calculates isotopic ratios and ages. Final ages for relatively young (Phanerozoic) zircons are based on a weighted average of the calculated $^{206}\text{Pb}/^{238}\text{U}$ ages for 10-15 individual analyses. Final interpretation and plotting of the analytical results employ the ISOPLOT software written by K.R. Ludwig.

SAMPLE LOCATIONS AND DESCRIPTIONS

Two samples of massive granite of the Cassiar batholith were collected from roadcuts on the north side of the Alaska Highway (Fig. 2). Sample 94-M-150 is a medium-grained, equigranular biotite-muscovite granite collected 2.6 km east of Canyon Creek (12.6 km east of the Upper Rancheria River) (UTM 6662082N, 411358E; all coordinates are NAD 1983, zone 9). Sample 94-M-152 was collected 3.1 km east of Canyon Creek (UTM 6661682N, 412008E), and consists of fractured and chloritized biotite granite with K-feldspar phenocrysts up to 3 cm in length. Both zircon and abundant monazite were recovered from this sample. A third sample (00-M-115) was collected near the western margin of the Cassiar batholith, from a zone of strongly foliated biotite granite with K-feldspar augen up to 1.5 cm long on the east side of Porcupine Creek, 3.4 km east of the Upper Rancheria River (UTM 6661394N, 387721E). This sample yielded only zircon.

Two samples were dated from the Seagull batholith (Fig. 2). Sample 2005-TL-7 is a fine-grained megacrystic biotite granite containing K-feldspar phenocrysts up to

1.5 cm in length, and was collected on a northeast-trending spur approximately 2 km south of Dorsey Lake (UTM 6669582N, 357865E). This sample contains ~15% fresh black biotite. Sample 2005-RAS-70 was collected on Peak 1727 m, approximately 4.5 km north of the outlet of Dorsey Lake (UTM 6676481N, 354299E). It is an aplitic biotite granite containing ~10% biotite. Both samples yielded abundant zircon and monazite.

ANALYTICAL RESULTS

The two samples of massive granite from the Cassiar batholith each yielded a small amount of zircon, which consisted of clear, pale yellow, equant to stubby prismatic grains, some of which contained visible cloudy cores. Three fractions of zircon were selected from sample 94-M-150, taking care to avoid grains with visible cores. The three analyses all yielded discordant analyses (Fig. 3a) with relatively old Pb/Pb ages (up to 1181 Ma), indicating that inherited cores were present in at least some of the grains in each fraction. The data do not define a linear array, and, therefore, meaningful upper and lower concordia intercept ages cannot be calculated. Both samples also yielded abundant monazite, occurring as

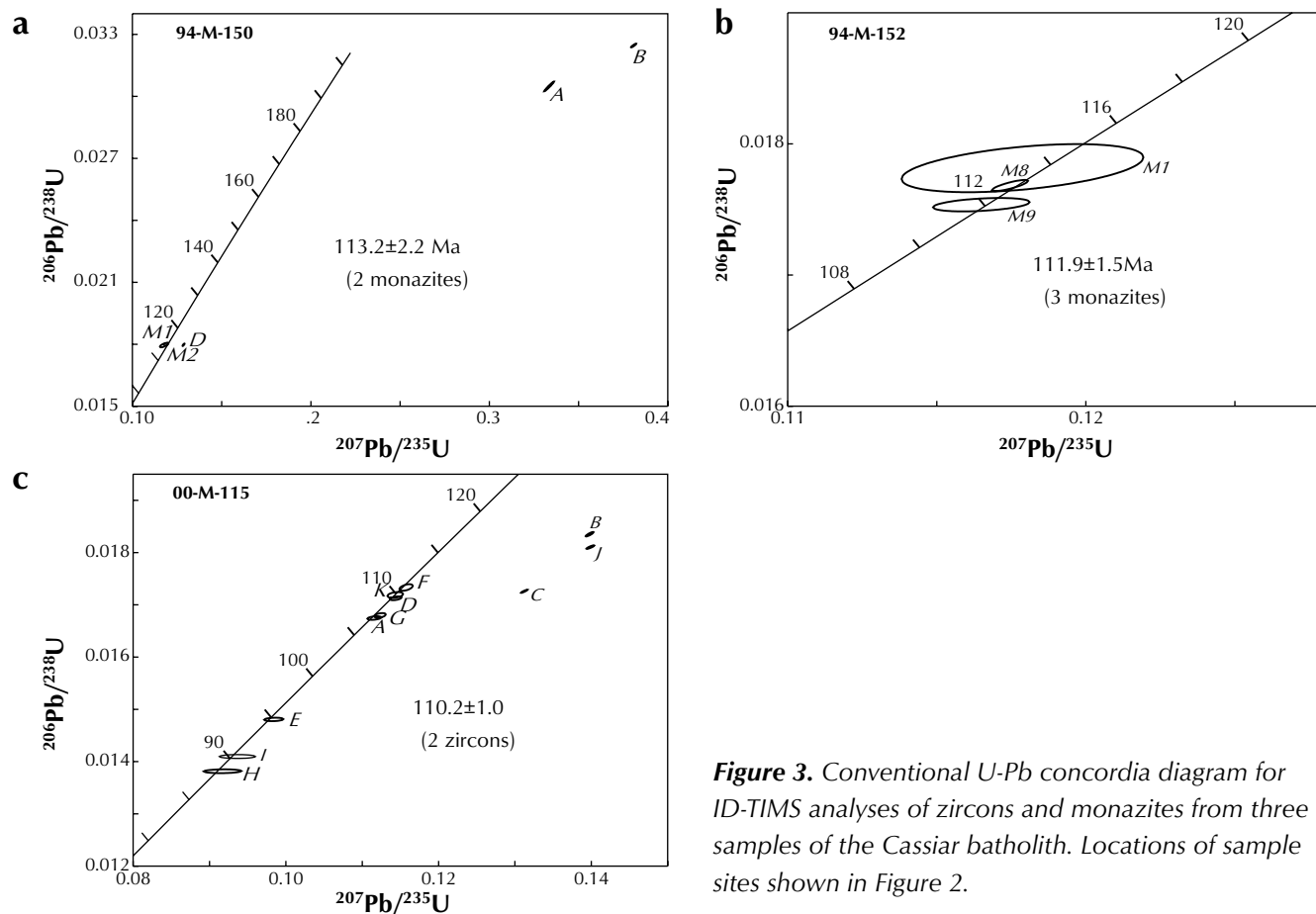


Figure 3. Conventional U-Pb concordia diagram for ID-TIMS analyses of zircons and monazites from three samples of the Cassiar batholith. Locations of sample sites shown in Figure 2.

equant, multifaceted pale yellow grains. Two fractions of monazite were analysed from sample 94-M-150, and both analyses lie slightly above concordia, presumably a result of disequilibrium amounts of ^{206}Pb present. The total range of $^{207}\text{Pb}/^{235}\text{U}$ ages of the two monazite fractions (113.2 ± 2.2 Ma) is taken as the best estimate for the crystallization age of the sample. Only monazite was analysed from the second sample (94-M-152). Three fractions lie on or immediately above concordia (Fig. 3b), and the total range of $^{207}\text{Pb}/^{235}\text{U}$ ages for the three fractions (111.9 ± 1.5 Ma) is taken as the best estimate for the crystallization age.

The sample of strongly foliated and lineated K-feldspar augen gneiss from near the western edge of the Cassiar batholith (sample 00-M-115, Fig. 2) yielded only zircon. Zircons from this sample include some grains that are similar in appearance to those in the previous two samples, along with a larger population of square elongate prisms with simple terminations. Previous work on zircon populations with significant inheritance has shown that this latter morphological population is less likely to contain inherited cores. A total of 12 strongly abraded fractions from the prismatic population were analysed, and a considerable amount of scatter is evident in the data (Fig. 3c). Three of the analyses (B, C and J) are strongly discordant with Pb/Pb ages up to 454 Ma and are interpreted to have contained a significant inherited zircon component. The rest of the analyses fall on, or immediately below, concordia with a considerable amount of scatter in the $^{206}\text{Pb}/^{238}\text{U}$ ages. This scatter is interpreted to reflect the effects of post-crystallization Pb-loss, which is not surprising in light of the very high U-contents of these samples (up to 3843 ppm; Table 1). The best estimate for the crystallization age of the sample is given by the total range of $^{206}\text{Pb}/^{238}\text{U}$ ages for fractions D, F and K, at 110.2 ± 1.5 Ma. There is a small degree of scatter between these three analyses, however, and we cannot preclude the possibility that some or all of these fractions have also experienced minor Pb-loss. The age should therefore be considered to be a minimum estimate for the crystallization age of the gneissic granite.

LA-ICP-MS methods were used to date the two samples from the Seagull batholith. Both samples yielded abundant zircon as well as abundant monazite. The zircon grains range from clear, pale yellow, stubby multifaceted prisms, some of which contain cloudy cores, to elongate square prisms, with simple terminations and rare to abundant clear inclusions. Twenty of the elongate prismatic population were selected from each of the two

Seagull samples and mounted in epoxy pucks along with several grains of the FC-1 zircon standard. The grains were examined on a cathodoluminescence stage to confirm that no cores were present. A total of 11 analyses were done on sample 2005-TL-7 and 12 analyses on sample 2005-RAS-70. Results are shown in Figure 4, in the form of a compilation of measured $^{206}\text{Pb}/^{238}\text{U}$ ages. The individual analyses are relatively imprecise as compared to conventional TIMS analyses, and the assigned ages are based on weighted means of all or most of the $^{206}\text{Pb}/^{238}\text{U}$ ages. Results indicate an age of 95.7 ± 2.1 Ma for sample 2005-TL-7 (Fig. 4a; megacrystic biotite granite phase) and 99.3 ± 2.2 Ma for sample 2005-RAS-70 (Fig. 4b; aplitic biotite granite phase). All eleven analyses were included in the weighted average age for sample 2005-TL-7. However, two analyses from sample 2005-RAS-70 give significantly older ages than the rest, and are interpreted

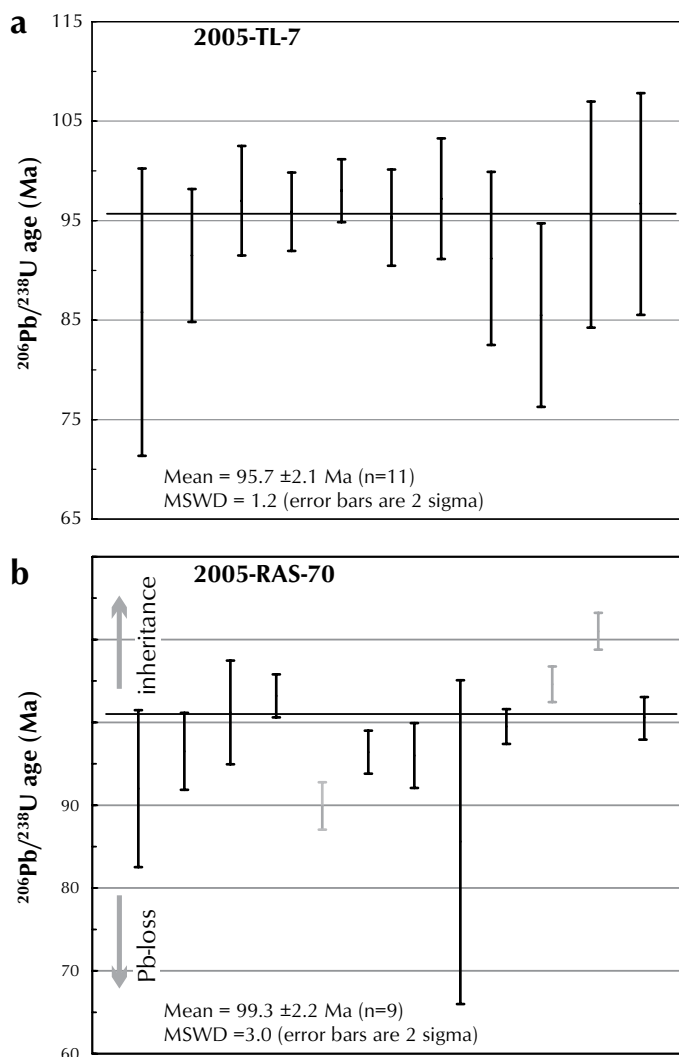


Figure 4. Plot of $^{206}\text{Pb}/^{238}\text{U}$ ages for individual LA-ICP-MS analyses from two samples of the Seagull batholith.

Table 1. U-Pb analytical data for Cassiar Batholith samples (ID-TIMS).

Sample description ¹	weight (mg)	U (ppm)	Pb ² (ppm)	²⁰⁶ Pb/ ²⁰⁴ Pb (measured) ³	total common Pb (pg)	% ²⁰⁸ Pb ²	²⁰⁶ Pb/ ²³⁸ U ⁴ (± % 1σ)	²⁰⁷ Pb/ ²³⁵ U ⁴ (± % 1σ)	²⁰⁷ Pb/ ²⁰⁶ Pb ⁴ (± % 1σ)	²⁰⁶ Pb/ ²³⁸ U age (Ma; ± % 2σ)	²⁰⁷ Pb/ ²⁰⁶ Pb age (Ma; ± % 2σ)
Sample 94-M-150											
A: N2,+104	0.080	834	25.4	14 490	9	7.1	0.08239(0.39)	0.3335(0.42)	0.07935(0.09)	193.6(1.5)	1181.0(3.4)
B: N2,+104	0.062	773	26.1	6517	15	10.2	0.03246(0.14)	0.3809(0.20)	0.08509(0.08)	205.9(0.6)	1317.7(3.2)
D: N2,+104	0.048	1033	18.2	5447	10	7.5	0.01798(0.16)	0.1287(0.23)	0.05191(0.11)	114.9(0.4)	281.4(5.1)
M1: +134,u	0.051	2691	352.4	231	710	87.5	0.01796(0.30)	0.1178(0.99)	0.04754(0.80)	113.0(2.1)5	76.6(38.2)
M2: +134,u	0.046	2647	385.7	437	326	88.8	0.01801(0.19)	0.1190(0.59)	0.04790(0.49)	114.1(1.3)5	94.4(23.0)
Sample 94-M-152											
M1: +104,u	0.009	1167	170.9	593	20	89.0	0.01782(0.51)	0.1179(1.72)	0.04799(1.56)	113.1(3.7)5	98.7(73.8)
M4: +104,u	0.019	2629	337.0	2200	24	87.7	0.01743(0.14)	0.1156(0.24)	0.04810(0.16)	111.0(0.5)5	104.4(7.6)
M8: +104,u	0.024	2010	250.2	1352	39	87.1	0.01768(0.12)	0.1175(0.26)	0.04818(0.17)	112.8(0.6)5	107.9(8.2)
M9: +104,u	0.035	1890	236.4	1185	62	87.3	0.01754(0.15)	0.1165(0.70)	0.04818(0.65)	111.9(1.5)5	108.1(30.9)
Sample 00-M-115											
A: N2,+134,p	0.050	840	15.2	3366	13	16.6	0.01675(0.10)	0.1116(0.41)	0.04832(0.38)	107.1(0.2)	115.1(18.2)
B: N2,+134,p	0.084	1318	25.3	5882	21	13.3	0.01835(0.12)	0.1398(0.19)	0.05524(0.10)	117.2(0.3)	421.9(4.4)
C: N2,+134,p	0.086	1516	27.4	8192	17	13.4	0.01726(0.09)	0.1312(0.16)	0.05514(0.09)	110.3(0.2)	417.8(3.8)
D: N2,+134,p	0.074	1226	23.2	6512	15	18.3	0.01713(0.10)	0.1144(0.34)	0.04844(0.31)	109.5(0.2)	120.8(14.4)
E: N2,+134,t	0.022	2840	42.9	2319	25	11.6	0.01480(0.11)	0.0994(0.21)	0.04869(0.13)	94.7(0.2)	133.1(6.0)
F: N2,+104,p	0.015	1472	28.2	3986	6	16.6	0.01771(0.17)	0.1190(0.21)	0.04870(0.16)	113.2(0.4)	133.5(7.4)
G: N2,+104,p	0.018	1725	31.9	4385	7	17.9	0.01680(0.13)	0.1123(0.34)	0.04850(0.31)	107.4(0.3)	123.6(14.4)
H: N2,+104,p	0.048	2413	34.2	576	177	12.0	0.01382(0.13)	0.0917(1.34)	0.04814(1.33)	88.5(0.2)	106.1(62.9)
I: N2,+104,p	0.042	3843	56.5	1253	114	13.5	0.01410(0.13)	0.0936(1.26)	0.04817(1.27)	90.3(0.2)	107.8(59.2)
J: N2,+104,p	0.018	1771	34.2	3425	10	14.9	0.01811(0.09)	0.1399(0.19)	0.05603(0.11)	115.7(0.2)	453.6(5.0)
K: N2,+104,p	0.015	1299	23.3	1679	12	14.3	0.01719(0.16)	0.1148(0.27)	0.04846(0.22)	109.8(0.4)	121.7(10.5)
L: N2,+104,p	0.037	658	12.8	1399	19	18.7	0.01751(0.10)	0.1178(0.25)	0.04879(0.18)	111.9(0.2)	137.8(8.2)

¹ N2 = non-magnetic at 2 degrees side-slope on Frantz magnetic separator; grain size given in microns; p = elongate square prisms; sp = stubby prisms; mf = equant multifaceted grains; t = tips broken off prisms; u = unabraded.

² radiogenic Pb; corrected for blank, initial common Pb, and spike

³ corrected for spike and fractionation

⁴ corrected for blank Pb and U, and common Pb

⁵ ²⁰⁷Pb/²³⁵U ages given for monazite analyses

to have included a minor inherited component. In addition, one fraction gives a younger age and is interpreted to have experienced post-crystallization Pb-loss. These three fractions were excluded from the calculated average age.

DISCUSSION

The classification of plutonic rocks into suites is an important first step in assessing their role in regional tectonic history and metallogeny. Plutons of Early and mid-Cretaceous age in the northern Cordillera have been subdivided into various plutonic suites on the basis of age, lithology and geochemistry. Those southwest of the

Tintina Fault, including the Cassiar and Seagull batholiths, comprise the Cassiar suite (Mortensen *et al.*, 2000), one of three suites included in the Anvil-Hyland-Cassiar belt by Hart (2004) and Hart *et al.* (2004). These three sites have mainly felsic, weakly to moderately peraluminous compositions.

Establishing common parentage between intrusions in the Cassiar Terrane and those intrusions northeast of the Tintina Fault is complicated by the ~450 km of early Tertiary dextral slip between them. Furthermore, the U-Pb ages for the Cassiar batholith reported here are identical to the 110-113 Ma age range obtained from several large intrusions that were emplaced into the Yukon-Tanana Terrane in the Finlayson Lake District of southeastern

Yukon (Mortensen, unpublished data); and those are included in the Anvil plutonic suite. The Seagull batholith is distinct in age and composition from both the Cassiar batholith and most bodies of the Anvil plutonic suite. Liverton and Alderton (1994), and Hart *et al.* (2004) considered it to represent an ultra-fractionated sub-suite of the Cassiar suite. We suggest that the Seagull batholith is akin to the Tungsten plutonic suite of eastern Yukon and southwestern Northwest Territories (Mortensen *et al.*, 2000; Hart *et al.*, 2004) because our new U-Pb ages for the Seagull batholith (99.3 ± 2.2 Ma and 95.7 ± 2.1 Ma) overlap with ages obtained for various intrusions of the Tungsten suite (Mortensen *et al.*, 2000; Mortensen, unpublished data; Hart, 2004). At this point, however, there are insufficient data available for other intrusions

Table 2. U-Pb analytical data for Seagull Batholith samples (LA-ICP-MS)

Sample number	$^{206}\text{Pb}/^{238}\text{U}$ age (Ma)	Error (Ma, 1 sigma)
	85.8	7.22
2005-TL-7a	91.5	3.34
2005-TL-7b	97	2.75
2005-TL-7c	95.9	1.97
2005-TL-7d	98	1.58
2005-TL-7e	95.3	2.42
2005-TL-7f	97.2	3.03
2005-TL-7g	91.2	4.35
2005-TL-7h	85.5	4.61
2005-TL-7i	95.6	5.68
2005-TL-7j	96.7	5.56
2005-RAS-70a	92	4.74
2005-RAS-70b	96.5	2.32
2005-RAS-70c	101.2	3.13
2005-RAS-70d	103.2	1.3
2005-RAS-70e	89.9	1.43
2005-RAS-70f	96.4	1.3
2005-RAS-70g	96	1.96
2005-RAS-70h	85.6	9.74
2005-RAS-70i	99.5	1.05
2005-RAS-70j	104.6	1.08
2005-RAS-70k	111	1.11
2005-RAS-70l	100.6	1.23

within the Cassiar Terrane to further speculate on possible genetic linkages between the various intrusions.

The age and origin of the strong ductile deformation that affected the western margin of the Cassiar batholith remains unresolved. The deformation is presumably associated with the Cassiar fault; however, since contacts between massive phases of the batholith and ductile deformed phases are not exposed, we cannot prove that the deformation is actually synplutonic. At this point, the minimum age for the fabric development is only constrained to be older than the 89 ± 4 Ma K-Ar muscovite age from the sheared Cassiar batholith granite that was reported by Wanless *et al.* (1972), and younger than both the Rb-Sr whole-rock isochron age of 112 ± 4 Ma (unpublished) and the 110 ± 1.5 Ma zircon age reported here.

A somewhat similar scenario was described by Mortensen and Hansen (1992) at the northwest end of the Nisutlin batholith in west-central Quiet Lake map area, approximately 200 km northwest of the current study area. At this locality, granodioritic orthogneiss yielded a U-Pb zircon and monazite crystallization age of 110.8 ± 0.4 Ma, and a $^{40}\text{Ar}/^{39}\text{Ar}$ cooling age for biotite of 100.0 ± 1.0 Ma. This orthogneiss unit was interpreted to represent an early phase of Cassiar suite magmatism that experienced ductile deformation prior to 100 Ma, and prior to the intrusion of the massive phases of the Nisutlin batholith, which cross-cut the ductile fabrics. Foliations in the gneissic rocks adjacent to the Nisutlin batholith dip gently to the northeast, and kinematic indicators record top-to-the-southeast (or dextral) displacement, which differs somewhat from that of fabrics in the western margin of the Cassiar batholith.

The Anvil-Cassiar suite is regionally associated with proximal tungsten (\pm molybdenum) and zinc-lead skarn mineralization, and more distal silver-lead-zinc veins (Mortensen *et al.*, 2000; Hart, 2004). In southern and central Wolf Lake map area, there are numerous occurrences that are hosted within or immediately adjacent to the Cassiar batholith (Yukon MINFILE, Deklerk and Traynor, 2005). Most of these are polymetallic veins, along with several examples of tungsten, molybdenum and zinc-lead skarns. None of these occurrences have been dated thus far, and therefore we cannot confidently state that they are genetically associated with the Cassiar batholith.

The metallogenic signature of the Seagull batholith is very different from that of the Cassiar batholith. Mineralization

within or immediately adjacent to the Seagull batholith consists of tin (\pm tungsten) skarns and greisens, along with several zinc-lead skarns. The most significant of these occurrences is the JC skarn system (105B 040, Yukon MINFILE, Deklerk and Traynor, 2005) with a drilled reserve of 1.25 Mt of 0.2% Sn (Layne and Spooner, 1991). The nature of the spatially associated mineralization near the Seagull batholith is consistent with its 'ultrafractionated' composition, and it has been assumed (although unproven) that most or all of the skarn and greisen mineralization is temporally and genetically related to the batholith.

CONCLUSIONS

- The age of the Cassiar batholith is now narrowly confined between 110 and 113 Ma, confirming an unpublished Rb-Sr age and revealing that the two K-Ar dates on biotite were too young.
- The U-Pb zircon age for the Seagull batholith confirms earlier K-Ar dates that suggest it is distinctly younger than the Cassiar suite. However, the older date for the less common aplitic phase (99.3 ± 2.2 Ma) and younger date on the common megacrystic phase (95.7 ± 2.1 Ma) are the converse of what is normally expected in a large batholith. The distribution and timing of phases within Seagull batholith warrant further investigation, and is a promising avenue of research in granite petrology and metallogeny.

REFERENCES

- Baadsgaard, H., Folinsbee, R.E. and Lipson, J., 1961. Caledonian or Acadian granites of the northern Yukon Territory. *In: Geology of the Arctic*, G.O. Raasch (ed.), University of Toronto Press, p. 458-465.
- Deklerk, R. and Traynor, S. (compilers), 2005. Yukon MINFILE – A database of mineral occurrences. Yukon Geological Survey, CD-ROM.
- Driver, L.A., Creaser, R.A., Chacko, T. and Erdmer, P., 2000. Petrogenesis of the Cretaceous Cassiar batholith, Yukon-British Columbia, Canada: Implications for magmatism in the North American Cordilleran interior. *Geological Society of America Bulletin*, vol. 112, p. 1119-1133.
- Gabrielse, H., 1969. Geology of Jennings River map area, British Columbia.(104O). Geological Survey of Canada, Paper 68-55, 37 p.
- Hart, C.J.R., 2004. Mid-Cretaceous magmatic evolution and intrusion-related metallogeny of the Tintina Gold Province, Yukon and Alaska. Unpublished Ph.D. thesis, University of Western Australia, Perth, Australia.
- Hart, C.J.R., Goldfarb, R.J., Lewis, L.L. and Mair, J.L., 2004. The northern Cordilleran mid-Cretaceous plutonic province: Ilmenite/magnetite series granitoids and intrusion-related mineralization. *Resource Geology*, vol. 54, p. 253-280.
- Liverton, T. and Alderton, D.H.M., 1994. Plutonic rocks of the Thirtymile Range, Dorsey Terrane: Ultrafractionated tin granites in the Yukon. *Canadian Journal of Earth Sciences*, vol. 31, p. 1557-1568.
- Liverton, T. and Botelho, N.F. 2001. Fractionated alkaline rare-metal granites: two examples. *Journal of Asian Earth Sciences*, vol. 19, p. 399-412.
- Liverton, T., Thirlwall, M.F. and McClay, K.R., 2001. Tectonic significance of plutonism in the Thirtymile Range, southern Yukon. *In: Yukon Exploration and Geology 2000*, D.S. Emond and L.H. Weston (eds.), Exploration and Geological Services Division, Yukon Region, Indian and Northern Affairs Canada, p. 171-180.
- Liverton, R., Mortensen, J.K. and Roots, C.F., 2005. Character and metallogeny of Permian, Jurassic and Cretaceous plutons in the southern Yukon-Tanana Terrane. *In: Yukon Exploration and Geology 2004*, D.S. Emond, L.L. Lewis and G.D. Bradshaw (eds.), Yukon Geological Survey, p. 147-165.
- Lowdon, J.A. 1961. Age determinations by the Geological Survey of Canada: Report 2, Isotopic ages. *Geological Survey of Canada, Paper 61-17*, 127 p.
- Mato, G., Ditson, G. and Godwin, C.I., 1983. Geology and geochronometry of tin mineralization associated with the Seagull batholith, south-central Yukon Territory. *Canadian Institute of Mining and Metallurgy Bulletin*, vol. 76, p. 43-49.
- Mortensen, J.K. and Hansen, V.L., 1992. U-Pb and ^{40}Ar - ^{39}Ar geochronology of granodioritic orthogneiss in the western Pelly Mountains, Yukon Territory. *In: Radiogenic Age and Isotopic Studies: Report 6*, Geological Survey of Canada, Paper 1992-2, p. 125-128.

Mortensen, J.K., Ghosh, D. and Ferri, F., 1995. U-Pb age constraints of intrusive rocks associated with copper-gold porphyry deposits in the Canadian Cordillera. *In: Porphyry Deposits of the Northwestern Cordillera of North America*, T.G. Schroeter (ed.), CIM Special Volume 46, p. 142-158.

Mortensen, J.K., Hart, C.J.R., Murphy, D.C. and Heffernan, S., 2000. Temporal evolution of Early and mid-Cretaceous magmatism in the Tintina Gold Belt. *In: The Tintina Gold Belt: Concepts, Exploration and Discoveries*, J. Jambor (ed.), British Columbia and Yukon Chamber of Mines, Special Volume 2, p. 49-57.

Poole, W.H., Roddick, J.A. and Green, L.H., 1960. Geology, Wolf Lake, Yukon Territory. Geological Survey of Canada, Map 10-1960 (1:253 440 scale, with marginal notes).

Wanless, R.K., Stevens, R.D., Lachance, G.R. and Delabio, R.N., 1972. Age determinations and geological studies: K-Ar isotopic ages, Report 10. Geological Survey of Canada, Paper 71-2.

Stratigraphy summary for southeast Yukon (NTS 95D/8 and 95C/5)

*Lee C. Pigage*¹
Yukon Geological Survey

Pigage, L.C., 2006. Stratigraphy summary for southeast Yukon (95D/8 and 95C/5). *In*: Yukon Exploration and Geology 2005, D.S. Emond, G.D. Bradshaw, L.L. Lewis and L.H. Weston (eds.), Yukon Geological Survey, p. 267-285.

ABSTRACT

Sedimentary strata located within NTS map sheets 95C/5 and 95D/8, southeast Yukon, have a combined thickness ranging between 5000 and 15 000 m and depositional ages ranging from Proterozoic to Paleocene. They can be grouped into eight successions with formations within each succession indicating either similar depositional environments or a horizontal or vertical lithological facies zonation. Early to middle Paleozoic successions are best exposed; Proterozoic, Late Paleozoic, Mesozoic and Cenozoic successions are only locally exposed. Many of the successions are bounded by unconformities; some also contain internal depositional hiatuses. The deposition and preservation of the successions reflect the regional tectonic framework of the Canadian Cordillera from Neoproterozoic to present.

RÉSUMÉ

Les strates de roches sédimentaires dans les régions des cartes 95C/5 et 95D/8 du SNRC, au sud-est du Yukon, ont une épaisseur combinée variant de 5000 à 15 000 m, et ont été déposées du Protérozoïque au Paléocène. Elles peuvent être groupées en sept successions stratigraphiques, qui contiennent chacune des formations indiquant soit des milieux de sédimentation similaires ou une zonation horizontale ou verticale du lithofaciès. Les successions datant du Paléozoïque précoce à moyen sont les mieux exposées; les successions datant du Protérozoïque, du Paléozoïque tardif, du Mésozoïque et du Cénozoïque ne sont apparentes que par endroits. Plusieurs des successions sont limitées par des discordances; certaines comportent également des lacunes de sédimentation internes. La stratification lithologique et les discordances qui séparent les strates peuvent être sommairement interprétées comme des cycles de transgression-régression. La sédimentation et la préservation des successions reflètent le cadre mégatectonique de la Cordillère canadienne depuis le Néoprotérozoïque jusqu'au présent.

¹lee.pigage@gov.yk.ca

INTRODUCTION

The Central Foreland Ancient Pacific Margin National Mapping (NATMAP) project was a multi-disciplinary collaborative geological mapping project initiated to better define the stratigraphy, structure, and mineral and hydrocarbon potential of the Foothills of the Rocky Mountains in northeastern British Columbia, and the Liard Basin region of the southern Northwest Territories and southeast Yukon Territory. The Yukon Geology Program (YGP) joined the Central Foreland NATMAP Project during the 2000 field season and continued to participate during the 2001 and 2002 field seasons. NTS map sheet 95C/5 (Pool Creek) was the primary field area (Fig. 1) for YGP during the 2000 and 2001 field seasons. Bedrock mapping in the western half of NTS map sheet 95C constituted the final field season for YGP in the NATMAP project in 2002.

Yukon Geological Survey (YGS) continued field work (Fig. 1) in NTS map sheet 95D/8 during the 2003-2005 field seasons. The 95D/8 geology mapping was a small-scale program designed to further explore stratigraphy and structure delineated as part of the earlier geological mapping.

This paper summarizes the stratigraphy and facies relations documented as a result of the geology mapping completed by the Yukon Geological Survey during 2000-2005. A more detailed report of the geology of the map areas is in preparation and will be published as a YGS bulletin.

LOCATION AND PHYSIOGRAPHY

NTS map sheets 95C/5 (Pool Creek) and 95D/8 (Fig. 1) are located 150 km west-northwest of Fort Liard, Northwest Territories and 155 km east-northeast of

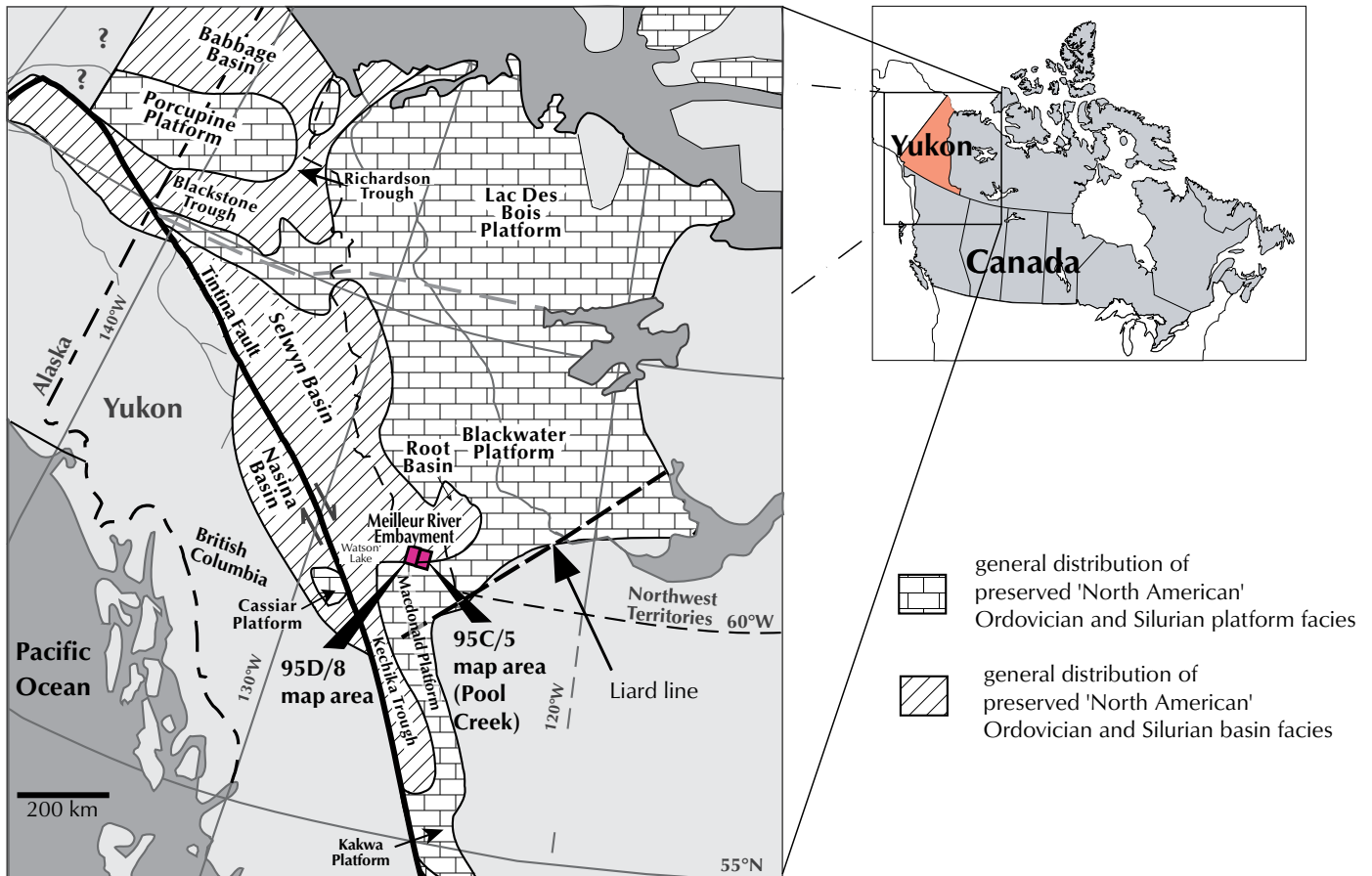


Figure 1. Location of NTS map sheets 95D/8 and 95C/5 in southeast Yukon. General distribution of Ordovician-Silurian platform carbonate and basinal shale facies for Canadian Cordillera and Alaska are indicated. Modified from Cecile et al. (1997).

Watson Lake, Yukon Territory. Topography in both map sheets consists of low rounded hills with incised stream drainages. Elevations range from 1500 feet (460 m) to 4600 feet (1400 m) asl (above sea level). The area is heavily forested with a single, north-trending ridge in the Pool Creek map area extending above tree line for 8 km. Beaver River flows from northwest to southeast through the area into the Liard River and then into the Mackenzie River which drains northward to the Beaufort Sea. Bedrock exposure is 10% or less, with most outcrops occurring as exposures along streams and rivers. Map sheet 95D/8 area contains scattered large lakes which drain southward into the Smith River and then the Liard River, or northward into the Beaver River.

Access was by helicopter from Fort Liard (95C/5) and Watson Lake (95D/8). A fixed-wing aircraft on floats from Watson Lake was used to mobilize and demobilize camps established adjacent to the larger lakes in map sheet 95D/8. Fieldwork was completed primarily by foot and boat traverses from base camps. Spot checks and short foot traverses were completed in other areas where helicopter landing was feasible.

PREVIOUS WORK

The Geological Survey of Canada completed 1:253 440-scale geological bedrock mapping in La Biche River map area (95C) in 1957 as part of Operation Mackenzie (Douglas and Norris, 1959). The geology of the area was further updated based on subsequent fieldwork and compilations completed in adjacent map areas (Douglas, 1976). Framework geological bedrock mapping in Coal River map area (95D) was completed at 1:253 440 scale by the Geological Survey of Canada, largely during 1967 (Gabrielse and Blusson, 1969).

Mineral exploration in 95C/5 between 1973 and 1986 identified U-Th-REE prospects in the contact metamorphic aureole of the Pool Creek syenite, sedimentary-exhalative (SEDEX) targets in lower Paleozoic shales and carbonates, and barite veins in Devonian carbonates (Deklerk and Traynor, 2005). Mineral exploration has been limited since 1986. No mineral claims have been staked in 95D/8; the single MINFILE occurrence in 95D/8 (Deklerk and Traynor, 2005) resulted from the regional mapping completed by Gabrielse and Blusson (1969). Oil and gas exploration activities within Yukon have been largely east and north of the map area.

Preliminary research studies on geology of the map area as part of the Central Foreland NATMAP have been

published in various Yukon Geological Survey Open Files and reports (Allen and Pigage, 2000; Allen *et al.*, 2001; Pigage and Allen, 2001; Pigage, 2004; Pigage and MacNaughton, 2004) and one NATMAP volume (Pigage and Mortensen, 2004). Updated geology maps for adjacent areas in the La Biche River map sheet (NTS 95C) have recently been completed (MacNaughton and Pigage, 2003; Fallas *et al.*, 2004, 2005).

REGIONAL GEOLOGY

NTS map areas 95C/5 and 95D/8 (Fig. 1) are located in southeast Yukon in the Cordilleran miogeocline, a depositional prism of sedimentary rocks of Precambrian to Middle Jurassic age along the relatively stable western continental margin of ancestral North America (Abbott *et al.*, 1986). The map area contains eight successions of sedimentary rocks, ranging from Proterozoic to Paleocene in age. Regional unconformities have been identified between several of these successions, and some of the successions also contain internal unconformities. Early to Middle Paleozoic stratigraphic successions are best preserved in the map area, with younger strata being only locally preserved. Sparse outcrop precluded seeing detailed contact relations between formations in many places. Lateral facies relations are commonly inferred from distribution of the lithologies and time equivalence of the different formations. It is assumed that lithologic facies older than Jurassic are part of a regional west- to southwest-facing marine passive margin of ancestral North America. Sedimentary successions younger than Jurassic are depositionally linked to Cordilleran deformation caused by accretion of exotic terranes to the western margin of North America (Coney *et al.*, 1980).

Figure 2 is a schematic cross-section illustrating the sedimentary formations and successions for the area of interest. The formations and successions are illustrated in time-stratigraphic columns in Figures 3 and 4. These latter figures also indicate the fossil control available for the different formations in the map area.

Intrusive igneous activity in Neoproterozoic and Eocene occurred in close proximity in the map area (Pigage and Mortensen, 2004). Extrusive volcanic rocks are dated stratigraphically or with isotopic age dating as Proterozoic, Cambrian to Ordovician, and Paleocene. Fossil constraints on extrusive activity are locally very poor.

STRATIGRAPHY

SUCCESSION 1 (PROTEROZOIC STRATA)

Succession 1 (Figs. 2,3,4) is exposed in the immediate hanging wall of the Beaver River Thrust in the western part of map sheet 95C/5 (Pigage and Allen, 2001) and consists of two units, a lower siliciclastic unit (Ps) and an upper volcanoclastic unit (Pls). An interpreted fault separates the two units, and stratigraphic relations between them are therefore unknown. Succession 1 strata are unconformably overlain by Crow map unit (unit COc of Pigage and Allen, 2001) belonging to succession 2. Both units Ps and Pls share a common folding deformation, which is not present in any of the younger strata.

Unit Ps

Unit Ps (Allen *et al.*, 2001; their units 1 and 2) consists of interbedded light to dark grey quartzose sandstone and siltstone capped by calc-silicate rock. A minimum exposed stratigraphic thickness for this unit is approximately 500 m; the stratigraphic base is not exposed, and the upper contact is eroded. Sandstones and siltstones are typically finely planar-laminated with laminae being 1-2 mm thick spaced about every 1 cm. Minor intervals up to 1 m thick contain soft-sediment deformation folds.

Planar bedding denotes deposition in quiet water below wave-base. Soft-sediment deformation folds indicate local transport on a slight slope. A proximal offshore depositional environment is indicated because of the thick accumulation of sand-sized material.

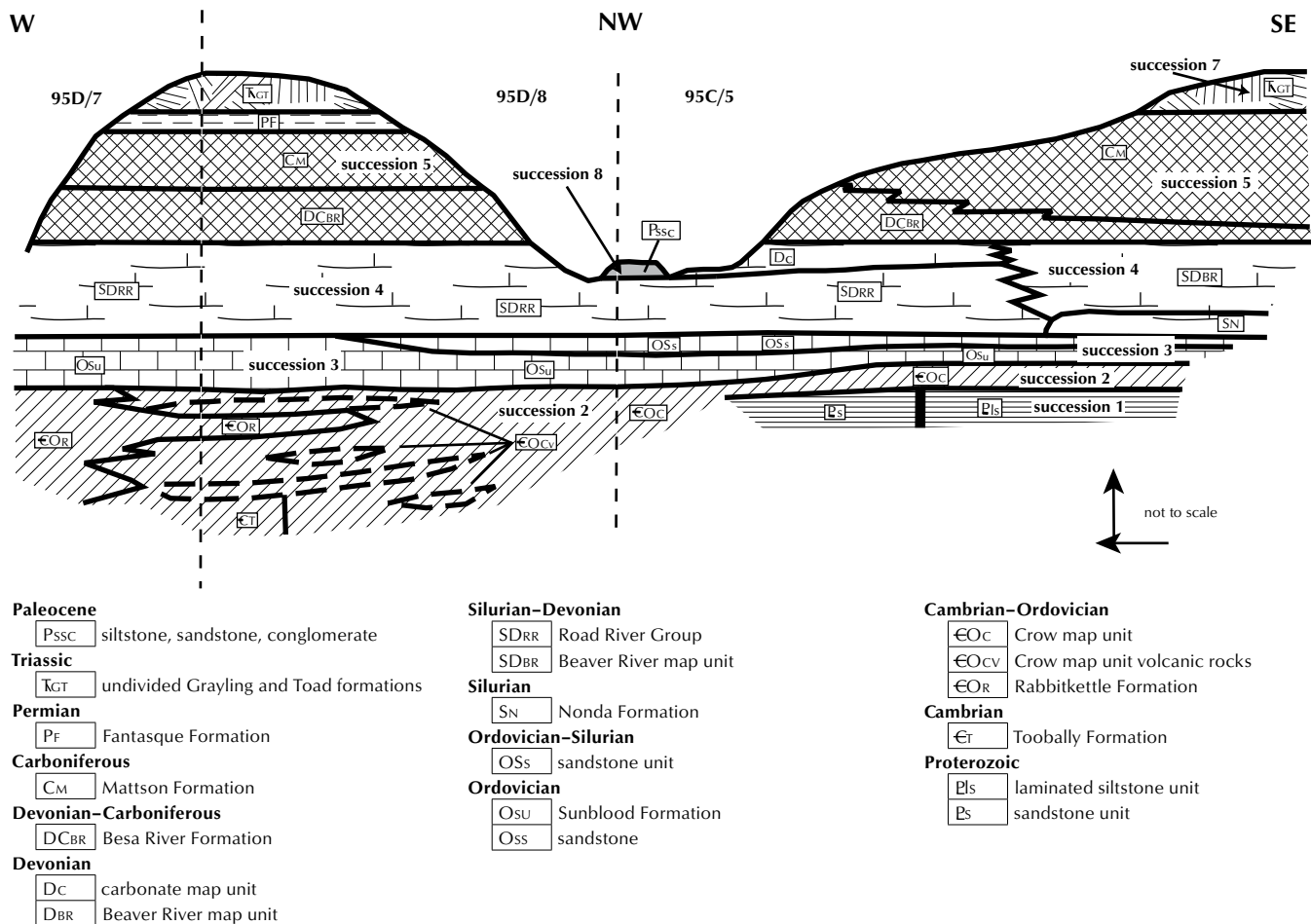


Figure 2. Schematic cross-section for geology contained in 95C/5 and 95D/8. Not to scale. Western part of section oriented east-west; eastern part oriented northwest-southeast. Modified from Fallas *et al.*, (2004).

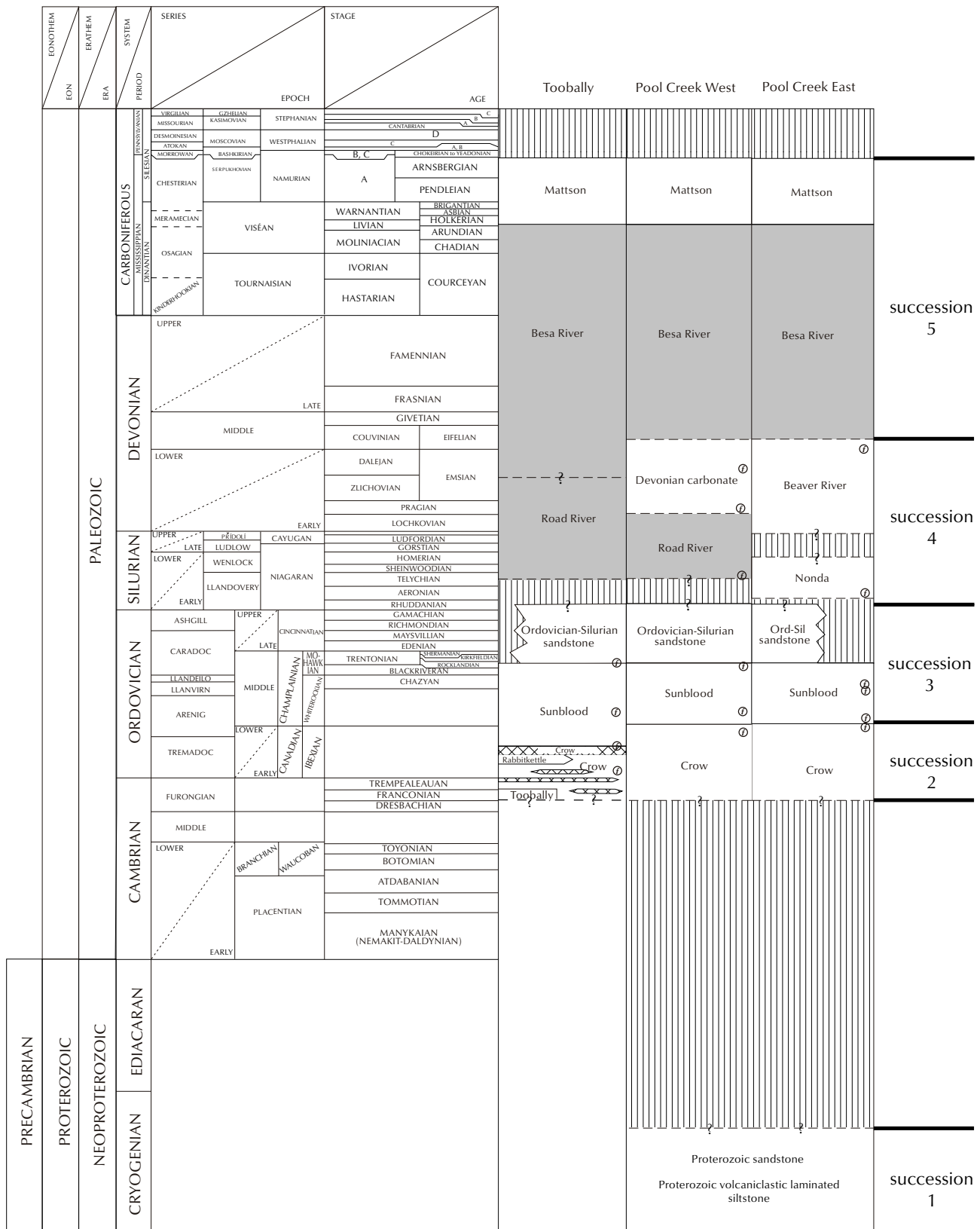


Figure 3. Stratigraphy-time column for Proterozoic, Lower and Middle Paleozoic formations in Figure 2. Fossil control (small 'f' in circle) from McCracken (2003a, 2003b), A.D. McCracken (pers. comm., 2003), Norford (2001, 2002), Nowlan (2004), L.J. Pyle (unpublished data, 2001, 2004). Time scale from Okulitch (2001).

GEOLOGICAL FIELDWORK

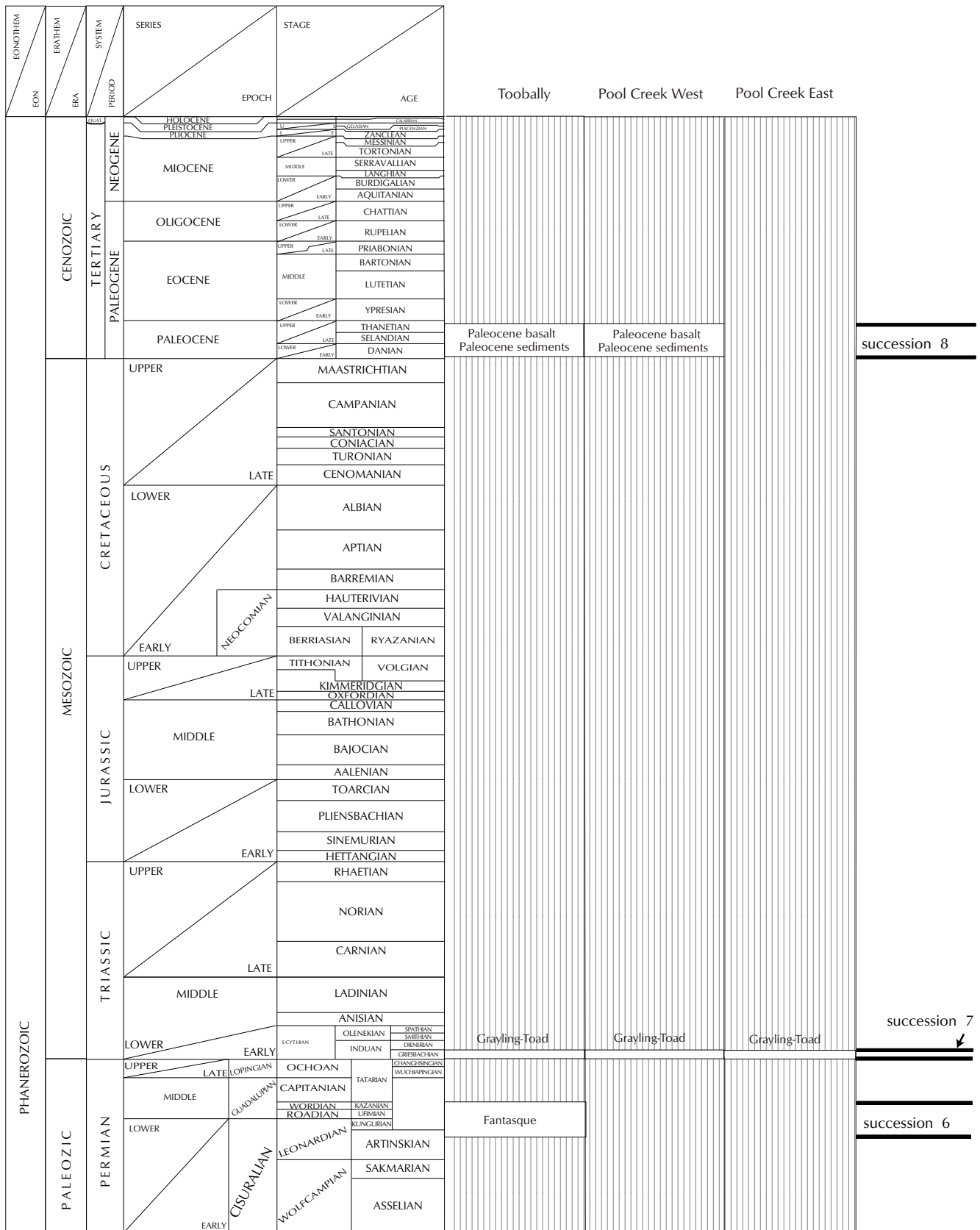


Figure 4. Stratigraphy-time column for Upper Paleozoic, Mesozoic, and Cenozoic formations in Figure 2. Time scale from Okulitch (2001).



Figure 5. Polymictic diamictite, Toobally Formation.

Unit Ps is nonfossiliferous. It is intruded and hornfelsed by the Pool Creek syenite and correlative dykes, which have been isotopically dated at 650 Ma (Pigage and Mortensen, 2004). Isotopic dating of detrital zircons from one sample of Unit Ps provides a maximum depositional age of 1832 ± 23 Ma (G. Gehrels, pers. comm., 2005).

Unit Pls

Unit Pls consists predominantly of pale green argillaceous siltstone with thin, cream, locally calcareous, very fine-grained sandstone interbeds (Allen *et al.*, 2001; their unit 3). The sandstone interbeds are 1-5 cm thick and generally make up 5-50% of the siltstone. Lesser lithologies in unit Pls include green, poorly sorted, matrix- to clast-supported basalt breccias and a brown to green, crudely bedded, poorly to moderately sorted basalt conglomerate (unit 3a in Allen *et al.*, 2001).

As with unit Ps, a minimum exposed stratigraphic thickness for unit Pls is approximately 500 m, with the stratigraphic base not being exposed, and the upper contact being eroded. Unit Pls locally contains isoclinal slump folds oriented at a low angle to bedding (Allen *et al.*, 2001).

No fossils have been noted in unit Pls. It is thought to be older than 650 Ma because of the occurrence of metamorphic epidote and actinolite, which is considered to be due to hornfelsing caused by intrusion of the Pool Creek syenite. Deposition was in quiet water, as indicated by the fine grain size and planar bedding. The occurrence of slumping and massive breccia beds suggests deposition on a slope. These features are

consistent with deposition in a slope-shelf or uppermost slope setting (Allen *et al.*, 2001).

SUCCESSION 2

Toobally Formation, Crow map unit, and Rabbitkettle Formation constitute succession 2 (Figs. 2,3,4). In 95C/5, succession 2 consists entirely of Crow map unit, and it unconformably overlies unit Pls and Pool Creek syenite. In west 95D/8, the lower contact of succession 2 is structural and consists of the Toobally fault (Pigage, 2004).

Toobally Formation occurs immediately west of north Toobally Lake in 95D/8. Crow map unit occurs in both 95C/5 and 95D/8. In westernmost 95D/8, a tongue of Rabbitkettle Formation was mapped within the uppermost Crow map unit (unit Os in Pigage, 2004). The upper contact of succession 2 is diachronous, as Crow map unit is overlain by Sunblood Formation of different ages in 95D/8 and 95C/5 (Fig. 3).

Toobally Formation

Toobally Formation (Pigage and MacNaughton, 2004) consists of massive, orange-weathering, polymictic, matrix-supported conglomerates to pebbly mudstones (Fig. 5) with a minimum inferred thickness of 1800 m. Bedding cannot generally be recognized within this unit. Clasts consist of a variety of rock types, including sandstones, siltstones, dolostones, limestones, and rare volcanic rocks. In one locality a large, finely laminated dolostone olistolith, at least 20 m thick, was mapped overlying outcrop exposures of diamictite.

Pigage and MacNaughton (2004) interpreted the Toobally Formation as being produced by relatively viscous, sediment-gravity flows, probably debris flows. They also noted its similarity to Neoproterozoic glacial diamictites in the Canadian Cordillera and tentatively considered it to be correlative with the Ice Brook and Vreeland formations. Further mapping in 2005 determined that Crow map unit sandstones occur along strike immediately north of Toobally Formation exposures in the central part of 95D/8. Crow map unit, therefore, both overlies the Toobally Formation and occurs along strike with it. This map pattern has important consequences for the ages of both the Toobally Formation and the lower Crow map unit; the ages of these units will be discussed further in the section on the Crow map unit (see below).



Figure 6. Subarkosic quartz sandstone, Crow map unit. Bedding dips gently to the right in the photo.



Figure 7. Clast-supported conglomerate, Crow map unit. Predominant clasts are white, pink and grey quartz sandstones. 95C/5 map sheet. Swiss Army knife for scale (circled).

Crow map unit

The Crow map unit consists predominantly of poorly sorted, thick-bedded to massive, coarse- to fine-grained, pebbly, variably subarkosic sandstones with subangular to subround monocrystalline quartz clasts (Fig. 6). The sandstones are typically indistinctly bedded with bed thicknesses ranging from 20-70 cm. Locally scattered through the sandstone are well rounded quartz pebbles, up to 2 cm across (1-3%), consisting largely of monocrystalline quartz.

Interbedded with the pebbly sandstone on map sheet 95C/5 are lesser intervals of white to light grey, noncalcareous, clast-supported, cobble conglomerate (Fig. 7). Cobbles are well rounded and consist dominantly of quartz sandstone in shades of grey and pink. The matrix for the cobbles is medium- to coarse-grained quartz sand. In one location, the conglomerate has a minimum thickness of 9 m. Imbrication of the cobbles is not visible.

Minor dark maroon, silty argillite is interbedded with the above coarse siliciclastic rock. Dolostone and limestone interbeds are scattered throughout the upper part of the formation in map sheet 95D/8. One prominent, 200-m-thick fossiliferous carbonate horizon occurs about 530 m below the top of the formation in the west part of 95D/8. Carbonate horizons do not occur within Crow map unit in the 95C/5; some intervals of sandstone and siltstone in that map sheet, however, are calcareous.

West of north Toobally Lake, in map sheet 95D/8, the Crow map unit contains dark purplish green, amygdaloidal to vesicular, massive to pillowed alkali basalts and interbedded, thick-bedded to massive, lapilli tuffs occurring at four stratigraphic levels. No volcanic rocks were recognized in the formation in 95C/5. The most prominent of these horizons (horizon 2) is about 890 m thick and has been mapped laterally along strike for a distance of slightly greater than 15 km. Previously, these volcanic horizons (Goodfellow *et al.*, 1995) have informally been referred to as the Toobally (horizon 2) and Gusty volcanics (horizon 4). Geochemistry of the basalts is consistent with the volcanic horizons being within-plate alkali basalts (Pigage and MacNaughton, 2004).

The upper and lower contacts of the Crow map unit are not directly exposed. In 95C/5, the lower contact is unconformable as the Crow map unit overlies both succession 1 strata and the Pool Creek syenite. In 95C/5, thickness of the Crow map unit is approximately 300 m;



Figure 8. Desiccation cracks and ripples in subarkosic sandstone, Crow map unit.

in the west part of 95D/8, it has an interpreted thickness in excess of 5700 m if the unit is structurally intact.

The occurrence of poorly sorted, fine- to coarse-grained, locally cross-bedded sandstones interbedded with pebbly sandstones, cobble conglomerates, maroon siltstones and argillites, and fossiliferous carbonates indicates a shallow water marine to subaerial fluvial depositional environment. The common presence of desiccation cracks, herringbone cross-bedding and ripples (Fig. 8) also indicates a shallow to intertidal to subaerial depositional environment. Subangular shapes for grains and subarkosic composition suggest an immature clastic succession.

Conodont fossil collections from the upper part of the Crow map unit and the overlying Sunblood Formation indicate the upper contact is diachronous, ranging from earliest Whiterockian to Tremadocian (Fig. 3). A maximum age for the lower part of the Crow map unit has not been defined through fossils. Given a total thickness of 4000 to 5700 m for the Crow map unit in 95D/8, it is reasonable to assume that the lower part of the map unit is Cambrian. A Cambrian age, however, is at variance with the interpreted age of Neoproterozoic for the Toobally Formation, which is directly along strike with it (Pigage, 2004).

Figure 9 illustrates three possible stratigraphic and structural scenarios for interpreting the map pattern for the Toobally Formation and Crow map unit. Scenarios 9a and 9b retain the Neoproterozoic age for the Toobally Formation. A major unconformity is required at the base of the volcanic horizon immediately above the Toobally

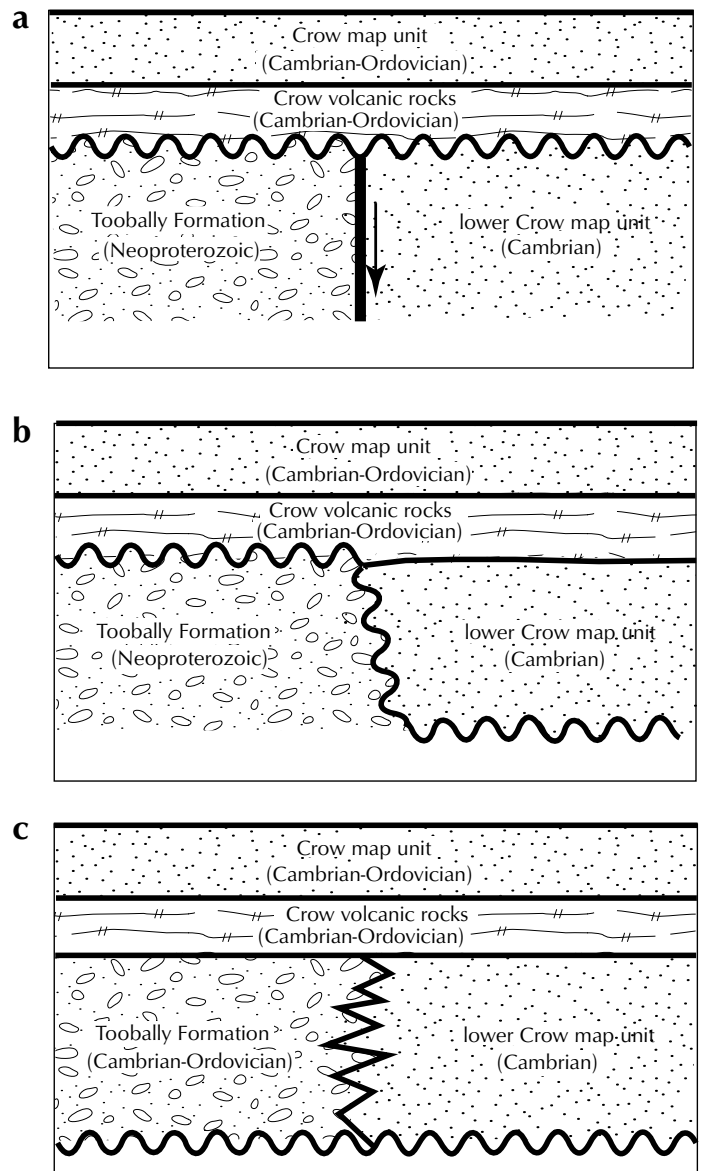


Figure 9. Interpreted stratigraphic and structural relations between Toobally Formation and Crow map unit. In (a) and (b), Toobally Formation is Neoproterozoic and lower Crow map unit is Cambrian. In (c), Toobally Formation and Crow map unit are Cambrian-Ordovician.

Formation to account for the volcanic horizon being uninterrupted along strike. In scenario 9a, the lateral contact between Toobally Formation and Crow map unit is an early, pre-unconformity fault. The unconformity at the top of the Toobally Formation is internal to the Crow map unit in the northern part of 95D/8. With scenario 9b, the unconformity at the top of the Toobally Formation has erosional relief, cutting down through the Toobally Formation in a northward direction. In this interpretation,

the unconformity remains at the base of the Crow map unit throughout the map area. Scenario 9c introduces the possibility that the correlation of Toobally Formation with Neoproterozoic glacial diamictites is in error, and the along-strike contact between Toobally Formation and Crow map unit is a lateral facies change. The major unconformity at the base of the Crow map unit in 95C/5 is inferred to occur at the base of the Toobally Formation in 95D/8.

All three interpretations have geological challenges. With 9a, the Crow map unit contains an internal unconformity representing a time interval of over 30 million years with identical lithologies above and below the unconformity surface. With 9b, the unconformity at the base of the Crow map unit has an erosional relief of some 1400 m within a 1-km lateral distance. With interpretation 9c, the expected interbedding of Toobally diamictite and Crow map unit sandstone close to the lateral transition between the two units has not been seen in the field. In support of interpretation 9c, the Toobally Formation lacks readily visible bedding and dropstones (primary sedimentary features which are present in both Ice Brook and Vreeland formations), making a lithologic correlation of the Toobally with these units less compelling. I have inferred interpretation 9c in Figure 3; further work is needed to properly constrain the ages of the Toobally Formation and lower Crow map unit.

Rabbitkettle Formation

In the western part of 95D/8, the upper part of the Crow map unit contains an interval of thin-bedded, brownish grey, slightly dolomitic siltstone approximately 750 m



Figure 10. Nodular limestone beds in dolomitic siltstone, Rabbitkettle Formation.

thick. The uppermost part of the siltstone contains distinctive interbeds of nodular, medium-grey limestone (Fig. 10). Neither upper and lower contacts are exposed. I have interpreted this interval as a tongue of Rabbitkettle Formation (Gabrielse *et al.*, 1973) based on age and lithologic characteristics. The Rabbitkettle Formation thins rapidly and disappears to the south, as it was not observed in the southern part of 95D/8 (Pigage, 2004). It also was not observed in the east-half of 95D/8, nor in 95C/5. Mapping by Gabrielse and Blusson (1969) confirmed that Rabbitkettle Formation increases significantly in thickness to the west and north, and Crow map unit is absent in the same directions. The schematic cross-section in Figure 2 therefore interprets a lateral facies change from shallow-water, coarse clastics of Crow map unit to deeper water, fine clastics of Rabbitkettle Formation towards the west and north.

Fossils collected regionally from the Rabbitkettle Formation encompass Late Cambrian (Franconian) through Early Ordovician (Gabrielse *et al.*, 1973; Tipnis *et al.*, 1978; Cecile, 1982). The formation in the type area is bounded by unconformities at both its lower and upper contacts. The lower unconformity is angular and marks a major stratigraphic break, as regionally, the Rabbitkettle Formation overlies strata as old as the Precambrian-Lower Cambrian Hyland Group (Gabrielse *et al.*, 1973). This major unconformity is presumed to be at the base of the Crow map unit in Figures 2, 3 and 9c. In the map area, fossil control constrains the Rabbitkettle tongue in 95D/8 as being Tremadocian (Fig. 3).

SUCCESSION 3

Succession 3 is comprised of the Sunblood Formation, conformably overlain by interbedded sandstones, shales, and bioturbated siltstones of unit OSs. West of the map area unit OSs is absent (Gabrielse and Blusson, 1969).

Sunblood Formation

In the map area, the Sunblood Formation (Kingston, 1951) consists of medium to dark grey, tan to tan-grey weathering, fine-grained, interbedded dolostones and limestones (Fig. 11). It is a resistant unit and locally forms cliffs over 30 m high. Beds typically range between 5 cm and 1 m in thickness. Dolostone is the predominant lithology; limestone intervals within the dolostone range up to 60 m thick. Both limestone and dolostone are essentially monomineralic, with only very minor amounts of opaque minerals and quartz.



Figure 11. Mottled bedding plane surface, Sunblood Formation. Mottling caused by burrowing.



Figure 12. Interbedded sandstone and dolomitic siltstone, unit OSs. Bedding dips back into the photo. Intervals with rough, recessive outcrop are dolomitic siltstone. Previously published as Figure 14 in Allen *et al.* (2001).

Interpreted thickness of the Sunblood Formation in 95C/5 ranges from 150 to 550 m (Pigage and Allen, 2001). The formation is thinnest in the south-central part of 95C/5. It increases in thickness to the west, with an interpreted thickness of greater than 2000 m in the western part of 95D/8 (Pigage, 2004).

The lower contact of the Sunblood Formation is diachronous, ranging in age from earliest Middle Ordovician (Whiterockian) in 95C/5 to early Early Ordovician (middle Tremadocian) in 95D/8 (Fig. 3). Conodonts from the uppermost part of the Sunblood Formation give an early Late Ordovician (early to middle Caradocian) age.

Sunblood Formation is exposed in Northwest Territories and Yukon over a widespread area north and west of the map area. Sunblood carbonates were deposited in a shallow, dominantly sublittoral (0-100 m depth) environment on a carbonate platform up to 100 km wide (Ludvigson, 1975). The formation is bounded on the southwest by deeper water, dark grey to black shale facies of Selwyn Basin (Cecile *et al.*, 1997); this facies transition is located west of the map area.

Unit OSs

Unit OSs occurs as scattered outcrops of sandstone and pebbly sandstone, with lesser interbeds of pebble to cobble conglomerate, bioturbated dolomitic siltstone, and dark grey, silty shale (Fig. 12). It has an interpreted thickness of 160 to 200 m. The lower contact with

Sunblood Formation is conformable and is marked by an abrupt, but gradational change from dolostone through calcareous sandstone to sandstone. The upper contact is not exposed, but is marked by a rapid change to black, silty, graptolitic shales and limestones of the Road River Group. This upper contact is considered to be an unconformity because of the time gap inferred from fossil control (Fig. 3).

Unit OSs is described in more detail as unit 6 in Allen *et al.* (2001). Dolomitic siltstone and dark grey to black shale lithotypes decrease in abundance to the southeast in 95C/5. Outcrops along the Beaver River in the central part of 95C/5 consist entirely of quartz sandstone, and approximately 50% of the unit in the northwest corner of 95C/5 consists of dolomitic siltstone and interbedded grey shale.

Unit OSs does not contain diagnostic fossils for determining an age of deposition. It is considered to be Ordovician to possibly earliest Silurian because it conformably overlies the Ordovician Sunblood Formation and underlies the Silurian Road River Group (see below).

Extensive *Teichichnus*, *Phycodes* and *Planolites* ichnogenera and bioturbation indicate the depositional environment contained abundant nutrients and was most likely in the offshore transitional zone between fair-weather and storm wave bases (MacNaughton, 2002a). The common occurrence of sand and locally coarser clastic sediments suggests a proximal rather than distal depositional environment.

SUCCESSION 4

Succession 4 contains the lateral facies transition from carbonate platform sediments of Macdonald Platform to fine clastic, basinal sediments of Selwyn Basin (Cecile *et al.*, 1997; Fig. 1). The facies transition occurs in 95C/5 with shales of the Road River Group being restricted to the northwest corner of the map sheet, and time-equivalent thick carbonate rocks of the Nonda Formation, Beaver River map unit and the Devonian carbonate map unit occurring south and east of the Road River shale outcrops. The transition is rapid, but is also foreshortened by thrust faults in the area of the transition.

The carbonate Macdonald Platform is represented by, from oldest to youngest, the Nonda Formation, Beaver River map unit and the Devonian carbonate map unit. This succession of carbonates is 1300 m to 1400 m thick.

Nonda Formation

The lowermost Nonda Formation (Norford *et al.*, 1966) is a dark, fetid dolostone, locally with cherts. Its lower contact is sharp and is marked by an abrupt change from thick-bedded dolostones of the underlying Sunblood Formation to thin-bedded dolostones. Interpreted thickness of the Nonda Formation ranges from 90 m to 200 m. Fossil control for the age of the Nonda Formation is not available from the map area. Regionally, both upper and lower contacts are unconformable; in the type area, the formation is late Llandovery (Early Silurian) in age (Norford *et al.*, 1966).



Figure 13. Thick-bedded dolostone cliffs of Silurian-Devonian carbonates, Beaver River Formation. Bedding dips moderately to right in photo. Outcrop occurs in canyon along the Beaver River. Height from Beaver River to top of ridge is about 335 m.

Beaver River map unit

Dolostones of the Nonda Formation are overlain by a 1200-m-thick, monotonous succession of thick-bedded, generally nonfossiliferous, medium-grey, tan-weathering dolostones (Fig. 13) of the Beaver River map unit (Pigage, unpublished data). Its occurrence is restricted to east and south parts of 95C/5. Beds range from 10 cm to greater than 7 m thick, generally being 1-2 m thick. The uppermost 120 m of Beaver River map unit is fossiliferous, with visible two-hole crinoids. Based on fossil control, this uppermost part of the carbonate succession is middle Devonian (Fig. 3). The Beaver River map unit is correlated with Muncho-McConnell, Stone and Dunedin formations in northeastern British Columbia (Taylor and Mackenzie, 1970). The early Devonian Muncho-McConnell Formation unconformably overlies the Nonda Formation in northeastern British Columbia; by correlation, the maximum age of the Beaver River map unit is considered to be early Devonian, and its lower contact is also possibly unconformable (Fig. 3).

Devonian carbonate map unit

The Devonian carbonate map unit overlies the Road River Group and occurs northwest of the Beaver River map unit (Pigage and Allen, 2001). It is laterally equivalent to the uppermost fossiliferous part of the Beaver River map unit and the Dunedin Formation. Both limestone and dolostone occur within this unit. Limestone intervals consist of interbedded argillaceous limestones and fossiliferous grainstones. Dolostones commonly contain irregular black chert lenses. The maximum extent of the Devonian carbonate unit to the northwest occurs in nearby map sheets 95C/12, 95C/11, and 95C/14 (Fallas *et al.*, 2005). Fossils indicate a Middle Devonian age for this unit (Fig. 3).

Road River Group

Road River Group (Jackson and Lentz, 1962; Gordey and Anderson, 1993) is restricted to the northwestern corner of 95C/5 and eastern exposures in 95D/8. It is a heterolithic unit with the dominant lithology being a dark grey, noncalcareous to calcareous, graptolitic, silty shale. Interbeds within the shale include dark grey to black limestone and tan-weathering sandstone and siltstone. Overwhelmingly, the distinctive characteristics of the Road River Group are the presence of dark grey to black, organic material and the common occurrence of graptolites (Fig. 14). In the northwest corner of 95C/5,



Figure 14. Graptolites on bedding plane surface of dark grey limestone, Road River Group.



Figure 15. Dark grey to black, siliceous shale of Besa River Formation.

however, the upper part of Road River is a dark grey to black siliceous shale without graptolites.

Graptolites and conodonts collected from Road River Group indicate an age range of late Llandoveryan (late Early Silurian) to Lochkovian (Early Devonian). The lower contact is unconformable because of the time gap inferred from the fossil control (Fig. 3). The upper contact is abrupt; fossil collections have not been systematic enough to determine if it is conformable. Interpreted thickness of the Road River Group in the map area is 950 m.

SUCCESSION 5

Succession 5 consists of the dark grey to black, siliceous shales and bedded cherts of the Besa River Formation, overlain by the sandstones with lesser shales and limestones of the Mattson Formation.

Besa River Formation

Besa River Formation (Kidd, 1963) is generally recessive. It consists of dark grey to black bedded cherts and interbedded light grey-weathering, siliceous, carbonaceous shales (Fig. 15). Locally, the shales contain large limestone concretions. It has an interpreted thickness of 250 m to 750 m. The lower contact is not exposed. The upper contact is gradational with the Mattson Formation sandstones. Sandstone near the contact contains interbeds of dark grey shale typical of Besa River Formation.

The Besa River Formation is Middle Devonian to late Viséan (Lower Carboniferous) in age (Richards, 1989). Both upper and lower contacts are diachronous, with the age of the lower contact increasing, and the age of the upper contact decreasing from east to west. Macrofossils were not found in the Besa River Formation in the Pool Creek area. Conodont collections from limestone interbeds within the formation indicate Middle Devonian ages.

Deposition of Besa River shales was in a dysaerobic marine basin at moderate water depths (Richards, 1989). Richards (1989) suggested that shale and chert resulted from a combination of hemipelagic sedimentation and deposition from weak, gravity-assisted suspension currents.

Mattson Formation

Mattson Formation (Patton, 1958) in 95D/8 consists of fine-grained, thick-bedded, grey quartz sandstone. It has an interpreted thickness of 1450 m. In 95C/5, Mattson Formation becomes much thicker, ranging from 1850 m to 2850 m in interpreted thickness. It can be divided into two members in 95C/5, a lower member consisting of quartz sandstone with interbedded black shales (Fig. 16), and an upper member consisting predominantly of thick-bedded quartz sandstones with minor interbedded limestones. The upper contact is unconformable with a significant time gap before deposition of the overlying Fantasque Formation or undivided Grayling and Toad formations (Figs. 3 and 4).



Figure 16. Interbedded grey sandstone and dark grey siliceous shale, lower Mattson Formation.

East of the present map area, the interpreted depositional environment for the Mattson Formation is a south- to southwest-prograding delta complex with interbedded eolian sands, coals, fluvial deposits, channel-fill deposits, submarine channels, and delta shoreline deposits (Richards *et al.*, 1993). Exposures in the map area are clean quartz arenites, and therefore are not typical prodelta deposits; more sedimentological research is required to delineate the depositional environment. Age definitive fossils were not found in the area of interest. Fossils from thicker intervals to the east indicate the formation is upper Viséan to Serpukhovian (Richards *et al.*, 1993).



Figure 17. Siliceous, dark grey shales, Fantasque Formation. Beds dip moderately left in photo. Interval of change between bedded and thin bedded in centre of photo contains numerous carbonate concretions.

SUCCESSION 6

Succession 6 consists of siliceous shales and limestones of the Permian Fantasque Formation. It is preserved in the map area only in one structural panel forming the immediate footwall to the Toobally fault (Pigage, 2004) in 95D/8.

Fantasque Formation

Fantasque Formation (Harker, 1961) consists of siliceous shale with one interbed of thin-bedded, dark grey limestone. The shales are internally bedded on a scale of 5 to 20 cm (Fig. 17); nodular limestone beds occur scattered through the shale succession. Interpreted thickness of the unit is approximately 1700 m. In this structural panel, the Fantasque Formation disconformably overlies the Mattson Formation (Fig. 4) and is disconformably overlain by Triassic Grayling and Toad formations (Figs. 3 and 4).

Lateral areal exposure of the Fantasque Formation is much less extensive than that of the earlier successions, most likely indicating more extensive erosion after deposition. Regionally, the Fantasque Formation is late Artinskian (Early Permian) through Wordian (Late Permian; Henderson *et al.*, 1993) in age. One conodont collection from the area of interest had a broadly Permian age (L.J. Pyle, unpublished data, 2004). Depositional environment is presumed to be similar to that of the Besa River Formation, consisting of a dysaerobic marine basin at moderate water depths.



Figure 18. Soft, grey shales of the undivided Triassic Grayling and Toad formations.

SUCCESSION 7

Grayling and Toad formations

Dark grey, soft recessive shales with lesser interbedded thin, tan-weathering sandstones (Fig. 18) constitute Triassic sedimentary rocks in the map area. Since outcrop control is sparse, Triassic siliciclastic sedimentary rocks have generally been mapped as consisting of undivided Grayling and Toad formations (Kindle, 1944; Fallas and Lane, 2001). Shales are preserved mainly in synclinal fold keels, and in the immediate footwall of thrust faults in southern 95C/5 and central 95D/8. Interpreted thicknesses in the map area are very subjective, depending on assumed orientations of the overlying thrust faults and cross-sectional interpretation of the synclinal fold pattern. Interpreted sections within the map area have an inferred thickness ranging from a minimum of 150 m to a maximum of 850 m (Pigage, 2004). Regionally, within southwest 95C, interpreted thicknesses range from 1000 m to 1500 m (Fallas *et al.*, 2004).

Pollen samples for the undivided Grayling and Toad formations in southeast Yukon were identified as Griesbachian (Early Triassic; Utting *et al.*, 2005). Fossils from underlying and overlying sediments indicate both upper and lower contacts for Triassic siliciclastic rocks are disconformities. Detailed stratigraphic studies of the Early Triassic section in Mount Martin (95C/1) and Mount Merrill (95C/2) areas indicate that deposition of the Triassic sediments was in a nearshore shallow marine environment (MacNaughton, 2002b; Utting *et al.*, 2005).

SUCCESSION 8

Unit Pssc

Succession 8 consists of a slightly greater than 160-m-thick succession of horizontal, tan, noncalcareous, poorly consolidated, siltstones, sandstones, and conglomerates. They underlie an east-trending, ridge-length of approximately 5 km in the northwest corner of 95C/5, and possibly extend slightly into 95D/8. In one small area, the sedimentary rocks are conformably overlain by a 15- to 20-m-thick, dark brown, columnar-jointed, massive to slightly vesicular basalt flow. The conglomerate immediately beneath the basalt flow is baked and therefore more resistant to erosion, resulting in an inverted topography, as poorly consolidated sediments have been removed by erosion from other areas. The sediments unconformably overlie folded Silurian-Devonian Road River Group strata.

The sandstones contain thinner interbeds of clay siltstone to mudstone and highly variable 'red beds'. Siltstone intervals consist of well sorted clayey siltstone to mudstone. Lithologies are discontinuous across the section, occurring as thin lenses up to 20 m long. Locally abundant organic material, much of which is coalified, occurs as small lenses. Red-bed intervals consist dominantly of a dark-red-stained, matrix-supported conglomerate with a strongly to moderately cemented sand-silt matrix. Lesser discontinuous interbeds within the conglomerate include well sorted siltstone, sandstone, and fine conglomerate. Marginal contacts are gradational or sharp and are typically irregular.

The presence of columnar jointing in the basalt, the occurrence of red beds and coal in the sediments, and the widespread presence of gravels and sands with interbedded discontinuous silts and sands, all indicate a fluvial depositional environment, probably a clastic braided river environment (I.R. Smith, pers. comm., 2001). Imbrication and bar forms, and columnar leaning in the basalt all indicate a paleoflow direction of east to east-southeast.

A sample of the basalt flow was dated with $^{39}\text{Ar}/^{40}\text{Ar}$ methods by Dr. M. Villeneuve of the Geological Survey of Canada Geochronology Laboratory as $56.2 \pm 0.8 \text{ Ma}$ (2σ) (M. Villeneuve, pers. comm., 2003). The basalt flow is therefore Late Paleocene, and underlying sediments are also assumed to be Paleocene.

DISCUSSION AND SUMMARY

The various sedimentary formations of 95C/5 and 95D/8 areas have been presented above as eight major stratigraphic successions, ranging from Proterozoic to Paleocene, with a combined thickness on the order of 5000 m to 15 000 m. Early to Middle Paleozoic stratigraphic successions are best preserved in the map area with later strata being only locally preserved. Each succession contains one or more formations with related lithologic facies and depositional environments. In many cases, these successions are separated by unconformities, mostly marking significant hiatuses. Internally, the successions also locally contain unconformities.

The sedimentary successions record vertical and lateral changes in the depositional environment through time. In a broad sense, discussion of the stratigraphy in this format is similar to, but not as detailed as, a sequence stratigraphy approach (Cantuneanu, 2003). The variations in the sedimentary depositional environment are caused by an interplay of tectonics, eustasy and climate (Cantuneanu, 2003).

Succession 1 is older than 650 Ma and younger than about 1830 Ma. Exposed Proterozoic sedimentary rocks in the Canadian Cordillera have been divided into three successions A, B, C (Young *et al.*, 1979). Given the above age constraints, succession 1 is a possible correlative with any of Sequences A, B or C. Additional detrital zircon research may further restrict the age of deposition of succession 1 strata and better constrain possible regional correlations.

Without tighter age constraints, it is difficult to determine if this succession is associated in any way with the early rifting of Laurentia (Bond and Kominz, 1984; Ross, 1991; Colpron *et al.*, 2002). The absence of coarse clastic rocks in unit Ps suggests this succession may predate Proterozoic to Cambrian rifting. Alternatively, volcanic rocks and coarse breccias and conglomerates in unit Pls may record volcanism and rifting during initial breakup of Laurentia.

Successions 2 through 5 record miogeoclinal sedimentation on the western margin of ancestral North America. Both successions 2 and 4 contain a horizontal facies zonation westward from a shallow marine depositional setting to a deeper water marine depositional environment. In succession 2, proximal sedimentation is dominated by quartzose siliciclastic rocks, and in succession 4, the transition is marked by a

rapid lateral facies change from shallow marine carbonates to deeper water marine shales.

Succession 3 in the map area consists predominantly of shallow-water platform carbonates of the Sunblood Formation. The facies transition to marine basinal shales occurs farther west than the area of interest (Cecile *et al.*, 1997).

Succession 2 in southeast Yukon reflects a large measure of local and/or regional tectonic control. The upper part of the Crow map unit is time-correlative with the early to middle Ordovician Mackenzie carbonate platform, to basinal shale transition in central Yukon (Abbott *et al.*, 1986), and a similar transition between Macdonald Platform carbonates and Kechika Trough basinal shales in northeastern British Columbia (Pyle and Barnes, 2000). The Early Ordovician, coarse siliciclastic sedimentary rocks of the Crow map unit are unique to southeast Yukon and do not occur along strike to the north or south. Dramatic thickening of the Crow map unit between map sheets 95C/5 (300 m) and 95D/8 (5700 m) suggests a local paleohigh in 95C/5, possibly related to faulting. It is interesting to note that Cecile *et al.* (1997) identified the Liard Line (Fig. 1), slightly south of the map area of interest, as a major northeast-trending ancestral transfer fault, with substantial uplift occurring south of it during early Paleozoic.

Succession 5 records a shallowing-upward trend, with coarse clastic rocks of the Mattson Formation conformably overlying carbonaceous shales of the Besa River Formation. The lateral facies transition from basinal shales of the Besa River Formation to carbonates of the Flett and upper Banff formations (Richards, 1989) occurs east of the map area in the east side of 95C.

Permian (succession 6), Triassic (succession 7) and Paleocene (succession 8) sedimentary rocks are only locally preserved in the map area. The absence of Permian to Paleocene sedimentary rocks indicates that substantial erosion occurred in the map area as a result of contractional deformation and consequent structural thickening that caused mountain building and associated development of foredeeps (Stott *et al.*, 1993). This east-verging deformation was caused by collision and accretion of exotic terranes to the western margin of North America starting in Jurassic time (Coney *et al.*, 1980).

ACKNOWLEDGEMENTS

Jordin Barclay, Annie Daigle, Kristen Kennedy, Jesse Kirkby, André Lebel, Janis Lloyd, Andrew McNeill, Mark Ponto and Kyle McWilliam assisted in the field. Tammy Allen spent two field summers working on the project as a senior geological assistant. Rob MacNaughton measured a detailed stratigraphic section in the area, and Rod Smith completed regional and detailed studies on the recent Tertiary and glacial history. Helicopter support was provided by Talon Helicopters (2000), Wildcat Helicopters (2001), Mustang Helicopters (2002) and Trans North Air (2004-2005). Northern Rockies Air Charter mobilized and demobilized our camps into 95D/8 (2003-2005). Logistical support (2000-2002) was provided by the Central Foreland NATMAP project under the supervision of Larry Lane, Research Scientist, Geological Survey of Canada, Calgary, Alberta. Continuation of the project during the 2003-2005 seasons was under the auspices of the Yukon Geological Survey.

Extensive discussions concerning map details with Karen Fallas (Geological Survey of Canada, Calgary, Alberta) were illuminating. Rob MacNaughton (Geological Survey of Canada, Calgary, Alberta) offered stratigraphic consultation. Discussions concerning the regional tectonic framework with Don Murphy (Yukon Geological Survey) clarified the big picture. The manuscript was reviewed by Rob MacNaughton, Research Scientist, Geological Survey of Canada, Calgary, Alberta.

REFERENCES

- Abbott, J.G., Gordey, S.P. and Tempelman-Kluit, D.J., 1986. Setting of stratiform, sediment-hosted lead-zinc deposits in Yukon and northeastern British Columbia. *In: Mineral Deposits of Northern Cordillera*, J.A. Morin (ed.), Canadian Institute of Mining and Metallurgy, Special Volume 37, p. 1-18.
- Allen, T.L. and Pigage, L.C., 2000. Geological map of Pool Creek (NTS 95C/5), southeastern Yukon (1:50 000 scale). Exploration and Geological Services Division, Yukon Region, Indian and Northern Affairs Canada, Open File 2000-11.
- Allen, T.L., Pigage, L.C. and MacNaughton, R.B., 2001. Preliminary geology of the Pool Creek map area (95C/5), southeastern Yukon. *In: Yukon Exploration and Geology 2000*, D.S. Emond and L.H. Weston (eds.), Exploration and Geological Services Division, Yukon Region, Indian and Northern Affairs Canada, p. 53-72.
- Bond, G.C. and Kominz, M.A., 1984. Construction of tectonic subsidence curves for the early Paleozoic miogeocline, southern Canadian Rocky Mountains: Implications for subsidence mechanisms, age of breakup, and crustal thinning. *Geological Society of America Bulletin*, vol. 95, p. 155-173.
- Cantuneanu, O., 2003. Sequence stratigraphy of clastic systems. Geological Association of Canada, Short Course Notes, vol. 16, 248 p.
- Cecile, M.P., 1982. The Lower Paleozoic Misty Creek embayment, Selwyn Basin, Yukon and Northwest Territories. *Geological Survey of Canada, Bulletin 335*, 78 p.
- Cecile, M.P., Morrow, D.W. and Williams, G.K., 1997. Early Paleozoic (Cambrian to Early Devonian) tectonic framework, Canadian Cordillera. *Bulletin of Canadian Petroleum Geology*, vol. 45, p 54-74.
- Colpron, M., Logan, J.M. and Mortensen, J.K., 2002. U-Pb zircon age constraint for late Neoproterozoic rifting and initiation of the lower Paleozoic passive margin of western Laurentia. *Canadian Journal of Earth Sciences*, vol. 39, p. 133-143.
- Coney, P.J., Jones, D.L. and Monger, J.W.H., 1980. Cordilleran suspect terranes. *Nature*, vol. 288, p. 329-333.
- Deklerk, R. and Traynor, S., 2005. Yukon MINFILE – A database of mineral occurrences. Yukon Geological Survey, CD-ROM.
- Douglas, R.J.W., 1976. Geology of La Biche River map area (95C), District of Mackenzie. Geological Survey of Canada, "A" Series Map 1380A, 1:250 000 scale.
- Douglas, R.J.W. and Norris, D.K., 1959. Fort Liard and La Biche map-areas, Northwest Territories and Yukon 95B and 95C. Geological Survey of Canada, Paper 59-6, 23 p.
- Fallas, K.M. and Lane, L.S., 2001. Geology of the Mount Martin, Fisherman Lake, and Mount Flett map areas, Yukon Territory and Northwest Territories. Geological Survey of Canada, Current Research 2001-A5, 11 p.
- Fallas, K.M., Pigage, L.C. and MacNaughton, R.B. (compilers), 2004. Geology, southwest La Biche River (95C/SW), Yukon Territory and British Columbia. Geological Survey of Canada, Open File 4664, 1:100 000-scale map and cross-sections.

- Fallas, K.M., Pigage, L.C. and Lane, L.S. (compilers), 2005. Geology, La Biche River northwest (95C/NW), Yukon and Northwest Territories. Geological Survey of Canada, Open File 5018, 1:100 000 scale.
- Gabrielse, H. and Blusson, S.L., 1969. Geology of Coal River map-area, Yukon Territory and District of Mackenzie (95D). Geological Survey of Canada, Paper 68-38, 22 p.
- Gabrielse, H., Blusson, S.L. and Roddick, J.A., 1973. Geology of Flat River, Glacier Lake, and Wrigley Lake map-areas, District of Mackenzie and Yukon Territory. Geological Survey of Canada, Memoir 366 (Parts I and II), 421 p.
- Goodfellow, W.D., Cecile, M.P. and Leybourne, M.I., 1995. Geochemistry, petrogenesis and tectonic setting of lower Paleozoic alkalic and potassic volcanic rocks, Northern Canadian Cordilleran miogeocline. *Canadian Journal of Earth Sciences*, vol. 32, p. 1236-1254.
- Gordey, S.P. and Anderson, R.G., 1993. Evolution of the Northern Cordilleran miogeocline, Nahanni map area (105I), Yukon and Northwest Territories. Geological Survey of Canada, Memoir 428, 214 p.
- Harker, P., 1961. Summary account of Carboniferous and Permian formations, southwestern District of Mackenzie. Geological Survey of Canada, Paper 61-1, 25 p.
- Henderson, C.M., Bamber, E.W., Richards, B.C., Higgins, A.C. and McGugan, A., 1993. Permian; Subchapter 4F. *In: Sedimentary Cover of the Craton in Canada*, D.F. Stott and J.D. Aitken (eds.), Geological Survey of Canada, Geology of Canada, no. 5, p. 272-293.
- Jackson, D.E. and Lenz, A.C., 1962. Zonation of Ordovician and Silurian graptolites in northern Yukon, Canada. *American Association of Petroleum Geologists Bulletin*, vol. 46, p. 30-45.
- Kidd, F.A., 1963. The Besa River Formation. *Bulletin of Canadian Petroleum Geology*, vol. 11, p. 369-372.
- Kindle, E.D., 1944. Geological reconnaissance along Fort Nelson, Liard, and Beaver Rivers, northeastern British Columbia and southeastern Yukon. Geological Survey of Canada, Paper 44-16, 19 p.
- Kingston, D.R., 1951. Stratigraphic reconnaissance along the upper South Nahanni River, NWT. *American Association of Petroleum Geologists Bulletin*, vol. 35, no. 11, p. 2409-2426.
- MacNaughton, R.B., 2002a. Report on one sample from Ordovician strata, Pool Creek map area, Yukon Territory, collected by Lee Pigage (Yukon Geology Program) and submitted for trace-fossil identification: NTS 95C/5. Geological Survey of Canada, Report 001-RBM-2002, 3 p.
- MacNaughton, R.B., 2002b. Sedimentology of Triassic siliciclastic strata, Mount Martin and Mount Merrill map areas, Yukon Territory. Geological Survey of Canada, Current Research 2002-A4, 10 p.
- MacNaughton, R.B. and Pigage, L.C., 2003. Geology, Larsen Lake (95C/4), Yukon Territory and British Columbia. Geological Survey of Canada, Open File 1797, 1:50 000 scale.
- McCracken, A.D., 2003a. Report on 12 conodont samples (Con. No. 1762) from Middle Ordovician and Devonian strata from British Columbia collected by A. Khudoley and L. Pigage and submitted by L. Lane (GSC-C). NTS 94G/12, 95C/04, 95C/05, 95C/11, 95C/12, 95C/13. Geological Survey of Canada, Report 6-ADM-2003, 8 p.
- McCracken, A.D., 2003b. Report on one conodont sample (Con. No. 1674) from Middle Ordovician strata from southeastern Yukon Territory collected by R.B. MacNaughton (GSC-C) NTS 95C/05. Geological Survey of Canada, Report 7-ADM-2003, 4 p.
- Norford, B.S., 2001. Report on six collections from the Trutch and La Biche River map areas, northern British Columbia and adjacent Yukon Territory submitted by Dr. L.S. Lane in 2001 (NTS 94G/04, 95C/05). Geological Survey of Canada, Report S-3 BSN 2001, 2 p.
- Norford, B.S., 2002. Report on two lots of fossils from the La Biche River map-area, southern Yukon Territory, collected by Mr. Lee Pigage and Ms. Tammy Allen in 2001 and submitted by Dr. L.S. Lane, 2001 (95C/5). Geological Survey of Canada, Report S-1-BSN-2002, 2 p.
- Norford, B.S., Gabrielse, H. and Taylor, G.C., 1966. Stratigraphy of Silurian carbonate rocks of the Rocky Mountains, northern British Columbia. *Bulletin of Canadian Petroleum Geology*, vol. 14, p. 504-519.

- Nowlan, G.S., 2004. Report on eighteen samples from Cambrian, Ordovician, Silurian and possibly Devonian strata in the southeastern part of Yukon Territory submitted for conodonts analysis by Larry Lane, Rob MacNaughton and Karen Fallas (Geological Survey of Canada, Calgary) and Lee Pigage and Tammy Allen (Yukon Geological Survey); NTS 0095C/05; CON #1657. Geological Survey of Canada, Report 002-GSN-2004, 10 p.
- Okulitch, A.V., 2001. Geological time scale, 2001. Geological Survey of Canada, Open File 3040 (National Earth Science Series, Geological Atlas) – REVISION.
- Patton, W.J.H., 1958. Mississippian succession in South Nahanni River area, Northwest Territories. *In: Jurassic and Carboniferous of Western Canada*, A.J. Goodman (ed.), American Association of Petroleum Geologists, John Andrew Allan Memorial Volume, p. 309-326.
- Pigage, L.C., 2004. Preliminary geology of NTS 95D/8 (north Toobally Lakes area), southeast Yukon (1:50 000 scale). Yukon Geological Survey, Open File 2004-19.
- Pigage, L.C. and Allen, T.L., 2001. Geological map of Pool Creek (NTS 95C/5), southeastern Yukon (1:50 000 scale). Exploration and Geological Services Division, Yukon Region, Indian and Northern Affairs Canada, Open File 2001-32.
- Pigage, L.C. and MacNaughton, R.B., 2004. Reconnaissance geology of northern Toobally Lake (95D/8), southeast Yukon. *In: Yukon Exploration and Geology 2003*, D.S. Emond. and L.L. Lewis (eds.), Yukon Geological Survey, p. 199-219.
- Pigage, L.C. and Mortensen, J.K., 2004. Superimposed Neoproterozoic and early Tertiary alkaline magmatism in the La Biche River area, southeast Yukon Territory. *Bulletin of Canadian Petroleum Geology*, vol. 52, p. 325-342.
- Pyle, L.J. and Barnes, C.R., 2000. Upper Cambrian to Lower Silurian stratigraphic framework of platform-to-basin facies, northeastern British Columbia. *Bulletin of Canadian Petroleum Geology*, vol. 48, p. 123-149.
- Richards, B.C., 1989. Uppermost Devonian and lower Carboniferous stratigraphy, sedimentation, and diagenesis, southwestern District of Mackenzie and southeastern Yukon Territory. *Geological Survey of Canada, Bulletin 390*.
- Richards, B.C., Bamber, E.W., Higgins, A.C. and Utting, J., 1993. Carboniferous; Subchapter 4E. *In: Sedimentary Cover of the Craton in Canada*, D.F. Stott and J.D. Aitken (eds.), Geological Survey of Canada, *Geology of Canada*, no. 5, p. 202-271.
- Ross, G.M., 1991. Tectonic setting of the Windermere Supergroup revisited. *Geology*, vol. 19, p. 1125-1128.
- Stott, D.F., Caldwell, W.G.E., Cant, D.J., Christopher, J.E., Dixon, J., Koster, E.H., McNeil, D.H. and Simpson, F., 1993. Cretaceous, Subchapter 4I. *In: Sedimentary Cover of the Craton in Canada*, D.F. Stott and J.D. Aitken (eds.), Geological Survey of Canada, *Geology of Canada*, no. 5, p. 358-438.
- Tipnis, R.S., Chatterton, B.D.E. and Ludvigsen, R., 1978. Ordovician conodont biostratigraphy of the southern District of Mackenzie, Canada. *In: Western and Arctic Canadian biostratigraphy*, C.R. Stelck and B.D.E. Chatterton (eds.), Geological Association of Canada, Special Paper 18, p. 39-91.
- Utting, J., Zonneveld, J.P., MacNaughton, R.B. and Fallas, K.M., 2005. Palynostratigraphy, lithostratigraphy and thermal maturity of the Lower Triassic Toad and Grayling, and Montney formations of western Canada, and comparisons with coeval rocks of the Sverdrup Basin, Nunavut. *Bulletin of Canadian Petroleum Geology*, vol. 53, p. 5-24.
- Young, G.M., Jefferson, C.W., Delaney, G.D. and Yeo, G.M., 1979. Middle and Late Proterozoic evolution of the northern Canadian cordillera and shield. *Geology*, vol. 7, p. 125-128.

Geochronological and lithogeochemical studies of intrusive rocks in the Nahanni region, southwestern Northwest Territories and southeastern Yukon

Kirsten L. Rasmussen and James K. Mortensen

Department of Earth and Ocean Sciences, University of British Columbia¹

Hendrik Falck

Geological Survey of Canada/Northwest Territories Geoscience Office²

Rasmussen, K.L., Mortensen, J.K. and Falck, H., 2006. Geochronological and lithogeochemical studies of intrusive rocks in the Nahanni region, southwestern Northwest Territories and southeastern Yukon. *In: Yukon Exploration and Geology 2005*, D.S. Emond, G.D. Bradshaw, L.L. Lewis and L.H. Weston (eds.), Yukon Geological Survey, p. 287-298.

ABSTRACT

Magmatism in the Nahanni region, which defines the eastern extent of the Tintina Gold Province, is generally associated with tungsten mineralization and/or gold-copper-antimony-bismuth-lead-zinc metal occurrences. Intrusions are subalkaline, granitic to granodioritic, and contain several types of textural variations and highly evolved phases. The intrusions range from large composite batholiths to small stocks with associated felsic dykes and veins. Initial U-Pb and Ar-Ar geochronology reveals ages of 97.5-95 Ma with short (0.5-1.5 m.y.) cooling periods, although the intrusion associated with the Cantung tungsten-skarn orebody cooled over a relatively long period (3 m.y.). Magmatism in the area has been interpreted as crustally derived, however, the rare earth element primitive-mantle-normalized profile revealed negative niobium, tantalum and titanium anomalies suggesting an arc-type setting. Furthermore, the granites lack volumetrically significant, primary peraluminous mineralogies characteristic of S-type granites.

RÉSUMÉ

Dans la région de Nahanni, le magmatisme qui détermine la limite est de la Province aurifère de Tintina est généralement associé à une minéralisation en tungstène et/ou à des occurrences minérales d'or-cuivre-antimoine-bismuth-plomb-zinc. Les intrusions sont subalkalines, de granitiques à granodioritiques, contient plusieurs types de variations texturales et se répartissent en plusieurs phases très complexes. Les intrusions varient de grands batholithes composites à de petits stocks auxquels sont associés des dykes et des filons felsiques. La géochronologie initiale U-Pb et Ar-Ar révèle des âges de 97,5 à 95 Ma avec de brèves périodes (0,5 à 1,5 Ma) de refroidissement, bien qu'une période relativement longue (3 Ma) ait été nécessaire au refroidissement de l'intrusion associée au corps minéralisé de skarn tungsténifère de Cantung. On interprète le magmatisme de la région comme étant d'origine crustale. Cependant, le profil en terres rares normalisé au manteau primitif révèle des anomalies négatives en Nb, Ta et Ti, indiquant un cadre de type arc. De plus, les granites sont exempts d'importants volumes des principaux minéraux hyperalumineux, caractéristiques des granites de type S.

¹6339 Stores Road, Vancouver, British Columbia, Canada V6T 1Z4

²P.O. Box 1500, 4601-B 52nd Avenue, Yellowknife, Northwest Territories, Canada X1A 2R3

INTRODUCTION

A study of intrusive rocks and the potential for related mineralization in southwestern Northwest Territories and southeastern Yukon was initiated as one component of the 2004-2006 Nahanni Mineral and Energy Resource Assessment (MERA). The study area covers the South Nahanni River watershed, which originates in the eastern Selwyn Mountains and transects the southern Mackenzie Mountains in the Northwest Territories (Fig. 1). Magmatism in the study area is confined to the western portion of the watershed near the Yukon border, however, sampling was extended outside the watershed to include several more intrusions further west within Yukon (Fig. 2). Intrusions in the study area represent the southeastern extent of the Tintina Gold Province (TGP), an elongate band of Early to Late Cretaceous magmatism that extends northwest from the study area across Yukon and into central Alaska (Fig. 1). The TGP is characterized by numerous precious and base metal occurrences and deposits that are spatially and genetically related to well defined, metalliferous, mid- and Late Cretaceous plutonic suites (Mortensen *et al.*, 2000). A few intrusion-related deposits are present within the study

Figure 2. (next page) Mid-Cretaceous granitic intrusions (grey) within, and adjacent to, the Nahanni MERA study area. Radiometric ages (Ma) are reported for several granitoids sampled in 2003 (large closed circles) as ID-TIMS U-Pb (U) and Ar-Ar (A) ages, with 2-sigma errors in brackets. Locations for the 2003 and 2005 samples currently being analyzed for U-Pb geochronology by the laser ablation ICP-MS method are indicated by open circles. Sample locations from Heffernan (2004) for which geochronological analyses are available are also indicated. The Cantung mine area, outlined with a dashed line, is expanded in the inset for greater detail. Figure 3 photo locations are plotted as the figure notation in a box. NWT mineral occurrence locations from the NORMIN database, www.nwtgeoscience.ca/normin. Map modified from Gordey and Makepeace (2003).

area, but the rugged topography and lack of road access has hindered exploration efforts to date. The potential for additional intrusion-related mineralization in much of the study area has not been previously investigated in detail despite the presence of widespread mineral occurrences.

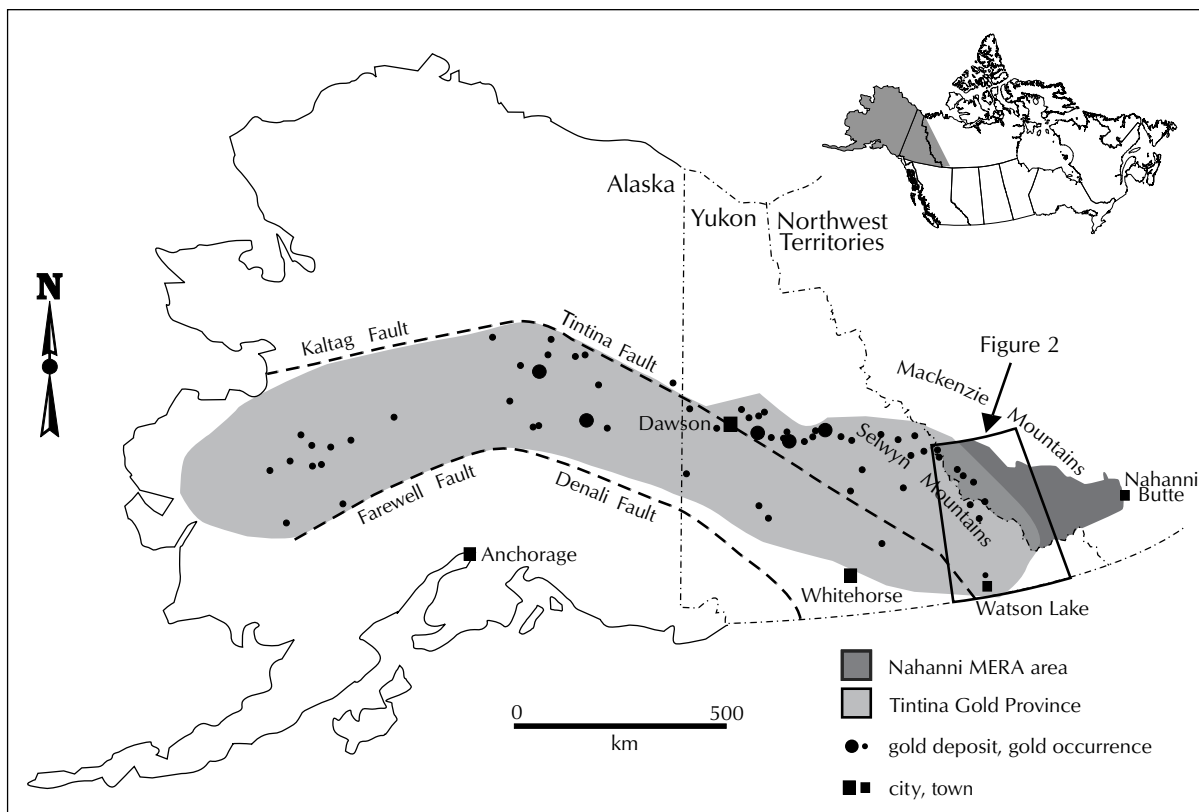


Figure 1. Location of the Nahanni MERA study area (dark grey), relative to Alaska, Yukon, and Northwest Territories. The Tintina Gold Province (TGP) is shaded in light grey and the area where the MERA and TGP areas overlap is shaded in medium grey. The location of Figure 2 is outlined in black. Map modified from Mortensen *et al.* (2000).

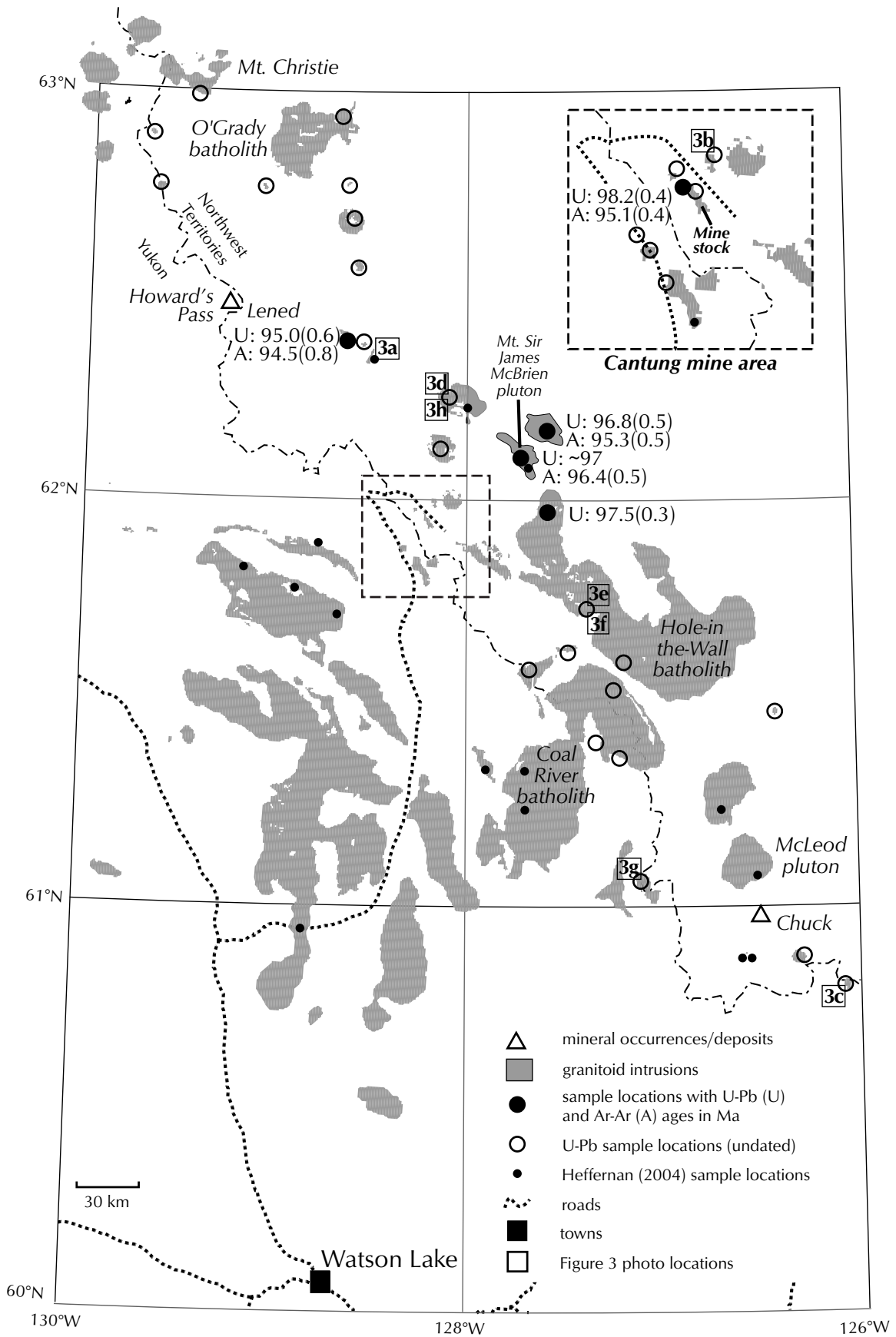


Figure 2. (caption on facing page)

Mineralization in the study area (Fig. 2) comprises five main deposit styles: (1) syngenetic sediment-hosted base metals (e.g., Howard's Pass zinc-lead, Yukon MINFILE 1051 012, Deklerk and Traynor, 2005); (2) fault-controlled, vein-hosted base metals (e.g., Prairie Creek zinc-lead-silver quartz-carbonate vein, NORMIN.DB 095FNE 0001-0003, 0009-0013); (3) placer gold originating from disseminated sediment or intrusive-hosted gold (e.g., Selina Creek placer; Chuck gold-showing, NORMIN.DB 095DNE 0007-0010); (4) intrusion-related proximal skarn, or distal quartz vein hosted base/precious metals (e.g., Lened tungsten-skarn, NORMIN.DB 105ISE 0003); and (5) intrusion-related or hosted precious/base metals and precious stones in evolved intrusive phases (e.g., Mt. Christie copper-lead-arsenic quartz veins; O'Grady gem tourmaline in miarolitic cavities). The most significant mineralization styles with respect to this study are placer, intrusion-related and intrusion-hosted mineralization. These mineralization styles consist of placer gold potentially derived from intrusion-related bedrock sources; intrusion- and sediment-hosted mineralized quartz veins or stockworks; intrusion-hosted sheeted gossanous fractures (\pm quartz veins) with anomalous precious and base metal contents; precious stones hosted in quartz veins or miarolitic cavities; and skarn mineralization in country rock adjacent to intrusions. Economically significant tungsten skarn deposits (e.g., Cantung mine, Fig. 2) and abundant tungsten (e.g., Lened showing, Fig. 2), copper, lead and zinc showings, many of which have been drilled, are spatially associated with the intrusions in the western portion of the MERA area. However, in much of the study area, the potential for intrusion-related precious and/or base metal mineralization is still uncertain.

The focus of this study is to identify intrusions or intrusive phases that have significant potential for genetically related mineralization within the Nahanni MERA area. This contribution will provide preliminary interpretations of magnetic susceptibility and lithogeochemical data recently obtained for several of the intrusive rocks from the study area. In addition, initial U-Pb (zircon and monazite) and Ar-Ar (biotite) ages for several of the intrusions within the study area are reported and discussed. Finally, this paper will describe ongoing and future work aimed at defining the potential of intrusion-related mineralization in the study area. This study builds on previous studies of intrusive rocks in the region (Heffernan, 2004), intrusive rocks in the immediate vicinity of the Cantung mine (Rasmussen, 2004), as well as regional geological studies

in the northern Cordillera (Gordey and Anderson, 1993; Mortensen *et al.*, 2000; Lang *et al.*, 2001; Jefferson and Spirito, 2003; Hart *et al.*, 2004).

GEOLOGIC OVERVIEW

The study area is underlain by Neoproterozoic (~800 Ma) to Late Cretaceous (~100 Ma) platformal to basinal strata that was deposited along the western margin of the early North American continent. The sedimentary rocks were intruded by minor Devonian (350 Ma) granitoid rocks and subsequently deformed into fold and thrust belts spanning the Middle Jurassic to Cretaceous time periods. During the mid-Cretaceous, a later magmatic event in this portion of the northern Cordillera was interpreted to be a result of syn- to post-collisional partial melting of miogeoclinal strata within the thickened crustal material (Woodsworth *et al.*, 1991). Mid-Cretaceous, felsic intrusive rocks underlie a significant portion of the MERA area and range from large batholithic bodies (e.g., the Coal River and Hole-in-the-Wall batholiths), to small stocks (e.g., the Mine stock, Cantung mine) and contemporaneous felsic dykes (Fig. 2). Most of the mid-Cretaceous intrusions have relatively restricted mineralogies and have been classified on this basis by Anderson (1983) as biotite-hornblende-bearing, biotite-bearing, and biotite-muscovite-bearing plutons.

Plutonic contacts are shallow- to steep-dipping, but dominantly conformable to, and typically overlain by, the adjacent strata (Fig. 3a). Adjacent, sub-parallel or concentric dykes and sills are commonly observed along the margins of the intrusions, intruding both plutonic and sedimentary rocks (Fig. 3b). Several textural variations, ranging from fine-grained, dioritic, quartz-feldspar porphyry phases (Fig. 3c), to K-feldspar megacrystic granite and syenite phases (Fig. 3d), are observed within the intrusions. Development of one or more late, volatile-rich phases in many of the felsic intrusions is indicated by the presence of the following: 1) miarolitic cavities in granites (Fig. 3e); 2) leucocratic dykes infilled with graphic-textured tourmaline (Fig. 3f); 3) quartz-(tourmaline) veins and aplite-pegmatite dykes (Fig. 3g); 4) sheeted gossanous fractures cutting plutons (Fig. 3h); and 5), one example of a late-stage, marginal breccia in the Circular stock at the Cantung mine. Many of the intrusions are composite; this is established from both internal contacts and textural, mineralogical, and magnetic susceptibility variations, or by age differences between different portions of the larger intrusions.

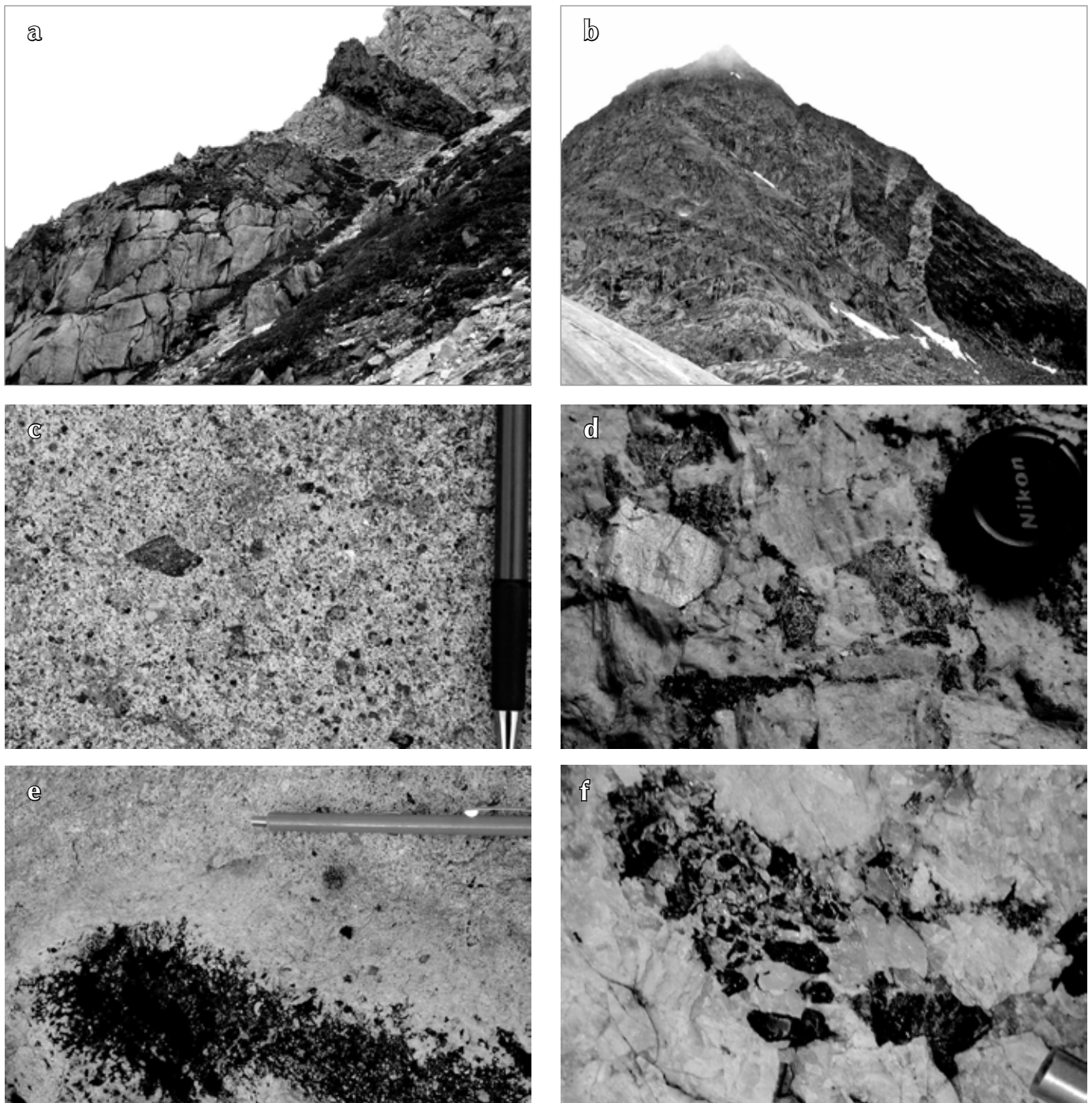


Figure 3. Photographs of structural and textural features of intrusive rocks (photo locations displayed on Figure 2). **(a)** Stepped pluton-country rock (lower left half of photo) with overlying strata dipping to the right (upper right half of photo); dark beds are mineralized skarn (outcrop is ~20 m high). **(b)** Stepped pluton-country rock contact with marginal dykes (granite is on left side of photo; bedding in country rock is sub-parallel to slope of hill; hill expresses ~100 m of relief). **(c)** Fine-grained, dioritic, quartz-feldspar porphyry phase (pen for scale). **(d)** Granitic, K-feldspar megacrystic phase; K-feldspar grains are represented by the large white phenocrysts (lens cap is 3 cm across). **(e)** Mirolitic cavity with aplitic margin and infilled with coarse-grained schorl, in granite (pen magnet for scale). **(f)** Relatively fine-grained pegmatitic dyke with graphic-textured K-feldspar and schorl (pen magnet tip for scale in bottom right corner of photograph). (Figure 3 continued on next page.)

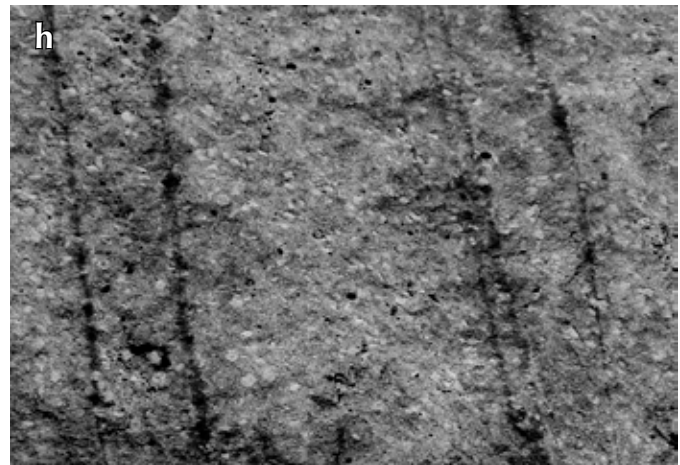


Figure 3. (continued) (g) Aplite dyke (vertical) cross-cut by quartz-tourmaline vein with gossanous margin (sub-horizontal) in garnet-muscovite-bearing granite (hammer for scale). (h) Typical sheeted, sub-vertical, gossanous fracture set cutting granitic pluton (0.25- and 1-m spacing between fractures).

PRELIMINARY RESULTS

MAGNETIC SUSCEPTIBILITY

Average magnetic susceptibility was measured in the field for many of the intrusive phases. Measured magnetic susceptibility values are based on an average of 10, randomly oriented readings on flat surfaces of each sample using a KT-9 Kappameter. Values ranged widely between intrusive phases within a single pluton, therefore the magnetic susceptibility of only the dominant intrusive phase in each pluton was selected for interpretation. In general, most of the magnetic susceptibility values are less than 0.5×10^{-3} SI units), but several intrusions have values as high as 16.4.

LITHOGEOCHEMISTRY

A total of 51 plutonic and aplitic samples collected during the 2003 and 2005 field seasons were analysed for major, trace and rare earth element composition by ALS Chemex Labs Ltd., North Vancouver. Major element oxides were obtained by both X-ray fluorescence and inductively coupled plasma atomic emission spectroscopy (ICP-AES), and trace and rare earth element concentrations were determined through a combination of ICP-AES and inductively coupled plasma mass spectroscopy (ICP-MS). The accuracy reproducibility of the analyses at the ALS Chemex facility was monitored by repeat analyses of several in-house standards of known composition.

The major element data suggests that intrusions in the study area are predominantly granitic and granodioritic in composition as is shown by the total alkali-silica diagram (Le Bas *et al.*, 1986; Fig. 4a). Samples that plot within the diorite field and low SiO_2 end of the granodiorite field are dominantly fine-grained porphyry phases. Magmatism in the area is subalkaline according to the Irvine and Baragar (1971) classification (Fig. 4a) and the felsic intrusions have a low to moderate peraluminous signature using Shand's Index, after Maniar and Piccoli (1989; Fig. 4b). Many of the northernmost and easternmost intrusions that have more alkaline compositions plot as distinctly metaluminous or weakly peraluminous; several of these intrusions are dioritic porphyries and K-feldspar porphyritic syenites (Fig. 4a,b). The extended trace element diagram of the plutonic bodies, normalized to the primitive mantle values of Sun and McDonough (1989), has a steep profile with distinct negative Ba, Nb, Ta, P, and Ti anomalies and a strong positive Pb anomaly (Fig. 5). On two tectonic discrimination diagrams (Y+Nb vs. Rb and Yb+Ta vs. Rb; Pearce *et al.*, 1984), the granitoids plot on the border between the volcanic arc granite (VAG) and syn-collisional granite (syn-COLG) fields (Fig. 6).

GEOCHRONOLOGY

Of the 51 samples collected for geochemical analysis, a total of 38 samples were selected for U-Pb dating (Fig. 2); many of these samples will also be dated by Ar-Ar, and (U-Th)-He geochronological analysis. The initial geochronological results for five of the plutonic samples

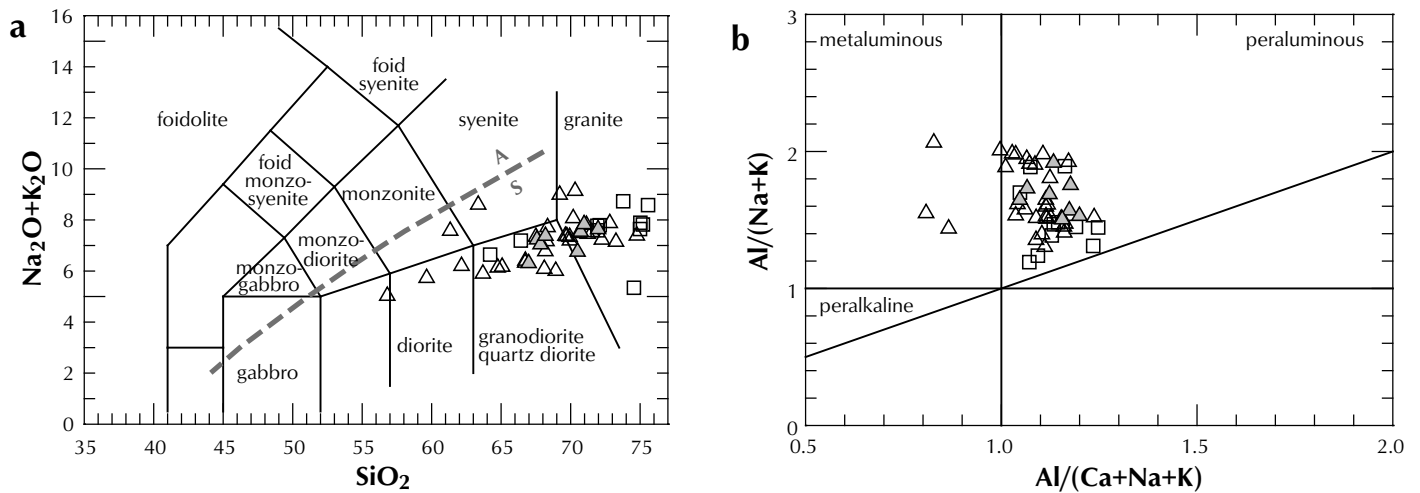


Figure 4. Geochemistry of the plutonic and aplitic samples. **(a)** Silica versus total alkali plot (Le Bas et al., 1986) displaying the range of plutonic rock types sampled (2003 – grey triangles; 2005 – white triangles) and aplitic dykes sampled (white squares); $n = 51$. The Irvine and Baragar (1971) alkalic-subalkalic discrimination line is indicated by the grey dashed line (A = alkaline; S = subalkaline). **(b)** $\text{Al}/(\text{Ca}+\text{Na}+\text{K})$ versus $\text{Al}/(\text{Na}+\text{K})$ plot based on Shand's Index, after Maniar and Piccoli (1989); intrusions have a predominantly low to moderate peraluminous signature.

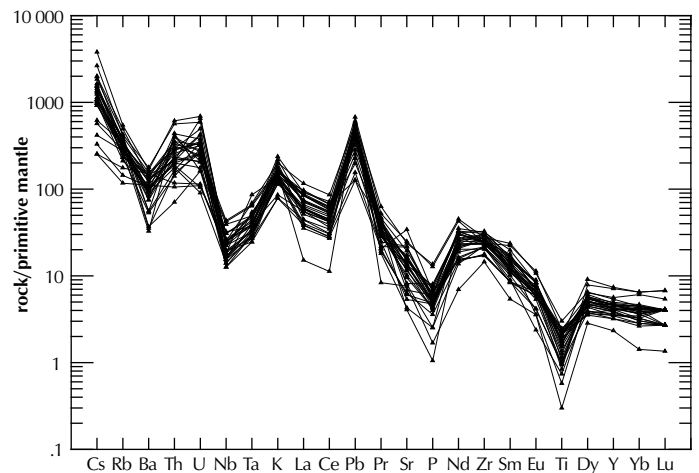


Figure 5. Primitive-mantle-normalized extended trace element diagram of the 2005 plutonic samples; $n = 31$. Mantle-normalized values from Sun and McDonough, 1989.

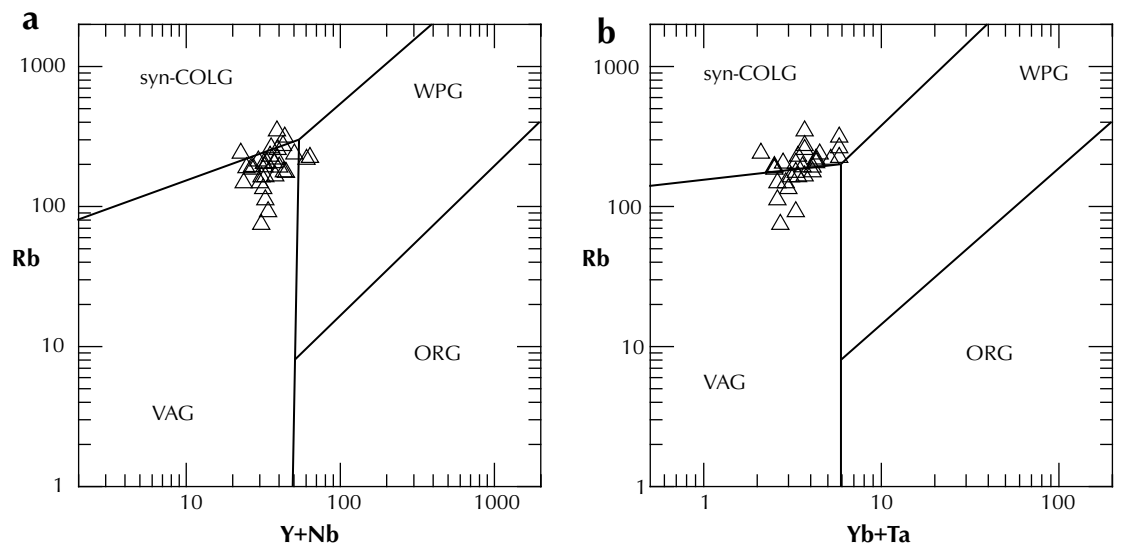


Figure 6. Tectonic discrimination diagrams for 2005 plutonic samples; $n = 31$. Diagrams are after Pearce et al., 1984. **(a)** $\text{Y}+\text{Nb}$ vs. Rb . **(b)** $\text{Yb}+\text{Ta}$ vs. Rb .

collected in 2003 are plotted in Figure 2, and include U-Pb zircon or monazite crystallization ages determined by the isotope dilution-thermal ionization mass spectrometry (ID-TIMS) method and four $^{40}\text{Ar}/^{39}\text{Ar}$ cooling ages for biotite. Zircon and monazite grains from the 2005 samples are currently being analysed for U-Pb geochronology by the laser ablation ICP-MS method.

DISCUSSION

The magnetic susceptibility data provides an indication of the redox state for granitoid intrusions sampled in the study area. Based on work by Hart *et al.* (2004) in Alaska and Yukon, the mid-Cretaceous intrusions in the northern Cordillera with magnetic susceptibility values less than 0.5 ($\times 10^{-3}$ SI units) are interpreted to reflect reduced ilmenite-series granitoids, and greater than 0.5 are interpreted to reflect more oxidized magnetite-series granitoids. The majority of the intrusions in the MERA study area are classified as ilmenite-series granitoids. However, several of the intrusions, particularly at the northern and eastern extremities of the study area, have magnetic susceptibility values greater than 0.5 , which classifies these intrusions as magnetite-series granitoids. The ilmenite/magnetite-series classification of granitic magmatism is linked to the type of mineralization that may be associated with an intrusion. In the Tintina Gold Province (TGP) throughout Yukon and Alaska, ilmenite-series magmatism is generally associated with tungsten, antimony, gold, silver-lead-zinc polymetallic veins, and tin mineralization related to very reduced intrusions. In contrast, magnetite-series magmatism is associated with copper-gold-iron(-molybdenum), and alkalic intrusion-related uranium-thorium(-copper-gold) enrichment (Hart *et al.*, 2004). The dominantly reduced, subalkaline intrusions within the study area are, therefore, most prospective for tungsten-antimony-gold-lead-zinc(-tin) mineralization, which is consistent with the majority of known intrusion-related mineral occurrences; however, there is some potential for mineralization typically associated with magnetite-series granitoids in outermost portions of the study area.

One important aspect of the lithochemical results is the constraint on the source of the granitoids. Granitic magmatism in the inboard portion of the northern Cordillera has been interpreted by several authors to be dominantly S-type, post-collisional magmatism produced by crustal thickening and subsequent melting in the outer miogeoclinal strata, followed by upper crustal extension

late in the orogeny (Woodsworth *et al.*, 1991; Hart *et al.*, 2004). Consistent with S-type magmas, accessory apatite, zircon, and ilmenite are abundant in the intrusions within the study area, and monazite and tourmaline may even be present in place of zircon and biotite, respectively. However, field observations and lithochemical data indicate that the majority of intrusions in the study area lack clear S-type characteristics, such as a strong peraluminosity and a diagnostic mineralogy (e.g., aluminous minerals), that are typically associated with magmas sourced from sedimentary material (e.g., shale or greywacke) (Christiansen and Keith, 1996). Magmatic aluminous minerals, such as muscovite and especially garnet, are rare in the majority of the intrusions, and where observed, appear to be volumetrically insignificant. Also, the observed negative niobium, tantalum and titanium anomalies on the extended trace element diagram (Fig. 5) are more characteristic of I-type magmas formed in subduction zone environments, and these magmas, in general, are derived from igneous source material (Christiansen and Keith, 1996). Other studies have also noted similarly anomalous geochemical signatures (van Middelaar, 1988; Driver *et al.*, 2000; Mortensen *et al.*, 2000; Lang *et al.*, 2001; Heffernan, 2004; Rasmussen, 2004), but most researchers have postulated a crustally derived origin for the mid-Cretaceous magmatism in the area. An alternative interpretation based on recent work has demonstrated that I-type geochemical signatures may also result from partial melting of rocks that initially formed in a subduction zone environment, or from partial melting of immature sedimentary rocks eroded from arc material (Christiansen and Keith, 1996; Morris *et al.*, 2000). Thus, tectonic discrimination plots such as that of Pearce *et al.* (1984), which suggest a volcanic arc setting for at least some of the Nahanni MERA area intrusions, must be used with caution.

The U-Pb zircon and monazite age results for five of the samples collected for this study (Fig. 2), together with those reported by Heffernan (2004) for the adjoining area to the southwest, indicate a narrow range of mid-Cretaceous crystallization ages of plutonic rocks within the region. These ages, together with lithological and geochemical characteristics of the rocks, permit individual intrusions in the study area to be correlated with three of the plutonic suites defined in the TGP further to the northwest by Mortensen *et al.* (2000). Metaluminous to weakly peraluminous intrusions with crystallization ages of 95-89 Ma are correlated with the Tombstone suite, those with ages in the 98-96 Ma range are correlated with

the Tay River suite, and intrusions with more strongly peraluminous compositions and crystallization ages of 97-92 Ma are assigned to the Tungsten suite. In the TGP, the metallogenic associations of these three suites are distinct: Tombstone suite intrusions are associated with gold and bismuth mineralization, commonly as structurally controlled sets of sheeted veins (e.g., Dublin Gulch), as well as tungsten skarns (e.g., Ray Gulch) and silver-lead-zinc veins (e.g., Keno Hill); Tay River suite intrusions are generally not associated with mineralization; and Tungsten suite intrusions are associated with tungsten skarn mineralization (e.g., MacTung; Deklerk and Traynor, 2005).

In the study area, metallogenic associations are more complex. In particular, tungsten skarns (together with volumetrically insignificant sheeted, tungsten-rich, gossanous fractures or veins) are associated with moderately peraluminous intrusions of the Tungsten suite (e.g., the Lened pluton), but also occur with intrusions assigned to the Tay River suite in terms of age and mineralogy (e.g., the Mine stock, Cantung mine). For example, biotite is the only primary mica observed in the main intrusions at the Cantung mine; although muscovite and, rarely, garnet occur in highly fractionated aplitic dykes, they are secondary mineral phases (Rasmussen, 2004). In fact, the Mine stock at Cantung is only moderately peraluminous with an aluminum saturation index, or $Al/(Ca+Na+K)$ ratio, of ~ 1.1 . In addition, the U-Pb zircon age of 98.2 ± 0.4 Ma for the Mine stock (Fig. 2) is significantly older than plutons adjacent to tungsten-skarn mineralization farther to the north at Lened (95.0 ± 0.6 Ma, the Lened pluton; this study) and MacTung (95.4 Ma, the Cirque Lake pluton; Mortensen, unpublished data). Although it is possible that younger intrusions are responsible for mineralization at MacTung, an older mineralization age of 97.5 ± 0.5 Ma (Re-Os isochron age, molybdenite; Selby *et al.*, 2003) indicates that an older unidentified intrusion closer in age to the Mine stock at the Cantung mine is a more likely source for the metals. Many of the intrusions with related tungsten mineralization provided the basis for the initial definition of the Tungsten suite (Mortensen *et al.*, 2000); however, the actual metallogenic, mineralogical, lithogeochemical and geochronological relationships observed appear to be somewhat more complicated. Although the Cantung mine rates within the 90th percentile of tungsten-skarn deposits based on grade (Lentz, 1998) and is one of the two most significant tungsten resources in the TGP, the older age of the Mine stock intrusion, combined with a low peraluminous geochemical signature and a lack of

primary aluminous minerals, indicate that this intrusion is not a member of the Tungsten suite. The nature and origin of the Tungsten suite and its relationship with tungsten mineralization in the southeastern Yukon and southwestern Northwest Territories is still uncertain and it appears that this suite may have to be redefined.

Initial U-Pb zircon geochronological results for three separate felsic intrusions sampled underground at the Cantung mine place firm constraints on the timing of tungsten and trace amounts of localized molybdenum mineralization. The Mine stock underlying the orebody and a scheelite- and pyrrhotite-bearing aplite dyke that cuts the stock, yield essentially identical ages of 98.2 ± 0.4 Ma and 98.3 ± 0.3 Ma, respectively. A separate felsic dyke that intrudes underground along one of several low-displacement normal faults and cuts the massive orebody, but does not contain scheelite or pyrrhotite (only trace molybdenite) is younger at 97.4 ± 0.3 Ma. Combined, these results indicate that the main tungsten mineralization coincided with emplacement of the Mine stock and associated aplite dykes, which is consistent with the results of Rasmussen (2004). Subsequent molybdenum mineralization is associated with a slightly younger phase of felsic magmatism.

As noted earlier in this report, the presence of multiple phases in many of the intrusions is independent of the size of the intrusion, whether large batholiths or smaller stocks. One example of this is demonstrated by zircons from two sample locations in the Mt. Sir James McBrien pluton (Fig. 2) that yielded U-Pb crystallization ages of 97.7 ± 0.2 Ma (Heffernan, 2004) and 96.8 ± 0.5 Ma (this study). These ages, both resulting from ID-TIMS, are statistically different at the 2-sigma error level and indicate that this body is composed of more than one granitic phase of intrusion. Similarly, U-Pb zircon ages reported previously by Heffernan (2004) for two separate samples from the southern portion of Coal River batholith (Fig. 2; 95.6 ± 0.4 Ma and 96.9 ± 0.4 Ma) are also different outside of error. These results are not unexpected, particularly in larger intrusive bodies where several phases of plutonism are distinguished by defined ranges of magnetic susceptibilities. For example, continuous magnetic susceptibility measurements over a 3-km traverse near the northeastern contact of the McLeod pluton (Fig. 2) have resolved at least six mineralogically and texturally distinct phases with unique magnetic susceptibility value ranges between ~ 0.3 and ~ 25 ($\times 10^{-3}$ SI units).

The ^{40}Ar - ^{39}Ar results for biotite from various intrusions suggest moderately rapid, post-emplacment cooling from magmatic temperatures of 850-900°C (indicated by zircon saturation thermometry) to the closure temperature of the argon system in biotite (~300°C). Cooling periods for three of the five intrusions sampled are indicated by precise U-Pb (zircon and monazite) and Ar-Ar (biotite) ages ranging from 1-1.5 m.y. (Fig. 2). This suggests rapid cooling due to a relatively shallow level of emplacement in the crust, which has important implications for the probability of a long-lasting magmatic-hydrothermal system that could lead to significant mineralization. One exception to this is the Mine stock at the Cantung mine, which cooled over a longer period of approximately 3 m.y. This correlates well with recent data from Yuwan *et al.* (2004) that presents pressure estimates of 2-3 kilobars for mineralized quartz veins located about 500 m above the intrusive stock; elevated pressure conditions are expected for large tungsten deposits as crystallization at deeper crustal levels allows for the longer cooling periods that are generally considered necessary for significant tungsten mineralization (Keith *et al.*, 1989). Surprisingly, the Lened pluton, which is also associated with a large tungsten resource, cooled quickly from emplacement at approximately 95.0 Ma to about 300°C in less than 1 m.y. However, as most or all of the intrusions in the area are composite, and several compositional phases were recognized within the Lened pluton by Gordey and Anderson (1993), it is possible that the phase sampled for dating was not directly associated with the tungsten skarn mineralization.

WORK IN PROGRESS

In addition to the geochronological and geochemical aspects of this study, the authors are investigating halogen (F, Cl, S) contents in igneous apatites and micas within the various intrusions in order to determine which intrusive phases may have exsolved a potentially mineralizing volatile phase. Results of this study will help identify intrusions and regions within the Nahanni MERA area that have higher potential for intrusion-related mineralization. If proven successful, the scope of this portion of the study will be expanded to include intrusions northwest to the Macmillan Pass area and into a study area immediately to the southwest (see Heffernan, 2004).

Lead isotopic compositions will be determined for igneous feldspars from the intrusions and for sulphide minerals from many of the known mineral occurrences

throughout the area, in order to test possible genetic relationships between mineralization and magmatism. These compositions will also help to determine the nature and origin (magmatic or sedimentary) of mineral occurrences that are not obviously associated with magmatism.

Some P-T-t studies, including investigations of metamorphic mineral assemblages in contact aureoles, as well as aluminum-in-hornblende geobarometry and (U-Th)-He dating of apatite, are underway to better constrain the depths of emplacement for various intrusions and their cooling histories. The resulting data will provide additional criteria useful in assessing which intrusions have good potential for genetically related mineralization.

A final aspect of the study will be the examination of the morphology and composition of placer gold grains from drainages in the MERA area, particularly the Selina Creek/Caribou River region in the southwest portion of the study area. Over 40 panned samples (collected in 2005), together with grains obtained from heavy mineral concentrate samples for the Nahanni MERA area (collected in 2005), and panned grains previously recovered from the study area by C. Jefferson (collected in 1986 and 1987; Jefferson and Spirito, 2003) will be compared to a larger database of gold grain morphologies and compositions being compiled on placer gold from the Klondike (Mortensen *et al.*, 2005). The resulting data will be used to assess the style of lode mineralization from which the placer gold grains were derived, and the approximate distance that they traveled from their source.

CONCLUSIONS

The focus of this study is to determine which intrusions or intrusive phases within the Nahanni MERA area are genetically related to mineralization. To date, field observations, combined with litho-geochemistry and geochronology of intrusions within the study area, have provided a basic understanding of the widespread magmatism that underlies the region and extends northwest into the Tintina Gold Province. Initial mid-Cretaceous U-Pb zircon and monazite crystallization ages (97.5-95 Ma) allow us to classify the intrusions as Tungsten and/or Tay River suites, with short 0.5-1.5 m.y. cooling periods from magmatic temperatures (850-900°C) down to ~300°C for several of the intrusions. The exception to this is the Mine stock at the world-class Cantung tungsten mine, for which a longer cooling period

(~3 m.y.) indicates a deeper emplacement level. Several uncertainties have arisen from the initial data reported here, including what the source(s) of the granitoid melt were and how valid the definition of the Tungsten plutonic suite is. Further work is necessary to answer these, among other questions, the most important of which is: which of the intrusions in the Nahanni MERA area have significant potential for intrusion-related mineralization?

ACKNOWLEDGEMENTS

We thank Jason Yuvan for his assistance in the field. We would also like to thank the pilots and operators of Great Slave Helicopters, Trans North Helicopters, Prism Helicopters, South Nahanni Airways, and Alkan Air for their experienced and professional air support throughout this project. Further thanks is extended to Canadian Zinc Corporation, North American Tungsten, Pacifica Resources and the many employees of these companies for their hospitality and shared knowledge over the 2003 and 2005 field seasons. Critical reviews of this paper were kindly provided by J.S. Scoates (University of British Columbia) and S. Cairns (Northwest Territories Geoscience Office). Funding for this project was provided by an NSERC Discovery Grant to Dr. J.K. Mortensen (University of British Columbia), Parks Canada, Natural Resources Canada, and the Northwest Territories Geoscience Office.

REFERENCES

- Anderson, R.G., 1983. Selwyn plutonic suite and its relationship to tungsten skarn mineralization, southeastern Yukon and District of Mackenzie. *Current Research, Part B*, Geological Survey of Canada, Paper 83-1B, p. 1151-163.
- Christiansen, E.H. and Keith, J.D., 1996. Trace element systematics in silicic magmas: a metallogenic perspective. *In: Trace Element Geochemistry of Volcanic Rocks: Applications for Massive Sulfide Exploration*, Geological Association of Canada, Short Course Notes, D.A. Wyman (ed.), vol. 12, p. 115-151.
- Deklerk, R. and Traynor, S., 2005. Yukon MINFILE – A database of mineral occurrences. Yukon Geological Survey, CD-ROM.
- Driver, L.A., Creaser, R.A., Chacko, T. and Erdmer, P., 2000. Petrogenesis of the Cretaceous Cassiar batholith, Yukon-British Columbia, Canada: implications for magmatism in the North American cordilleran interior. *Geological Society of America Bulletin*, vol. 112, p. 1119-1133.
- Gordey, S.P. and Anderson, R.L., 1993. Evolution of the northern cordilleran miogeocline, Nahanni map area (1051), Yukon and Northwest Territories. *Geological Survey of Canada, Memoir 428*, 214 p.
- Gordey, S.P. and Makepeace, A.J. (compilers), 2003. Yukon digital geology. Geological Survey of Canada, Open File 1749, and Exploration and Geological Services Division, Yukon Region, Open File 2003-9D.
- Hart, C.J.R., Goldfarb, R.J., Lewis, L.L. and Mair, J.L., 2004. The northern cordilleran mid-Cretaceous plutonic province: ilmenite/magnetite-series granitoids and intrusion-related mineralization. *Resource Geology*, vol. 54, p. 253-280.
- Heffernan, R.S., 2004. Temporal, geochemical, isotopic and metallogenic studies of mid-Cretaceous magmatism in the Tintina Gold Province, southeastern Yukon and southwestern Northwest Territories, Canada. Unpublished MSc thesis, University of British Columbia, Vancouver, BC, 83 p.
- Irvine, T.N. and Baragar, W.R.A., 1971. A guide to the chemical classification of the common volcanic rocks. *Canadian Journal of Earth Sciences*, vol. 8, p. 523-548.
- Jefferson, C.W. and Spirito, W.A. (eds.), 2003. Mineral and energy resource assessment of the Tlogotsho Plateau, Nahanni Karst, Ragged Ranges and adjacent areas under consideration for expansion of Nahanni National Park Reserve, Northwest Territories. Open File 1686, 1 CD-ROM.
- Keith, J.D., van Middelaar, W., Clark, A.H. and Hodgson, C.J., 1989. Granitoid textures, compositions, and volatile fugacities associated with the formation of tungsten-dominated skarn deposits. *In: Reviews in Economic Geology*, J.A. Whitney and A.J. Naldrett (eds.), vol. 4: Ore Deposition Associated with Magmas, p. 235-250.

- Lang, J., Thompson, J.F.H., Mortensen, J.K., Baker, T., Coulson, I., Duncan, R., Maloof, T., James, J.J., Friedman, R. and Lepitre, M., 2001. Regional and system-scale controls on the formation of copper and/or gold magmatic-hydrothermal mineralization. *In: Mineral Deposit Research Unit Special Publication No. 2*, J. Lang (ed.), Mineral Deposits Research Unit, 115 p.
- Le Bas, M.J., Le Maitre, R.W., Streckeisen, A. and Zanettin, B., 1986. A chemical classification of volcanic rocks based on the total alkali-silica diagram. *Journal of Petrology*, vol. 27, p. 745-750.
- Lentz, D.R. (comp.), 1998. Appendix: grade and tonnage models of skarns. *In: Mineralized Intrusion-Related Skarn Systems*, D.R. Lentz (ed.), Mineralogical Association of Canada Short Course Series, vol. 26, 663 p.
- Maniar, P.D. and Piccoli, P.M., 1989. Tectonic discrimination of granitoids. *Geological Society of America Bulletin*, vol. 101, p. 635-643.
- Morris, G.A., Larson, P.B. and Hooper, P.R., 2000. 'Subduction style' magmatism in a non-subduction setting: the Colville igneous complex, NE Washington State, USA. *Journal of Petrology*, vol. 41, p. 43-67.
- Mortensen, J.K., Hart, C.J.R., Murphy, D.C. and Heffernan, S., 2000. Temporal evolution of Early and mid-Cretaceous magmatism in the Tintina Gold Belt. *In: The Tintina Gold Belt: Concepts, Exploration and Discoveries*, British Columbia and Yukon Chamber of Mines, Special Volume 2, J. Jambor (ed.), p. 49-57.
- Mortensen, J.K., Chapman, R., LeBarge, W. and Jackson, L., 2005. Application of placer and lodegold geochemistry to gold exploration in western Yukon. *In: Yukon Exploration and Geology 2004*, D.S. Emond, L.L. Lewis and G.D. Bradshaw (eds.), Yukon Geological Survey, p. 205-212.
- Mortensen, J.K., Chapman, R., LeBarge, W. and Crawford, E., 2006 (this volume). Compositional studies of placer and lode gold from western Yukon: Implications for lode sources. *In: Yukon Exploration and Geology 2005*, D.S. Emond, G.D. Bradshaw, L.L. Lewis and L.H. Weston (eds.), Yukon Geological Survey, p. 247-255.
- Mortensen, J.K., Sluggett, C., Liverton, T. and Roots, C.F., 2006 (this volume). U-Pb zircon and monazite ages for the Seagull and Cassiar batholiths, Wolf Lake map area, southern Yukon. *In: Yukon Exploration and Geology 2005*, D.S. Emond, G.D. Bradshaw, L.L. Lewis and L.H. Weston (eds.), Yukon Geological Survey, p. 257-266.
- NORMIN.DB – The Northern Minerals Database. Northwest Territories Geoscience office.
- Pearce, J.A., Harris, N.B.W. and Tindle, A.G., 1984. Trace element discrimination diagrams for the tectonic interpretation of granitic rocks. *Journal of Petrology*, vol. 25, p. 956-983.
- Rasmussen, K.L., 2004. The aplitic dykes of the Cantung Mine, NWT: Petrology, geochemistry, and implications for the mineralization process. Unpublished BSc thesis, University of Calgary, Alberta, Canada, 128 p.
- Selby, D., Creaser, R.A., Heaman, L.M. and Hart, C.J.R., 2003. Re-Os and U-Pb geochronology of the Clear Creek, Dublin Gulch, and Mactung deposits, Tombstone Gold Belt, Yukon, Canada: absolute timing relationships between plutonism and mineralization. *Canadian Journal of Earth Sciences*, vol. 40, no. 12, p. 1839-1852.
- Sun, S.S. and McDonough, W.F., 1989. Chemical and isotope systematics of oceanic basalts: implications for mantle compositions and processes. *In: Magmatism in Ocean Basins*, Geological Society, London, Special Publications, A.D. Saunders, and M.J. Norry (eds.), vol. 42, p. 313-345.
- Van Middelaar, W.T., 1988. Alteration and mica chemistry of the granitoid associated with the Cantung scheelite skarn, Tungsten, Northwest Territories, Canada. Unpublished PhD thesis, University of Georgia, Georgia, 245 p.
- Woodsworth, G.J., Anderson, R.G. and Armstrong, R.L., 1991. Plutonic regimes. *In: Geology of the Cordilleran Orogen in Canada*, GSC Geology of Canada, H. Gabrielse and C.J. Yorath (eds.), no. 4, p. 491-531.
- Yuvan, J.G., Shelton, K.L., Falck, H. and Marshall, D.D., 2004. High-grade quartz-scheelite veins in the Cantung mine, Northwest Territories: a late magmatic-hydrothermal event. 32nd Annual Yellowknife Geoscience Forum, November 16-18, Abstracts Volume, p. 85.

Paleomagnetism of the ~91 Ma Deadman pluton: Post-mid-Cretaceous tectonic motion in central Yukon

David T.A. Symons^{1,2} and Michael J. Harris^{2,3}
Department of Earth Sciences, University of Windsor²
Department of Geology, James Madison University³

Craig J.R. Hart
Yukon Geological Survey⁴

Phil J.A. McCausland
Department of Earth Sciences, University of Windsor²
Department of Geological Sciences, University of Michigan⁵

Symons, D.T.A., Harris, M.J., Hart, C.J.R. and McCausland, P.J.A., 2006. Paleomagnetism of the ~91 Ma Deadman pluton: Post-mid-Cretaceous tectonic motion in central Yukon. *In: Yukon Exploration and Geology 2005*, D.S. Emond, G.D. Bradshaw, L.L. Lewis and L.H. Weston (eds.), Yukon Geological Survey, p. 299-313.

ABSTRACT

The 92 ± 1 Ma Deadman pluton is a massive, circular, felsic intrusion of alkalic composition that is part of the Tombstone plutonic suite. It intrudes Neoproterozoic Hyland Group strata within the Dawson thrust sheet in the northernmost Selwyn Basin. Paleomagnetic determinations have isolated a stable characteristic remanent magnetization (ChRM) direction, in magnetite, for 237 specimens from 23 sites. The sites are in three plutonic phases, in three dykes cutting the pluton as well as their contact zones, and in the pluton's contact-zone skarn. The ChRM at all sites is coeval with pluton crystallization. The ChRM directions of all sites form one population with a mean direction of declination = 333.0°, inclination = 76.8° ($\alpha_{95} = 2.6^\circ$, $k = 139$, $N = 23$), giving a paleopole of 144.9°E, 78.5°N ($\delta_p = 4.5^\circ$, $\delta_m = 4.8^\circ$) that is significantly different, at 95% confidence, from the coeval North American cratonic paleopole. This discordance is attributed to post-emplacement, northward displacement of at least several tens of kilometres of the Dawson thrust sheet, possibly along the Dawson thrust fault. The result is the 'beheading' of the Deadman pluton and rotating its 'head' as it was driven up the curved frontal ramp of the thrust fault. This evidence indicates at least local, but significant, post-mid-Cretaceous deformation within rocks underlying northern Selwyn Basin.

RÉSUMÉ

Le pluton de Deadman, datant de 92±1 Ma, est une intrusion felsique massive et circulaire de composition alcaline qui fait partie du cortège plutonique de Tombstone. Il pénètre les strates du Groupe de Hyland, datant du Néoprotérozoïque, à l'intérieur de la nappe de charriage de Dawson, dans la partie la plus septentrionale du bassin de Selwyn. Les analyses paléomagnétiques ont permis d'isoler une direction stable d'aimantation rémanente caractéristique (ChRM), dans la magnétite, pour 237 spécimens prélevés en 23 sites. Les sites se répartissent en trois phases plutoniques : à l'intérieur de trois dykes recoupant le pluton ainsi que leurs zones de contact, et dans le skarn de la zone de contact du pluton. Dans tous les sites, la ChRM est contemporaine de la cristallisation du pluton. Les directions de la ChRM appartiennent à une même population statistique avec une direction moyenne de déclinaison = 333,0°, une inclinaison = 76,8° ($\alpha_{95} = 2,6^\circ$, $k = 139$, $N = 23$), indiquant une position du paléopôle par 144,9° E. et 78,5° N. ($\delta_p = 4,5^\circ$, $\delta_m = 4,8^\circ$), ce qui représente un écart significatif, à un niveau de confiance de 95 %, par rapport au paléopôle du craton nord-américain d'âge identique. Cet écart est attribuable au déplacement vers le nord de la nappe de charriage de Dawson, après la mise en place, sur au moins plusieurs dizaines de kilomètres le long de la faille de chevauchement de Dawson. Ainsi, le pluton de Deadman's Gulch a été « étêté », sa « tête » subissant une rotation tandis qu'elle était poussée vers le haut contre la rampe frontale incurvée de la faille de chevauchement. Ces constatations indiquent que les roches du protocontinent nord-américain, en général et le long de la faille de Dawson en particulier, ont subi une déformation importante, à tout le moins par endroits, ultérieure au Crétacé.

¹dsymons@uwindsor.ca

⁴Box 2703 (K-102), Whitehorse, Yukon, Canada Y1A 2C6

²Windsor, Ontario, Canada N9B 3P4

⁵C.C. Little Building, 425 East University Avenue, Ann Arbor, MI, USA 48109-1063

³Harrisonburg, VA, USA 22807

INTRODUCTION

Previous paleomagnetic studies of Mesozoic rocks in the northern Canadian Cordillera have indicated significant displacements and rotations of those more outboard tectonic elements (i.e., terranes) in the western and central Cordillera (e.g., Irving and Wynne, 1992). In order to provide a local mid-Cretaceous paleopole, the Deadman pluton was chosen to provide a paleopole for the North American craton close to the large, transcurrent Tintina Fault, which represents the craton's edge and boundary with the allochthonous accreted terranes, including Yukon-Tanana Terrane (YTT) (Figs. 1, 2). This aim was based on the geologic rationale that the rocks of the Selwyn Basin that host the Deadman pluton had been a stable entity since the middle Cretaceous. However, since the study began and samples were taken in 2000, several lines of geophysical evidence have emerged to support the opposite hypothesis – that the basin has been involved in active orogenesis since the pluton's emplacement (Symons *et al.*, 2005). This paper provides a test of conflicting hypotheses regarding the participation, mobility and timing of deformation in the miogeoclinal strata above the cratonic basement.

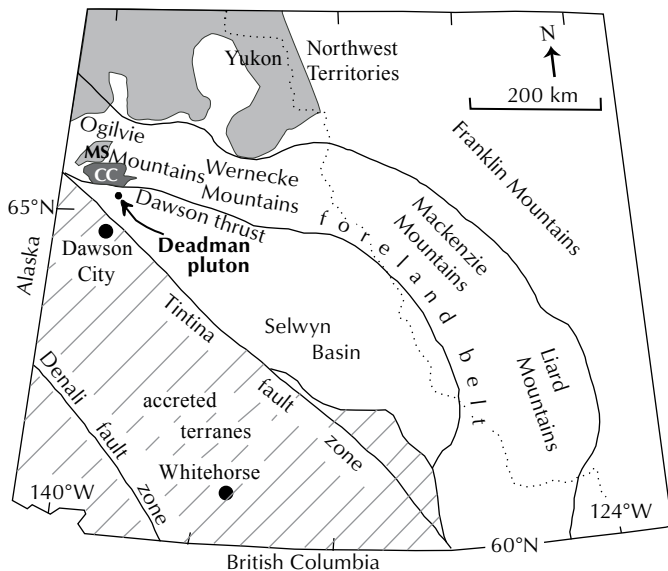


Figure 1. Location map for Deadman pluton, and assorted tectonic elements of Yukon (modified after Gordey and Makepeace, 2003). Accreted terranes are shown with diagonal hatching; the ancient North American cratonic margin in white; dark shade is the Proterozoic Coal Creek (CC) inlier; light shade is Cretaceous basins, including the Monster synclinorium (MS).

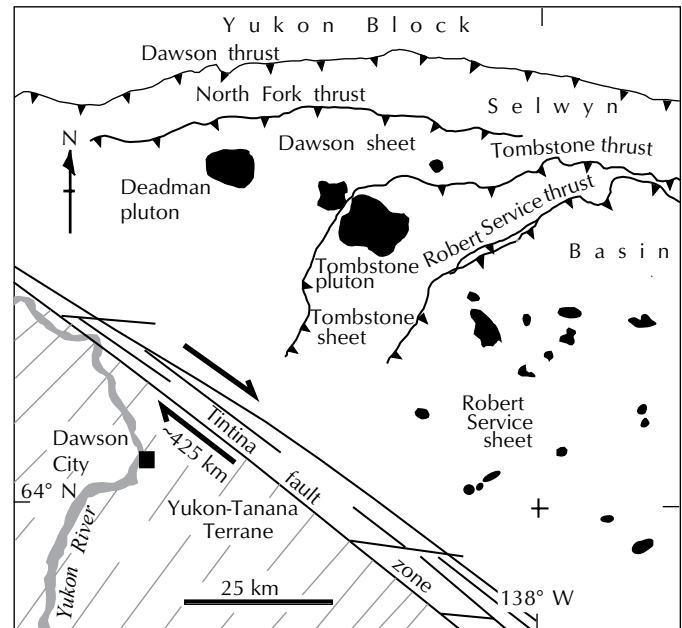


Figure 2. Regional geology after Gordey and Makepeace (2003) showing the northwestern end of the Tombstone plutonic suite and major faults. The plutons are represented by the solid black polygons. The barbs on the thrust faults indicate the downdip direction, and the Tintina Fault has a right-lateral displacement of ~425 km. The accreted Yukon-Tanana Terrane has diagonal hatching.

Within the framework of Lithoprobe, Canada's National Geoscience Project (Clowes *et al.*, 1999), the Slave-Northern Cordillera Lithospheric Evolution (SNORCLE) transect provided support for multidisciplinary studies aimed at examining the complex relationships within and between terranes in northwestern Canada. This study of the Deadman pluton in Yukon is one of a series of paleomagnetic studies begun under SNORCLE's aegis (Symons *et al.*, 2005).

GEOLOGY

The Deadman pluton is located about 55 km north of Dawson City, Yukon (Fig. 2). The stock is the most northerly member of a northwest-trending string of five mid-Cretaceous plutons and numerous assorted stocks, dykes and sills that parallel the Tintina Fault, which is ~35 km to the south-southwest (Anderson, 1987; Hart *et al.*, 2004). The plutons comprise the Tombstone plutonic suite, which are essentially defined by their alkalic compositions (Hart *et al.*, 2005). The plutons intrude deformed but weakly metamorphosed strata of

the Selwyn Basin that represent the most outboard components of the western North American miogeocline. Selwyn Basin assemblages at this location includes Neoproterozoic coarse clastic Hyland Group; lower Paleozoic Road River Group black shales and chert; Mississippian quartzite; Permian shale and chert; Triassic quartzite, calcareous siltstone, limestone and gabbro; and Jurassic black shale. These Selwyn Basin rocks are juxtaposed across the Dawson Fault against the Yukon Block (Abbott, 1997) where Proterozoic assemblages of the Coal Creek inlier are exposed beneath Lower Paleozoic dolostone and shale. The Coal Creek inlier includes three dominantly sedimentary assemblages: the Paleoproterozoic Wernecke Supergroup (Gillespie Lake and Quartet groups), Mesoproterozoic Pinguicula/Fifteen-Mile Group and Neoproterozoic Mt. Harper Group volcanic strata (Thompson *et al.*, 1992; Abbott, 1997). Paleozoic rocks include Ordovician to Devonian dolostone of the Bouvette Formation and time-equivalent black shale and chert of the Road River Group, and Devonian-Mississippian black shale, chert and siliciclastic rocks of the Earn Group. North of the Coal Creek inlier, the Earn Group is overlain by a succession of Carboniferous, Permian and Triassic shale, limy shale and limestone. Triassic strata are unconformably overlain by Cretaceous siliciclastic rocks of the Monster Formation in the Monster synclinorium (Ricketts, 1988).

Plutons of the Tombstone plutonic suite intrude the Selwyn Basin strata. The Deadman pluton is circular, about 7 km in diameter and has steep sides (Fig. 3). It is a concentrically zoned multiphase alkalic pluton composed mostly of medium- to coarse-grained alkali-feldspar syenite and biotite-hornblende monzonite, with lesser amounts of quartz monzonite and pseudoleucite-phyric tinguaita (Anderson, 1987). Vein, skarn and disseminated uranium-thorium-fluorine, antimony-arsenic-gold, tin-silver and gold-copper-bismuth mineralization occur within and adjacent to the Tombstone suite plutons (Hart *et al.*, 2005). In the Deadman pluton, uranium-thorium mineralization is associated with the tinguaita, a silica-undersaturated, highly potassic leucite porphyry. The stock is dated at 91 ± 1 Ma by the U-Pb SHRIMP method on zircons that are large and mostly unzoned (C. Hart, unpublished). This date is similar to determinations from other plutons in the suite, and similar K-Ar dates from the adjacent Tombstone pluton (Fig. 2) indicate that the plutons cooled rapidly within a few million years (Anderson, 1987; Hart *et al.*, 2005). Based on petrography and slightly elevated aeromagnetic responses and magnetic susceptibility values, Hart *et al.*, (2004) deem the Tombstone suite to be

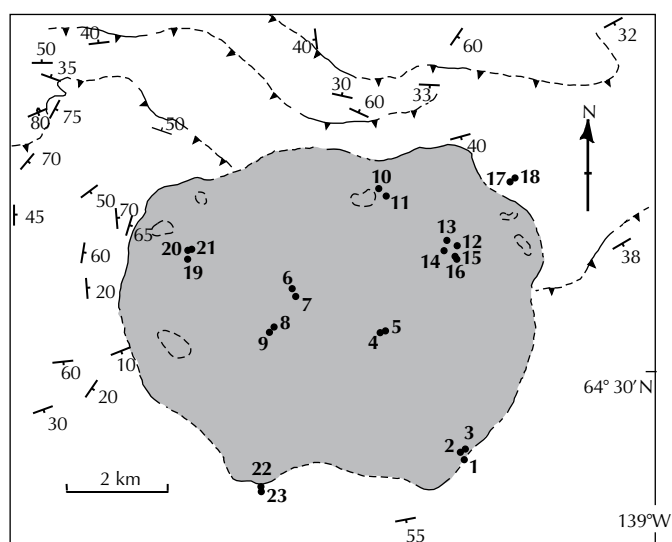


Figure 3. Location of sampling sites (solid circles) in, and adjacent to, the Deadman pluton (shaded). The surrounding host rocks belong to the Precambrian Hyland Group (clear) but have been hornfelsed within the pluton's contact aureole. Strikes and dips are shown for these strata, as are subsidiary thrust faults of the Dawson thrust with barbs pointing down-dip. Modified from Thompson *et al.*, (1992).

magnetite-series granitoids (Ishihara, 1981). They correlate the suite with the Livengood suite in east-central Alaska to form the Livengood-Tombstone plutonic belt, which requires ~425 km of post-emplacment dextral displacement on the Tintina fault zone.

Folds with west- to northwest-trending fold axes and related thrust faults deform the Selwyn Basin assemblages (Thompson, 1995; Murphy, 1997), and to a lesser degree those of the Yukon Block. The Dawson, Tombstone and Robert Service faults are thought to be low-angle thrust faults (Fig. 2) and account for most of the northward displacement (Tempelman-Kluit, 1982; Thompson *et al.*, 1992; Murphy, 1997; Mair *et al.*, in press). Regional metamorphism is at sub-greenschist levels. Deformation is dated at pre-Late Jurassic by macrofossils from deformed Jurassic rocks in the footwall of the Tombstone thrust fault (Poulton and Tempelman-Kluit, 1982), and at pre-105 Ma by Ar-Ar dates on metamorphic micas in deformed Hyland Group in the Robert Service thrust sheet (Mair *et al.*, in press). Deformation in Selwyn Basin, at surface, predates emplacement of the Tombstone suite plutons based on the massive non-foliated character of the

plutons (Anderson, 1987) and their mapped cross-cutting relationships with folds and thrust faults (Tempelman-Kluit, 1970; Thompson *et al.*, 1992; Murphy, 1997). For example, undeformed Tombstone suite plutons cut both the Tombstone and Robert Service thrust faults. The Deadman pluton intrudes thrust-faulted Hyland Group strata in the Dawson thrust sheet and presumably cuts the south-dipping Dawson thrust fault at depth (Fig. 2).

EXPERIMENTAL METHODS

SAMPLING

The Deadman pluton forms an isolated rugged 2000 m mountain peak rising about 1000 m above the adjacent valley floors. Outcrops are accessible by helicopter, and most are exposed in cirques. Six or seven 2.54-cm diameter cores were drilled, oriented by sun compass or by magnetic compass in a few cases, and collected from each of twenty-three sites (Fig. 3). Of these sites, 8 were located in monzonite, 5 in syenite, 1 in tinguaitite, 3 in felsic dykes cutting the pluton, 2 in dyke contact zones, and 4 in skarns of in the Precambrian host rocks around the pluton. From 8 to 13 standard paleomagnetic specimens with a 2.20-cm length were sliced from the cores to represent each site (Table 1). The specimens were stored in a magnetically shielded room with an ambient field of about 0.2% of the Earth's magnetic field intensity for about three months before measurement to allow their unwanted viscous remanent magnetization (VRM) components to substantially decay. VRM are unstable easily changed magnetization components in a specimen that are produced by the Earth's ambient magnetic field in the field or laboratory.

NATURAL REMANENT MAGNETIZATIONS

The natural remanent magnetizations (NRM) of the specimens were measured on a Canadian Thin Films DRM-420 cryogenic magnetometer with a sensitivity of $\sim 10^{-6}$ A/m. The median (M) NRM intensities by rock type were monzonite, $M = 2.2 \times 10^{-1}$ A/m, $N = 100$ specimens; syenite, $M = 1.2 \times 10^{-1}$ A/m, $N = 49$; tinguaitite, $M = 4.4 \times 10^{-1}$ A/m, $N = 13$; felsic dykes, $M = 0.46 \times 10^{-1}$ A/m, $N = 37$; dyke contact zones, $M = 1.5 \times 10^{-1}$ A/m, $N = 15$; and, host rock skarns, $M = 2.3 \times 10^{-1}$ A/m. Excluding the skarn specimens, the overall NRM intensity for the pluton is $M = 1.6 \times 10^{-1}$ A/m with first and third quartile values of $Q_1 = 0.65 \times 10^{-1}$ A/m and $Q_3 = 3.2 \times 10^{-1}$ A/m.

Table 1. Site mean remanence directions.

Site	Rock unit	N m, e	D °	I °	α_{95} °	k
1	Pm	10, 8	332.8	72.1	3.1	323
2	Pc	11, 11	348.2	74.4	11.1	18.0
3	df	11, 11	329.4	72.2	5.9	60.5
4	Pm	13, 13	354.9	71.6	3.8	119
5	Pm	12, 10	295.5	67.3	7.7	40.2
6	Pm	8, 8	8.7	67.9	6.9	65.9
7	Ps	8, 8	322.7	76.4	2.0	745
8	Ps	8, 8	320.0	74.0	4.5	154
9	Ps	8, 8	342.0	83.5	5.1	119
10	Pt	9, 9	304.3	75.2	2.4	465
11	Pm	10, 10	311.1	82.1	6.8	51.0
12	Pm	11, 10	306.0	80.3	6.6	55.2
13	Pm	12, 12	324.7	75.7	7.5	34.1
14	Pm	13, 13	338.5	75.5	3.6	130
15	Pc	14, 14	313.9	75.5	4.8	69.7
16	df	9, 8	325.4	77.1	4.8	137
17	H	8, 8	318.8	78.9	19.4	9.14
18	H	8, 8	321.0	83.9	10.9	26.8
19	Ps	12, 12	26.6	76.7	6.4	51.8
20	Ps	10, 10	337.1	79.5	2.9	271
21	df	11, 10	344.8	78.0	5.0	93.5
22	H	11, 11	346.4	72.9	2.6	310
23	H	10, 9	347.2	72.9	2.5	438

Rock unit abbreviations: c = contact zone, d = dyke, f = felsic, H = host rock, m = monzonite, P = pluton, s = syenite, t = tinguaitite. Number (N) of specimens measured (m) and used endpoint directions (e). Mean Declination (D), Inclination (I) and Radius of Cone of 95% Confidence (α_{95}) in degrees (°) and precision parameter (k) of Fisher (1953).

STEP DEMAGNETIZATION

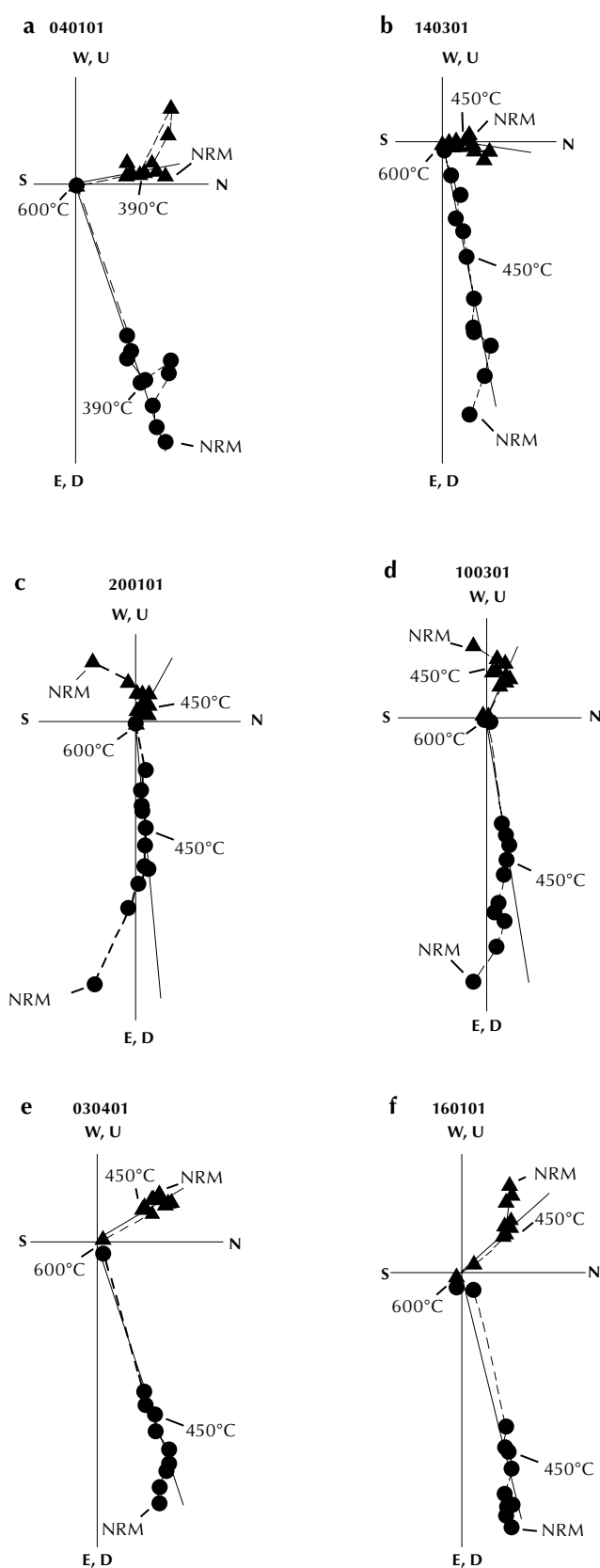
Two specimens with typical NRM intensities and directions were selected from each site and subjected to thermal demagnetization in 12 steps up to 600°C using a Magnetic Measurements MMTD-80 thermal demagnetizer. The NRM is the vector sum of the remanent magnetization components present in a specimen when it is first measured. The steps were preferentially concentrated in the 260 to 330°C and 500 to 600°C temperature ranges that are diagnostic for thermally demagnetizing pyrrhotite and magnetite, respectively. A further two typical specimens from each

site were alternating field (AF) demagnetized in 12 steps up to 130 mT using a Sapphire Instruments SI-4 AF demagnetizer. Based on the results from these four specimens per site, the remaining specimens from each site were step demagnetized using one of three regimens. Specimens from two baked contact zones of dykes (sites 2 and 15) were thermally demagnetized following the 12-step pattern used for the initial two specimens. Specimens from five sites (12, 13, 14, 19 and 22) were thermally demagnetized in 10 steps between 390 and 600°C, and those from the remaining 16 sites were AF-demagnetized in 6 steps between 20 mT and 70 to 110 mT.

The characteristic remanent magnetization (ChRM) directions of the 237 specimens were determined using visual inspection of vector component plots (Zijderveld, 1967) and calculated using the least-squares fitting method (Kirschvink, 1980). The ChRM component is the stable remanence of geologic interest that is preserved by a specimen. As evident from the 97% of specimens yielding endpoint ChRM directions that were used (Table 1), nearly all of the specimens gave normal directions with maximum angular deviation values of $\leq 10^\circ$ over several steps. Examples of specimens from the various petrologic phases of the pluton that show this reliable paleomagnetic behaviour on thermal and AF step demagnetization are given in Figures 4 and 5, respectively. The steep decrease in intensity on thermal demagnetization above 500°C shows that the ChRM resides mostly in magnetite or very low-titanium titanomagnetite.

Host rock sites 22 and 23 are within ~200 m of the observed contact with the Deadman pluton and sites 17

Figure 4. Thermal step demagnetization of example specimens from phases of the Deadman pluton: **(a)** monzonite, site 4; **(b)** monzonite, site 14; **(c)** syenite, site 20; **(d)** tinguaitite, site 10, **(e)** felsic dyke, site 3; and **(f)** felsic dyke, site 16. The characteristic remanent magnetization (ChRM) vector is projected onto the horizontal plane (triangles; north (N), east (E), south (S), and west (W) axes) and vertical plane (circles; up (U), north (N), down (D), and south (S) axes). The axial values are the ratio of the measured ChRM intensity (J) to the initial natural remanent magnetization (NRM) intensity (J_0), and the J_0 values in 10^{-1} A/m are: **(a)** 0.548; **(b)** 1.29; **(c)** 3.03; **(d)** 4.29; **(e)** 0.206; and **(f)** 0.166. The temperatures of some demagnetizing steps are given in °C.



and 18 are about 300 to 400 m from the contact, but all four sites are in skarn within the pluton's contact aureole. Most of the specimens gave normal steeply downward northwesterly ChRM directions (Fig. 6a,b). Thermal step demagnetization shows that the ChRM resides in magnetite in most cases (Fig. 6c), except for some specimens from the skarn at site 17, in which it resides in pyrrhotite (Fig. 6d).

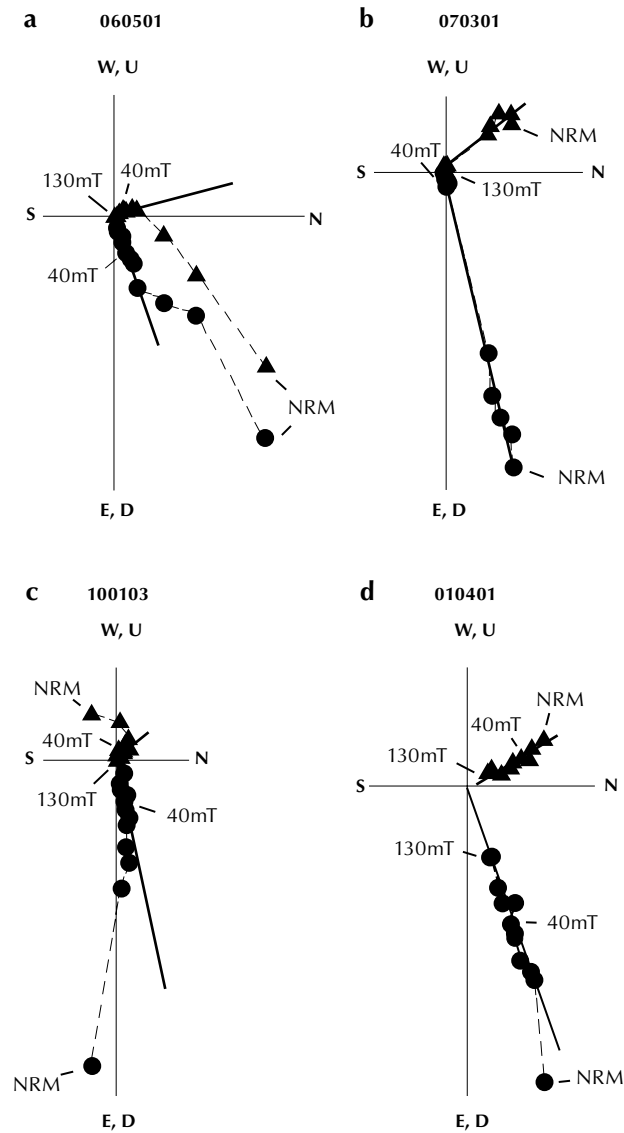


Figure 5. Alternating-field (AF) step demagnetization of example specimens from phases of Deadman pluton: (a) monzonite, site 6; (b) syenite, site 7; (c) tinguaitaite, site 10; and (d) felsic dyke, site 1. Conventions as in Figure 3. The J_0 values in 10^{-1} A/m are: (a) 6.42; (b) 0.281; (c) 3.38; and (d) 2.79. The intensity of some demagnetizing steps are given in mT.

SATURATION REMANENCE

Saturation isothermal remanent magnetization (SIRM) testing was done on 12 specimens to better characterize the magnetic minerals in the various rock types. A given magnetic mineral, such as pyrrhotite, reaches magnetic saturation in a distinctive range of applied direct-field intensities, and the rates of SIRM acquisition and demagnetization are indicative of the dominant domain sizes present in the mineral. The specimens were pulse magnetized in 12 steps up to 900 mT using a Sapphire

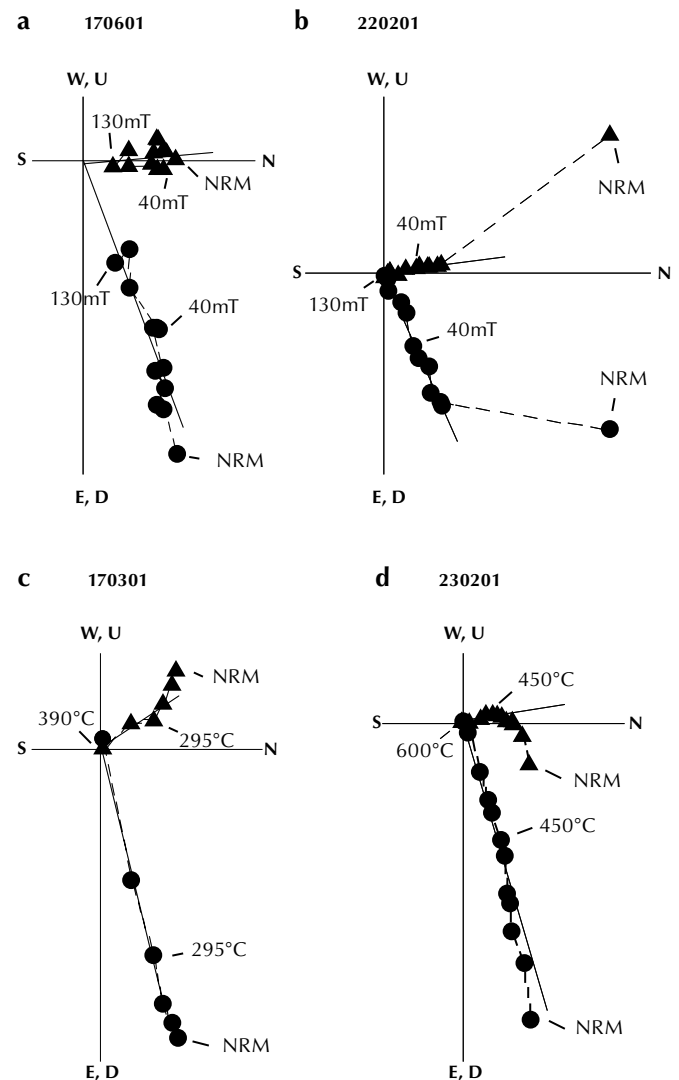


Figure 6. Alternating-field and thermal step demagnetization of example specimens from the host rock skarn of the Deadman pluton from: (a) site 17; (b) site 22; (c) site 17; and (d) site 23. Conventions as in Figure 3 and 4. The J_0 values in 10^{-1} A/m are: (a) 0.591; (b) 0.253; (c) 4.01; and (d) 5.50.

Instruments SI-6 direct-field pulse magnetizer to define their SIRM acquisition. In all cases, the specimens saturated by ~250 mT, indicating that their remanence is carried mainly by magnetite (Fig. 7a). The specimens were then AF demagnetized in 12 steps to 150 mT. The decay rates of their SIRM intensities, when plotted against type curves for magnetite, indicate that the ChRM is carried mostly by single and pseudosingle domain magnetite (Fig. 7b). In general, single or pseudosingle domain magnetite is carried by inclusions in the major minerals of an igneous rock and, therefore, is the most likely remanence component to retain a stable primary ChRM. Also, when the axial values for the crossover points are compared to type curves for magnetite (Fig. 7c) (Symons and Cioppa, 2000), the lithologies all give comparable intensity ratio values (J/J_{900}) of 0.32 ± 0.04 (pluton, 0.33 ± 0.04 ; dykes, 0.30 ± 0.04 ; skarn, 0.31). These values all indicate considerable interaction between the magnetic fields of the individual magnetite crystals in the specimens, thereby decreasing the values from a non-interacting ideal value of 0.50. Finally, the crossover points yield a mean value of 22 ± 12 mT for the magnetizing and demagnetizing fields in the nine pluton specimens, indicating that they carry mostly pseudosingle domain magnetite, with lesser amounts of single and multidomain magnetite. Similarly, the two dyke specimens and the skarn specimen give values of 23 ± 3 mT and 32 mT, respectively, indicating that their magnetization is carried mostly by pseudosingle domain magnetite.

SITE/UNIT MEAN CHRMs DIRECTIONS

The site mean ChRM directions were calculated from the 229 accepted specimen directions using methods described by Fisher (1953). Only 8 specimens, or 3%, gave an aberrant ChRM direction or failed to give a reliable direction. Nearly all sites had well clustered specimen directions, giving a median value for the radii of their cones at 95% confidence (α_{95}) of 5.0° and for their precision parameters (k) of 93.5. Site 17 in the host rock skarn was the sole exception and gave loosely clustered directions with $\alpha_{95} = 19.4^\circ$ and $k = 9.14$. This is the site in which the ChRM resided in both pyrrhotite and magnetite, suggesting that the two minerals acquired their remanence at different times and that either apparent polar wander or tectonic tilt occurred during the intervening time.

Plotted on a stereonet (Fig. 8), the site mean ChRM directions form a coherent cluster. Therefore, the test of McFadden and Lowes (1981) was used sequentially to

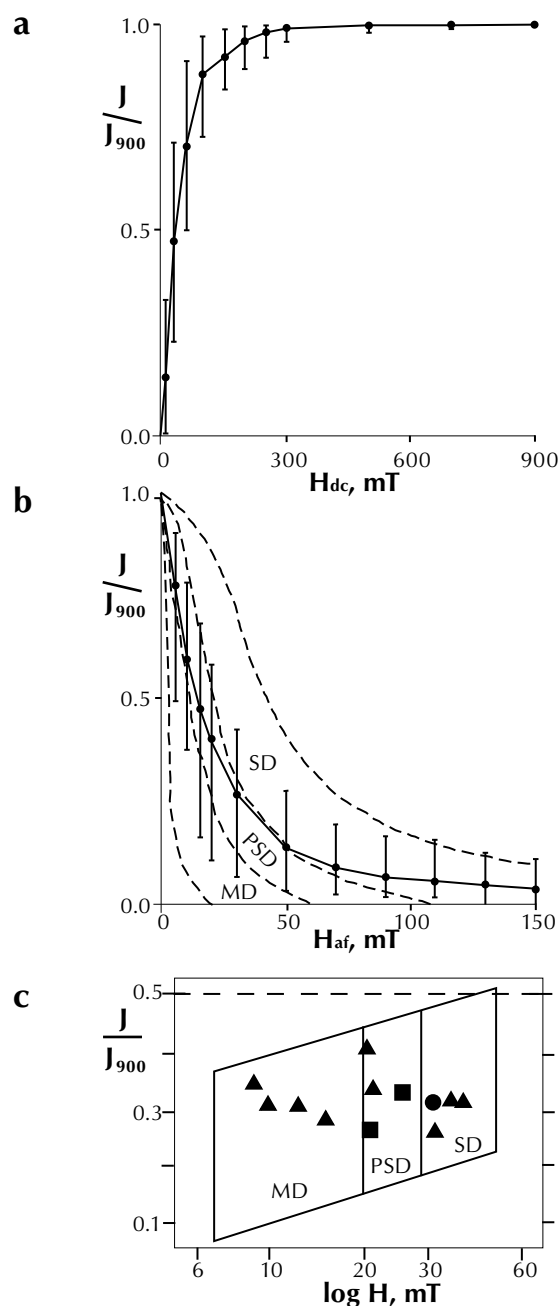


Figure 7. Saturation isothermal remanent magnetization (SIRM) data for example specimens of various lithologies: (a) SIRM acquisition; (b) AF demagnetization of SIRM; and (c) crossover points for the acquisition and decay curves. The magnetizing H_{dc} and demagnetizing H_{af} field axes are labeled in mT and the y-axis is the ratio of the measured intensity (J) to the saturation intensity at 900 mT (J_{900}). The reference curves are for magnetite: SD = single domain, PSD = pseudosingle domain, and MD = multidomain. The symbols denote specimens from the \blacktriangle pluton, \blacksquare dykes, and \bullet host rock skarn.

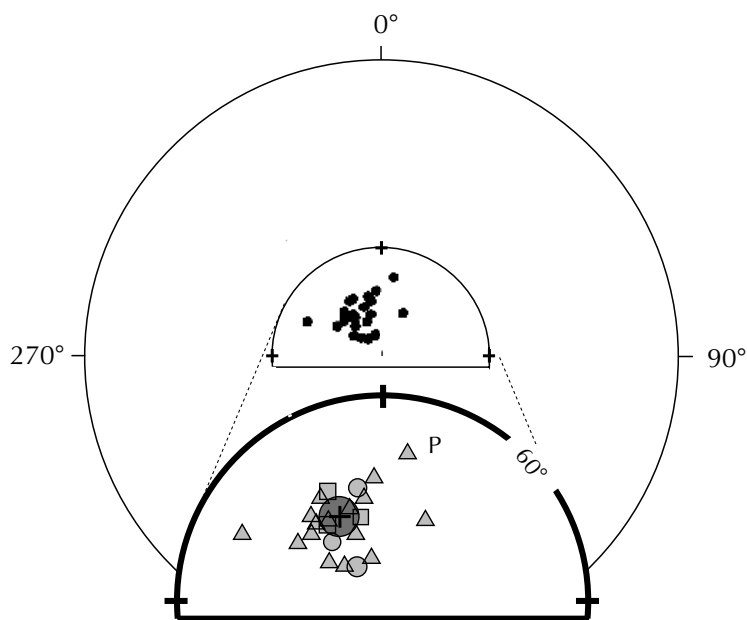


Figure 8. Equal-area stereonet showing the site mean directions for the Deadman pluton collection. Site symbols: \blacktriangle pluton, \blacksquare dykes, \bullet host rock skarn. The inset shows the central portion of the stereonet at inclinations of $>60^\circ$ for added clarity, along with the population mean (+) and its cone of 95% (2σ) confidence. The present Earth's magnetic field direction is shown by a "P".

compare the mean directions for the various lithologies, to see if they represented statistically different populations at $>95\%$ confidence. The test showed that: a) the pluton's 8 monzonite site mean directions are indistinguishable from the 5 syenite site mean directions, that is, they may share a common mean and thus the two populations may be combined; b) the tinguaitite site's direction is indistinguishable from the 13 monzonite and syenite sites' population and can thus be added to it; c) the 3 dyke sites form a directional population that is indistinguishable from the 14 site population from the pluton; d) similarly, the 2 sites from the contact zones of two of the dykes have directions that are indistinguishable from both the 14 site population of the pluton and the 3 site population from the dykes; thus all 19 sites may be combined to form a single population; and e) the directions from the 4 sites in the host rock skarns form a population that is indistinguishable from the 19 site population within the pluton. This sequential analysis shows that the mean directions for all 23 sites may be combined to form a single population to represent the Deadman pluton. The pluton yields a unit mean ChRM direction of declination

$D = 333.0^\circ$ and inclination $I = 76.8^\circ$ with a cone radius of 95% confidence $\alpha_{95} = 2.6^\circ$, precision parameter of Fisher (1953) $k = 139$, and number of sites $N = 23$.

There is no evidence to suggest that the Deadman pluton has been remagnetized since emplacement, therefore, it is deemed to have retained a primary thermoremanent magnetization (TRM) in magnetite. The associated dykes intruded and cooled with a primary TRM, and likely remagnetized their baked contact zones with a partial TRM. The host rocks of the Hyland Group were altered to skarn and calc-silicate within the pluton's contact zone and underwent thermochemical remagnetization, all within a few million years, and probably very much less, as the dykes are likely simply a late phase of the pluton. All of these magnetizations have a normal polarity, consistent with their acquisition during the Cretaceous normal polarity superchron from 119 to 84 Ma (Opdyke and Channell, 1996).

DISCUSSION

POLE POSITION

Using a mean location for the 23 sites of 220.88°E , 64.51°N , the unit mean ChRM direction for the Deadman pluton gives a pole position of 144.9°E , 78.5°N , $dp = 4.5^\circ$, $dm = 4.8^\circ$ (longitude, latitude, semi-axes of the oval of 95% confidence along and perpendicular to the site-pole great circle) (Fig. 9). If the Deadman pluton has not moved since being emplaced into a "stable" North American craton, then the pluton should give a paleopole that is concordant with the craton's paleopole at 91 Ma. From the recently computed apparent polar wander path (APWP) of Besse and Courtillot (2002) for the North American craton, the expected paleopole would be located at 205.0°E , 75.7°N ($A_{95} = 5.4^\circ$), where A_{95} is the radius of the cone of 95% confidence about the expected paleopole. Clearly, the determined and expected paleopoles for the pluton are significantly different at $\gg 95\%$ confidence (Fig. 9). Several hypotheses merit consideration to explain the discordance between the paleopoles. These are considered in turn in the following sections.

RAPID COOLING OF THE PLUTON

One possibility is that the Deadman pluton cooled sufficiently fast that secular variation in the Earth's magnetic field was not sufficiently averaged out, as happens in a lava flow. In general, it is deemed that a

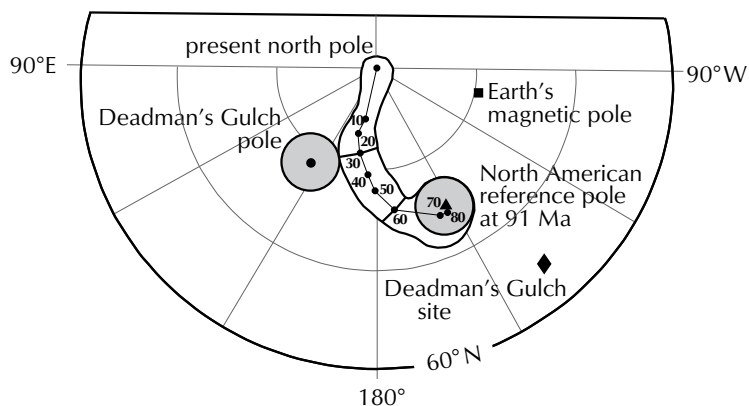


Figure 9. North polar projection showing the Apparent Polar Wander Path for the North American craton of Besse and Courtillot (2002) after 91 Ma, the 91 Ma reference paleopole (▲), and the Deadman pluton’s paleopole (●) with their 1σ confidence limits. To a close approximation, if the 1σ bounds of two populations do not cross, then the two populations are significantly different with >95% confidence. The diamond (◆) is the pluton’s location, and square (■) the Earth’s present magnetic pole.

paleopole should represent a time period in excess of a few thousand years (i.e., 10^3 - 10^4 years) to average out the biasing effects of secular variation (Merrill and McElhinny, 1983). The pluton’s sites were located between the perimeter and core of the pluton (Fig. 3). Following Carlsaw and Jaeger (1959) and Jaeger (1964), the magnetic minerals in rocks from the perimeter sites would cool through the $\sim 600^\circ\text{C}$ to $\sim 400^\circ\text{C}$ blocking temperature range of magnetite in less than a year. In contrast, using a vertical cylinder model and assuming a minimal ambient host rock temperature of $\sim 100^\circ\text{C}$ or depth to top of the pluton of ~ 3 km, the rock in the core sites of this 7-km-diameter pluton would pass through the same blocking temperature range about 10^5 years later. Thus, it appears that rapid cooling of the pluton is an improbable explanation for the pluton’s deviant paleopole.

POST-EMPLACEMENT REMAGNETIZATION

Remagnetization of the Deadman pluton to give its discordant paleopole is an unlikely explanation for two fundamental reasons. First, the rocks show no petrologic evidence of post-emplacement alteration by either metamorphism to generate a partial thermal remagnetization overprint or hydrothermal fluid flow to

generate a partial chemical overprint. Second, in the absence of any subsequent tectonic activity, a remagnetization should give a pole position on the apparent polar wander path at some time after 91 Ma. In contrast, the ChRM of the Deadman pluton gives a pole position that is significantly off the 91 Ma to Recent path for North America (Fig. 9).

ALLOCHTHONOUS TERRANE TECTONICS

Another way to bring the Deadman pluton and 91 Ma North America reference paleopoles into concordancy would be to translate the terrane hosting the pluton northward (i.e., poleward) to its present North American location. This would require that the pluton’s host terrane originated $12.8^\circ \pm 5.7^\circ$ or 1420 ± 600 km to the south-southeast along North America’s western margin in present-day southern British Columbia (BC). If the host terrane was part of what is known as the allochthonous Baja BC terranes (Irving, 1985; Irving et al., 1996), it could have been translated northward, coupled with the Kula plate between 91 Ma and 52 Ma with the rest of Baja BC. This explanation is improbable for two reasons. First, the host rocks of the Hyland Group correlate well with miogeoclinal strata that extend far into the adjacent craton and there is no geological evidence, such as faults, that would permit this solution. Second, although the translation distance agrees closely with the value of $8.3^\circ \pm 7.0^\circ$ calculated in a recent analysis of paleomagnetic data for Baja BC by Symons et al., (2005), the $9^\circ \pm 23^\circ$ vertical-axis counterclockwise rotation estimate since mid Cretaceous for the Deadman pluton conflicts significantly from the $51^\circ \pm 14^\circ$ clockwise rotation found in most Intermontane regions of Baja BC.

TECTONIC TILT

Another possibility is that the Deadman pluton was tilted after cooling. This requires correction for a tilt of 7.1° down to the southeast about a horizontal axis striking at $N55.6^\circ\text{E}$ to bring the pluton’s paleopole into agreement with the North American reference paleopole. The required correction is significant at $\gg 95\%$ confidence as the pluton’s ChRM vector direction is significantly different from the vector direction of $D = 341.6^\circ$, $I = 83.8^\circ$, $\alpha_{95} = 2.7^\circ$ that is required at the sampling site to give the reference paleopole. The obvious question is whether or not this post-emplacement tilt is geologically reasonable.

The Deadman pluton intrudes the Dawson thrust sheet (Fig. 2). Strata north of the Dawson thrust fault strike at about $N80^\circ\text{E}$ (Fig. 2), and strata in the overlying

Tombstone thrust sheet to the southeast strike at about N30°E. The pluton is located about half-way between these two thrust faults in a complex structural zone that may reflect interference between these structural trends. A horizontal tilt axis about half-way between these two trends, or about N55°E, is possible. Further, it should be noted that there are numerous intervening subsidiary thrust faults, such as the larger North Fork Thrust (Fig. 2), as well as several others that are crosscut by the pluton (Fig. 3). Cross-sections and map patterns of the thrust faults indicate moderate to shallow dips to the south and southeast (Tempelman-Kluit, 1970; Thompson *et al.*, 1992) (Fig. 3), which favour a downward tilt to the south and east.

DISPLACEMENT

If the Deadman pluton has been tilted southeasterly by tilting of the Dawson thrust sheet, it is important to consider the nature of that displacement. Three constraints are important. First, the pluton crosscuts several thrust faults without evident displacement of its contacts. This suggests that the thrust faulting predates emplacement of the pluton but requires that tilting occurred as the result of reactivation of the Dawson thrust fault, or movement of the Dawson sheet along another structure, but without substantial disruption of the internal part of the Dawson thrust sheet during motion. The second constraint is that the pluton is ~7 km in diameter, which means that its entire exposed area, along with the surrounding area of host rock contact aureole and skarn, had to be tilted by 7.1° to give the determined result. The third constraint is the typical geometry of regional thrust faults and the paleomagnetic imperative of rotation about a horizontal axis. Simple linear displacement of a thrust sheet along a shallowly dipping thrust fault will not cause a pluton's ChRM vector to rotate (Fig. 10a). For example, displacement of 111 km on a flat-lying sole fault of a pluton towards the Earth's pole position, as is the case here, is required to cause the pluton's paleopole to deviate by an insignificant 1° from the corresponding reference paleopole. What is required is that the thrust sheet hosting the pluton be pushed up the curving frontal ramp of a thrust fault so that the thrust sheet's dip is increased by 7.1° throughout the entire sampled area on average (Fig. 10b).

The geometry of the Dawson thrust is not well constrained. This is an old, extensional structure that controlled facies variations throughout the Proterozoic, and which marked the limit between basinal and

platformal deposition through Neoproterozoic and early Paleozoic time (Roots and Thompson, 1992; Abbott, 1997). Abbott (1997) considers the structure to have been a moderately steep south-dipping normal fault originally. However, Mesozoic inversion of Selwyn Basin reactivated the normal fault as a reverse fault over much of its length. Maps of the Dawson Thrust show dips ranging from flat to moderately steep (60°) and the cross-sections of Abbott (1997), from 100 km to the east, indicate a southerly shallowing of dip angles. The Dawson thrust sheet is composed mostly of strata of the 4000-m-thick Upper Proterozoic Hyland Group and emerges about 15 km

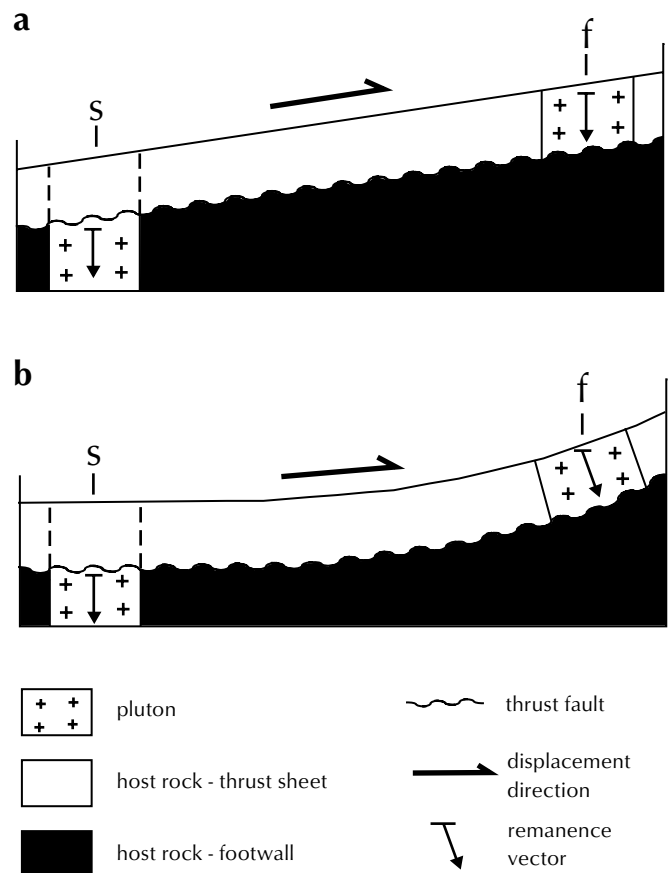


Figure 10. Schematic depiction, not to scale, of the head of a beheaded pluton being pushed up a thrust fault ramp that is: (a) linear; and, (b) curved. Note in **a** that the ChRM vector in the head and its host rocks in the thrust sheet are unchanged in inclination from the start (s) of displacement to its final (f) position, whereas in **b** that the vector's inclination shallows as the curved ramp's inclination steepens and the sheet moves towards the paleopole. Deadman pluton likely endured various amounts of both types of displacement before reaching its current location.

north of Deadman pluton (Fig. 2), suggesting that much of the fault beneath the pluton is flat-lying. These observations imply that the Deadman pluton would have had to be displaced by tens of kilometres northward on the Dawson Thrust after 91 Ma to achieve the required 7.1° tilt rotation. Furthermore they also imply that the pluton is now the head of a beheaded pluton.

There is, however, little evidence for significant post-Cretaceous displacement on the Dawson fault. Displacement of the Dawson thrust sheet, and associated tilting above thrust ramps, could otherwise have occurred along a master detachment that continued northward into the Yukon Block. This fault cut the Proterozoic Coal Creek inlier at depth, and migrated progressively north and east during later stages of Late Cretaceous deformation into the interior. As an example, deformation of the Monster synclinorium strata, north of the Coal Creek inlier, post-dates Monster Formation deposition (Ricketts, 1988), such that rocks as young as Cenomanian (99-93 Ma, Gradstein *et al.*, 2004) are folded, requiring some uncertain amount of deformation and potential tilting after the intrusion of the Deadman pluton.

TECTONIC STABILITY AFTER 91 MA?

The post-mid-Cretaceous tectonic history of the Selwyn Basin and adjacent Ogilvie-Wernecke-Mackenzie foreland belt (Fig. 1) is based on very limited geologic data. First, the youngest deformed strata observed in the foreland belt is Late Cretaceous (Yorath, 1992; McMechan *et al.*, 1992). Second, intrusions of the mid-Cretaceous Selwyn plutonic suites are massive and show little sign of post-emplacement deformation. Most deformation is deemed to be Early Cretaceous or earlier (McMechan *et al.*, 1992; Tempelman-Kluit *et al.*, 1992; Murphy, 1997), partly because of the lack of strata that is younger than 91 Ma in the Selwyn Basin to be deformed. The Cenomanian Monster Formation and Paleocene-Eocene strata in the northern Ogilvie, Wernecke and Franklin ranges are folded, which indicates that deformation continued into the Tertiary. The dearth of strata younger than 91 Ma south of the Dawson thrust indicates that they were either never deposited or since eroded, implying continual uplift and erosion since ~91 Ma. In the absence of post-91 Ma strata in the immediate study area, but indications of inboard deformation of Late Cretaceous strata, we speculate that horizontal motion occurred on sole faults or other horizontal detachment zones after 91 Ma in the Selwyn Basin and the adjacent foreland belt.

ACTIVE TECTONISM AFTER 91 MA

Curiously, there is considerable geophysical evidence to support the existence of post-91 Ma motion. Current global positioning system (GPS) data show that Whitehorse, located on the accreted terranes (Fig. 1) of the Intermontane Belt (IMB), is moving east-northeastwards (ENE) towards Yellowknife on the craton at 5.2 ± 2.2 mm/a (Fletcher and Freymueller, 1999). Combining GPS and earthquake seismology data, Mazzotti and Hyndman (2002) calculated a northeasterly maximum rate of 4.5 ± 2.5 mm/a through Whitehorse, and that changes to ENE through Yellowknife and north through the Ogilvie Mountains. They argued that the shortening was caused by the impact of the Yakutat plate on the Alaskan coastline and was being accommodated by crustal detachments exposed as thrust faults in the Mackenzie Mountains. Further, Lewis *et al.*, (2002) found from analysis of heat flow data in the northern Cordillera that the upper crust is sufficiently cool and rigid to be pushed ENE over top of the hot, and more fluid, lower crust on detachment zones. Additionally, continued ENE thrust-fault motion provides an explanation for the much higher rate of earthquake energy release in the northern foreland belt when compared to the southern foreland belt (Sweeney *et al.*, 1992). It also provides an explanation for the highly negative -80 to -120 mgal Bouguer gravity values found in the Mackenzie Mountains (Lowe *et al.*, 1994; Cook *et al.*, 2001), which are consistent with relatively rapid long-term uplift. Furthermore, the Lithoprobe SNORCLE seismic profiles across the northern Cordillera show the presence of well defined near-horizontal discontinuities that indicate that strata of the IMB terranes overlie a westward-thinning ramp of cratonic Proterozoic strata (Snyder *et al.*, 2002; Cook *et al.*, 2004). These profiles are thought to record thin-skin tectonics with the IMB strata having moved ENE over and up the marginal ramp. Such motion may also explain geological features such as: 1) the arcuate shape of the Mackenzie Arch, assuming maximum ENE displacement occurred on a vector about through Whitehorse; 2) the relative dearth of post-91 Ma intrusive and extrusive rocks in the northern Cordillera compared to the southern IMB because of continuing compression and uplift that records substantial extension (Souther and Yorath, 1992); and 3) the inboard offset from their probable mantle source regions of alkaline basalts of the northern Cordillera, as suggested by geochemical and isotopic signatures of mantle xenoliths (Abraham *et al.*, 2001).

Since the first suggestion that Eocene and younger paleomagnetic pole positions from the IMB could be recording thin-skin tectonics of the IMB rotating clockwise over the craton on sole faults (Symons *et al.*, 2000), the evidence has been accumulating and its paleomagnetic analysis has evolved (Symons *et al.*, 2003, 2005). In summary, the paleomagnetic data now indicate that the northern IMB rotated $16^\circ \pm 6^\circ$ (2σ), or at $0.29 \pm 0.11^\circ/\text{Ma}$, clockwise on top of the cratonic ramp during the past 54 Ma, with insignificant $2^\circ \pm 4^\circ$ (220 ± 440 km) northward translation (Symons *et al.*, 2005). Using a pivot point near the Peace River arch in north-central British Columbia, where extension in the southern IMB appears to change to compression in the northern IMB, leads to a calculated compressional ENE shortening of 305 ± 125 km. If the two GPS estimates for the current ENE compression of 5.2 ± 2.2 and 4.5 ± 2.5 mm/a are valid for the past 54 Ma, then they give comparable ENE shortening estimates of 280 ± 120 km and 240 ± 135 km, respectively. Further, the paleopoles for the IMB show that it was rotated an additional $35^\circ \pm 14^\circ$ clockwise and translated $8.3^\circ \pm 7.0^\circ$ (2σ) (915 ± 775 km) northward during the time interval from 102 ± 14 and 54 Ma. The northward motion suggests that the IMB terranes were being carried on the Kula plate, and the rotation suggests that they were being driven against and onto the cratonic ramp, thereby being the driving force for the Laramide orogeny from earliest Cretaceous to Early Eocene time. How much compressive shortening occurred prior to, or post, 91 Ma is uncertain given the presently available paleomagnetic data base. It is likely, however, that substantial ENE shortening continued after 91 Ma because the Kula plate was still active.

The obvious question then is “why are abundant Late Cretaceous and Tertiary rock units of the IMB terranes not found in the Selwyn Basin or Mackenzie Arch?” The answer could be that these areas northeast of the Tintina fault zone have undergone more rapid uplift than those on the southwest side because of continuing ENE compression against, and thrust faulting in, the more competent carbonate plateau strata of the Mackenzie Mountains. Thus, the Late Cretaceous and Tertiary strata of the IMB that likely overrode the proto-Tintina fault zone to cover a large area on its northeastern side have since been eroded except for the wedge of accreted terranes in southeastern Yukon that presumably overlies cratonic strata of the Selwyn Basin (Fig. 1).

Within this scenario, the Deadman pluton paleomagnetic result provides an additional line of evidence. It supports

a post-91 Ma transport direction to the north as Mazzotti and Hyndman (2002) observed in the GPS and earthquake seismicity data. It further suggests that the pluton moved at least several tens of kilometres, and perhaps much further, within the Dawson thrust sheet and possibly along the Dawson fault. This is consistent with existing geological estimates of at least 20 km of shortening in the Dawson sheet, at least 100 km of structural overlap in the Tombstone and Robert Service thrust sheets, and perhaps much more shortening overall (Tempelman-Kluit *et al.*, 1992). Also consistent with these estimates of substantial post-91 Ma northward motion is the displacement found on the adjacent Tintina fault zone. It shows a dextral displacement of about 425 km, of which about 125 km is thought to be post-Eocene (Gabrielse, 1985; Murphy and Mortensen, 2003). Accepting the transmission of transtensional stress across the Tintina fault zone, both the northward displacement of the thrust sheets, and of the southwest side of the Tintina Fault, could well be part of the same long-term Late Cretaceous-to-present tectonic process.

CONCLUSIONS

This paleomagnetic study shows that the Deadman pluton, crosscutting dykes, and adjacent host-rock skarn retain a ChRM that resides in magnetite and has a direction of $D = 333.0^\circ$, $I = 76.8^\circ$ ($\alpha_{95} = 2.6^\circ$, $k = 139$, $N = 23$). The ChRM is considered to be a primary TRM in the plutonic phases, including the late phase dykes, and a secondary thermochemical remagnetization in the skarn that were all acquired at 91 ± 1 Ma. The pluton's paleopole of 144.9°E , 78.5°N ($\delta_p = 4.5^\circ$, $\delta_m = 4.8^\circ$) is significantly different at $>>95\%$ confidence from the expected coeval paleopole for the North American craton. The difference is interpreted to reflect tilting of the pluton and surrounding host rocks of the Dawson thrust sheet as they were driven northward and up a curved frontal ramp of a thrust fault, likely the Dawson fault. Geometrical considerations suggest that the northward displacement amounts to a few tens of kilometres at least and perhaps much more. This requires the Deadman pluton to be the head of a beheaded pluton that is far removed from its source. Tilting likely occurred as deformation moved progressively inboard during Late Cretaceous, but a growing body of evidence increasingly supports active tectonism in Yukon from mid-Cretaceous to the present.

ACKNOWLEDGEMENTS

The authors gratefully thank Peter Kelly of Fireweed Helicopters Ltd. for his skilled help in collecting samples; the Yukon Geological Survey for logistical support of this study; Kazuo Kawasaki for his help with the manuscript preparation; the LITHOPROBE-SNORCLE transect project for financial support (to D.T.A. Symons); and the Ontario government for scholarship support (to P.J.A. McCausland). Reviews and comments by Grant Abbott are particularly appreciated, as is editorial assistance by Geoff Bradshaw.

REFERENCES

- Abbott, G., 1997. Geology of the upper Hart River area, eastern Ogilvie Mountains, Yukon Territory (116 A/10, 11). Exploration and Geological Services Division, Yukon Region, Indian and Northern Affairs Canada, Bulletin 9, 76 p., plus appendices.
- Abraham, A.C., Francis, D. and Polvé, M., 2001. Recent alkaline basalts as probes of the lithospheric mantle roots of the Northern Canadian Cordillera. *Chemical Geology*, vol. 175, p. 361-386.
- Anderson, R.G., 1987. Plutonic rocks in the Dawson map area, Yukon Territory. *In: Current Research, Part A*, Geological Survey of Canada, Paper 87-1A, p. 689-697.
- Besse, J. and Courtillot, V., 2002. Apparent and true polar wander and the geometry of the geomagnetic field over the last 200 Myr. *Journal of Geophysical Research*, vol. 107 (B 11), p. 1-31.
- Carslaw, H.S. and Jaeger, J.C., 1959. *Conduction of Heat in Solids*, 2nd edition, Oxford University Press, New York, 510 p.
- Clowes, R.M., Cook, F., Hajnal, Z., Hall, J., Lewry, J., Lucas, S. and Wardle, R., 1999. Canada's LITHOPROBE Project (collaborative, multidisciplinary geoscience research leads to new understanding of continental evolution). *Episodes*, vol. 22, p. 3-20.
- Cook, F.A., Clowes, R.M., Snyder, D.B., van der Velden, A.J., Hall, K.W., Erdmer, P. and Evenchick, C.A., 2001. Lithoprobe seismic reflection profiling of the northern Canadian Cordillera: First results of SNORCLE profiles 2 and 3. *Lithoprobe Report* 79, p. 36-49.
- Cook, F.A., Clowes, R.M., Snyder, D.B., van der Velder, A.J., Erdmer, P. and Evenchick, C.A., 2004. Precambrian crust beneath the Mesozoic northern Canadian Cordillera discovered by Lithoprobe seismic reflection profiling. *Tectonics*, vol. 23: TC2010, doi:10.1029/2002TC001412, 28 p.
- Fisher, R.A., 1953. Dispersion on a sphere. *Proceedings of the Royal Society of London*, vol. A217, p. 295-305.
- Fletcher, H.J. and Freymueller, J.T., 1999. New GPS constraints on the motion of the Yakutat block. *Geophysical Research Letters*, vol. 26, p. 3029-3032.
- Gabrielse, H., 1985. Major dextral tanscurrent displacements along the northern Rocky Mountain Trench and related lineaments in north-central British Columbia. *Geological Society of America Bulletin*, vol. 96, p. 1-14.
- Gordey, S.P. and Makepeace, A.J. (compilers), 2003. Yukon digital geology. Geological Survey of Canada, Open File 1749, and Yukon Geological Survey, Open File 2003-9(D), 2 CD-ROMs.
- Gradstein, F.M., Ogg, J.G. and Smith, G.A. and 37 others, 2004. *A Geologic Time Scale 2004*. Cambridge University Press, 589 p.
- Hart, C.J.R., Goldfarb, R.J., Lewis, L.L. and Mair, J.L., 2004. The northern Cordilleran mid-Cretaceous plutonic province: Ilmenite/magnetite series granitoids and intrusion-related mineralization. *Resource Geology*, vol. 54, p. 253-280.
- Hart, C.J.R., Mair, J.L., Goldfarb, R.J. and Groves D.I., in press. Source and redox controls of intrusion-related metallogeny, Tombstone-Tungsten Belt, Yukon, Canada. *In: Fifth Hutton Symposium on the Origin of Granites and Related Rocks*, Transactions of the Royal Society of Edinburgh: Earth Sciences.
- Irving, E., 1985. Whence British Columbia? *Nature*, vol. 314, p. 673-674.
- Irving, E. and Wynne, P.J. 1992. Chapter 3, Paleomagnetism: review and tectonic implications. *In: Geology of the Cordilleran Orogen in Canada*, H. Gabrielse and C.J. Yorath (eds.), Geological Survey of Canada, *Geology of Canada*, no. 4, p. 63-86.

- Irving, E., Wynne, P.J., Thorkelson, D.J. and Schiarizza, P., 1996. Large (1000 to 4000 km) northward movements of tectonic domains in the northern Cordillera, 83 to 45 Ma. *Journal of Geophysical Research*, vol. 101, p. 17901-17916.
- Ishihara, S., 1981. The granitoid series and mineralization. *Economic Geology*, 75th Anniversary Volume, p. 458-484.
- Jaeger, J.C., 1964. Thermal effects of intrusions. *Reviews in Geophysics*, vol. 2, p. 443-466.
- Kirschvink, J.L., 1980. The least squares line and plane and the analysis of paleomagnetic data. *Geophysical Journal of the Royal Astronomical Society*, vol. 62, p. 699-718.
- Lewis, T.J., Hyndman, R.D. and Flueck, P., 2002. Thermal controls on present tectonics in the northern Canadian Cordillera. *Lithoprobe Report* 82, p. 15-16.
- Lowe, C., Horner, R.B., Mortensen, J.K., Johnston, S.T. and Roots, C.F., 1994. New geophysical data from the northern Cordillera: Preliminary interpretations and implications for the tectonics and deep geology. *Canadian Journal of Earth Sciences*, vol. 31, p. 891-904.
- Mair, J.L., Hart, C.J.R. and Stephens, J., in press, 2006. Deformation history of the western Selwyn Basin, Yukon, Canada: Implications for orogen evolution and mid-Cretaceous magmatism. *Geological Association of America*, vol. 118.
- Mazzotti, S. and Hyndman, R.D., 2002. Yakutat collision and strain transfer across the northern Canadian Cordillera. *Geology*, vol. 30, p. 495-498.
- McFadden, P.L. and Lowes, F.J., 1981. The discrimination of mean directions drawn from Fisher distributions. *Geophysical Journal of the Royal Astronomical Society*, vol. 67, p. 19-33.
- McMechan, M.E., Thompson, R.I., Cook, D.G., Gabrielse, H. and Yorath, C.J., 1992. Structural Styles: Foreland Belt. *In: Geology of the Cordilleran Orogen in Canada*, H. Gabrielse and C.J. Yorath (eds.), Geological Survey of Canada, *Geology of Canada*, no. 4, p. 634-650.
- Merrill, R.T. and McElhinny, M.W., 1983. The Earth's Magnetic Field: Its History, Origin and Planetary Perspective. Academic Press, London, U.K., 401 p.
- Murphy, D.C., 1997. Geology of the McQuesten River region, northern McQuesten and Mayo map areas, Yukon Territory (115P/14, 15, 16; 105M/13, 14) Exploration and Geological Services Division, Yukon Region, Indian and Northern Affairs Canada, *Bulletin* 6, 122 p.
- Murphy, D.C. and Mortensen, J.K., 2003. Late Paleozoic and Mesozoic features constrain displacement on Tintina Fault and limit large-scale orogen-parallel displacement in the Northern Cordillera. *In: Geological Association of Canada/ Mineralogical Association of Canada Joint Annual Meeting, Vancouver, BC, Program with Abstracts*, vol. 28, CD-ROM.
- Opdyke, N.D. and Channell, J.E.T., 1996. *Magnetic Stratigraphy*. Academic Press Inc., San Diego, U.S.A., 364 p.
- Poulton, T.P. and Tempelman-Kluit, D.J., 1982. Recent discoveries of Jurassic fossils in the Lower Schist Division of central Yukon. *In: Current Research, Part C*, Geological Survey of Canada, Paper 82-1C, p. 91-94.
- Ricketts, B.D., 1988. The Monster Formation: A coastal fan system of Late Cretaceous age, Yukon Territory. Geological Survey of Canada, Paper 86-14, p. 27
- Roots, C.F. and Thompson, R.I., 1992. Long-lived basement weak zones and their role in extensional magmatism in the Ogilvie Mountains, Yukon Territory. *In: Basement Tectonics 8: Characterization and Comparison of Ancient and Mesozoic Continental Margins*, M.J. Bartholomew, D.W. Hyndman, D.W. Mogk and R. Mason (eds.), Kluwer Academic Publishers, Dordrecht, The Netherlands, p. 359-372.
- Snyder, D.B., Clowes, R.M., Cook, F.A., Erdmer, P., Evanchick, C.A., van der Velden, A.J. and Hall, K.W., 2002. Proterozoic prism arrests suspect terranes: Insights in the ancient Cordilleran margin from seismic reflection data. *GSA Today*, vol. 12, no. 10, p. 4-10.
- Souther, J.G. and Yorath, C.J., 1992. Neogene assemblages. *In: Geology of the Cordilleran Orogeny in Canada*, H. Gabrielse and C.D. Yorath (eds.), Geological Survey of Canada, no. 4, p. 375-401.
- Sweeney, J.F., Stephenson, R.A., Currie, R.G. and DeLaurier, J.M., 1992. Crustal Geophysics. *In: Geology of the Cordilleran Orogeny of Canada*, H. Gabrielse and C.D. Yorath (eds.), Geological Survey of Canada, no. 4, p. 39-59.

- Symons, D.T.A. and Cioppa, M.T., 2000. Crossover plots: A useful method for displaying SIRM data in paleomagnetism. *Geophysical Research Letters*, vol. 27, p. 1779-1782.
- Symons, D.T.A., Harris, M.J., Gabites, J.E. and Hart, C.J.R., 2000. Eocene (51 Ma) end to northward translation of the Coast Plutonic Complex: Paleomagnetism and K-Ar dating of the White Pass dykes. *Tectonophysics*, vol. 326, p. 93-109.
- Symons, D.T.A., Erdmer, P. and McCausland, P.J.A., 2003. New 42 Ma cratonic North American paleomagnetic pole from the Yukon shows post-Eocene mobility of the Canadian Cordilleran terranes. *Canadian Journal of Earth Sciences*, vol. 40, p. 1321-1334.
- Symons, D.T.A., Harris, M.J., McCausland, P.J.A., Blackburn, W.H. and Hart, C.J.R., 2005. Mesozoic-Cenozoic paleomagnetism of the Intermontane and Yukon-Tanana Terranes, Canadian Cordillera. *Canadian Journal of Earth Sciences*, vol. 42, p. 1163-1185.
- Tempelman-Kluit, D.J., 1970. Stratigraphy and structure of the 'Keno Hill Quartzite' in Tombstone River-Upper Klondyke River map areas, Yukon Territory (116B/7,B/8). *Geological Survey of Canada, Bulletin 180*, 103 p., 2 maps at 1:506 880 and 1:63 360 scale.
- Tempelman-Kluit, D.J. and 16 other authors, 1992. Structural styles: Omineca Belt. *In: Geology of the Cordilleran Orogen in Canada*, H. Gabrielse and C.D. Yorath (eds.), *Geological Survey of Canada, Geology of Canada*, no. 4, p. 603-634.
- Thompson, R.I., 1995. Geological Compilation (1:250 000) map of the Dawson map area (116B, C) (northeast of the Tintina Trench). *Geological Survey of Canada, Open File*, 3223.
- Thompson, R.I., Roots, C.F. and Mustard, P., 1992. Geology of the Dawson map area (116B,C) (northeast of the Tintina Trench). *Geological Survey of Canada, Open File 2849*, 12 selected 1:50 000 map sheets plus legend.
- Yorath, C.J., 1992. Upper Jurassic to Paleogene assemblages. *In: Geology of the Cordilleran Orogen in Canada*, H. Gabrielse and C.D. Yorath (eds.), *Geological Survey of Canada, Geology of Canada*, no. 4, p. 331-371.
- Zijderveld, J.D.A., 1967. A.C. demagnetization of rocks: analysis of results. *In: Methods in Paleomagnetism: Amsterdam*, D.W. Collinson, K.M. Creer and S.K. Runcorn (eds.), Elsevier, Amsterdam, p. 254-286.

Structural constraints for oil and gas assessment in the Whitehorse Trough: New results from seismic profiling¹

Donald White

Geological Survey of Canada, Central Canada Division

Maurice Colpron²

Yukon Geological Survey

Grant Buffett and Brian Roberts

Geological Survey of Canada, Central Canada Division

White, D., Colpron, M., Buffett, G. and Roberts, B., 2006. Structural constraints for oil and gas assessment in the Whitehorse Trough: New results from seismic profiling. *In: Yukon Exploration and Geology 2005*, D.S. Emond, G.D. Bradshaw, L.L. Lewis and L.H. Weston (eds.), Yukon Geological Survey, p. 315-323.

ABSTRACT

The Whitehorse Trough is a Mesozoic sedimentary basin in south-central Yukon that has been identified as an immature, gas-prone basin, based on a limited geoscience database. A total of 170 km of regional, multi-channel, multi-component Vibroseis seismic reflection data were acquired in 2004 across the northern Whitehorse Trough in order to improve understanding of its structural architecture. The shallow seismic images appear to depict broad antiformal and synformal structures, truncated by relatively steep faults. Strata interpreted as the Lewes River and Laberge groups seem to attain a maximum thickness of 6000-7000 m toward the west side of the Trough, with interpreted Laberge Group accounting for up to ~3000 m of this total. Maximum vertical relief of the structures is ~4000 m.

RÉSUMÉ

Le bassin de Whitehorse est un bassin sédimentaire d'âge Mésozoïque dans le centre-sud du Yukon. Il fût identifié, sur la base de données géoscientifiques limitées, comme étant un bassin immature ayant un potentiel pour le gaz naturel. Des données de levé sismique Vibroseis régional multicanal et multicomposante ont été acquises sur 170 kilomètres en 2004 sur la partie septentrionale de la cuvette de Whitehorse, dans le but d'améliorer notre compréhension de son architecture structurale. Les images sismiques à faible profondeur semblent révéler des structures antiformes et synformes de grande amplitude recoupées par des failles de fort pendage. Les strates interprétées comme étant les groupes de Lewes River et de Laberge atteignent une épaisseur maximale de 6000 à 7000 mètres vers le côté ouest du bassin, le Groupe de Laberge représentant jusqu'à 3000 mètres de cette épaisseur totale. L'extension maximale de ces structures suivant la verticale est d'environ 4000 mètres.

¹GSC Contribution No. 2005543

²maurice.colpron@gov.yk.ca

INTRODUCTION

The Whitehorse Trough is an elongated, northwest-trending Mesozoic marine sedimentary basin which extends some 650 km from just north of Carmacks, Yukon, to near Dease Lake, British Columbia (Fig. 1). It originated as a forearc basin in the Middle to Late Triassic, adjacent to the emerging Lewes River Arc, and had received more than 7000 m of clastic deposits by Middle Jurassic time (e.g., Wheeler, 1961; Tempelman-Kluit, 1979). It is underlain by late Paleozoic and early Mesozoic arc volcanic rocks of Stikinia and is structurally overlain, in southern Yukon and northern British Columbia, by the oceanic Cache Creek Terrane (Fig. 1). The Whitehorse Trough overlies Stikinia at its northern apex, where it is bounded on three sides by polydeformed and metamorphosed mid- to late Paleozoic rocks of the Yukon-Tanana Terrane.

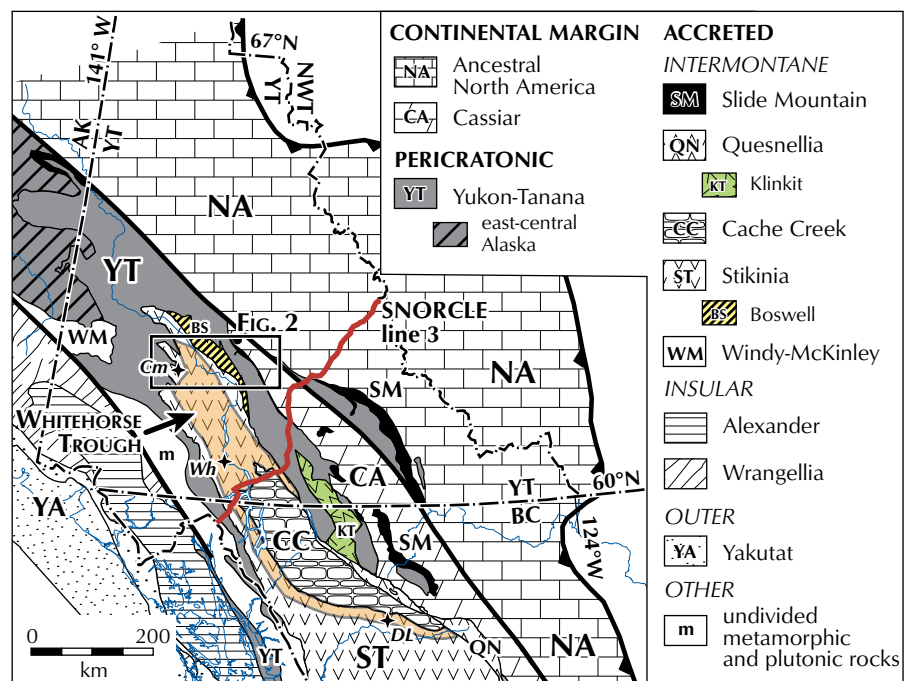
The Whitehorse Trough has been identified as an immature, gas-prone basin in which potential source rocks, reservoirs and seals occur (National Energy Board, 2001). Potential for some 7.3 trillion cubic feet (Tcf) (210 billion m³) of gas, and possibly some oil, is estimated for the basin, with 2.6 to 4.8 Tcf (74 to 140 billion m³) in Yukon (K. Ozadetz, pers. comm., 2004). Structural traps associated with clastic or carbonate reservoirs (Lewes River and Laberge groups) are proposed as having significant hydrocarbon potential with surface-defined anticlines posing the best primary drilling targets (National

Energy Board, 2001). However, current assessments of hydrocarbon potential in the Whitehorse Trough rely on limited stratigraphic studies and are based on conceptual plays. No private seismic surveys or wells have been completed in this region. A recent Lithoprobe seismic survey crosses the central part of Whitehorse Trough near the Yukon-British Columbia boundary (SNORCLE line 3, Fig. 1; Cook *et al.*, 2004) and provides an interpretation of the crustal structure in the area. However, the Lithoprobe survey was designed primarily to image deep crustal features and offers limited information about the upper crust, and thus is of little use for hydrocarbon potential assessment. In 2004, the Yukon Geological Survey and Geological Survey of Canada commissioned a regional, multi-channel, multi-component Vibroseis seismic reflection survey across the northern part of Whitehorse Trough and into adjacent terranes (Fig. 2), with the aim of enhancing the geoscience database of the area for use in future hydrocarbon potential assessments. The survey comprises two seismic profiles, totaling 170 km in length, acquired along the Robert Campbell and North Klondike highways (Fig. 2). An initial interpretation of the shallow part of these crustal sections is presented here.

GEOLOGICAL SETTING

The Canadian Cordillera consists of a collage of terranes that were accreted to the western margin of the North American craton between late Paleozoic and early

Figure 1. Terrane map of Yukon and adjacent northern British Columbia. The grey-shaded area in northern Stikinia indicates regional distribution of the Whitehorse Trough. Cm = Carmacks, DL = Dease Lake, Wh = Whitehorse.



Cenozoic time (Coney *et al.*, 1980; Gabrielse *et al.*, 1991; Price and Monger, 2000 and references therein). The largest of these terranes, Stikinia, comprises Late Devonian to Middle Jurassic volcanic and sedimentary strata, as well as comagmatic plutonic rocks (Monger *et al.*, 1991). Paleozoic assemblages are mostly known in northern British Columbia (e.g., Logan *et al.*, 2000). The northern portion of Stikinia is composed of Upper Triassic arc volcanic and sedimentary rocks of the Lewes River Group and Lower to Middle Jurassic sedimentary strata of the Laberge Group (e.g., Wheeler, 1961; Fig. 3). Sedimentary facies of the Lewes River (Aksala formation) and Laberge groups define the

Whitehorse Trough in Yukon (e.g., Wheeler, 1961; Hart, 1997). The Lewes River Group at its base comprises calc-alkaline basalts, andesites and agglomerates of the Povoas formation (Tempelman-Kluit, 1984; Hart, 1997). The Povoas locally overlies Paleozoic greenstones of the Takhini assemblage west of Whitehorse (Hart, 1997). The Povoas is conformably overlain by heterogeneous clastic strata (mainly sandstone, greywacke and argillite), limestone and minor conglomerate of the Aksala formation (Tempelman-Kluit, 1984; Hart, 1997).

The Laberge Group consists of conglomerate, sandstone, siltstone, argillite and tuff. In the northern Whitehorse Trough, near Carmacks (Fig. 2), the Laberge Group

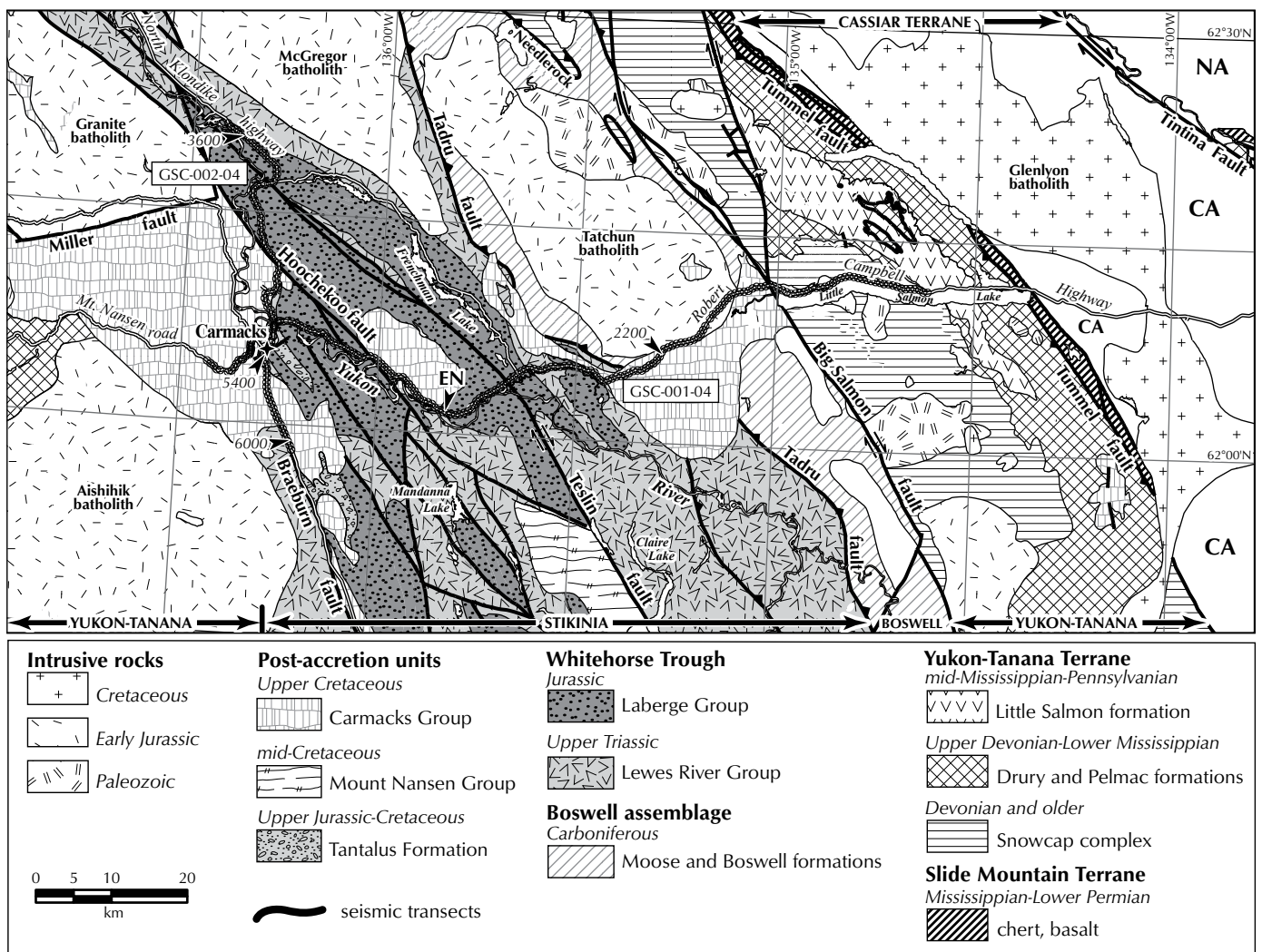


Figure 2. Geological map of the northern Whitehorse Trough and surrounding region compiled from Tempelman-Kluit (1984) and Colpron *et al.* (2002). Heavy black lines show location of seismic transects along the Robert Campbell (GSC-001-04, Line 1) and North Klondike highways (GSC-002-04, Line 2). Numbers and arrows along transects indicate station numbers near end-points for parts of the sections shown in Figure 4. “EN” points to location of Eagle’s Nest Bluff along Line 1. NA = Ancestral North America; CA = Cassiar Terrane.

slip fault with up to 56 km of Late Cretaceous(?) dextral displacement (Colpron *et al.*, 2003; Fig. 2).

The Yukon-Tanana Terrane comprises a metasedimentary basement complex (Snowcap complex), intruded by Mississippian plutons, and unconformably overlain by Carboniferous arc-derived metaclastic rocks (Drury and Pelmac formations) and mafic metavolcanic rocks (Little Salmon formation). To the east, Yukon-Tanana Terrane is juxtaposed with Cassiar Terrane along the Tummel fault, a ~3 km-wide zone of imbricate fault slices of Slide Mountain Terrane (chert, basalt, serpentinite) and synorogenic metaclastic rocks (Colpron *et al.*, 2005; Fig. 2).

Rocks of Yukon-Tanana Terrane, Boswell assemblage and Lewes River Group are intruded by large Early Jurassic batholiths (Fig. 2) that are, in part, coeval with deposition of Laberge Group strata in the Whitehorse Trough. Cretaceous plutons intrude rocks of Stikinia near Whitehorse, but are absent from the northern Whitehorse Trough (Gordey and Makepeace, 2001). In this region, Cretaceous plutons are mainly restricted to Yukon-Tanana and Cassiar terranes (Fig. 2).

Rocks of the northern Whitehorse Trough are extensively faulted and folded by broad, open to southwest-vergent folds (Fig. 2; Tempelman-Kluit, 1984). The overall structure is that of a broad anticlinorium, occupied by strata of the Lewes River Group, flanked by two synclinoria of the Laberge Group. These structures are dissected by an array of brittle faults with a complex kinematic history.

Basalt and agglomerate of the Upper Cretaceous Carmacks Group overlie all terranes along the transect area (Fig. 2; Tempelman-Kluit, 1984). The Carmacks Group occurs as a series of erosional remnants, along the survey transect, which are typically only a few hundred metres thick, with the thickest accumulation (~800 m) west of Carmacks. The Carmacks Group clearly postdates some of the major faults in the area (Tadru and Braeburn faults, Fig. 2), but is possibly affected by late brittle deformation along some of the other faults (e.g., Big Salmon, Hoochekoo and Miller faults).

SURVEY DESIGN

The seismic survey was designed to transect three distinct geological terranes: the Yukon-Tanana Terrane, the Boswell assemblage, and Stikinia, which envelop the Whitehorse Trough. Two regional profiles were acquired in the winter, 2004: Line GSC-001-04 (Line 1) is a 117-km

east-west transect across the northern Whitehorse Trough, along the Robert Campbell Highway, beginning at the midpoint of Little Salmon Lake, and ending 13 km west of the town of Carmacks on Mt. Nansen road (Fig. 2). This line transects all terranes, generally at a high angle to the regional structures. It starts well to the east of the Whitehorse Trough in order to test whether Mesozoic strata extend in the subsurface beneath Paleozoic rocks of the Boswell assemblage and Yukon-Tanana Terrane. Line GSC-002-04 (Line 2) is 53 km in length, starting 35 km north of Carmacks and ending 18 km south of the town, entirely along the western edge of the Whitehorse Trough on the North Klondike Highway (Fig. 2). A 2.64-km section on the North Klondike Highway is common to both lines. Data recording parameters were chosen to obtain optimal resolution in the upper 5 km, while allowing sufficient depth penetration to image crustal-scale features.

RECORDING PARAMETERS

During the survey, standard operating procedures were followed which precluded vibrating in the immediate vicinity of buildings, wells or other infrastructure. While traversing the town of Carmacks, data receivers were deployed to record reflections from vibration points located outside of town, but no vibration operations were conducted through the town. This expectantly reduced data quality somewhat near Carmacks. However, due to low population density this approach was necessary only once per line and did not affect the overall data acquisition integrity. Acquisition parameters are summarized in Table 1, with Table 2 providing the sequence of processes applied to obtain the seismic images presented here. In addition to the processes listed in Table 2, tests of prestack partial migration (or dip-moveout processing) and prestack time migration were made but without significant improvement of the seismic images.

PRELIMINARY INTERPRETATION

The preliminary interpretation of the seismic reflection profiles presented here focuses on the shallow structures of the Whitehorse Trough (upper 3 seconds (s); Fig. 4). An example of the migrated seismic data for the centre of the Whitehorse Trough is shown in Figure 5, overlain with a preliminary geological interpretation. Summary interpretation schematics for Lines 1 and 2 are included in Figure 4.

Table 1. Data acquisition parameters

Field crew	Kinetex Inc., Calgary.
Date	February-April, 2004
Clients	Geological Survey of Canada/ Yukon Geological Survey
Instrumentation	I/O Vectorseis® System IV
Traces/record	600
Record length	33 seconds (extended correlation)
Sample rate	2 ms
Anti-alias filter	½ Nyquist
Nominal CDP fold	100
Vibroseis source parameters	
Source type	4 Vibrators (IVI Y2400 Buggy Mount)
Source array	4 Vibrators in-line
Pattern length	100 m
VP interval	60 m
# sweeps/VP	6 or 10 (with 3 vibrators operational)
Sweep length	24 seconds
Sweep type	Linear upsweep
Sweep frequency	10-84 Hz
Receiver array parameters	
Group interval	20 m
Geophones/group	1 (3C Sensor Buried)

Table 2. Data processing flow

Data preparation	Diversity stacking of unstacked sweeps Vibroseis self-tapering extended correlation Crooked-line geometry application First breaks manually picked
Pre-stack processing	AGC: 500ms mean window Top mute application Velocity analysis: semblance and constant velocity stack Refraction statics correction: final datum elevation: 750 m, replacement velocity: 4800 m/s Normal moveout correction: Stretch mute tolerance of 50% Residual statics correction CDP Stack: Method for trace summing: mean
Post-stack processing	Phase-shift migration Semblance smoothing Amplitude threshold applied (values < 1.5*RMS are set to zero)

Interpretation of the seismic lines is complicated by the variable orientation of the profiles relative to the regional strike of the regional geology in this area which is approximately southeast. Recognizing this, it is important to keep in mind that the dips observed on the seismic sections are apparent dips and that changes in apparent attitude may in some cases be caused by changes in the direction of the seismic lines.

The interpretations presented in Figure 4 hinge on observations made along the central part of Line 1 (Fig. 5) where the seismic data correlate very well with observed surface geology. A seismically defined antiform corresponds with a geologically mapped anticline, and a highly reflective package projects up-dip to exposed Upper Triassic limestone of the Lewes River Group at Eagle's Nest bluff. The reflection fabrics observed in the upper 5-6 km are interpreted as primarily representing original stratigraphic layering as rocks of the Whitehorse Trough have experienced relatively low-grade metamorphism. Based on correlation with outcrops (along the central part of Line 1 and the northern end of Line 2), and the more diverse composition of the Lewes River Group relative to the Laberge Group, as a general rule, the zones of higher subsurface reflectivity are interpreted as Lewes River Group (Fig. 5). The shallow seismic images depict broad antiformal and synformal structures punctuated by relatively steep faults where reflectivity is abruptly truncated (e.g., Teslin fault in Fig. 5). The vertical extent of interpreted strata of Lewes River and Laberge groups attains a maximum thickness of 6000-7000 m toward the west side of the Trough, with interpreted Laberge Group accounting for up to ~3000 m of this total. Maximum vertical relief is ~4000 m as indicated by the amplitude of the interpreted fold structures, with less structural relief observed along-strike on Line 2 (Fig. 4).

Several prominent fault zones within or along the boundaries of the Whitehorse Trough are crossed along Lines 1 and 2, including the Tadru, Teslin, Hoochekoo and Braeburn faults. These faults have variable expression on the seismic sections. The Tadru fault does not have a distinct shallow expression, but the interpreted location of this fault in the seismic data is based primarily on the surface projection of a prominent east-dipping zone of reflectivity that can be followed to mid-crustal depths (not shown). The Teslin fault is identified by truncation of a prominent package of west-dipping reflections (Fig. 5), defining a relatively steep fault trace to a two-way traveltime of ~2 s. At greater depth, it is interpreted to dip

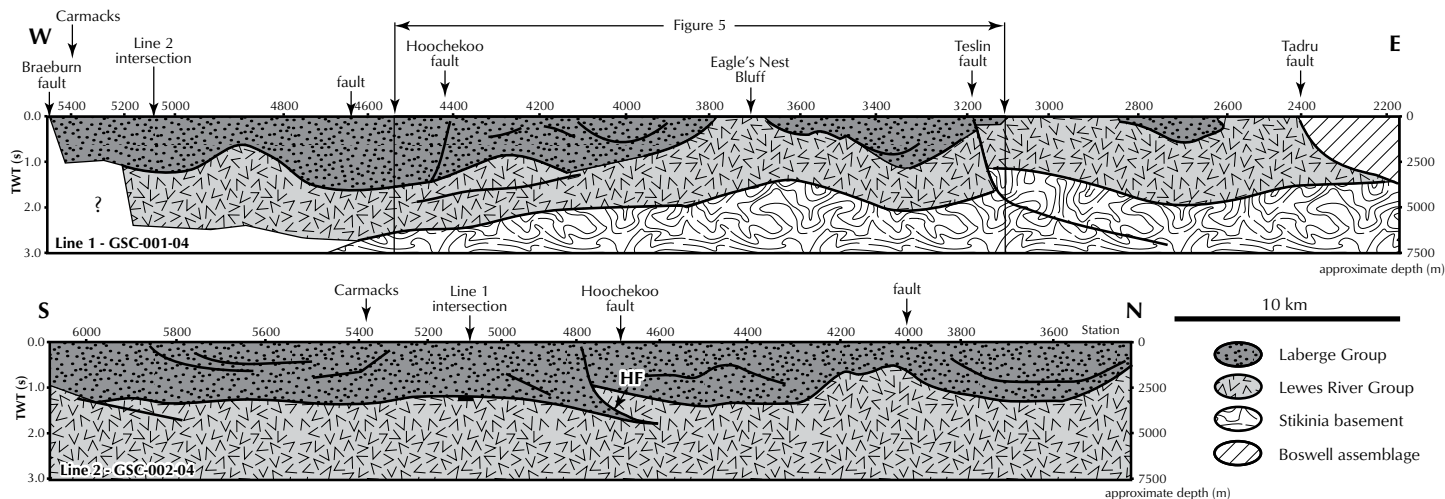


Figure 4. Schematic interpretations for Lines 1 and 2. The surface locations of major faults are indicated. Also shown are the locations of the town of Carmacks, Eagle's Nest Bluff and point of intersection of the two lines. Detailed image for the central part of Line 1 is shown in Figure 5. "HF" on Line 2 points to subsurface expression of the Hoochekoo fault. Note that the depth of the bottom of the Lewes River Group along Line 2 is uncertain, although it is shown continuing to 7500 m depth. TWT = two-way travelttime (in seconds).

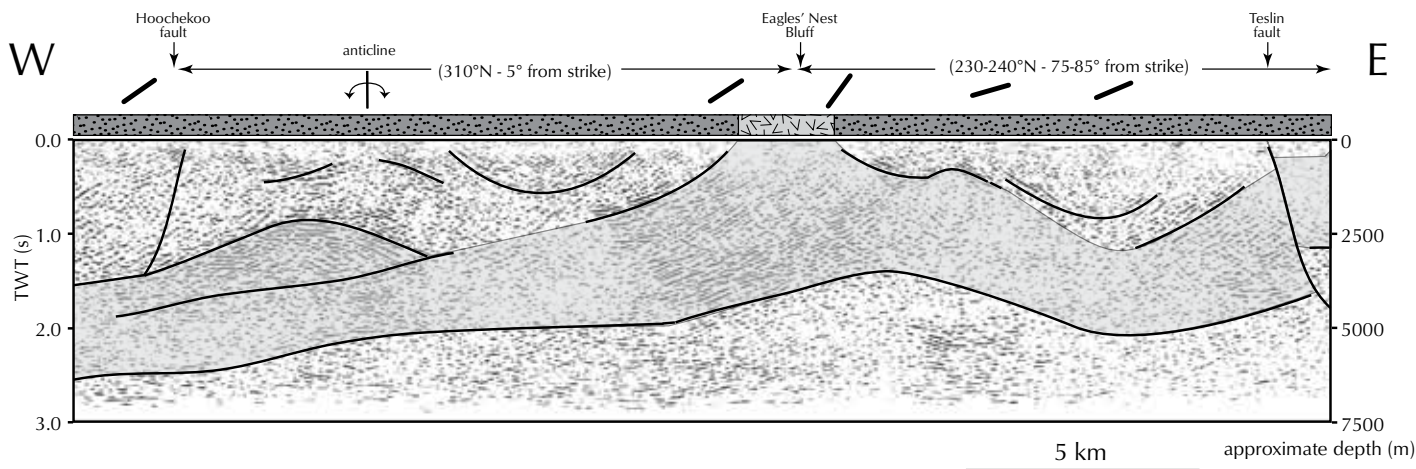


Figure 5. Preliminary interpretation of migrated seismic data from the central segment of Line 1. Indicated along the top of the plot are the following: 1) the distribution of rock types as mapped at the surface (patterns correspond to legend in Fig. 4); 2) apparent dip of bedding measured on outcrops near the profile (solid bars); 3) orientation of the seismic line with respect to regional strike of structures in Whitehorse Trough (~315°N); 4) surface location of major faults; 5) surface projection of an anticlinal structure mapped north of the profile (Tempelman-Kluit, 1984); and 6) location of Eagle's Nest Bluff, where Upper Triassic limestone of the Lewes River Group is exposed. Note that the road takes a 90° bend near the bluff (Fig. 2). Grey-shaded area in subsurface shows distribution of interpreted Lewes River Group extrapolated from surface exposure. The approximate depth scale indicated on the right vertical axis assumes a mean subsurface seismic velocity of 5000 m/s. TWT = two-way travelttime (in seconds).

eastward to at least the middle crust and perhaps deeper (Fig. 4). The interpreted subsurface trajectory of the Hoochekoo fault is based primarily on the image from Line 2 (not shown) where a prominent zone of reflectivity projects at the surface to near the location of the fault as indicated by the surface geology (Figs. 2, 4). This fault extends to 2 s two-way traveltime where it appears to sole out. It should be noted that the seismic interpretation of Line 2 suggests that the surface location of the Hoochekoo fault is actually several kilometres south of its currently mapped position (Fig. 4). The nature of the Braeburn fault is not obvious in the seismic data, due largely to the crooked nature of the profiles where this fault is crossed.

SUMMARY

Preliminary images from the Whitehorse Trough seismic survey provide a first look at the crustal architecture of the region. Preliminary interpretation of the shallow seismic images indicates broad antiformal and synformal structures truncated by relatively steep faults. Interpreted strata of the Lewes River and Laberge groups attain a maximum thickness of 6000-7000 m toward the west side of the Trough, with interpreted Laberge Group accounting for up to ~3000 m of this total. Maximum vertical relief of the structures is ~4000 m. Interpreted results will be studied against current geological models to assess the hydrocarbon potential of the Whitehorse Trough and advance the understanding of the tectonic history and structural framework of central Yukon.

ACKNOWLEDGEMENTS

We thank Grant Abbott, Steve Gordey, Craig Hart, Steve Israel, Larry Lane, Grant Lowey, Don Murphy, Kirk Ozadetz, Lee Pigage and Derek Thorkelson for input into this preliminary interpretation. Gilles Bellefleur who helped supervise the seismic acquisition crew is also thanked. The support of the local population and workforce during survey acquisition is greatly appreciated. Steve Piercey provided comments on an early version of the manuscript.

REFERENCES

- Bostock, H.S., 1936. Carmacks district, Yukon. Geological Survey of Canada, Memoir 189, 67 p.
- Colpron, M., Murphy, D.C., Nelson, J.L., Roots, C.F., Gladwin, K., Gordey, S.P., Abbott, G. and Lipovsky, P.S., 2002. Preliminary geological map of Glenlyon (105L/1-7,11-14) and northeast Carmacks (115I/9,16) areas, Yukon Territory (1:125 000 scale). Exploration and Geological Services Division, Yukon Region, Indian and Northern Affairs Canada, Open File 2002-9.
- Colpron, M., Murphy, D.C., Nelson, J.L., Roots, C.F., Gladwin, K., Gordey, S.P. and Abbott, J.G., 2003. Yukon Targeted Geoscience Initiative, Part 1: Results of accelerated bedrock mapping in Glenlyon (105L/1-7, 11-14) and northeast Carmacks (115I/9,16) areas, central Yukon. *In: Yukon Exploration and Geology 2002*, D.S. Emond and L.L. Lewis (eds.), Exploration and Geological Services Division, Yukon Region, Indian and Northern Affairs Canada, p. 85-108.
- Colpron, M., Gladwin, K., Johnston, S.T., Mortensen, J.K. and Gehrels, G.E., 2005. Geology and juxtaposition history of Yukon-Tanana, Slide Mountain and Cassiar terranes in the Glenlyon area of central Yukon. *Canadian Journal of Earth Sciences*, vol. 42, p. 1431-1448.
- Coney, P.J., Jones, D.L. and Monger, J.W.H., 1980. Cordilleran suspect terranes. *Nature*, vol. 288, p. 329-333.
- Cook, F.A., Clowes, R.M., Snyder, D.B., van der Velden, A.J., Hall, K.W., Erdmer, P. and Evenchick, C.A., 2004. Precambrian crust beneath the Mesozoic northern Canadian Cordillera discovered by Lithoprobe seismic reflection profiling. *Tectonics*, vol. 23, p. 18-19.
- Gabrielse, H., Monger, J.W.H., Wheeler, J.O. and Yorath, C.J., 1991. Part A. Morphogeological belts, tectonic assemblages and terranes (Chapter 2). *In: Geology of the Cordilleran Orogen in Canada*, H. Gabrielse and C.J. Yorath (eds.). Geological Survey of Canada, *Geology of Canada*, no. 4, p. 15-28.
- Gordey, S.P. and Makepeace, A.J. (compilers), 2001. Bedrock geology, Yukon Territory. Geological Survey of Canada, Open File 3754, 1:1 000 000 scale.

- Hart, C.J.R., 1997. A transect across northern Stikinia: Geology of the northern Whitehorse map area, southern Yukon Territory (105D/13-16). Exploration and Geological Services Division, Yukon Region, Indian and Northern Affairs Canada, Bulletin 8, 112 p.
- Logan, J.M., Drobe, J.R. and McClelland, W.C., 2000. Geology of the Forrest Kerr–Mess Creek area, northwestern British Columbia (NTS 104B/10, 15 & 104G/2 & 7W). B.C. Ministry of Energy and Mines, Bulletin 104, 164 p.
- Long, D.G.F., 2005. Sedimentology and hydrocarbon potential of fluvial strata in the Tantalus and Aksala formations, northern Whitehorse Trough, Yukon. *In: Yukon Exploration and Geology 2004*, D.S. Emond, L.L. Lewis and G. Bradshaw (eds.), Yukon Geological Survey, p. 167-176.
- Lowey, G.W., 2004. Preliminary lithostratigraphy of the Laberge Group (Jurassic), south-central Yukon: Implications concerning the petroleum potential of the Whitehorse Trough. *In: Yukon Exploration and Geology 2003*, D.S. Emond and L.L. Lewis (eds.), Yukon Geological Survey, p. 129-142.
- Lowey, G.W., 2005. Sedimentology, stratigraphy and source rock potential of the Richthofen formation (Jurassic), northern Whitehorse Trough, Yukon. *In: Yukon Exploration and Geology 2004*, D.S. Emond, L.L. Lewis and G. Bradshaw (eds.), Yukon Geological Survey, p. 177-191.
- Monger, J.W.H., Wheeler, J.O., Tipper, H.W., Gabrielse, H., Harms, T., Struik, L.C., Campbell, R.B., Dodds, C.J., Gehrels, G.E. and O'Brien, J., 1991. Part B. Cordilleran terranes, Upper Devonian to Middle Jurassic assemblages (Chapter 8). *In: Geology of the Cordilleran orogen in Canada*, H. Gabrielse and C.J. Yorath (eds.), Geological Survey of Canada, Geology of Canada, no. 4, p. 281-327.
- National Energy Board, 2001. Petroleum Resource Assessment of the Whitehorse Trough, Yukon Territory, Canada. Oil and Gas Resources Branch, Department of Economic Development, Government of Yukon, 59 p.
- Price, R.A. and Monger, J.W.H., 2000. A transect of the southern Canadian Cordillera from Calgary to Vancouver. Geological Association of Canada, Cordilleran Section, Field Trip Guidebook, 164 p.
- Simard, R.-L., 2003. Geological map of southern Semenof Hills (part of NTS 105E/1,7,8), south-central Yukon (1:50 000 scale). Yukon Geological Survey, Open File 2003-12.
- Tempelman-Kluit, D. J., 1979. Transported cataclasite, ophiolite and granodiorite in Yukon: Evidence of Arc-Continent Collision. Geological Survey of Canada, Paper 79-14, 27 p.
- Tempelman-Kluit, D. J., 1984. Geology, Laberge (105E) and Carmacks (105I), Yukon Territory. Geological Survey of Canada, Open File 1101, 1:250 000 scale.
- Wheeler, J.O., 1961. Whitehorse map-area, Yukon Territory, 105D. Geological Survey of Canada, Memoir 312, 156 p.

Sediment-hosted disseminated gold occurrence, northeast Mayo Lake area

*Gregory Lynch*¹
Consulting Geologist

Lynch, G., 2006. Sediment-hosted disseminated gold occurrence, northeast Mayo Lake area. In: Yukon Exploration and Geology 2005, D.S. Emond, G.D. Bradshaw, L.L. Lewis and L.H. Weston (eds.), Yukon Geological Survey, p. 327-339.

ABSTRACT

Low to moderate levels of gold are widely distributed within a distinct member of the Mississippian Keno Hill Quartzite northeast of Mayo Lake, demonstrating characteristics of sediment-hosted disseminated gold deposits. Alteration is pervasively developed within a 20-m-thick, moderately dipping quartzite interval that can be traced along strike for 4 km. The unit is distinct in texture and appearance due to the effects of hydrothermal alteration. The altered sandstone is highly porous due to secondary leaching (decalcification), producing a friable unit. Also striking is the bleached white appearance (decarbonatation), which contrasts with the dark grey to black of unaltered graphitic quartzite. Sericite and illite are widespread secondary products of the alteration, and trace amounts of pyrite have been largely oxidized into rusty streaks. Abundant, regular, steep, northeast-striking, vuggy quartz veins are stratabound to the porous interval along its entire length – likely resulting from *in-situ* hydrofracturing due to elevated pore fluid pressure.

RÉSUMÉ

Des concentrations en or faibles à modérées sont largement répandues à l'intérieur d'un membre distinct du Quartzite de Keno Hill du Mississipien, au nord-est du lac Mayo, qui présente des propriétés propres à des dépôts d'or disséminés dans des sédiments. L'altération est répandue à l'intérieur d'une couche de quartzite modérément inclinée d'une épaisseur de 20 m qui peut être suivie sur une distance de 4 km. L'unité est distincte en texture et en apparence en raison des effets de l'altération hydrothermale. Le grès altéré est hautement perméable en raison d'un lessivage secondaire (décalcification), résultant en une unité friable. L'aspect blanc décoloré (décarbonatation) est frappant et contraste avec la couleur gris-sombre à noire du quartzite graphitique inaltéré. La séricite et l'illite, issues de l'altération, sont des produits secondaires largement répandus, et des quantités traces de pyrite ont été en grande partie oxydées en traînées rouillées. D'abondantes et régulières veines de quartz vacuolaire fortement inclinées au nord-est sont stratiformes dans l'intervalle perméable sur toute sa longueur – découlant vraisemblablement de la fracturation hydraulique *in situ* due à la pression interstitielle élevée des fluides.

¹5839 Dalcastle Drive, NW, Calgary, Alberta, Canada T3A 1Z2, tglynch@telusplanet.net

INTRODUCTION

The study area is situated 20 km southeast of the Keno Hill mining district (Fig. 1), along the northern fringe of the Selwyn Basin, within map sheet 105 M/15 (Green, 1971). Distinct gold-bearing altered members of the Mississippian Keno Hill Quartzite unit are the subject of this investigation. Mapping and sampling were conducted northeast of Mayo Lake (105 M/15) at a scale of 1:10 000 in order to trace the key altered units along 4 km of strike of exposed bedrock. Two detailed maps are presented. Samples of both altered host rock and vein material were taken; assay results are tabulated and discussed within the paper. Although the gold assays returned modest results, the values are distinctly anomalous.

Recently, in considering the regional setting of the Selwyn Basin and its associated plutonic rocks, it has been suggested that sediment-hosted disseminated gold deposits may be prospective in this area of the Yukon (Poulsen et al., 1997; Roots, 1997). However, an important

class of gold vein deposits has now been defined for this region which relate to Cretaceous granitic bodies, comprising the Tombstone Gold Belt (Stephens et al., 2004). In addition, zoned, large-scale polymetallic hydrothermal vein systems, such as at Keno Hill and Dublin Gulch, occur within the district (Boyle, 1965; Lynch, 1989a,b).

Sediment-hosted disseminated gold deposits comprise a diverse class of deposits whose characteristics continue to be refined world-wide as research and exploration progress (Bagby and Berger, 1985; Arehart, 1996; Ilchick and Barton, 1997; Peters, 2004). Most famously, in the Carlin district of Nevada, deposits are typically hosted within Paleozoic-aged impure silty carbonaceous carbonates and feature discrete clay mineral and silica alteration patterns. These rocks contain disseminated gold deposits which are amenable to bulk mining (Bagby and Berger, 1985). However, host rock types are known to be variable and can include carbonaceous sandstone and chert, among others. Regional lineaments and structure,

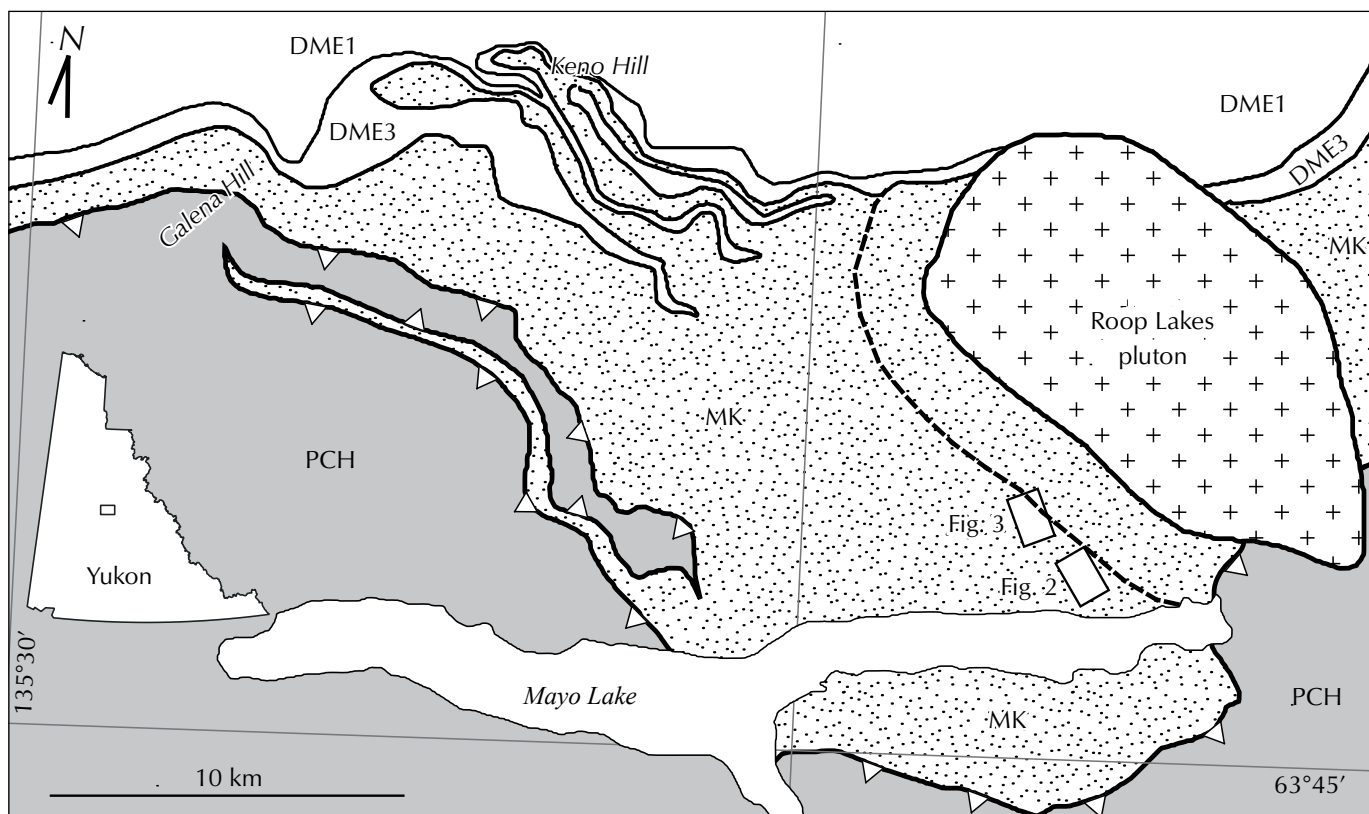


Figure 1. Location map of study areas displaying map sites of Figures 2 and 3 southeast of Keno Hill mining district and immediately west of the Roop Lakes pluton. Map and units are taken from Yukon Geological Survey website; DME1 corresponds to Devono-Mississippian Earn Group unit 1, DME3 to Earn Group unit 3, MK is Mississippian Keno Hill Quartzite, and PCH refers to Neoproterozoic Hyland Group. Unit descriptions can be found in Roots (1997). Dashed line is the outer limit of contact metamorphic halo adjacent to the Roop Lakes pluton.

large-scale hydrothermal circulation, as well as proximity to granitic bodies are also thought to be key (Bagby and Berger, 1985; Arehart, 1996; Lefebure et al., 1999).

Nonetheless, reports of sediment-hosted disseminated gold occurrences remain rare for the Selwyn Basin, owing possibly to the often subtle nature of this type of mineralization, or to difficulties and ambiguities related to classification. This report describes an altered member of the Keno Hill Quartzite unit displaying stratabound alteration and veining with associated disseminated gold values. From a descriptive standpoint, designation for this unit as a sediment-hosted disseminated gold occurrence seems reasonable. However, the example presented here displays mesothermal characteristics, whereas those from type areas tend to be more commonly, though not uniquely, epithermal in character. This paper will identify and characterize a new type of mineralization for the area, which may ultimately help guide further exploration and research.

GEOLOGICAL SETTING

The Mississippian Keno Hill Quartzite (Tempelman-Kluit, 1970; Mortenson and Thompson, 1990; Roots and Murphy, 1992; Roots, 1997) is contained within the ancient continental margin succession of the Paleoproterozoic to Paleozoic western North American miogeocline, near the northern edge of the Selwyn Basin (Abbott et al., 1986; Gordey and Anderson, 1993). The region forms the northern extension of the Omenica Crystalline Belt (Monger et al., 1982) and has been affected by late Jurassic to middle Cretaceous deformation, metamorphism and igneous activity (Roots, 1997). The Keno Hill Quartzite extends continuously along strike for 220 km, from the Tintina Fault in the west, to central Yukon in the east (Tempelman-Kluit, 1970). Strata dip generally south as a result of northerly thrusting; the quartzite may be as much as 1 km thick where affected by imbrication and structural thickening. The southern flank of the quartzite is bound by the Robert Service thrust which juxtaposes Neoproterozoic to Cambrian units of the Hyland Group onto the Mississippian Keno Hill Quartzite (Roots and Murphy, 1992; Thompson, 1995; Roots, 1997). Regional considerations constrain the thrusting between the deformed middle Jurassic strata and Late Cretaceous granitoid magmatism, which postdates deformation. Middle Triassic gabbro and diorite sills are dispersed within the Keno Hill Quartzite and underlying

units (Mortensen and Thompson, 1990) and have been strongly affected by shearing during thrusting.

The deformed sedimentary rocks of the region are cross-cut by a northwest-trending belt of Cretaceous granitic plutons and dykes termed the Tombstone plutonic suite (Anderson, 1987; Poulsen et al., 1997), which was dated by U-Pb zircon geochronology at 90-95 Ma (Mortensen et al., 1996). The Tombstone plutonic suite includes the large Roop Lakes pluton, dated at 92.8 ± 0.5 Ma (Roots, 1997), which intrudes the quartzite east of the Keno Hill mining district. The Keno Hill Quartzite unit comprises a number of lithologies, including dark grey to black, graphitic quartzite containing variable amounts of muscovite, chlorite, tourmaline, carbonate and detrital zircon. Calcareous quartzite also occurs (Roots, 1997), though thin limestone beds are minor to rare. Interbedded schist and graphitic phyllite are common. Tuffaceous metavolcanic rocks are contained within the Keno Hill Quartzite succession (Roots, 1997).

A contact metamorphic halo within the Keno Hill Quartzite extends as much as 4 km away from exposures of the Roop Lakes pluton (Lynch, 1989a,b). Sillimanite schist at the contact passes outwards to garnet-staurolite-plagioclase-biotite-muscovite schist, whereas the outermost halo is characterized by graphite-andalusite schist, or locally biotite-muscovite schist. Porphyroblasts within the metamorphic halo typically overgrow earlier deformation fabrics. Mineral assemblages within the halo permit characterization of pressure and temperature conditions during emplacement of the Roop Lakes pluton. Microprobe analyses for coexisting garnet-staurolite-plagioclase-biotite-muscovite-quartz returned pressure-temperature determinations, based on the intersection point of three independent reactions (Berman, 1991) near 3500 bar and 530°C (Lynch, unpublished data). As a lithostatic pressure determination, 3500 bar reflects a similar crustal depth to the 1500 bar pressure determination for hydrostatic conditions recorded in the veins of the Keno Hill mining district (Lynch, 1989b; Lynch et al., 1990).

Fault- and fracture-controlled hydrothermal veins within the quartzite extend from the margin of the metamorphic halo toward the west into the Keno Hill mining district, forming a vein system distributed across 40 km. Hydrothermal alteration along the veins in the mining district has been dated at 84 Ma by K-Ar analysis of wallrock alteration (Sinclair et al., 1980). Typically, veins are coarse-grained, vuggy, with euhedral to subhedral crystals displaying banding textures, are structurally

discordant, and locally may have well developed alteration haloes. Much of the vein material is unstrained, but parts of some veins contain sheared and deformed crystals, whereas other portions display cyclical brecciation and cementation, indicating contemporaneity between veining, hydrothermal circulation and brittle faulting.

In the study area, the Roop Lakes pluton (Roots, 1997) dominates the centre of map 105 M/15, and is the largest granitic body within the Tombstone plutonic suite. From east to west, veining is zoned away from the pluton, with changing hydrothermal assemblages interpreted to reflect evolving physical-chemical conditions in the fluids (Lynch et al., 1990). Seven mineralogical zones have been defined, which are described in Lynch (1989a,b). Quartz-feldspar-tourmaline veins occur immediately west of this intrusive body, whereas a tungsten skarn is found at its southeastern contact. Outward from the quartz-feldspar veins are vuggy quartz-calcite veins. Further west still, this family of veins transitions into the sulphide-rich, quartz-siderite veins of the Keno Hill silver-lead-zinc mining district. The regional zoning pattern suggests that gold may be found between the Roop Lakes pluton and the Keno Hill district (Lynch, 1986). District-scale zoning in the Keno Hill system is also reflected in the tetrahedrite-freibergite solid solution, with tetrahedrite occurring in the east and changing gradually to freibergite in the west (Lynch, 1989a; Sack et al., 2003). Veins in the mining district display a regular paragenetic association by their growth textures and cross-cutting relationships. These are characterized mainly by early, coarse-grained quartz, followed by siderite and sulphides, and at the western end of the system, a late, fine-grained quartz stage overgrows the middle siderite stage. Furthermore, tetrahedrite has been shown to be a useful petrogenetic indicator; compositions of this mineral in the Keno Hill veins indicate hydrothermal mineralization occurred predominantly within the range of 250° to 310°C, although some analyses indicate that temperatures in the veins may have reached up to approximately 400°C (Sack et al., 2003).

SUGAR MEMBER: GEOLOGY, ALTERATION AND MINERALIZATION

Two detailed maps (1:10 000 scale) of the adjacent study areas are presented in Figures 2 and 3; these maps include the areas surrounding the Sugar and Honey claim groups respectively. The first map (Fig. 2) covers an area

along a stream gully situated at the northeast end of Mayo Lake. At this location, the sloping ridge face above the lake provides adequate outcrop exposure from 3000-4500 ft (914.4-1372.6 m) asl. Five mapable units from within the Keno Hill Quartzite unit can be defined at the present scale of work. These are in ascending order: (1) interbedded, grey-black quartzite, graphitic schist and phyllite, with minor greenstone; (2) a unit of thinly bedded, competent, dark green, tuffaceous volcanic rocks and trachytic andesite; (3) pervasively altered, porous, white sandstone; (4) interbedded, silver-grey and brown-coloured schist and phyllite; and (5) foliated to massive, feldspathic greenstone or metadiorite. Because of deformation and lack of top indicators, the true stratigraphic position of these units remains uncertain, and the sequence of 1-5 above represents the present relative positions of the layered sequence. All, except unit five above, are thought to be subdivisions of the Mississippian Keno Hill Quartzite unit. The greenstone-metadiorite is likely Triassic in age (Mortensen and Thompson, 1990). The principal unit of interest is the pervasively altered, porous, white sandstone which was informally labelled the Sugar member during the course of fieldwork, because in places it has the appearance of granulated white sugar.

Bedding strikes north-northwest and dips moderately east-northeast (Figs. 2, 4, 5). Two penetrative fabrics are generally preserved within the micaceous units, and to varying degrees within the more competent rocks. The earliest and strongest foliation is parallel, or sub-parallel to bedding, and is characterized by aligned mica and locally a schistose fabric. The fabric is axial planar to isoclinal folds, which are sometimes observed at hand sample or outcrop scales. Highly sheared, detached, intrafolial folds, boudins, and fault rock were observed at a contact along a series of outcrops in the centre of the map area (Fig. 2), which has been interpreted as a thrust fault. This fault was extended to a mylonitized greenstone outcrop in the north-centre part of the map area. The second fabric comprises an upright-spaced cleavage which strikes northwest-southeast, and is axial planar to open folds which plunge moderately to the southeast. The two stages of deformation are well known in the district and can be related, in succession, to early thrusting in association with the Robert Service Thrust, followed by later upright folding in association with the Mayo Lake anticline.

The Sugar member stands out as a distinct white sandstone band (Fig. 5, 6) within the layered sequence,

represented by a number of outcrops exposed along the slope and obliquely across the stream gully (Fig. 2, 5). The unit is approximately 20 m thick and is underlain by a competent, well bedded, dark-coloured volcanic lapilli and ash tuff, or locally trachytic andesite. A number of characteristics make the Sugar member unique. The rock is porous, white, and has been almost entirely bleached of

graphite or dark organic matter. Rare, remnant patches of grey-black graphite are present in some outcrops, indicating hints of the protolith, but the graphite is entirely absent in proximity of quartz veins, as well as along alteration haloes which affect most of the unit. The rock has clearly been decarbonized. The porous nature of the rock is also peculiar; the intergranular porosity is

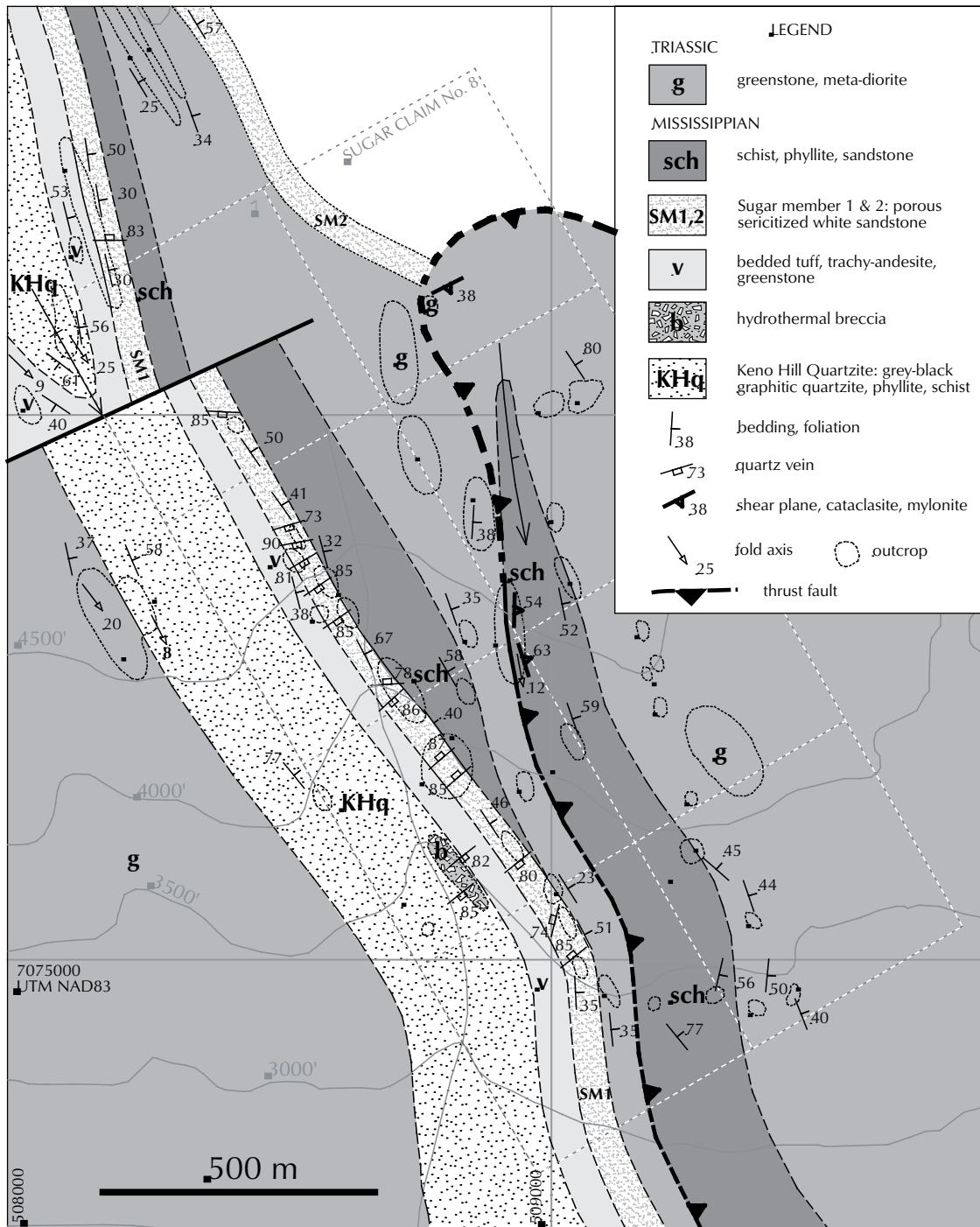


Figure 2. Geological map of area surrounding Sugar claim group.

PROPERTY DESCRIPTION

estimated to be up to 10% and greater. When water is poured onto the rock, it is readily absorbed by the unit. It should be emphasized that sandstone which has been deformed and metamorphosed to the degree that these rocks have, cannot retain any primary porosity. A lack of flattening or annealing gives rise to the distinct high porosity of this unit. It should be noted however, that

irregularly oriented stylolites with black organic-rich seams are sometimes observed, indicating some degree of flattening. All porosity is likely the effect of secondary leaching and postdates penetrative deformation. Removal of organic matter would have contributed to only a small portion of the porosity. Leaching of a cement such as calcite (decalcification) likely contributed to most of the

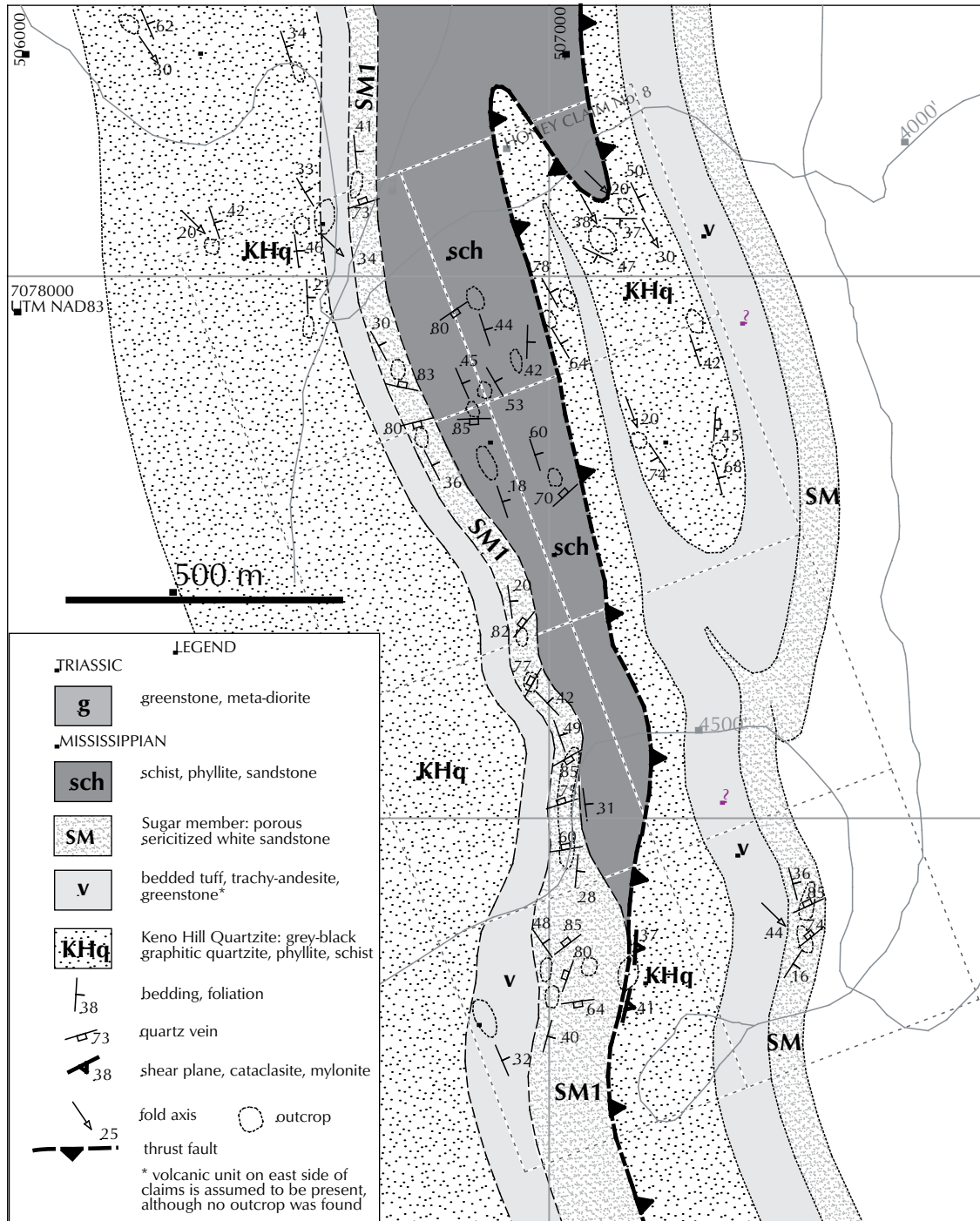


Figure 3. Geological map of area surrounding Honey claim group.

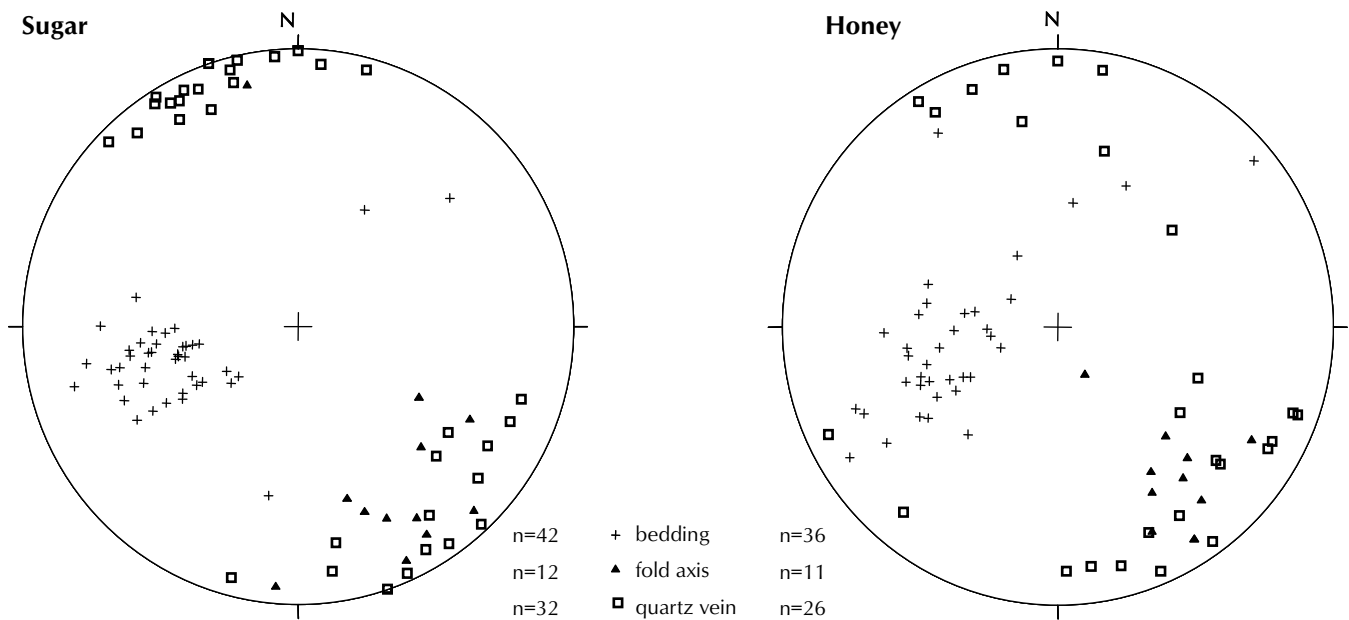


Figure 4. Lower hemisphere equal area stereonet plots of poles to bedding, poles to quartz veins, as well as trend and plunge of late stage fold axes, for areas covering Sugar claim group (Fig. 2) and Honey claim group (Fig. 3).

porosity; calcite is locally an important component of the Keno Hill Quartzite (Green, 1971; Roots, 1997). A further consequence of the secondary porosity is the generally friable nature of the rock, which crumbles between the hands in the case of some samples. Outcrops have rounded, as opposed to angular weathering profiles. Rock competency is variable due to widespread sericitization and patchy silicification, however, overall outcrop exposure is good. Small flakes of satin-white to transparent muscovite/sericite are disseminated throughout the Sugar member. Locally, apple green flakes of Cr-muscovite, or fuchsite are observed, which is consistent with the generally high chromium assay values recorded throughout the unit (Fig. 7). A very light brown to buff colouration is common from the weathering of small quantities of disseminated pyrite. This unit is thought to be equivalent to the hydrothermally altered 'powdery sandstone' of Roots (1997) described from a locality near Mount Albert, and the 'crush breccias' of Green (1971).

Quartz veins are abundant along the entire strike of the Sugar member. The veins are often vuggy with comb texture (Fig. 6), and are very regularly oriented as near-vertical, northeast-southwest-striking, fracture-controlled, planar features (Fig. 4, 6). Fractures and joints which control the veins are oriented approximately perpendicular to late-stage, southeast-plunging fold axes (Fig. 4). Folding appears to have influenced fracture

orientations. Veins terminate at the upper and lower contacts of the Sugar member. Overlying and underlying units are almost entirely barren of veins. One exception is an irregular quartz vein breccia body hosted in the underlying grey-black Keno Hill Quartzite beneath the Sugar member at the south end of the map (Fig. 2). It is clear that the intense vein system is largely stratabound to the Sugar member. Mineralogically, subhedral to euhedral quartz is the dominant mineral in the veins, however, grey-brown botryoidal crusts occur along the walls of some veins, and white clay minerals have been observed as a late vug filling. A black mineral, possibly tourmaline, was observed, but remains to be confirmed.

It is noteworthy that a second occurrence of the Sugar member was mapped (Fig. 2) and is located at an outcrop situated on the upper ridge at the margin of the map area and to the north. It is uncertain if this is a second independent occurrence of the same facies in the normal stratigraphic succession, or if it is a structural repetition of a single unit. The available outcrop distribution does not allow for a clear distinction to be made. Nonetheless, the unit shows the same attributes of alteration and veining as the Sugar member elsewhere in the map area.

Figure 3 is a map of the Sugar member extending northwest from Figure 2. The area covers a portion of the ridge top to the north of Mayo Lake where the topography is flatter. In this area, outcrops are more

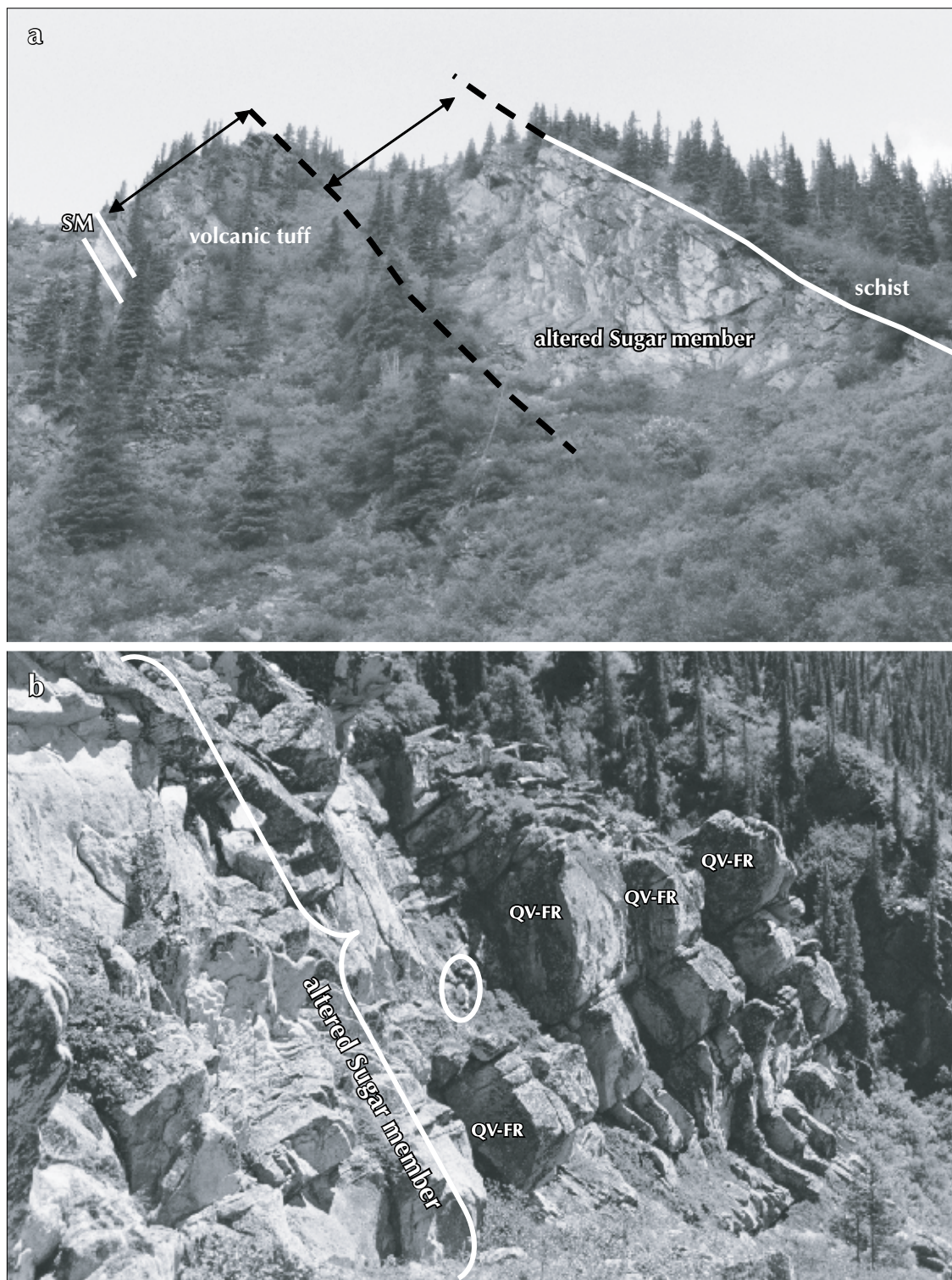


Figure 5. (a) View looking northwest of Sugar member outcrop profile, sandwiched between overlying schist and underlying volcanic tuff units. Light-coloured Sugar member is highly altered and crosscut by numerous fractures and quartz veins. SM refers to a 3-m-thick band of Sugar member contained within bedded volcanic interval below main outcrop. (b) Variably altered white Sugar member with regular set of quartz vein fractures (QV-FR). Note person standing in middle of outcrop (circled) for scale, where Sugar member is at least 20 m thick.

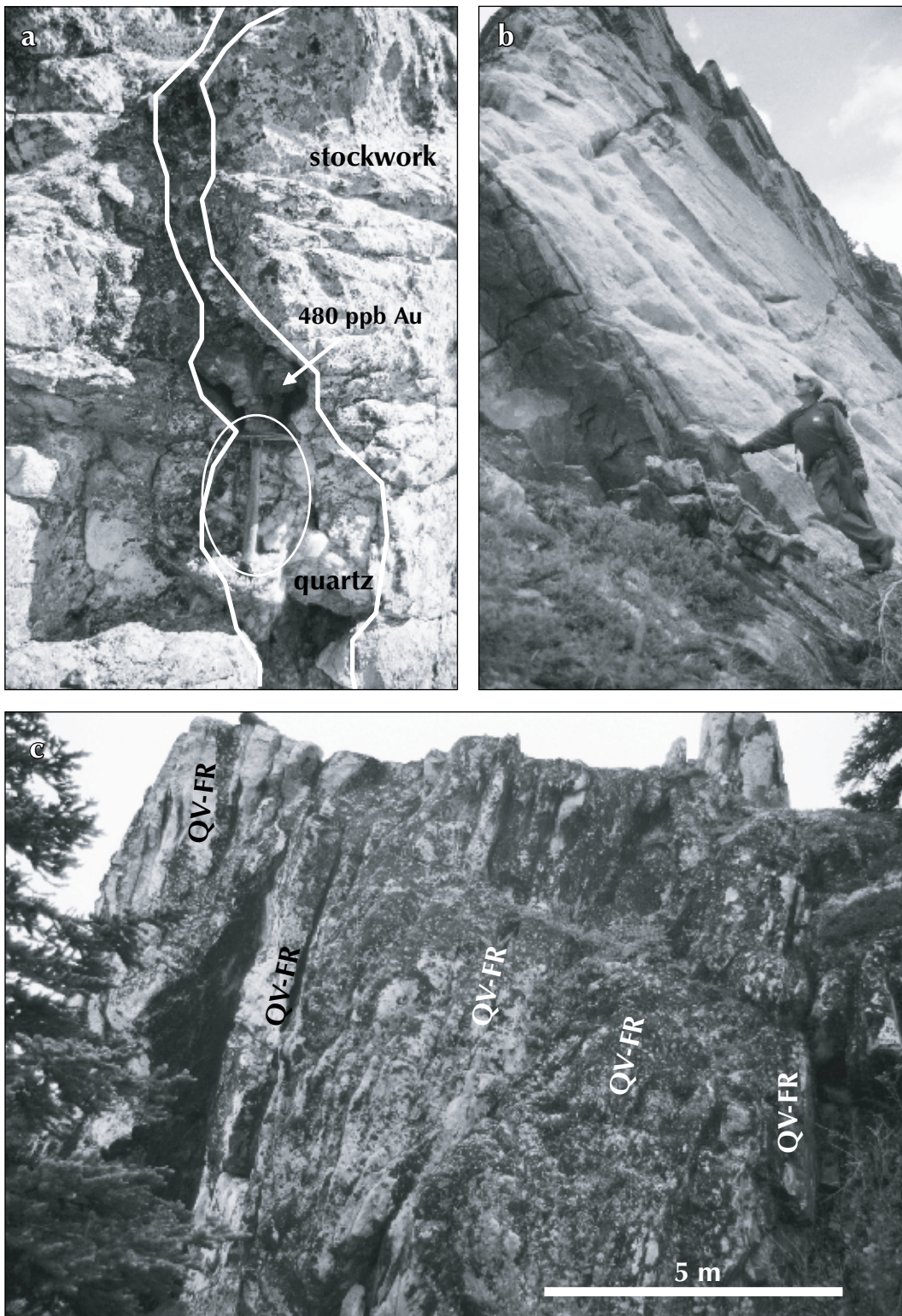


Figure 6. (a) Close up of coarse, vuggy quartz vein within highly altered Sugar member cross-cut by quartz vein stockwork. Composite sample of quartz vein, host rock, and limonite rim returned a value of 480 ppb Au. Circled hammer used for scale. (b) Three-metre-thick subunit of Sugar member within volcanic tuff unit below main Sugar member interval (see SM on Figure 5a). Note rounded weathering profile of porous, crumbly, altered rock compared to brittle, resistant, tight volcanic unit. (c) Parallel, high-density quartz vein fracture (QV-FR) set within altered Sugar member.

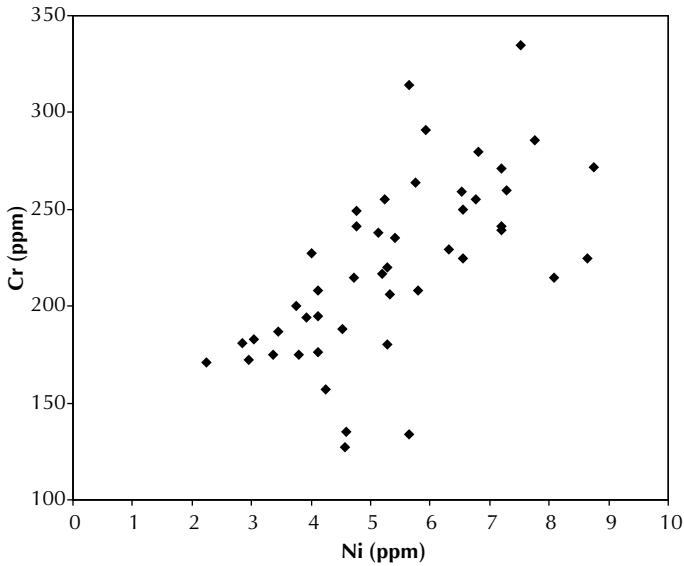


Figure 7. Cross-plot of Cr versus Ni for all samples collected from the study area.

scattered, however, the Sugar member is well exposed in a series of outcrops located along the west side of the map area. In a large outcrop which is continuous for at least 100 m, the unit was measured to be 15 m thick, though this is a minimum since upper and lower contacts are not exposed. Underlying rocks consist of green metavolcanic and greenstone units, which are above grey-black quartzite and phyllite. Overlying rocks are dominated by metasedimentary lithologies consisting of graphitic quartzite, schist and phyllite, as well as one occurrence of sandstone-pebble conglomerate. In contrast to the mapped area to the southeast, a broad continuous unit of greenstone above the Sugar member does not occur in this part of the study area. However, a second unit of the porous, altered and bleached Sugar member is mapped in both the southeast and northwest portions of the study area (Figs. 2 and 3). Structurally, the rocks dip moderately to the east-northeast (Fig. 3, 4). An early, micaceous, bedding-parallel fabric is also recorded. A sheared contact at the top of the Sugar member with detached isoclinal intrafolial folds is found in the southwest portion of the map area and is interpreted to be an early deformation-stage thrust fault. Later, upright, southeast-plunging, open folds are observed in outcrop overprinting the earlier fabrics, and locally have an associated upright-spaced cleavage. A map-scale fold has been interpreted from outcrop exposures. Alteration of the Sugar member is pervasive throughout the southwest portion of the map area and displays a bleached white appearance, sericite alteration and crumbly texture with

intense quartz veining within a porous sandstone. Planar, sub-vertical, northeast-southwest-striking, vuggy quartz veins are abundant and stratabound to the member (Fig. 4). The orientation of the veins in the northwest is remarkably consistent with the veins in the area to the southeast. Disseminated pyrite has been largely oxidized to rust streaks in the rock, or occurs along vein margins.

Interestingly, one occurrence of andalusite within black graphitic schist has been found at the northeast corner of the map area of Figure 3. Andalusite is characteristic of the outer contact metamorphic halo to the Roop Lakes pluton (Lynch, 1989b), and indicates a certain proximity to, and influence from, the underlying pluton.

GEOCHEMISTRY AND ASSAY RESULTS

A total of 45 samples were analysed by inductively coupled plasma mass spectrometry (ICP-MS) for 31 elements; gold was analysed separately by fire assay. Fist-sized samples were collected from the altered Sugar member, including altered hostrock and mixed vein/hostrock materials. Samples were collected in order to cover the entire mapped length of the unit. Within the detection limits, gold ranges from 5 to 50 ppb, with one

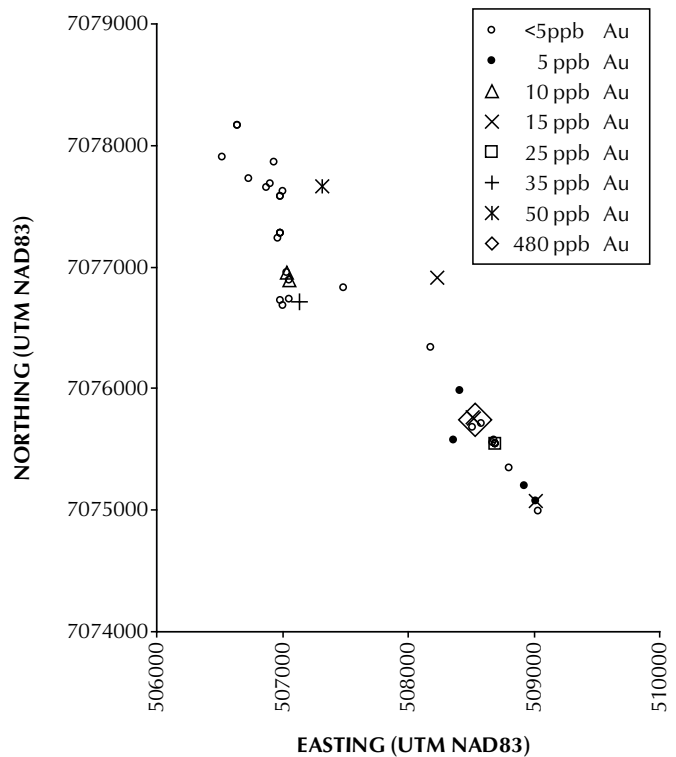


Figure 8. Grid map (UTM NAD83 grid) displaying gold assay results across the two map areas.

outlier that returned a value of 480 ppb (Fig. 8). In total, 14 samples returned gold values distributed along much of the 4-km-long strike length of the unit, although the northwest end appears to be barren. The anomalous value of 480 ppb is from a distinct sample which consists of quartz vein material, altered host rock, and a 1-cm-thick, grey-brown botryoidal goethite rim along the vein margin. None of the other samples include the botryoidal goethite, though this material was noted in the field at other localities such as within the hydrothermal breccia underlying the southernmost end of the Sugar member (Fig. 3); further sampling of this site is necessary now that it has been established that the goethite is gold bearing. Sampling was originally conducted to test for the possibility of widespread, low-grade gold values, in order to determine the potential for bulk mining.

Positive correlations were not established between gold and the other elements. Most of the other metals occur in very low concentrations in the samples. An exception is chromium, which is typically high and correlates positively with nickel (Fig. 7). Values for chromium range up to 335 ppm, well above any concentrations which may arise from contamination by the chromium-molybdenum crusher and are above background values from control samples. Furthermore, the crusher used does not contain nickel, and so the positive correlation between nickel and chromium indicates a natural trend. The likely source of chromium in the rocks is from muscovite, which is known to contain up to 6% naturally occurring Cr_2O_3 . Muscovite is also reported to be chromium-bearing in metasedimentary rocks elsewhere in the Rockies (Heinrich, 1965). High chromium mica, termed fuchsite, is a common alteration product in certain gold districts. However, further mineralogical work is needed to confirm the composition of the muscovite.

In considering the geochemical results and assays, it is important to take into account the particular nature of the host rock. The Sugar member is abnormally porous and susceptible to the effects of surface waters, as well as groundwater. Water is readily absorbed into the unit which has undoubtedly been thoroughly flushed over the years. Samples taken from surface outcrops are largely representative of the present day vadose zone where strong geochemical gradients and element remobilization are common. Consequently, a representative evaluation of the Sugar member would require sampling in drill core from below the water table. Gold associated with pyrite, such as is typical in sediment-hosted disseminated deposits, is largely remobilized in surface exposures,

while most of the pyrite has oxidized to rust streaks. A higher gold content in association with the botryoidal limonite crust for one sample indicates that gold was indeed remobilized in the low-temperature oxidizing environment; refractory ore is postulated at depth.

DISCUSSION AND SUMMARY

This paper describes a new type of gold occurrence east of the Keno Hill mining district, along the northern fringe of the Selwyn Basin. The occurrence may be classified as a sediment-hosted disseminated gold deposit, on the basis of the stratabound nature of the alteration and veining, the disseminated low-grade gold values, as well as on the basis of the observed decarbonatization and apparent decalcification. However, characteristics suggest that the hydrothermal activity occurred within the mesothermal regime by virtue of the coarse-grained, euhedral morphology of quartz crystals within veins, and predominance of sericite-pyrite (phyllic) alteration. This contrasts with the more epithermal character of well established, sediment-hosted disseminated gold deposits, whereby fine-grained cherty quartz and clay (argillic) alteration are more prevalent (Bagby and Berger, 1985; Lefebure et al., 1999), though characteristics of deeper-seated deposits are also known (Peters, 2004).

The exact timing of hydrothermal activity is uncertain, however, alteration and veining post-date stages of penetrative deformation. Furthermore, the porous nature of the altered rock precludes flattening which was observed in the surrounding units. These relationships roughly place a Jurassic age as the lower limit on the timing of events. It is more likely that the hydrothermal circulation is coincident with the adjacent Roop Lakes pluton of mid-Cretaceous age, which also post-dates deformation. Consequently, the veins and altered host rocks may be linked to the Tombstone Gold Belt.

It is also worth considering the position of the altered Sugar member relative to the zoned Keno Hill hydrothermal system (Lynch, 1989 a,b). The site occupies a position at the outer fringe of the contact metamorphic halo which surrounds the Roop Lakes pluton (Fig. 1), a position inboard of quartz-calcite veins which are widespread immediately to the west of the present study area and overlap with the veins of the Keno Hill silver-lead-zinc district. It is noteworthy that calcite veins typically form a halo surrounding sediment-hosted disseminated gold deposits in the Carlin district, which have been affected by decalcification (Bagby and Berger, 1985).

From a mass balance perspective, decalcification in the orebodies is matched by calcite precipitation in veins adjacent to the deposits. This principle may also apply here where decalcification of the Sugar member and surrounding rocks is countered with calcite veining immediately west of the study area, and points toward the possible scale of the system to which alteration in the Sugar member is linked. As a porous hydrothermal aquifer, the Sugar member and similar units may have acted as important conduits for regional hydrothermal circulation. The regular set of fractures, as well as the confined stratabound nature of associated quartz veins within the Sugar member, suggest that the interparticle porosity was present during hydrothermal circulation, creating elevated pore fluid pressures which promoted *in situ* fracturing (e.g., Sibson, 2004). Very high, lateral permeability within the unit would be expected from the presence of such a fracture system. In contrast, the immediately overlying and underlying stratigraphy are not fractured and veined because of their lack of associated porosity and very low pore fluid pressures; alternatively they acted as seals and aquicludes. Such a stratified flow system may have created the underlying feeder network to discordant fault-controlled veins in the region.

ACKNOWLEDGEMENTS

Funding was received from the Yukon Mining Incentives Program (YMIP), which has made this work possible. Patrick Lynch provided support and assistance during the course of fieldwork.

REFERENCES

- Abbott, J.G., Gordey, S.P. and Tempelman-Kluit, D.J., 1986. Setting of stratiform, sediment-hosted lead-zinc deposits in Yukon and northeastern British Columbia. *In: Mineral Deposits of the Northern Cordillera*, J.A. Morin (ed.), Canadian Institute of Mining and Metallurgy, Special Volume 37, p. 1-18.
- Anderson, R.G., 1987. Plutonic rocks of the Dawson map area, Yukon Territory. *In: Current Research*, Geological Survey of Canada Paper 97-1A, p. 689-697.
- Arehart, G.B., 1996. Characteristics and origin of sediment-hosted disseminated gold deposits: a review. *Ore Geology Reviews*, vol. 11, p. 383-403.
- Bagby, W.C. and Berger, B.R., 1985. Geologic characteristics of sediment-hosted, disseminated precious-metal deposits in the western United States. *In: Geology and Geochemistry of Epithermal Systems*, B.R. Berger and P.M. Bethke (eds.), *Reviews in Economic Geology*, vol. 2, Society of Economic Geologists, p. 169-202.
- Berman, R.G., 1991. Thermobarometry using multi-equilibrium calculations: A new technique, with petrological applications. *The Canadian Mineralogist*, vol. 29, p. 833-856.
- Boyle, R.W., 1965. Keno Hill-Galena Hill lead-zinc-silver deposits, Yukon Territory. *Geological Survey of Canada, Bulletin 111*, 302 p.
- Gordey, S.P. and Anderson, R.G., 1993. Evolution of the Northern Cordilleran miogeocline, Nahanni map area (1051), Yukon and Northwest Territories. *Geological Survey of Canada, Memoir 428*, 214 p.
- Green, L.H., 1971. Geology of Mayo Lake, Scougale Creek and McQuesten Lake map-areas, Yukon Territory. *Geological Survey of Canada, Memoir 357*, 72 p.
- Heinrich, W.E., 1965. Further information on the geology of chromian muscovites. *American Mineralogist*, vol. 50, p. 758-762.
- Ilchick, R.P. and Barton, M.D., 1997. An amagmatic origin of Carlin-type gold deposits. *Economic Geology*, vol. 92, p. 269-288.
- Lefebvre, D.V., Brown, D.A. and Ray, G.E., 1999. The British Columbia sediment-hosted gold project. *In: Geological Fieldwork 1998*, B.C. Ministry of Energy and Mines, Paper 1999-1, p. 165-178.
- Lynch, G., 1986. Mineral zoning in the Keno Hill Ag-Pb-Zn mining district, Yukon. *In: Yukon Exploration and Geology 1985*, D.S. Emond and J.A. Morin (eds.), Exploration and Geological Services Division, Yukon Region, Indian and Northern Affairs Canada, p. 89-97.
- Lynch, J.V.G., 1989a. Large-scale hydrothermal zoning reflected in the tetrahedrite-freibergite solid solution, Keno Hill Ag-Pb-Zn district, Yukon. *The Canadian Mineralogist*, vol. 27, p. 383-400.
- Lynch, J.V.G., 1989b. Hydrothermal zoning in the Keno Hill Ag-Pb-Zn vein system: a study in structural geology, mineralogy, fluid inclusions and stable isotope geochemistry. Unpublished PhD thesis, University of Alberta, Edmonton, Alberta, Canada, 219 p.

- Lynch, J.V.G., Longstaffe, F.J. and Nesbitt, B.E., 1990. Stable isotopic and fluid inclusion indications of large-scale hydrothermal paleoflow, boiling and fluid mixing in the Keno Hill Ag-Pb-Zn district, Yukon Territory, Canada. *Geochimica et Cosmochimica Acta*, vol. 54, p. 1045-1059.
- Monger, J.W.H., Price, R.A. and Tempelman-Kluit, D.J., 1982. Tectonic accretion and origin of the two major metamorphic and plutonic belts in the Canadian Cordillera. *Geology*, vol. 10, p. 70-75.
- Mortensen, J.K. and Thompson, R.I., 1990. A U-Pb zircon-baddeleyite age for a differentiated mafic sill in the Ogilvie Mountains, west-central Yukon Territory. *In: Radiogenic Age and Isotope Studies, Report 3, Geological Survey of Canada Paper 89-2*, p. 23-28.
- Mortensen, J.K., Murphy, D.C., Poulsen, K.H. and Bremner, T., 1996. Intrusion-related gold and base metal mineralization associated with the Early Cretaceous Tombstone plutonic suite, Yukon and east-central Alaska. *In: New Mineral Deposit Models of the Canadian Cordillera, 1996 Cordilleran Roundup Short Course Notes, section L*, 13 p.
- Peters, S.G., 2004. Syn-deformational features of Carlin-type Au deposits. *Journal of Structural Geology*, vol. 26, p. 1007-1023.
- Poulsen, K.H., Mortensen, J.K. and Murphy, D.C., 1997. Styles of intrusion-related gold mineralization in the Dawson-Mayo area, Yukon Territory. *In: Current Research 1997-A, Geological Survey of Canada*, p. 1-10.
- Roots, C.F., 1997. Geology of the Mayo Map Area, Yukon Territory (105M). Exploration and Geological Services Division, Yukon, Indian and Northern Affairs Canada, Bulletin 7, 82 p.
- Roots, C.F. and Murphy, D.C., 1992. New developments in the geology of the Mayo map area, Yukon Territory. *In: Current Research, Part A, Geological Survey of Canada, Paper 92-1A*, p. 163-171.
- Sack, R.O., Lynch, J.V.G. and Foit, F. Jr., 2003. Fahlore as a petrogenetic indicator: Keno Hill Ag-Pb-Zn District, Yukon, Canada. *Mineralogical Magazine*, vol. 67, p. 1023-1038.
- Sibson, R.H., 2004. Controls on maximum fluid overpressure defining conditions for mesozonal mineralisation. *Journal of Structural Geology*, vol. 26, p. 1127-1136.
- Sinclair, A.J., Tessari, O.J. and Harakal, J.E., 1980. Age of Ag-Pb-Zn mineralization, Keno Hill-Galena Hill area, Yukon Territory. *Canadian Journal of Earth Sciences*, vol. 17, p. 1100-1103.
- Stephens, J.R., Mair, J.L., Oliver, N.H.S., Hart, C.J.R. and Baker, T., 2004. Structural and mechanical controls on intrusion-related deposits of the Tombstone Gold Belt, Yukon, Canada, with comparisons to other vein-hosted ore-deposit types. *Journal of Structural Geology*, vol. 26, p. 1025-1041.
- Tempelman-Kluit, D.J., 1970. Stratigraphy and structure of the "Keno Hill Quartzite" in Tombstone River, Upper Klondike River map areas, Yukon Territory (116 B/7, B/8). *Geological Survey of Canada, Bulletin 180*, 102 p.
- Thompson, R.I., 1995. Geological compilation (1:250 000) of Dawson map area (11B, C) northeast of Tintina Trench. *Geological Survey of Canada, Open File 3223*, 1:250 000 scale.

